# Electromagnetic Scattering in Microwave Remote Sensing and Fluctuation Electrodynamics

by

Mohammadreza Sanamzadehkarimabad

A dissertation submitted in partial fulfillment
of the requirements for the degree of
Doctor of Philosophy
(Electrical Engineering)
in The University of Michigan
2020

Doctoral Committee:

Professor Leung Tsang, Chair
Professor Eric Michielssen
Professor Kamal Sarabandi
Associate Professor Kai Sun

Mohammadreza Sanamzadehkarimabad
mrsanam@umich.edu
ORCID iD: 0000-0002-6818-856X

*To the memory of my father Davoud,* and
*To my mother Zahra;*
*Thank you for all that you've been to me, for all you've done for me, and for all that you are.*

# ACKNOWLEDGMENTS

I don't know if it is possible to convey in words the sense of gratitude I feel. Foremost, I would like to express my sincere gratitude to my advisor Prof. Leung Tsang for the continuous support of my Ph.D study and research, for his patience, motivation, enthusiasm, and immense knowledge. His willingness to give his time so generously and responding to my questions and queries so promptly have been very much appreciated.

I would like to give special thanks to my dissertation committee Prof. Kamal Sarabandi, Prof. Eric Michielssen, and Prof. Kai Sun for their support, feedback, insightful comments, and encouragement.

A special warm thank you to Prof. Joel Johnson (Ohio State University) who generously accommodated me in the Ultra-wideband Software-Defined Microwave Radiometer (UWBRAD) project. His great support, huge work experience, and patience were necessary for finishing this thesis.

The funding received from the National Aeronautics and Space Administration (NASA) Earth Science Division through UWBRAD project (NNH13ZDA001N-IIP) and National Science Foundation (NSF, F039963) is deeply appreciated. I am also grateful to the funding received from the University of Michigan to undertake my PhD.

I owe a great debt of gratitude to my former mentors at Sharif University of Technology, in particular, Prof. Khashayar Mehrany, Prof. Hamid Behroozi , and Prof. Vahid Karimipour for their mentorship, help, and encouragement.

My time at Michigan was made enjoyable in large part due to the many friends that became a part of my life. I am grateful for time spent with colleagues and friends for providing support and friendship that I needed.

Last but not the least, I would like to thank my family: my parents and brothers for supporting me spiritually throughout my life.

# TABLE OF CONTENTS

# LIST OF FIGURES

# LIST OF TABLES

# LIST OF APPENDICES



-

# ABSTRACT

Application of the electromagnetic scattering theory to the physical models of microwave remote sensing of natural targets including but not limited to polar ice sheets, soil surface, vegetated area, etc. and fluctuation electrodynamic as well as microwave resonators are presented in this thesis. Advancement of the remote sensing technology led the radar and radiometry measurement to a level of accuracy that correct interpretation of the measurement outcomes and relating those to the unknown parameters under study requires the physical models that are capable of resembling the real life situation as close and accurate as possible. Along with accuracy, the model should be simple enough for the purpose of real time implementation. This is where the analytical solution of the physical problem manifest itself against pure numerical methods in terms of the fast evaluation and more importantly the insight that is not available in a numerical approach. Scattering from random rough interferences is studied throughout the first part of the thesis. Also, beyond the small perturbation method, the T-matrix method is also studied as an alternative approach that works for larger surface heights. Beside these, an alternative partially coherent approach is also introduced to significantly reduce the computational cost of the problem of layered media with random permittivity profile. The finite coherency length of the propagating wave inside the layered media is considered to divide the layered media into smaller blocks and then combine the block's responses afterward. In the second part we consider fast and broad band computation of the Green's function inside the cavity of irregular shape. Conventional way of computing the Green's function of an irregular shaped cavity is the numerical methods such as surface integral equation or finite element methods which can obtain the response at single frequency with intensive computational cost. The proposed method utilizes the imaginary wave number extraction of the Green's function from itself to develop a broad band and at the same time fast converging hybrid spatial-spectral expansion to achieve a highly accurate result for the Green's function whereas in computing the Green's function of cavity using numerical methods, a fine sweep over the frequency band is required to capture individual resonance line, the broad band solution provide the solution thousand times faster than the competitor methods. The last part of the thesis includes a classical electromagnetic treatment of the Casimir self-stress on nano tubes. Although the Casimir force on the parallel plates can be regularized by throwing away the bulk part of the full Green's function, it is shown that such a regularization does not remove divergence of zero-point energy and the final stress is computed by applying further regularizations.

# Chapter 1

# Fluctuation-Dissipation Theorem and Brightness Temperature

## 1.1 Introduction

Every object at non-zero temperature $T$ radiates electromagnetic wave Spontaneously and continuously. This electromagnetic radiation is often called the thermal radiation as the radiation spectrum is stronger over the Infrared band. Thermal radiation from an object is strongly dependent on the physical properties of the object[1, 2]. In order to simplify the subject, people often define an imaginary object that radiates perfectly (In term of far field radiation) which is know as *Blackbody*. Perfect radiator here stands for an object that achieves maximum possible radiated power when it is in equilibrium with a thermal bath at temperature $T$. Assuming such an object separates out the dependence of the thermal radiation from the physical characteristics of the radiator. Planck's radiation law expresses how the thermal radiation depends on the temperature of the radiator object and what would be the frequency content of the radiated field.

## 1.2 Planck's Radiation Law

The radiated power from an object primarily depends on the size of the object, the direction in which power being measured, the bandwidth of the receiver, and the distance between the receiver and the radiator. In order to quantify radiated power in general, a normalized quantity can be defined that elevates the above dependencies. Radiated power from a unit surface area of an object at thermal equilibrium at frequency of $\omega$ within unit solid angle of emission is called the *Radiance* of the object. For a blackbody at fixed temperature $T$, the radiance $I_B(\omega,T)$ is given by the Planck's law[3–6],

$$I_B(\omega,T)=\frac{\hbar\omega^3}{2\pi^2c^2}\frac{1}{e^{\hbar\omega/kT}-1} \tag{1.2.1}$$

With unit of $[I_B]=\mathrm{W}\cdot\mathrm{m}^{-2}\cdot\mathrm{Sr}^{-1}\cdot\mathrm{Hz}$. Note that this is the maximum possible radiance for an ideal object that can deliver whole thermal energy to the radiation field. Now, for an arbitrary imperfect object (Gray object) we introduce the emissivity function $0\leq e(\Omega,\omega)\leq 1$, which is its effectiveness in radiating the thermal energy, as [4]

$$I_G(\omega,T)=e(\Omega,\omega)I_B(\omega,T) \tag{1.2.2}$$

The thermal radiation in general is not polarized. However, the emissivity $e(\Omega,\omega)$ for different states of polarization can be different that changes the radiated power polarization.

Figure. 1.1 plots the radiance spectrum for different body temperatures. The frequency

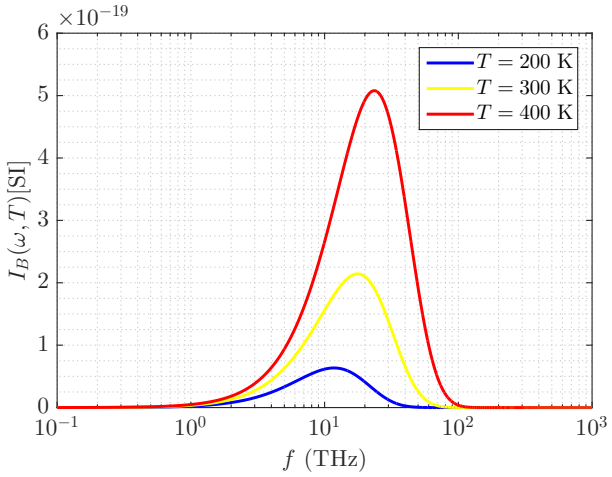


FIGURE 1.1: Radiance of a blackbody at temperature $T$ vs frequency for different temperature.

at which maximum radiance occurs shifts to higher frequencies as temperature increases in a linear fashion ($f_{\max} \propto T$). This shows that a light bulb should works at very high temperature to have a good visible radiation at optical frequencies. For temperatures in the order of room temperature, maximum radiation falls within the IR band (300 GHz - 430 THz) where the radiation can be absorbed greatly and produce heat. That's why blackbody radiation is known as thermal radiation.

If we have a receiver with infinite bandwidth that integrates the radiated power over all frequencies, the result is interesting. Power radiated by surface $\mathrm{d}A$ of a blackbody through solid angle of $\mathrm{d}\Omega$ and frequency band $\mathrm{d}\omega/(2\pi)$ is $\mathrm{d}P(T) = I_B(T,\omega)\mathrm{d}A\mathrm{d}\omega/(2\pi)\mathrm{d}\Omega$. The blackbody can be placed face up inside a sphere ($\hat{z}$ is normal to the surface). Then the power flux through a surface element on the sphere would be $I_B(T,\omega)\mathrm{d}A\mathrm{d}\omega/(2\pi)\cos\theta\mathrm{d}\Omega$ and total radiated power over all bandwidth [7]

$$\begin{aligned}\frac{\mathrm{d}P(T)}{\mathrm{d}A} &= \int_0^\infty \frac{\mathrm{d}\omega}{2\pi} \int_{(2\pi)^+} \mathrm{d}\Omega \cos\theta I_B(T,\omega) \\ &= \frac{\hbar}{4\pi^2\hbar^3c^2} \int_0^\infty \mathrm{d}\omega \frac{(\hbar\omega)^3}{e^{\hbar\omega/kT}-1} \\ &= \frac{\pi^2(k_BT)^4}{60\hbar^3c^2}\end{aligned} \tag{1.2.3}$$

where the last integral can be computed using the Gamma function. Therefore, broadband radiated power per unit area of the blackbody is [8, 9]

$$\frac{P(T)}{A} = \sigma T^4 \tag{1.2.4}$$

where $\sigma = \dfrac{\pi^2 k_B^4}{60\hbar^3c^2}$ is the Stefan-Boltzmann constant ($[\sigma] = \mathrm{W}\cdot\mathrm{m}^{-2}\cdot\mathrm{K}^{-4}$). This is the Stefan-Boltzmann law which shows the broadband radiated power from unit area of the blackbody is proportional to $T^4$. This law was discovered before Planck discover the black body radiation spectrum.

### 1.2.1 Black Body as a Bosonic Gas

The black body can be considered as a photon gas in equilibrium with the cavity. The photon gas is actually collection of simple harmonic oscillators with different natural frequencies that construct the modes inside the cavity. The dispersion relation of each mode of oscillation is

$$\omega = ck \tag{1.2.5}$$

The density of states of the electromagnetic waves as a function of $k$ is the number of modes with wave number between $k$ and $k+\mathrm{d}k$. Considering a cavity of volume $L^3$ with periodic boundary condition, each mode occupies the volume of $(2\pi/L)^3$ in $k-$space, while the volume of a spherical shell of thickness $\mathrm{d}k$ at $k$ in spectral space is $4\pi k^2\mathrm{d}k$. In addition, in the volume that occupied with a single mode, there are two electromagnetic modes with two polarizations. Therefore, the density of states can be expressed as,

$$g(k)\mathrm{d}k = \frac{4\pi k^2}{(2\pi/L)^3} \times 2 = V\frac{k^2\mathrm{d}k}{\pi^2} \tag{1.2.6}$$

where $V$ is the volume of cavity. Density od states can be equivalently expressed in term of $\omega$ through

$$g(\omega) = g(k)\Big|_{k=\omega/c}\frac{\mathrm{d}k}{\mathrm{d}\omega} \tag{1.2.7}$$

and hence,

$$g(\omega)\mathrm{d}\omega = V\frac{\omega^2\mathrm{d}\omega}{\pi^2c^3} \tag{1.2.8}$$

The density of states $g(\omega)\mathrm{d}\omega$ shows number of photons in the box with volume $V$, that have oscillation frequency between $\omega$ and $\omega+\mathrm{d}\omega$. According to Bose-Einstein statistic for photons in equilibrium at temperature $T$, average number of photons in state $\omega$ is given by,

$$N(\omega) = \frac{1}{e^{\hbar\omega/kT}-1} \tag{1.2.9}$$

Then the energy of all of the system in state $\omega$ is $(N(\omega)+1/2)\hbar\omega$ as the Hamiltonian of the system can be written as $H=(N+1/2)\hbar\omega$ ant $N$ is the particle number operator. Considering the density of state, total electromagnetic energy of the system is given by

$$U = \int_0^\infty \mathrm{d}\omega g(\omega)\hbar\omega\left(\frac{1}{2}+\frac{1}{e^{\hbar\omega/kT}-1}\right) \tag{1.2.10}$$

The constant term of $1/2$ corresponds to the zero point energy of the vacuum which results in a divergent result for the energy. However, this term can be ignored by redefining the reference of the energy (normal ordering). Therefore, renormalized energy can be written as

$$U = V\frac{\hbar}{\pi^2c^3}\int_0^\infty \mathrm{d}\omega\frac{\omega^3}{e^{\hbar\omega/kT}-1} \tag{1.2.11}$$

The energy per unit volume $u=:U/V$

$$u=\frac{\hbar}{\pi^2c^3}\int_0^\infty \mathrm{d}\omega \frac{\omega^3}{e^{\hbar\omega/kT}-1} \tag{1.2.12}$$

From the energy density, the radiated power would be $cu$. If we express the frequency integral in terms of $\nu$

$$P=\frac{\hbar}{\pi^2c^3}\int_0^\infty 2\pi\mathrm{d}\nu \frac{\omega^3}{e^{\hbar\omega/kT}-1} \tag{1.2.13}$$

Normalizing the integrand by $4\pi$ gives power density per unit solid angle. In fact, before discovery of Planck, people tried to do inversely, i.e. somehow finding a radiation spectrum $I_B(\omega,T)$ from the Stefan-Boltzmann law in a compatible way. From (1.2.13), the specific intensity of the radiation can be identified as

$$I_B(\omega,T)=\frac{\hbar}{2\pi^2c^3}\frac{\omega^3}{e^{\hbar\omega/kT}-1} \tag{1.2.14}$$

which is the Planck's radiation law of the black body.

## 1.3 Fluctuation-Dissipation Theorem

Although Planck's radiation law describes radiation intensity of a black body object in thermal equilibrium at temperature $T$, for small objects compared to the thermal wavelength $\lambda_T$, radiated energy differs from black body radiation because of interference of radiation with the object itself. In other words, the emission from the object depends on the other physical parameters of the object in addition to its temperature. The thermal wavelength $\lambda_T$ comes to the picture by considering a photon with oscillation frequency of $\omega$. Assigned energy $\hbar\omega$ corresponds to thermal energy of $k_BT$ that gives a thermal wavelength of $\lambda_T=\hbar c/k_BT$ (thermal wavelength is approximately $7\mu$m at room temperature).

Another question regarding the thermal radiation of the black body comes about the polarization of the radiated wave. Experiments have shown that the radiated heat can be polarized depending on the size of the object (aspect ratio). As we can predict, thermal radiation is nothing but the radiation from the fluctuating particles inside the object. If we have a wire like object with radius smaller than the thermal wavelength, it is expected to mostly have polarized electric field along the wire. Actually it is the case, as the wire length tends to zero, radiation becomes fully polarized along the wire [1].

If instead of radiation intensity, the excitations sources inside the object are known in a consistent manner, then radiation formulation can account for the radiation properties like polarization, near field radiation and physical parameters of the radiating object. Fluctuation-dissipation theorem provides a consistent inversion of the radiation intensity to find the source of radiation.

### 1.3.1 Classical Response Function

Consider a system consists of dipole moments $\overline{P}(s)$ with Hamiltonian $H_0(s)$ where $s=(q_i,p_i)\in\Omega$ is a point in the phase space of the system where $q_i$'s and $p_i$'s are coordinates and conjugate momenta, respectively. The probability density of any physical quantity of

the system (including dipole moment) to be in the state $s$ in equilibrium at temperature $T$, is classically given by the Boltzmann distribution [10],

$$f_{eq}(s) \propto e^{-\beta H_0(s)} \tag{1.3.1}$$

where $\beta = 1/k_B T$. Statistical average of the dipole moment $\overline{P}$ in equilibrium over the whole phase space can be obtained as

$$\langle \overline{P} \rangle = \frac{\int_\Omega \mathrm{d}s \overline{P}(s) e^{-\beta H_0(s)}}{\int_\Omega \mathrm{d}s e^{-\beta H_0(s)}} \tag{1.3.2}$$

If perturbation electric field $\overline{E}(\overline{r},t)$ interacts with the system, the Hamiltonian become perturbed $H = H_0 + \delta H$ where the perturbation Hamiltonian contains interaction of the applied electric field with the dipole moment of the system,

$$\delta H = -\int_V \mathrm{d}\overline{r} \overline{P}(\overline{r},t) \cdot \overline{E}(\overline{r},t) \tag{1.3.3}$$

If we consider an object with physical dimension smaller than the thermal wave length, then we can approximate the object by it's dipole moment (which is independent of location) and write

$$\delta H = -\overline{P}(t) \cdot \overline{E}(t) \tag{1.3.4}$$

Due to this perturbation, the expected value of the dipole moment changes $\langle \delta \overline{P} \rangle(t) = \langle \overline{P}(t) \rangle - \langle \overline{P} \rangle_{\mathrm{eq}}$ where $\langle \overline{P}(t) \rangle$ is the expected value after applying the perturbation at time $t$. If we assume the change in the dipole moment expectation is small and is linearly proportional to the perturbation electric field, the change in the dipole moment of the system can be written as [10, 11],

$$\langle \delta \overline{P} \rangle(t) = \int_{-\infty}^{\infty} \mathrm{d}t' \, \overline{\overline{\chi}}(t,t') \cdot \overline{E}(t') \tag{1.3.5}$$

where, $\overline{\overline{\chi}}$ is the linear response function of the system. For a perturbation electric field which is constant $\overline{E}_0$ before $t$ and vanishes afterward,

$$\langle \delta \overline{P} \rangle(t) = \left[ \int_t^{\infty} \mathrm{d}t' \, \overline{\overline{\chi}}(t') \right] \cdot \overline{E}_0 \tag{1.3.6}$$

where, causality of the response function ($\overline{\overline{\chi}}(t) = 0$ for $t < 0$) and stationary time response is applied. Equation (1.3.6) can be solved for the response function to find

$$\chi_{ij}(t) = -\frac{1}{E_{0j}} U(t) \frac{\mathrm{d}}{\mathrm{d}t} \langle \delta P_i \rangle(t) \tag{1.3.7}$$

Here, $U(t)$ is the unit step function to enforce causality. The response function $\chi_{ij}(t)$ can be determined by knowing the time derivative of $\delta \langle \overline{P} \rangle(t)$. The expectation value of the dipole moment $\overline{P}$ after perturbation can be evaluated using Boltzmann distribution with perturbed Hamiltonian $H_0 + \delta H$ [12]

$$f(s) \propto e^{-\beta(H_0 + \delta H)} = f_{eq}(s) e^{-\beta \delta H} \approx f_{eq}(s) \left[ 1 - \beta \delta H \right] \tag{1.3.8}$$

Therefore the expectation value of the dipole moment after applying perturbation would be

$$\begin{aligned}\langle\overline{P}(t)\rangle&=\frac{\langle\overline{P}\rangle_{\rm eq}-\beta\langle\overline{P}\delta H\rangle_{\rm eq}}{\langle 1-\beta\delta H\rangle_{\rm eq}}\\&=\Big(\langle\overline{P}\rangle_{\rm eq}-\beta\langle\overline{P}\delta H\rangle_{\rm eq}\Big)\Big[1+\beta\langle\delta H\rangle_{\rm eq}\Big]\end{aligned}\tag{1.3.9}$$

Keeping the terms up to the first order of applied field,

$$\langle\overline{P}(t)\rangle=\langle\overline{P}\rangle_{\rm eq}-\beta\langle\overline{P}(t)\delta H\rangle_{\rm eq}+\beta\langle\delta H\rangle_{\rm eq}\langle\overline{P}(t)\rangle_{\rm eq}\tag{1.3.10}$$

or,

$$\langle\delta\overline{P}\rangle(t)=-\beta\langle\overline{P}(t)\delta H\rangle_{\rm eq}+\beta\langle\delta H\rangle_{\rm eq}\langle\overline{P}(t)\rangle_{\rm eq}\tag{1.3.11}$$

For the perturbation at time $t=0$, $\delta H=-\overline{P}(0)\cdot\overline{E}_0$

$$\begin{aligned}\langle\delta\overline{P}\rangle(t)&=\beta\Big[\langle\overline{P}(t)\overline{P}(0)\rangle_{\rm eq}-\langle\overline{P}(t)\rangle_{\rm eq}\langle\overline{P}(0)\rangle_{\rm eq}\Big]\cdot\overline{E}_0\\&=\beta\Big\langle\Big[\overline{P}(t)-\langle\overline{P}\rangle_{\rm eq}\Big]\Big[\overline{P}(0)-\langle\overline{P}\rangle_{\rm eq}\Big]\Big\rangle_{\rm eq}\cdot\overline{E}_0\\&=\beta\Big\langle\delta\overline{P}(t)\delta\overline{P}(0)\Big\rangle_{\rm eq}\cdot\overline{E}_0\end{aligned}\tag{1.3.12}$$

Note that the expectation value $\langle\delta\overline{P}\rangle(t)$ is over non-equilibrium states while the above result is in term of equilibrium expectation. Substituting in Eq. (1.3.7) results in

$$\overline{\overline{\chi}}(t)=-\beta U(t)\frac{\rm d}{{\rm d}t}\Big\langle\delta\overline{P}(t)\delta\overline{P}(0)\Big\rangle_{\rm eq}\tag{1.3.13}$$

However, it is assumed that the response function is stationary in time, thus

$$\overline{\overline{\chi}}(t)=-\beta U(t)\frac{\rm d}{{\rm d}t}\Big\langle\delta\overline{P}(t+\tau)\delta\overline{P}(\tau)\Big\rangle_{\rm eq}\tag{1.3.14}$$

In general, being stationary in time implies uncorrelated spectrum in frequency domain, except at a point. Assuming Fourier transform of dipole moment,

$$\delta\overline{P}(t)=\int\frac{{\rm d}\omega}{2\pi}e^{-i\omega t}\delta\overline{P}(\omega)\tag{1.3.15}$$

and the response function as

$$\overline{\overline{\chi}}(t)=\int\frac{{\rm d}\omega}{2\pi}e^{-i\omega t}\overline{\overline{\chi}}(\omega)\tag{1.3.16}$$

then, correlation of frequency components yields

$$\begin{aligned}\Big\langle\delta\overline{P}(t+\tau)\delta\overline{P}(\tau)\Big\rangle&=\int\frac{{\rm d}\omega}{2\pi}\int\frac{{\rm d}\omega'}{2\pi}\Big\langle\delta\overline{P}(\omega)\delta\overline{P}(\omega')\Big\rangle e^{-i\omega(t+\tau)}e^{-i\omega'\tau}\\&=\int\frac{{\rm d}\omega}{2\pi}\int\frac{{\rm d}\omega'}{2\pi}\Big\langle\delta\overline{P}(\omega)\delta\overline{P}(\omega')\Big\rangle e^{-i(\omega+\omega')\tau}e^{-i\omega t}\end{aligned}\tag{1.3.17}$$

Left hand side does not depends on $\tau$. Right hand side becomes independent of $\tau$ if

$$\left\langle \delta\overline{P}(\omega)\delta\overline{P}(\omega')\right\rangle \propto \delta(\omega+\omega') \tag{1.3.18}$$

Assuming this proportionality,and since $\delta\overline{P}(t)$ is a real quantity

$$\frac{\mathrm{d}}{\mathrm{d}t}\left\langle \delta\overline{P}(t+\tau)\delta\overline{P}(\tau)\right\rangle_{\mathrm{eq}} = \int \frac{\mathrm{d}\omega}{2\pi}(-i\omega)\left\langle \delta\overline{P}(\omega)\delta\overline{P}^{*}(\omega)\right\rangle e^{-i\omega t} \tag{1.3.19}$$

Fourier Transform of the response function is convolution of spectrum of step and spectral density of the dipole moment,

$$\begin{aligned}\overline{\overline{\chi}}(\omega) &= -\beta U(\omega) \star \frac{-i\omega}{2\pi}\left\langle \delta\overline{P}(\omega)\delta\overline{P}^{*}(\omega)\right\rangle \\ &= -\beta\left[-\frac{1}{i\omega}+\pi\delta(\omega)\right]\star(-i\omega)\left\langle \delta\overline{P}(\omega)\delta\overline{P}^{*}(\omega)\right\rangle\end{aligned} \tag{1.3.20}$$

Finding the imaginary part of the response function is less difficult.

$$2\mathrm{Im}\ \overline{\overline{\chi}}(\omega) = 2\pi\frac{\omega}{k_B T}\left\langle \delta\overline{P}(\omega)\delta\overline{P}^{*}(\omega)\right\rangle \tag{1.3.21}$$

If we call the $\delta\overline{P}(\omega)$ noise polarization $\overline{P}_N(\omega)$ caused by perturbation, then

$$\left\langle \overline{P}_N(\omega)\overline{P}_N^{*}(\omega')\right\rangle = \frac{k_B T}{\pi\omega}\mathrm{Im}\ \overline{\overline{\chi}}(\omega)\delta(\omega-\omega') \tag{1.3.22}$$

This derivation is based on classical physics. In order to transit to the quantum limit, classical average energy of $k_B T$ per degree of freedom should be replaced by energy of the harmonic oscillator

$$E(\omega,T) = \left(n(\omega)+\frac{1}{2}\right)\hbar\omega = \hbar\omega\left(\frac{1}{e^{\beta\hbar\omega}-1}+\frac{1}{2}\right) \tag{1.3.23}$$

Henceforth, Spectral density of the noise polarization is given by [2, 13]

$$\begin{aligned}\left\langle \overline{P}_N(\omega)\overline{P}_N^{*}(\omega')\right\rangle &= \frac{\hbar}{\pi}\mathrm{Im}\ \overline{\overline{\chi}}(\omega)\left(\frac{1}{e^{\beta\hbar\omega}-1}+\frac{1}{2}\right)\delta(\omega-\omega') \\ &= \frac{\hbar}{2\pi}\mathrm{Im}\ \overline{\overline{\chi}}(\omega)\coth\left(\frac{\hbar\omega}{2k_B T}\right)\delta(\omega-\omega')\end{aligned} \tag{1.3.24}$$

In our derivation, $\overline{\overline{\chi}}$ is response of polarization to the external electric field which means $\mathrm{Im}\overline{\overline{\chi}} = \varepsilon_0\overline{\overline{\varepsilon}}''$ and $\mathrm{Re}\overline{\overline{\chi}} = \varepsilon_0(\overline{\overline{\varepsilon}}'-\overline{\overline{I}})$. It turns out that for a local medium, the noise polarization at different points in space is uncorrelated. For an isotropic, local material at temperature $T$

$$\left\langle \overline{P}_N(\overline{r},\omega)\overline{P}_N^{*}(\overline{r}',\omega')\right\rangle = \frac{\hbar\varepsilon_0}{2\pi}\varepsilon''(\overline{r},\omega)\coth\left(\frac{\hbar\omega}{2k_B T}\right)\delta(\omega-\omega')\delta(\overline{r}-\overline{r}')\overline{\overline{I}} \tag{1.3.25}$$

using $\overline{D}=\varepsilon_0\overline{E}+\overline{P}$ microscopic Maxwell's law in the dielectric medium reads

$$\nabla\times\overline{H}=\overline{J}(\overline{r})+\varepsilon_0\frac{\partial\overline{E}}{\partial t}+\frac{\partial\overline{P}}{\partial t}+\frac{\partial\overline{P}_N}{\partial t} \tag{1.3.26}$$

The noise current density $\overline{J}_N$ is related to the noise polarization through $\overline{J}_N=\partial\overline{P}_N/\partial t$ and therefore,

$$\left\langle\overline{J}_N(\overline{r},\omega)\overline{J}_N^*(\overline{r}',\omega')\right\rangle=\frac{\hbar\omega^2\varepsilon_0}{2\pi}\varepsilon''(\overline{r},\omega)\coth\left(\frac{\hbar\omega}{2k_BT}\right)\delta(\omega-\omega')\delta(\overline{r}-\overline{r}')\overline{\overline{I}} \tag{1.3.27}$$

This is the statement of *Fluctuation-Dissipation* Theorem (FDT) [13, 14]. Note that here we considered positive and negative frequencies. Single sideband power spectral density would have additional factor of 2. This is the correlation of fluctuating current density as a result of loss in the medium. According to Fluctuation-dissipation theorem, fluctuations and loss in the medium are always tied together. All the physical media are lossy, as having a lossless media contradict the Kramers–Kronig relations and consequently the causality principle. Therefore having a fluctuation or excitation in the medium comes with dissipations. On the other hand, wherever there is loss (always), there should be some fluctuations in the medium that is given by FDT.

## 1.4 Radiated Electric Field From an Object at Temperature $T$

Utilizing the Fluctuation-Dissipation theorem, statistics of fluctuating current inside the object at temperature $T$ is known. Therefore, finding the radiated electric field is a classical problem of radiation from a statistical source.

Consider an object that occupies volume $V_1$ with permittivity of $\varepsilon_0\varepsilon_1$ and the rest of space $V_0=\mathbb{R}^3-V_1$ is vacuum. In order to relate the fluctuating current inside the object to the radiated field in $V_0$, the dyadic Green's function can be utilized. For a current density $\overline{J}(\overline{r},\omega)$ inside the object, the radiated field satisfies the homogeneous wave equation of

$$\nabla\times\nabla\times\overline{E}_0(\overline{r},\omega)-\omega^2\mu_0\varepsilon_0\overline{E}_0(\overline{r},\omega)=0 \tag{1.4.1}$$

Here, $\overline{r}\in V_0$ but the source is inside the object. In order to find the surface fields as boundary conditions for the radiated field, one should solve the wave equation inside the object

$$\nabla\times\nabla\times\overline{E}_1(\overline{r},\omega)-\omega^2\mu_0\varepsilon_0\varepsilon_1\overline{E}_1(\overline{r},\omega)=i\omega\mu_0\overline{J}(\overline{r},\omega) \tag{1.4.2}$$

Finding the radiated field requires solution of both Eqs. (1.4.1) and (1.4.2) together. Equivalently, we can define dyadic Green's function as propagator of the field to $V_0$ and $V$ via

$$\begin{aligned}\nabla\times\nabla\times\overline{\overline{G}}^{[01]}(\overline{r},\overline{r}',\omega)-\omega^2\mu_0\varepsilon_0\overline{\overline{G}}^{[01]}(\overline{r},\overline{r}',\omega)&=0\\ \nabla\times\nabla\times\overline{\overline{G}}^{[11]}(\overline{r},\overline{r}',\omega)-\omega^2\mu_0\varepsilon_0\varepsilon\overline{\overline{G}}^{[11]}(\overline{r},\overline{r}',\omega)&=i\omega\mu_0\overline{J}(\overline{r},\omega)\end{aligned} \tag{1.4.3}$$

Here, $\overline{\overline{G}}^{[01]}(\overline{r},\overline{r}',\omega)$, $\overline{\overline{G}}^{[11]}(\overline{r},\overline{r}',\omega)$ refer to the Green's propagator with source in the region 1 and observation points in region 0 and 1 (inside and outside the object), respectively.

Assuming known Green's functions for the problem of interest, we can find the radiated field into region 0 as

$$\overline{E}_0(\overline{r},\omega)=i\omega\mu_0\int_{V_1}\mathrm{d}\overline{r}'\overline{\overline{G}}^{[01]}(\overline{r},\overline{r}',\omega)\cdot\overline{J}(\overline{r}',\omega) \tag{1.4.4}$$

One of the advantages of the dyadic Green's function formulation is that although the current density and radiated field are stochastic processes, the Green's function itself is deterministic and this isolates the physical parameters of the problem from the statistical properties. The current density is unknown, but fluctuation-dissipation theorem provides it's spectral density. Assuming that $\overline{J}(\overline{r},\omega)$ is a stationary Gaussian stochastic process over space, knowledge of its first two moments is enough for determination of the process. Power spectral density of the radiated field can be found as

$$\begin{aligned}\left\langle\overline{E}_0(\overline{r},\omega)\overline{E}_0^*(\overline{r}',\omega')\right\rangle&=\omega^2\mu_0^2\left\langle\int_{V_1}\mathrm{d}\overline{s}\int_{V_1}\mathrm{d}\overline{u}\;\overline{\overline{G}}^{[01]}(\overline{r},\overline{s},\omega)\cdot\overline{J}(\overline{s},\omega)\left[\overline{\overline{G}}^{[01]}(\overline{r}',\overline{u},\omega)\right]^*\cdot\overline{J}^*(\overline{u},\omega)\right\rangle \\ &=\omega^2\mu_0^2\int_{V_1}\mathrm{d}\overline{s}\int_{V_1}\mathrm{d}\overline{u}\;\overline{\overline{G}}^{[01]}(\overline{r},\overline{s},\omega)\cdot\left\langle\overline{J}(\overline{s},\omega)\overline{J}^*(\overline{u},\omega)\right\rangle\cdot\left[\overline{\overline{G}}^{[01]}(\overline{r}',\overline{u},\omega)\right]^\dagger\end{aligned} \tag{1.4.5}$$

Using the expression of power spectral density of the fluctuating current, we arrive at,

$$\begin{aligned}\left\langle\overline{E}_0(\overline{r},\omega)\overline{E}_0^*(\overline{r}',\omega')\right\rangle&=\omega^2\mu_0^2\frac{\hbar\omega^2\varepsilon_0}{2\pi}\coth\left(\frac{\hbar\omega}{2k_BT}\right)\delta(\omega-\omega') \\ &\times\int_{V_1}\mathrm{d}\overline{s}\;\varepsilon''(\overline{s},\omega)\overline{\overline{G}}^{[01]}(\overline{r},\overline{s},\omega)\cdot\left[\overline{\overline{G}}^{[01]}(\overline{r}',\overline{s},\omega)\right]^\dagger\end{aligned} \tag{1.4.6}$$

Since the medium is reciprocal, The Green's function manifest the reciprocity through $\left[\overline{\overline{G}}^{[01]}(\overline{r}',\overline{s},\omega)\right]^\dagger=\left[\overline{\overline{G}}^{[10]}(\overline{s},\overline{r}',\omega)\right]^*$, where, the observation and source medium are swapped [3, 15],

$$\begin{aligned}\left\langle\overline{E}_0(\overline{r},\omega)\overline{E}_0^*(\overline{r}',\omega')\right\rangle&=\omega^2\mu_0^2\frac{\hbar\omega^2\varepsilon_0}{2\pi}\coth\left(\frac{\hbar\omega}{2k_BT}\right)\delta(\omega-\omega') \\ &\times\int_{V_1}\mathrm{d}\overline{s}\;\varepsilon''(\overline{s},\omega)\overline{\overline{G}}^{[01]}(\overline{r},\overline{s},\omega)\cdot\overline{\overline{G}}^{[10]*}(\overline{s},\overline{r}',\omega)\end{aligned} \tag{1.4.7}$$

This expression can be simplified using an integral identity as follows.

**Theorem:**

The dyadic Green's function in a reciprocal medium of Fig. 1.2 satisfies the following integral identity.

$$\omega^2\mu_0\varepsilon_0\int_{V_1}\mathrm{d}\overline{s}\;\mathrm{Im}\varepsilon_1(\overline{s},\omega)\overline{\overline{G}}^{[01]}(\overline{r},\overline{s},\omega)\cdot\overline{\overline{G}}^{[10]*}(\overline{s},\overline{r}',\omega)=\mathrm{Im}\overline{\overline{G}}^{[00]}(\overline{r},\overline{r}',\omega) \tag{1.4.8}$$

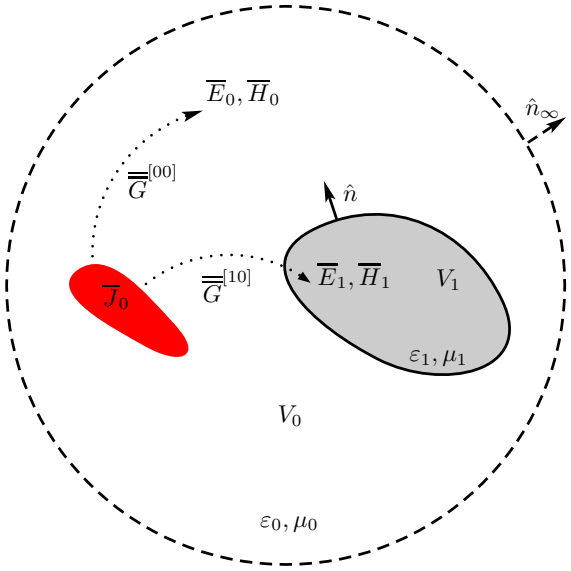


FIGURE 1.2: Configuration of the object for the complex reciprocity theorem.

**Proof: Complex Reciprocity**

This proof is similar to the reciprocity theorem but with taking complex conjugate of the fields. Consider a current density $\overline{J}_0(\overline{r})$ locate in region 0 that produce EM fields $(\overline{E}_0,\overline{H}_0)$ in region 0 and $(\overline{E}_1,\overline{H}_1)$ in region 1 as depicted in Fig. 1.2. The Maxwell's equations in region 0 reads

$$\nabla\times\overline{E}_0=i\omega\mu_0\overline{H}_0 \tag{1.4.9}$$
$$\nabla\times\overline{H}_0=J_0(\overline{r})-i\omega\varepsilon_0\overline{E}_0 \tag{1.4.10}$$

Multiplying Eq. (1.4.9) and Eq. (1.4.10) by $\overline{H}_0^*$ and $\overline{E}_0^*$ respectively and subtract the results yields

$$\nabla\cdot(\overline{E}_0^*\times\overline{H}_0)=i\omega\mu_0\overline{H}_0\cdot\overline{H}_0^*-\overline{J}_0\cdot\overline{E}_0^*+i\omega\varepsilon_0\overline{E}_0\cdot\overline{E}_0^* \tag{1.4.11}$$

taking the real part of the above equation and integrating over the volume $V_0$ gives

$$2\mathrm{Re}\Big[-\oint_S \mathrm{d}S\hat{n}\cdot(\overline{E}_0^*\times\overline{H}_0)+\oint_{S_\infty}\mathrm{d}S\hat{n}_\infty\cdot(\overline{E}_0^*\times\overline{H}_0)\Big]=-\int_{V_0}\mathrm{d}\overline{r}(\overline{J}_0\cdot\overline{E}_0^*+\overline{J}_0^*\cdot\overline{E}_0) \tag{1.4.12}$$

where $\hat{n}$ is the unit normal pointing out of region 1 to the interface and $\hat{n}_\infty$ is normal to a sphere at infinity. The integral over the sphere at infinity vanishes by virtue of the radiation condition (sources are localized). Then,

$$2\mathrm{Re}\oint_S \mathrm{d}S\hat{n}\cdot(\overline{E}_0^*\times\overline{H}_0)=\int_{V_0}\mathrm{d}\overline{r}(\overline{J}_0\cdot\overline{E}_0^*+\overline{J}_0^*\cdot\overline{E}_0) \tag{1.4.13}$$

By the same argument about fields in region 1 due to the current density $\overline{J}_0$ in region 0, we have

$$2\mathrm{Re}\oint_S \mathrm{d}S\hat{n}\cdot(\overline{E}_1^*\times\overline{H}_1)=i\omega\varepsilon_0\int_{V_1}\mathrm{d}\overline{r}\Big[\varepsilon_1(\overline{r})-\varepsilon_1^*(\overline{r})\Big]\overline{E}_1\cdot\overline{E}_1^* \tag{1.4.14}$$

However, over the interface $\hat{n}\cdot(\overline{E}_1^*\times\overline{H}_1)=\hat{n}\cdot(\overline{E}_0^*\times\overline{H}_0)$ and therefore,

$$i\omega\varepsilon_0\int_{V_1}\mathrm{d}\overline{r}\Big[\varepsilon_1(\overline{r})-\varepsilon_1^*(\overline{r})\Big]\overline{E}_1(\overline{r})\cdot\overline{E}_1^*(\overline{r})=\int_{V_0}\mathrm{d}\overline{r}\Big[\overline{J}_0(\overline{r})\cdot\overline{E}_0^*(\overline{r})+\overline{J}_0^*(\overline{r})\cdot\overline{E}_0(\overline{r})\Big] \tag{1.4.15}$$

Expressing the fields in terms of the dyadic Green's function results in,

$$\begin{aligned}\overline{E}_0(\overline{r})&=i\omega\mu_0\int_{V_0}\mathrm{d}\overline{r}'\overline{\overline{G}}^{[00]}(\overline{r},\overline{r}')\cdot\overline{J}_0(\overline{r}')\\ \overline{E}_1(\overline{r})&=i\omega\mu_0\int_{V_0}\mathrm{d}\overline{r}'\overline{\overline{G}}^{[10]}(\overline{r},\overline{r}')\cdot\overline{J}_0(\overline{r}')\end{aligned} \tag{1.4.16}$$

and the right hand side would be,

$$\begin{aligned}\Big[\overline{J}_0(\overline{r})\cdot\overline{E}_0^*(\overline{r})+\overline{J}_0^*(\overline{r})\cdot\overline{E}_0(\overline{r})\Big]&=i\omega\mu_0\int_{V_0}\mathrm{d}\overline{r}'\overline{J}_0^*(\overline{r})\cdot\overline{\overline{G}}^{[00]}(\overline{r},\overline{r}')\cdot\overline{J}_0(\overline{r}')\\ &\quad-\overline{J}_0(\overline{r})\cdot\overline{\overline{G}}^{[00]*}(\overline{r},\overline{r}')\cdot\overline{J}_0^*(\overline{r}')\\ &=-2\omega\mu_0\int_{V_0}\mathrm{d}\overline{r}'\overline{J}_0^*(\overline{r})\cdot\mathrm{Im}\Big[\overline{\overline{G}}^{[00]}(\overline{r},\overline{r}')\Big]\cdot\overline{J}_0(\overline{r}')\end{aligned} \tag{1.4.17}$$

where the symmetry properties of $\overline{\overline{G}}^{[00]}$ are used. On the other hand

$$\begin{aligned}\overline{E}_1(\overline{r})\cdot\overline{E}_1^*(\overline{r})&=\omega^2\mu_0^2\int_{V_0}\mathrm{d}\overline{r}'\int_{V_0}\mathrm{d}\overline{s}\ \left(\overline{\overline{G}}^{[10]}(\overline{r},\overline{s})\cdot\overline{J}_0(\overline{s})\right)^*\cdot\left(\overline{\overline{G}}^{[10]}(\overline{r},\overline{r}')\cdot\overline{J}_0(\overline{r}')\right)\\ &=\omega^2\mu_0^2\int_{V_0}\mathrm{d}\overline{r}'\int_{V_0}\mathrm{d}\overline{s}\ \overline{J}_0^*(\overline{s})\cdot\overline{\overline{G}}^{[01]*}(\overline{s},\overline{r})\cdot\overline{\overline{G}}^{[10]}(\overline{r},\overline{r}')\cdot\overline{J}_0(\overline{r}')\end{aligned}$$

Putting everything together,

$$\begin{aligned}&\omega^2\mu_0\varepsilon_0\int_{V_1}\mathrm{d}\overline{r}\mathrm{Im}\varepsilon_1(\overline{r})\int_{V_0}\mathrm{d}\overline{r}'\int_{V_0}\mathrm{d}\overline{s}\ \overline{J}_0^*(\overline{s})\cdot\overline{\overline{G}}^{[01]*}(\overline{s},\overline{r})\cdot\overline{\overline{G}}^{[10]}(\overline{r},\overline{r}')\cdot\overline{J}_0(\overline{r}')\\ &\quad=\int_{V_0}\mathrm{d}\overline{r}'\int_{V_0}\mathrm{d}\overline{r}\overline{J}_0^*(\overline{r})\cdot\mathrm{Im}\Big[\overline{\overline{G}}^{[00]}(\overline{r},\overline{r}')\Big]\cdot\overline{J}_0(\overline{r}')\end{aligned}$$

Interchanging $\overline{s}$ and $\overline{r}$ on the left hand side

$$\begin{aligned}\int_{V_0}\mathrm{d}\overline{r}'\int_{V_0}\mathrm{d}\overline{r}\overline{J}_0^*(\overline{r})\cdot\Bigg[&\omega^2\mu_0\varepsilon_0\int_{V_1}\mathrm{d}\overline{s}\mathrm{Im}\varepsilon_1(\overline{s})\ \overline{\overline{G}}^{[01]*}(\overline{r},\overline{s})\cdot\overline{\overline{G}}^{[10]}(\overline{s},\overline{r}')\\ &=\mathrm{Im}\Big[\overline{\overline{G}}^{[00]}(\overline{r},\overline{r}')\Big]\Bigg]\cdot\overline{J}_0(\overline{r}')\end{aligned} \tag{1.4.18}$$

Since the current density $\overline{J}_0(\overline{r})$ is arbitrary function of position

$$\omega^2\mu_0\varepsilon_0\int_{V_1}\mathrm{d}\overline{s}\mathrm{Im}\varepsilon_1(\overline{s})\;\overline{\overline{G}}^{[01]*}(\overline{r},\overline{s})\cdot\overline{\overline{G}}^{[10]}(\overline{s},\overline{r}')=\mathrm{Im}\left[\overline{\overline{G}}^{[00]}(\overline{r},\overline{r}')\right] \tag{1.4.19}$$

The quantity on the right hand side is real and does not change with complex conjugation

$$\omega^2\mu_0\varepsilon_0\int_{V_1}\mathrm{d}\overline{s}\mathrm{Im}\varepsilon_1(\overline{s})\;\overline{\overline{G}}^{[01]}(\overline{r},\overline{s})\cdot\overline{\overline{G}}^{[10]*}(\overline{s},\overline{r}')=\mathrm{Im}\left[\overline{\overline{G}}^{[00]}(\overline{r},\overline{r}')\right] \tag{1.4.20}$$

The proof is completed.

Using the integral identity of theorem 1.4, Eq. (1.4.8) can be rewritten as

$$\begin{aligned}\left\langle\overline{E}_0(\overline{r},\omega)\overline{E}_0^*(\overline{r}',\omega')\right\rangle&=\frac{\hbar\omega^2}{2\pi c^2\varepsilon_0}\coth\left(\frac{\hbar\omega}{2k_BT}\right)\delta(\omega-\omega')\mathrm{Im}\left[\overline{\overline{G}}^{[00]}(\overline{r},\overline{r}',\omega)\right]\\&=\frac{\omega}{\pi c^2\varepsilon_0}E(T,\omega)\delta(\omega-\omega')\mathrm{Im}\left[\overline{\overline{G}}^{[00]}(\overline{r},\overline{r}',\omega)\right]\end{aligned} \tag{1.4.21}$$

where,

$$E(T,\omega)=\hbar\omega\left(\frac{1}{e^{\hbar\omega/kT}-1}+\frac{1}{2}\right)$$

is the average energy of harmonic quantum oscillator with frequency $\omega$. This is an interesting result. The radiated field into region 0 is only dependent on the dyadic Green's function of region 0. All the dielectric properties of the region 1 will emerge into the picture through the $\overline{\overline{G}}^{[00]}(\overline{r},\overline{r}',\omega)$ as it is continuous on the boundary.

## 1.5 Energy Density of Radiated Field

For the energy density $W(\overline{r},t)$ of the fluctuating radiated field into vacuum at time $t$ [2, 10],

$$W(\overline{r},t)=\frac{\varepsilon_0}{2}\overline{E}_0(\overline{r},t)\cdot\overline{E}_0(\overline{r},t)+\frac{\mu_0}{2}\overline{H}_0(\overline{r},t)\cdot\overline{H}_0(\overline{r},t) \tag{1.5.1}$$

Upon taking statistical average by assuming stationary fluctuations in time and introducing correlation functions of the fields as

$$\begin{aligned}R_E(\tau)&=\left\langle\overline{E}_0(\overline{r},t)\cdot\overline{E}_0(\overline{r},t+\tau)\right\rangle\\R_H(\tau)&=\left\langle\overline{H}_0(\overline{r},t)\cdot\overline{H}_0(\overline{r},t+\tau)\right\rangle\end{aligned} \tag{1.5.2}$$

the energy density can be written as

$$\langle W(\overline{r},t)\rangle=\frac{\varepsilon_0}{2}R_E(0)+\frac{\mu_0}{2}R_H(0) \tag{1.5.3}$$

Power spectral density of the electric and magnetic fields is related to the correlation function through,

$$S_E(\omega)=\int_{-\infty}^{\infty}\mathrm{d}\tau\ e^{i\omega\tau}R_E(\tau) \tag{1.5.4}$$

Now, correlation function at $\tau=0$ can be expressed as

$$R_E(0)=\int\frac{\mathrm{d}\omega}{2\pi}S_E(\omega)=\int\frac{\mathrm{d}\omega}{2\pi}\int\mathrm{d}\tau e^{i\omega\tau}R_E(\tau) \tag{1.5.5}$$

Therefore the energy density has the following spectral expansion

$$\begin{aligned}\langle W(\overline{r},t)\rangle=\int_{-\infty}^{\infty}\frac{\mathrm{d}\omega}{2\pi}\Bigg[\int_{-\infty}^{\infty}\mathrm{d}\tau e^{i\omega\tau}\Bigg(\frac{\varepsilon_0}{2}\Big\langle\overline{E}_0(\overline{r},t)\cdot\overline{E}_0(\overline{r},t+\tau)\Big\rangle \\ +\frac{\mu_0}{2}\Big\langle\overline{H}_0(\overline{r},t)\cdot\overline{H}_0(\overline{r},t+\tau)\Big\rangle\Bigg)\Bigg]=\int_{-\infty}^{\infty}\mathrm{d}\omega S(\omega)\end{aligned} \tag{1.5.6}$$

where the energy spectral density is given by,

$$S(\omega)=\frac{1}{2\pi}\int_{-\infty}^{\infty}\mathrm{d}\tau e^{i\omega\tau}\Bigg(\frac{\varepsilon_0}{2}\Big\langle\overline{E}_0(\overline{r},t)\cdot\overline{E}_0(\overline{r},t+\tau)\Big\rangle+\frac{\mu_0}{2}\Big\langle\overline{H}_0(\overline{r},t)\cdot\overline{H}_0(\overline{r},t+\tau)\Big\rangle\Bigg)$$

Substituting for the fields in terms of Fourier transforms to write the energy spectral density in terms of the fields spectral densities, we get

$$\begin{aligned}\int_{-\infty}^{\infty}\mathrm{d}\tau e^{i\omega\tau}\Big\langle\overline{E}_0(\overline{r},t)\cdot\overline{E}_0(\overline{r},t+\tau)\Big\rangle=\int_{-\infty}^{\infty}\mathrm{d}\tau e^{i\omega\tau}\int_{-\infty}^{\infty}\frac{\mathrm{d}\omega'}{2\pi} \\ e^{-i\omega' t}\int_{-\infty}^{\infty}\frac{\mathrm{d}\omega''}{2\pi}e^{-i\omega''(t+\tau)}\Big\langle\overline{E}_0(\overline{r},\omega')\cdot\overline{E}_0(\overline{r},\omega'')\Big\rangle\end{aligned} \tag{1.5.7}$$

Based on assumption of stationary fluctuations, the left hand side does not depend on time $t$, so the spectral average on the right hand side contains $\delta(\omega'+\omega'')$ and

$$\begin{aligned}\int_{-\infty}^{\infty}\mathrm{d}\tau e^{i\omega\tau}\Big\langle\overline{E}_0(\overline{r},t)\cdot\overline{E}_0(\overline{r},t+\tau)\Big\rangle&=\int_{-\infty}^{\infty}\mathrm{d}\tau e^{i(\omega-\omega')\tau}\int_{-\infty}^{\infty}\frac{\mathrm{d}\omega'}{2\pi}\Big\langle\overline{E}_0(\overline{r},\omega')\cdot\overline{E}_0^*(\overline{r},\omega')\Big\rangle \\ &=\delta(\omega-\omega')\int_{-\infty}^{\infty}\mathrm{d}\omega\Big\langle\overline{E}_0(\overline{r},\omega)\cdot\overline{E}_0^*(\overline{r},\omega')\Big\rangle\end{aligned} \tag{1.5.8}$$

Therefore energy spectral density becomes

$$S(\omega)\delta(\omega-\omega')=\frac{\varepsilon_0}{2}\Big\langle\overline{E}_0(\overline{r},\omega)\cdot\overline{E}_0^*(\overline{r},\omega')\Big\rangle+\frac{\mu_0}{2}\Big\langle\overline{H}_0(\overline{r},\omega)\cdot\overline{H}_0^*(\overline{r},\omega')\Big\rangle \tag{1.5.9}$$

### 1.5.1 Planck's Black body Radiation Revisited

From fluctuation-dissipation theorem,

$$\Big\langle\overline{E}_0(\overline{r},\omega)\cdot\overline{E}_0^*(\overline{r},\omega')\Big\rangle=\frac{\omega}{\pi c^2\varepsilon_0}E(T,\omega)\delta(\omega-\omega')\lim_{\overline{r}\to\overline{r}'}\mathrm{Im}\Big[\mathrm{Tr}\,\overline{\overline{G}}^{[00]}(\overline{r},\overline{r}',\omega)\Big] \tag{1.5.10}$$

In free space the energy in the electric and magnetic fields are equal and the imaginary part of the dyadic Green's function is regular [16] (it will be shown later) and the energy spectral density can be written as

$$S(\omega)=\frac{\omega}{\pi c^2}E(T,\omega)\mathrm{Im}\Big[\mathrm{Tr}\,\overline{\overline{G}}^{[00]}(\overline{r},\overline{r},\omega)\Big] \tag{1.5.11}$$

The averaged energy of the fluctuating electromagnetic field is given by

$$\langle W\rangle=\int_{-\infty}^{\infty}\mathrm{d}\omega S(\omega) \tag{1.5.12}$$

The average energy of quantum oscillator $E(T,\omega)$ is an odd function of $\omega$. On the other hand, $\mathrm{Im}\overline{\overline{G}}^{[00]}(\overline{r},\overline{r},\omega)=-\mathrm{Im}\overline{\overline{G}}^{[00]}(\overline{r},\overline{r},-\omega)$ which shows the imaginary part of Green's function is also an odd function of frequency (as the Green's function is real in time domain). Therefore, the energy can be written in terms of one sided spectral density $S_+(\omega)$ where

$$S_+(\omega)=\frac{2\omega}{\pi c^2}E(T,\omega)\mathrm{Im}\Big[\mathrm{Tr}\,\overline{\overline{G}}^{[00]}(\overline{r},\overline{r},\omega)\Big] \tag{1.5.13}$$

and,

$$\langle W\rangle=\int_{0}^{\infty}\mathrm{d}\omega S_+(\omega) \tag{1.5.14}$$

The energy spectral density can be decomposed into $S_+(\omega)=E(T,\omega)N(\overline{r},\omega)$ where $N(\overline{r},\omega)$ shows the density of states that depends on $\overline{r}$. In contrast to the equilibrium case, when density of states is independent of spatial coordinates, here local density of states can be identified as [10, 16, 17]

$$N(\overline{r},\omega)=\frac{2\omega}{\pi c^2}\mathrm{Im}\Big[\mathrm{Tr}\,\overline{\overline{G}}^{[00]}(\overline{r},\overline{r},\omega)\Big] \tag{1.5.15}$$

In free space, the dyadic Green's function is given by

$$\overline{\overline{G}}^{[00]}(\overline{r},\overline{r}',\omega)=\overline{\overline{G}}_0(\overline{r},\overline{r}',\omega)=\Big[\overline{\overline{I}}+\frac{\nabla\nabla}{k_0^2}\Big]\frac{e^{ik_0|\overline{r}-\overline{r}'|}}{4\pi|\overline{r}-\overline{r}'|} \tag{1.5.16}$$

then,

$$\mathrm{Im}\Big[\mathrm{Tr}\,\overline{\overline{G}}^{[00]}(\overline{r},\overline{r},\omega)\Big]=\mathrm{Im}\Big[3+\frac{\nabla\cdot\nabla}{k_0^2}\Big]\frac{e^{ik_0|\overline{r}-\overline{r}'|}}{4\pi|\overline{r}-\overline{r}'|} \tag{1.5.17}$$

but from the wave equation

$$\nabla^2\frac{e^{ik_0|\overline{r}-\overline{r}'|}}{4\pi|\overline{r}-\overline{r}'|}=-\delta(\overline{r}-\overline{r}')-k_0^2\frac{e^{ik_0|\overline{r}-\overline{r}'|}}{4\pi|\overline{r}-\overline{r}'|} \tag{1.5.18}$$

The delta function does not contribute to the imaginary part. Therefore,

$$\mathrm{Im}\Big[\mathrm{Tr}\,\overline{\overline{G}}^{[00]}(\overline{r},\overline{r},\omega)\Big]=2\lim_{\overline{r}\to\overline{r}'}\frac{\sin k_0|\overline{r}-\overline{r}'|}{4\pi|\overline{r}-\overline{r}'|}=\frac{k_0}{2\pi}=\frac{\omega}{2\pi c} \tag{1.5.19}$$

The density of states becomes

$$N(\overline{r},\omega)=\frac{2\omega}{\pi c^2}\mathrm{Im}\left[\mathrm{Tr}\,\overline{\overline{G}}^{[00]}(\overline{r},\overline{r},\omega)\right]=\frac{\omega^2}{\pi^2 c^3} \tag{1.5.20}$$

Now the Planck's radiation law is recovered from the Fluctuation dissipation theorem. This reveals that the fluctuation dissipation theorem is an answer to the question of inversion of Planck's radiation spectrum to obtain source of radiations. This is also generalization of Planck's radiation for non-equilibrium condition. In such a condition, density of states is position dependent and should be calculated using the Green's function of the system. The position dependent density of states provides a way to manipulate the radiation from the object by changing the Green's function. For example by bringing another object close to the surface of radiating object, the density of states increases near the surface and thermal radiation becomes orders of magnitude larger than radiation in free space as the radiation becomes dominant by the evanescent modes that can tunnel between the object, which is the essence of the radiative heat transfer [9, 18, 19].

## 1.6 Brightness Temperature

All the objects at temperature greater than absolute zero radiate electromagnetic energy. This fact brings up the idea of measuring the electromagnetic radiation of an object to obtain some information about the radiating object. Of course, in order to do this inversion, it is required to isolate radiation of object of interest from other radiating bodies. Measurement of radiation from a specific object is possible by an antenna that can resolve between object and surrounding medium well. This would remove line of sight radiation from undesired bodies but multiple scattering contribution cannot be separated in general. Consider a surface element $\mathrm{d}A$ at $\overline{r}$ and the intensity passing through it in $\hat{s}$ direction (Fig.

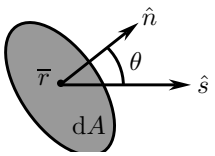


FIGURE 1.3: Power flow in direction $\hat{s}$ through surface $\hat{n}\mathrm{d}A$

1.3). Specific intensity $I(\overline{r},\hat{s})$ is a quantity that the power passing through this surface in frequency interval $(f,f+\mathrm{d}f)$ can be written as,

$$\mathrm{d}P=I(\overline{r},\hat{s})\cos\theta\mathrm{d}A\mathrm{d}\Omega\mathrm{d}f \tag{1.6.1}$$

Consider an imaginary object in thermal equilibrium with surrounding medium at temperature $T$. When $k_BT\gg hf$, Planck's radiation law can be approximated as (Rayleigh-Jean's approximation)

$$I=\frac{hf^3}{c^2}\frac{1}{e^{hf/k_BT}-1}\approx\frac{k_BT}{\lambda^2} \tag{1.6.2}$$

Let's examine when approximation of $k_BT\gg\hbar\omega$ is valid. As an example, for temperature in the oder of room temperature $t$=300 K, corresponding frequency that satisfies $k_BT=\hbar\omega$

would be $f^*=k_BT/h=6.2$ THz. As long as our operation frequency is very small compared to $f^*$, the approximation is valid. At room temperature and operational frequency of 100 GHz, the relative error in the intensity is less than 0.7 percent. Now, for any different configuration, the brightness temperature $T_B$ is defined in terms of the measured specific intensity $I$ by

$$T_B=\frac{\lambda^2 I}{k_B} \tag{1.6.3}$$

If the receiver if Fig. 1.4 measure power $P$ with bandwidth of $\Delta f$ then measured specific

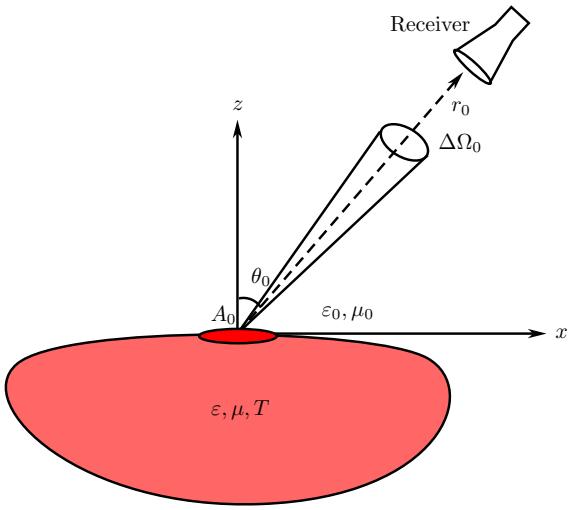


FIGURE 1.4: Measurement of the brightness temperature.

intensity can be related to measured power through

$$I=\frac{P}{A_0\Delta f\cos\theta_0\Delta\Omega_0} \tag{1.6.4}$$

Therefore, the brightness temperature can be obtained as

$$T_B=\frac{\lambda^2}{k_B}\frac{P}{A_0\Delta f\cos\theta_0\Delta\Omega_0} \tag{1.6.5}$$

Depending on the polarization of the receiving antenna, power can be measured for two polarizations, namely vertical and horizontal. Thus, a polarization can also be assigned to the brightness temperature.

$$T_B^\alpha=\frac{\lambda^2}{k_B}\frac{P^\alpha}{A_0\Delta f\cos\theta_0\Delta\Omega_0} \tag{1.6.6}$$

where $P^\alpha$ is power measured in channel $\alpha=$ TE, TM (or $h$ and $v$, respectively).

### 1.6.1 Brightness Temperature of a Dielectric Half Space

Consider a half space of lossy dielectric material in equilibrium at temperature $T$. Based on the Fluctuation-Dissipation theorem, there is a fluctuating current density inside the

lossy half space with zero mean and power spectral density of

$$\left\langle \overline{J}(\overline{r},\omega)\overline{J}^{*}(\overline{r}',\omega')\right\rangle = \frac{\hbar\omega^{2}\varepsilon_{0}}{2\pi}\varepsilon''(\overline{r},\omega)\coth\left(\frac{\hbar\omega}{2k_{B}T}\right)\delta(\omega-\omega')\delta(\overline{r}-\overline{r}')\overline{\overline{I}} \tag{1.6.7}$$

Again, for $\hbar\omega \ll k_B T$, $\coth(\hbar\omega/2k_BT) \approx 2k_BT/\hbar\omega$ and,

$$\left\langle \overline{J}(\overline{r},\omega)\overline{J}^{*}(\overline{r}',\omega')\right\rangle = \frac{\omega k_{B}T\varepsilon_{0}}{\pi}\varepsilon''(\overline{r},\omega)\delta(\omega-\omega')\delta(\overline{r}-\overline{r}')\overline{\overline{I}} \tag{1.6.8}$$

Note that this is double side band power spectral density. In order to make it single sideband, a factor of 4 should be inserted. From now on, we work with single side band spectral density.

$$\left\langle \overline{J}(\overline{r},\omega)\overline{J}^{*}(\overline{r}',\omega')\right\rangle = \frac{4\omega k_{B}T\varepsilon_{0}}{\pi}\varepsilon''(\overline{r},\omega)\delta(\omega-\omega')\delta(\overline{r}-\overline{r}')\overline{\overline{I}} \quad , \quad \text{Single side band} \tag{1.6.9}$$

Utilizing the dyadic Green's function $\overline{\overline{G}}^{[01]}(\overline{r},\overline{r}')$ we can find the electric field in the region

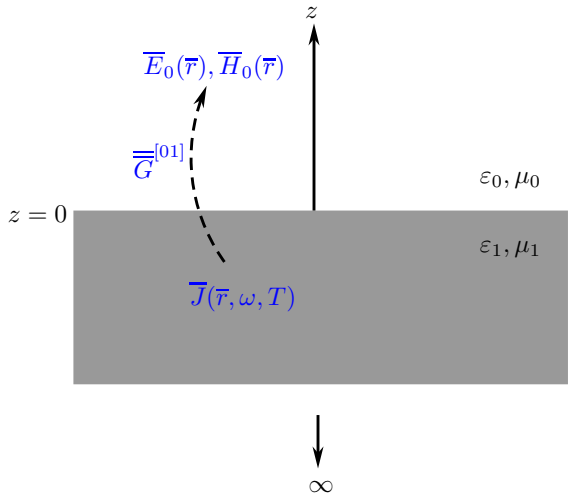


FIGURE 1.5: Fluctuating current inside the lossy dielectric half space give rise to radiated power into region 0.

0 from Eq. (1.4.7) as

$$\begin{aligned}\left\langle \overline{E}_{0}(\overline{r},\omega)\overline{E}_{0}^{*}(\overline{r},\omega')\right\rangle &= \frac{4\omega^{3}}{\pi c^{4}\varepsilon_{0}}k_{B}T\delta(\omega-\omega')\int_{V_1}\mathrm{d}\overline{r}'\ \varepsilon''(\overline{r}',\omega)\overline{\overline{G}}^{[01]}(\overline{r},\overline{r}',\omega)\cdot\overline{\overline{G}}^{[10]*}(\overline{r}',\overline{r},\omega)\\ &= \frac{4\omega^{3}}{\pi c^{4}\varepsilon_{0}}k_{B}T\delta(\omega-\omega')\int_{V_1}\mathrm{d}\overline{r}'\ \varepsilon''(\overline{r}',\omega)\overline{\overline{G}}^{[01]}(\overline{r},\overline{r}',\omega)\cdot\overline{\overline{G}}^{[01]*}(\overline{r},\overline{r}',\omega)\end{aligned} \tag{1.6.10}$$

From the reciprocity of the dyadic Green's function we have

$$\overline{\overline{G}}^{[01]}(\overline{r},\overline{r}',\omega) = \left[\overline{\overline{G}}^{[10]}(\overline{r}',\overline{r},\omega)\right]^{T} \tag{1.6.11}$$

For different Green's functions, we consider following expression in spectral domain

$$\overline{\overline{G}}(\overline{r}',\overline{r},\omega)=\frac{i}{2}\int\frac{\mathrm{d}^2\overline{k}_\perp}{(2\pi)^2}e^{i\overline{k}_\perp\cdot(\overline{r}-\overline{r}')}\overline{\overline{g}}(\overline{k}_\perp,z,z') \tag{1.6.12}$$

Then, spectral component of the different Green's function can be expanded as (see Appendix [2])

$$\begin{aligned}
\overline{\overline{g}}^{[10]}(\overline{k}_\perp,z,z')&=\frac{1}{k_{1z}}\Big[T_e\hat{e}_1^-\hat{e}_0^-+T_h\hat{h}_1^-\hat{h}_0^-\Big]e^{-ik_{1z}z+ik_zz'} \\
\overline{\overline{g}}_S^{[00]}(\overline{k}_\perp,z,z')&=\frac{1}{k_z}\Big[R_e\hat{e}_0^+\hat{e}_0^-+R_h\hat{h}_0^+\hat{h}_0^-\Big]e^{ik_zz+ik_zz'} \\
\overline{\overline{g}}_0(\overline{k}_\perp,z,z')&=\frac{1}{k_z}\Big[\hat{e}_0^-\hat{e}_0^-+\hat{h}_0^-\hat{h}_0^-\Big]e^{-ik_zz+ik_zz'}
\end{aligned} \tag{1.6.13}$$

Continuity of the tangential component of the Green's function over the boundary at $z=0$ requires,

$$\begin{aligned}
\frac{1}{k_1}T_h&=\frac{1}{k}(1-R_h) \\
\frac{1}{k_{1z}}T_e&=\frac{1}{k_z}(1+R_e)
\end{aligned} \tag{1.6.14}$$

Also, continuity of the tangential magnetic field gives,

$$\begin{aligned}
T_e&=1-R_e \\
\frac{k_1}{k_{1z}}T_h&=\frac{k}{k_z}(1+R_h)
\end{aligned} \tag{1.6.15}$$

Solution of these equations are the Fresnel reflection coefficients of

$$\begin{aligned}
R_e&=\frac{k_z-k_{1z}}{k_z+k_{1z}} \\
R_h&=\frac{k_1^2k_z-k^2k_{1z}}{k_1^2k_z+k^2k_{1z}} \\
T_e&=\frac{2k_{1z}}{k_z+k_{1z}} \\
T_h&=\frac{k_1}{k}\frac{2k^2k_{1z}}{k_1^2k_z+k^2k_{1z}}
\end{aligned}$$

For spectral component of the dyadic Green's function, swapping $\overline{r}$ and $\overline{r}'$ is equivalent to $\overline{\overline{g}}(\overline{k}_\perp,z,z')\to\overline{\overline{g}}(-\overline{k}_\perp,z',z)$. Therefore using reciprocity to find the propagator $\overline{\overline{G}}^{[01]}(\overline{r},\overline{r}',\omega)$ from $\overline{\overline{G}}^{[10]}(\overline{r},\overline{r}',\omega)$ results in

$$\begin{aligned}
\overline{\overline{G}}^{[01]}(\overline{r},\overline{r}',\omega)&=\left[\overline{\overline{G}}^{[10]}(\overline{r}',\overline{r},\omega)\right]^{\mathrm{T}} \\
&=\frac{i}{2}\int\frac{\mathrm{d}^2\overline{k}_\perp}{(2\pi)^2}e^{i\overline{k}_\perp\cdot(\overline{r}-\overline{r}')}\left[\overline{\overline{g}}^{[10]}(-\overline{k}_\perp,z',z)\right]^{\mathrm{T}} \\
&=\frac{i}{2}\int\frac{\mathrm{d}^2\overline{k}_\perp}{(2\pi)^2}e^{i\overline{k}_\perp\cdot(\overline{r}-\overline{r}')}\frac{1}{k_{1z}}\Big[T_e\hat{e}_0^+\hat{e}_1^++T_h\hat{h}_0^+\hat{h}_1^+\Big]e^{-ik_{1z}z'+ik_zz}
\end{aligned} \tag{1.6.16}$$

Where we have used that under transformation $\overline{k}_\perp \to -\overline{k}_\perp$, TM polarization unit vectors changes as $\hat{h}^\pm \to \hat{h}^\mp$ and TE unit vector are always equal, $\hat{e}^+ = \hat{e}^-$. Using the stationary phase approximation of the spectral integral to find the far field Green's function we have,

$$\overline{\overline{G}}^{[01]}_{\rm FF}(\overline{r},\overline{r}',\omega) = \frac{e^{ikr}}{4\pi r} e^{-i\overline{k}_\perp\cdot\overline{r}'} \frac{k_z}{k_{1z}} \Big[ T_e \hat{e}_0^+ \hat{e}_1^+ + T_h \hat{h}_0^+ \hat{h}_1^+ \Big] e^{-i\overline{k}_\perp\cdot\overline{r}' - ik_{1z}z'} \Big|_{\overline{k}=\overline{k}_{\rm s}} \tag{1.6.17}$$

Where the stationary spectral point is given by

$$\begin{aligned} k_x &= k\sin\theta\cos\phi \\ k_y &= k\sin\theta\sin\phi \\ k_z &= k\cos\theta \end{aligned}$$

for observation point in direction of $(\theta,\phi)$ in the far field. Different components of the far field Green's function are given by,

$$\begin{aligned} \hat{e}_0^+ \cdot \overline{\overline{G}}^{[01]}_{\rm FF}(\overline{r},\overline{r}',\omega) &= \frac{e^{ikr}}{4\pi r} \frac{k_z}{k_{1z}} T_e \hat{e}_1^+ e^{-i\overline{k}_\perp\cdot\overline{r}' - ik_{1z}z'} \\ \hat{h}_0^+ \cdot \overline{\overline{G}}^{[01]}_{\rm FF}(\overline{r},\overline{r}',\omega) &= \frac{e^{ikr}}{4\pi r} \frac{k_z}{k_{1z}} T_h \hat{h}_1^+ e^{-i\overline{k}_\perp\cdot\overline{r}' - ik_{1z}z'} \end{aligned} \tag{1.6.18}$$

Integration the absolute squared of the Green's function components over the volume of half space $z'<0$, it yields,

$$\begin{aligned} \int_{V_1} {\rm d}\overline{r}' \Big| \hat{e}_0^+ \cdot \overline{\overline{G}}^{[01]}_{\rm FF}(\overline{r},\overline{r}',\omega) \Big|^2 &= \frac{A}{16\pi^2 r^2} |T_e|^2 \frac{k_z^2}{|k_{1z}|^2} \int_{-\infty}^0 {\rm d}z' e^{2{\rm Im}(k_{1z})z'} \\ &= \frac{A}{16\pi^2 r^2} \frac{k_z^2}{|k_{1z}|^2} \frac{|T_e|^2}{2{\rm Im}(k_{1z})} \\ \int_{V_1} {\rm d}\overline{r}' \Big| \hat{h}_0^+ \cdot \overline{\overline{G}}^{[01]}_{\rm FF}(\overline{r},\overline{r}',\omega) \Big|^2 &= \frac{A}{16\pi^2 r^2} \frac{|k_{1z}|^2 + k_\perp^2}{|k_1|^2} \frac{k_z^2}{|k_{1z}|^2} \frac{|T_h|^2}{2{\rm Im}(k_{1z})} \end{aligned} \tag{1.6.19}$$

Now, the brightness temperature can be computed as

$$T_B^\alpha = T \frac{16\pi^2 k}{A\cos\theta_0} \lim_{r\to\infty} r^2 \int_{V_1} {\rm d}\overline{r}' \; \varepsilon''(\overline{r}',\omega) \Big| \hat{\alpha} \cdot \overline{\overline{G}}^{[01]}(\overline{r},\overline{r}',\omega) \Big|^2 \tag{1.6.20}$$

$$\begin{aligned} T_B^e &= T \frac{k\varepsilon_1''}{\cos\theta_0} \frac{k_z^2}{|k_{1z}|^2} \frac{|T_e|^2}{2{\rm Im}(k_{1z})} \\ T_B^h &= T \frac{k\varepsilon_1''}{\cos\theta_0} \frac{|k_{1z}|^2 + k_\perp^2}{|k_1|^2} \frac{k_z^2}{|k_{1z}|^2} \frac{|T_h|^2}{2{\rm Im}(k_{1z})} \end{aligned} \tag{1.6.21}$$

These brightness temperature formulas can be cast into another form which provides greater insight into the brightness temperature of the half space. From $k_1^2 = k^2\varepsilon_1$ and balancing the imaginary parts we have $k^2\varepsilon'' = 2k_1'k_1''$ that simplifies brightness temperature expressions to

$$\begin{aligned} T_B^e &= T \frac{k_1'k_1''}{k_z k_{1z}''} \frac{k_z^2}{|k_{1z}|^2} |T_e|^2 \\ T_B^h &= T \frac{k_1'k_1''}{k_z k_{1z}''} \frac{|k_{1z}|^2 + k_\perp^2}{|k_1|^2} \frac{k_z^2}{|k_{1z}|^2} |T_h|^2 \end{aligned} \tag{1.6.22}$$

For TE polarization,

$$1-|R_e|^2=\frac{4k_zk'_{1z}}{|k_z+k_{1z}|^2}=\frac{k_zk'_{1z}}{|k_{1z}|^2}|T_e|^2 \tag{1.6.23}$$

or,

$$|T_e|^2=(1-|R_e|^2)\frac{|k_{1z}|^2}{k_zk'_{1z}} \tag{1.6.24}$$

Also, balancing real and imaginary parts of $k_{1z}^2=k_1^2-k_\perp^2$ gives another identity $k'_1k''_1=k'_{1z}k''_{1z}$ and therefore

$$T_B^e=T\frac{k'_{1z}}{k_z}\frac{k_z^2}{|k_{1z}|^2}(1-|R_e|^2)\frac{|k_{1z}|^2}{k_zk'_{1z}}=T(1-|R_e|^2) \tag{1.6.25}$$

Brightness temperature of an object at temperature is simply it's physical temperature times it's emissivity. Here TE emissivity of the half space is $e^{\mathrm{TE}}=1-|R_e|^2$. The same argument holds true for the TM channel.

## 1.7 Absorption and Emission

If an object at temperature $T$ radiate energy into surrounding medium, the temperature of the object eventually decreases. This is a non-equilibrium problem where Planck's radiation law does not apply. However, after enough amount of time, thermal equilibrium between object and environment will be established. In thermal equilibrium, amount of radiated energy from the object should be balanced with the absorbed energy from the environment. Therefore for an object at equilibrium with a thermal bath at temperature $T$, rate of absorption and emission should be the same, otherwise the object's temperature would increase or decrease to achieve a new equilibrium state [20].

If we consider the example of half space at equilibrium with temperature $T$, we can find the amount of absorption by the half space from an external source of radiation. For a point source in the region 0 , spectral component of the dyadic Green's function has been calculated as

$$\begin{aligned}
\overline{\overline{g}}^{[10]}(\overline{k}_\perp,z,z')&=\frac{1}{k_{1z}}\left[T_e\hat{e}_1^-\hat{e}_0^-+T_h\hat{h}_1^-\hat{h}_0^-\right]e^{-ik_{1z}z+ik_zz'} \\
\overline{\overline{g}}_S^{[00]}(\overline{k}_\perp,z,z')&=\frac{1}{k_z}\left[R_e\hat{e}_0^+\hat{e}_0^-+R_h\hat{h}_0^+\hat{h}_0^-\right]e^{ik_zz+ik_zz'} \\
\overline{\overline{g}}_0(\overline{k}_\perp,z,z')&=\frac{1}{k_z}\left[\hat{e}_0^-\hat{e}_0^-+\hat{h}_0^-\hat{h}_0^-\right]e^{-ik_zz+ik_zz'}
\end{aligned} \tag{1.7.1}$$

where the spatial counterpart can be synthesized by

$$\overline{\overline{G}}(\overline{r}',\overline{r},\omega)=\frac{i}{2}\int\frac{\mathrm{d}^2\overline{k}_\perp}{(2\pi)^2}e^{i\overline{k}_\perp\cdot(\overline{r}-\overline{r}')}\overline{\overline{g}}(\overline{k}_\perp,z,z') \tag{1.7.2}$$

The Green's function at each spectral point $\overline{k}_\perp$ is the response of the medium to a plane wave that propagating in direction determined by $\overline{k}_\perp$ and $k_z=k^2-k_\perp^2$. Our goal here is to find the absorptivity of the half space and therefore the propagating wave in the dielectric half

space is proportional to $\overline{\overline{G}}^{[10]}(\overline{r},\overline{r}')$. More precisely, for a current source with polarization of $\hat{\alpha}$ and magnitude $J_0(\overline{r}_0)$, where $\overline{r}_0$ is located far away from the surface such that incident wave is a plane wave. This incident plane wave causes a transmitted plane wave in the region 1 that is given by

$$\begin{aligned}\overline{E}_1(\overline{r}) &= i\omega\mu J_0 \int \mathrm{d}\overline{r}' \overline{\overline{G}}^{[10]}(\overline{r},\overline{r}')\cdot\hat{\alpha}\delta(\overline{r}'-\overline{r}_0) \\ &= \overline{\overline{G}}^{[10]}(\overline{r},\overline{r}_0)\cdot\hat{\alpha}\end{aligned} \tag{1.7.3}$$

where we have normalized $i\omega\mu J_0=1$. Using the far field approximation of the Green's function as $r_0\to\infty$ by applying the stationary phase approximation to the spectral integral,

$$\lim_{r_0\to\infty} \overline{\overline{G}}^{[10]}(\overline{r},\overline{r}_0) = \frac{e^{ikr_0}}{4\pi r_0}\frac{k_z}{k_{1z}}\left[T_e\hat{e}_1^-\hat{e}_0^- + T_h\hat{h}_1^-\hat{h}_0^-\right]e^{i\overline{k}_\perp\cdot\overline{r}-ik_{1z}z} \tag{1.7.4}$$

Therefore the propagating wave in the region 1 can be written in terms of the Green's function as

$$\lim_{r_0\to\infty} \overline{\overline{G}}^{[10]}(\overline{r},\overline{r}_0)\cdot\hat{\alpha} = \frac{e^{ikr_0}}{4\pi r_0}\overline{E}_1(\overline{r}) \tag{1.7.5}$$

Now, we are in position to find the power absorbed by the half space. The TE absorbed power in the half space is given by

$$\begin{aligned}P_a^e &= \frac{1}{2}\omega\varepsilon_0\int_{V_1}\mathrm{d}\overline{r}\varepsilon_1''|\overline{E}_1(\overline{r})|^2 \\ &= \frac{1}{2}\omega\varepsilon_0 A_0\varepsilon_1''\frac{k_z^2}{|k_{1z}|^2}\frac{|T_e|^2}{2\mathrm{Im}(k_{1z})}|\hat{e}_0^-\cdot\hat{\alpha}|^2\end{aligned} \tag{1.7.6}$$

However, the incident electric field on the surface is proportional to $\overline{\overline{G}}_0\cdot\hat{\alpha}$ and is given by

$$\overline{E}_{\mathrm{inc}}(\overline{r}) = \left[\hat{e}_0^-\hat{e}_0^- + \hat{h}_0^-\hat{h}_0^-\right]\cdot\hat{\alpha}e^{-i\overline{k}\cdot\overline{r}} \tag{1.7.7}$$

Therefore, the incident power in TE channel is given by

$$P_i^e = \frac{1}{2\eta}\cos\theta_0\int\mathrm{d}S|\overline{E}_{\mathrm{inc}}|^2 = \frac{A_0}{2\eta}\cos\theta_0|\hat{e}_0^-\cdot\hat{\alpha}|^2 \tag{1.7.8}$$

The ratio of absorbed power to the incident power can be found as

$$\frac{P_a^e}{P_{\mathrm{inc}}^e} = \frac{k\varepsilon_1''}{\cos\theta_0}\frac{k_z^2}{|k_{1z}|^2}\frac{|T_e|^2}{2\mathrm{Im}(k_{1z})} = 1-|R_e|^2 \tag{1.7.9}$$

Comparing Eq.(1.7.9) with Eq.(1.6.21) shows that the amount of absorbed power from the incident field is equal to the emissivity of the surface. This relation also holds for the TM polarization and in general any arbitrary polarization of the electric field. This example demonstrates a bridge between absorption and emission from an object in the thermal equilibrium. The equality of the absorptivity and emissivity connects active and passive microwave remote sensing scenarios. If one has information about the reflectivity of the object (which can be measured by a polarimetry radar) then the absorptivity is known

and the emission from the object at equilibrium can be found and vice versa. However, the emissivity for complex objects is not as simple as the half space and there are several parameters contributing in the functionality of the emissivity.

This result is not restricted to the flat boundary half space. For a general surface in addition to specular reflection and transmission, diffused scattered field should be taken into account. If reflectivity of the surface is expressed by $\gamma_{\alpha\beta}(\theta,\phi;\theta',\phi')$ that corresponds to reflected power in channel $\alpha$ in direction $(\theta,\phi)$ off the surface when $\beta-$polarized incident field in direction $(\theta',\phi')$ is impinging on the surface, then the total reflection coefficient when surface is illuminated by $\beta$-polarized field is given by

$$R_\beta(\theta',\phi')=\sum_{\alpha=e,h}\int_0^{\pi/2}\mathrm{d}\theta\sin\theta\int_0^{2\pi}\mathrm{d}\phi\gamma_{\alpha\beta}(\theta,\phi;\theta',\phi') \tag{1.7.10}$$

Then, the $\beta-$ channel emissivity of the surface in direction $(\theta',\phi')$ is given by

$$e_\beta(\theta',\phi')=1-R_\beta(\theta',\phi') \tag{1.7.11}$$

Similarly, measured $\beta-$polarized power in direction $(\theta',\phi')$ would be proportional to the $e_\beta(\theta',\phi')$ according to reciprocity.

## 1.8 UWBRAD: Brightness temperature of ice-sheets

UWBRAD's goal of retrieving ice sheet internal temperatures from 0.5-2 GHz brightness temperature data requires that an accurate and robust forward model for ice sheet thermal emission be available. Extensive efforts throughout the project have been conducted to create the required model, as described in this section.

Because ice particle grain sizes are very small compared to UWBRAD's 0.5-2 GHz wavelengths, volume scattering effects should be small. Variations in firn density over cm to m length scales however can cause significant effects. Both incoherent and coherent models have been used to examine these effects [21]. Incoherent models include a "cloud model" that neglects any reflections internal to the ice sheet (Jezek et al., 2015), and the DMRT-ML [22] and MEMLS [23] radiative transfer codes that are publicly available. The coherent model is based on the layered medium implementation of the fluctuation dissipation theorem for thermal microwave radiation from a medium having a nonuniform temperature. Density profiles including random fluctuations (which in part account for daily variations in accumulation and other meteorological forcing) must be modeled using a stochastic approach, with model predictions then averaged over a large number of realizations to take into account an averaging over the radiometer footprint. Density profiles are described by combining a smooth average density profile with a spatially correlated random process to model density fluctuations. It is shown that coherent model results after ensemble averaging depend on the correlation lengths of the vertical density fluctuations. If the correlation length is moderate or long compared with the wavelength ( 0.6x longer or greater for Gaussian correlation function without regard for layer thinning due to compaction), coherent and incoherent model results are similar (within 1K). However, when the correlation length is short compared to the wavelength, coherent model results are significantly different from the incoherent model by several tens of kelvins. For example, for a 10cm correlation length, the differences are significant between 0.5 and 1.1GHz, and less for 1.1GHz to 2GHz. Predictions of the coherent model have been shown to be able to match v-pol SMOS data (1.4 GHz) closely and also predict h-pol data well for small observation angles. The higher h-pol brightness temperatures than model predictions observed at large angles are explained by the presence of multi-layered roughness between ice layers. Roughness introduces angular and polarization coupling that increases h-pol emissivities at large angles [24, 25]. To promote efficiency of the forward model so that model-based retrieval is more feasible, a partially coherent model has been designed in which the fully coherent model is applied after dividing the ice sheet into blocks [26]. Within each block the coherent model applies, but within adjacent blocks the radiative transfer theory is used for incoherent cascading of block parameters. By using a block size of several wavelengths, the partially coherent approach reproduces the results of fully coherent results but requires a much smaller number of realizations to reach convergence. The partially coherent model, when combined with a two-scale density variation model, predicts angular brightness temperatures that also agree well with the 1.4 GHz SMOS observations over Greenland's Summit station. The partially coherent model also enables the inclusion of rough interface effects, which can couple emissions among angles and polarizations.

### 1.8.1 The Effects of Multi-layered Roughness

The effects of interface roughness were also explored under project forward modeling studies. Density variations near the top of the ice sheet can also introduce interface roughness [27], which can perturb reflections and modulate ice sheet emissions. In particular, interface roughness can cause angular and polarization coupling not present with flat interfaces. The partially coherent approach also allows an effective method for characterizing multi-layer roughness effects within the same block using coherent wave analysis. A full wave small perturbation method up to second order (SPM2) was developed to examine interface roughness effects. The SPM2 has the advantage of conserving energy [24, 25]. Numerical results have been reported in checking energy conservation and in illustrating the angular and polarization coupling effects arising due to interface roughness. In Figure 1.6, roughness effects are examined by modeling the L-band SMOS angular brightness temperatures at Dome C, Antarctica centered on Concordia Base [28]. The SMOS data are averaged over 4 months between November 2012 and March 2013, over a total of 274 images. There is good consistency between the SMOS data and DOMEX-2 ground-based radiometer observations. Airborne data were also acquired during the DomeC Air campaign confirming the same trends with differences of around 1-2K.

The DMRT-ML model predictions agree with the vertical-pol SMOS observations quite well with an RMS about 2.7K and mean difference of 2.5K. The RMS difference is on the level of the standard deviation of SMOS data. The model predictions also follow the horizontal-pol observations up to 35° with difference less than 1.7K. However, as the observation angle continues to increase, the predictions fall below the observations to 20K at 60°. The higher h-pol brightness temperature observed implies an over-estimation of reflections at large observation angles, which is possibly due to the roughness of interfaces [21]. In Figure 1.6, the SPM2 model is applied to compute the emission from an equivalent ice sheet with 20 rough interfaces. The roughness is independent among layers and is each characterized by a Gaussian correlation function with rms height 1.5cm and correlation length 25cm. The ice sheet is assumed to have a constant temperature of 228K, close to the upward emission from below the near surface density fluctuations of the ice sheet at Dome C. The brightness angular patterns are compared in Figure 9(b) for both flat and rough interfaces. Results show that roughness has little effect on vertical polarization emission. However, it significantly increases the horizontal polarization emission at large observation angles. The v-pol and h-pol emissions agree with each other at nadir as expected, and nadir emission from the rough interfaces is only slightly larger than the flat counterpart. The roughness effects are through angular coupling and polarization coupling associated with the rough interfaces. With roughness, the model predictions show better agreement with SMOS brightness temperatures at large angles for h-pol [24].

The project's studies also formulated a Sommerfeld integration path in the SPM2 formulation to facilitate coherent model computations when waveguide modes occur in random density fluctuations where a dense layer is sandwiched between two less dense layers [84]. A T-matrix formulation for multi-layered rough surface scattering was also developed for cases when the SPM2 approximation degrades and to validate the partially coherent approach [89, 90]. Given the limited influence of interface roughness for the nadiral geometries where UWBRAD operates, interface roughness was neglected in subsequent UWBRAD retrieval analyses.

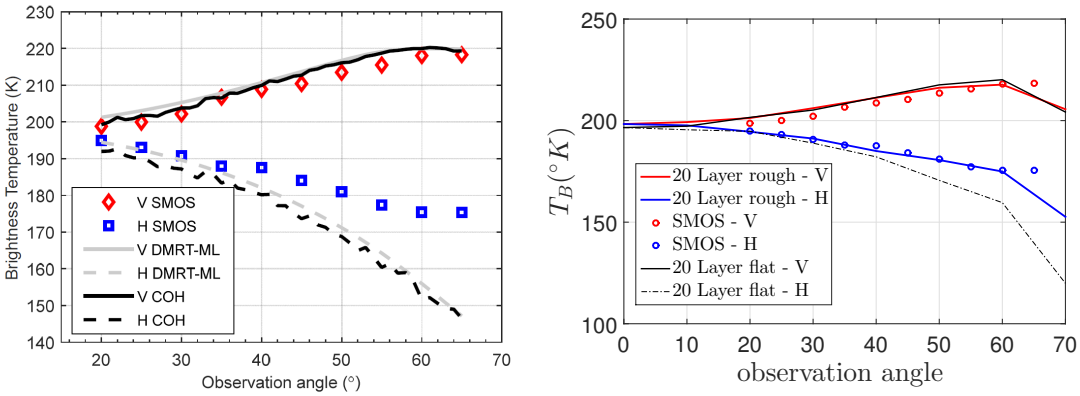


FIGURE 1.6: Comparison of model prediction of brightness temperature with L band (1.4GHz) SMOS angular data at Dome C, Antarctica. (a) Flat layers are assumed. The ice sheet temperature is characterized by the Robin temperature model that fits the borehole temperature profile well. Results are computed from 1000 Monte Carlo simulations using the coherent model. (b) Emission from an equivalent ice sheet with 20 rough interfaces. The roughness is independent among layers and is each characterized by a Gaussian correlation function with rms height 1.5cm and correlation length 25cm. The ice sheet is assumed a constant temperature of 228K, close to the upward emission from below the near surface density fluctuations of the ice sheet at Dome C. The results are computed from 400 Monte Carlo simulations over random density and layer thickness realization with SPM2.

# Chapter 2

# 2D scattering From Dielectric Layered Media with Random Rough Interfaces, Small Perturbation Method

## 2.1 Introduction

The small perturbation method has been studied for random rough surface scattering extensively [24, 29–39]. Recently, the method has been studied for multi-layered random rough surfaces [24, 30, 34] as an analytical method which has advantages over numerical methods for multiple rough interfaces. As the number of layers increases, Numerical methods become costly in CPU and memory [40]. An application of the multi-layered medium is microwave remote sensing of ice sheets in the Arctic and Antarctica, where the snow layers have multi-layering of fluctuations of permittivity due to the snow accumulation patterns as well as rough interfaces between layers [41].

The small perturbation method must be carried out to the second order[24] for energy conservation in emissivity calculations. In carrying out the Small Perturbation Method, the higher order field is expressed in terms of a convolution of the layered medium Green's function with the lower order field, where the convolution is performed in the spectral domain. To calculate the emissivity, the energy is decomposed into the incoherent intensity and the coherent intensity followed by the spectral integration. In the incoherent intensity, integration is to be carried out over the visible radiation spectrum. However, In the coherent intensity, integration is to be carried out over the entire $k$ domain spectrum.

Analytical methods provide approximate solutions. There are generally two classical approaches[3**?** ]. The high frequency method known as Kirchhoff approach and low frequency method known as small perturbation method (SPM). Higher order perturbation method has been studied in [37] up to the fourth order. Also the fourth order perturbative solution of the two layer rough surfaces has been studied recently in [32, 38]. Other analytical methods include the AIEM method [42] and the Small slope approximation (SSA) [43].

In recent years, there are numerical methods based on surface integral equations [40, 40, 44–48], the extended boundary condition methods [49, 50] and the finite difference time domain method [51]. However, for large number of rough interfaces, the dielectric contrasts between layers are usually weak, and numerical methods suffer from discretization errors. It is particularly difficult to achieve energy conservation using numerical methods for large

number of rough interfaces with small dielectric contrasts between adjacent layers. Energy conservation in scattering from 2D multilayer rough surfaces has been studied recently [39]. However we need to have solution for actual physical problem of 3D electromagnetic scattering from multilayer medium with random rough interfaces that conserve energy.

In this chapter, we study energy conservation and emissivity in scattering process of electromagnetic waves from 2D multi-layer media with a large number random rough interfaces using the second order small perturbation method (SPM2). The formulation is based on extinction theorem and developing integral equation for surface fields in spectral domain. Using SPM2, we calculate the scattered and transmitted coherent fields and incoherent fields. Energy conservation is calculated by integration of the coherent and incoherent reflected and transmitted power in the spectral domain. In this chapter, we show that the kernel function of each rough interface obeys the energy conservation. This means that energy is conserved independent of the statistics of the random rough surfaces nor the spectral densities of the rough profile of each interface. Results of this strong condition are illustrated numerically for up to 5 rough interfaces.

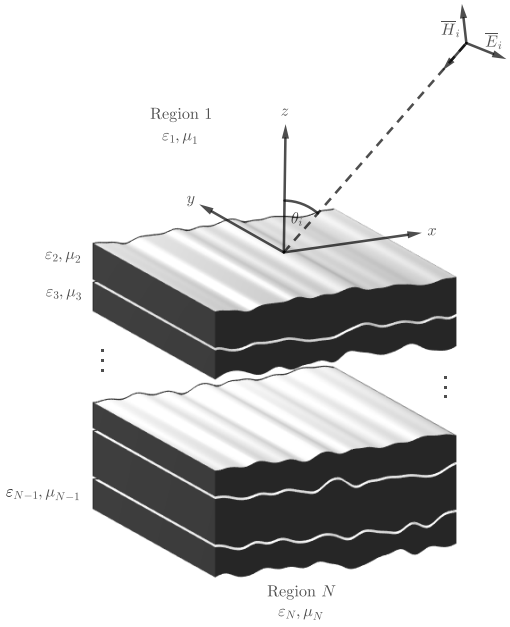


FIGURE 2.1: Dielectric layered media with 2D random rough interfaces excited by a TE polarized incident field.

## 2.2 Electric Field Integral Equation

### 2.2.1 Extinction of Downward Propagating Wave in Region 1

Upon placing the observation point in the extinction theorem [3, 52] just below the first interface, total field with wave number $k_1$ in lower media would be zero and,

$$\psi_i(\overline{\rho}) - \int_{z'=f_1(x')} \mathrm{d}l' \Big( g_1(\overline{\rho},\overline{\rho}')\hat{n}_1' \cdot \nabla' \psi_1(\overline{\rho}') - \psi_1(\overline{\rho}')\hat{n}_1' \cdot \nabla' g_1(\overline{\rho},\overline{\rho}') \Big) = 0 \tag{2.2.1}$$

We can define the surface field variables on the first surface as $a_1(x)\mathrm{d}x=\mathrm{d}l\hat{n}\cdot\nabla\psi_1$ and $b_1(x)=\psi_1(x)$ to get

$$\psi_i(\overline{\rho})-\int_{z'=f_1(x')}\mathrm{d}x'\Big(g_1(\overline{\rho},\overline{\rho}')a_1(x')-b_1(x')\frac{\mathrm{d}l'}{\mathrm{d}x'}\hat{n}_1'\cdot\nabla' g_1(\overline{\rho},\overline{\rho}')\Big)=0 \tag{2.2.2}$$

Notice that measure of integration is changed to the flat line integral from the general curved path. From plane wave expansion of the Green's function for $z<z'$,

$$g_1(z<z')=\frac{i}{4\pi}\int\mathrm{d}k_x\frac{1}{k_{1z}}e^{ik_x(x-x')-ik_{1z}(z-z')} \tag{2.2.3}$$

then normal derivative of Green's function becomes

$$\hat{n}_1'\cdot\nabla' g_1(z<z')=\frac{1}{\sqrt{1+f_{x'}^2}}\frac{i}{4\pi}\int\mathrm{d}k_x\frac{1}{k_{1z}}\Big[ik_{1z}+ik_x f_1'(x')\Big]e^{ik_x(x-x')-ik_{1z}(z-f_1(x'))} \tag{2.2.4}$$

Note that for the spectral expansion of the Green's function we assumed that the observation point is somewhere that for all values of $z'$, the condition $z<z'$ is true. Such an observation point cannot be on the boundary surface unless the boundary is flat. Because of the fact that here we are putting the observation point on another surface than the actual surface, this method of solving the integral equation using the spectral expansion is called *Extended Boundary Condition Method* (EBCM)[53–56]. Substituting the spectral expansion of the Green's function and its derivative into the Extinction integral equation of (2.2.2), it yields

$$\psi_i(\overline{\rho})-\frac{i}{4\pi}\int\mathrm{d}k_x\frac{1}{k_{1z}}e^{ik_x x-ik_{1z}z}\int\mathrm{d}x'e^{-ik_x x'+ik_{1z}f_1(x')}\Big(a_1(x')-b_1(x')\Big[ik_{1z}+ik_x f_1'(x')\Big]\Big)=0 \tag{2.2.5}$$

Notice that the surface fields $a_1(x)$,$b_1(x)$ are defined in such a way that the surface profile length element (which depends on the surface profile non-linearly) is not present in the integral equation of (2.2.5). Inserting the Fourier representation of the downward propagating incident field $\psi_i$ in the above equation and noting that plane wave with different wave numbers are eigenfunction of the Hermitian operator of the wave function and are independent, we arrive at

$$\psi_i(k_x)-\frac{i}{4\pi k_{1z}}\int\mathrm{d}x'e^{-ik_x x'+ik_{1z}f_1(x')}\Big(a_1(x')-b_1(x')\Big[ik_{1z}+ik_x f_1'(x')\Big]\Big)=0 \tag{2.2.6}$$

Defining the Fourier transform of the surface fields as

$$a_1(x')=\int\mathrm{d}k_x' A_1(k_x')e^{ik_x' x'} \tag{2.2.7}$$

$$\psi_i(k_x)-\frac{i}{4\pi k_{1z}}\int\mathrm{d}k_x'\int\mathrm{d}x'e^{-i(k_x-k_x')x'+ik_{1z}f_1(x')}\Big\{A_1(k_x')-B_1(k_x')\Big[ik_{1z}+ik_x f_1'(x')\Big]\Big\}=0 \tag{2.2.8}$$

There is a term in the integrand that depends on the derivative of the profile. performing the by part integration on this term yields,

$$\begin{aligned}\int\mathrm{d}x'e^{-i(k_x-k_x')x'+ik_{1z}f_1}ik_x f_1'(x')=&\frac{k_x}{k_{1z}}\int\mathrm{d}\Big[e^{-i(k_x-k_x')x'+ik_{1z}f_1}\Big]\\&+i(k_x-k_x')\frac{k_x}{k_{1z}}\int\mathrm{d}x'e^{-i(k_x-k_x')x'+ik_{1z}f_1}\end{aligned} \tag{2.2.9}$$

Assuming periodic boundary condition on the surface (with very large period that simulate an infinitely large surface), the first term vanishes and

$$\int \mathrm{d}x' e^{-i(k_x-k'_x)x'+ik_{1z}f_1(x')}\Big[ik_{1z}+ik_x f'_1(x')\Big]=i\frac{k_1^2-k_xk'_x}{k_{1z}}\int \mathrm{d}x' e^{-i(k_x-k'_x)x'+ik_{1z}f_1(x')} \tag{2.2.10}$$

Furthermore, if the scattering potential $I^-_{11}(k_x,k'_x)$ for the downward propagating wave in the region 1 that is scattered from the first surface defined as

$$I^-_{11}(k_x,k'_x)=\frac{1}{2\pi}\int \mathrm{d}x' e^{-i(k_x-k'_x)x'}\Big[e^{ik_{1z}f_1(x')}-1\Big] \tag{2.2.11}$$

Then, the integral equation describing the Fourier transform of the surface fields over the boundary $z=f_1(x)$ can be written as follows,

$$\psi_i(k_x)-\frac{i}{2k_{1z}}\left[A_1(k_x)-ik_{1z}B_1(k_x)+\int \mathrm{d}k'_x I^-_{11}(k_x,k'_x)\left\{A_1(k'_x)-B_1(k'_x)i\frac{k_1^2-k_xk'_x}{k_{1z}}\right\}\right]=0 \tag{2.2.12}$$

The scattering potential is completely responsible for the presence of the roughness in the problem. If the surface is flat, then the scattering potential vanishes and the integral equation becomes an algebraic equation.

### 2.2.2 Extinction of Upward propagating Wave in Region $m$

$$\begin{aligned}\int_{z'=-d_{m-1}+f_{m-1}(x')} \mathrm{d}l'\Big(g_m(\overline{\rho},\overline{\rho}')\hat{n}'\cdot\nabla'\psi_m(\overline{\rho}')-\psi_m(\overline{\rho}')\hat{n}'\cdot\nabla'g_m(\overline{\rho},\overline{\rho}')\Big) \\ -\int_{z'=-d_m+f_m(x')} \mathrm{d}l'\Big(g_m(\overline{\rho},\overline{\rho}')\hat{n}'\cdot\nabla'\psi_m(\overline{\rho}')-\psi_m(\overline{\rho}')\hat{n}'\cdot\nabla'g_m(\overline{\rho},\overline{\rho}')\Big)=0\end{aligned} \tag{2.2.13}$$

Utilizing the boundary conditions to express the surface fields in the first integral in terms of neighborer layer fields, we arrive at

$$\begin{aligned}\int \mathrm{d}x'\Big(g_m(\overline{\rho},\overline{\rho}')\gamma_{m-1,m}a_{m-1}(x')-b_{m-1}(x')\hat{n}'\cdot\nabla'g_m(\overline{\rho},\overline{\rho}')\Big) \\ -\int \mathrm{d}x'\Big(g_m(\overline{\rho},\overline{\rho}')a_m(x')-b_m(x')\hat{n}'\cdot\nabla'g_m(\overline{\rho},\overline{\rho}')\Big)=0\end{aligned} \tag{2.2.14}$$

Using the spectral expansion of the Green's function in the region $m$ as

$$g_m(z>z')=\frac{i}{4\pi}\int \mathrm{d}k_x\frac{1}{k_{mz}}e^{ik_x(x-x')+ik_{mz}(z-z')} \tag{2.2.15}$$

and normal derivative of Green's function over $m$ and $(m-1)$th interfaces,

$$\begin{aligned}\hat{n}'_{m-1}\cdot\nabla'g_m&=\frac{1}{\sqrt{1+f'^2_{m-1}}}\frac{i}{4\pi}\int \mathrm{d}k_x\frac{1}{k_{mz}}\Big[-ik_{mz}+ik_xf'_{m-1}\Big]e^{ik_x(x-x')+ik_{mz}(z-f_{m-1})}e^{ik_{mz}d_{m-1}} \\ \hat{n}'_{m}\cdot\nabla'g_m&=\frac{1}{\sqrt{1+f'^2_{m}}}\frac{i}{4\pi}\int \mathrm{d}k_x\frac{1}{k_{mz}}\Big[-ik_{mz}+ik_xf'_{m}\Big]e^{ik_x(x-x')+ik_{mz}(z-f_m(x'))}e^{ik_{mz}d_m}\end{aligned} \tag{2.2.16}$$

The integral equation for the upward propagating field in the region $m$ can be obtained by following the same procedure as region 1 (Inserting Fourier transform of the fields and performing by part integration) as

$$e^{ik_{mz}d_{m-1}}\Bigg[\gamma_{m-1,m}A_{m-1}(k_x)+ik_{mz}B_{m-1}(k_x)+\int \mathrm{d}k'_x I^+_{m,m-1}(k_x,k'_x)\Bigg\{\gamma_{m-1,m}A_{m-1}(k'_x) \\ +B_{m-1}(k'_x)i\frac{k_m^2-k_xk'_x}{k_{mz}}\Bigg\}\Bigg]-e^{ik_{mz}d_m}\Bigg[A_m(k_x)+ik_{mz}B_m(k_x) \\ +\int \mathrm{d}k'_x I^+_{m,m}(k_x,k'_x)\Bigg\{A_m(k'_x)+B_m(k'_x)i\frac{k_m^2-k_xk'_x}{k_{mz}}\Bigg\}\Bigg]=0 \tag{2.2.17}$$

Here $2\leq m\leq N-1$ and scattering potentials are defined as

$$I^+_{m,m-1}(k_x,k'_x)=\frac{1}{2\pi}\int \mathrm{d}x' e^{-i(k_x-k'_x)x'}\left[e^{-ik_{mz}f_{m-1}(x')}-1\right] \tag{2.2.18}$$
$$I^+_{m,m}(k_x,k'_x)=\frac{1}{2\pi}\int \mathrm{d}x' e^{-i(k_x-k'_x)x'}\left[e^{-ik_{mz}f_{m}(x')}-1\right].$$

### 2.2.3 Extinction of Downward propagating Wave in Region $m$

The extinction relation here is the same as upward propagating wave in the region $m$. The only difference is the spectral expansion of the Green's function. In order to extinct downward propagating wave in region $m$, the observation point should be placed under the surface $z=-d_m+f_m(x)$ to satisfy the condition $z<z'$ for all of the source point on the surface. The Green's function can be expanded as

$$g_m(z<z')=\frac{i}{4\pi}\int \mathrm{d}k_x \frac{1}{k_{mz}}e^{ik_x(x-x')-ik_{mz}(z-z')} \tag{2.2.19}$$

Following the same procedure as extinction of the upward propagating wave, we arrive at

$$e^{-ik_{mz}d_{m-1}}\Bigg[\gamma_{m-1,m}A_{m-1}(k_x)-ik_{mz}B_{m-1}(k_x)+\int \mathrm{d}k'_x I^-_{m,m-1}(k_x,k'_x)\Bigg\{\gamma_{m-1,m}A_{m-1}(k'_x) \\ -B_{m-1}(k'_x)i\frac{k_m^2-k_xk'_x}{k_{mz}}\Bigg\}\Bigg]-e^{-ik_{mz}d_m}\Bigg[A_m(k_x)-ik_{mz}B_m(k_x) \\ +\int \mathrm{d}k'_x I^-_{m,m}(k_x,k'_x)\Bigg\{A_m(k'_x)-B_m(k'_x)i\frac{k_m^2-k_xk'_x}{k_{mz}}\Bigg\}\Bigg]=0 \tag{2.2.20}$$

with the scattering potentials $I^-_{m,m}(k_x,k'_x)$ and $I^-_{m,m-1}(k_x,k'_x)$ defined as

$$I^-_{m,m-1}(k_x,k'_x)=\frac{1}{2\pi}\int \mathrm{d}x' e^{-i(k_x-k'_x)x'}\left[e^{ik_{mz}f_{m-1}(x')}-1\right] \tag{2.2.21}$$
$$I^-_{m,m}(k_x,k'_x)=\frac{1}{2\pi}\int \mathrm{d}x' e^{-i(k_x-k'_x)x'}\left[e^{ik_{mz}f_{m}(x')}-1\right].$$

### 2.2.4 Extinction of Upward Propagating Wave in region $N$

Application of the extinction theorem to the last half space gives similar results to that of single interface problem described in Chapter 1. The final integral equation of the surface fields on the last boundary in the spectral domain can be written as

$$\gamma_{N-1,N}A_{N-1}+ik_{Nz}B_{N-1}+\int \mathrm{d}k'_x I^+_{N,N-1}\left\{\gamma_{N-1,N}A_{N-1}(k'_x)+B_{N-1}(k'_x)i\frac{k_N^2-k_xk'_x}{k_{Nz}}\right\}=0$$

where the scattering potential $I^+_{N,N-1}(k_x,k'_x)$ is defined as

$$I^+_{N,N-1}(k_x,k'_x)=\frac{1}{2\pi}\int \mathrm{d}x' e^{-i(k_x-k'_x)x'}\left[e^{-ik_{Nz}f_{N-1}(x')}-1\right]. \tag{2.2.22}$$

For middle layers where $2\leq m\leq N-1$, the surface field variables can be related through the Lippmann-Schwinger type equation of

$$\overline{\overline{G}}^u_{0,m-1}\overline{\psi}_{m-1}(k_x)+\int \mathrm{d}k'_x\overline{\overline{S}}^u_{m-1}(k_x,k'_x)\overline{\psi}_{m-1}(k'_x)=\overline{\overline{G}}^d_{0,m}\overline{\psi}_m(k_x)+\int \mathrm{d}k'_x\overline{\overline{S}}^d_m(k_x,k'_x)\overline{\psi}_m(k'_x) \tag{2.2.23}$$

where $\overline{\overline{G}}^u_{0,m-1}$ and $\overline{\overline{G}}^d_{0,m}$ are the propagation operator of the surface field over the flat surfaces

$$\begin{aligned}\overline{\overline{G}}^u_{0,m-1}&=\begin{bmatrix}e^{ik_{mz}d_{m-1}}\gamma_{m-1,m} & e^{ik_{mz}d_{m-1}}ik_{mz}\\ e^{-ik_{mz}d_{m-1}}\gamma_{m-1,m} & -e^{-ik_{mz}d_{m-1}}ik_{mz}\end{bmatrix}\\ \overline{\overline{G}}^d_{0,m}&=\begin{bmatrix}e^{ik_{mz}d_m} & e^{ik_{mz}d_m}ik_{mz}\\ e^{-ik_{mz}d_m} & -e^{-ik_{mz}d_m}ik_{mz}\end{bmatrix}\end{aligned} \tag{2.2.24}$$

and $\overline{\overline{S}}^u_{m-1}$ and $\overline{\overline{S}}^d_m$ are scattering operators that incorporate scattering effect of the $(m-1)$th and $m$th rough interfaces, respectively and are given by,

$$\begin{aligned}\overline{\overline{S}}^u_{m-1}&=\begin{bmatrix}e^{ik_{mz}d_{m-1}}\gamma_{m-1,m}I^+_{m,m-1} & e^{ik_{mz}d_{m-1}}i\frac{k_m^2-k_xk'_x}{k_{mz}}I^+_{m,m-1}\\ e^{-ik_{mz}d_{m-1}}\gamma_{m-1,m}I^-_{m,m-1} & -e^{-ik_{mz}d_{m-1}}i\frac{k_m^2-k_xk'_x}{k_{mz}}I^-_{m,m-1}\end{bmatrix}\\ \overline{\overline{S}}^d_m&=\begin{bmatrix}e^{ik_{mz}d_m}I^+_{m,m} & e^{ik_{mz}d_m}i\frac{k_m^2-k_xk'_x}{k_{mz}}I^+_{m,m}\\ e^{-ik_{mz}d_m}I^-_{m,m} & -e^{-ik_{mz}d_m}i\frac{k_m^2-k_xk'_x}{k_{mz}}I^-_{m,m}\end{bmatrix}\end{aligned} \tag{2.2.25}$$

The superscripts $u$ and $d$ are here to distinguish two operators and finally, the unknown surface fields on the $m$th boundary are placed in the column vector $\overline{\psi}_m$ and is defined as

$$\overline{\psi}_m(k_x)=\begin{bmatrix}A_m(k_x)\\ B_m(k_x)\end{bmatrix} \tag{2.2.26}$$

The extinction relations of two half spaces (region 1 and region $N$) can be combined together and written as

$$\overline{\overline{G}}_{0,E}(k_x)\overline{\psi}_E(k_x)+\int \mathrm{d}k'_x\overline{\overline{S}}_E(k_x,k'_x)\overline{\psi}_E(k'_x)=\overline{\psi}_i \tag{2.2.27}$$

Here $E$ refers to the External layers. Again, $\overline{\overline{G}}_{0,E}$ is the propagator of the surface fields over the first and the last interfaces with zero roughness,

$$\overline{\overline{G}}_{0,E}(k_x)=\begin{bmatrix} \frac{i}{2k_{1z}} & \frac{1}{2} & 0 & 0 \\ 0 & 0 & \gamma_{N-1,N} & ik_{Nz} \end{bmatrix} \tag{2.2.28}$$

and $\overline{\overline{S}}_E(k_x,k'_x)$ is the partial scattering operator that is partially responsible for scattering from the first and last interfaces due to the presence of roughness.

$$\overline{\overline{S}}_E(k_x,k'_x)=\begin{bmatrix} \frac{i}{2k_{1z}}I_{11}^- & \frac{k_1^2-k_xk'_x}{2k_{1z}^2}I_{11}^- & 0 & 0 \\ 0 & 0 & \gamma_{N-1,N}I_{N,N-1}^+ & i\frac{k_N^2-k_xk'_x}{k_{Nz}}I_{N,N-1}^+ \end{bmatrix} \tag{2.2.29}$$

and the external surface field vector is defined as,

$$\overline{\psi}_E(k_x)=\begin{bmatrix} A_1(k_x) \\ B_1(k_x) \\ A_{N-1}(k_x) \\ B_{N-1}(k_x) \end{bmatrix} \tag{2.2.30}$$

## 2.3 Solution of the Surface Fields

### 2.3.1 Zeroth Order Solution

Up to the zeroth order of the surface roughness, the scattering operators are all set to zero and propagation relation of middle layers can be written as

$$\overline{\overline{G}}^u_{0,m-1}\overline{\psi}^{(0)}_{m-1}(k_x)=\overline{\overline{G}}^d_{0,m}\overline{\psi}^{(0)}_m(k_x) \tag{2.3.1}$$

Also, for the external layers,

$$\overline{\overline{G}}_{0,E}(k_x)\overline{\psi}^{(0)}_E(k_x)=\delta(k_x-k_{ix})\overline{\psi}_i \tag{2.3.2}$$

The surface fields over the last boundary can be related to the surface fields over the first boundary by a recursive relation through

$$\overline{\psi}^{(0)}_m(k_x)=\left[\overline{\overline{G}}^d_{0,m}\right]^{-1}\overline{\overline{G}}^u_{0,m-1}\overline{\psi}^{(0)}_{m-1}(k_x) \tag{2.3.3}$$

to obtain,

$$\begin{aligned}\overline{\psi}^{(0)}_{N-1}(k_x)&=\left(\left[\overline{\overline{G}}^d_{0,N-1}\right]^{-1}\overline{\overline{G}}^u_{0,N-2}\right)\left(\left[\overline{\overline{G}}^d_{0,N-2}\right]^{-1}\overline{\overline{G}}^u_{0,N-3}\right)\cdots\left(\left[\overline{\overline{G}}^d_{0,1}\right]^{-1}\overline{\overline{G}}^u_{0,0}\right)\overline{\psi}^{(0)}_0(k_x)\\ &:=\overline{\overline{G}}^{(0)}\overline{\psi}^{(0)}_0\end{aligned}$$

Here, $\overline{\overline{G}}_0$ is defined as product of all propagation operators and relates the surface fields of the first boundary to the last one. Combining the middle and external equations, the obtained a matrix equation for the $\overline{\psi}_E$ as

$$\begin{bmatrix} & \overline{\overline{G}}_{0,E}(k_x) & \\ \overline{\overline{G}}^{(0)} & & -\overline{\overline{I}} \end{bmatrix}\overline{\psi}^{(0)}_E(k_x)=\delta(k_x-k_{ix})\overline{\psi}_i \tag{2.3.4}$$

which provides the surface fields solution over the first and last interfaces that enable us to calculated both scattered and transmitted fields. The requirement for the finite solution of the surface fields is that the matrix on the left hand side should be invertible at $k_x=k_{ix}$.

### 2.3.2 First Order Solution

Balancing (2.2.23) and (2.2.27) up to the first order of surface roughness gives

$$\overline{\overline{G}}^{u}_{0,m-1}\overline{\psi}^{(1)}_{m-1}(k_x)+\int \mathrm{d}k'_x \overline{\overline{S}}^{u(1)}_{m-1}(k_x,k'_x)\overline{\psi}^{(0)}_{m-1}(k'_x)=\overline{\overline{G}}^{d}_{0,m}\overline{\psi}^{(1)}_{m}(k_x)+\int \mathrm{d}k'_x \overline{\overline{S}}^{d(1)}_{m}(k_x,k'_x)\overline{\psi}^{(0)}_{m}(k'_x)$$

$$\overline{\overline{G}}_{0,E}(k_x)\overline{\psi}^{(1)}_{E}(k_x)+\int \mathrm{d}k'_x \overline{\overline{S}}^{(1)}_{E}(k_x,k'_x)\overline{\psi}^{(0)}_{E}(k'_x)=0 \tag{2.3.5}$$

Since the zeroth order solution exists only in specular spectral point $k_x=k_{ix}$, the integrals will be sifted by the delta function and

$$\begin{aligned}\overline{\overline{G}}^{u}_{0,m-1}\overline{\psi}^{(1)}_{m-1}(k_x)+\overline{\overline{S}}^{u(1)}_{m-1}(k_x,k_{ix})\overline{\psi}^{(0)}_{m-1}&=\overline{\overline{G}}^{d}_{0,m}\overline{\psi}^{(1)}_{m}(k_x)+\overline{\overline{S}}^{d(1)}_{m}(k_x,k_{ix})\overline{\psi}^{(0)}_{m}\\ \overline{\overline{G}}_{0,E}(k_x)\overline{\psi}^{(1)}_{E}(k_x)+\overline{\overline{S}}^{(1)}_{E}(k_x,k_{ix})\overline{\psi}^{(0)}_{E}&=0\end{aligned} \tag{2.3.6}$$

We can solve for the first order surface fields and noting that the zeroth order solution of surface fields are known over all of the interfaces, a recursive relation can be obtained as

$$\begin{aligned}\overline{\psi}^{(1)}_{m}(k_x)=&\left[\overline{\overline{G}}^{d}_{0,m}(k_x)\right]^{-1}\overline{\overline{G}}^{u}_{0,m-1}\overline{\psi}^{(1)}_{m-1}(k_x)\\ &+\left[\overline{\overline{G}}^{d}_{0,m}(k_x)\right]^{-1}\left(\overline{\overline{S}}^{u(1)}_{m-1}(k_x,k_{ix})\overline{\psi}^{(0)}_{m-1}-\overline{\overline{S}}^{d(1)}_{m}(k_x,k_{ix})\overline{\psi}^{(0)}_{m}\right)\end{aligned} \tag{2.3.7}$$

Observing that the first order approximation of the scattering potentials are related to the interfaces spectrum through,

$$\overline{\overline{S}}^{u(1)}_{m-1}(k_x,k_{ix})=\begin{bmatrix}e^{ik_{mz}d_{m-1}}\gamma_{m-1,m}(-ik_{mz}) & e^{ik_{mz}d_{m-1}}i\frac{k_m^2-k_xk'_x}{k_{mz}}(-ik_{mz})\\ e^{-ik_{mz}d_{m-1}}\gamma_{m-1,m}(ik_{mz}) & -e^{-ik_{mz}d_{m-1}}i\frac{k_m^2-k_xk'_x}{k_{mz}}(ik_{mz})\end{bmatrix}F_{m-1}(k_x-k_{ix}) \tag{2.3.8}$$

$$\overline{\overline{S}}^{d(1)}_{m}(k_x,k_{ix})=\begin{bmatrix}e^{ik_{mz}d_{m}}(-ik_{mz}) & e^{ik_{mz}d_{m}}i\frac{k_m^2-k_xk'_x}{k_{mz}}(-ik_{mz})\\ e^{-ik_{mz}d_{m}}(ik_{mz}) & -e^{-ik_{mz}d_{m}}i\frac{k_m^2-k_xk'_x}{k_{mz}}(ik_{mz})\end{bmatrix}F_{m}(k_x-k_{ix})$$

The first order surface field over the $m$th interface can be decomposed into

$$\overline{\psi}^{(1)}_{m}(k_x)=\overline{\overline{G}}^{(1)}_{m}\overline{\psi}^{(1)}_{m-1}+\overline{D}^{u}_{m-1}F_{m-1}+\overline{D}^{d}_{m}F_{m} \tag{2.3.9}$$

where, the following intermediate vectors are introduced for convenience

$$\begin{aligned}\overline{\overline{G}}^{(1)}_{m}(k_x)&=\left[\overline{\overline{G}}^{d}_{0,m}(k_x)\right]^{-1}\overline{\overline{G}}^{u}_{0,m-1}\\ \overline{D}^{u}_{m-1}(k_x)&=\left[\overline{\overline{G}}^{d}_{0,m}(k_x)\right]^{-1}\tilde{\overline{\overline{S}}}^{u(1)}_{m-1}(k_x,k_{ix})\overline{\psi}^{(0)}_{m-1}\\ \overline{D}^{d}_{m}(k_x)&=-\left[\overline{\overline{G}}^{d}_{0,m}(k_x)\right]^{-1}\tilde{\overline{\overline{S}}}^{d(1)}_{m}(k_x,k_{ix})\overline{\psi}^{(0)}_{m}\end{aligned} \tag{2.3.10}$$

Now we are in position to solve recursive relation of the surface fields to relate first and the last surface fields together

$$\begin{aligned}\overline{\psi}_m^{(1)}(k_x)=&\overline{\overline{G}}_m^{(1)}\left(\overline{\overline{G}}_{m-1}^{(1)}\overline{\psi}_{m-2}^{(1)}+\overline{D}_{m-2}^{u}F_{m-2}+\overline{D}_{m-1}^{d}F_{m-1}\right)+\overline{D}_{m-1}^{u}F_{m-1}+\overline{D}_{m}^{d}F_{m}\\ =&\overline{\overline{G}}_m^{(1)}\overline{\overline{G}}_{m-1}^{(1)}\overline{\psi}_{m-2}^{(1)}+\overline{\overline{G}}_m^{(1)}\overline{D}_{m-2}^{u}F_{m-2}+\overline{\overline{G}}_m^{(1)}\overline{D}_{m-1}^{d}F_{m-1}+\overline{D}_{m-1}^{u}F_{m-1}+\overline{D}_{m}^{d}F_{m}\\ =&\overline{\overline{G}}_m^{(1)}\overline{\overline{G}}_{m-1}^{(1)}\overline{\psi}_{m-2}^{(1)}+\overline{\overline{G}}_m^{(1)}\overline{D}_{m-2}^{u}F_{m-2}+\left[\overline{\overline{G}}_m^{(1)}\overline{D}_{m-1}^{d}+\overline{D}_{m-1}^{u}\right]F_{m-1}+\overline{D}_{m}^{d}F_{m}\end{aligned}$$

also

$$\overline{\psi}_{m-2}^{(1)}(k_x)=\overline{\overline{G}}_{m-2}^{(1)}\overline{\psi}_{m-3}^{(1)}+\overline{D}_{m-3}^{u}F_{m-3}+\overline{D}_{m-2}^{d}F_{m-2} \tag{2.3.11}$$

and as a result of substitution, we obtain,

$$\begin{aligned}\overline{\psi}_m^{(1)}(k_x)=&\overline{\overline{G}}_m^{(1)}\overline{\overline{G}}_{m-1}^{(1)}\left(\overline{\overline{G}}_{m-2}^{(1)}\overline{\psi}_{m-3}^{(1)}+\overline{D}_{m-3}^{u}F_{m-3}+\overline{D}_{m-2}^{d}F_{m-2}\right)\\ &+\overline{\overline{G}}_m^{(1)}\overline{D}_{m-2}^{u}F_{m-2}+\left[\overline{\overline{G}}_m^{(1)}\overline{D}_{m-1}^{d}+\overline{D}_{m-1}^{u}\right]F_{m-1}+\overline{D}_{m}^{d}F_{m}\\ =&\overline{\overline{G}}_m^{(1)}\overline{\overline{G}}_{m-1}^{(1)}\overline{\overline{G}}_{m-2}^{(1)}\overline{\psi}_{m-3}^{(1)}+\overline{\overline{G}}_m^{(1)}\overline{\overline{G}}_{m-1}^{(1)}\overline{D}_{m-3}^{u}F_{m-3}+\overline{\overline{G}}_m^{(1)}\overline{\overline{G}}_{m-1}^{(1)}\overline{D}_{m-2}^{d}F_{m-2}\\ &+\overline{\overline{G}}_m^{(1)}\overline{D}_{m-2}^{u}F_{m-2}+\left[\overline{\overline{G}}_m^{(1)}\overline{D}_{m-1}^{d}+\overline{D}_{m-1}^{u}\right]F_{m-1}+\overline{D}_{m}^{d}F_{m}\end{aligned} \tag{2.3.12}$$

or

$$\begin{aligned}\overline{\psi}_m^{(1)}(k_x)=&\overline{\overline{G}}_m^{(1)}\overline{\overline{G}}_{m-1}^{(1)}\overline{\overline{G}}_{m-2}^{(1)}\overline{\psi}_{m-3}^{(1)}+\overline{\overline{G}}_m^{(1)}\overline{\overline{G}}_{m-1}^{(1)}\overline{D}_{m-3}^{u}F_{m-3}\\ &+\overline{\overline{G}}_m^{(1)}\left[\overline{\overline{G}}_{m-1}^{(1)}\overline{D}_{m-2}^{d}+\overline{D}_{m-2}^{u}\right]F_{m-2}+\left[\overline{\overline{G}}_m^{(1)}\overline{D}_{m-1}^{d}+\overline{D}_{m-1}^{u}\right]F_{m-1}+\overline{D}_{m}^{d}F_{m}\end{aligned} \tag{2.3.13}$$

This recursive relation can be generalized to for arbitrary number of layers through,

$$\begin{aligned}\overline{\psi}_{N-1}^{(1)}(k_x)=&\overline{\overline{G}}_{N-1}^{(1)}\overline{\overline{G}}_{N-2}^{(1)}\cdots\overline{\overline{G}}_{2}^{(1)}\overline{\psi}_{1}^{(1)}\\ &+\overline{\overline{G}}_{N-1}^{(1)}\overline{\overline{G}}_{N-2}^{(1)}\cdots\overline{\overline{G}}_{3}^{(1)}\left[\overline{D}_{1}^{u}F_1+\overline{D}_{2}^{d}F_2\right]\\ &+\overline{\overline{G}}_{N-1}^{(1)}\overline{\overline{G}}_{N-2}^{(1)}\cdots\overline{\overline{G}}_{4}^{(1)}\left[\overline{D}_{2}^{u}F_2+\overline{D}_{3}^{d}F_3\right]\\ &+\overline{\overline{G}}_{N-1}^{(1)}\overline{\overline{G}}_{N-2}^{(1)}\cdots\overline{\overline{G}}_{5}^{(1)}\left[\overline{D}_{3}^{u}F_3+\overline{D}_{4}^{d}F_4\right]\\ &\vdots\\ &+\overline{\overline{G}}_{N-1}^{(1)}\left[\overline{D}_{N-3}^{u}F_{N-3}+\overline{D}_{N-2}^{d}F_{N-2}\right]\\ &+\left[\overline{D}_{N-2}^{u}F_{N-2}+\overline{D}_{N-1}^{d}F_{N-1}\right]\\ :=&\overline{\overline{G}}^{(1)}\overline{\psi}_{1}^{(1)}+\sum\overline{D}_{j}^{(1)}F_j\end{aligned} \tag{2.3.14}$$

On the other hand, for external layers,

$$\overline{\overline{G}}_{0,E}(k_x)\overline{\psi}_{E}^{(1)}(k_x)+\overline{\overline{S}}_{E}^{(1)}(k_x,k_{ix})\overline{\psi}_{E}^{(0)}=0 \tag{2.3.15}$$

where,

$$\overline{\overline{S}}_E^{(1)}(k_x,k_x')=\begin{bmatrix} -\frac{1}{2}F_1 & i\frac{k_1^2-k_xk_x'}{2k_{1z}}F_1 & 0 & 0 \\ 0 & 0 & -i\gamma_{N-1,N}k_{Nz}F_{N-1} & (k_N^2-k_xk_x')F_{N-1} \end{bmatrix} \tag{2.3.16}$$

Combination of (2.3.14) and (2.3.15) provides necessary system of equations to solve the surface fields on the external interfaces,

$$\begin{bmatrix} \overline{\overline{G}}_{0,E} & \\ -\overline{\overline{G}}^{(1)} & \overline{\overline{I}} \end{bmatrix} \overline{\psi}_E^{(1)} = \begin{bmatrix} -\overline{\overline{S}}_E^{(1)}(k_x,k_{ix})\overline{\psi}_E^{(0)} \\ \sum \overline{D}_j^{(1)}F_j \end{bmatrix} \tag{2.3.17}$$

### 2.3.3 Second Order Solution

Balancing (2.2.23) up to the second order of surface roughness result in,

$$\begin{aligned} &\overline{\overline{G}}_{0,m-1}^{u}\overline{\psi}_{m-1}^{(2)}(k_x)+\int \mathrm{d}k_x'\overline{\overline{S}}_{m-1}^{u(1)}(k_x,k_x')\overline{\psi}_{m-1}^{(1)}(k_x')+\int \mathrm{d}k_x'\overline{\overline{S}}_{m-1}^{u(2)}(k_x,k_x')\overline{\psi}_{m-1}^{(0)}(k_x') \\ &\quad=\overline{\overline{G}}_{0,m}^{d}\overline{\psi}_m^{(2)}(k_x)+\int \mathrm{d}k_x'\overline{\overline{S}}_m^{d(1)}(k_x,k_x')\overline{\psi}_m^{(1)}(k_x')+\int \mathrm{d}k_x'\overline{\overline{S}}_m^{d(2)}(k_x,k_x')\overline{\psi}_m^{(0)}(k_x') \end{aligned} \tag{2.3.18}$$

Before proceeding to the solution second order perturbation of scattering operator are as following

$$\overline{\overline{S}}_{m-1}^{u(2)}(k_x,k_x')=-\frac{1}{2}k_{mz}^2\begin{bmatrix} e^{ik_{mz}d_{m-1}}\gamma_{m-1,m} & e^{ik_{mz}d_{m-1}}i\frac{k_m^2-k_xk_x'}{k_{mz}} \\ e^{-ik_{mz}d_{m-1}}\gamma_{m-1,m} & -e^{-ik_{mz}d_{m-1}}i\frac{k_m^2-k_xk_x'}{k_{mz}} \end{bmatrix} F_{m-1}^{(2)}(k_x-k_x') \tag{2.3.19}$$

$$\overline{\overline{S}}_m^{d(2)}(k_x,k_x')=-\frac{1}{2}k_{mz}^2\begin{bmatrix} e^{ik_{mz}d_m} & e^{ik_{mz}d_m}i\frac{k_m^2-k_xk_x'}{k_{mz}} \\ e^{-ik_{mz}d_m} & -e^{-ik_{mz}d_m}i\frac{k_m^2-k_xk_x'}{k_{mz}} \end{bmatrix} F_m^{(2)}(k_x-k_x')$$

Inserting specular zeroth order solution yields

$$\begin{aligned} &\overline{\overline{G}}_{0,m-1}^{u}\overline{\psi}_{m-1}^{(2)}(k_x)+\int \mathrm{d}k_x'\overline{\overline{S}}_{m-1}^{u(1)}(k_x,k_x')\overline{\psi}_{m-1}^{(1)}(k_x')+\overline{\overline{S}}_{m-1}^{u(2)}(k_x,k_{ix})\overline{\psi}_{m-1}^{(0)} \\ &\quad=\overline{\overline{G}}_{0,m}^{d}\overline{\psi}_m^{(2)}(k_x)+\int \mathrm{d}k_x'\overline{\overline{S}}_m^{d(1)}(k_x,k_x')\overline{\psi}_m^{(1)}(k_x')+\overline{\overline{S}}_m^{d(2)}(k_x,k_{ix})\overline{\psi}_m^{(0)} \end{aligned} \tag{2.3.20}$$

From the first order solution of the surface fields, $\overline{\psi}_m^{(1)}$ can be decomposed as contribution of the different interfaces as

$$\overline{\psi}_m^{(1)}=\sum \overline{\psi}_{m,j}^{(1)}F_j \tag{2.3.21}$$

thus,

$$\begin{aligned} &\overline{\overline{G}}_{0,m-1}^{u}\overline{\psi}_{m-1}^{(2)}(k_x)+\sum_j\int \mathrm{d}k_x'\tilde{\overline{\overline{S}}}_{m-1}^{u(1)}(k_x,k_x')\overline{\psi}_{m-1,j}^{(1)}(k_x')F_{m-1}(k_x-k_x')F_j(k_x'-k_{ix}) \\ &\qquad+\tilde{\overline{\overline{S}}}_{m-1}^{u(2)}(k_x,k_{ix})F_{m-1}^{(2)}(k_x-k_{ix})\overline{\psi}_{m-1}^{(0)} \\ &=\overline{\overline{G}}_{0,m}^{d}\overline{\psi}_m^{(2)}(k_x)+\sum_j\int \mathrm{d}k_x'\tilde{\overline{\overline{S}}}_m^{d(1)}(k_x,k_x')\overline{\psi}_{m,j}^{(1)}(k_x')F_m(k_x-k_x')F_j(k_x'-k_{ix}) \\ &\qquad+\tilde{\overline{\overline{S}}}_m^{d(2)}(k_x,k_{ix})F_m^{(2)}(k_x-k_{ix})\overline{\psi}_m^{(0)} \end{aligned} \tag{2.3.22}$$

Upon taking statistical average, the second order surface fields become simplified for further derivations. Using the second spectral moments of the surface profiles [57] as

$$\begin{aligned}\langle F_j^{(2)}(k_x-k_{ix})\rangle&=\delta(k_x-k_{ix})\int \mathrm{d}k_x' W_j(k_x'-k_{ix})\\ \langle F_j(k_x-k_x')F_j(k_x'-k_{ix})\rangle&=\delta(k_x-k_{ix})W_j(k_x'-k_{ix})\end{aligned} \tag{2.3.23}$$

and assuming uncorrelated surfaces $\langle F_j(k_x-k_x')F_j(k_x'-k_{ix})\rangle=0$ we arrive at

$$\begin{aligned}&\overline{\overline{G}}_{0,m}^{d}\left\langle\overline{\psi}_m^{(2)}(k_x)\right\rangle+\int \mathrm{d}k_x'\overline{\overline{\tilde{S}}}_m^{d(1)}(k_x,k_x')\overline{\psi}_{m,m}^{(1)}(k_x')\delta(k_x-k_{ix})W_m(k_x'-k_{ix})\\ &\qquad+\overline{\overline{\tilde{S}}}_m^{d(2)}(k_x,k_{ix})\overline{\psi}_m^{(0)}\delta(k_x-k_{ix})\int \mathrm{d}k_x' W(k_x'-k_{ix})\\ =&\overline{\overline{G}}_{0,m-1}^{u}\left\langle\overline{\psi}_{m-1}^{(2)}(k_x)\right\rangle+\delta(k_x-k_{ix})\int \mathrm{d}k_x'\overline{\overline{\tilde{S}}}_{m-1}^{u(1)}(k_x,k_x')\overline{\psi}_{m-1,m-1}^{(1)}(k_x')W_{m-1}(k_x'-k_{ix})\\ &\qquad+\overline{\overline{\tilde{S}}}_{m-1}^{u(2)}(k_x,k_{ix})\overline{\psi}_{m-1}^{(0)}\delta(k_x-k_{ix})\int \mathrm{d}k_x' W_{m-1}(k_x'-k_{ix})\end{aligned} \tag{2.3.24}$$

This is a recursive relation that relates the surface field on the neighbor interfaces that can be written as

$$\left\langle\overline{\psi}_m^{(2)}\right\rangle=\overline{\overline{G}}_m^{(2)}\left\langle\overline{\psi}_{m-1}^{(2)}\right\rangle+\overline{D}_{m-1}^{u}+\overline{D}_m^{d} \tag{2.3.25}$$

where the vector and dyadic quantities $\overline{D}_m^d$, $\overline{D}_{m-1}^u$, and $\overline{\overline{G}}_m^{(2)}$ are defined as

$$\begin{aligned}\overline{\overline{G}}_m^{(2)}&=\left[\overline{\overline{G}}_{0,m}^{d}\right]^{-1}\overline{\overline{G}}_{0,m-1}^{u}\\ \overline{D}_m^d&=-\delta(k_x-k_{ix})\left[\overline{\overline{G}}_{0,m}^{d}\right]^{-1}\int \mathrm{d}k_x'\left\{\overline{\overline{\tilde{S}}}_m^{d(1)}\overline{\psi}_{m,m}^{(1)}(k_x')+\overline{\overline{\tilde{S}}}_m^{d(2)}\overline{\psi}_m^{(0)}\right\}W_m(k_x'-k_{ix})\\ \overline{D}_{m-1}^u&=\delta(k_x-k_{ix})\left[\overline{\overline{G}}_{0,m}^{d}\right]^{-1}\int \mathrm{d}k_x'\left\{\overline{\overline{\tilde{S}}}_{m-1}^{u(1)}\overline{\psi}_{m-1,m-1}^{(1)}(k_x')+\overline{\overline{\tilde{S}}}_{m-1}^{u(2)}\overline{\psi}_{m-1}^{(0)}\right\}W_{m-1}(k_x'-k_{ix})\end{aligned} \tag{2.3.26}$$

The averaged second order surface fields on the last boundary $\left\langle\overline{\psi}_{N-1}^{(2)}\right\rangle$ can be written in terms of that of first boundary using the recursive relation (2.3.26), similar to the procedure

used in the first order solution,

$$\begin{aligned}\left\langle\overline{\psi}_{N-1}^{(2)}\right\rangle=&\overline{\overline{G}}_{N-1}^{(2)}\overline{\overline{G}}_{N-2}^{(2)}\cdots\overline{\overline{G}}_{1}^{(2)}\left\langle\overline{\psi}_{0}^{(2)}\right\rangle\\&+\overline{\overline{G}}_{N-1}^{(2)}\overline{\overline{G}}_{N-2}^{(2)}\cdots\overline{\overline{G}}_{2}^{(2)}\overline{D}_{0}^{u}F_0\\&+\overline{\overline{G}}_{N-1}^{(2)}\overline{\overline{G}}_{N-2}^{(2)}\cdots\overline{\overline{G}}_{3}^{(2)}\left[\overline{\overline{G}}_{2}^{(2)}\overline{D}_{1}^{d}+\overline{D}_{1}^{u}\right]\\&+\overline{\overline{G}}_{N-1}^{(2)}\overline{\overline{G}}_{N-2}^{(2)}\cdots\overline{\overline{G}}_{4}^{(2)}\left[\overline{\overline{G}}_{3}^{(2)}\overline{D}_{2}^{d}+\overline{D}_{2}^{u}\right]\\&\vdots\\&+\overline{\overline{G}}_{N-1}^{(2)}\left[\overline{\overline{G}}_{N-2}^{(2)}\overline{D}_{N-3}^{d}+\overline{D}_{N-3}^{u}\right]\\&+\left[\overline{\overline{G}}_{N-1}^{(2)}\overline{D}_{N-2}^{d}+\overline{D}_{N-2}^{u}\right]\\&+\overline{D}_{N-1}^{d}\\&:=\overline{\overline{G}}^{(2)}\overline{\psi}_{0}^{(2)}+\sum\overline{D}_{j}^{(2)}\end{aligned}\tag{2.3.27}$$

where the overall zeroth order propagator from the first to the last boundary is defined as

$$\overline{\overline{G}}^{(2)}=\overline{\overline{G}}_{N-1}^{(2)}\overline{\overline{G}}_{N-2}^{(2)}\cdots\overline{\overline{G}}_{1}^{(2)}\tag{2.3.28}$$

Now that we have a relation between the first and last surface fields, using the exterior equations we can derive another relation between the first and last region surface fields. From the second order approximation of the exterior field integral equation,

$$\overline{\overline{G}}_{0,E}(k_x)\overline{\psi}_{E}^{(2)}(k_x)+\overline{\overline{S}}_{E}^{(2)}(k_x,k_{ix})\overline{\psi}_{E}^{(0)}+\int\mathrm{d}k_x'\overline{\overline{S}}_{E}^{(1)}(k_x,k_x')\overline{\psi}_{E}^{(1)}(k_x')=0\tag{2.3.29}$$

Here the second order perturbation of scattering operator becomes

$$\overline{\overline{S}}_{E}^{(2)}(k_x,k_x')=-\frac{1}{2}\begin{bmatrix}\frac{i}{2}k_{1z}F_1^{(2)} & \frac{k_1^2-k_xk_x'}{2}F_1^{(2)} & 0 & 0\\ 0 & 0 & \gamma_{N-1,N}(k_{Nz}^2F_{N-1}^{(2)}) & ik_{Nz}(k_N^2-k_xk_x')F_{N-1}^{(2)}\end{bmatrix}$$

The second order scattering operator can be decomposed into contribution of the first and last interfaces as,

$$\begin{aligned}\overline{\overline{S}}_{E}^{(2)}(k_x,k_x')=&\overset{\sim}{\overline{\overline{S}}}_{E,0}^{(2)}(k_x,k_x')F_0^{(2)}+\overset{\sim}{\overline{\overline{S}}}_{E,N-1}^{(2)}(k_x,k_x')F_{N-1}^{(2)}\\\overline{\overline{S}}_{E}^{(1)}(k_x,k_x')=&\overset{\sim}{\overline{\overline{S}}}_{E,0}^{(1)}(k_x,k_x')F_0+\overset{\sim}{\overline{\overline{S}}}_{E,N-1}^{(1)}(k_x,k_x')F_{N-1}\end{aligned}\tag{2.3.30}$$

In addition, the first order surface field $\overline{\psi}_{E}^{(1)}$ has two components proportional to the first and the last surface spectrum,

$$\overline{\psi}_{E}^{(1)}=\overline{\psi}_{E,0}^{(1)}F_0+\overline{\psi}_{E,N-1}^{(1)}F_{N-1}\tag{2.3.31}$$

Plugging the first and zeroth order solutions in (2.3.29) we will arrive at

$$\overline{\overline{G}}_{0,E}(k_x)\left\langle\overline{\psi}_{E}^{(2)}\right\rangle=-\delta(k_x-k_{ix})\int\mathrm{d}k_x'\left[W_0(k_x'-k_{ix})\overline{D}_{E,0}^{(2)}+W_{N-1}(k_x'-k_{ix})\overline{D}_{E,N-1}^{(2)}\right]\tag{2.3.32}$$

where,

$$\overline{D}^{(2)}_{E,0}(k'_x)=\overline{\overline{S}}^{(2)}_{E,0}(k_x,k_{ix})\overline{\psi}^{(0)}_{E}+\overline{\overline{S}}^{(1)}_{E,0}(k_{ix},k'_x)\overline{\psi}^{(1)}_{E,0}(k'_x) \tag{2.3.33}$$
$$\overline{D}^{(2)}_{E,N-1}(k'_x)=\overline{\overline{S}}^{(2)}_{E,N-1}(k_x,k_{ix})\overline{\psi}^{(0)}_{E}+\overline{\overline{S}}^{(1)}_{E,N-1}(k_{ix},k'_x)\overline{\psi}^{(1)}_{E,N-1}(k'_x)$$

Now, using general recursive relation of the second order surface field of (2.3.27), it can be rewritten as

$$\left\langle\overline{\psi}^{(2)}_{N-1}\right\rangle-\overline{\overline{G}}^{(2)}\left\langle\overline{\psi}^{(2)}_{0}\right\rangle=\delta(k_x-k_{ix})\sum_j\int \mathrm{d}k'_x W_j(k'_x-k_{ix})\overline{C}^{(2)}_j(k'_x) \tag{2.3.34}$$

The governing system of equation for the averaged second order fields on the first and last surfaces are as follows

$$\begin{bmatrix}\overline{\overline{G}}_{0,E}(k_{ix}) & \\ -\overline{\overline{G}}^{(2)} & \overline{\overline{I}}\end{bmatrix}\left\langle\overline{\psi}^{(2)}_{E}\right\rangle=\delta(k_x-k_{ix})\int \mathrm{d}k'_x\overline{R}(k'_x) \tag{2.3.35}$$

$$\overline{R}(k'_x)=\begin{bmatrix}-W_0(k'_x-k_{ix})\overline{D}^{(2)}_{E,0}-W_{N-1}(k'_x-k_{ix})\overline{D}^{(2)}_{E,N-1}\\ \\ \sum_j\int \mathrm{d}k'_x W_j(k'_x-k_{ix})\overline{C}^{(2)}_j(k'_x)\end{bmatrix} \tag{2.3.36}$$

Presence of the delta function on the right hand side shows that the average second order surface fields are only non-zero in the specular direction.

## 2.4 Scattered and Transmitted Fields

Using the equivalence principle we can find the scattered field into the region 1 as

$$E_s(k_x)=-\frac{i}{2k_{1z}}\left[A_10(k_x)+ik_{1z}B_1(k_x)+\int \mathrm{d}k'_x I^{+}_{11}(k_x,k'_x)\left\{A_1(k'_x)+B_1(k'_x)i\frac{k_1^2-k_xk'_x}{k_{1z}}\right\}\right] \tag{2.4.1}$$

where the scattering potential for the upward propagating scattered field is defined through,

$$I^{+}_{11}(k_x,k'_x)=\frac{1}{2\pi}\int \mathrm{d}x' e^{-i(k_x-k'_x)x'}\left[e^{-ik_{1z}f_1(x')}-1\right] \tag{2.4.2}$$

and the transmitted field into region $N$ can be found by the equivalence principle to the last half space that results in

$$E_t(k_x)=\frac{i}{2k_{Nz}}e^{-ik_{Nz}d_{N-1}}\left[\gamma_{N-1,N}A_{N-1}(k_x)-ik_{Nz}B_{N-1}(k_x)\right. \tag{2.4.3}$$
$$\left.+\int \mathrm{d}k'_x I^{-}_{N,N-1}(k_x,k'_x)\left\{\gamma_{N-1,N}A_{N-1}(k'_x)-B_{N-1}(k'_x)i\frac{k_N^2-k_xk'_x}{k_{Nz}}\right\}\right]$$

with relevant scattering potential of

$$I^{-}_{N,N-1}(k_x,k'_x)=\frac{1}{2\pi}\int \mathrm{d}x' e^{-i(k_x-k'_x)x'}\left[e^{+ik_{Nz}f_{N-1}(x')}-1\right]. \tag{2.4.4}$$

Upon defining the scattered field vector $\overline{\psi}_s$ as

$$\overline{\psi}_s(k_x)=\begin{bmatrix}E_s(k_x)\\E_t(k_x)\end{bmatrix} \tag{2.4.5}$$

The scattered field can be written in terms of the external surface field vector $\overline{\psi}_E$ as

$$\overline{\psi}_s(k_x)=\overline{\overline{G}}^0_s(k_x)\overline{\psi}_E(k_x)+\int \mathrm{d}k'_x\ \overline{\overline{S}}_s(k_x,k'_x)\overline{\psi}_E(k'_x) \tag{2.4.6}$$

where $\overline{\overline{G}}^0_s(k_x)$ is the flat surface propagator of the scattered field

$$\overline{\overline{G}}^0_s(k_x)=\begin{bmatrix}-\frac{i}{2k_{1z}} & \frac{1}{2} & 0 & 0\\ 0 & 0 & \frac{i}{2k_{Nz}}e^{-ik_{Nz}d_{N-1}}\gamma_{N-1,N} & \frac{1}{2}e^{-ik_{Nz}d_{N-1}}\end{bmatrix} \tag{2.4.7}$$

and $\overline{\overline{S}}_s(k_x,k'_x)$ is the proper scattering operator of the scattered field defined by,

$$\overline{\overline{S}}_s=\begin{bmatrix}-\frac{i}{2k_{1z}}I^{+}_{11} & \frac{k_1^2-k_xk'_x}{2k_{1z}^2}I^{+}_{00} & 0 & 0\\ 0 & 0 & \frac{i}{2k_{Nz}}e^{-ik_{Nz}d_{N-1}}\gamma_{N-1,N}I^{-}_{N,N-1} & e^{-ik_{Nz}d_{N-1}}\frac{k_N^2-k_xk'_x}{2k_{Nz}^2}I^{-}_{N,N-1}\end{bmatrix} \tag{2.4.8}$$

### 2.4.1 Zeroth order scattered field

Balancing (2.4.6) up to the zeroth order of the surface roughness yields,

$$\overline{\psi}^{(0)}_s(k_x)=\delta(k_x-k_{ix})\overline{\overline{G}}^0_s(k_{ix})\overline{\psi}^{(0)}_E \tag{2.4.9}$$

Notice that no inversion operation is involved in calculation of the scattered fields.

### 2.4.2 First Order Scattered Field

Collecting the terms f order one in (2.4.6) and using the first order solution of the surface fields, results in

$$\overline{\psi}^{(1)}_s(k_x)=\overline{\overline{G}}^0_s(k_x)\overline{\psi}^{(1)}_E(k_x)+\overline{\overline{S}}^{(1)}_s(k_x,k_{ix})\overline{\psi}^{(0)}_E \tag{2.4.10}$$

In addition, the first order external surface fields can be expanded in terms of contributions of individual interfaces as

$$\overline{\psi}^{(1)}_E(k_x)=\sum\overline{\psi}^{(1)}_{E,j}(k_x)F_j(k_x-k_{ix}) \tag{2.4.11}$$

On the other side the scattering operator of the first order can be decomposed into the first and the last interfaces contributions,

$$\overline{\overline{S}}^{(1)}_s(k_x,k_{ix})=\overline{\overline{S}}^{(1)}_{s,1}(k_x,k_{ix})F_1(k_x-k_{ix})+\overline{\overline{S}}^{(1)}_{s,N-1}(k_x,k_{ix})F_{N-1}(k_x-k_{ix}) \tag{2.4.12}$$

Separating different surface spectrum contributions gives

$$\begin{aligned}\overline{\psi}_s^{(1)}(k_x)=&\left[\overline{\overline{G}}_s^0(k_x)\overline{\psi}_{E,1}^{(1)}(k_x)+\overline{\overline{S}}_{s,1}^{(1)}(k_x,k_{ix})\overline{\psi}_E^{(0)}\right]F_1\\&+\left[\overline{\overline{G}}_s^0(k_x)\overline{\psi}_{E,N-1}^{(1)}(k_x)+\overline{\overline{S}}_{s,N-1}^{(1)}(k_x,k_{ix})\overline{\psi}_E^{(0)}\right]F_{N-1}\\&+\sum_{j\neq 1,N-1}\overline{\overline{G}}_s^0(k_x)\overline{\psi}_{E,j}^{(1)}(k_x)F_j(k_x-k_{ix})\end{aligned}\tag{2.4.13}$$

where,

$$\overline{\overline{S}}_{s,1}^{(1)}(k_x,k_{ix})=\begin{bmatrix}-\frac{1}{2} & -i\frac{k_1^2-k_xk_{ix}}{2k_{1z}} & 0 & 0\\ 0 & 0 & 0 & 0\end{bmatrix}\tag{2.4.14}$$

$$\overline{\overline{S}}_{s,N-1}^{(1)}(k_x,k_{ix})=\begin{bmatrix}0 & 0 & 0 & 0\\ 0 & 0 & -\frac{1}{2}e^{-ik_{Nz}d_{N-1}}\gamma_{N-1,N} & e^{-ik_{Nz}d_{N-1}}i\frac{k_N^2-k_xk_{ix}}{2k_{Nz}}\end{bmatrix}\tag{2.4.15}$$

### 2.4.3 Second Order Scattered Field

Balancing (2.4.6) up to the second order of the surface roughness and substituting the zeroth and first order surface fields gives,

$$\begin{aligned}\overline{\psi}_s^{(2)}(k_x)=&\overline{\overline{G}}_s^0(k_x)\overline{\psi}_E^{(2)}(k_x)+\overline{\overline{\tilde{S}}}_{s,1}^{(2)}(k_x,k_{ix})\overline{\psi}_E^{(0)}F_1^{(2)}+\overline{\overline{\tilde{S}}}_{s,N-1}^{(2)}(k_x,k_{ix})\overline{\psi}_E^{(0)}F_{N-1}^{(2)}\\&+\sum_{i=1,N-1;j}\int \mathrm{d}k_x'\ \overline{\overline{\tilde{S}}}_{s,i}^{(1)}(k_x,k_x')F_i(k_x-k_x')\overline{\psi}_{E,j}^{(1)}(k_x')F_j(k_x'-k_{ix})\end{aligned}\tag{2.4.16}$$

Upon taking the statistical average and assuming uncorrelated surfaces

$$\begin{aligned}\left\langle\overline{\psi}_s^{(2)}\right\rangle=&\overline{\overline{G}}_s^0(k_x)\left\langle\overline{\psi}_E^{(2)}\right\rangle+\delta(k_x-k_{ix})\left[\overline{\overline{\tilde{S}}}_{s,1}^{(2)}(k_x,k_{ix})\overline{\psi}_E^{(0)}\int \mathrm{d}k_x'W_1(k_x'-k_{ix})\right.\\&+\overline{\overline{\tilde{S}}}_{s,N-1}^{(2)}(k_x,k_{ix})\overline{\psi}_E^{(0)}\int \mathrm{d}k_x'W_{N-1}(k_x'-k_{ix})\\&+\int \mathrm{d}k_x'\ \overline{\overline{\tilde{S}}}_{s,1}^{(1)}(k_x,k_x')\overline{\psi}_{E,1}^{(1)}(k_x')W_1(k_x'-k_{ix})\\&\left.+\int \mathrm{d}k_x'\ \overline{\overline{\tilde{S}}}_{s,N-1}^{(1)}(k_x,k_x')\overline{\psi}_{E,N-1}^{(1)}(k_x')W_{N-1}(k_x'-k_{ix})\right]\end{aligned}\tag{2.4.17}$$

Utilizing averaged second order surface field expression as

$$\left\langle\overline{\psi}_E^{(2)}\right\rangle=\delta(k_x-k_{ix})\sum_j\int \mathrm{d}k_x'\overline{\psi}_{E,j}^{(2)}(k_x')W_j(k_x'-k_{ix})\tag{2.4.18}$$

the second order scattered field in spectral domain can be obtained as

$$\begin{aligned}\left\langle\overline{\psi}_s^{(2)}\right\rangle=&\delta(k_x-k_{ix})\int \mathrm{d}k_x'\left[\sum_{j\neq 0,N-1}\overline{\overline{G}}_s^0(k_x)\overline{\psi}_{E,j}^{(2)}(k_x')W_j(k_x'-k_{ix})\right.\\&+\left\{\overline{\overline{\tilde{S}}}_{s,1}^{(2)}(k_x,k_{ix})\overline{\psi}_E^{(0)}+\overline{\overline{\tilde{S}}}_{s,1}^{(1)}(k_x,k_x')\overline{\psi}_{E,1}^{(1)}(k_x')+\overline{\overline{G}}_s^0(k_x)\overline{\psi}_{E,1}^{(2)}(k_x')\right\}W_1\\&\left.+\left\{\overline{\overline{\tilde{S}}}_{s,N-1}^{(2)}(k_x,k_{ix})\overline{\psi}_E^{(0)}+\overline{\overline{\tilde{S}}}_{s,N-1}^{(1)}(k_x,k_x')\overline{\psi}_{E,N-1}^{(1)}(k_x')+\overline{\overline{G}}_s^0(k_x)\overline{\psi}_{E,N-1}^{(2)}(k_x')\right\}W_{N-1}\right]\end{aligned}\tag{2.4.19}$$

## 2.5 Scattered and Transmitted Power

The scattered field in spatial coordinate can be obtained from the spectral representation through,

$$\psi_s(\overline{r}) = \int \mathrm{d}k_x \psi_s(k_x) e^{ik_x x + ik_{1z} z} \tag{2.5.1}$$

and for different orders of the scattered field we have

$$\begin{aligned} \psi_s^{(0)}(\overline{r}) &= \psi_s^{(0)}(k_{ix}) e^{ik_{ix} + ik_{iz} z} \\ \psi_s^{(1)}(\overline{r}) &= \sum_j \int \mathrm{d}k_x e^{ik_x x + ik_{1z} z} \psi_{s,j}^{(1)}(k_x) F_j(k_x - k_{ix}) \\ \langle \psi_s^{(2)}(\overline{r}) \rangle &= e^{ik_{ix} + ik_{iz}} \sum_j \int \mathrm{d}k_x' \langle \psi_s^{(2)} \rangle_j W_j(k_x' - k_{ix}) \end{aligned} \tag{2.5.2}$$

Here $\psi_s = E_{sy}$. The scattered power density can be expressed in terms of pilot electric field $E_{sy}$ as

$$\langle \overline{S}_s \cdot \hat{z} \rangle = -\frac{1}{2} \mathrm{Im} \left[ \frac{1}{k\eta} E_{sy} \left( \hat{z} \cdot \nabla E_{sy}^* \right) \right] = -\frac{1}{2} \mathrm{Im} \left[ \frac{1}{k\eta} \left\langle E_{sy} \frac{\partial E_{sy}^*}{\partial z} \right\rangle \right] \tag{2.5.3}$$

The zeroth and second oder scattered field are coherent. Therefore the coherent power consists of

$$\begin{aligned} \langle \overline{S}_s \cdot \hat{z} \rangle_{\mathrm{coh}} &= -\frac{1}{2} \mathrm{Im} \left[ \frac{1}{k\eta} \left\langle E_{sy}^{(0)} \frac{\partial E_{sy}^{(0)*}}{\partial z} + E_{sy}^{(0)} \frac{\partial E_{sy}^{(2)*}}{\partial z} + E_{sy}^{(2)} \frac{\partial E_{sy}^{(0)*}}{\partial z} \right\rangle \right] \\ &= \frac{1}{2} \mathrm{Re} \left[ \frac{k_{iz}}{k\eta} \left\langle E_{sy}^{(0)} \partial E_{sy}^{(0)*} + E_{sy}^{(0)} E_{sy}^{(2)*} + E_{sy}^{(2)} E_{sy}^{(0)*} \right\rangle \right] \\ &= \frac{1}{2} \mathrm{Re} \left[ \frac{k_{iz}}{k\eta} \left( |E_{sy}^{(0)}|^2 + 2 \langle E_{sy}^{(2)} \rangle E_{sy}^{(0)*} \right) \right] \end{aligned} \tag{2.5.4}$$

The coherent power can be decomposed into the zeroth order and second order as

$$\begin{aligned} \langle \overline{S}_s \cdot \hat{z} \rangle_{\mathrm{coh}}^{(0)} &= \frac{1}{2} \mathrm{Re} \left[ \frac{k_{iz}}{k\eta} |E_{sy}^{(0)}|^2 \right] \\ \langle \overline{S}_s \cdot \hat{z} \rangle_{\mathrm{coh}}^{(2)} &= \mathrm{Re} \left[ \frac{k_{iz}}{k\eta} \langle E_{sy}^{(2)} \rangle E_{sy}^{(0)*} \right] \end{aligned} \tag{2.5.5}$$

The zeroth order is that of flat interfaces and the second order is given by

$$\langle \overline{S}_s \cdot \hat{z} \rangle_{\mathrm{coh}}^{(2)} = \sum_j \int \mathrm{d}k_x' \mathrm{Re} \left[ \frac{k_{iz}}{k\eta} \psi_s^{(0)*}(k_{ix}) \langle \psi_s^{(2)} \rangle_j W_j(k_x' - k_{ix}) \right] \tag{2.5.6}$$

On the order hand, the incoherent power originates from the first order scattered field (which has zero coherence) that can be computed as

$$\begin{aligned} \langle \overline{S}_s \cdot \hat{z} \rangle_{\mathrm{incoh}} &= -\frac{1}{2} \mathrm{Im} \left[ \frac{1}{k\eta} \left\langle E_{sy}^{(1)} \frac{\partial E_{sy}^{(1)*}}{\partial z} \right\rangle \right] = \frac{1}{2} \mathrm{Re} \left[ \frac{k_z}{k\eta} \left\langle E_{sy}^{(1)} E_{sy}^{(1)*} \right\rangle \right] \\ &= \frac{1}{2k\eta} \mathrm{Re}(k_z) \sum_j \int \mathrm{d}k_x |\psi_{s,j}^{(1)}(k_x)|^2 W_j(k_x - k_{ix}) \end{aligned} \tag{2.5.7}$$

The Transmitted power can be computed in a similar way. The final results are given below. Note that the last region can be lossy (as opposed to the first region with usually is considered to be vacuum). For coherent transmitted power density,

$$\langle \overline{S}_t \cdot (-\hat{z}) \rangle_{\rm coh}^{(0)} = \frac{1}{2} {\rm Re}\left[ \frac{k_{Niz}}{k_N \eta_N} |E_{ty}^{(0)}|^2 \right] \tag{2.5.8}$$

$$\langle \overline{S}_t \cdot (-\hat{z}) \rangle_{\rm coh}^{(2)} = {\rm Re}\left[ \frac{k_{Niz}}{k_N \eta_N} \langle E_{ty}^{(2)} \rangle E_{ty}^{(0)*} \right]$$

$$\langle \overline{S}_t \cdot \hat{z} \rangle_{\rm coh}^{(2)} = \sum_j \int {\rm d}k_x' {\rm Re}\left[ \frac{k_{Niz}}{k_N \eta_N} \psi_t^{(0)*}(k_{ix}) \langle \psi_t^{(2)} \rangle_j W_j(k_x' - k_{ix}) \right]$$

and the incoherent power density is given by

$$\langle \overline{S}_t \cdot (-\hat{z}) \rangle_{\rm incoh} = \frac{1}{2k_N \eta_N} {\rm Re}(k_{Nz}) \sum_j \int {\rm d}k_x |\psi_{t,j}^{(1)}(k_x)|^2 W_j(k_x - k_{ix}) \tag{2.5.9}$$

## 2.6 Strong Statement of Energy Conservation

For a lossless media, energy conservation mandates that total scattered and transmitted power balance up the incident power to the structure. This is always the case for the exact solution of the Maxwell's equations. However, for an approximate solution of the problem, it is not clear that approximate solution respects the energy conservation. One may verify this by considering a special spectral density $W_j(k_x)$ for the rough interfaces and calculate the different components of the scattered and transmitted powers. The power conservation is critical in computation of the emissivity of the surface as computation of the scattered field is easier than taking care of the transmitted and lost power within the media.

It can be shown that the SPM2 provides an approximate solution that always satisfies the energy conservation criteria, irrespective of the surface statistics [24]. Even when the approximations that are made in SPM perturbation solution are not valid, the SPM2 solution respects energy conservation. The zeroth order solution is exact solution of the same problem with flat interfaces. Therefore, the zeroth order scattered and transmitted power balance up the incident power. The remaining power terms, including the coherent and incoherent scattered and transmitted powers should sum up to zero. Therefore, energy is conserved within the solution if

$$\langle \overline{S}_t \cdot (-\hat{z}) \rangle_{\rm incoh} + \langle \overline{S}_t \cdot (-\hat{z}) \rangle_{\rm coh}^{(2)} + \langle \overline{S}_s \cdot (\hat{z}) \rangle_{\rm incoh} + \langle \overline{S}_s \cdot (\hat{z}) \rangle_{\rm coh}^{(2)} = 0 \tag{2.6.1}$$

All of the power density terms are in terms of spectral integral of a spectral function times spectral density of the surfaces. If we define the power spectral coefficients $\mathcal{S}_{sj,tj}^{\rm coh/incoh}$ of the

$j$-th surface such that

$$\langle \overline{S}_t \cdot (-\hat{z}) \rangle_{\text{incoh}} = \sum_j \int \mathrm{d}k_x \; \mathcal{S}_{tj}^{\text{incoh}}(k_x) W_j(k_x - k_{ix}) \tag{2.6.2}$$

$$\langle \overline{S}_t \cdot (-\hat{z}) \rangle_{\text{coh}} = \sum_j \int \mathrm{d}k_x \; \mathcal{S}_{tj}^{\text{coh}}(k_x) W_j(k_x - k_{ix})$$

$$\langle \overline{S}_s \cdot (\hat{z}) \rangle_{\text{incoh}} = \sum_j \int \mathrm{d}k_x \; \mathcal{S}_{sj}^{\text{incoh}}(k_x) W_j(k_x - k_{ix})$$

$$\langle \overline{S}_s \cdot (\hat{z}) \rangle_{\text{coh}} = \sum_j \int \mathrm{d}k_x \; \mathcal{S}_{sj}^{\text{coh}}(k_x) W_j(k_x - k_{ix})$$

Then, the energy conservation can be achieved if

$$\sum_j \int \mathrm{d}k_x \; W_j(k_x - k_{ix}) \Big[ \mathcal{S}_{tj}^{\text{incoh}}(k_x) + \mathcal{S}_{tj}^{\text{coh}}(k_x) + \mathcal{S}_{sj}^{\text{incoh}}(k_x) + \mathcal{S}_{sj}^{\text{coh}}(k_x) \Big] = 0 \tag{2.6.3}$$

Since the spectral density of the surface can be selected arbitrarily, the energy conservation is satisfied if the integrand identically vanishes

$$\mathcal{S}_{tj}^{\text{incoh}}(k_x) + \mathcal{S}_{tj}^{\text{coh}}(k_x) + \mathcal{S}_{sj}^{\text{incoh}}(k_x) + \mathcal{S}_{sj}^{\text{coh}}(k_x) = 0 \quad , \quad \forall k_x \in \mathbb{R}, j = 1,2,\cdots,N-1 \tag{2.6.4}$$

at all of the spectral points and for individual interface index $j$. We will show that for the SPM2 solution, (2.6.4) is true at all spectral points and for all surfaces (two interfaces here) that translate to energy conservation irrespective of the statistical shape of the interface (even when surface parameters do not meet SPM2 criteria, for example, large height). Consider a dielectric layered media of Fig.[] with dielectric constant of $\varepsilon_r = [1, 1.5, 2.8, 3.5, 4.3]$ from the top (the top medium is vacuum) to the bottom and mean position of rough interfaces at $d = [0, .5, 0.8, 1.6]\lambda$. The structure is illuminated with a TE polarized wave with $\theta_i = 40^\circ$ with the wave length of $\lambda$. Figure. 2.2 plots the power spectral coefficients of the all rough interfaces (with unit of $\mathrm{W/m^4}$) versus the normalized spectral variable $k_x/k = k_x\lambda/2\pi$. Summation of all power spectral coefficients is identical to zero (up to the machine precision) for individual interfaces which is plotted with dashed black line. This shows that the SPM2 solution always satisfies the energy conservation irrespective of the surface roughness statistics.

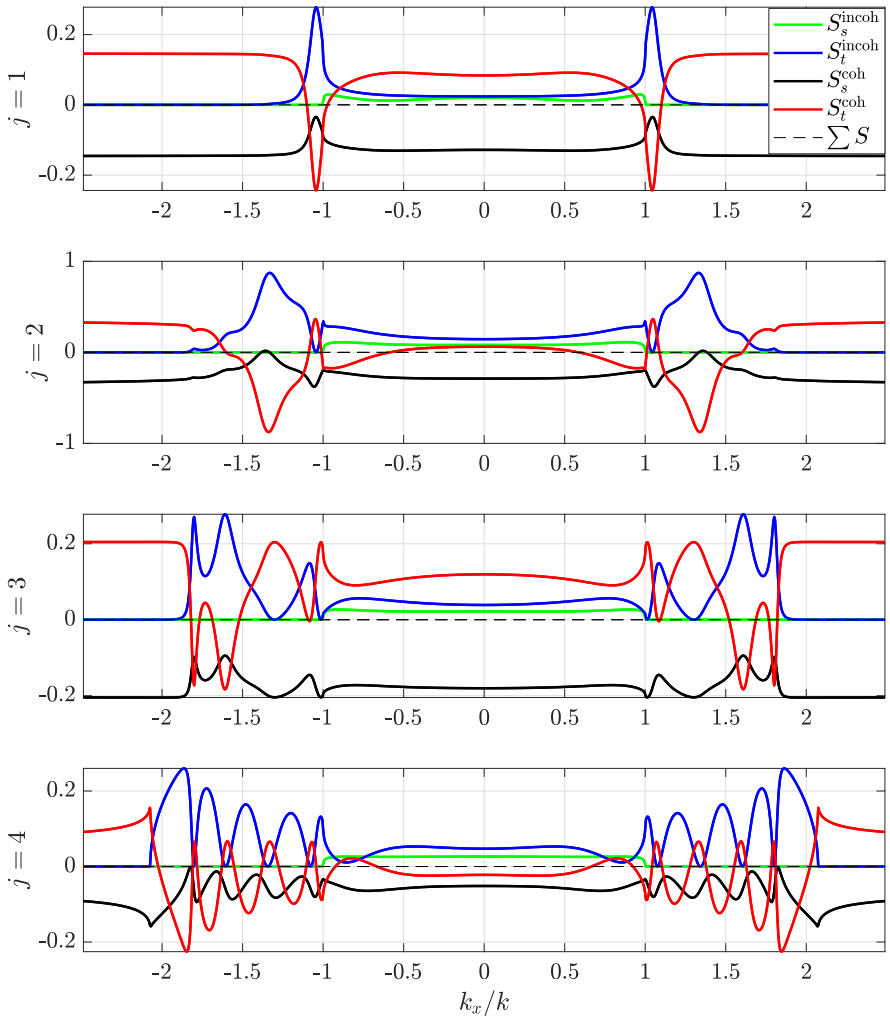


FIGURE 2.2: Coherent and incoherent power spectral coefficients of the all interfaces ($j$=1,$\cdots$,4) (with unit of W/m$^4$) for a TE plane wave incidence along $\theta_i$=40° on a 2D dielectric rough interface with dielectric constant of $\varepsilon_r$=[1,1.5,2.8,3.5,4.3] from the top (top medium is vacuum) and mean rough interfaces position of $d$=[0,.5,0.8,1.6]$\lambda$.

# Chapter 3

# 2D scattering From Dielectric Layered Media with Periodic Interfaces, $T$-matrix Approach

## 3.1 Introduction

The solution is based on the integral equation with periodic Green's function as he kernel of the integral equation [56, 58–60]. However, in contrast to the usual surface integral equation that is mapped on the boundary surface itself [61–63], the integral equation is mapped on another surface which completely include the scatterer. This extension of boundaries originates in the fact that the spectral expansion of the Green's function can be used if the source and observation positions are globally differentiated (source position always lower or upper than the observation point). Mapping the integral equation on this surface with is extended beyond the actual surface is called *Extended Boundary Condition Method* [54, 55, 62]. Once we consider this, it naturally results in the presence of only upward going waves on top of the surface. This is the same as considering the upward propagating waves in the expansion of the scattered field. This assumption that neglect downward propagating waves on top of the surface is known as *Rayleigh Hypothesis*. So the Rayleigh Hypothesis is essentially the same as extended boundary condition method [53]. The Rayleigh hypothesis is a good approximation for the surfaces without shadow area. Generally, it is valid when the surface slop does not exceed certain value [64]. If the average slope is such that some downward going modes should be present in the scattered field expansion, i.e. the included modes are not enough to correctly represent the scattered field. If one wants to somehow compensate lake of shadow modes by increasing the number of included modes, nothing will be added to the response. The coefficients of the additional modes would be around zero and the problem becomes ill-conditioned.

## 3.2 Bloch Theorem for 2D Periodic Surfaces

Assume a 2D periodic surface that is uniform along $y$ direction and variation along $x$ is described by a periodic function $z=f(x)$ with period $L$ such that

$$f(x+L)=f(x) \tag{3.2.1}$$

Consider a plane wave with unit amplitude $\overline{E}_i(\overline{r})=\hat{e}_i e^{i\overline{k}_i\cdot\overline{r}}$ that is impinging upon the periodic surface from the top, where $\hat{e}_i$ is the polarization of the incident field and

$$\overline{k}_i=k_{ix}\hat{x}+k_{iy}\hat{y}-k_{iz}\hat{z} \tag{3.2.2}$$

is the incident wave vector. Since the periodic surface is uniform along $y$ direction, all field quantities have dependence of $e^{ik_{iy}y}$ by setting $\partial/\partial y=ik_{iy}$ in the Maxwell's equations. In order to see why all field quantities have such a dependence, consider a plane wave that is propagating along the uniform direction of the surface which is $y$ direction. Then, due to the continuity of the tangential component of the wave vector, wave in both regions (top and bottom of surface) have the same wave vectors which shows that $e^{ik_{iy}y}$ is conserved for both scattered field and transmitted field (and also for surface fields).

Therefore, without loss of generality, assume that the incident plane wave is propagating in $x-z$ plane with wave vector $\overline{k}_i=k_{ix}\hat{x}-k_{iz}\hat{z}$. Also for TE problem assume that the incident electric field polarization is along $y$ direction. With this assumption we only have $y$- directed electric field in the medium as there is no depolarization for electric field since electric field does not cross the corrugations. Thus, in each medium $\overline{E}=E_y\hat{y}$ should satisfies the 2D wave equation of

$$\left(\frac{\partial^2}{\partial x^2}+\frac{\partial^2}{\partial z^2}\right)E_y+k^2E_y=0 \tag{3.2.3}$$

In order to solve for Eq. (3.2.3) corresponding free space Green's function can be introduced by

$$\left(\frac{\partial^2}{\partial x^2}+\frac{\partial^2}{\partial z^2}\right)g(x,z;x',z')+k^2g(x,z;x',z')=-\delta(x-x')\delta(z-z') \tag{3.2.4}$$

subject to the Sommerfeld radiation condition at infinity. The differential equation of (3.2.4) can be integrated in the cylindrical coordinate in a closed form to obtain

$$g(\overline{\rho},\overline{\rho}')=\frac{i}{4}H_0^{(1)}(k|\overline{\rho}-\overline{\rho}'|) \tag{3.2.5}$$

where $\overline{\rho}=x\hat{x}+z\hat{z}$. Alternatively, (3.2.4) can be solved in Cartesian coordinate by applying one Fourier transform over $x$ dimension to obtain the spectral expansion of

$$g(\overline{\rho},\overline{\rho}')=\frac{i}{4\pi}\int \mathrm{d}k_x\,\frac{1}{k_z}e^{ik_x(x-x')+ik_z|z-z'|} \tag{3.2.6}$$

Applying 2D Green's second identity results in,

$$\oint_{\partial S}\mathrm{d}l\hat{n}\cdot\Big(g(\overline{\rho},\overline{\rho}')\nabla E_y(\overline{\rho})-E_y(\overline{\rho})\nabla g(\overline{\rho},\overline{\rho}')\Big)=\begin{cases}E_y(\overline{\rho}') & \overline{\rho}'\in S\\ 0 & \overline{\rho}'\notin S\end{cases} \tag{3.2.7}$$

Here $\hat{n}$ is a unit normal pointing outward from the region $S$. Now take the region $S$ to be the half space defined by $z>f(x)$. Upon reversing direction of the unit normal as $\hat{n}\to-\hat{n}$ (points into region $S$) and swapping the primed and unprimed coordinates it yields

$$-\oint_{\partial S}\mathrm{d}l'\hat{n}'\cdot\Big(g(\overline{\rho},\overline{\rho}')\nabla' E_y(\overline{\rho}')-E_y(\overline{\rho}')\nabla' g(\overline{\rho},\overline{\rho}')\Big)=\begin{cases}E_y(\overline{\rho}) & \overline{\rho}\in S\\ 0 & \overline{\rho}\notin S\end{cases} \tag{3.2.8}$$

This is the statement of the Extinction theorem for scalar wave $E_y(\overline{\rho})$. The boundary integral over $\partial S$ consists of two part. One segment is the integral over the boundary surface $z=f(x)$ and another integral is over a large closing path at infinity $C_\infty$,

$$-\left[\int_{z=f(x)}+\int_{C_\infty}\right]\mathrm{d}l'\hat{n}'\cdot\Big(g(\overline{\rho},\overline{\rho}')\nabla' E_y(\overline{\rho}')-E_y(\overline{\rho}')\nabla' g(\overline{\rho},\overline{\rho}')\Big)=\begin{cases}E_y(\overline{\rho}) & \overline{\rho}\in S\\ 0 & \overline{\rho}\notin S\end{cases} \tag{3.2.9}$$

Now for a moment assume that there is no scatterer and everywhere is vacuum. The extinction theorem is still valid and the first integral has no contribution. With this assumption, the electric field anywhere is the incident electric field

$$-\int_{C_\infty}\mathrm{d}l'\hat{n}'\cdot\Big(g(\overline{\rho},\overline{\rho}')\nabla' E_y(\overline{\rho}')-E_y(\overline{\rho}')\nabla' g(\overline{\rho},\overline{\rho}')\Big)=E_{iy}(\overline{\rho}) \tag{3.2.10}$$

Therefore, the value of the integral over $C_\infty$ is now determined. Substituting back in the extinction theorem we have

$$E_{iy}(\overline{\rho})-\int_{z=f(x)}\mathrm{d}l'\hat{n}'\cdot\Big(g(\overline{\rho},\overline{\rho}')\nabla' E_y(\overline{\rho}')-E_y(\overline{\rho}')\nabla' g(\overline{\rho},\overline{\rho}')\Big)=\begin{cases}E_y(\overline{\rho}) & ,\overline{\rho}\in S\\ 0 & ,\overline{\rho}\notin S\end{cases} \tag{3.2.11}$$

where $E_{iy}(\overline{\rho})=e^{ik_{ix}x-ik_{iz}z}$. In what follows, a simple proof of the Floquet-Bloch theorem for the periodic surface is derived based on integral equation formalism. Let's restrict the observation point to be on the periodic surface but slightly above it, i.e. $z=f(x)^+$, then

$$E_{iy}(x,z=f(x))-\int_{z'=f(x')}\mathrm{d}l'\hat{n}'\cdot\Big(g(\overline{\rho},\overline{\rho}')\nabla' E_y(\overline{\rho}')-E_y(\overline{\rho}')\nabla' g(\overline{\rho},\overline{\rho}')\Big)=E_y(\overline{\rho}) \tag{3.2.12}$$

Note that the normal length element on the surface is given by $\mathrm{d}l'\hat{n}'=(\hat{z}-f_{x'}\hat{x})\mathrm{d}x'$. Therefore,

$$e^{ik_{ix}x-ik_{iz}f(x)}=E_y(\overline{\rho})+\int_{-\infty}^{\infty}\mathrm{d}x'\Big(\hat{z}-\frac{\mathrm{d}f(x')}{\mathrm{d}x'}\hat{x}\Big)\cdot\Big(g(\overline{\rho},\overline{\rho}')\nabla' E_y(\overline{\rho}')-E_y(\overline{\rho}')\nabla' g(\overline{\rho},\overline{\rho}')\Big) \tag{3.2.13}$$

The notation will be simplified by defining an integro-differential operator $\mathcal{G}$ as

$$\mathcal{G}u(\overline{\rho})=u(\rho)+\int_{-\infty}^{\infty}\mathrm{d}x'\Big(\hat{z}-\frac{\mathrm{d}f(x')}{\mathrm{d}x'}\hat{x}\Big)\cdot\Big(g(\overline{\rho},\overline{\rho}')\nabla' u(\overline{\rho}')-u(\overline{\rho}')\nabla' g(\overline{\rho},\overline{\rho}')\Big) \tag{3.2.14}$$

then

$$e^{ik_{ix}x-ik_{iz}f(x)}=\mathcal{G}E_y(\overline{\rho}) \tag{3.2.15}$$

From the periodicity of $f(x)$, left hand side transforms under $x\to x+L$ as

$$e^{ik_{ix}(x+L)-ik_{iz}f(x+L)}=e^{ik_{ix}(x+L)-ik_{iz}f(x)}=e^{ik_{ix}L}\Big(e^{ik_{ix}x-ik_{iz}f(x)}\Big) \tag{3.2.16}$$

Lets apply the same transformation on the right hand side of (3.2.15) to see what will happen. Since the primed coordinate is a dummy variable we can also let $x'\to x'+L$ as well. However, since Green's function is translational invariant, i.e. $g(x+x_0,y;x'+x_0,y')=g(x,y;x',y')$, $\mathcal{G}$ does not change under the transformation. As a result [65]

$$E_y(x+L,f(x))=e^{ik_{ix}L}E_y(x,f(x)) \tag{3.2.17}$$

Apart from the phase factor, the surface electric field is a periodic function with the same period as the surface. This is the statement of the Floquet-Bloch theorem [66] for the surface fields on a periodic surface.

## 3.3 Integral Equation Formulation

Assume a TE polarized incidence electric field of $\overline{E}_i = \hat{y} e^{i\overline{k}_i \cdot \overline{r}}$ and the polarization vector $\hat{y}$ is parallel to the uniform dimension of the surface. The pilot electric field component satisfies the wave equation of

$$\nabla^2 E_{jy} + k_j^2 E_{jy} = 0 \tag{3.3.1}$$

in each region labeled by $j$. Here $k_j^2 = \omega^2 \mu_j \varepsilon_j$ and $E_{jy}$ is electric field in region $j$. Since the structure is uniform along $y$, all field quantities preserve the dependence on $y$ the same as the incident field and $\frac{\partial}{\partial y} = ik_{iy}$ in all of the Maxwell's equations. In particular, the wave equation becomes a 2D wave equation of

$$\nabla_t^2 E_{jy} + k_{jt}^2 E_{jy} = 0 \tag{3.3.2}$$

where $k_{jt}^2 = k_j^2 - k_{iy}^2$. We define the Green's function for the equation (3.3.2) by the same operator as

$$\nabla_t^2 G_j + k_{jt}^2 G_j = -\delta(\overline{\rho} - \overline{\rho}') \tag{3.3.3}$$

Using the Green's identity and integrating the result over the surface $S_0$ which is the top half-space, we have

$$\oint_{S_0} \mathrm{d}l \left( G_0 \frac{\partial E_{0y}}{\partial n} - E_{0y} \frac{\partial G_0}{\partial n} \right) = \begin{cases} E_{0y}(\overline{\rho}'), & \overline{\rho}' \in S_0 \\ 0 \qquad\quad , & \overline{\rho}' \notin S_0 \end{cases} \tag{3.3.4}$$

here $\hat{n}$ has a negative $z$ component and pointing outside of $S_0$. The boundary integral consists of two parts. An integral over the first surface which is described by $z = f_0(x)$ and an integral over a closing path at infinity $C_\infty$. There are two way of introducing the incident electric field into the integral equation. One is beginning with the inhomogeneous wave equation with a forcing function which gives the incident field upon convolution with the Green's function inside the integral equation. The other way is to start from the homogeneous wave equation for the electric field and assuming the source of the incident field is somewhere at infinity, which is the approach here. The integral equation of (3.3.4) is a general statement. If we assume that everywhere filled with vacuum (free space), the boundary integral over the periodic surface $z = f_0(x)$ vanishes and total electric field everywhere is the incident electric field. Therefore,

$$\int_{C_\infty} \mathrm{d}l \left( G_0 \frac{\partial E_{0y}}{\partial n} - E_{0y} \frac{\partial G_0}{\partial n} \right) = E_{iy}(\overline{\rho}') \tag{3.3.5}$$

Swapping the primed and unprimed coordinates and also change the direction of unit normal to pointing into the region 0 (upward), results in

$$E_{iy}(\overline{\rho}) - \int_{z'=f_0(x')} \mathrm{d}l_0' \left( G_0 \frac{\partial E_{0y}}{\partial n_0'} - E_{0y} \frac{\partial G_0}{\partial n_0'} \right) = \begin{cases} E_{0y}(\overline{\rho}) & z > f_0(x) \\ 0 & z < f_0(x) \end{cases} \tag{3.3.6}$$

The extinction equations (3.3.6) can be written as

$$E_{iy}(\overline{\rho}) + E_{0sy}(\overline{\rho}) = \begin{cases} E_{0y}(\overline{\rho}) & z > f_0(x) \\ 0 & z < f_0(x) \end{cases} \tag{3.3.7}$$

where the scattered field propagated by $G_0$ is given by

$$E_{0sy}(\overline{\rho})=-\int_{z'=f_0(x')}\mathrm{d}l_0'\left(G_0\frac{\partial E_{0y}}{\partial n_0'}-E_{0y}\frac{\partial G_0}{\partial n_0'}\right) \tag{3.3.8}$$

Applying the extinction equation to the region 1, results in the similar sort of equations,

$$E_{1sy}^u(\overline{\rho})+E_{1sy}^d(\overline{\rho})=\begin{cases}0 & z>f_0(x)\\ E_{1y} & f_0(x)>z>-d+f_1(x)\\ 0 & z<-d+f_1(x)\end{cases} \tag{3.3.9}$$

where the upward and downward propagating scattered field in region 1 given in terms of boundary integrals of

$$\begin{aligned}E_{1sy}^u(\overline{\rho})&=\int_{z'=f_0(x')}\mathrm{d}l_0'\left(G_1\frac{\partial E_{1y}}{\partial n_0'}-E_{1y}\frac{\partial G_1}{\partial n_0'}\right)\\ E_{1sy}^d(\overline{\rho})&=-\int_{z'=f_1(x')}\mathrm{d}l_1'\left(G_1\frac{\partial E_{1y}}{\partial n_1'}-E_{1y}\frac{\partial G_1}{\partial n_1'}\right)\end{aligned} \tag{3.3.10}$$

Here, $\hat{n}_1$ is unit vector normal to the surface $z=f_1(x)$ that pointing upward. Application of the extinction theorem to the last region which is region 2 gives

$$E_{2sy}=\begin{cases}E_{2y} & z<f_1(x)-d\\ 0 & z>f_1(x)-d\end{cases} \tag{3.3.11}$$

where the scattered field in the region 2 is given by

$$E_{2sy}(\overline{\rho})=\int_{z'=f_1(x')}\mathrm{d}l_1'\left(G_2\frac{\partial E_{2y}}{\partial n_1'}-E_{2y}\frac{\partial G_2}{\partial n_1'}\right) \tag{3.3.12}$$

### 3.3.1 2D Periodic Green's Function

Different scattered fields can be expressed in terms of condensed integrals over one period using the periodic Green's function as a propagator. Considering a typical boundary integral over the $j$-th region as

$$E_s(\overline{\rho})=\int_{z'=f_j(x')}\mathrm{d}l_1'\left(G_j(\overline{\rho},\overline{\rho}')\frac{\partial E_{jy}(\overline{\rho}')}{\partial n_j'}-E_{jy}(\overline{\rho}')\frac{\partial G_j(\overline{\rho},\overline{\rho}')}{\partial n_j'}\right) \tag{3.3.13}$$

The integral can be divided into sum of the integrals over individual periods,

$$E_s(\overline{\rho})=\sum_{n=-\infty}^{\infty}\int_{(n-1)L_j}^{nL_j}\mathrm{d}l_1'\left(G_j(\overline{\rho},\overline{\rho}')\frac{\partial E_{jy}(\overline{\rho}')}{\partial n_j'}-E_{jy}(\overline{\rho}')\frac{\partial G_j(\overline{\rho},\overline{\rho}')}{\partial n_j'}\right) \tag{3.3.14}$$

By shifting $x'$ in all of the segments to the interval $[0,L_j]$ and noting that the surface fields follow the Bloch condition of [67]

$$E_{jy}(x+L_j,z)=E_{jy}(x,z)e^{ik_{ix}L_j} \tag{3.3.15}$$

and the Green's function is translational invariant, the scattered field boundary integral can be written as

$$E_s(\overline{\rho})=\int_0^{L_j} \mathrm{d}l_1' \left( G_{jp}(\overline{\rho},\overline{\rho}') \frac{\partial E_{jy}(\overline{\rho}')}{\partial n_j'} - E_{jy}(\overline{\rho}') \frac{\partial G_{jp}(\overline{\rho},\overline{\rho}')}{\partial n_j'} \right) \tag{3.3.16}$$

where the periodic Green's function of the region $j$ is defined by

$$G_{jp}(\overline{\rho},\overline{\rho}')=\sum_{n=-\infty}^{\infty} G_j(x,z,x'+nL_j,z') e^{ik_{ix}nL_j} \tag{3.3.17}$$

where $L_j$ is period of the $j$-th surface. The 2D Green's function $G_j$ has a closed form solution of

$$G_j(\overline{\rho},\overline{\rho}')=\frac{i}{4} H_0^{(1)}\left(k_{jt}|\overline{\rho}-\overline{\rho}'|\right) \tag{3.3.18}$$

In order to evaluate the periodic Green's function we can use the spatial solution of (3.3.18) in the summation to get

$$G_{jp}(\overline{\rho},\overline{\rho}')=\frac{i}{4} \sum_{n=-\infty}^{\infty} H_0^{(1)}\left(k_{jt}\sqrt{(x-x'-nL_j)^2+(z-z')^2}\right) e^{ink_{ix}L_j} \tag{3.3.19}$$

However this series has a slow convergence as the tail of the Hankel function $H_0(x)$ falls like $1/\sqrt{x}$ that makes the spatial expansion essentially not a useful one. However, if the problem of interest has some amount of loss, then the spatial summation would have an exponential convergence. The other approach of calculating the periodic Green's function is using the spectral expansion of the 2D free space Green's function as

$$H_0^{(1)}\left(k_{jt}|\overline{\rho}-\overline{\rho}'|\right)=\frac{1}{\pi}\int_{-\infty}^{\infty} \mathrm{d}k_x \frac{1}{k_{jz}} e^{ik_x(x-x')} e^{ik_{jz}|z-z'|} \tag{3.3.20}$$

Substituting in the periodic Green's function expression of (3.3.17) gives,

$$G_{jp}=\frac{i}{4\pi}\int_{-\infty}^{\infty} \mathrm{d}k_x \frac{1}{k_{jz}} e^{ik_x(x-x')} e^{ik_{jz}|z-z'|} \sum_{n=-\infty}^{\infty} e^{i(k_{ix}-k_x)nL_j} \tag{3.3.21}$$

Now from the Fourier expansion of the impulse train we can obtain the following identity

$$\sum_{n=-\infty}^{\infty} e^{i\alpha nL}=\frac{2\pi}{L}\sum_{n=-\infty}^{\infty}\delta\left(\alpha-\frac{2n\pi}{L}\right) \tag{3.3.22}$$

Using this summation in periodic Green's function expression, the delta function samples the integral at $k_x=k_{ix}+\frac{2\pi n}{L_j}$ that results in

$$G_{jp}=\frac{i}{2L_j}\sum_{n=-\infty}^{\infty}\frac{1}{k_{jnz}} e^{ik_{nx}(x-x')} e^{ik_{jnz}|z-z'|} \tag{3.3.23}$$

where the Bloch wave numbers

$$\begin{aligned} k_{jnx}&=k_{ix}+\frac{2\pi n}{L_j} \\ k_{jnz}&=\sqrt{k_j^2-k_{jnx}^2} \end{aligned} \tag{3.3.24}$$

are the possible values of the wave number components. Notice that the periodicity of the structure leads to a discrete spectrum of the plane wave. This discrete spectrum is result of the constructive interference of different periods of the structure and the individual plane waves of order $n$ with the wave vector $\overline{k}_n = k_{jnx}\hat{x} + k_{jnz}\hat{z}$ are called the *Bragg Modes* of the structure. Notice that the periodic Green's function here, is the collective response of the empty lattice sites. The periodic Green's function is similar to the array factor in the antenna theory where it accounts for the collective response and interaction of individual elements in an array, but the element can be an arbitrary radiator.

## 3.4 Integral Equations Using Periodic Green's Function

Using the periodic Green's function instead of free space Green's function, the surface integrals over the boundary can be shrunk over one period of the surface. Therefore, we only need to replace

$$\int_{z'=f_i(x')} \mathrm{d}l_i' \, G_j(\overline{\rho},\overline{\rho}')\,[\cdot] \Longrightarrow \int_{\langle L_i\rangle} \mathrm{d}l_i' \, G_{jp}(\overline{\rho},\overline{\rho}')\,[\cdot] \tag{3.4.1}$$

Then scattered field expressions using the periodic Green's function reduce to

$$\begin{aligned}
E_{0sy}(\overline{\rho}) &= -\int_{\langle L_0\rangle} \mathrm{d}x' \sqrt{1+f_0'^2}\left(G_{0p}\frac{\partial E_{0y}}{\partial n_0'} - E_{0y}\frac{\partial G_{0p}}{\partial n_0'}\right) \\
E_{1sy}^{u}(\overline{\rho}) &= +\int_{\langle L_0\rangle} \mathrm{d}x' \sqrt{1+f_0'^2}\left(G_{1p}\frac{\partial E_{1y}}{\partial n_0'} - E_{1y}\frac{\partial G_{1p}}{\partial n_0'}\right) \\
E_{1sy}^{d}(\overline{\rho}) &= -\int_{\langle L_1\rangle} \mathrm{d}x' \sqrt{1+f_1'^2}\left(G_{1p}\frac{\partial E_{1y}}{\partial n_1'} - E_{1y}\frac{\partial G_{1p}}{\partial n_1'}\right) \\
E_{2sy}(\overline{\rho}) &= +\int_{\langle L_1\rangle} \mathrm{d}x' \sqrt{1+f_1'^2}\left(G_{2p}\frac{\partial E_{2y}}{\partial n_1'} - E_{2y}\frac{\partial G_{2p}}{\partial n_1'}\right)
\end{aligned} \tag{3.4.2}$$

Now we have 4 extinction equations and 6 unknowns $E_{jy}$ and $\hat{n}\cdot\nabla E_{jy} (j=0,1,2)$. These unknowns are not independent and can be related through the boundary conditions on the fields.

First, continuity of the tangential electric field eliminates one of the unknowns since at the interfaces $E_{0y}=E_{1y}$ and $E_{1y}=E_{2y}$. Also we need to apply continuity of the magnetic field over a dielectric boundary. Magnetic field can be expressed in terms of the pilot electric field component as

$$\overline{H}_{jt} = \frac{-i\omega\varepsilon_j}{k_{jt}^2}\nabla_t \times (E_{jy}\hat{y}) \tag{3.4.3}$$

and also $H_{jy} = 0$. We need to impose $\hat{n}\times\overline{H}_{jt}$ to be continuous across the boundary,

$$\hat{n}\times\overline{H}_{jt} = \frac{-i\omega\varepsilon_j}{k_{jt}^2}\hat{n}\times[\nabla_t\times(E_{jy}\hat{y})] = \frac{i\omega\varepsilon_j}{k_{jt}^2}\hat{n}\cdot\nabla_t E_{jy}\hat{y} \tag{3.4.4}$$

Therefore, magnetic field s continuous across the boundaries if

$$\begin{aligned}
\frac{\varepsilon_0}{k_{0t}^2}\hat{n}_0\cdot\nabla_t E_{0y} &= \frac{\varepsilon_1}{k_{1t}^2}\hat{n}_0\cdot\nabla_t E_{1y} \\
\frac{\varepsilon_1}{k_{1t}^2}\hat{n}_1\cdot\nabla_t E_{1y} &= \frac{\varepsilon_2}{k_{2t}^2}\hat{n}_1\cdot\nabla_t E_{2y}
\end{aligned} \tag{3.4.5}$$

We choose two surface fields as $\hat{n}_0\cdot\nabla_t E_{0y}$ and $\hat{n}_1\cdot\nabla_t E_{1y}$ as unknowns fields.

$$\begin{aligned}\frac{\varepsilon_0 k_{1t}^2}{\varepsilon_1 k_{0t}^2}\frac{\partial E_{0y}}{\partial n_0'}&=\frac{\partial E_{1y}}{\partial n_0'}\\ \frac{\varepsilon_1 k_{2t}^2}{\varepsilon_2 k_{1t}^2}\frac{\partial E_{1y}}{\partial n_1'}&=\frac{\partial E_{2y}}{\partial n_1'}\end{aligned}\tag{3.4.6}$$

Using the boundary conditions to eliminate region 2 fields, the scattered fields expressions can be written as

$$\begin{aligned}E_{0sy}(\overline{\rho})&=-\int_{\langle L_0\rangle}\mathrm{d}x'\sqrt{1+f_0'^2}\left(G_{0p}\frac{\partial E_{0y}}{\partial n_0'}-E_{0y}\frac{\partial G_{0p}}{\partial n_0'}\right)\\ E_{1sy}^u(\overline{\rho})&=+\int_{\langle L_0\rangle}\mathrm{d}x'\sqrt{1+f_0'^2}\left(\left(\frac{\varepsilon_0 k_{1t}^2}{\varepsilon_1 k_{0t}^2}\right)G_{1p}\frac{\partial E_{0y}}{\partial n_0'}-E_{0y}\frac{\partial G_{1p}}{\partial n_0'}\right)\\ E_{1sy}^d(\overline{\rho})&=-\int_{\langle L_1\rangle}\mathrm{d}x'\sqrt{1+f_1'^2}\left(G_{1p}\frac{\partial E_{1y}}{\partial n_1'}-E_{1y}\frac{\partial G_{1p}}{\partial n_1'}\right)\\ E_{2sy}(\overline{\rho})&=+\int_{\langle L_1\rangle}\mathrm{d}x'\sqrt{1+f_1'^2}\left(\left(\frac{\varepsilon_1 k_{2t}^2}{\varepsilon_2 k_{1t}^2}\right)G_{2p}\frac{\partial E_{1y}}{\partial n_1'}-E_{1y}\frac{\partial G_{2p}}{\partial n_1'}\right)\end{aligned}\tag{3.4.7}$$

We can generalize the approach to the multilayer periodic media in the next section.

### 3.4.1 Extinction of Downward Propagating Wave in Region 0

Here, we assume that all of the surfaces in the problem have the same period $L$. Inserting spectral expansion of the periodic Green's function into (3.4.7), extinction of the incident field can be written as

$$E_{iy}+\sum_n b_n^{10}e^{i(k_{nx}x-k_{nz}^0 z)}=0\tag{3.4.8}$$

where $b_n^{10}$ is amplitude of Floquet modes that are excited to cancel the incident field in the lower regions (the superscript 10 refers to the source|observation media) that is given by

$$\begin{aligned}b_n^{10}=&-\frac{i}{2Lk_{nz}^0}\int_L\mathrm{d}x'\left[\sqrt{1+f'^2}\hat{n}'\cdot\nabla' E_{0y}\right]e^{-i(k_{nx}x'-k_{nz}^0 z')}\\ &+\frac{i}{2Lk_{nz}^0}\int_L\mathrm{d}x' E_{0y}\left[ik_{nx}f'(x')+ik_{0nz}\right]e^{-i(k_{nx}x'-k_{nz}^0 z')}\end{aligned}\tag{3.4.9}$$

### 3.4.2 Extinction of Upward Propagating Wave in Region $m$

The periodic Green's function in region $m$, where $1\leq m\leq N-1$ for $z<z'$ can be expanded as

$$G_{mp}(z>z')=\frac{i}{2L}\sum_n\frac{1}{k_{nz}^m}e^{i(k_{nx}x+k_{nz}^m z)}e^{-i(k_{nx}x'+k_{nz}^m z')}\tag{3.4.10}$$

and normal its derivative,

$$\hat{n}_m'\cdot\nabla' G_{mp}(z>f)=\frac{1}{\sqrt{1+f_{m-1}'^2}}\frac{i}{2L}\sum_n\frac{1}{k_{nz}^m}e^{i(k_{nx}x+k_{nz}^m z)}\left[ik_{nx}f_{m-1}'(x')-ik_{nz}^m\right]e^{-i(k_{nx}x'+k_{nz}^m z')}\tag{3.4.11}$$

Substituting in upward scattered field of region $m$ with source on the upper layer ($u$), $E^u_{msy}(\overline{\rho})$ we have

$$E^u_{msy}=\int_L \mathrm{d}x'\sqrt{1+f'^2_{m-1}}\Big(\frac{\varepsilon_{m-1}k^2_{m-1,t}}{\varepsilon_m k^2_{m-1,t}}\Big)\hat{n}'\cdot\nabla' E_{m-1,y}\frac{i}{2L}\sum_n\frac{1}{k^m_{nz}}e^{i(k_{nx}x+k^m_{nz}z)}e^{-i(k_{nx}x'+k^m_{nz}z')} \tag{3.4.12}$$
$$-\int_L \mathrm{d}x' E_{m-1,y}\frac{i}{2L}\sum_n\frac{1}{k^m_{nz}}e^{i(k_{nx}x+k^m_{nz}z)}\Big[ik_{nx}f'_{m-1}(x')-ik^m_{nz}\Big]e^{-i(k_{nx}x'+k^m_{nz}z')}$$

Note that it is an expansion in terms of upward propagating spatial harmonics $e^{i(k_{nx}x+k^m_{nz}z)}$. Also for contribution of the bottom surface of region $m$, $E^d_{msy}$,

$$E^d_{msy}=-\int_L \mathrm{d}x'\sqrt{1+f'^2_m}\hat{n}'\cdot\nabla' E_{my}\frac{i}{2L}\sum_n\frac{1}{k^m_{nz}}e^{i(k_{nx}x+k^m_{nz}z)}e^{-i(k_{nx}x'+k^m_{nz}z')} \tag{3.4.13}$$
$$+\int_L \mathrm{d}x' E_{my}\frac{i}{2L}\sum_n\frac{1}{k_{mnz}}e^{i(k_{nx}x+k^m_{nz}z)}\Big[ik_{nx}f'_m(x')-ik^m_{nz}\Big]e^{-i(k_{nx}x'+k^m_{nz}z')}$$

Again, this is an expansion in terms of the upward propagating harmonics $e^{i(k_{nx}x+k^m_{nz}z)}$. Putting everything together, the extinction relation of the wave in region $m$, which is sum of the two contributions can be written as

$$E^u_{msy}(z>z')+E^d_{msy}(z>z')=\sum_n b^{m-1,m}_n e^{i(k_{nx}x+k^m_{nz}z)}=0 \tag{3.4.14}$$

where the harmonic coefficients $b^{m-1,m}_n$ are defined by

$$b^{m-1,m}_n=\frac{i}{2Lk^m_{nz}}\int_L \mathrm{d}x'\sqrt{1+f'^2_{m-1}}\Big(\frac{\varepsilon_{m-1}k^2_{m,t}}{\varepsilon_m k^2_{m-1,t}}\Big)\hat{n}'\cdot\nabla' E_{m-1,y}e^{-i(k_{nx}x'+k^m_{nz}z')} \tag{3.4.15}$$
$$-\frac{i}{2Lk^m_{nz}}\int_L \mathrm{d}x' E_{m-1,y}\Big[ik_{nx}f'_{m-1}(x')-ik^m_{nz}\Big]e^{-i(k_{nx}x'+k^m_{nz}z')}$$
$$-\frac{i}{2Lk^m_{nz}}\int_L \mathrm{d}x'\sqrt{1+f'^2_m}\hat{n}'_m\cdot\nabla' E_{my}e^{-i(k_{nx}x'+k^m_{nz}z')}$$
$$+\frac{i}{2Lk^m_{nz}}\int_L \mathrm{d}x' E_{my}\Big[ik_{nx}f'_m(x')-ik^m_{nz}\Big]e^{-i(k_{nx}x'+k^m_{nz}z')}$$

### 3.4.3 Extinction of Downward Propagating Wave in Region $m$

Following the same procedure as extinction of upward propagating wave n region $m$, but here the periodic Green's function need to be expanded with condition $z<z'$ as

$$G_{mp}(z<z')=\frac{i}{2L}\sum_n\frac{1}{k^m_{nz}}e^{i(k_{nx}x-k^m_{nz}z)}e^{-i(k_{nx}x'-k^m_{nz}z')} \tag{3.4.16}$$

Inserting the Green's function expansion into the extinction equation of region $m$ with observation point in lower regions results in

$$E^u_{msy}(z<z')+E^d_{msy}(z<z')=\sum b^{m+1,m}_n e^{i(k_{nx}x-k^m_{nz}z)}=0 \tag{3.4.17}$$

where,

$$E^u_{msy}(\overline{\rho})=\int_L \mathrm{d}x'\sqrt{1+f'^2_{m-1}}\Big(\Big(\frac{\varepsilon_{m-1}k^2_{m,t}}{\varepsilon_m k^2_{m-1,t}}\Big)\frac{i}{2L}\sum_n \frac{1}{k^m_{nz}}e^{i(k_{nx}x-k^m_{nz}z)}e^{-i(k_{nx}x'-k^m_{nz}z')}\frac{\partial E_{m-1,y}}{\partial n'_{m-1}} \tag{3.4.18}$$

$$-E_{m-1,y}\frac{1}{\sqrt{1+f'^2_{m-1}}}\frac{i}{2L}\sum_n \frac{1}{k^m_{nz}}e^{i(k_{nx}x-k^m_{nz}z)}\Big[ik_{nx}f'_{m-1}(x')+ik^m_{nz}\Big]e^{-i(k_{nx}x'-k^m_{nz}z')}\Big)$$

$$E^d_{msy}(\overline{\rho})=-\int_L \mathrm{d}x'\sqrt{1+f'^2_{m}}\Big(\frac{i}{2L}\sum_n \frac{1}{k^m_{nz}}e^{i(k_{nx}x-k^m_{nz}z)}e^{-i(k_{nx}x'-k^m_{nz}z')}\frac{\partial E_{my}}{\partial n'_{m}}$$

$$-E_{my}\frac{1}{\sqrt{1+f'^2_{m}}}\frac{i}{2L}\sum_n \frac{1}{k^m_{nz}}e^{i(k_{nx}x-k^m_{nz}z)}\Big[ik_{nx}f'_{m}(x')+ik^m_{nz}\Big]e^{-i(k_{nx}x'-k^m_{nz}z')}\Big)$$

and the spectral coefficients $b^{m+1,m}_n$ are given by

$$b^{m+1,m}_n=\frac{i}{2Lk^m_{nz}}\int_{\langle L_{m-1}\rangle}\mathrm{d}x'\sqrt{1+f'^2_{m-1}}\frac{\partial E_{m-1,y}}{\partial n'_{m-1}}\Big(\frac{\varepsilon_{m-1}k^2_{m,t}}{\varepsilon_m k^2_{m-1,t}}\Big)e^{-i(k_{nx}x'-k^m_{nz}z')} \tag{3.4.19}$$

$$-\frac{i}{2Lk^m_{nz}}\int_{\langle L_{m-1}\rangle}\mathrm{d}x'E_{m-1,y}\Big[ik_{nx}f'_{m-1}(x')+ik^m_{nz}\Big]e^{-i(k_{nx}x'-k^m_{nz}z')}$$

$$-\frac{i}{2Lk^m_{nz}}\int_{\langle L_m\rangle}\mathrm{d}x'\sqrt{1+f'^2_{m}}\frac{\partial E_{my}}{\partial n'_{m}}e^{-i(k_{nx}x'-k^m_{nz}z')}$$

$$+\frac{i}{2Lk^m_{nz}}\int_{\langle L_m\rangle}\mathrm{d}x'E_{my}\Big[ik_{nx}f'_{m}(x')+ik^m_{nz}\Big]e^{-i(k_{nx}x'-k^m_{nz}z')}$$

### 3.4.4 Extinction of Upward Propagating Wave in Region $N$

For extinction of wave in the last region, the observation point is considered to be on a place that is always above the last interface, namely $z>-d_{N-1}+f_{N-1}(x)$. Under this condition, the periodic Green's function can be expanded as

$$G_{Np}(z>z')=\frac{i}{2L}\sum_n \frac{1}{k^N_{nz}}e^{i(k_{nx}x+k^N_{nz}z)}e^{-i(k_{nx}x'+k^N_{nz}z')} \tag{3.4.20}$$

following the same procedure as before and substituting the periodic Green's function in the extinction equation of the last region yields

$$\sum_n b^{N-1,N}_n e^{i(k_{nx}x+k^N_{nz}z)}=0 \tag{3.4.21}$$

where the Bloch amplitude of the upward propagating waves is given by

$$b^{N-1,N}_n=\frac{i}{2Lk^N_{nz}}\int_L \mathrm{d}x'\sqrt{1+f'^2_{N-1}}\Big(\frac{\varepsilon_{N-1}k^2_{N,t}}{\varepsilon_N k^2_{N-1,t}}\Big)\hat{n}'\cdot\nabla' E_{N-1,y}e^{-i(k_{nx}x'+k^N_{nz}z')} \tag{3.4.22}$$

$$-\frac{i}{2Lk^N_{nz}}\int_L \mathrm{d}x'E_{N-1,y}\Big[ik_{nx}f'_{N-1}(x')-ik^N_{nz}\Big]e^{-i(k_{nx}x'+k^N_{nz}z')}$$

Notice that the surface fields in (3.4.22) are those of region $N-1$ that replaced the fields of region $N$ using continuity conditions. The extinction relation in all of the layers are

obtained as a harmonic expansions of,

$$\begin{aligned} E_{iy}+\sum_n b_n^{10} e^{i(k_{nx}x-k_{nz}^0 z)}&=0 \\ \sum_n b_n^{m-1,m} e^{i(k_{nx}x+k_{nz}^m z)}&=0 \\ \sum b_n^{m+1,m} e^{i(k_{nx}x-k_{nz}^m z)}&=0 \\ \sum_n b_n^{N-1,N} e^{i(k_{nx}x+k_{nz}^N z)}&=0 \end{aligned} \tag{3.4.23}$$

Since the Bloch modes are orthogonal in space, i.e. for two mode index $p$,$q$, the inner product of two modes can be computed as

$$\begin{aligned} \langle p,q\rangle &= \int_L \mathrm{d}x e^{i(k_{px}x+k_{pz}z)} e^{-i(k_{qx}x+k_{qz}z)} \\ &= e^{i(k_{pz}-k_{qz})z} \int_L \mathrm{d}x e^{2\pi i(p-q)/L} \\ &= L\delta_{pq} \end{aligned} \tag{3.4.24}$$

Which shows two different modes are spatially orthogonal. Based on this, $b_n^{01}=b_n^{m+1,m}=b_n^{m-1,m}=b_n^{N-1,N}=0$ for all values of $n$ and $1\leq m\leq N-1$. Also, assuming incidence electric field of $E_{iy}=e^{ik_{ix}x-ik_{iz}z}$ for $b_n^{10}$ we have

$$e^{ik_{ix}x-ik_{iz}z}+\sum_n b_n^{10} e^{i(k_{nx}x-k_{0nz}z)}=0 \tag{3.4.25}$$

Since the electric field is directed along the zeroth spatial harmonic the only non zero component of $b^{10}$ is $b_0^{10}$ with $b_0^{10}=-1$ and $b_{n\neq 0}^{10}=0$ for all other $n$'s. Now that the coefficients $b$ are known completely, surface fields in the definition of the spectral coefficients are the unknown quantities to be determined. In order to solve for the surface fields, using the fact that surface fields are periodic with the period of the surface, the surface fields can be expanded in a Fourier series. For the surface fields on the $q$-th surface, the expansion reads,

$$\begin{aligned} E_{qy}(x') &= \sum_m \alpha_m^q e^{ik_{mx}x'} \\ \sqrt{1+f_q'^2}\hat{n}_q'\cdot\nabla' E_{qy} &= \sum_m \beta_m^q e^{ik_{mx}x'} \end{aligned} \tag{3.4.26}$$

for $q=0,1,\cdots N-1$. Notice that the length scale of the surface is included in the unknowns as its all we need to compute the fields everywhere. substituting surface fields Fourier expansions and noting that $z'=f_0(x')$ for the first surface and $z'=-d_q+f_q(x)$ for the $q$-th surface ($1\leq q\leq N-1$) we arrive at

$$\begin{aligned} b_n^{10} = &-\frac{i}{2Lk_{nz}^0}\sum_m \beta_m^0 \int_L \mathrm{d}x' e^{i(k_{mx}-k_{nx})x'+ik_{nz}^0 z'} \\ &+\frac{i}{2Lk_{nz}^0}\sum_m \alpha_m^0 \int_L \mathrm{d}x' \Big[ik_{nx}f'(x')+ik_{nz}^0\Big] e^{i(k_{mx}-k_{nx})x'+ik_{nz}^0 z'} \end{aligned} \tag{3.4.27}$$

$$b_n^{q-1,q}=\frac{i}{2Lk_{nz}^q}\sum_m\beta_m^{q-1}\int_L\mathrm{d}x'\Big(\frac{\varepsilon_{q-1}k_{q,t}^2}{\varepsilon_q k_{q-1,t}^2}\Big)e^{i(k_{mx}-k_{nx})x'-ik_{nz}^q z'} \tag{3.4.28}$$
$$-\frac{i}{2Lk_{nz}^q}\sum_m\alpha_m^{q-1}\int_L\mathrm{d}x'\Big[ik_{nx}f'_{q-1}(x')-ik_{nz}^q\Big]e^{i(k_{mx}-k_{nx})x'-ik_{nz}^q z'}$$
$$-\frac{i}{2Lk_{nz}^q}\sum_m\beta_m^{q}\int_L\mathrm{d}x'e^{i(k_{mx}-k_{nx})x'-ik_{nz}^q z'}$$
$$+\frac{i}{2Lk_{nz}^q}\sum_m\alpha_m^{q}\int_L\mathrm{d}x'\Big[ik_{nx}f'_{q}(x')-ik_{nz}^q\Big]e^{i(k_{mx}-k_{nx})x'-ik_{nz}^q z'}$$

$$b_n^{q+1,q}=\frac{i}{2Lk_{nz}^q}\sum_m\beta_m^{q-1}\int_L\mathrm{d}x'\Big(\frac{\varepsilon_{q-1}k_{q-1,t}^2}{\varepsilon_q k_{q-1,t}^2}\Big)e^{i(k_{mx}-k_{nx})x'+ik_{nz}^q z'} \tag{3.4.29}$$
$$-\frac{i}{2Lk_{nz}^q}\sum_m\alpha_m^{q-1}\int_L\mathrm{d}x'\Big[ik_{nx}f'_{q-1}(x')+ik_{nz}^q\Big]e^{i(k_{mx}-k_{nx})x'+ik_{nz}^q z'}$$
$$-\frac{i}{2Lk_{nz}^q}\sum_m\beta_m^{q}\int_L\mathrm{d}x'e^{i(k_{mx}-k_{nx})x'+ik_{nz}^q z'}$$
$$+\frac{i}{2Lk_{nz}^q}\sum_m\alpha_m^{q}\int_L\mathrm{d}x'\Big[ik_{nx}f'_{q}(x')+ik_{nz}^q\Big]e^{i(k_{mx}-k_{nx})x'+ik_{nz}^q z'}$$

$$b_n^{N-1,N}=\frac{i}{2Lk_{nz}^N}\sum_m\beta_m^{N-1}\int_L\mathrm{d}x'\Big(\frac{\varepsilon_{N-1}k_{N,t}^2}{\varepsilon_N k_{N-1,t}^2}\Big)e^{i(k_{mx}-k_{nx})x'-ik_{nz}^N z'} \tag{3.4.30}$$
$$-\frac{i}{2Lk_{nz}^N}\sum_m\alpha_m^{N-1}\int_L\mathrm{d}x'\Big[ik_{nx}f'_{N-1}(x')-ik_{nz}^N\Big]e^{i(k_{mx}-k_{nx})x'-ik_{nz}^N z'}$$

The integrals that have the derivative of the surface profile in the integrand can be simplified using a by part integration. For example,

$$\int_L\mathrm{d}x'ik_{nx}f'(x')e^{i(k_{mx}-k_{nx})x'-ik_{1nz}f(x')}=+\frac{ik_{nx}(k_{mx}-k_{nx})}{k_{1nz}}\int_L\mathrm{d}x'e^{i(k_{mx}-k_{nx})x'-ik_{1nz}f(x')} \tag{3.4.31}$$

Using this technique to simplify the integrations and upon defining the following integrals,

$$I_{00}^{-}[m,n]=\int_L\mathrm{d}x'e^{i(k_{mx}-k_{nx})x'+ik_{nz}^0 f_0(x')} \tag{3.4.32}$$
$$I_{q,q-1}^{\pm}[m,n]=\int_L\mathrm{d}x'e^{i(k_{mx}-k_{nx})x'\mp ik_{nz}^q f_{q-1}(x')}$$
$$I_{q,q}^{\pm}[m,n]=\int_L\mathrm{d}x'e^{i(k_{mx}-k_{nx})x'\mp ik_{nz}^q f_{q}(x')}$$
$$I_{N,N-1}^{+}[m,n]=\int_L\mathrm{d}x'e^{i(k_{mx}-k_{nx})x'-ik_{nz}^N f_{N-1}(x')}$$

The governing system of coupled equation for the Fourier coefficients of the surface fields on the boundaries can be written as

$$b_n^{10} = -\frac{i}{2Lk_{nz}^0}\sum_m \beta_m^0 I_{00}^-[m,n] + \frac{i}{2Lk_{nz}^0}\sum_m \alpha_m^0 i\frac{k_{t0}^2 - k_{nx}k_{mx}}{k_{nz}^0} I_{00}^-[m,n] \tag{3.4.33}$$

$$\begin{aligned} b_n^{q-1,q} = &\frac{i}{2Lk_{nz}^q}\sum_m \beta_m^{q-1}\Big(\frac{\varepsilon_{q-1}k_{q,t}^2}{\varepsilon_q k_{q-1,t}^2}\Big)e^{ik_{nz}^q d_{q-1}} I_{q,q-1}^+[m,n] \\ &-\frac{i}{2Lk_{nz}^q}\sum_m \alpha_m^{q-1}(-i)\frac{k_{q,t}^2 - k_{nx}k_{mx}}{k_{nz}^q} e^{ik_{nz}^q d_{q-1}} I_{q,q-1}^+[m,n] \\ &-\frac{i}{2Lk_{nz}^q}\sum_m \beta_m^q e^{ik_{nz}^q d_q} I_{qq}^+[m,n] + \frac{i}{2Lk_{nz}^q}\sum_m \alpha_m^q e^{ik_{nz}^q d_q}(-i)\frac{k_{qt}^2 - k_{nx}k_{mx}}{k_{nz}^q} I_{qq}^+[m,n] \end{aligned} \tag{3.4.34}$$

$$\begin{aligned} b_n^{q+1,q} = &\frac{i}{2Lk_{nz}^q}\sum_m \beta_m^{q-1}\Big(\frac{\varepsilon_{q-1}k_{q,t}^2}{\varepsilon_q k_{q-1,t}^2}\Big)e^{-ik_{nz}^q d_{q-1}} I_{q,q-1}^-[m,n] \\ &-\frac{i}{2Lk_{nz}^q}\sum_m \alpha_m^{q-1} i\frac{k_{q-1,t}^2 - k_{nx}k_{mx}}{k_{nz}^q} e^{-ik_{nz}^q d_{q-1}} I_{q,q-1}^-[m,n] \\ &-\frac{i}{2Lk_{nz}^q}\sum_m \beta_m^q e^{-ik_{nz}^q d_q} I_{qq}^-[m,n] + \frac{i}{2Lk_{nz}^q}\sum_m \alpha_m^q e^{-ik_{nz}^q d_q} i\frac{k_{q,t}^2 - k_{nx}k_{mx}}{k_{nz}^q} I_{qq}^-[m,n] \end{aligned} \tag{3.4.35}$$

$$\begin{aligned} b_n^{N-1,N} = &\frac{i}{2Lk_{nz}^N}\sum_m \beta_m^{N-1} e^{ik_{nz}^N d_{N-1}}\Big(\frac{\varepsilon_{N-1}k_{N,t}^2}{\varepsilon_N k_{N-1,t}^2}\Big) I_{N,N-1}^+[m,n] \\ &-\frac{i}{2Lk_{nz}^N}\sum_m \alpha_m^{N-1} e^{ik_{nz}^N d_{N-1}}(-i)\frac{k_{N,t}^2 - k_{nx}k_{mx}}{k_{nz}^N} I_{N,N-1}^+[m,n] \end{aligned}$$

Note that the integrals defined in (3.4.32) are similar to the scattering potentials in the formulation of the SPM2 for layered media with rough interfaces. For the case of flat interfaces, the integrals in (3.4.32) becomes degenerate to $I[m,n]=L\delta_{mn}$ that does not allow mode mixing (similar to the scattering potentials that vanish for the flat surface case).

## 3.5 Solution of Surface Fields

In order to solve for the Fourier coefficients of the surface fields $\alpha_m^q$ and $\beta_m^q$, we need to connect surface fields of different layers with propagation matrices recursively. Using the extinction equations of the middle layers which are given for $b_n^{q-1,q}$ and $b_n^{q+1,q}$ we can extract surface field propagation matrices that relates surface fields of neighbor layers as

$$\begin{bmatrix} \overline{\overline{M}}_{q-1}^{u+} & \overline{\overline{N}}_{q-1}^{u+} \\ \overline{\overline{M}}_{q-1}^{u-} & \overline{\overline{N}}_{q-1}^{u-} \end{bmatrix} \begin{bmatrix} \overline{\alpha}^{q-1} \\ \overline{\beta}^{q-1} \end{bmatrix} = \begin{bmatrix} \overline{\overline{M}}_q^{d+} & \overline{\overline{N}}_q^{d+} \\ \overline{\overline{M}}_q^{d-} & \overline{\overline{N}}_q^{d-} \end{bmatrix} \begin{bmatrix} \overline{\alpha}^q \\ \overline{\beta}^q \end{bmatrix} \tag{3.5.1}$$

or

$$\overline{\overline{D}}_{q-1}^u \begin{bmatrix} \overline{\alpha}^{q-1} \\ \overline{\beta}^{q-1} \end{bmatrix} = \overline{\overline{D}}_q^d \begin{bmatrix} \overline{\alpha}^q \\ \overline{\beta}^q \end{bmatrix} \tag{3.5.2}$$

where $q=1,2,\cdots,N-1$ and sub-matrices of $\overline{\overline{M}}$, and $\overline{\overline{N}}$ for different layers are defined through,

$$\begin{aligned}
\left[\overline{\overline{N}}^{u+}_{q-1}\right]_{nm} &= \frac{i}{2Lk^q_{nz}}\left(\frac{\varepsilon_{q-1}k^2_{q,t}}{\varepsilon_q k^2_{q-1,t}}\right)e^{ik^q_{nz}d_{q-1}}I^+_{q,q-1}[m,n] \\
\left[\overline{\overline{M}}^{u+}_{q-1}\right]_{nm} &= -\frac{i}{2Lk^q_{nz}}(-i)\frac{k^2_{q,t}-k_{nx}k_{mx}}{k^q_{nz}}e^{ik^q_{nz}d_{q-1}}I^+_{q,q-1}[m,n] \\
\left[\overline{\overline{N}}^{d+}_{q}\right]_{nm} &= \frac{i}{2Lk^q_{nz}}e^{ik^q_{nz}d_q}I^+_{qq}[m,n] \\
\left[\overline{\overline{M}}^{d+}_{q}\right]_{nm} &= -\frac{i}{2Lk^q_{nz}}e^{ik^q_{nz}d_q}(-i)\frac{k^2_{qt}-k_{nx}k_{mx}}{k^q_{nz}}I^+_{qq}[m,n]
\end{aligned} \tag{3.5.3}$$

and

$$\begin{aligned}
\left[\overline{\overline{N}}^{u-}_{q-1}\right]_{nm} &= \frac{i}{2Lk^q_{nz}}\left(\frac{\varepsilon_{q-1}k^2_{q,t}}{\varepsilon_q k^2_{q-1,t}}\right)e^{-ik^q_{nz}d_{q-1}}I^-_{q,q-1}[m,n] \\
\left[\overline{\overline{M}}^{u-}_{q-1}\right]_{nm} &= -\frac{i}{2Lk^q_{nz}}i\frac{k^2_{q,t}-k_{nx}k_{mx}}{k^q_{nz}}e^{-ik^q_{nz}d_{q-1}}I^-_{q,q-1}[m,n] \\
\left[\overline{\overline{N}}^{d-}_{q}\right]_{nm} &= \frac{i}{2Lk^q_{nz}}e^{-ik^q_{nz}d_q}I^-_{qq}[m,n] \\
\left[\overline{\overline{M}}^{d-}_{q}\right]_{nm} &= -\frac{i}{2Lk^q_{nz}}e^{-ik^q_{nz}d_q}i\frac{k^2_{q,t}-k_{nx}k_{mx}}{k^q_{nz}}I^-_{qq}[m,n]
\end{aligned} \tag{3.5.4}$$

Using propagation matrices we can connect the first and last surface fields components to each other. Also, the extinction relation of the incident field and the last region can be combined together to get,

$$\begin{aligned}
b^{10}_n &= \overline{\overline{M}}^-_0\,\overline{\alpha}^0 + \overline{\overline{N}}^-_0\,\overline{\beta}^0 \\
\overline{0} &= \overline{\overline{M}}^+_{N-1}\overline{\alpha}^{N-1} + \overline{\overline{N}}^+_{N-1}\overline{\beta}^{N-1}
\end{aligned} \tag{3.5.5}$$

where matrix entries are given by,

$$\begin{aligned}
\left[\overline{\overline{M}}^-_0\right]_{nm} &= \frac{i}{2Lk^0_{nz}}i\frac{k^2_{t0}-k_{nx}k_{mx}}{k^0_{nz}}I^-_{00}[m,n] \\
\left[\overline{\overline{N}}^-_0\right]_{nm} &= -\frac{i}{2Lk^0_{nz}}I^-_{00}[m,n] \\
\left[\overline{\overline{M}}^+_{N-1}\right]_{nm} &= -\frac{i}{2Lk^N_{nz}}e^{ik^N_{nz}d_{N-1}}(-i)\frac{k^2_{N,t}-k_{nx}k_{mx}}{k^N_{nz}}I^+_{N,N-1}[m,n] \\
\left[\overline{\overline{N}}^+_{N-1}\right]_{nm} &= \frac{i}{2Lk^N_{nz}}e^{ik^N_{nz}d_{N-1}}\left(\frac{\varepsilon_{N-1}k^2_{N,t}}{\varepsilon_N k^2_{N-1,t}}\right)I^+_{N,N-1}[m,n]
\end{aligned} \tag{3.5.6}$$

From the recursive relation of middle layers of (3.5.2) the surface fields over the $(N-1)$-th surface can be expressed in terms of the zeroth surface as

$$\begin{aligned}
\begin{bmatrix}\overline{\alpha}^{N-1}\\ \overline{\beta}^{N-1}\end{bmatrix} &= \left(\left(\overline{\overline{D}}^d_{N-1}\right)^{-1}\overline{\overline{D}}^u_{N-2}\right)\left(\left(\overline{\overline{D}}^d_{N-2}\right)^{-1}\overline{\overline{D}}^u_{N-3}\right)\cdots\left(\left(\overline{\overline{D}}^d_{1}\right)^{-1}\overline{\overline{D}}^u_{0}\right)\begin{bmatrix}\overline{\alpha}^0\\ \overline{\beta}^0\end{bmatrix} \\
&:= \overline{\overline{D}}\begin{bmatrix}\overline{\alpha}^0\\ \overline{\beta}^0\end{bmatrix}
\end{aligned} \tag{3.5.7}$$

where the total propagation matrix $\overline{\overline{D}}$ is defined as connection between the zeroth and last boundary surface fields. Using the extinction of the zeroth and the last layer if (3.5.5), a consistent system of equations for the Fourier coefficients of the surface fields over the zeroth and last boundary can be obtained as

$$\begin{bmatrix} \overline{\overline{M}}_0^- & \overline{\overline{N}}_0^- & \overline{\overline{0}} & \overline{\overline{0}} \\ \overline{\overline{0}} & \overline{\overline{0}} & \overline{\overline{M}}_{N-1}^+ & \overline{\overline{N}}_{N-1}^+ \\ & \overline{\overline{D}} & & -\overline{\overline{I}} \end{bmatrix} \begin{bmatrix} \overline{\alpha}^0 \\ \overline{\beta}^0 \\ \overline{\alpha}^{N-1} \\ \overline{\beta}^{N-1} \end{bmatrix} = \begin{bmatrix} \overline{b}^{10} \\ \overline{0} \\ \overline{0} \\ \overline{0} \end{bmatrix} \tag{3.5.8}$$

Once (3.5.8) is solved for the Fourier coefficients of the surface fields, the actual surface fields can be synthesized by the Fourier series. In order to find the surface fields on other boundaries than the zeroth and last boundaries, one can apply the propagation matrices of (3.5.2) to obtain all of the surface field variables.

## 3.6 Scattered and Transmitted Fields

Once the surface fields are known through their Fourier coefficients of (3.5.8), the equivalence principle can be applied to the surface fields over the zeroth boundary to find the scattered field as

$$E_{sy}(\overline{\rho}) = -\int_L \mathrm{d}l' \Big[ G_{0p}(\overline{\rho},\overline{\rho}')\hat{n}'\cdot\nabla' E_{0y}(\overline{\rho}') - E_{0y}(\overline{\rho}')\hat{n}'\cdot\nabla' G_{0p}(\overline{\rho},\overline{\rho}') \Big] \quad , \quad z>f(x) \tag{3.6.1}$$

Here, the observation point is placed somewhere in the region 0 that satisfies $z>f_0(x)$ fo all values of $x$. Given this observation point, the periodic Green's function of the region 0 can be expanded as

$$G_{0p}(z>f) = \frac{i}{2L}\sum_n \frac{1}{k_{nz}^0} e^{i(k_{nx}x+k_{nz}^0 z)} e^{-i(k_{nx}x'+k_{nz}^0 z')} \tag{3.6.2}$$

and for its derivative,

$$\hat{n}'\cdot\nabla' G_{0p}(z>f) = \frac{1}{\sqrt{1+f'^2}} \frac{i}{2L}\sum_n \frac{1}{k_{nz}^0} e^{i(k_{nx}x+k_{nz}^0 z)} \Big[ ik_{nx}f'(x') - ik_{nz}^0 \Big] e^{-i(k_{nx}x'+k_{nz}^0 z')} \tag{3.6.3}$$

Inserting the periodic Green's function expansion into the scattered field expression of (3.6.1), results in an expansion of the scattered field in terms of the upward propagating harmonics of

$$E_{sy} = \sum_n B_n e^{i(k_{nx}x+k_{nz}^0 z)} \tag{3.6.4}$$

where $B_n$ is the amplitude of the $n$-th order scattered Bloch mode and is equal to

$$\begin{aligned} B_n = &-\frac{i}{2Lk_{nz}^0}\int_L \mathrm{d}x' \sqrt{1+f'^2}\hat{n}'\cdot\nabla' E_{0y} e^{-i(k_{nx}x'+k_{nz}^0 z')} \\ &+\frac{i}{2Lk_{nz}^0}\int_L \mathrm{d}x' E_{0y}\Big[ ik_{nx}f'(x') - ik_{nz}^0 \Big] e^{-i(k_{nx}x'+k_{nz}^0 z')} \end{aligned} \tag{3.6.5}$$

Using the Fourier expansion of the surface fields, which are known after solving (3.5.8), the scattered field mode coefficient $B_n$ can be written as

$$\begin{aligned} B_n = &-\frac{i}{2Lk_{nz}^0}\sum_m \beta_m^0 \int_L \mathrm{d}x' e^{i(k_{mx}-k_{nx})x'-ik_{nz}^0 f(x')} \\ &+\frac{i}{2Lk_{nz}^0}\sum_m \alpha_m^0 \int_L \mathrm{d}x' \Big[ik_{nx}f'(x')-ik_{nz}^0\Big] e^{i(k_{mx}-k_{nx})x'-ik_{nz}^0 f(x')} \end{aligned} \tag{3.6.6}$$

Performing the by part on the first term of the second integrand and defining the following potential integral of the scattered field as

$$I_{00}^+[m,n] = \int_L \mathrm{d}x' e^{i(k_{mx}-k_{nx})x'-ik_{nz}^0 f(x')} \tag{3.6.7}$$

the scattered field coefficient can be written as

$$B_n = -\frac{i}{2Lk_{nz}^0}\sum_m \beta_m^0 I_{00}^+[m,n] + \frac{i}{2Lk_{nz}^0}\sum_m \alpha_m^0 \frac{i(k_{nx}k_{mx}-k_{0t}^2)}{k_{nz}^0} I_{00}^+[m,n] \tag{3.6.8}$$

or in matrix form of,

$$\overline{B} = \overline{\overline{M}}_{00}^{0,+}\overline{\alpha}^0 + \overline{\overline{N}}_{00}^{0,+}\overline{\beta}^0 \tag{3.6.9}$$

Similarly, for the transmitted field, the equivalence principle should apply to the last region as

$$E_{ty} = \int_L \mathrm{d}l' \Big[ G_{Np}(\overline{\rho},\overline{\rho}')\hat{n}'\cdot\nabla' E_{Ny}(\overline{\rho}') - E_{Ny}(\overline{\rho}')\hat{n}'\cdot\nabla' G_{Np}(\overline{\rho},\overline{\rho}') \Big] \quad , \quad z<-d_{N-1}+f_{N-1}(x) \tag{3.6.10}$$

where $E_{ty}$ is the transmitted electric field into region $N$. Using region $N$ periodic Green's function expansion when $z<z'=-d_{N-1}+f_{N-1}(x)$ we have

$$G_{Np}(z<z') = \frac{i}{2L}\sum_n \frac{1}{k_{nz}^N} e^{i(k_{nx}x-k_{nz}^N z)} e^{-i(k_{nx}x'-k_{nz}^N z')} \tag{3.6.11}$$

and for its derivative,

$$\hat{n}'\cdot\nabla' G_{Np} = \frac{1}{\sqrt{1+f_{N-1}'^2}} \frac{i}{2L}\sum_n \frac{1}{k_{nz}^N} e^{i(k_{nx}x-k_{nz}^N z)} \Big[ik_{nx}f_{N-1}'(x')+ik_{nz}^N\Big] e^{-i(k_{nx}x'-k_{nz}^N z')} \tag{3.6.12}$$

Substituting the periodic Green's function expansion in the transmitted field expression yields a downward propagating Bloch mode expansion of the transmitted field as

$$E_{ty} = \sum_n A_n e^{i(k_{nx}x-k_{nz}^N z)} \tag{3.6.13}$$

where

$$\begin{aligned} A_n = &\int_L \mathrm{d}x' \sqrt{1+f_{n-1}'^2}\,\hat{n}'\cdot\nabla' E_{Ny} \frac{i}{2L}\sum_n \frac{1}{k_{nz}^N} e^{-i(k_{nx}x'-k_{nz}^N z')} \\ &-\int_L \mathrm{d}x' E_{Ny} \frac{i}{2L}\sum_n \frac{1}{k_{nz}^N}\Big[ik_{nx}f_{N-1}'(x')+ik_{nz}^N\Big] e^{-i(k_{nx}x'-k_{nz}^N z')} \end{aligned} \tag{3.6.14}$$

Using continuity condition of the tangential electric and magnetic fields across the last boundary,

$$E_{Ny}=E_{N-1,y} \tag{3.6.15}$$
$$\hat{n}\cdot\nabla_t E_{N,y}=\frac{k_{N,t}^2}{k_{N-1,t}^2}\frac{\varepsilon_{N-1}}{\varepsilon_N}\hat{n}\cdot\nabla_t E_{N-1,y}$$

and solution of the surface fields Fourier series, the mode coefficient of the transmitted field can be obtained as

$$A_n=\frac{i}{2Lk_{nz}^N}\left(\frac{k_{N,t}^2}{k_{N-1,t}^2}\frac{\varepsilon_{N-1}}{\varepsilon_N}\right)e^{-ik_{nz}^N d_{N-1}}\sum_m \beta_m^{N-1}\int_L \mathrm{d}x' e^{i(k_{mx}-k_{nx})x'+ik_{nz}^N f_{N-1}(x')} \tag{3.6.16}$$
$$-\frac{i}{2Lk_{nz}^N}e^{-ik_{nz}^N d_{N-1}}\sum_m \alpha_m^{N-1}\frac{i(k_{N,t}^2-k_{nx}k_{mx})}{k_{nz}^N}\int_L \mathrm{d}x' e^{i(k_{mx}-k_{nx})x'+ik_{nz}^N f_{N-1}(x')}$$

or in a matrix form,

$$\overline{A}=\overline{\overline{M}}^-_{N,N-1}\overline{\alpha}^{N-1}+\overline{\overline{N}}^-_{N,N-1}\overline{\beta}^{N-1} \tag{3.6.17}$$

where

$$\left[\overline{\overline{M}}^-_{N,N-1}\right]_{nm}=e^{-ik_{nz}^N d_{N-1}}\frac{(k_{N,t}^2-k_{nx}k_{mx})}{2Lk_{nz}^{N\,2}}I^-_{N,N-1}[m,n] \tag{3.6.18}$$
$$\left[\overline{\overline{N}}^-_{N,N-1}\right]_{nm}=e^{-ik_{nz}^N d_{N-1}}\frac{i}{2Lk_{nz}^N}\left(\frac{k_{N,t}^2}{k_{N-1,t}^2}\frac{\varepsilon_{N-1}}{\varepsilon_N}\right)I^-_{N,N-1}[m,n]$$

and potential integral for the transmitted field is defined as

$$I^-_{N,N-1}[m,n]=\int_L \mathrm{d}x' e^{i(k_{mx}-k_{nx})x'+ik_{nz}^N f_{N-1}(x')} \tag{3.6.19}$$

## 3.7 Scattered and Transmitted Power

From the surface fields solution, the scattered and transmitted electric fields are obtained as a sum of the Bloch modes in region 0 and $N$, respectively. Since for TE polarization the only non-zero component of the electric field is $E_y$ we can compute the associated magnetic field as

$$\overline{H}=\frac{1}{ik\eta}\nabla E_y\times\hat{y} \tag{3.7.1}$$

Therefore, the time averaged poynting vector becomes

$$\overline{S}=\frac{1}{2}\mathrm{Re}\left[E_y\hat{y}\times\left(\frac{1}{ik\eta}\nabla E_y\times\hat{y}\right)^*\right]=-\frac{1}{2}\mathrm{Im}\left[\frac{1}{k\eta}E_y\hat{y}\times\left(\nabla E_y^*\times\hat{y}\right)\right]=-\frac{1}{2}\mathrm{Im}\left[\frac{1}{k\eta}E_y\nabla E_y^*\right] \tag{3.7.2}$$

For the scattered field we are interested to the power flow in $+\hat{z}$ direction. Therefore,

$$\overline{S}_s\cdot\hat{z}=-\frac{1}{2}\mathrm{Im}\left[\frac{1}{k\eta}E_{sy}\left(\hat{z}\cdot\nabla E_{sy}^*\right)\right]=-\frac{1}{2}\mathrm{Im}\left[\frac{1}{k\eta}E_{sy}\frac{\partial E_{sy}^*}{\partial z}\right] \tag{3.7.3}$$

However, from the Bloch expansion of the scattered field,

$$\frac{\partial E_{sy}}{\partial z}=\sum_n ik_{nz}^0 B_n e^{i(k_{nx}x+k_{nz}^0 z)} \tag{3.7.4}$$

therefore,

$$\begin{aligned}\overline{S}_s\cdot\hat{z}&=-\frac{1}{2k\eta}\mathrm{Im}\left[\left(\sum_m B_m e^{i(k_{mx}x+k_{mz}^0 z)}\right)\left(\sum_n ik_{nz}^0 B_n e^{i(k_{nx}x+k_{nz}^0 z)}\right)^*\right] \\ &=-\frac{1}{2k\eta}\sum_m\sum_n \mathrm{Im}\left[(-ik_{nz}^{0\,*})B_m B_n^* e^{i(k_{mx}x+k_{mz}^0 z)}e^{-i(k_{nx}x+k_{nz}^{0\,*} z)}\right] \\ &=-\frac{1}{2k\eta}\sum_m\sum_n \mathrm{Im}\left[(-ik_{nz}^{0\,*})B_m B_n^* e^{i(k_{mx}-k_{nx})x}e^{i(k_{mz}^0-k_{nz}^{0\,*})z}\right]\end{aligned} \tag{3.7.5}$$

The scattered power can be obtained by integration of power density over one period,

$$P_s=\int_L \mathrm{d}x\,\overline{S}_s\cdot\hat{z}=-\frac{1}{2k\eta}\sum_m\sum_n \mathrm{Im}\left[(-ik_{nz}^{0\,*})B_m B_n^*\int_L \mathrm{d}x\,e^{i(k_{mx}-k_{nx})x}e^{i(k_{mz}^0-k_{nz}^{0\,*})z}\right] \tag{3.7.6}$$

But $e^{i(k_{mx}-k_{nx})x}=e^{i(m-n)2\pi x/L}$ is a periodic function and

$$\int_L \mathrm{d}x\,e^{i(k_{mx}-k_{nx})x}=\int_0^L \mathrm{d}x\,e^{i(m-n)2\pi x/L}=L\delta_{mn} \tag{3.7.7}$$

Thus,

$$\begin{aligned}P_s&=\int_L \mathrm{d}x\,\overline{S}_s\cdot\hat{z}=-\frac{L}{2k\eta}\sum_n |B_n|^2\mathrm{Im}\left[(-ik_{nz}^{0\,*})\right]e^{-2\mathrm{Im}(k_{nz}^0)z} \\ &=\frac{L}{2k\eta}\sum_n |B_n|^2\mathrm{Re}(k_{nz}^0)e^{-2\mathrm{Im}(k_{nz}^0)z}=\frac{L}{2\omega\mu_0}\sum_n |B_n|^2\mathrm{Re}(k_{nz}^0)\end{aligned} \tag{3.7.8}$$

Similarly, the transmitted power can be obtained as

$$P_t=\int_L \mathrm{d}x\,\overline{S}_t\cdot(-\hat{z})=\frac{L}{2\omega\mu_N}\sum_n |A_n|^2\mathrm{Re}(k_{nz}^N) \tag{3.7.9}$$

Presence of the factors $\mathrm{Re}(k_{nz}^0)$ and $\mathrm{Re}(k_{nz}^N)$ in scattered and transmitted power expressions shows that only propagating Bloch mode contributes to the power transfer. Also note that above derivation is for non-magnetic materials. Assuming a unit amplitude incident electric field, associated power flow along $-\hat{z}$ direction is $k_{iz}/2k\eta$ and the incident power is

$$P_{\mathrm{inc}}=\int_L \mathrm{d}x\,\frac{k_{iz}}{2k\eta}=\frac{Lk_{iz}}{2k\eta} \tag{3.7.10}$$

Then, the fraction of power which is reflected (total reflectivity) and transmitted (total transmissivity) are given by

$$\begin{aligned}S&=\frac{P_s}{P_{\mathrm{inc}}}=\sum_n |B_n|^2\frac{\mathrm{Re}(k_{nz^0})}{k_{iz}} \\ T&=\frac{P_t}{P_{\mathrm{inc}}}=\frac{\mu_0}{\mu_N}\sum_n |A_n|^2\frac{\mathrm{Re}(k_{nz}^N)}{k_{iz}}\end{aligned} \tag{3.7.11}$$

Notice that the above formula for the scattered and transmitted power considers lossless materials. For a general lossy materials

$$P_s = \frac{L}{2}\sum_n |B_n|^2 \mathrm{Im}\left[\frac{ik_{nz}^{0\ *}}{k\eta}\right] e^{-2\mathrm{Im}(k_{nz}^0)z} \tag{3.7.12}$$
$$= \frac{L}{2}\sum_n |B_n|^2 \mathrm{Re}\left[\frac{k_{nz}^{0\ *}}{k\eta}\right] e^{-2\mathrm{Im}(k_{nz}^0)z}$$

Two differences appear here, one is the loss exponential factor if the power at another plane is desired, and the second one is the propagating real power is no longer attributed to the propagating Bloch modes if $k\eta$ has an imaginary part. This only happens for lossy magnetic materials where $\mu$ is complex.

## 3.8 Numerical Considerations

Theoretically, for a given medium, there are finite number of propagating Bloch modes. However, inclusion of the propagating modes is not enough to correctly represent the surface field. Although the evanescent modes does not contribute to power transfer, they are critical in correct representation of the surface fields such that satisfy the proper border conditions.

However, one cannot and should not include all of them in a numerical procedure. On one side system of matrix equation should be finite.

The $T$-matrix solution or Extended Boundary Condition or equivalently using the Rayleigh Hypothesis assume that the scattered field is constitute of only upward propagating waves (same as mapping the integral equation to a surface above and below the boundary surface) and only consider those [68]. In turn if the properties of the boundary surface is such that allows for backward propagating wave, this phenomena is not captured within the formulation. Therefore, there is a limit of the shape and slope of the surface to be eligible for application of this method. If the surface is not a proper surface for applying the extended boundary condition method, one may want to try increasing number of included modes to overcome the neglected backward waves, but since upward and downward propagating waves are independent, increasing number of modes is not only useful but also makes the system of equations ill-condition. The reason of ill-condition system is by including more and more evanescent modes that have imaginary $k_{nz}$, the factor $e^{\pm ik_{nz}z}$ that appears in the propagation equations, becomes very large or very small number even for small values of $z$. Therefore this results in a matrix that has very large condition number to be inverted. Therefore, we need to include evanescent mode such that results in the well conditioned matrix equations. A key to find the proper number of included modes is by monitoring the energy conservation and condition number of the involved matrices for the corresponding lossless problem.

## 3.9 TM Excitation Case

The TM incident field is better represented through the magnetic field of $\overline{H} = \hat{y}H_{iy}$ and now the pilot component of the field is $H_y$ in each region. We can obtain the solution of TM problem using the duality transformation as

$$\begin{array}{c} E_y \Longrightarrow H_y \\ \mu \Longleftrightarrow \varepsilon \end{array} \tag{3.9.1}$$

# Chapter 4

# 3D Scattering From Dielectric Layered Media with Random Rough Interfaces, Small Perturbation Method (SPM2)

## 4.1 Introduction

Scattering of electromagnetic waves by random rough surfaces has broad applications in optical and microwave remote sensing, imaging, Nano photonic, plasmonic, radiative heat transfer and many other areas of science and engineering [3, 44, 49, 69–72] In particular, the problem of multi-layers with multiple interfaces have drawn attention recently [29–31, 34, 73]. There is a particular interest in applications where there are a large number of rough interfaces.

Analytical methods provide approximate solutions. There are generally two classical approaches[3]. The high frequency method known as Kirchhoff approach and low frequency method known as small perturbation method (SPM). Higher order perturbation method has been studied in [37] up to the fourth order. Also the fourth order perturbative solution of the two layer rough surfaces has been studied recently in [32, 38]. Other analytical methods include the AIEM method [42] and the Small Slope Approximation (SSA) [43].

In recent years, there are numerical methods based on surface integral equations [44–47], the extended boundary condition methods [49, 50] and the finite difference time domain method [51, 74]. However, for large number of rough interfaces, the dielectric contrasts between layers are usually weak, and numerical methods suffer from discretization errors. It is particularly difficult to achieve energy conservation using the numerical methods for large number of rough interfaces with small dielectric contrasts between adjacent layers where the numerical noise can dominate over the layers contrasts. The energy conservation in scattering from 2D multilayer rough surfaces has been studied recently [39]. However we need to have solution for actual physical problem of 3D electromagnetic scattering from multilayer medium with random rough interfaces that conserve energy as 2D layered media predicts different emissivities for TE and TM channels for observation angle normal to the surface.

In this chapter, we study energy conservation and emissivity in scattering process of electromagnetic waves from 3D multi-layer media with a large number random rough interfaces using the second order small perturbation method (SPM2). The formulation is

based on extinction theorem and developing integral equation for surface fields in spectral domain. Using SPM2, we calculate the scattered and transmitted coherent fields and incoherent fields. Energy conservation is calculated by integration of the coherent and incoherent reflected and transmitted power over the 2D $(k_x,k_y)$ spectral domain. It is shown that each of the coherent, and incoherent reflected and transmitted intensities consists of a summation of the contributions from each rough interface. For each interface in the integrand, the contribution is a product of the spectral density of roughness of the interface and the kernel function of $k_x,k_y$. In this paper we show that the kernel function of each rough interface obeys energy conservation. This means that energy is conserved independent of the statistics of the random rough surfaces nor the spectral densities of the rough profile of each interface. Results of this strong condition are illustrated numerically for up to 50 rough interfaces without the need of specifying any spectral density of the roughness. The methodology is also applied to study the effect of roughness on brightness temperature of Antarctic ice sheets. In the Antarctica, because of the pattern of accumulation o snow, the layered media consists of many layers with varying densities of ice giving rise to permittivity variations. The dielectric contrasts between adjacent layers are weak. The brightness temperature were previously studied for a multilayer model without roughness [41]. Comparisons of the multilayer SPM2 simulations are made with brightness temperatures measurements of SMOS (Soil Moisture Ocean Salinity ) satellite showing that theoretical simulations are in good agreement with experimental measurements. The outline of this chapter is as follows:

In section 4.2 , the integral equations for the surface fields on each rough interfaces using the Extinction theorem are developed. Section 4.5 dedicated to expansion of the integral equations in the spectral space and applying perturbation method up to the second order to find the surface fields and then scattered and transmitted fields. In section 4.6, coherent and incoherent, scattered and transmitted power have been discussed and then in section 4.7, the energy conservation constraint is derived and it is shown for the 50 layer case as an example. Application of the problem to the physical model of emission from the Antarctic ice sheets is discussed in the section 4.8 . The last section includes the energy conservation verification and the effect of roughness on scattering and transmission of power for a 1-D photonic crystal.

## 4.2 Problem Geometry

Consider closed region $V$ with boundary surface $\partial V$ with macroscopic parameters $\mu,\epsilon$ and region $V_1=\mathbb{R}^3-V$ that filled with $\mu_1,\epsilon_1$. Assume an incident wave $\overline{E}_{inc}(\overline{r})$ impinging upon closed region $V$ from exterior region.
For such a geometry, statement of Ewald-Osean Extinction theorem [3] reads

$$\overline{E}_{inc}(\overline{r})+\int_S \mathrm{d}S'\Big\{ik\eta\overline{\overline{G}}(\overline{r},\overline{r}')\cdot[\hat{n}'\times\overline{H}(\overline{r}')] \\ +\nabla\times\overline{\overline{G}}(\overline{r},\overline{r}')\cdot[\hat{n}'\times\overline{E}(\overline{r}')]\Big\}=\begin{cases}0, & \overline{r}\in V\\ \overline{E}(\overline{r}), & \overline{r}\notin V\end{cases} \tag{4.2.1}$$

where $\overline{\overline{G}}(\overline{r},\overline{r}')$ is electric field dyadic Green's function for unbounded space with wavenumber $k$

$$\overline{\overline{G}}(\overline{r},\overline{r}')=\left(\overline{\overline{I}}+\frac{\nabla\nabla}{k^2}\right)\frac{e^{ik|\overline{r}-\overline{r}'|}}{4\pi|\overline{r}-\overline{r}'|} \tag{4.2.2}$$

and $\hat{n}'(\overline{r}'_\perp)$ is local unit normal vector pointing outward of region $V$.

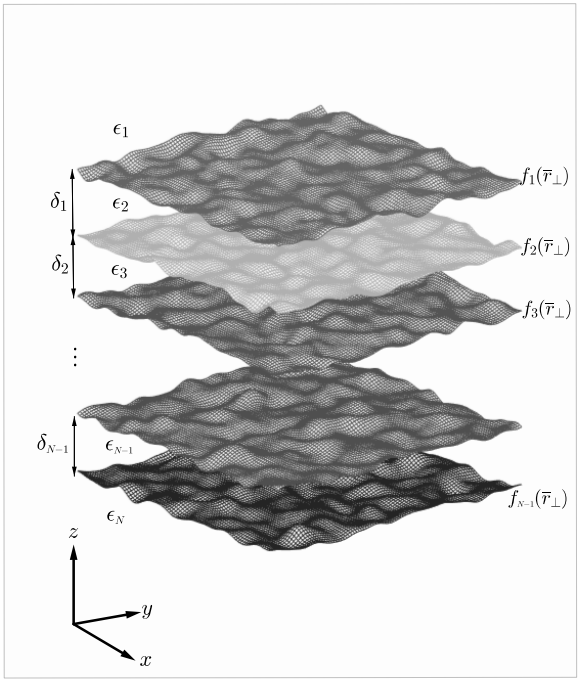


FIGURE 4.1: Geometry of Multi-layer structure with random rough interfaces. Every surface is extended to infinity on both $x$ and $y$ directions.

For the present problem we have $N$ distinct media. Figure 4.1 shows the geometry of the problem. There are $N$ homogeneous mediums such that common interface between two adjacent mediums is a random rough surface. The last media is a semi-infinite half space that is extended to $-\infty$ in $z$ direction. Assume an incident wave impinging upon the structure from the uppermost region (region 1). Incident wave that is propagating with wavenumber $k_1$ cannot exist in the other mediums (such as region 2 ) with different wavenumbers. Thus another field should be excited in that region (region 2) with wavenumber $k_1$ such that cancels out the incident field.

### 4.2.1 Incident Field in Spectral Domain

For an arbitrary incident wave of $\overline{E}_i(\overline{r})$ , it can be expanded in terms of a spectrum of plane waves as

$$\overline{E}_i(\overline{r})=\int \mathrm{d}\overline{k}_\perp \overline{E}_i(\overline{k})e^{i(k_{ix}x+k_{iy}y-k_{iz}z)} \tag{4.2.3}$$

where, $E_i(\overline{k})$ loosely represents the strength of the plane wave with wave vector $\overline{k}$ in the expansion. If the incident field is a single plane wave of $\overline{E}_i(\overline{r})=\hat{e}_i e^{i(\overline{k}_{i\perp}\cdot\overline{r}_\perp-k_{iz}z)}$ with definite wave vector $\overline{k}_i$, then

$$\overline{E}_i(\overline{r})=\hat{e}_i e^{i(\overline{k}_{i\perp}\cdot\overline{r}_\perp-k_{iz}z)}=\int \mathrm{d}\overline{k}_\perp \hat{e}_i\delta(\overline{k}_{i\perp}-\overline{k}_\perp)e^{i(k_{i\perp}\cdot\overline{r}_\perp-k_{iz}z)} \tag{4.2.4}$$

and spectrum of the incident field becomes,

$$\overline{E}_{inc}(\overline{k})=\hat{e}_i\delta(\overline{k}_{i\perp}-\overline{k}_{\perp}) \tag{4.2.5}$$

If incident field originated from a dipole source in $\hat{\alpha}$ direction at $\overline{r}_0=(0,0,z_0)$, we should solve the wave equation to obtain the incident field,

$$\nabla\times\nabla\times\overline{E}_i(\overline{r})-k^2\overline{E}_i(\overline{r})=ik\eta Il\hat{\alpha}\delta(\overline{r}_{\perp})\delta(z-z_0) \tag{4.2.6}$$

The incident field that satisfies the above vector wave equation, can be obtained by the dyadic Green's function of free space $\overline{\overline{G}}(\overline{r},\overline{r}')$ that satisfies the same vector wave equation (and radiation condition at infinity)

$$\overline{E}(\overline{r})=ik\eta Il\overline{\overline{G}}(\overline{r},\overline{r}')\cdot\hat{\alpha} \tag{4.2.7}$$

Since we are interested in plane wave expansion of the incident field, we can use plane wave expansion of the dyadic Green's function. If we assume that the source is radiating to the region of interest from above (like satellite), for $z<z'$ we have

$$\overline{\overline{G}}(\overline{r},\overline{r}')=\frac{i}{2(2\pi)^2}\int\frac{1}{k_z}\mathrm{d}k_{\perp}\ \left[\hat{h}(-k_z)\hat{h}(-k_z)+\hat{e}(-k_z)\hat{e}(-k_z)\right]e^{i\overline{k}_{\perp}\cdot(\overline{r}_{\perp}-\overline{r}'_{\perp})-ik_z(z-z')} \tag{4.2.8}$$

Therefore,

$$\overline{E}_i(\overline{r})=-\frac{k\eta Il}{2(2\pi)^2}\int\frac{1}{k_z}\mathrm{d}k_{\perp}\ \left[\hat{h}(-k_z)\hat{h}(-k_z)+\hat{e}(-k_z)\hat{e}(-k_z)\right]\cdot\hat{\alpha}e^{i\overline{k}_{\perp}\cdot\overline{r}_{\perp}-ik_z(z-z_0)} \tag{4.2.9}$$

Comparing (4.2.9) with the original expansion of (4.2.3), spectral representation of the incident field can be identified as

$$\overline{E}_i(\overline{k})=-\frac{k\eta Il}{2(2\pi)^2}\frac{1}{k_z}\ \left[\hat{h}(-k_z)\hat{h}(-k_z)+\hat{e}(-k_z)\hat{e}(-k_z)\right]\cdot\hat{\alpha}e^{ik_zz_0} \tag{4.2.10}$$

For example if we have a horizontal dipole aligned along $\hat{\alpha}=\hat{x}$, the TE and TM components of the incident field spectrum are proportional to

$$\begin{aligned}\hat{e}(-k_z)\cdot\hat{x}&=\frac{1}{k_\rho}(\hat{x}k_y-\hat{y}k_x)\cdot\hat{x}=\frac{k_y}{k_\rho}\\ \hat{h}(-k_z)\cdot\hat{x}&=\left[\frac{k_z}{kk_\rho}(\hat{x}k_x+\hat{y}k_y)+\frac{k_\rho}{k}\hat{z}\right]\cdot\hat{x}=\frac{k_xk_z}{kk_\rho}\end{aligned} \tag{4.2.11}$$

Note that a horizontal dipole produce both TM and TE polarizations. Using (4.2.11) in (4.2.10) results in

$$\overline{E}_i(\overline{k})=-\frac{k\eta Il}{2(2\pi)^2}\frac{e^{ik_zz_0}}{k_z}\ \left[\frac{k_xk_z}{kk_\rho}\hat{h}(-k_z)+\frac{k_y}{k_\rho}\hat{e}(-k_z)\right] \tag{4.2.12}$$

On the other hand, a vertical dipole ($z$-directed) only radiates vertical polarized (TM) electric field.

## 4.3 Integral Equation for the Surface Fields

In this section, we formulate the problem using integral equation in terms of the electric and magnetic surface currents on the interfaces. We assume the electric and magnetic fields over the boundaries and according to the Extinction theorem, the surface currents should satisfy certain constraints from where the surface currents can be obtained.

### 4.3.1 Extinction of Downward Propagating Wave in region 1

According to the extinction theorem, the incident wave propagating in region 1 with the wave number $k_1$ cannot be present in other regions as it is not solution of the Maxwell's equations. Therefore, a set of surface current should exist over the dielectric boundary such that upon propagation with region 1 Green's function cancel the incident field in other regions. Mathematically [47, 52],

$$\overline{E}_{inc}(\overline{r})+\int_{S_1}\mathrm{d}S'\Big\{ik_1\eta_1\overline{\overline{G}}_1(\overline{r},\overline{r}')\cdot[\hat{n}_1\times\overline{H}_1(\overline{r}')]+\nabla\times\overline{\overline{G}}_1(\overline{r},\overline{r}')\cdot[\hat{n}_1\times\overline{E}_1(\overline{r}')]\Big\}=0, z<f_1(\overline{r}_\perp) \tag{4.3.1}$$

where, $\overline{E}_1(\overline{r})$ and $\overline{H}_1(\overline{r})$ are electromagnetic fields in the region 1, $\hat{n}_1$ is the unit normal to the boundary (that points into region 1), and $\overline{\overline{G}}_1(\overline{r},\overline{r}')$ is the free space dyadic Green's function (that satisfies the radiation condition at infinity) in region 1, i.e. with wave number $k_1=\omega\sqrt{\mu_1\varepsilon_1}$. In the above integral equation the unknowns are tangential electric and magnetic fields at the boundary $z=f_1(x,y)$. Here, the surface fields are unambiguously defined as the boundary condition on the tangential electromagnetic fields of region 1 and 2 requires that

$$\begin{aligned}\hat{n}_1\times\overline{E}_1(\overline{r}')&=\hat{n}_1\times\overline{E}_2(\overline{r}')\\ \hat{n}_1\times\overline{H}_1(\overline{r}')&=\hat{n}_1\times\overline{H}_2(\overline{r}')\end{aligned} \tag{4.3.2}$$

Defining the surface field variables of $\overline{a}_1(x,y)$ and $\overline{b}_1(x,y)$ over the boundary in terms of region 1 tangential fields according to

$$\begin{aligned}\overline{a}_1(x,y)\mathrm{d}x'\mathrm{d}y'&=\hat{n}_1\times\eta_1\overline{H}_1(\overline{r}')\mathrm{d}S'\\ \overline{b}_1(x,y)\mathrm{d}x'\mathrm{d}y'&=\hat{n}_1\times\overline{E}_1(\overline{r}')\mathrm{d}S'\end{aligned} \tag{4.3.3}$$

Note that Using this definition, both unknown fields $\overline{a}_1(x,y)$ and $\overline{b}_1(x,y)$ have dimension of the electric field. Second, the measure of integration is changed from the general surface element $\mathrm{d}S$ to the Cartesian surface element $\mathrm{d}x\mathrm{d}y$ that simplifies dealing with the surface Jacobian. The statement of the extinction theorem in terms of the ne surface field variables can be written as

$$\overline{E}_{inc}(\overline{r})+\int\mathrm{d}\overline{r}'_\perp\Big\{ik_1\overline{\overline{G}}_1(\overline{r},\overline{r}')\cdot\overline{a}_1(\overline{r}'_\perp)+\nabla\times\overline{\overline{G}}_1(\overline{r},\overline{r}')\cdot\overline{b}_1(\overline{r}'_\perp)\Big\}=0, z<f_1(\overline{r}_\perp) \tag{4.3.4}$$

where $\overline{r}_\perp=(x,y)$. Assuming the observation point is placed somewhere below the boundary surface such that $z<f_1(\overline{r}_\perp)$ for all values of $\overline{r}_\perp$ ($z<\min\limits_{\overline{r}_\perp} f_1(\overline{r}_\perp)$), we can expand the dyadic Green's function under condition $z<z'$ in spectral domain (see Appendix B) as

$$\overline{\overline{G}}_1(\overline{r},\overline{r}')=\frac{i}{2(2\pi)^2}\int\mathrm{d}k_\perp\frac{1}{k_{1z}}\Big[\hat{e}(-k_{1z})\hat{e}(-k_{1z})+\hat{h}(-k_{1z})\hat{h}(-k_{1z})\Big]e^{i\overline{k}_\perp\cdot(\overline{r}_\perp-\overline{r}'_\perp)-ik_{1z}(z-z')} \tag{4.3.5}$$

Notice that here the observation point is restricted to always be below the source location (which is on the surface). Only under this condition the spectral expansion of (4.3.5) is valid. The integral equation of (4.3.4) is not a surface integral equation as the observation point is not on the boundary surface. The observation point is placed on an extension of the boundary surface, not itself. That is why the integral equation formulation of(4.3.4) sometimes is called *Extended Boundary Condition Method* (EBCM). Within EBCM, in order to use the spectral expansion of the dyadic Green's function, a definite direction for radiation of the surface field is taken (for (4.3.5) it is downward) which means that counter propagating wave are neglected. The EBCM is closely related to the *Rayleigh Hypothesis* about the scattering from a surface. According to the Rayleigh hypothesis, the scattered field from a surface can be written in terms of a linear combination of upward propagating waves in that region. As it is clear, the properties of the surface can be in such a way that allows for the backward wave toward the surface, like a shadowed surface and Rayleigh hypothesis is not correct in general. However, if we put an upper limit on the slop of the surface, then the backwards scattered wave toward the surface is unlikely or if it happens the effect would be negligible. It can be shown that the Rayleigh hypothesis and extended boundary condition method are equivalent formulations that results in the same answer for scattering from the rough interfaces. However, since we consider the problem with small height and slope, the extended boundary condition formulation would be highly dependable.

Going back to the extinction relation (4.3.4), we also need to determine the expression of $\nabla\times\overline{\overline{G}}_1(\overline{r},\overline{r}')$. By operating $\nabla\times$ on both sides of (4.3.5), utilizing that plane waves are eigenvectors of the $\nabla$,

$$\nabla\times\left\{\hat{e}(-k_{1z})\hat{e}(-k_{1z})e^{i\overline{k}_\perp\cdot(\overline{r}_\perp-\overline{r}'_\perp)-ik_{1z}(z-z')}\right\}=i\overline{K}_1\times\left\{\hat{e}(-k_{1z})\hat{e}(-k_{1z})e^{i\overline{k}_\perp\cdot(\overline{r}_\perp-\overline{r}'_\perp)-ik_{1z}(z-z')}\right\} \tag{4.3.6}$$

and using the definition of the polarization unit vectors (Chapter 1) it can be written as

$$\nabla\times\overline{\overline{G}}_1(\overline{r},\overline{r}')=-\frac{1}{2(2\pi)^2}\int \mathrm{d}k_\perp\frac{k_1}{k_{1z}}\Big[-\hat{h}(-k_{1z})\hat{e}(-k_{1z})+\hat{e}(-k_{1z})\hat{h}(-k_{1z})\Big]e^{i\overline{k}_\perp\cdot(\overline{r}_\perp-\overline{r}'_\perp)-ik_{1z}(z-z')} \tag{4.3.7}$$

Where $\overline{K}_1=k_{1x}\hat{x}+k_{1y}\hat{y}-k_{1z}\hat{z}$ is the wave vector of a downward propagating wave in region 0. For the upward and downward propagating plane waves, the triplets $\{\hat{h}(k_{1z}),\hat{e}(k_{1z}),\hat{k}_1\}$ and $\{\hat{h}(-k_{1z}),\hat{e}(-k_{1z}),\hat{K}_1\}$ constitute a right handed orthogonal unit vectors, respectively. Inserting the Green's function and its derivative expansions into the extinction relation of the incident field and noting that the plane waves with different values of $\overline{k}_\perp$ are orthogonal and in turn independent, we arrive at

$$\begin{aligned}
\overline{E}_{inc}(\overline{k})&-\frac{1}{2}\frac{k_1}{k_{1z}}\hat{e}(-k_{1z})\hat{e}(-k_{1z})\cdot\frac{1}{(2\pi)^2}\int \mathrm{d}\overline{r}'_\perp\overline{a}_1(\overline{r}'_\perp)e^{-i\left(\overline{k}_\perp\cdot\overline{r}'_\perp-k_{1z}f_1(\overline{r}'_\perp)\right)}\\
&-\frac{1}{2}\frac{k_1}{k_{1z}}\hat{h}(-k_{1z})\hat{h}(-k_{1z})\cdot\frac{1}{(2\pi)^2}\int \mathrm{d}\overline{r}'_\perp\overline{a}_1(\overline{r}'_\perp)e^{-i\left(\overline{k}_\perp\cdot\overline{r}'_\perp-k_{1z}f_1(\overline{r}'_\perp)\right)}\\
&+\frac{1}{2}\frac{k_1}{k_{1z}}\hat{h}(-k_{1z})\hat{e}(-k_{1z})\cdot\frac{1}{(2\pi)^2}\int \mathrm{d}\overline{r}'_\perp\overline{b}_1(\overline{r}'_\perp)e^{-i\left(\overline{k}_\perp\cdot\overline{r}'_\perp-k_{1z}f_1(\overline{r}'_\perp)\right)}\\
&-\frac{1}{2}\frac{k_1}{k_{1z}}\hat{e}(-k_{1z})\hat{h}(-k_{1z})\cdot\frac{1}{(2\pi)^2}\int \mathrm{d}\overline{r}'_\perp\overline{b}_1(\overline{r}'_\perp)e^{-i\left(\overline{k}_\perp\cdot\overline{r}'_\perp-k_{1z}f_1(\overline{r}'_\perp)\right)}=0
\end{aligned} \tag{4.3.8}$$

Here we used the fact that the polarization unit vectors $\hat{e}(-k_z)$ and $\hat{h}(-k_z)$ are not functions of spatial coordinates they can be swept out of the spatial integration. To convert integrals

to the Fourier type integrals and separating the roughness part from that of flat surface, the factor in the integrand can be decomposed to

$$e^{-i\left(\overline{k}_\perp\cdot\overline{r}'_\perp-k_{1z}f_1(\overline{r}'_\perp)\right)}=e^{-i\overline{k}_\perp\cdot\overline{r}'_\perp}\left[e^{ik_{1z}f_1(\overline{r}'_\perp)}-1\right]+e^{-i\overline{k}_\perp\cdot\overline{r}'_\perp} \tag{4.3.9}$$

The first term vanishes for the case of flat surface. Considering a Fourier pair for the surface fields as

$$\begin{aligned}\overline{A}_1(\overline{k}_\perp)&=\frac{1}{(2\pi)^2}\int \mathrm{d}\overline{r}'_\perp\,\overline{a}_1(\overline{r}'_\perp)e^{-i\overline{k}_\perp\cdot\overline{r}'_\perp}\\ \overline{a}_1(\overline{r}'_\perp)&=\int \mathrm{d}\overline{k}'_\perp\,\overline{A}_1(\overline{k}'_\perp)e^{i\overline{k}'_\perp\cdot\overline{r}'_\perp}\end{aligned} \tag{4.3.10}$$

and inserting Fourier transform of the fields in the extinction relation of (4.3.8), it can be written as

$$\begin{aligned}\overline{E}_{inc}(\overline{k})&-\frac{1}{2}\frac{k_1}{k_{1z}}\hat{e}(-k_{1z})\hat{e}(-k_{1z})\cdot\left\{\overline{A}_1(\overline{k}_\perp)+\int \mathrm{d}\overline{k}'_\perp\, I_{11}^-(\overline{k}_\perp;\overline{k}'_\perp)\overline{A}_1(\overline{k}'_\perp)\right\}\\ &-\frac{1}{2}\frac{k_1}{k_{1z}}\hat{h}(-k_{1z})\hat{h}(-k_{1z})\cdot\left\{\overline{A}_1(\overline{k}_\perp)+\int \mathrm{d}\overline{k}'_\perp\, I_{11}^-(\overline{k}_\perp;\overline{k}'_\perp)\overline{A}_1(\overline{k}'_\perp)\right\}\\ &+\frac{1}{2}\frac{k_1}{k_{1z}}\hat{h}(-k_{1z})\hat{e}(-k_{1z})\cdot\left\{\overline{B}_1(\overline{k}_\perp)+\int \mathrm{d}\overline{k}'_\perp\, I_{11}^-(\overline{k}_\perp;\overline{k}'_\perp)\overline{B}_1(\overline{k}'_\perp)\right\}\\ &-\frac{1}{2}\frac{k_1}{k_{1z}}\hat{e}(-k_{1z})\hat{h}(-k_{1z})\cdot\left\{\overline{B}_1(\overline{k}_\perp)+\int \mathrm{d}\overline{k}'_\perp\, I_{11}^-(\overline{k}_\perp;\overline{k}'_\perp)\overline{B}_1(\overline{k}'_\perp)\right\}=0\end{aligned} \tag{4.3.11}$$

Here, the kernel of integral equation $I_{11}^-(\overline{k}_\perp;\overline{k}'_\perp)$ is the scattering potential (in conjunction with the Lippmann-Schwinger equations in quantum scattering) experienced by the downward propagating wave in region 1 in scattering from the first surface and is defined as

$$I_{11}^-(\overline{k}_\perp;\overline{k}'_\perp)=\frac{1}{(2\pi)^2}\int \mathrm{d}\overline{r}'_\perp\, e^{-i\left[(k_x-k'_x)x'+(k_y-k'_y)y'\right]}\left[e^{ik_{1z}f_1(\overline{r}'_\perp)}-1\right] \tag{4.3.12}$$

The first subscript shows it is related to the wave propagating (wavenumber) in region 1 and second one stands for the first rough surface. the minus sign shows that it is responsible for a downward propagating wave (respect to $z$).Note that if interface $z=f_1(x,y)$ is a flat surface at $z=0$, the scattering potential is equal to zero.

Equation 4.3.11 is a vector equation for vector unknowns $\overline{A}_1$ and $\overline{B}_1$. However, it cannot be solved directly in $\mathbb{R}^3$ as it contains only two independent equation. Although unknown surface fields have a representation in 3 dimension, they are really 2D objects. Therefore, solving (4.3.11) directly in $\mathbb{R}^3$ is not possible. We can obtain the scalar components by projecting the equation on the unit vectors $\hat{e}(-k_{1z})$ and $\hat{h}(-k_{1z})$. For TE and TM components of the extinction equation, (4.3.11) should be pre-multiplied by polarization unit vectors to get two scalar integral equations,

$$\begin{aligned}\hat{e}(-k_{1z})\cdot\tilde{\overline{E}}_{inc}(\overline{k}_\perp)&-\frac{1}{2}\frac{k_1}{k_{1z}}\hat{e}(-k_{1z})\cdot\left\{\overline{A}_1(\overline{k}_\perp)+\int \mathrm{d}\overline{k}'_\perp\, I_{11}^-(\overline{k}_\perp;\overline{k}'_\perp)\overline{A}_1(\overline{k}'_\perp)\right\}\\ &-\frac{1}{2}\frac{k_1}{k_{1z}}\hat{h}(-k_{1z})\cdot\left\{\overline{B}_1(\overline{k}_\perp)+\int \mathrm{d}\overline{k}'_\perp\, I_{11}^-(\overline{k}_\perp;\overline{k}'_\perp)\overline{B}_1(\overline{k}'_\perp)\right\}=0\end{aligned} \tag{4.3.13}$$

$$\hat{h}(-k_{1z})\cdot\tilde{\overline{\overline{E}}}_{inc}(\overline{k}_\perp)-\frac{1}{2}\frac{k_1}{k_{1z}}\hat{h}(-k_{1z})\cdot\left\{\overline{A}_1(\overline{k}_\perp)+\int \mathrm{d}\overline{k}'_\perp I_{11}^-(\overline{k}_\perp;\overline{k}'_\perp)\overline{A}_1(\overline{k}'_\perp)\right\} \tag{4.3.14}$$
$$+\frac{1}{2}\frac{k_1}{k_{1z}}\hat{e}(-k_{1z})\cdot\left\{\overline{B}_1(\overline{k}_\perp)+\int \mathrm{d}\overline{k}'_\perp I_{11}^-(\overline{k}_\perp;\overline{k}'_\perp)\overline{B}_1(\overline{k}'_\perp)\right\}=0$$

In order to extract scalar components of the surface fields, we can use another right handed set of unit vector in the spectral domain $\{\hat{p}(\overline{k}_\perp),\hat{q}(\overline{k}_\perp),\hat{z}\}$ that are defined at any point $\overline{k}_\perp=(k_x,k_y)$ as

$$\hat{p}(\overline{k}_\perp)=\frac{k_x\hat{x}+k_y\hat{y}}{k_\perp} \tag{4.3.15}$$
$$\hat{p}(\overline{k}_\perp)=\frac{-k_y\hat{x}+k_x\hat{y}}{k_\perp}$$

Inserting a unit dyad $\overline{\overline{I}}=\hat{p}(\overline{k}_\perp)\hat{p}(\overline{k}_\perp)+\hat{q}(\overline{k}_\perp)\hat{q}(\overline{k}_\perp)+\hat{z}\hat{z}$ between the dot products results in a set of scalar integral equations for scalar surface fields unknowns,

$$\hat{e}(-k_{1z})\cdot\tilde{\overline{\overline{E}}}_{inc}(\overline{k}_\perp)-\frac{1}{2}\frac{k_1}{k_{1z}}\Big\{A_{1q}(\overline{k}_\perp)+\int \mathrm{d}\overline{k}'_\perp I_{11}^-(\overline{k}_\perp;\overline{k}'_\perp)\hat{e}(-k_{1z})\cdot\hat{p}(\overline{k}'_\perp)A_{1p}(\overline{k}'_\perp) \tag{4.3.16}$$
$$+\int \mathrm{d}\overline{k}'_\perp I_{11}^-(\overline{k}_\perp;\overline{k}'_\perp)\hat{e}(-k_{1z})\cdot\hat{q}(\overline{k}'_\perp)A_{1q}(\overline{k}'_\perp)\Big\}$$
$$-\frac{1}{2}\frac{k_1}{k_{1z}}\Big\{\frac{k_{1z}}{k_1}B_{1p}(\overline{k}_\perp)+\frac{k_\rho}{k_1}B_{1z}(\overline{k}_\perp)$$
$$+\int \mathrm{d}\overline{k}'_\perp I_{11}^-(\overline{k}_\perp;\overline{k}'_\perp)\hat{h}(-k_{1z})\cdot\hat{p}(\overline{k}'_\perp)B_{1p}(\overline{k}'_\perp)$$
$$+\int \mathrm{d}\overline{k}'_\perp I_{11}^-(\overline{k}_\perp;\overline{k}'_\perp)\hat{h}(-k_{1z})\cdot\hat{q}(\overline{k}'_\perp)B_{1q}(\overline{k}'_\perp)$$
$$+\int \mathrm{d}\overline{k}'_\perp I_{11}^-(\overline{k}_\perp;\overline{k}'_\perp)\hat{h}(-k_{1z})\cdot\hat{z}\,B_{1z}(\overline{k}'_\perp)\Big\}=0$$

$$\hat{h}(-k_{1z})\cdot\tilde{\overline{\overline{E}}}_{inc}(\overline{k}_\perp)-\frac{1}{2}\frac{k_1}{k_{1z}}\Big\{\frac{k_{1z}}{k_1}A_{1p}(\overline{k}_\perp)+\frac{k_\rho}{k_1}A_{1z}(\overline{k}_\perp) \tag{4.3.17}$$
$$+\int \mathrm{d}\overline{k}'_\perp I_{11}^-(\overline{k}_\perp;\overline{k}'_\perp)\hat{h}(-k_{1z})\cdot\hat{p}(\overline{k}'_\perp)A_{1p}(\overline{k}'_\perp)$$
$$+\int \mathrm{d}\overline{k}'_\perp I_{11}^-(\overline{k}_\perp;\overline{k}'_\perp)\hat{h}(-k_{1z})\cdot\hat{q}(\overline{k}'_\perp)A_{1q}(\overline{k}'_\perp)$$
$$+\int \mathrm{d}\overline{k}'_\perp I_{11}^-(\overline{k}_\perp;\overline{k}'_\perp)\hat{h}(-k_{1z})\cdot\hat{z}\,A_{1z}(\overline{k}'_\perp)\Big\}$$
$$+\frac{1}{2}\frac{k_1}{k_{1z}}\Big\{B_{1q}(k_x,k_y)+\int \mathrm{d}\overline{k}'_\perp I_{11}^-(\overline{k}_\perp;\overline{k}'_\perp)\hat{e}(-k_{1z})\cdot\hat{p}(\overline{k}'_\perp)B_{1p}(\overline{k}'_\perp)$$
$$+\int \mathrm{d}\overline{k}'_\perp I_{11}^-(\overline{k}_\perp;\overline{k}'_\perp)\hat{e}(-k_{1z})\cdot\hat{q}(\overline{k}'_\perp)B_{1q}(\overline{k}'_\perp)\Big\}=0$$

Notice that the surface field vectors $\overline{A}$ and $\overline{B}$ are essentially 2 dimensional objects in the coordinate system that is attached to the surface and changing from a point to others.

However, here we used three components to describe them in another coordinate system but it is still a 2 dimensional object. Therefore, all three components cannot be independent and this is indeed the case. Since these are tangential surface fields, $\hat{n}_1\cdot\overline{A}_1=\hat{n}_1\cdot\overline{B}_1=0$ and this provides another description to the extinction equations to have a consistent system. Equivalently, one may use the orthogonality condition for the spatial fields $\hat{n}_1\cdot\overline{a}_1(\overline{r}_\perp)=\hat{n}_1\cdot\overline{b}_1(\overline{r}_\perp)=0$ to write

$$\frac{\hat{z}-\nabla_\perp f_1(\overline{r}_\perp)}{\sqrt{1+|\nabla_\perp f_1|^2}}\cdot\overline{a}_1(\overline{r})=0 \tag{4.3.18}$$

or

$$\overline{a}_1(\overline{r}_\perp)\cdot\hat{z}=\nabla_\perp f_1(\overline{r}_\perp)\cdot\overline{a}_1(\overline{r}_\perp) \tag{4.3.19}$$

that yields the $z$-component in terms of the transverse components of the surface fields. Therefore, each surface field vector brings two scalar unknowns into the system of equations. Equation. 4.3.19 can be transformed to the spectral domain to get

$$\overline{A}_1(\overline{k}_\perp)\cdot\hat{z}=\int \mathrm{d}\overline{k}_\perp i(\overline{k}_\perp-\overline{k}'_\perp)\cdot\overline{A}_1(\overline{k}'_\perp)F_1(\overline{k}_\perp-\overline{k}'_\perp) \tag{4.3.20}$$

where, $F_1(\overline{k}_\perp)$ is the Fourier transform of the boundary surface.

### 4.3.2 Extinction of Upward Propagating Wave in Region $m$

Similar to the extinction of the wave in region 1, the extinction theorem for the wave propagating in region $m$ can be written as

$$\begin{aligned}0=&-\oint_{\partial V_m}\mathrm{d}S'\left\{ik_m\eta_m\overline{\overline{G}}_m(\overline{r},\overline{r}')\cdot[\hat{n}'\times\overline{H}_m(\overline{r}')]+\nabla\times\overline{\overline{G}}_m(\overline{r}',\overline{r})\cdot[\hat{n}'\times\overline{E}_m(\overline{r}')]\right\} \\ =&-\int_{S_{m-1}}\mathrm{d}S'\left\{ik_m\eta_m\overline{\overline{G}}_m(\overline{r},\overline{r}')\cdot[\hat{n}'_{m-1}\times\overline{H}_m(\overline{r}')]+\nabla\times\overline{\overline{G}}_m(\overline{r}',\overline{r})\cdot[\hat{n}'_{m-1}\times\overline{E}_m(\overline{r}')]\right\} \\ &+\int_{S_m}\mathrm{d}S'\left\{ik_m\eta_m\overline{\overline{G}}_m(\overline{r},\overline{r}')\cdot[\hat{n}'_m\times\overline{H}_m(\overline{r}')]+\nabla\times\overline{\overline{G}}_m(\overline{r}',\overline{r})\cdot[\hat{n}'_m\times\overline{E}_m(\overline{r}')]\right\}\end{aligned} \tag{4.3.21}$$

Here, $\overline{\overline{G}}_m$ is the dyadic Green's function in region $m$, $S_m$ and $S_{m-1}$ are the lower and upper boundary surfaces of region $m$ and $\hat{n}_m$ is the unit normal to the surface $S_m$ that has a positive component along $z$. Over the boundary at $z=-d_{m-1}+f_{m-1}(x,y)$, we can define the surface fields in terms of region $m-1$ fields (surface fields are continuous across the boundary)

$$\begin{aligned}\mathrm{d}S'\hat{n}'_m\times\eta_{m-1}\overline{H}_m(\overline{r}')=\mathrm{d}S'\eta_{m-1}\hat{n}'_{m-1}\times\overline{H}_{m-1}(\overline{r}')=\mathrm{d}x'\mathrm{d}y'\overline{a}_{m-1}(x',y') \\ \mathrm{d}S'\hat{n}'_m\times\overline{E}_m(\overline{r}')=\mathrm{d}S'\hat{n}'_{m-1}\times\overline{E}_{m-1}(\overline{r}')=\mathrm{d}x'\mathrm{d}y'\overline{b}_{m-1}(x',y')\end{aligned} \tag{4.3.22}$$

and for second boundary of $z=-d_m+f_m(x,y)$ we use region $m$ fields to define the surface field variables as

$$\begin{aligned}\mathrm{d}S'\hat{n}'_m\times\eta_m\overline{H}_m(\overline{r}')=\mathrm{d}x'\mathrm{d}y'\overline{a}_m(x',y') \\ \mathrm{d}S'\hat{n}'_m\times\overline{E}_m(\overline{r}')=\mathrm{d}x'\mathrm{d}y'\overline{b}_m(x',y')\end{aligned} \tag{4.3.23}$$

Note that unit normal vectors for the upper and lower boundaries are different but we include their differences as a part of unknown surface fields. Also for Non-magnetic material case $k\eta=k_m\eta_m=k_{m-1}\eta_{m-1}=\omega\mu$, so that the integral equation (4.3.21) becomes

$$\begin{aligned}0=&-\int_{S_{m-1}}\mathrm{d}\overline{r}'_\perp\left\{ik_{m-1}\overline{\overline{G}}_m(\overline{r},\overline{r}')\cdot\overline{a}_{m-1}(\overline{r}'_\perp)]+\nabla\times\overline{\overline{G}}_m(\overline{r}',\overline{r})\cdot\overline{b}_{m-1}(\overline{r}'_\perp)\right\}\\&+\int_{S_m}\mathrm{d}\overline{r}'_\perp\left\{ik_m\overline{\overline{G}}_m(\overline{r},\overline{r}')\cdot\overline{a}_m(\overline{r}'_\perp)+\nabla\times\overline{\overline{G}}_m(\overline{r}',\overline{r})\cdot\overline{b}_m(\overline{r}'_\perp)\right\}\end{aligned}\tag{4.3.24}$$

For the wave that goes up to the upper regions, i.e. the observation point placed in the upper regions always $z>z'$ and we can expand the dyadic Green's function in region $m$ as

$$\overline{\overline{G}}_m(\overline{r},\overline{r}')=\frac{i}{2(2\pi)^2}\int\frac{1}{k_{mz}}\mathrm{d}\overline{k}_\perp\ \left[\hat{e}(k_{mz})\hat{e}(k_{mz})+\hat{h}(k_{mz})\hat{h}(k_{mz})\right]e^{i\overline{k}_\perp\cdot(\overline{r}_\perp-\overline{r}'_\perp)+ik_{mz}(z-z')}\tag{4.3.25}$$

Substituting the Green's function and its derivative into the integral equation (4.3.24), utilizing independence of the plane waves at different points, and introducing the Fourier transform of the surface fields, the integral equation can be written as

$$\begin{aligned}&+\frac{1}{2}\frac{k_{m-1}}{k_{mz}}e^{ik_{mz}d_{m-1}}\left[\hat{e}(k_{mz})\hat{e}(k_{mz})\right]\cdot\left\{\overline{A}_{m-1}(\overline{k}_\perp)+\int\mathrm{d}\overline{k}'_\perp I^+_{m,m-1}(\overline{k}_\perp;\overline{k}'_\perp)\overline{A}_{m-1}(\overline{k}'_\perp)\right\}\\&+\frac{1}{2}\frac{k_{m-1}}{k_{mz}}e^{ik_{mz}d_{m-1}}\left[\hat{h}(k_{mz})\hat{h}(k_{mz})\right]\cdot\left\{\overline{A}_{m-1}(\overline{k}_\perp)+\int\mathrm{d}\overline{k}'_\perp I^+_{m,m-1}(\overline{k}_\perp;\overline{k}'_\perp)\overline{A}_{m-1}(\overline{k}'_\perp)\right\}\\&+\frac{1}{2}\frac{k_m}{k_{mz}}e^{ik_{mz}d_{m-1}}\left[-\hat{h}(k_{mz})\hat{e}(k_{mz})\right]\cdot\left\{\overline{B}_{m-1}(\overline{k}_\perp)+\int\mathrm{d}\overline{k}'_\perp I^+_{m,m-1}(\overline{k}_\perp;\overline{k}'_\perp)\overline{B}_{m-1}(\overline{k}'_\perp)\right\}\\&+\frac{1}{2}\frac{k_m}{k_{mz}}e^{ik_{mz}d_{m-1}}\left[\hat{e}(k_{mz})\hat{h}(k_{mz})\right]\cdot\left\{\overline{B}_{m-1}(\overline{k}_\perp)+\int\mathrm{d}\overline{k}'_\perp I^+_{m,m-1}(\overline{k}_\perp;\overline{k}'_\perp)\overline{B}_{m-1}(\overline{k}'_\perp)\right\}\\&-\frac{1}{2}\frac{k_m}{k_{mz}}e^{ik_{mz}d_m}\left[\hat{e}(k_{mz})\hat{e}(k_{mz})\right]\cdot\left\{\overline{A}_m(\overline{k}_\perp)+\int\mathrm{d}\overline{k}'_\perp I^+_{mm}(\overline{k}_\perp;\overline{k}'_\perp)\overline{A}_m(\overline{k}'_\perp)\right\}\\&-\frac{1}{2}\frac{k_m}{k_{mz}}e^{ik_{mz}d_m}\left[\hat{h}(k_{mz})\hat{h}(k_{mz})\right]\cdot\left\{\overline{A}_m(\overline{k}_\perp)+\int\mathrm{d}\overline{k}'_\perp I^+_{mm}(\overline{k}_\perp;\overline{k}'_\perp)\overline{A}_m(\overline{k}'_\perp)\right\}\\&-\frac{1}{2}\frac{k_m}{k_{mz}}e^{ik_{mz}d_m}\left[-\hat{h}(k_{mz})\hat{e}(k_{mz})\right]\cdot\left\{\overline{B}_m(\overline{k}_\perp)+\int\mathrm{d}\overline{k}'_\perp I^+_{mm}(\overline{k}_\perp;\overline{k}'_\perp)\overline{B}_m(\overline{k}'_\perp)\right\}\\&-\frac{1}{2}\frac{k_m}{k_{mz}}e^{ik_{mz}d_m}\left[\hat{e}(k_{mz})\hat{h}(k_{mz})\right]\cdot\left\{\overline{B}_m(\overline{k}_\perp)+\int\mathrm{d}\overline{k}'_\perp I^+_{mm}(\overline{k}_\perp;\overline{k}'_\perp)\overline{B}_m(\overline{k}'_\perp)\right\}=0\end{aligned}\tag{4.3.26}$$

Where different scattering potentials for presence of roughness at $(m-1)$ and $m$-th boundary are defined through,

$$\begin{aligned}I^+_{mm}(\overline{k}_\perp;\overline{k}'_\perp)&=\frac{1}{(2\pi)^2}\int\mathrm{d}\overline{r}'_\perp e^{-i(\overline{k}_\perp-\overline{k}'_\perp)\cdot\overline{r}'_\perp}\left[e^{-ik_{mz}f_m(\overline{r}'_\perp)}-1\right]\\I^+_{m,m-1}(\overline{k}_\perp;\overline{k}'_\perp)&=\frac{1}{(2\pi)^2}\int\mathrm{d}\overline{r}'_\perp e^{-i(\overline{k}_\perp-\overline{k}'_\perp)\cdot\overline{r}'_\perp}\left[e^{-ik_{mz}f_{m-1}(\overline{r}'_\perp)}-1\right]\end{aligned}\tag{4.3.27}$$

The first subscript stands for wave propagating in region $m$ (with wavenumber $k_m$) and second one label the boundary ($m-1$ for the upper surface and $m$ for the lower surface), and plus sign is also for upward propagating wave. Similar to the region1 case, (4.3.26) can be projected over the TE and TM polarization unit vectors in region $m$ to get two sets of

scalar equations but still for vector unknowns.

$$
\begin{aligned}
&+\frac{1}{2}\frac{k_{m-1}}{k_{mz}}e^{ik_{mz}d_{m-1}}\left\{\hat{e}(k_{mz})\cdot\overline{A}_{m-1}(\overline{k}_\perp)+\int \mathrm{d}\overline{k}'_\perp \hat{e}(k_{mz})\cdot\overline{A}_{m-1}(\overline{k}'_\perp)I^+_{m,m-1}(\overline{k}_\perp;\overline{k}'_\perp)\right\}\\
&+\frac{1}{2}\frac{k_{m}}{k_{mz}}e^{ik_{mz}d_{m-1}}\left\{\hat{h}(k_{mz})\cdot\overline{B}_{m-1}(\overline{k}_\perp)+\int \mathrm{d}\overline{k}'_\perp \hat{h}(k_{mz})\cdot\overline{B}_{m-1}(\overline{k}'_\perp)I^+_{m,m-1}(\overline{k}_\perp;\overline{k}'_\perp)\right\}\\
&-\frac{1}{2}\frac{k_{m}}{k_{mz}}e^{ik_{mz}d_{m}}\left\{\hat{e}(k_{mz})\cdot\overline{A}_{m}(\overline{k}_\perp)+\int \mathrm{d}\overline{k}'_\perp \hat{e}(k_{mz})\cdot\overline{A}_{m}(\overline{k}'_\perp)I^+_{mm}(\overline{k}_\perp;\overline{k}'_\perp)\right\}\\
&-\frac{1}{2}\frac{k_{m}}{k_{mz}}e^{ik_{mz}d_{m}}\left\{\hat{h}(k_{mz})\cdot\overline{B}_{m}(\overline{k}_\perp)+\int \mathrm{d}\overline{k}'_\perp \hat{h}(k_{mz})\cdot\overline{B}_{m}(\overline{k}'_\perp)I^+_{mm}(\overline{k}_\perp;\overline{k}'_\perp)\right\}=0
\end{aligned}
\tag{4.3.28}
$$

$$
\begin{aligned}
&+\frac{1}{2}\frac{k_{m-1}}{k_{mz}}e^{ik_{mz}d_{m-1}}\left\{\hat{h}(k_{mz})\cdot\overline{A}_{m-1}(\overline{k}_\perp)+\int \mathrm{d}\overline{k}'_\perp \hat{h}(k_{mz})\cdot\overline{A}_{m-1}(\overline{k}'_\perp)I^+_{m,m-1}(\overline{k}_\perp;\overline{k}'_\perp)\right\}\\
&-\frac{1}{2}\frac{k_{m}}{k_{mz}}e^{ik_{mz}d_{m-1}}\left\{\hat{e}(k_{mz})\cdot\overline{B}_{m-1}(\overline{k}_\perp)+\int \mathrm{d}\overline{k}'_\perp \hat{e}(k_{mz})\cdot\overline{B}_{m-1}(\overline{k}'_\perp)I^+_{m,m-1}(\overline{k}_\perp;\overline{k}'_\perp)\right\}\\
&-\frac{1}{2}\frac{k_{m}}{k_{mz}}e^{ik_{mz}d_{m}}\left\{\hat{h}(k_{mz})\cdot\overline{A}_{m}(\overline{k}_\perp)+\int \mathrm{d}\overline{k}'_\perp \hat{h}(k_{mz})\cdot\overline{A}_{m}(\overline{k}'_\perp)I^+_{mm}(\overline{k}_\perp;\overline{k}'_\perp)\right\}\\
&+\frac{1}{2}\frac{k_{m}}{k_{mz}}e^{ik_{mz}d_{m}}\left\{\hat{e}(k_{mz})\cdot\overline{B}_{m}(\overline{k}_\perp)+\int \mathrm{d}\overline{k}'_\perp \hat{e}(k_{mz})\cdot\overline{B}_{m}(\overline{k}'_\perp)I^+_{mm}(\overline{k}_\perp;\overline{k}'_\perp)\right\}=0
\end{aligned}
\tag{4.3.29}
$$

In addition, expansion of the surface field in terms of the $pq$ unit vectors provides the scalar equations for scalar unknowns.

### 4.3.3 Extinction of Downward Propagating Wave in Region $m$

The extinction relation here is the same as the case of Downward propagating wave in region $m$ of (4.3.21). The only difference is that here the observation point is placed in below regions such that always $z<z'$ where $z'$ is the $z$-component of the location of the surface source reside on both surfaces $S_m$ and $S_{m-1}$. The dyadic Green's function can be expanded in spectral domain as a superposition of downward propagating plane waves

$$
\overline{\overline{G}}_m(\overline{r},\overline{r}')=\frac{i}{2(2\pi)^2}\int\frac{1}{k_{mz}}\mathrm{d}\overline{k}_\perp\ \left[\hat{e}(-k_{mz})\hat{e}(-k_{mz})+\hat{h}(-k_{mz})\hat{h}(-k_{mz})\right]e^{i\overline{k}_\perp\cdot(\overline{r}_\perp-\overline{r}'_\perp)-ik_{mz}(z-z')}
\tag{4.3.30}
$$

Following similar procedure as upward propagating case, we can obtain TE and TM scalar integral equations for the surface fields. the TE part of the integral equation reads,

$$
\begin{aligned}
&+\frac{1}{2}\frac{k_{m-1}}{k_{mz}}e^{-ik_{mz}d_{m-1}}\hat{e}(-k_{mz})\cdot\left\{\overline{A}_{m-1}(\overline{k}_\perp)+\int \mathrm{d}\overline{k}'_\perp I^-_{m,m-1}(\overline{k}_\perp;\overline{k}'_\perp)\overline{A}_{m-1}(\overline{k}'_\perp)\right\}\\
&+\frac{1}{2}\frac{k_{m}}{k_{mz}}e^{-ik_{mz}d_{m-1}}\hat{h}(-k_{mz})\cdot\left\{\overline{B}_{m-1}(\overline{k}_\perp)+\int \mathrm{d}\overline{k}'_\perp I^-_{m,m-1}(\overline{k}_\perp;\overline{k}'_\perp)\overline{B}_{m-1}(\overline{k}'_\perp)\right\}\\
&-\frac{1}{2}\frac{k_{m}}{k_{mz}}e^{-ik_{mz}d_{m}}\hat{e}(-k_{mz})\cdot\left\{\overline{A}_{m}(\overline{k}_\perp)+\int \mathrm{d}\overline{k}'_\perp I^-_{mm}(\overline{k}_\perp;\overline{k}'_\perp)\overline{A}_{m}(\overline{k}'_\perp)\right\}\\
&-\frac{1}{2}\frac{k_{m}}{k_{mz}}e^{-ik_{mz}d_{m}}\hat{h}(-k_{mz})\cdot\left\{\overline{B}_{m}(\overline{k}_\perp)+\int \mathrm{d}\overline{k}'_\perp I^-_{mm}(\overline{k}_\perp;\overline{k}'_\perp)\overline{B}_{m}(\overline{k}'_\perp)\right\}=0
\end{aligned}
\tag{4.3.31}
$$

whereas for TM part,

$$
\begin{aligned}
&+\frac{1}{2}\frac{k_{m-1}}{k_{mz}}e^{-ik_{mz}d_{m-1}}\hat{h}(-k_{mz})\cdot\Big\{\overline{A}_{m-1}(\overline{k}_\perp)+\int \mathrm{d}\overline{k}'_\perp I^-_{m,m-1}(\overline{k}_\perp;\overline{k}'_\perp)\overline{A}_{m-1}(\overline{k}'_\perp)\Big\}\\
&-\frac{1}{2}\frac{k_m}{k_{mz}}e^{-ik_{mz}d_{m-1}}\hat{e}(-k_{mz})\cdot\Big\{\overline{B}_{m-1}(\overline{k}_\perp)+\int \mathrm{d}\overline{k}'_\perp I^-_{m,m-1}(\overline{k}_\perp;\overline{k}'_\perp)\overline{B}_{m-1}(\overline{k}'_\perp)\Big\}\\
&-\frac{1}{2}\frac{k_m}{k_{mz}}e^{-ik_{mz}d_m}\hat{h}(-k_{mz})\cdot\Big\{\overline{A}_m(\overline{k}_\perp)+\int \mathrm{d}\overline{k}'_\perp I^-_{mm}(\overline{k}_\perp;\overline{k}'_\perp)\overline{A}_m(\overline{k}'_\perp)\Big\}\\
&+\frac{1}{2}\frac{k_m}{k_{mz}}e^{-ik_{mz}d_m}\hat{e}(-k_{mz})\cdot\Big\{\overline{B}_m(\overline{k}_\perp)+\int \mathrm{d}\overline{k}'_\perp I^-_{mm}(\overline{k}_\perp;\overline{k}'_\perp)\overline{B}_m(\overline{k}'_\perp)\Big\}=0
\end{aligned}
\tag{4.3.32}
$$

Here, the relevant scattering potentials are $I^-_{m,m-1}(\overline{k}_\perp;\overline{k}'_\perp)$ and $I^-_{m,m}(\overline{k}_\perp;\overline{k}'_\perp)$ which are defined through,

$$
\begin{aligned}
I^-_{m,m-1}(\overline{k}_\perp;\overline{k}'_\perp)&=\frac{1}{(2\pi)^2}\int \mathrm{d}\overline{r}'_\perp e^{-i(\overline{k}_\perp-\overline{k}'_\perp)\cdot\overline{r}'_\perp}\left[e^{ik_{mz}f_{m-1}(\overline{r}'_\perp)}-1\right]\\
I^-_{m,m}(\overline{k}_\perp;\overline{k}'_\perp)&=\frac{1}{(2\pi)^2}\int \mathrm{d}\overline{r}'_\perp e^{-i(\overline{k}_\perp-\overline{k}'_\perp)\cdot\overline{r}'_\perp}\left[e^{ik_{mz}f_m(\overline{r}'_\perp)}-1\right]
\end{aligned}
\tag{4.3.33}
$$

### 4.3.4 Extinction of Upward Propagating Wave in Region $N$

The statement of the extinction theorem applied to the last half space is given by (the minus sign is due to the way of selecting the normal vector pointing upward over the last interface)

$$
\begin{aligned}
-\int_{\partial V_N}\mathrm{d}S'\Big\{&ik_N\eta_N\overline{\overline{G}}_N(\overline{r},\overline{r}')\cdot[\hat{n}'_N\times\overline{H}_N(\overline{r}')]\\
&+\nabla\times\overline{\overline{G}}_N(\overline{r},\overline{r}')\cdot[\hat{n}'_N\times\overline{E}_N(\overline{r}')]\Big\}=\begin{cases}\overline{E}_N(\overline{r}) & \overline{r}\in\text{region N}\\ 0 & \overline{r}\notin\text{region N}\end{cases}
\end{aligned}
\tag{4.3.34}
$$

where $\partial V_N$ is the last rough boundary described with equation $z=-d_{N-1}+f_{N-1}(x,y)$. In order maintain number of unknown surface fields such that (4.3.34) does not introduce a new surface field variable, we define surface fields in terms of region $N-1$ fields and noting that for non-magnetic mediums $k_N\eta_N=k_{N-1}\eta_{N-1}$, on the last boundary

$$
\begin{aligned}
\mathrm{d}S'\hat{n}'_N\times\eta_{N-1}\overline{H}_{N-1}(\overline{r}')&=\mathrm{d}x'\mathrm{d}y'\overline{a}_{N-1}(x',y')\\
\mathrm{d}S'\hat{n}'_N\times\overline{E}_{N-1}(\overline{r}')&=\mathrm{d}x'\mathrm{d}y'\overline{b}_{N-1}(x',y')
\end{aligned}
\tag{4.3.35}
$$

and if the observation point is placed in upper regions such that $z>z'$ is always true, the integral equation becomes

$$
\int_{\partial V_N}\mathrm{d}\overline{r}'_\perp\Big\{ik_{N-1}\overline{\overline{G}}_N(\overline{r},\overline{r}')\cdot\overline{a}_{N-1}(\overline{r}'_\perp)+\nabla\times\overline{\overline{G}}_N(\overline{r},\overline{r}')\cdot\overline{b}_{N-1}(\overline{r}'_\perp)\Big\}=0,\quad \overline{r}\notin\text{region } N
\tag{4.3.36}
$$

Given this condition the Green's function of the last layer can be spectrally expanded as

$$
\overline{\overline{G}}_N(\overline{r},\overline{r}')=\frac{i}{2(2\pi)^2}\int\frac{1}{k_{Nz}}\mathrm{d}\overline{k}_\perp\ \Big[\hat{e}(k_{Nz})\hat{e}(k_{Nz})+\hat{h}(k_{Nz})\hat{h}(k_{Nz})\Big]e^{i\overline{k}_\perp(\overline{r}_\perp-\overline{r}'_\perp)+ik_{Nz}(z-z')}
\tag{4.3.37}
$$

Following the same procedure as before, the set of TE and TM integral equations becomes,

$$\frac{1}{2}\frac{k_{N-1}}{k_{Nz}}\Big\{\hat{e}(k_{Nz})\cdot\overline{A}_{N-1}(\overline{k}_\perp)+\int \mathrm{d}\overline{k}'_\perp I^+_{N,N-1}(\overline{k}_\perp;\overline{k}'_\perp)\hat{e}(k_{Nz})\cdot\overline{A}_{N-1}(\overline{k}'_\perp)\Big\} \tag{4.3.38}$$
$$+\frac{1}{2}\frac{k_N}{k_{Nz}}\Big\{\hat{h}(k_{Nz})\cdot\overline{B}_{N-1}(\overline{k}_\perp)+\int \mathrm{d}\overline{k}'_\perp I^+_{N,N-1}(\overline{k}_\perp;\overline{k}'_\perp)\hat{h}(k_{Nz})\cdot\overline{B}_{N-1}(\overline{k}'_\perp)\Big\}=0$$

$$+\frac{1}{2}\frac{k_{N-1}}{k_{Nz}}\Big\{\hat{h}(k_{Nz})\cdot\overline{A}_{N-1}(\overline{k}_\perp)+\int \mathrm{d}\overline{k}'_\perp I^+_{N,N-1}(\overline{k}_\perp;\overline{k}'_\perp)\hat{h}(k_{Nz})\cdot\overline{A}_{N-1}(\overline{k}'_\perp)\Big\} \tag{4.3.39}$$
$$-\frac{1}{2}\frac{k_N}{k_{Nz}}\Big\{\hat{e}(k_{Nz})\cdot\overline{B}_{N-1}(\overline{k}_\perp)+\int \mathrm{d}\overline{k}'_\perp I^+_{N,N-1}(\overline{k}_\perp;\overline{k}'_\perp)\hat{e}(k_{Nz})\cdot\overline{B}_{N-1}(\overline{k}'_\perp)\Big\}=0$$

where the scattering potential $I^+_{N,N-1}(\overline{k}_\perp;\overline{k}'_\perp)$ for upward propagating wave in region $N$ that scattered from the last boundary is defined as

$$I^+_{N,N-1}(\overline{k}_\perp;\overline{k}'_\perp)=\frac{1}{(2\pi)^2}\int \mathrm{d}\overline{r}'_\perp e^{-i(\overline{k}_\perp-\overline{k}'_\perp)\cdot\overline{r}'_\perp}\Big[e^{-ik_{Nz}f_{N-1}(\overline{r}'_\perp)}-1\Big] \tag{4.3.40}$$

## 4.4 Scattered and Transmitted Fields

Once we have the surface field quantities, it is possible to compute the scattered field into region 0. Statement of the Equivalent principle (Extinction theorem) for the first boundary reads

$$\overline{E}_{inc}(\overline{r})+\int_{S_1}\mathrm{d}S'\Big\{ik_1\eta_1\overline{\overline{G}}_1(\overline{r},\overline{r}')\cdot[\hat{n}'_1\times\overline{H}_1(\overline{r}')]+\nabla\times\overline{\overline{G}}_1(\overline{r},\overline{r}')\cdot[\hat{n}'_1\times\overline{E}_1(\overline{r}')]\Big\}=\overline{E}_1(\overline{r}) \tag{4.4.1}$$

Therefore, the scattered field expression in terms of surface fields $\overline{a}_1(\overline{r}'_\perp)$ and $\overline{b}_1(\overline{r}'_\perp)$ that are defined in (4.3.3) is given by

$$\overline{E}_s(\overline{r})=\int_{S_1}\mathrm{d}S'\Big\{ik_1\overline{\overline{G}}_1(\overline{r},\overline{r}')\cdot\overline{a}_1(\overline{r}'_\perp)+\nabla\times\overline{\overline{G}}_1(\overline{r},\overline{r}')\cdot\overline{b}_1(\overline{r}'_\perp)\Big\},\ z>f_1(x,y) \tag{4.4.2}$$

This is the exact expression of the scattered field given the exact values for the surface fields. However, here again we apply the extended boundary condition to the integral equation of (4.4.2) by letting $z$ resides on a location that is always above the actual interface profile. Here, it will be clear that the idea of the extended boundary condition is the same as the Rayleigh hypothesis where the starting point ins considering an expansion for the scattered field in terms of the upward propagating waves in region 1. Utilizing the extended boundary condition guarantees that $z>z'$ and as a consequence it allows to expand the dyadic Green's function in term of the plane waves with definite propagation direction (which is upward here) as

$$\overline{\overline{G}}_1(\overline{r},\overline{r}')=\frac{i}{2(2\pi)^2}\int \mathrm{d}k_\perp\frac{1}{k_{1z}}\Big[\hat{e}(k_{1z})\hat{e}(k_{1z})+\hat{h}(k_{1z})\hat{h}(k_{1z})\Big]e^{i\overline{k}_\perp\cdot(\overline{r}_\perp-\overline{r}'_\perp)+ik_{1z}(z-z')} \tag{4.4.3}$$

Substituting the Green's function in the scattered field expression gives

$$\begin{aligned}\overline{E}_s(\overline{r})=&-\frac{1}{2(2\pi)^2}\int \mathrm{d}\overline{r}'_\perp \int \mathrm{d}\overline{k}_\perp \frac{k_1}{k_{1z}}\hat{e}(k_{1z})\hat{e}(k_{1z})\cdot\overline{a}_1(x',y')e^{i(\overline{k}_\perp\cdot\overline{r}_\perp+k_{1z}z)}e^{-i\left(\overline{k}_\perp\cdot\overline{r}'_\perp+k_{1z}f_1(\overline{r}'_\perp)\right)}\\ &-\frac{1}{2(2\pi)^2}\int \mathrm{d}\overline{r}'_\perp \int \mathrm{d}\overline{k}_\perp \frac{k_1}{k_{1z}}\hat{h}(k_{1z})\hat{h}(k_{1z})\cdot\overline{a}_1(\overline{r}'_\perp)e^{i(\overline{k}_\perp\cdot\overline{r}_\perp+k_{1z}z)}e^{-i\left(\overline{k}_\perp\cdot\overline{r}'_\perp+k_{1z}f_1(\overline{r}'_\perp)\right)}\\ &+\frac{1}{2(2\pi)^2}\int \mathrm{d}\overline{r}'_\perp \int \mathrm{d}\overline{k}_\perp \frac{k_1}{k_{1z}}\hat{h}(k_{1z})\hat{e}(k_{1z})\cdot\overline{b}_1(\overline{r}'_\perp)e^{i(\overline{k}_\perp\cdot\overline{r}_\perp+k_{1z}z)}e^{-i\left(\overline{k}_\perp\cdot\overline{r}'_\perp+k_{1z}f_1(\overline{r}'_\perp)\right)}\\ &-\frac{1}{2(2\pi)^2}\int \mathrm{d}\overline{r}'_\perp \int \mathrm{d}\overline{k}_\perp \frac{k_1}{k_{1z}}\hat{e}(k_{1z})\hat{h}(k_{1z})\cdot\overline{b}_1(\overline{r}'_\perp)e^{i(\overline{k}_\perp\cdot\overline{r}_\perp+k_{1z}z)}e^{-i\left(\overline{k}_\perp\cdot\overline{r}'_\perp+k_{1z}f_1(\overline{r}'_\perp)\right)}\end{aligned} \tag{4.4.4}$$

The scattered field in (4.4.4) is a superposition of upward propagating waves in region 1 [75] as

$$\overline{E}_s(\overline{r})=\int \mathrm{d}\overline{k}_\perp \overline{S}(\overline{k}_\perp)e^{i\overline{k}_\perp\cdot\overline{r}_\perp}e^{ik_{1z}z} \tag{4.4.5}$$

This is the starting point of the Rayleigh hypothesis that automatically comes out of extended boundary condition approach. Using the Rayleigh hypothesis, the field in each region will be expanded in terms of propagating waves (upward and downward) and then they ill be forced to satisfy the border conditions. Therefore, although the extended boundary condition integral equation is derived more rigorously, the assumption of the Rayleigh hypothesis coincides with the integral equation approach.

Changing order of spatial and spectral integrations and using spectral incident field as well as inserting Fourier transform of the surface fields into (4.4.4), the spectral representation of the scattered field becomes

$$\begin{aligned}\overline{E}_s(\overline{k})=&-\frac{1}{2}\frac{k_1}{k_{1z}}\hat{e}(k_{1z})\hat{e}(k_{1z})\cdot\left\{\overline{A}_1(\overline{k}_\perp)+\int \mathrm{d}k'_\perp I_{11}^+(\overline{k}_\perp;\overline{k}'_\perp)\overline{A}_1(\overline{k}'_\perp)\right\}\\ &-\frac{1}{2}\frac{k_1}{k_{1z}}\hat{h}(k_{1z})\hat{h}(k_{1z})\cdot\left\{\overline{A}_1(\overline{k}_\perp)+\int \mathrm{d}k'_\perp I_{11}^+(\overline{k}_\perp;\overline{k}'_\perp)\overline{A}_1(\overline{k}'_\perp)\right\}\\ &+\frac{1}{2}\frac{k_1}{k_{1z}}\hat{h}(k_{1z})\hat{e}(k_{1z})\cdot\left\{\overline{B}_1(\overline{k}_\perp)+\int \mathrm{d}k'_\perp I_{11}^+(\overline{k}_\perp;\overline{k}'_\perp)\overline{B}_1(\overline{k}'_\perp)\right\}\\ &-\frac{1}{2}\frac{k_1}{k_{1z}}\hat{e}(k_{1z})\hat{h}(k_{1z})\cdot\left\{\overline{B}_1(\overline{k}_\perp)+\int \mathrm{d}k'_\perp I_{11}^+(\overline{k}_\perp;\overline{k}'_\perp)\overline{B}_1(\overline{k}'_\perp)\right\}\end{aligned} \tag{4.4.6}$$

where the scattering potential for the scattered wave is defined as

$$I_{11}^+(\overline{k}_\perp;\overline{k}'_\perp)=\frac{1}{(2\pi)^2}\int \mathrm{d}\overline{r}'_\perp e^{-i(\overline{k}_\perp-\overline{k}'_\perp)\cdot\overline{r}'_\perp}\left[e^{-ik_{1z}f_1(\overline{r}'_\perp)}-1\right] \tag{4.4.7}$$

In accordance with the surface field solutions, the scattered field can be expressed through its TE/TM decomposition and in terms of the scalar components of the surface fields. Similarly, for transmitted field into region $N$, the equivalence principle can be applied to the last half space to get the transmitted field as

$$\overline{E}_t(\overline{r})=-\int_{S_{N-1}} \mathrm{d}\overline{r}'_\perp\left\{ik_{N-1}\overline{\overline{G}}_N(\overline{r},\overline{r}')\cdot\overline{a}_{N-1}(\overline{r}'_\perp)+\nabla\times\overline{\overline{G}}_N(\overline{r},\overline{r}')\cdot\overline{b}_{N-1}(\overline{r}'_\perp)\right\},\quad \overline{r}\in V_N \tag{4.4.8}$$

This is the exact transmitted field given that the surface fields are computed exactly. However, if we assume that the observation point placed in region $N$ such that always $z<z'$, we can use a unidirectional expansion of the dyadic Green's function in terms of downward propagating waves

$$\overline{\overline{G}}_N(\overline{r},\overline{r}')=\frac{i}{2(2\pi)^2}\int\frac{1}{k_{Nz}}\mathrm{d}\overline{k}_\perp\ \Big[\hat{e}(-k_{Nz})\hat{e}(-k_{Nz})+\hat{h}(-k_{Nz})\hat{h}(-k_{Nz})\Big]e^{i\overline{k}_\perp\cdot(\overline{r}_\perp-\overline{r}'_\perp)-ik_{Nz}(z-z')} \tag{4.4.9}$$

Therefore, the spectral component of the transmitted field into region $N$ can be obtained in terms of the Fourier transform of the surface fields as

$$\begin{aligned}
\tilde{\overline{E}}_t(\overline{k}_\perp)=&\frac{1}{2}\frac{k_{N-1}}{k_{Nz}}e^{-ik_{Nz}d_{N-1}}\big[\hat{e}(-k_{Nz})\hat{e}(-k_{Nz})\big]\cdot\Big\{\overline{A}_{N-1}(\overline{k}_\perp)+\int\mathrm{d}\overline{k}'_\perp\overline{A}_{N-1}(\overline{k}'_\perp)I^-_{N,N-1}\Big\}\\
&+\frac{1}{2}\frac{k_{N-1}}{k_{Nz}}e^{-ik_{Nz}d_{N-1}}\big[\hat{h}(-k_{Nz})\hat{h}(-k_{Nz})\big]\cdot\Big\{\overline{A}_{N-1}(\overline{k}_\perp)+\int\mathrm{d}\overline{k}'_\perp\overline{A}_{N-1}(\overline{k}'_\perp)I^-_{N,N-1}(\overline{k}_\perp;\overline{k}'_\perp)\Big\}\\
&+\frac{1}{2}\frac{k_N}{k_{Nz}}e^{-ik_{Nz}d_{N-1}}\big[-\hat{h}(-k_{Nz})\hat{e}(-k_{Nz})\big]\cdot\Big\{\overline{B}_{N-1}(\overline{k}_\perp)+\int\mathrm{d}\overline{k}'_\perp\overline{B}_{N-1}(\overline{k}'_\perp)I^-_{N,N-1}(\overline{k}_\perp;\overline{k}'_\perp)\Big\}\\
&+\frac{1}{2}\frac{k_N}{k_{Nz}}e^{-ik_{Nz}d_{N-1}}\big[\hat{e}(-k_{Nz})\hat{h}(-k_{Nz})\big]\cdot\Big\{\overline{B}_{N-1}(\overline{k}_\perp)+\int\mathrm{d}\overline{k}'_\perp\overline{B}_{N-1}(\overline{k}'_\perp)I^-_{N,N-1}(\overline{k}_\perp;\overline{k}'_\perp)\Big\}
\end{aligned}$$

where the scattering potential for the transmitted field in defined as

$$I^-_{N,N-1}(\overline{k}_\perp;\overline{k}'_\perp)=\frac{1}{(2\pi)^2}\int\mathrm{d}\overline{r}'_\perp e^{-i(\overline{k}_\perp-\overline{k}'_\perp)\cdot\overline{r}'_\perp}\Big[e^{+ik_{Nz}f_{N-1}(\overline{r}'_\perp)}-1\Big] \tag{4.4.10}$$

The TE component of transmitted field can be obtained by projection of the transmitted field on the TE polarization unit vectors.

## 4.5 Surface Fields Solution

From the extended boundary condition integral equations of (4.3.11), (4.3.26), (4.3.31), (4.3.32), (4.3.38), and (4.3.39) we have a system of integral equations to be solved for the surface fields. There are $N-1$ interfaces with two vector surface currents $\overline{A}$ and $\overline{B}$ on each interface that results in $2(N-1)$ vector unknowns. The vector surface fields are two dimensional objects and therefore number of scalar unknowns becomes $4(N-1)$. On the other hand, for $2\leq m\leq N-1$, the extinction relation of the middle layers provide us with $2(N-2)$ vector integral equations and the first and last layers also bring two additional vector equations that results in $2(N-1)$ vector equation that contain $4(N-1)$ scalar equations (TE and TM). Overall the system of boundary integral equations s consistent and ready to solve. Again, notice that these are the extended boundary condition integral equation to be applied to the surfaces that have a maximum acceptable slope.

The vector surface fields belong to the tangent space of the rough boundary, i.e. for a general interface labeled by $j$,

$$\hat{n}_j(\overline{r})\cdot\overline{a}_j(\overline{r}_\perp)=\hat{n}_j(\overline{r})\cdot\overline{b}_j(\overline{r}_\perp)=0\qquad,j=0,1,2,\ldots N-1 \tag{4.5.1}$$

where the normal to the boundary is related to the surface profile through,

$$\hat{n}_j(\overline{r})=\frac{\hat{z}-\nabla f_j(\overline{r}_\perp)}{\sqrt{1+||\nabla f_j(\overline{r}_\perp)||^2}} \tag{4.5.2}$$

Therefore, $z$-component of the surface field can be obtained from the transverse component through,

$$a_{j,z}(\overline{r}_\perp)=\nabla f_j(\overline{r}_\perp)\cdot\overline{a}_j(\overline{r}_\perp) \tag{4.5.3}$$

It can be written in spectral domain by a convolution integral of

$$A_{j,z}(\overline{k}_\perp)=\int \mathrm{d}\overline{k}'_\perp iF_j(\overline{k}_\perp-\overline{k}'_\perp)(\overline{k}_\perp-\overline{k}'_\perp)\cdot\overline{A}_{j\perp}(\overline{k}'_\perp) \tag{4.5.4}$$

### 4.5.1 Small Height and Slope Approximations

The *Small Perturbation Method* (SPM) is a perturbative solution of the boundary integral equations obtained in 4.3. Perturbation parameter is the surface height which is considered to be smaller than the operational wavelength $\lambda$. When the interfaces are considered to be random rough surfaces, the height would be characterized by the statistics of the surface processes. Here, we consider the interfaces to be a Gaussian processes with a given autocorrelation function. The autocorrelation function is defined through

$$\langle f(\overline{r}_\perp)f(\overline{r}'_\perp)\rangle=h^2C(\overline{r}_\perp-\overline{r}'_\perp) \tag{4.5.5}$$

Here, $h$ is the RMS height of the surface and $C(\overline{r}_\perp)$ is the normalized and dimensionless correlation function such that $C(\overline{0})=1$. The surface process is assumed to be a stationary process in a wide sense. The small perturbation method assumes that in general $|kh|\ll 1$ for all of the layers. More specifically, the approximation to be made is $|k_{jz}f_n(\overline{r}_\perp)|\ll 1$ for $n=j,j+1$ and all $\overline{r}_\perp$. Given that $|kh|$ is a small parameter, the solution can be expanded in terms of different orders as

$$\overline{A}_j=\sum_{m=0}^{\infty}\overline{A}_j^{(m)}=\overline{A}_j^{(0)}+\overline{A}_j^{(1)}+\overline{A}_j^{(2)}+\cdots \tag{4.5.6}$$

where different orders are related through $A^{(m)}\propto A^{(m-1)}|kh|$. This expansion is convergent if the perturbation parameter $|kh|$ is really smaller than unity and series would reach its value using a few terms. As $|kh|$ becomes close to unity, the convergence slows down and the solution becomes divergent. It is important to note that the perturbation series is an alternative series such that by adding one term it may overshoot or undershoot the final result. After considering a perturbation series for all of the surface field unknowns, terms of the same order can be collected on both sides. Starting from the zeroth order solution, we can continue o construct higher order terms iteratively.Small height is not the only approximation in the SPM as it uses *Small Slope Approximation* as well. The small slope approximation enters through,

$$\left|\left|\nabla f_j(\overline{r}_\perp)\right|\right|\ll 1 \tag{4.5.7}$$

for all values of $j$. Therefore, if we consider perturbation series $\overline{A}_j(\overline{k}_\perp)=\sum_{m=0}^{N}\overline{A}_j^{(m)}(\overline{k}_\perp)$ for the surface fields, $z$-component of the surface fields is one order smaller than the transverse part, i.e.

$$A_{j,z}^{(m)}(\overline{k}_\perp)=\int \mathrm{d}\overline{k}'_\perp iF_j(\overline{k}_\perp-\overline{k}'_\perp)(\overline{k}_\perp-\overline{k}'_\perp)\cdot\overline{A}_{j\perp}^{(m-1)}(\overline{k}'_\perp) \tag{4.5.8}$$

Computation of different orders of perturbation becomes more complicated for higher orders of solution. Usually the SPM would be useful if the perturbation parameter is small enough

that series converges with considering up to the second order of perturbation which is called SPM2. Different orders of the surface field will be computed in the next part.

### 4.5.2 Zeroth order Solution

For zeroth order solution is independent of surface roughness and therefore $F_j(\overline{k}_\perp)=0$ within the zeroth order solution. The zeroth order of the surface fields is one order smaller than the transverse part and therefore $z$-components of the fields vanishes within the zeroth order. Also, the scattering potentials are defined in such a way that they vanish for the flat surface case. TE and TM part of equations are isolated and can be solved separately. Balancing the integral equations up to the zeroth order gives the following equation for the TE part and after simplifying we obtain,

$$\hat{e}(-k_{1z})\cdot\tilde{\overline{E}}_{inc}(\overline{k})-\frac{1}{2}\frac{k_1}{k_{1z}}A^{(0)}_{1,q}(\overline{k}_\perp)-\frac{1}{2}B^{(0)}_{1,p}(\overline{k}_\perp)=0$$

$$\frac{k_{m-1}}{k_m}A^{(0)}_{m-1,q}(\overline{k}_\perp)-\frac{k_{mz}}{k_m}B^{(0)}_{m-1,p}(\overline{k}_\perp)=e^{ik_{mz}\delta_m}A^{(0)}_{m,q}(\overline{k}_\perp)-e^{ik_{mz}\delta_m}\frac{k_{mz}}{k_m}B^{(0)}_{m,p}(\overline{k}_\perp)$$
$$\frac{k_{m-1}}{k_m}A^{(0)}_{m-1,q}(\overline{k}_\perp)+\frac{k_{mz}}{k_m}B^{(0)}_{m-1,p}(\overline{k}_\perp)=e^{-ik_{mz}\delta_m}A^{(0)}_{m,q}(\overline{k}_\perp)+e^{-ik_{mz}\delta_m}\frac{k_{mz}}{k_m}B^{(0)}_{m,p}(\overline{k}_\perp)$$

$$\frac{k_{N-1}}{k_N}A^{(0)}_{N-1,q}(\overline{k}_\perp)-\frac{k_{Nz}}{k_N}B^{(0)}_{N-1,p}(\overline{k}_\perp)=0$$

Here, $\delta_m=d_m-d_{m-1}\quad,m=2,3,\cdots N-1$. Notice that the TE field variables are $A^{(0)}_q$ and $B^{(0)}_p$. The extinction relations of the middle layers can be casted into a propagation matrix type of equations as

$$\frac{k_{m-1}}{k_m}\begin{bmatrix}1 & -\frac{k_{mz}}{k_{m-1}}\\ 1 & \frac{k_{mz}}{k_{m-1}}\end{bmatrix}\begin{bmatrix}A^{(0)}_{m-1,q}\\ B^{(0)}_{m-1,p}\end{bmatrix}=\begin{bmatrix}e^{i\phi_m} & 0\\ 0 & e^{-i\phi_m}\end{bmatrix}\begin{bmatrix}1 & -\frac{k_{mz}}{k_m}\\ 1 & \frac{k_{mz}}{k_m}\end{bmatrix}\begin{bmatrix}A^{(0)}_{m,q}\\ B^{(0)}_{m,p}\end{bmatrix} \tag{4.5.9}$$

where the phase factor $\phi_m$ is the phase delay in propagation through the region $m$ and is defined as $\phi_m=k_{mz}\delta_m$. The surface fields of region $m$ can be related to that of region $m-1$ through,

$$\begin{bmatrix}A^{(0)}_{m,q}\\ B^{(0)}_{m,p}\end{bmatrix}=\frac{k_{m-1}}{k_m}\begin{bmatrix}1 & -\frac{k_{mz}}{k_m}\\ 1 & \frac{k_{mz}}{k_m}\end{bmatrix}^{-1}\begin{bmatrix}e^{-i\phi_m} & 0\\ 0 & e^{i\phi_m}\end{bmatrix}\begin{bmatrix}1 & -\frac{k_{mz}}{k_{m-1}}\\ 1 & \frac{k_{mz}}{k_{m-1}}\end{bmatrix}\begin{bmatrix}A^{(0)}_{m-1,q}\\ B^{(0)}_{m-1,p}\end{bmatrix} \tag{4.5.10}$$

By defining a propagation matrix $\overline{\overline{P}}^{[0,e]}_m$ that is responsible for propagation of the surface fields from the region $m-1$ to region $m$ as

$$\begin{bmatrix}A^{(0)}_{m,q}\\ B^{(0)}_{m,p}\end{bmatrix}=\overline{\overline{P}}^{[0,e]}_m\begin{bmatrix}A^{(0)}_{m-1,q}\\ B^{(0)}_{m-1,p}\end{bmatrix} \tag{4.5.11}$$

The surface fields on the last boundary can be related to the surface fields on the first boundary recursively,

$$\begin{bmatrix}A^{(0)}_{N-1,q}\\ B^{(0)}_{N-1,p}\end{bmatrix}=\prod_{j=2}^{N-1}\overline{\overline{P}}^{[0,e]}_j\begin{bmatrix}A^{(0)}_{1q}\\ B^{(0)}_{1p}\end{bmatrix}=\overline{\overline{P}}^{[0,e]}\begin{bmatrix}A^{(0)}_{1q}\\ B^{(0)}_{1p}\end{bmatrix} \tag{4.5.12}$$

where, $\overline{\overline{P}}^{[0,e]}$ is the total propagation matrix of the zeroth order TE fields from the first to the last surface. Also the extinction of the wave in two half spaces, can be combined to the recursive relation between the first and last interfaces to get a consistent system of equations of

$$\begin{bmatrix} \frac{1}{2}\frac{k_1}{k_{1z}} & \frac{1}{2} & 0 & 0 \\ 0 & 0 & \frac{k_{N-1}}{k_{Nz}} & -1 \\ P_{11}^{[0,e]} & P_{12}^{[0,e]} & -1 & 0 \\ P_{21}^{[0,e]} & P_{22}^{[0,e]} & 0 & -1 \end{bmatrix} \begin{bmatrix} A_{1q}^{(0)} \\ B_{1p}^{(0)} \\ A_{N-1,q}^{(0)} \\ B_{N-1,p}^{(0)} \end{bmatrix} = \begin{bmatrix} 1 \\ 0 \\ 0 \\ 0 \end{bmatrix} \hat{e}(-k_{1z}) \cdot \hat{e}_i \delta(\overline{k}_\perp - \overline{k}_{i\perp}) \tag{4.5.13}$$

Similarly, collecting the terms up to the zeroth order of surface roughness in TM set of equations, yields,

$$\hat{h}(-k_{1z}) \cdot \tilde{\overline{E}}_{inc}(\overline{k}) - \frac{1}{2} A_{1,p}^{(0)}(\overline{k}_\perp) + \frac{1}{2}\frac{k_1}{k_{1z}} B_{1,q}^{(0)}(\overline{k}_\perp) = 0$$

$$\begin{aligned} &+\frac{1}{2}\frac{k_{m-1}}{k_{mz}} e^{ik_{mz}d_{m-1}} \Big\{ -\frac{k_{mz}}{k_m} A_{m-1,p}^{(0)}(\overline{k}_\perp) \Big\} - \frac{1}{2}\frac{k_m}{k_{mz}} e^{ik_{mz}d_{m-1}} B_{m-1,q}^{(0)}(\overline{k}_\perp) \\ &-\frac{1}{2}\frac{k_m}{k_{mz}} e^{ik_{mz}d_m} \Big\{ -\frac{k_{mz}}{k_m} A_{m,p}^{(0)}(\overline{k}_\perp) \Big\} + \frac{1}{2}\frac{k_m}{k_{mz}} e^{ik_{mz}d_m} B_{m,q}^{(0)}(\overline{k}_\perp) = 0 \end{aligned}$$

$$\begin{aligned} &+\frac{1}{2}\frac{k_{m-1}}{k_{mz}} e^{-ik_{mz}d_{m-1}} \Big\{ \frac{k_{mz}}{k_m} A_{m-1,p}^{(0)}(\overline{k}_\perp) \Big\} - \frac{1}{2}\frac{k_m}{k_{mz}} e^{-ik_{mz}d_{m-1}} B_{m-1,q}^{(0)}(\overline{k}_\perp) \\ &-\frac{1}{2}\frac{k_m}{k_{mz}} e^{-ik_{mz}d_m} \Big\{ \frac{k_{mz}}{k_m} A_{m,p}^{(0)}(\overline{k}_\perp) \Big\} + \frac{1}{2}\frac{k_m}{k_{mz}} e^{-ik_{mz}d_m} B_{m,q}^{(0)}(\overline{k}_\perp) = 0 \end{aligned}$$

$$+\frac{1}{2}\frac{k_{N-1}}{k_{Nz}} e^{ik_{Nz}d_{N-1}} \Big\{ -\frac{k_{Nz}}{k_N} A_{N-1,p}^{(0)}(\overline{k}_\perp) \Big\} - \frac{1}{2}\frac{k_N}{k_{Nz}} e^{ik_{Nz}d_{N-1}} B_{N-1,q}^{(0)}(\overline{k}_\perp) = 0$$

From extinction relation of middle layers,

$$\begin{bmatrix} \frac{k_{m-1}k_{mz}}{k_m^2} & 1 \\ \frac{k_{m-1}k_{mz}}{k_m^2} & -1 \end{bmatrix} \begin{bmatrix} A_{m-1,p}^{(0)} \\ B_{m-1,q}^{(0)} \end{bmatrix} = \begin{bmatrix} e^{i\phi_m} & 0 \\ 0 & e^{-i\phi_m} \end{bmatrix} \begin{bmatrix} \frac{k_{mz}}{k_m} & 1 \\ \frac{k_{mz}}{k_m} & -1 \end{bmatrix} \begin{bmatrix} A_{m,p}^{(0)} \\ B_{m,q}^{(0)} \end{bmatrix} \tag{4.5.14}$$

a propagation matrix for the surface fields of TM set can be obtained as

$$\begin{bmatrix} A_{m,p}^{(0)} \\ B_{m,q}^{(0)} \end{bmatrix} = \begin{bmatrix} \frac{k_{mz}}{k_m} & 1 \\ \frac{k_{mz}}{k_m} & -1 \end{bmatrix}^{-1} \begin{bmatrix} e^{-i\phi_m} & 0 \\ 0 & e^{i\phi_m} \end{bmatrix} \begin{bmatrix} \frac{k_{m-1}k_{mz}}{k_m^2} & 1 \\ \frac{k_{m-1}k_{mz}}{k_m^2} & -1 \end{bmatrix} \begin{bmatrix} A_{m-1,p}^{(0)} \\ B_{m-1,q}^{(0)} \end{bmatrix} \tag{4.5.15}$$

or,

$$\begin{bmatrix} A_{m,p}^{(0)} \\ B_{m,q}^{(0)} \end{bmatrix} = \overline{\overline{P}}_m^{[0,h]} \begin{bmatrix} A_{m-1,p}^{(0)} \\ B_{m-1,q}^{(0)} \end{bmatrix} \tag{4.5.16}$$

where

$$\overline{\overline{P}}_m^{[0,h]} = \begin{bmatrix} \frac{k_{mz}}{k_m} & 1 \\ \frac{k_{mz}}{k_m} & -1 \end{bmatrix}^{-1} \begin{bmatrix} e^{-i\phi_m} & 0 \\ 0 & e^{i\phi_m} \end{bmatrix} \begin{bmatrix} \frac{k_{m-1}k_{mz}}{k_m^2} & 1 \\ \frac{k_{m-1}k_{mz}}{k_m^2} & -1 \end{bmatrix} \tag{4.5.17}$$

that can be used to connect the first and last surface fields together through

$$\begin{bmatrix} A^{(0)}_{N-1,p} \\ B^{(0)}_{N-1,q} \end{bmatrix} = \prod_{j=2}^{N-1} \overline{\overline{P}}^{[0,h]}_j \begin{bmatrix} A^{(0)}_{1p} \\ B^{(0)}_{1q} \end{bmatrix} = \overline{\overline{P}}^{[0,h]} \begin{bmatrix} A^{(0)}_{1p} \\ B^{(0)}_{1q} \end{bmatrix} \tag{4.5.18}$$

where $\overline{\overline{P}}^{[0,h]}$ is the total propagation matrix from the first surface fields to the last one. Using the two half spaces relation, a consistent system of equation for the surface fields will be obtained as

$$\begin{bmatrix} \frac{1}{2} & -\frac{1}{2}\frac{k_1}{k_{1z}} & 0 & 0 \\ 0 & 0 & \frac{k_{N-1}}{k_N}\frac{k_{Nz}}{k_N} & 1 \\ P^{[0,h]}_{11} & P^{[0,h]}_{12} & -1 & 0 \\ P^{[0,h]}_{21} & P^{[0,h]}_{22} & 0 & -1 \end{bmatrix} \begin{bmatrix} A^{(0)}_{1p} \\ B^{(0)}_{1q} \\ A^{(0)}_{N-1,p} \\ B^{(0)}_{N-1,q} \end{bmatrix} = \begin{bmatrix} 1 \\ 0 \\ 0 \\ 0 \end{bmatrix} \hat{h}(-k_{1z}) \cdot \hat{e}_i \delta(\overline{k}_\perp - \overline{k}_{i\perp}) \tag{4.5.19}$$

Note that due to the presence of the delta-function on the right hand side of (4.5.19), all of spectral quantities should be evaluated at $\overline{k}_\perp = \overline{k}_{i\perp}$. The surface fields on the intermediate layers can be found directly by applying the propagation matrices as

$$\begin{bmatrix} A^{(0)}_{m,q} \\ B^{(0)}_{m,p} \end{bmatrix} = \prod_{j=2}^{m} \overline{\overline{P}}^{[0,e]}_j \begin{bmatrix} A^{(0)}_{1q} \\ B^{(0)}_{1p} \end{bmatrix} \tag{4.5.20}$$

$$\begin{bmatrix} A^{(0)}_{m,p} \\ B^{(0)}_{m,q} \end{bmatrix} = \prod_{j=2}^{m} \overline{\overline{P}}^{[0,h]}_j \begin{bmatrix} A^{(0)}_{1p} \\ B^{(0)}_{1q} \end{bmatrix}$$

### 4.5.3 Zeroth Order Scattered and Transmitted Field

Since the zeroth order surface fields are specular at $\overline{k}_\perp = \overline{k}_{i\perp}$, we defines the zeroth order surface fields amplitudes through,

$$A^{(0)}_{m\alpha} = a^{(0)}_{m\alpha} \delta(\overline{k}_\perp - \overline{k}_{i\perp}) \tag{4.5.21}$$

then, the scattered field can be obtained by balancing the scattered field integral of (4.4.2) to find the scattered field as

$$\overline{E}^{(0)}_s(\overline{k}) = \left[ S^{(0)}_e \hat{e}(k_{1z}) + S^{(0)}_h \hat{h}(k_{1z}) \right] \delta(\overline{k}_\perp - \overline{k}_{i\perp}) \tag{4.5.22}$$

where

$$\begin{aligned} S^{(0)}_e &= -\frac{1}{2}\frac{k_1}{k_{1iz}} a^{(0)}_{1q} + \frac{1}{2} b^{(0)}_{1p} \\ S^{(0)}_h &= +\frac{1}{2} a^{(0)}_{1p} + \frac{1}{2}\frac{k_1}{k_{1iz}} b^{(0)}_{1q} \end{aligned} \tag{4.5.23}$$

The scattered field representation in the spatial domain can be obtained as

$$\overline{E}^{(0)}_s(\overline{r}) = \int \mathrm{d}\overline{k}_\perp \tilde{\overline{E}}_s(\overline{k}) e^{i\overline{k}_1 \cdot \overline{r}} = e^{i\overline{k}_{1i} \cdot \overline{r}} \left[ S^{(0)}_e \hat{e}(k_{1iz}) + S^{(0)}_h \hat{h}(k_{1iz}) \right] \tag{4.5.24}$$

with associated magnetics field of

$$\overline{H}_s^{(0)}(\overline{r})=\frac{1}{\eta_1}e^{i\overline{k}_{1i}\cdot\overline{r}}\Big[-S_e^{(0)}\hat{h}(k_{1iz})+S_h^{(0)}\hat{e}(k_{1iz})\Big] \tag{4.5.25}$$

that results in the scattered power density of

$$\overline{S}_s^{(0)}\cdot\hat{z}=\frac{1}{2}\mathrm{Re}\Big[\overline{E}_s^{(0)}(\overline{r})\times\overline{H}_s^{(0)*}(\overline{r})\Big]\cdot\hat{z}=\frac{1}{2k_1\eta_1}\Big[|S_e^{(0)}|^2+|S_h^{(0)}|^2\Big]\mathrm{Re}(k_{1iz}) \tag{4.5.26}$$

Similarly for the transmitted field into region $N$,

$$\tilde{\overline{E}}_t^{(0)}(\overline{k}_\perp)=e^{-ik_{Nz}d_{N-1}}\Big[T_e^{(0)}\hat{e}(-k_{Nz})+T_h^{(0)}\hat{h}(-k_{Nz})\Big]\delta(\overline{k}_\perp-\overline{k}_{i\perp}) \tag{4.5.27}$$

where,

$$\begin{aligned}T_e^{(0)}&=\frac{1}{2}\left[\frac{k_{N-1}}{k_{Niz}}a_{N-1,q}^{(0)}+b_{N-1,p}^{(0)}\right]\\ T_h^{(0)}&=\frac{1}{2}\left[\frac{k_{N-1}}{k_N}a_{N-1,p}^{(0)}-\frac{k_N}{k_{Niz}}b_{N-1,q}^{(0)}(\overline{k}_\perp)\right]\end{aligned} \tag{4.5.28}$$

Converting to the spatial domain gives

$$\overline{E}_t^{(0)}(\overline{r})=e^{-ik_{Niz}d_{N-1}}e^{i\overline{K}_{Ni}\cdot\overline{r}}\Big[T_e^{(0)}\hat{e}(-k_{Niz})+T_h^{(0)}\hat{h}(-k_{Niz})\Big] \tag{4.5.29}$$

and corresponding magnetic field of

$$\overline{H}_t^{(0)}(\overline{r})=\frac{1}{\eta_N}e^{-ik_{Niz}d_{N-1}}e^{i\overline{K}_{Ni}\cdot\overline{r}}\Big[-T_e^{(0)}\hat{h}(-k_{Niz})+T_h^{(0)}\hat{e}(-k_{Niz})\Big] \tag{4.5.30}$$

that yield the following power density for the transmitted field,

$$\overline{S}_t^{(0)}\cdot(-\hat{z})=\frac{1}{2}\mathrm{Re}\Big[\overline{E}_t^{(0)}(\overline{r})\times\overline{H}_t^{(0)*}(\overline{r})\Big]\cdot(-\hat{z})=\frac{1}{2}\mathrm{Re}\Big[\frac{k_{Niz}^*}{k_N^*\eta_N^*}|T_e^{(0)}|^2+\frac{k_{Niz}}{k_N\eta_N^*}|T_h^{(0)}|^2\Big] \tag{4.5.31}$$

Notice that the zeroth order scattered and transmitted fields are deterministic quantities and independent of the surface roughness.

### 4.5.4 First Order Solution

For convenience in later calculations, lets define the zeroth order surface field amplitudes $u_\alpha^{(0)}(\overline{k}_{\perp_i})$ as

$$U_\alpha^{(0)}(\overline{k}_\perp)=u_\alpha^{(0)}(\overline{k}_{\perp_i})\delta(\overline{k}_\perp-\overline{k}_{\perp_i}) \tag{4.5.32}$$

where $U\in\{A_i,B_i\}$ and $\alpha\in\{p,q\}$. Balancing the extinction integral equations up to the first order of surface roughness, using the first order approximation of the scattering potentials of

$$\begin{aligned}I_{11}^{-(1)}(\overline{k}_\perp;\overline{k}'_\perp)&=ik_{1z}F_1(\overline{k}_\perp-\overline{k}'_\perp)\\ I_{m,m-1}^{\pm(1)}(\overline{k}_\perp;\overline{k}'_\perp)&=\mp ik_{mz}F_{m-1}(\overline{k}_\perp-\overline{k}'_\perp)\\ I_{mm}^{\pm(1)}(\overline{k}_\perp;\overline{k}'_\perp)&=\mp ik_{mz}F_m(\overline{k}_\perp-\overline{k}'_\perp)\\ I_{N,N-1}^{+(1)}(\overline{k}_\perp;\overline{k}'_\perp)&=-ik_{Nz}F_{N-1}(\overline{k}_\perp-\overline{k}'_\perp)\end{aligned} \tag{4.5.33}$$

and expression of the $z$-component of the fields in terms of the transverse part,

$$A_{j,z}^{(1)}(\overline{k}_\perp)=iF_j(\overline{k}_\perp-\overline{k}_{i\perp})(\overline{k}_\perp-\overline{k}_{i\perp})\cdot\overline{a}_j^{(0)} \tag{4.5.34}$$
$$B_{j,z}^{(1)}(\overline{k}_\perp)=iF_j(\overline{k}_\perp-\overline{k}_{i\perp})(\overline{k}_\perp-\overline{k}_{i\perp})\cdot\overline{b}_j^{(0)}$$

it reveals that the first order surface fields are proportional to the spectrum of the interface profiles. By this token, lets define the new surface field variables $\tilde{A}_j^{(1)}$ by

$$A_j^{(1)}(\overline{k}_\perp)=iF_j(\overline{k}_\perp-\overline{k}_{i\perp})\tilde{A}_j^{(1)}(\overline{k}_\perp) \tag{4.5.35}$$

The TE part of the extinction equations in terms of the new surface field variables become,

$$-\frac{1}{2}\frac{k_1}{k_{1z}}\left\{\tilde{A}_{1q}^{(1)}(\overline{k}_\perp)+k_{1z}\hat{e}(-k_{1z})\cdot\overline{a}_1^{(0)}\right\} \tag{4.5.36}$$
$$-\frac{1}{2}\frac{k_1}{k_{1z}}\left\{\frac{k_{1z}}{k_1}\tilde{B}_{1p}^{(1)}(\overline{k}_\perp)+\frac{k_\rho}{k_1}(\overline{k}_\perp-\overline{k}_{i\perp})\cdot\overline{b}_1^{(0)}+k_{1z}\hat{h}(-k_{1z})\cdot\overline{b}_1^{(0)}\right\}=0$$

$$+\frac{1}{2}\frac{k_{m-1}}{k_{mz}}e^{ik_{mz}d_{m-1}}\left\{\tilde{A}_{m-1,q}^{(1)}(\overline{k}_\perp)-k_{mz}\hat{e}(k_{mz})\cdot\overline{a}_{m-1}^{(0)}\right\}F_{m-1}$$
$$+\frac{1}{2}\frac{k_m}{k_{mz}}e^{ik_{mz}d_{m-1}}\left\{-\frac{k_{mz}}{k_m}\tilde{B}_{m-1,p}^{(1)}(\overline{k}_\perp)+\frac{k_\rho}{k_m}(\overline{k}_\perp-\overline{k}_{i\perp})\cdot\overline{b}_{m-1}^{(0)}-k_{mz}\hat{h}(k_{mz})\cdot\overline{b}_{m-1}^{(0)}\right\}F_{m-1}$$
$$-\frac{1}{2}\frac{k_m}{k_{mz}}e^{ik_{mz}d_m}\left\{\tilde{A}_{m,q}^{(1)}(\overline{k}_\perp)-k_{mz}\hat{e}(k_{mz})\cdot\overline{a}_m^{(0)}(\overline{k}'_\perp)\right\}F_m$$
$$-\frac{1}{2}\frac{k_m}{k_{mz}}e^{ik_{mz}d_m}\left\{-\frac{k_{mz}}{k_m}\tilde{B}_{m,p}^{(1)}(\overline{k}_\perp)+\frac{k_\rho}{k_m}(\overline{k}_\perp-\overline{k}_{i\perp})\cdot\overline{b}_m^{(0)}-k_{mz}\hat{h}(k_{mz})\cdot\overline{b}_m^{(0)}\right\}F_m=0$$

$$+\frac{1}{2}\frac{k_{m-1}}{k_{mz}}e^{-ik_{mz}d_{m-1}}\left\{\tilde{A}_{m-1,q}^{(1)}(\overline{k}_\perp)+k_{mz}\hat{e}(-k_{mz})\cdot\overline{a}_{m-1}^{(0)}\right\}F_{m-1}$$
$$+\frac{1}{2}\frac{k_m}{k_{mz}}e^{-ik_{mz}d_{m-1}}\left\{\frac{k_{mz}}{k_m}\tilde{B}_{m-1,p}^{(1)}(\overline{k}_\perp)+\frac{k_\rho}{k_m}(\overline{k}_\perp-\overline{k}_{i\perp})\cdot\overline{b}_{m-1}^{(0)}+k_{mz}\hat{h}(-k_{mz})\cdot\overline{b}_{m-1}^{(0)}(\overline{k}'_\perp)\right\}F_{m-1}$$
$$-\frac{1}{2}\frac{k_m}{k_{mz}}e^{-ik_{mz}d_m}\left\{\tilde{A}_{m,q}^{(1)}(\overline{k}_\perp)+k_{mz}\hat{e}(-k_{mz})\cdot\overline{a}_m^{(0)}\right\}F_m$$
$$-\frac{1}{2}\frac{k_m}{k_{mz}}e^{-ik_{mz}d_m}\left\{\frac{k_{mz}}{k_m}\tilde{B}_{m,p}^{(1)}(\overline{k}_\perp)+\frac{k_\rho}{k_m}(\overline{k}_\perp-\overline{k}_{i\perp})\cdot\overline{b}_m^{(0)}+k_{mz}\hat{h}(-k_{mz})\cdot\overline{b}_m^{(0)}\right\}F_m=0$$

$$+\frac{1}{2}\frac{k_{N-1}}{k_{Nz}}e^{ik_{Nz}d_{N-1}}\left\{\tilde{A}_{N-1,q}^{(1)}(\overline{k}_\perp)-k_{Nz}\hat{e}(k_{Nz})\cdot\overline{a}_{N-1}^{(0)}\right\}$$
$$+\frac{1}{2}\frac{k_N}{k_{Nz}}e^{ik_{Nz}d_{N-1}}\left\{-\frac{k_{Nz}}{k_N}\tilde{B}_{N-1,p}^{(1)}(\overline{k}_\perp)+\frac{k_\rho}{k_N}(\overline{k}_\perp-\overline{k}_{i\perp})\cdot\overline{b}_{N-1}^{(0)}-k_{Nz}\hat{h}(k_{Nz})\cdot\overline{b}_{N-1}^{(0)}\right\}=0$$

From the middle layers relation for $2\leq m\leq N-1$, surface field over adjacent interfaces can be connected by

$$F_{m-1}\begin{bmatrix}\frac{k_{m-1}}{k_m} & -\frac{k_{mz}}{k_m}\\ \frac{k_{m-1}}{k_m} & +\frac{k_{mz}}{k_m}\end{bmatrix}\begin{bmatrix}\tilde{A}_{m-1,q}^{(1)}\\ \tilde{B}_{m-1,p}^{(1)}\end{bmatrix}+F_{m-1}\begin{bmatrix}u_m^{1e+}\\ u_m^{1e-}\end{bmatrix} \tag{4.5.37}$$
$$=F_m\begin{bmatrix}e^{i\phi_m} & 0\\ 0 & e^{-i\phi_m}\end{bmatrix}\begin{bmatrix}1 & -\frac{k_{mz}}{k_m}\\ 1 & +\frac{k_{mz}}{k_m}\end{bmatrix}\begin{bmatrix}\tilde{A}_{m,q}^{(1)}\\ \tilde{B}_{m,p}^{(1)}\end{bmatrix}+F_m\begin{bmatrix}c_m^{1e+}\\ c_m^{1e-}\end{bmatrix}$$

where $\delta_m = d_m - d_{m-1}$, $\phi_m = k_{mz}\delta_m$, and

$$u_m^{1e+} = -\frac{k_{m-1}}{k_m} k_{mz}\hat{e}(k_{mz})\cdot\overline{a}_{m-1}^{(0)} + \Big[\frac{k_\rho}{k_m}(\overline{k}_\perp - \overline{k}_{i\perp}) - k_{mz}\hat{h}(k_{mz})\Big]\cdot\overline{b}_{m-1}^{(0)} \tag{4.5.38}$$
$$u_m^{1e-} = \frac{k_{m-1}}{k_m} k_{mz}\hat{e}(-k_{mz})\cdot\overline{a}_{m-1}^{(0)} + \Big[\frac{k_\rho}{k_m}(\overline{k}_\perp - \overline{k}_{i\perp}) + k_{mz}\hat{h}(-k_{mz})\Big]\cdot\overline{b}_{m-1}^{(0)}$$

and

$$c_m^{1e+} = e^{i\phi_m}\Big\{-k_{mz}\hat{e}(k_{mz})\cdot\overline{a}_m^{(0)} + \Big[\frac{k_\rho}{k_m}(\overline{k}_\perp - \overline{k}_{i\perp}) - k_{mz}\hat{h}(k_{mz})\Big]\cdot\overline{b}_m^{(0)}\Big\} \tag{4.5.39}$$
$$c_m^{1e-} = e^{-i\phi_m}\Big\{k_{mz}\hat{e}(-k_{mz})\cdot\overline{a}_m^{(0)} + \Big[\frac{k_\rho}{k_m}(\overline{k}_\perp - \overline{k}_{i\perp}) + k_{mz}\hat{h}(-k_{mz})\Big]\cdot\overline{b}_m^{(0)}\Big\}$$

The matrix relation (4.5.37) can be used to explicitly express the surface fields on the $m$-th interface as

$$F_m\begin{bmatrix}\tilde{A}_{m,q}^{(1)}\\ \tilde{B}_{m,p}^{(1)}\end{bmatrix} = \overline{\overline{P}}_{m,m-1}^{[1e]} F_{m-1}\begin{bmatrix}\tilde{A}_{m-1,q}^{(1)}\\ \tilde{B}_{m-1,p}^{(1)}\end{bmatrix} + \overline{U}_m^{[1e]} F_{m-1} + \overline{C}_m^{[1e]} F_m \tag{4.5.40}$$

where,

$$\overline{\overline{P}}_{m,m-1}^{[1e]} = \begin{bmatrix}1 & -\frac{k_{mz}}{k_m}\\ 1 & +\frac{k_{mz}}{k_m}\end{bmatrix}^{-1}\begin{bmatrix}e^{-i\phi_m} & 0\\ 0 & e^{i\phi_m}\end{bmatrix}\begin{bmatrix}\frac{k_{m-1}}{k_m} & -\frac{k_{mz}}{k_m}\\ \frac{k_{m-1}}{k_m} & +\frac{k_{mz}}{k_m}\end{bmatrix} \tag{4.5.41}$$
$$\overline{C}_m^{[1e]} = -\begin{bmatrix}1 & -\frac{k_{mz}}{k_m}\\ 1 & +\frac{k_{mz}}{k_m}\end{bmatrix}^{-1}\begin{bmatrix}e^{-i\phi_m} & 0\\ 0 & e^{i\phi_m}\end{bmatrix}\begin{bmatrix}c_m^{1e+}\\ c_m^{1e-}\end{bmatrix}$$
$$\overline{U}_m^{[1e]} = \begin{bmatrix}1 & -\frac{k_{mz}}{k_m}\\ 1 & +\frac{k_{mz}}{k_m}\end{bmatrix}^{-1}\begin{bmatrix}e^{-i\phi_m} & 0\\ 0 & e^{i\phi_m}\end{bmatrix}\begin{bmatrix}u_m^{1e+}\\ u_m^{1e-}\end{bmatrix}$$

Equation. 4.5.40 can be used to recursively connect interface by interface to eventually have a relationship between the first and the last interface surface fields. This relation can

be found by induction and it is given by

$$
\begin{aligned}
F_{N-1}\begin{bmatrix}\tilde{A}^{(1)}_{N-1,q}\\ \tilde{B}^{(1)}_{N-1,p}\end{bmatrix} = & \prod_{j=2}^{N-1}\overline{\overline{P}}^{[1e]}_{j,j-1}F_1\begin{bmatrix}\tilde{A}^{(1)}_{1,q}\\ \tilde{B}^{(1)}_{1,p}\end{bmatrix} \\
& + \prod_{j=3}^{N-1}\overline{\overline{P}}^{[1e]}_{j,j-1}\overline{U}^{[1e]}_{2}F_1 \\
& + \prod_{j=4}^{N-1}\overline{\overline{P}}^{[1e]}_{j,j-1}\left(\overline{U}^{[1e]}_{3}+\overline{\overline{P}}^{[1e]}_{3,2}\overline{C}^{[1e]}_{2}\right)F_2 \\
& + \prod_{j=5}^{N-1}\overline{\overline{P}}^{[1e]}_{j,j-1}\left(\overline{U}^{[1e]}_{4}+\overline{\overline{P}}^{[1e]}_{4,3}\overline{C}^{[1e]}_{3}\right)F_3 \\
& + \prod_{j=6}^{N-1}\overline{\overline{P}}^{[1e]}_{j,j-1}\left(\overline{U}^{[1e]}_{5}+\overline{\overline{P}}^{[1e]}_{5,4}\overline{C}^{[1e]}_{4}\right)F_4 \\
& \vdots \\
& + \prod_{j=N-1}^{N-1}\overline{\overline{P}}^{[1e]}_{j,j-1}\left(\overline{U}^{[1e]}_{N-2}+\overline{\overline{P}}^{[1e]}_{N-2,N-3}\overline{C}^{[1e]}_{N-3}\right)F_{N-3} \\
& + \left(\overline{U}^{[1e]}_{N-1}+\overline{\overline{P}}^{[1e]}_{N-1,N-2}\overline{U}^{[1e]}_{N-2}\right)F_{N-2} \\
& + \overline{C}^{[1e]}_{N-1}F_{N-1}
\end{aligned}
\tag{4.5.42}
$$

By taking total propagation matrix corresponds to the flat interfaces between the first and last layers as

$$
\overline{\overline{P}}^{[1e]} = \prod_{j=2}^{N-1}\overline{\overline{P}}^{[1e]}_{j,j-1} \tag{4.5.43}
$$

which results in,

$$
F_{N-1}\begin{bmatrix}\tilde{A}^{(1)}_{N-1,q}\\ \tilde{B}^{(1)}_{N-1,p}\end{bmatrix} - \overline{\overline{P}}^{[1e]}F_1\begin{bmatrix}\tilde{A}^{(1)}_{1,q}\\ \tilde{B}^{(1)}_{1,p}\end{bmatrix} = \overline{R}^{[1e]} \tag{4.5.44}
$$

where,

$$\begin{aligned}\overline{R}^{[1e]}=&+\prod_{j=3}^{N-1}\overline{\overline{P}}^{[1e]}_{j,j-1}\overline{U}^{[1e]}_{2}F_1\\&+\prod_{j=4}^{N-1}\overline{\overline{P}}^{[1e]}_{j,j-1}\left(\overline{U}^{[1e]}_{3}+\overline{\overline{P}}^{[1e]}_{3,2}\overline{C}^{[1e]}_{2}\right)F_2\\&+\prod_{j=5}^{N-1}\overline{\overline{P}}^{[1e]}_{j,j-1}\left(\overline{U}^{[1e]}_{4}+\overline{\overline{P}}^{[1e]}_{4,3}\overline{C}^{[1e]}_{3}\right)F_3\\&+\prod_{j=6}^{N-1}\overline{\overline{P}}^{[1e]}_{j,j-1}\left(\overline{U}^{[1e]}_{5}+\overline{\overline{P}}^{[1e]}_{5,4}\overline{C}^{[1e]}_{4}\right)F_4\\&\vdots\\&+\prod_{j=N-1}^{N-1}\overline{\overline{P}}^{[1e]}_{j,j-1}\left(\overline{U}^{[1e]}_{N-2}+\overline{\overline{P}}^{[1e]}_{N-2,N-3}\overline{C}^{[1e]}_{N-3}\right)F_{N-3}\\&+\left(\overline{U}^{[1e]}_{N-1}+\overline{\overline{P}}^{[1e]}_{N-1,N-2}\overline{U}^{[1e]}_{N-2}\right)F_{N-2}\\&+\overline{C}^{[1e]}_{N-1}F_{N-1}\end{aligned}\tag{4.5.45}$$

In addition, from extinction relation of two half spaces,

$$\begin{aligned}\tilde{A}^{(1)}_{1q}(\overline{k}_\perp)+\frac{k_{1z}}{k_1}\tilde{B}^{(1)}_{1p}(\overline{k}_\perp)+C^{[1e]}_{12}=0\\\frac{k_{N-1}}{k_N}\tilde{A}^{(1)}_{N-1,q}(\overline{k}_\perp)-\frac{k_{Nz}}{k_N}\tilde{B}^{(1)}_{N-1,p}(\overline{k}_\perp)+C^{[1e]}_{N,N-1}=0\end{aligned}\tag{4.5.46}$$

where,

$$\begin{aligned}C^{[1e]}_{12}=&k_{1z}\hat{e}(-k_{1z})\cdot\overline{a}^{(0)}_1+\left[\frac{k_\rho}{k_1}(\overline{k}_\perp-\overline{k}_{i\perp})+k_{1z}\hat{h}(-k_{1z})\right]\cdot\overline{b}^{(0)}_1\\C^{[1e]}_{N,N-1}=&-\frac{k_{N-1}}{k_N}k_{Nz}\hat{e}(k_{Nz})\cdot\overline{a}^{(0)}_{N-1}+\left[\frac{k_\rho}{k_N}(\overline{k}_\perp-\overline{k}_{i\perp})-k_{Nz}\hat{h}(k_{Nz})\right]\cdot\overline{b}^{(0)}_{N-1}\end{aligned}\tag{4.5.47}$$

The matrix equation (4.5.44) together with external half spaces relation of (4.5.46) provides sufficient information to solve for the unknown first order TE surface fields. Similarly, for TM part of the first order extinction equations,

$$\begin{aligned}&-\frac{1}{2}\frac{k_1}{k_{1z}}\left\{\frac{k_{1z}}{k_1}\tilde{A}^{(1)}_{1p}(\overline{k}_\perp)+\frac{k_\rho}{k_1}(\overline{k}_\perp-\overline{k}_{i\perp})\cdot\overline{a}^{(0)}_1+k_{1z}\hat{h}(-k_{1z})\cdot\overline{a}^{(0)}_1\right\}\\&+\frac{1}{2}\frac{k_1}{k_{1z}}\left\{\tilde{B}^{(1)}_{1q}(k_x,k_y)+k_{1z}\hat{e}(-k_{1z})\cdot\overline{b}^{(0)}_1\right\}=0\end{aligned}\tag{4.5.48}$$

$$+\frac{1}{2}\frac{k_{m-1}}{k_{mz}}e^{ik_{mz}d_{m-1}}\Big\{-\frac{k_{mz}}{k_m}\tilde{A}^{(1)}_{m-1,p}(\overline{k}_\perp)+\frac{k_\rho}{k_m}(\overline{k}_\perp-\overline{k}_{i\perp})\cdot\overline{a}^{(0)}_{m-1}-k_{mz}\hat{h}(k_{mz})\cdot\overline{a}^{(0)}_{m-1}\Big\}F_{m-1} \tag{4.5.49}$$

$$-\frac{1}{2}\frac{k_m}{k_{mz}}e^{ik_{mz}d_{m-1}}\Big\{\tilde{B}^{(1)}_{m-1,q}(\overline{k}_\perp)-k_{mz}\hat{e}(k_{mz})\cdot\overline{b}^{(0)}_{m-1}\Big\}F_{m-1}$$
$$-\frac{1}{2}\frac{k_m}{k_{mz}}e^{ik_{mz}d_m}\Big\{-\frac{k_{mz}}{k_m}\tilde{A}^{(1)}_{m,p}(\overline{k}_\perp)+\frac{k_\rho}{k_m}(\overline{k}_\perp-\overline{k}_{i\perp})\cdot\overline{a}^{(0)}_{m}-k_{mz}\hat{h}(k_{mz})\cdot\overline{a}^{(0)}_{m}\Big\}F_{m}$$
$$+\frac{1}{2}\frac{k_m}{k_{mz}}e^{ik_{mz}d_m}\Big\{\tilde{B}^{(1)}_{m,q}(\overline{k}_\perp)-k_{mz}\hat{e}(k_{mz})\cdot\overline{b}^{(0)}_{m}\Big\}F_{m}=0$$

$$+\frac{1}{2}\frac{k_{m-1}}{k_{mz}}e^{-ik_{mz}d_{m-1}}\Big\{\frac{k_{mz}}{k_m}\tilde{A}^{(1)}_{m-1,p}(\overline{k}_\perp)+\frac{k_\rho}{k_m}(\overline{k}_\perp-\overline{k}_{i\perp})\cdot\overline{a}^{(0)}_{m-1}+k_{mz}\hat{h}(-k_{mz})\cdot\overline{a}^{(0)}_{m-1}\Big\}F_{m-1} \tag{4.5.50}$$

$$-\frac{1}{2}\frac{k_m}{k_{mz}}e^{-ik_{mz}d_{m-1}}\Big\{\tilde{B}^{(1)}_{m-1,q}(\overline{k}_\perp)+k_{mz}\hat{e}(-k_{mz})\cdot\overline{b}^{(0)}_{m-1}\Big\}F_{m-1}$$
$$-\frac{1}{2}\frac{k_m}{k_{mz}}e^{-ik_{mz}d_m}\Big\{\frac{k_{mz}}{k_m}\tilde{A}^{(1)}_{m,p}(\overline{k}_\perp)+\frac{k_\rho}{k_m}(\overline{k}_\perp-\overline{k}_{i\perp})\cdot\overline{a}^{(0)}_{m}+k_{mz}\hat{h}(-k_{mz})\cdot\overline{a}^{(0)}_{m}\Big\}F_{m}$$
$$+\frac{1}{2}\frac{k_m}{k_{mz}}e^{-ik_{mz}d_m}\Big\{\tilde{B}^{(1)}_{m,q}(\overline{k}_\perp)+k_{mz}\hat{e}(-k_{mz})\cdot\overline{b}^{(0)}_{m}\Big\}F_{m}=0$$

$$+\frac{1}{2}\frac{k_{N-1}}{k_{Nz}}e^{ik_{Nz}d_{N-1}}\Big\{-\frac{k_{Nz}}{k_N}\tilde{A}^{(1)}_{N-1,p}(\overline{k}_\perp)+\frac{k_\rho}{k_N}(\overline{k}_\perp-\overline{k}_{i\perp})\cdot\overline{a}^{(0)}_{N-1}-k_{Nz}\hat{h}(k_{Nz})\cdot\overline{a}^{(0)}_{N-1}\Big\} \tag{4.5.51}$$
$$-\frac{1}{2}\frac{k_N}{k_{Nz}}e^{ik_{Nz}d_{N-1}}\Big\{\tilde{B}^{(1)}_{N-1,q}(\overline{k}_\perp)-k_{Nz}\hat{e}(k_{Nz})\cdot\overline{b}^{(0)}_{N-1}\Big\}=0$$

The middle layers extinction relations (4.5.49), and (4.5.50) can be written as a matrix equation between surface fields of interface $m$ and $m-1$ as

$$\begin{bmatrix}-\frac{k_{m-1}}{k_m}\frac{k_{mz}}{k_m} & -1\\ +\frac{k_{m-1}}{k_m}\frac{k_{mz}}{k_m} & -1\end{bmatrix}F_{m-1}\begin{bmatrix}\tilde{A}^{(1)}_{m-1,p}\\ \tilde{B}^{(1)}_{m-1,q}\end{bmatrix}+F_{m-1}\begin{bmatrix}u^{1h+}_m\\ u^{1h-}_m\end{bmatrix}$$
$$=\begin{bmatrix}e^{i\phi_m} & 0\\ 0 & e^{-i\phi_m}\end{bmatrix}\begin{bmatrix}-\frac{k_{mz}}{k_m} & -1\\ \frac{k_{mz}}{k_m} & -1\end{bmatrix}F_m\begin{bmatrix}\tilde{A}^{(1)}_{m,p}\\ \tilde{B}^{(1)}_{m,q}\end{bmatrix}+F_m\begin{bmatrix}c^{1h+}_m\\ c^{1h-}_m\end{bmatrix}$$

where

$$u^{1h+}_m=\frac{k_{m-1}}{k_m}\Big[\frac{k_\rho}{k_m}(\overline{k}_\perp-\overline{k}_{i\perp})-k_{mz}\hat{h}(k_{mz})\Big]\cdot\overline{a}^{(0)}_{m-1}+k_{mz}\hat{e}(k_{mz})\cdot\overline{b}^{(0)}_{m-1} \tag{4.5.52}$$
$$u^{1h-}_m=\frac{k_{m-1}}{k_m}\Big[\frac{k_\rho}{k_m}(\overline{k}_\perp-\overline{k}_{i\perp})+k_{mz}\hat{h}(-k_{mz})\Big]\cdot\overline{a}^{(0)}_{m-1}-k_{mz}\hat{e}(-k_{mz})\cdot\overline{b}^{(0)}_{m-1}$$

and

$$c^{1h+}_m=e^{i\phi_m}\left(\Big[\frac{k_\rho}{k_m}(\overline{k}_\perp-\overline{k}_{i\perp})-k_{mz}\hat{h}(k_{mz})\Big]\cdot\overline{a}^{(0)}_{m}+k_{mz}\hat{e}(k_{mz})\cdot\overline{b}^{(0)}_{m}\right) \tag{4.5.53}$$
$$c^{1h-}_m=e^{-i\phi_m}\left(\Big[\frac{k_\rho}{k_m}(\overline{k}_\perp-\overline{k}_{i\perp})+k_{mz}\hat{h}(-k_{mz})\Big]\cdot\overline{a}^{(0)}_{m}-k_{mz}\hat{e}(-k_{mz})\cdot\overline{b}^{(0)}_{m}\right)$$

or by collecting the matrices involved into one matrix

$$F_m\begin{bmatrix}\tilde{A}^{(1)}_{m,p}\\ \tilde{B}^{(1)}_{m,q}\end{bmatrix}=\overline{\overline{P}}^{[1h]}_{m,m-1}F_{m-1}\begin{bmatrix}\tilde{A}^{(1)}_{m-1,p}\\ \tilde{B}^{(1)}_{m-1,q}\end{bmatrix}+\overline{U}^{1h}_m F_{m-1}+\overline{C}^{1h}_m F_m \tag{4.5.54}$$

where TM propagation matrix $\overline{\overline{P}}^{[1h]}_{m,m-1}$ and vectors $\overline{U}^{1h}_m$ and $\overline{C}^{1h}_m$ are defined through,

$$\begin{aligned}\overline{\overline{P}}^{[1h]}_{m,m-1}&=\begin{bmatrix}-\frac{k_{mz}}{k_m} & -1\\ \frac{k_{mz}}{k_m} & -1\end{bmatrix}^{-1}\begin{bmatrix}e^{-i\phi_m} & 0\\ 0 & e^{i\phi_m}\end{bmatrix}\begin{bmatrix}-\frac{k_{m-1}}{k_m}\frac{k_{mz}}{k_m} & -1\\ +\frac{k_{m-1}}{k_m}\frac{k_{mz}}{k_m} & -1\end{bmatrix}\\ \overline{U}^{1h}_m&=\begin{bmatrix}-\frac{k_{mz}}{k_m} & -1\\ \frac{k_{mz}}{k_m} & -1\end{bmatrix}^{-1}\begin{bmatrix}e^{-i\phi_m} & 0\\ 0 & e^{i\phi_m}\end{bmatrix}\begin{bmatrix}u^{1h+}_m\\ u^{1h-}_m\end{bmatrix}\\ \overline{C}^{1h}_m&=-\begin{bmatrix}-\frac{k_{mz}}{k_m} & -1\\ \frac{k_{mz}}{k_m} & -1\end{bmatrix}^{-1}\begin{bmatrix}e^{-i\phi_m} & 0\\ 0 & e^{i\phi_m}\end{bmatrix}\begin{bmatrix}c^{1h+}_m\\ c^{1h-}_m\end{bmatrix}\end{aligned} \tag{4.5.55}$$

The propagation relation (4.5.54) connects the surface fields over the interface $m$ to that of interface $m-1$. From that, the first and last interface surface fields can be connected through a linear relation that can be obtained by induction (similar to the TE case) as

$$F_{N-1}\begin{bmatrix}\tilde{A}^{(1)}_{N-1,p}\\ \tilde{B}^{(1)}_{N-1,q}\end{bmatrix}-\overline{\overline{P}}^{[1h]}F_1\begin{bmatrix}\tilde{A}^{(1)}_{1,p}\\ \tilde{B}^{(1)}_{1,q}\end{bmatrix}=\overline{R}^{[1h]}$$

where, the vector $\overline{R}^{[1h]}$ which contained the roughness effect is defined by

$$\begin{aligned}\overline{R}^{[1h]}=&\prod_{j=3}^{N-1}\overline{\overline{P}}^{[1h]}_{j,j-1}\overline{U}^{[1h]}_2F_1\\ &+\prod_{j=4}^{N-1}\overline{\overline{P}}^{[1h]}_{j,j-1}\left(\overline{U}^{[1h]}_3+\mathbb{P}^{[1h]}_{3,2}\overline{C}^{[1h]}_2\right)F_2\\ &+\prod_{j=5}^{N-1}\overline{\overline{P}}^{[1h]}_{j,j-1}\left(\overline{U}^{[1h]}_4+\mathbb{P}^{[1h]}_{4,3}\overline{C}^{[1h]}_3\right)F_3\\ &+\prod_{j=6}^{N-1}\overline{\overline{P}}^{[1h]}_{j,j-1}\left(\overline{U}^{[1h]}_5+\mathbb{P}^{[1h]}_{5,4}\overline{C}^{[1h]}_4\right)F_4\\ &\vdots\\ &+\prod_{j=N-1}^{N-1}\overline{\overline{P}}^{[1h]}_{j,j-1}\left(\overline{U}^{[1h]}_{N-2}+\mathbb{P}^{[1h]}_{N-2,N-3}\overline{C}^{[1h]}_{N-3}\right)F_{N-3}\\ &+\left(\overline{U}^{[1h]}_{N-1}+\overline{\overline{P}}^{[1h]}_{N-1,N-2}\overline{C}^{[1h]}_{N-2}\right)F_{N-2}\\ &+\overline{C}^{[1h]}_{N-1}F_{N-1}\end{aligned} \tag{4.5.56}$$

also from both ends extinction theorems we have

$$\begin{aligned}-\frac{k_{1z}}{k_1}\tilde{A}^{(1)}_{1p}(\overline{k}_\perp)+\tilde{B}^{(1)}_{1q}(\overline{k}_\perp)+C^{[1h]}_{12}=0\\ -\frac{k_{Nz}}{k_N}\tilde{A}^{(1)}_{N-1,p}(\overline{k}_\perp)-\tilde{B}^{(1)}_{N-1,q}(\overline{k}_\perp)+C^{[1h]}_{N,N-1}=0\end{aligned} \tag{4.5.57}$$

where

$$C_{12}^{[1h]} = -\left[\frac{k_\rho}{k_1}(\overline{k}_\perp - \overline{k}_{i\perp}) + k_{1z}\hat{h}(-k_{1z})\right]\cdot\overline{a}_1^{(0)} + k_{1z}\hat{e}(-k_{1z})\cdot\overline{b}_1^{(0)} \tag{4.5.58}$$
$$C_{N,N-1}^{[1h]} = \left[\frac{k_\rho}{k_N}(\overline{k}_\perp - \overline{k}_{i\perp}) - k_{Nz}\hat{h}(k_{Nz})\cdot\right]\overline{a}_{N-1}^{(0)} + k_{Nz}\hat{e}(k_{Nz})\cdot\overline{b}_{N-1}^{(0)}$$

Therefore, a complete set of equations for the TM part of the surface field can be written as

$$\begin{bmatrix} -\frac{k_{1z}}{k_1} & 1 & 0 & 0 \\ 0 & 0 & -\frac{k_{Nz}}{k_N} & -1 \\ -P_{11}^{[1h]} & -P_{12}^{[1h]} & 1 & 0 \\ -P_{21}^{[1h]} & -P_{22}^{[1h]} & 0 & 1 \end{bmatrix} \begin{bmatrix} F_1\tilde{A}_{1p}^{(1)} \\ F_1\tilde{B}_{1q}^{(1)} \\ F_{N-1}\tilde{A}_{N-1,p}^{(1)} \\ F_{N-1}\tilde{B}_{N-1,q}^{(1)} \end{bmatrix} = \begin{bmatrix} -F_1 C_{12}^{[1h]} \\ -F_{N-1} C_{N,N-1}^{[1h]} \\ R^{[1h]} \end{bmatrix} \tag{4.5.59}$$

As an aside, from the linear system of (4.5.59), since the vector $\overline{R}^{[1h]}$ linearly depends on all of the surfaces spectrum, the surface fields do depend linearly of all of the surfaces spectrum.

### 4.5.5 First Order Scattered and Transmitted Field

The scattered field can be computed using the equivalence principle applied to the region 1 with known surface fields. Balancing the TE scattered field expression up to the first order nd using the first order approximation of the scattering potential for the scattered field as

$$I_{11}^{+(1)}(\overline{k}_\perp,\overline{k}'_\perp)=-ik_{1z}F_1(\overline{k}_\perp-\overline{k}'_\perp) \tag{4.5.60}$$

we arrive at,

$$-2\frac{k_{1z}}{k_1}\hat{e}(k_{1z})\cdot\tilde{\overline{E}}_s^{(1)}(\overline{k})=iF_1(k_\perp-k_{\perp_i})\Big\{\tilde{A}_{1q}^{(1)}(\overline{k}_\perp)-k_{1z}\hat{e}(k_{1z})\cdot\overline{a}_1^{(0)} \tag{4.5.61}$$

$$-\frac{k_{1z}}{k_1}\tilde{B}_{1p}^{(1)}(\overline{k}_\perp)+\left(\frac{k_\rho}{k_1}(\overline{k}_\perp-\overline{k}_{\perp_i})-k_{1z}\hat{h}(k_{1z})\right)\cdot\overline{b}_1^{(0)}\Big\} \tag{4.5.62}$$

This expression can be further simplified if we use the extinction relation of the downward propagating wave in region 1 of (4.5.36) as

$$\tilde{A}_{1q}^{(1)}(\overline{k}_\perp)+\frac{k_{1z}}{k_1}\tilde{B}_{1p}^{(1)}(\overline{k}_\perp)+k_{1z}\hat{e}(-k_{1z})\cdot\overline{a}_1^{(0)}+\left(\frac{k_\rho}{k_1}(\overline{k}_\perp-\overline{k}_{\perp_i})+k_{1z}\hat{h}(-k_{1z})\right)\cdot\overline{b}_1^{(0)}=0 \tag{4.5.63}$$

which is essentially similar to the expression of the scattered field except it is a relation for a downward propagating field. Manipulating the signs by make a sign flip in the arguments of polarization unit vectors to be matched with scattered field and utilizing that

$$\hat{h}(-k_{1z})\cdot\overline{T}=-\hat{h}(k_{1z})\cdot\overline{T} \tag{4.5.64}$$

where $\overline{T}$ is transverse vector such that $\overline{T}\cdot\hat{z}=0$ and

$$\hat{e}(-k_{1z})=\hat{e}(k_{1z}) \tag{4.5.65}$$

(4.5.63) results in,

$$\tilde{A}_{1q}^{(1)}(\overline{k}_\perp)+k_{1z}\hat{e}(k_{1z})\cdot\overline{a}_1^{(0)}+\left(\frac{k_\rho}{k_1}(\overline{k}_\perp-\overline{k}_{\perp_i})-k_{1z}\hat{h}(k_{1z})\right)\cdot\overline{b}_1^{(0)}=-\frac{k_{1z}}{k_1}\tilde{B}_{1p}^{(1)}(\overline{k}_\perp) \tag{4.5.66}$$

that upon substitution in the scattered field expression results in a great simplification that leads to a factor of 2 to get

$$\hat{e}(k_{1z})\cdot\tilde{\overline{E}}_s^{(1)}(\overline{k})=-iF_1(k_\perp-k_{\perp_i})\frac{k_1}{k_{1z}}\left\{\tilde{A}_{1q}^{(1)}(\overline{k}_\perp)+\left(\frac{k_\rho}{k_1}(\overline{k}_\perp-\overline{k}_{\perp_i})-k_{1z}\hat{h}(k_{1z})\right)\cdot\overline{b}_1^{(0)}\right\}$$

Using TE surface fields solution, the solution of the first boundary surface fields is a linear combination of all of the surfaces spectra as

$$F_1(k_\perp-k_{\perp_i})\tilde{A}_{1q}^{(1)}(\overline{k}_\perp)=\tilde{A}_{1q,F1}^{(1)}F_1(k_\perp-k_{\perp_i})+\sum_{j\neq1}\tilde{A}_{q,F_j}^{(1)}F_j(k_\perp-k_{\perp_i}) \tag{4.5.67}$$

Therefore, the first order TE scattered field has $N-1$ spectral components in terms of individual interfaces

$$\hat{e}(k_z)\cdot\overline{E}_s^{(1)}(\overline{k})=\sum_{j=1}^{N-1}S_{e,F_j}^{(1)}(\overline{k}_\perp)F_j(k_\perp-k_{\perp_i}) \tag{4.5.68}$$

where contribution of each interface in the scattered field is given by

$$S^{(1)}_{e,F_j}(\overline{k}_\perp)=\begin{cases}-\dfrac{ik_1}{k_{1z}}\left[\tilde{A}^{(1)}_{1q,F_1}(\overline{k}_\perp)+\left(\dfrac{k_\rho}{k_1}(\overline{k}_\perp-\overline{k}_{\perp_i})-k_{1z}\hat{h}(k_{1z})\right)\cdot\overline{b}^{(0)}_1\right] & j=1\\ -\dfrac{ik_1}{k_{1z}}\tilde{A}^{(1)}_{1q,F_j}(\overline{k}_\perp) & j\neq 1\end{cases} \tag{4.5.69}$$

Similarly, the first order TM scattered field can be obtained as

$$\hat{h}(k_z)\cdot\overline{E}^{(1)}_s(\overline{k})=\sum_{j=1}^{N-1}S^{(1)}_{h,F_j}(\overline{k}_\perp)F_j(k_\perp-k_{\perp_i}) \tag{4.5.70}$$

where

$$S^{(1)}_{h,F_j}(\overline{k}_\perp)=\begin{cases}\dfrac{ik_1}{k_{1z}}\left[\tilde{B}^{(1)}_{1q,F_1}-\left(\dfrac{k_\rho}{k_1}(\overline{k}_\perp-\overline{k}_{\perp_i})-k_{1z}\hat{h}(k_{1z})\right)\cdot\overline{a}^{(0)}_1\right] & j=1\\ \dfrac{ik_1}{k_{1z}}\tilde{B}^{(1)}_{1q,F_j} & j\neq 1\end{cases} \tag{4.5.71}$$

Therefore, total first order scattered field can be written as

$$\overline{E}^{(1)}_s(\overline{k}_\perp)=\sum_{j=1}^{N-1}F_j(k_\perp-k_{\perp_i})\left[S^{(1)}_{e,F_j}(\overline{k}_\perp)\hat{e}(k_z)+S^{(1)}_{h,F_j}(\overline{k}_\perp)\hat{h}(k_z)\right] \tag{4.5.72}$$

Notice that the first order scattered field is linearly related to the surface spectra. Therefore, one may obtain the first order solution of the scattered field by considering a layered media with only one rough interface at a time and the rest of the interfaces to be flat to find contribution of each rough surface and add them up to get the final result. However, this would not be the case for higher orders of solution. Converting the scattered field to spatial domain representation,

$$\begin{aligned}\overline{E}^{(1)}_s(\overline{r})&=\int \mathrm{d}\overline{k}_\perp\tilde{\overline{E}}^{(1)}_s(\overline{k}_\perp)e^{i\overline{k}\cdot\overline{r}}\\ &=\sum_{j=1}^{N-1}\int \mathrm{d}\overline{k}_\perp e^{i\overline{k}\cdot\overline{r}}F_j(k_\perp-k_{\perp_i})\left[S^{(1)}_{e,F_j}(\overline{k}_\perp)\hat{e}(k_z)+S^{(1)}_{h,F_j}(\overline{k}_\perp)\hat{h}(k_z)\right]\end{aligned} \tag{4.5.73}$$

Equation (4.5.73) shows that the first order scattered and transmitted fields have a non-zero bandwidth in the spectral domain, which means scattered and transmitted fields involve continuous spectrum of plane waves in different directions.

Also it is worth to note that the spectrum of the scattered field (4.5.73) is filtered by the surface spectrum $F_j(\overline{k}_\perp)$. In other words, the scattered field from a random rough surface in a special directions does exist if the surface spectrum can provide a non-zero amplitude at that spectral frequency.

Another observation is that every rough interfaces has its own contribution to the scattered field that is true in the light of linearity of the problem. For zero mean processes, averaging over ensemble of Gaussian random surfaces give zero and therefore the first order scattered field has zero mean

$$\langle\overline{E}^{(1)}_s(\overline{r})\rangle=0 \tag{4.5.74}$$

So the first order fields are totally random. we will use higher order moments of first order fields solution in section 4.6. The second order averaged scattered field and transmitted field can be computed as (in section 4.6 we will see why we are interested in the average of second order scattered field). For the first order transmitted field, following a similar procedure as the scattered field we obtain

$$\overline{E}_t^{(1)}(\overline{k}_\perp)=\sum_{j=1}^{N-1} F_j(k_\perp-k_{\perp_i})\left[T_{e,F_j}^{(1)}(\overline{k}_\perp)\hat{e}(-k_{Nz})+T_{h,F_j}^{(1)}(\overline{k}_\perp)\hat{h}(-k_{Nz})\right] \tag{4.5.75}$$

where, each interface roughness contributes to the first order TE and TM transmitted field through

$$T_{e,F_j}^{(1)}(\overline{k}_\perp)=\begin{cases}\dfrac{ik_N}{k_{Nz}}\left[\dfrac{k_{N-1}}{k_N}\tilde{A}_{N-1,q,F_1}^{(1)}(\overline{k}_\perp)+\left(\dfrac{k_\rho}{k_N}(\overline{k}_\perp-\overline{k}_{\perp_i})+k_{Nz}\hat{h}(-k_{Nz})\right)\cdot\overline{b}_{N-1}^{(0)}\right] & j=1\\ \dfrac{ik_{N-1}}{k_{Nz}}\tilde{A}_{N-1,q,F_j}^{(1)}(\overline{k}_\perp) & j\neq 1\end{cases} \tag{4.5.76}$$

$$T_{h,F_j}^{(1)}(\overline{k}_\perp)=\begin{cases}\dfrac{ik_N}{k_{Nz}}\left[\dfrac{k_{N-1}}{k_N}\left(\dfrac{k_\rho}{k_N}(\overline{k}_\perp-\overline{k}_{\perp_i})+k_{Nz}\hat{h}(-k_{Nz})\right)\cdot\overline{a}_{N-1}^{(0)}-\tilde{B}_{N-1,q,F_1}^{(1)}\right] & j=1\\ -\dfrac{ik_N}{k_{Nz}}\tilde{B}_{N-1,q,F_j}^{(1)} & j\neq 1\end{cases} \tag{4.5.77}$$

The transmitted field representation in spatial domain can be obtained from (4.5.75) by a superposition integral as

$$\begin{aligned}\overline{E}_t^{(1)}(\overline{r})&=\int \mathrm{d}\overline{k}_\perp\,\overline{E}_t^{(1)}(\overline{k})e^{i\overline{k}_\perp\cdot\overline{r}_\perp-ik_{Nz}z}\\&=\sum_{j=1}^{N-1}\int \mathrm{d}\overline{k}_\perp e^{i\overline{k}_\perp\cdot\overline{r}_\perp-ik_{Nz}z}F_j(k_\perp-k_{\perp_i})\left[T_{e,F_j}^{(1)}(\overline{k}_\perp)\hat{e}(-k_{Nz})+T_{h,F_j}^{(1)}(\overline{k}_\perp)\hat{h}(-k_{Nz})\right]\end{aligned}$$

### 4.5.6 Second Order Solution

The second order solution is proportional to the interfaces spectra in a quadratic fashion and includes multiple scattering processes up to the second order within the solution. The transverse component of the surface fields are second order in the surface roughness parameter. Since the $z$-component of the fields are an order lower that the traverse fields, it would be from the first order within the second order solution and it can be expressed in terms of the first order solution as

$$Q_{j,z}^{(2)}(\overline{k}_\perp)=\int \mathrm{d}\overline{k}'_\perp iF_j(\overline{k}_\perp-\overline{k}'_\perp)(\overline{k}_\perp-\overline{k}'_\perp)\cdot\overline{Q}_{j,\perp}^{(1)}(\overline{k}'_\perp) \tag{4.5.78}$$

and using the first order tilde fields solution $\tilde{\overline{Q}}_{j,\perp}^{(1)}$, it can be written as

$$Q_{j,z}^{(2)}(\overline{k}_\perp)=-\int \mathrm{d}\overline{k}'_\perp F_j(\overline{k}_\perp-\overline{k}'_\perp)F_j(\overline{k}'_\perp-\overline{k}_{\perp_i})(\overline{k}_\perp-\overline{k}'_\perp)\cdot\tilde{\overline{Q}}_{j,\perp}^{(1)}(\overline{k}'_\perp) \tag{4.5.79}$$

where $Q$ can be an electric or magnetic surface field. For the second order solution the first and second order approximations of the scattering potentials are required. Within the second order approximation,

$$
\begin{aligned}
I_{11}^{\pm(2)}(\overline{k}_\perp;\overline{k}'_\perp)&=-\frac{1}{2}k_{1z}^2F_1^{(2)}(\overline{k}_\perp-\overline{k}'_\perp)\\
I_{m,m-1}^{\pm(2)}(\overline{k}_\perp;\overline{k}'_\perp)&=-\frac{1}{2}k_{mz}^2F_{m-1}^{(2)}(\overline{k}_\perp-\overline{k}'_\perp)\\
I_{mm}^{\pm(2)}(\overline{k}_\perp;\overline{k}'_\perp)&=-\frac{1}{2}k_{mz}^2F_m^{(2)}(\overline{k}_\perp-\overline{k}'_\perp)\\
I_{N,N-1}^{\pm(2)}(\overline{k}_\perp;\overline{k}'_\perp)&=-\frac{1}{2}k_{Nz}^2F_{N-1}^{(2)}(\overline{k}_\perp-\overline{k}'_\perp)
\end{aligned}
\tag{4.5.80}
$$

where $F^{(2)}=F\star F$ and $\star$ denotes 2D convolution. Balancing the extinction relations (4.3.11), (4.3.26), (4.3.31), (4.3.32), (4.3.38), and (4.3.39) up to the second order on both sides, inserting the zeroth and first order solutions of the surface field and scattering potentials, and lengthy simplifications, we arrive at the following relation between the TE part of the surface fields,

$$
\begin{aligned}
&A_{1q}^{(2)}(\overline{k}_\perp)+\frac{k_{1z}}{k_1}B_{1p}^{(2)}(\overline{k}_\perp)-\frac{1}{2}k_{1z}^2\left[\hat{e}(-k_{1z})\cdot\overline{a}_1^{(0)}+\hat{h}(-k_{1z})\cdot\overline{b}_1^{(0)}\right]F_1^{(2)}(\overline{k}_\perp-\overline{k}_{i\perp})\\
&\qquad+\int\mathrm{d}\overline{k}'_\perp(-)k_{1z}\hat{e}(-k_{1z})\cdot\tilde{\overline{A}}_1^{(1)}(\overline{k}'_\perp)F_1(\overline{k}_\perp-\overline{k}'_\perp)F_1(\overline{k}'_\perp-\overline{k}_{i\perp})\\
&-\frac{k_\rho}{k_1}\int\mathrm{d}\overline{k}'_\perp F_1(\overline{k}_\perp-\overline{k}'_\perp)F_1(\overline{k}'_\perp-\overline{k}_{\perp_i})(\overline{k}_\perp-\overline{k}'_\perp)\cdot\tilde{\overline{B}}_{1,\perp}^{(1)}(\overline{k}'_\perp)\\
&\qquad+\int\mathrm{d}\overline{k}'_\perp(-)k_{1z}\hat{h}(-k_{1z})\cdot\tilde{\overline{B}}_1^{(1)}(\overline{k}'_\perp)F_1(\overline{k}_\perp-\overline{k}'_\perp)F_1(\overline{k}'_\perp-\overline{k}_{i\perp})=0
\end{aligned}
\tag{4.5.81}
$$

$$
\begin{aligned}
&+\frac{k_{m-1}}{k_m}\left\{A_{m-1,q}^{(2)}(\overline{k}_\perp)-\frac{1}{2}k_{mz}^2F_{m-1}^{(2)}(\overline{k}_\perp-\overline{k}_{i\perp})\hat{e}(k_{mz})\cdot\overline{a}_{m-1}^{(0)}\right.\\
&\qquad\left.+\int\mathrm{d}\overline{k}'_\perp k_{mz}\hat{e}(k_{mz})\cdot\tilde{\overline{A}}_{m-1}^{(1)}(\overline{k}'_\perp)F_{m-1}(\overline{k}_\perp-\overline{k}'_\perp)F_{m-1}(\overline{k}'_\perp-\overline{k}_{i\perp})\right\}\\
&-\frac{k_{mz}}{k_m}B_{m-1,p}^{(2)}(\overline{k}_\perp)-\frac{k_\rho}{k_m}\int\mathrm{d}\overline{k}'_\perp F_{m-1}(\overline{k}_\perp-\overline{k}'_\perp)F_{m-1}(\overline{k}'_\perp-\overline{k}_{\perp_i})(\overline{k}_\perp-\overline{k}'_\perp)\cdot\tilde{\overline{B}}_{m-1,\perp}^{(1)}(\overline{k}'_\perp)\\
&-\frac{1}{2}k_{mz}^2F_{m-1}^{(2)}(\overline{k}_\perp-\overline{k}_{i\perp})\hat{h}(k_{mz})\cdot\overline{b}_{m-1}^{(0)}\\
&+\int\mathrm{d}\overline{k}'_\perp k_{mz}\hat{h}(k_{mz})\cdot\tilde{\overline{B}}_{m-1}^{(1)}(\overline{k}'_\perp)F_{m-1}(\overline{k}_\perp-\overline{k}'_\perp)F_{m-1}(\overline{k}'_\perp-\overline{k}_{i\perp})\\
&-e^{i\phi_m}\left\{A_{m,q}^{(2)}(\overline{k}_\perp)-\frac{1}{2}k_{mz}^2F_m^{(2)}(\overline{k}_\perp-\overline{k}_{i\perp})\hat{e}(k_{mz})\cdot\overline{a}_m^{(0)}\right.\\
&\qquad\left.+\int\mathrm{d}\overline{k}'_\perp k_{mz}\hat{e}(k_{mz})\cdot\tilde{\overline{A}}_m^{(1)}(\overline{k}'_\perp)F_m(\overline{k}_\perp-\overline{k}'_\perp)F_m(\overline{k}'_\perp-\overline{k}_{i\perp})\right\}\\
&-e^{i\phi_m}\left\{-\frac{k_{mz}}{k_m}B_{m,p}^{(2)}(\overline{k}_\perp)-\frac{k_\rho}{k_m}\int\mathrm{d}\overline{k}'_\perp F_m(\overline{k}_\perp-\overline{k}'_\perp)F_m(\overline{k}'_\perp-\overline{k}_{\perp_i})(\overline{k}_\perp-\overline{k}'_\perp)\cdot\tilde{\overline{B}}_{m,\perp}^{(1)}(\overline{k}'_\perp)\right.\\
&\qquad-\frac{1}{2}k_{mz}^2F_m^{(2)}(\overline{k}_\perp-\overline{k}_{i\perp})\hat{h}(k_{mz})\cdot\overline{b}_m^{(0)}\\
&\qquad\left.+\int\mathrm{d}\overline{k}'_\perp k_{mz}\hat{h}(k_{mz})\cdot\tilde{\overline{B}}_m^{(1)}(\overline{k}'_\perp)F_m(\overline{k}_\perp-\overline{k}'_\perp)F_m(\overline{k}'_\perp-\overline{k}_{i\perp})\right\}=0
\end{aligned}
\tag{4.5.82}
$$

$$
\begin{aligned}
&+\frac{k_{m-1}}{k_m}\Big\{A^{(2)}_{m-1,q}(\overline{k}_\perp)-\frac{1}{2}k_{mz}^2F^{(2)}_{m-1}(\overline{k}_\perp-\overline{k}_{i\perp})\hat{e}(-k_{mz})\cdot\overline{a}^{(0)}_{m-1} \qquad (4.5.83)\\
&\qquad\qquad+\int \mathrm{d}\overline{k}'_\perp(-)k_{mz}\hat{e}(-k_{mz})\cdot\tilde{\overline{A}}^{(1)}_{m-1}(\overline{k}'_\perp)F_{m-1}(\overline{k}_\perp-\overline{k}'_\perp)F_{m-1}(\overline{k}'_\perp-\overline{k}_{i\perp})\Big\}\\
&+\frac{k_{mz}}{k_m}B^{(2)}_{m-1,p}(\overline{k}_\perp)-\frac{k_\rho}{k_m}\int \mathrm{d}\overline{k}'_\perp F_{m-1}(\overline{k}_\perp-\overline{k}'_\perp)F_{m-1}(\overline{k}'_\perp-\overline{k}_{\perp_i})(\overline{k}_\perp-\overline{k}'_\perp)\cdot\tilde{\overline{B}}^{(1)}_{m-1,\perp}(\overline{k}'_\perp)\\
&-\frac{1}{2}k_{mz}^2F^{(2)}_{m-1}(\overline{k}_\perp-\overline{k}_{i\perp})\hat{h}(-k_{mz})\cdot\overline{b}^{(0)}_{m-1}\\
&+\int \mathrm{d}\overline{k}'_\perp(-)k_{mz}\hat{h}(-k_{mz})\cdot\tilde{\overline{B}}^{(1)}_{m-1}(\overline{k}'_\perp)F_{m-1}(\overline{k}_\perp-\overline{k}'_\perp)F_{m-1}(\overline{k}'_\perp-\overline{k}_{i\perp})\\
&-e^{-i\phi_m}\Big\{A^{(2)}_{m,q}(\overline{k}_\perp)-\frac{1}{2}k_{mz}^2F^{(2)}_{m}(\overline{k}_\perp-\overline{k}_{i\perp})\hat{e}(-k_{mz})\cdot\overline{a}^{(0)}_{m}\\
&\qquad\qquad+\int \mathrm{d}\overline{k}'_\perp(-)k_{mz}\hat{e}(-k_{mz})\cdot\tilde{\overline{A}}^{(1)}_{m}(\overline{k}'_\perp)F_{m}(\overline{k}_\perp-\overline{k}'_\perp)F_{m}(\overline{k}'_\perp-\overline{k}_{i\perp})\Big\}\\
&-e^{-i\phi_m}\Big\{\frac{k_{mz}}{k_m}B^{(2)}_{m,p}(\overline{k}_\perp)-\frac{k_\rho}{k_m}\int \mathrm{d}\overline{k}'_\perp F_{m}(\overline{k}_\perp-\overline{k}'_\perp)F_{m}(\overline{k}'_\perp-\overline{k}_{\perp_i})(\overline{k}_\perp-\overline{k}'_\perp)\cdot\tilde{\overline{B}}^{(1)}_{m,\perp}(\overline{k}'_\perp)\\
&\qquad\qquad-\frac{1}{2}k_{mz}^2F^{(2)}_{m}(\overline{k}_\perp-\overline{k}_{i\perp})\hat{h}(-k_{mz})\cdot\overline{b}^{(0)}_{m}\\
&\qquad\qquad+\int \mathrm{d}\overline{k}'_\perp(-)k_{mz}\hat{h}(-k_{mz})\cdot\tilde{\overline{B}}^{(1)}_{m}(\overline{k}'_\perp)F_{m}(\overline{k}_\perp-\overline{k}'_\perp)F_{m}(\overline{k}'_\perp-\overline{k}_{i\perp})\Big\}=0
\end{aligned}
$$

$$
\begin{aligned}
&\frac{k_{N-1}}{k_N}\Big\{A^{(2)}_{N-1,q}(\overline{k}_\perp)-\frac{1}{2}k_{Nz}^2F^{(2)}_{N-1}(\overline{k}_\perp-\overline{k}_{i\perp})\hat{e}(k_{Nz})\cdot\overline{a}^{(0)}_{N-1} \qquad (4.5.84)\\
&\qquad\qquad+\int \mathrm{d}\overline{k}'_\perp k_{Nz}\hat{e}(k_{Nz})\cdot\tilde{\overline{A}}^{(1)}_{N-1}(\overline{k}'_\perp)F_{N-1}(\overline{k}_\perp-\overline{k}'_\perp)F_{N-1}(\overline{k}'_\perp-\overline{k}_{\perp_i})\Big\}\\
&-\frac{k_{Nz}}{k_N}B^{(2)}_{N-1,p}(\overline{k}_\perp)-\frac{k_\rho}{k_N}\int \mathrm{d}\overline{k}'_\perp F_{N-1}(\overline{k}_\perp-\overline{k}'_\perp)F_{N-1}(\overline{k}'_\perp-\overline{k}_{\perp_i})(\overline{k}_\perp-\overline{k}'_\perp)\cdot\tilde{\overline{B}}^{(1)}_{N-1,\perp}(\overline{k}'_\perp)\\
&\qquad\qquad-\frac{1}{2}k_{Nz}^2F^{(2)}_{N-1}(\overline{k}_\perp-\overline{k}_{i\perp})\hat{h}(k_{Nz})\cdot\overline{b}^{(0)}_{N-1}\\
&\qquad\qquad+\int \mathrm{d}\overline{k}'_\perp k_{Nz}\hat{h}(k_{Nz})\cdot\tilde{\overline{B}}^{(1)}_{N-1}(\overline{k}'_\perp)F_{N-1}(\overline{k}_\perp-\overline{k}'_\perp)F_{N-1}(\overline{k}'_\perp-\overline{k}_{\perp_i})=0
\end{aligned}
$$

From the extinction relations (4.5.82) and (4.5.83), a propagation matrix relation between the adjacent layers surface fields can be obtained as

$$
\begin{bmatrix} e^{i\phi_m} & 0 \\ 0 & e^{-i\phi_m}\end{bmatrix}\begin{bmatrix} 1 & -\frac{k_{mz}}{k_m} \\ 1 & \frac{k_{mz}}{k_m}\end{bmatrix}\begin{bmatrix} A^{(2)}_{m,q} \\ B^{(2)}_{m,p}\end{bmatrix}=\begin{bmatrix} \frac{k_{m-1}}{k_m} & -\frac{k_{mz}}{k_m} \\ \frac{k_{m-1}}{k_m} & \frac{k_{mz}}{k_m}\end{bmatrix}\begin{bmatrix} A^{(2)}_{m-1,q} \\ B^{(2)}_{m-1,p}\end{bmatrix}+\begin{bmatrix} u^{2e+}_m \\ u^{2e-}_m\end{bmatrix}-\begin{bmatrix} c^{2e+}_m \\ c^{2e-}_m\end{bmatrix} \qquad (4.5.85)
$$

where the coefficients $c_m^{2e\pm}$ and $u_m^{2e\pm}$ are purely proportional to the surface roughness of interfaces and are defined by

$$\begin{aligned} u_m^{2e\pm} = & \frac{k_{m-1}}{k_m}\Big\{-\frac{1}{2}k_{mz}^2 F_{m-1}^{(2)}(\overline{k}_\perp - \overline{k}_{i\perp})\hat{e}(\pm k_{mz})\cdot\overline{a}_{m-1}^{(0)} \\ & \pm\int \mathrm{d}\overline{k}'_\perp k_{mz}\hat{e}(\pm k_{mz})\cdot\tilde{\overline{A}}_{m-1}^{(1)}(\overline{k}'_\perp)F_{m-1}(\overline{k}_\perp - \overline{k}'_\perp)F_{m-1}(\overline{k}'_\perp - \overline{k}_{i\perp})\Big\} \\ & -\frac{k_\rho}{k_m}\int \mathrm{d}\overline{k}'_\perp F_{m-1}(\overline{k}_\perp - \overline{k}'_\perp)F_{m-1}(\overline{k}'_\perp - \overline{k}_{\perp_i})(\overline{k}_\perp - \overline{k}'_\perp)\cdot\tilde{\overline{B}}_{m-1,\perp}^{(1)}(\overline{k}'_\perp) \\ & -\frac{1}{2}k_{mz}^2 F_{m-1}^{(2)}(\overline{k}_\perp - \overline{k}_{i\perp})\hat{h}(\pm k_{mz})\cdot\overline{b}_{m-1}^{(0)} \\ & \pm\int \mathrm{d}\overline{k}'_\perp k_{mz}\hat{h}(k_{mz})\cdot\tilde{\overline{B}}_{m-1}^{(1)}(\overline{k}'_\perp)F_{m-1}(\overline{k}_\perp - \overline{k}'_\perp)F_{m-1}(\overline{k}'_\perp - \overline{k}_{i\perp}) \end{aligned} \tag{4.5.86}$$

and

$$\begin{aligned} c_m^{2e\pm} = & +e^{i\phi_m}\Big\{-\frac{1}{2}k_{mz}^2 F_m^{(2)}(\overline{k}_\perp - \overline{k}_{i\perp})\hat{e}(k_{mz})\cdot\overline{a}_m^{(0)} \\ & \pm\int \mathrm{d}\overline{k}'_\perp k_{mz}\hat{e}(\pm k_{mz})\cdot\tilde{\overline{A}}_m^{(1)}(\overline{k}'_\perp)F_m(\overline{k}_\perp - \overline{k}'_\perp)F_m(\overline{k}'_\perp - \overline{k}_{i\perp}) \\ & -\frac{k_\rho}{k_m}\int \mathrm{d}\overline{k}'_\perp F_m(\overline{k}_\perp - \overline{k}'_\perp)F_m(\overline{k}'_\perp - \overline{k}_{\perp_i})(\overline{k}_\perp - \overline{k}'_\perp)\cdot\tilde{\overline{B}}_{m,\perp}^{(1)}(\overline{k}'_\perp) \\ & -\frac{1}{2}k_{mz}^2 F_m^{(2)}(\overline{k}_\perp - \overline{k}_{i\perp})\hat{h}(k_{mz})\cdot\overline{b}_m^{(0)} \\ & \pm\int \mathrm{d}\overline{k}'_\perp k_{mz}\hat{h}(\pm k_{mz})\cdot\tilde{\overline{B}}_m^{(1)}(\overline{k}'_\perp)F_m(\overline{k}_\perp - \overline{k}'_\perp)F_m(\overline{k}'_\perp - \overline{k}_{i\perp})\Big\} \end{aligned} \tag{4.5.87}$$

By defining the propagation matrix of the flat surface media $\overline{\overline{P}}_{m,m-1}^{[2e]}$ and vector functions $\overline{U}_m^{[2e]}$ and $\overline{C}_m^{[2e]}$ which are responsible for the roughness of the $m$-th interface as

$$\begin{aligned} \overline{\overline{P}}_{m,m-1}^{[2e]} &= + \begin{bmatrix} 1 & -\frac{k_{mz}}{k_m} \\ 1 & \frac{k_{mz}}{k_m} \end{bmatrix}^{-1} \begin{bmatrix} e^{-i\phi_m} & 0 \\ 0 & e^{i\phi_m} \end{bmatrix} \begin{bmatrix} \frac{k_{m-1}}{k_m} & -\frac{k_{mz}}{k_m} \\ \frac{k_{m-1}}{k_m} & \frac{k_{mz}}{k_m} \end{bmatrix} \\ \overline{U}_m^{[2e]} &= + \begin{bmatrix} 1 & -\frac{k_{mz}}{k_m} \\ 1 & \frac{k_{mz}}{k_m} \end{bmatrix}^{-1} \begin{bmatrix} e^{-i\phi_m} & 0 \\ 0 & e^{i\phi_m} \end{bmatrix} \begin{bmatrix} u_m^{2e+} \\ u_m^{2e-} \end{bmatrix} \\ \overline{C}_m^{[2e]} &= - \begin{bmatrix} 1 & -\frac{k_{mz}}{k_m} \\ 1 & \frac{k_{mz}}{k_m} \end{bmatrix}^{-1} \begin{bmatrix} e^{-i\phi_m} & 0 \\ 0 & e^{i\phi_m} \end{bmatrix} \begin{bmatrix} c_m^{2e+} \\ c_m^{2e-} \end{bmatrix} \end{aligned} \tag{4.5.88}$$

(4.5.85) can be written as,

$$\begin{bmatrix} A_{m,q}^{(2)} \\ B_{m,p}^{(2)} \end{bmatrix} = \overline{\overline{P}}_{m,m-1}^{[2e]} \begin{bmatrix} A_{m-1,q}^{(2)} \\ B_{m-1,p}^{(2)} \end{bmatrix} + \overline{U}_m^{[2e]} + \overline{C}_m^{[2e]} \tag{4.5.89}$$

For the second order solution of the surface fields, different quadratic forms of the surface spectra will appear in the solution which make the solution looks more complicated. However, as it will be discussed later[], we are only interested in the average of the second

order field (not itself in general). Therefore, taking statistical average of the unknowns before solving the linear system results in a great simplifications. If we assume uncorrelated surfaces, the surface roughness spectral functions simplify to

$$\begin{aligned} u_m^{2e\pm}=&-\frac{1}{2}k_{mz}^2F_{m-1}^{(2)}(\overline{k}_\perp-\overline{k}_{i\perp})\left[\frac{k_{m-1}}{k_m}\hat{e}(\pm k_{mz})\cdot\overline{a}_{m-1}^{(0)}+\hat{h}(\pm k_{mz})\cdot\overline{b}_{m-1}^{(0)}\right] \\ &+\int \mathrm{d}\overline{k}'_\perp F_{m-1}(\overline{k}_\perp-\overline{k}'_\perp)F_{m-1}(\overline{k}'_\perp-\overline{k}_{i\perp})\left[\pm\frac{k_{m-1}}{k_m}k_{mz}\hat{e}(\pm k_{mz})\cdot\tilde{\overline{A}}_{m-1,F_{m-1}}^{(1)}(\overline{k}'_\perp)\right. \\ &\left.-\frac{k_\rho}{k_m}(\overline{k}_\perp-\overline{k}'_\perp)\cdot\tilde{\overline{B}}_{m-1,\perp,F_{m-1}}^{(1)}(\overline{k}'_\perp)\pm k_{mz}\hat{h}(\pm k_{mz})\cdot\tilde{\overline{B}}_{m-1,F_{m-1}}^{(1)}(\overline{k}'_\perp)\right] \end{aligned} \tag{4.5.90}$$

$$\begin{aligned} c_m^{2e\pm}=&e^{i\phi_m}\left\{-\frac{1}{2}k_{mz}^2F_m^{(2)}(\overline{k}_\perp-\overline{k}_{i\perp})\left[\hat{e}(\pm k_{mz})\cdot\overline{a}_m^{(0)}+\hat{h}(\pm k_{mz})\cdot\overline{b}_m^{(0)}\right]\right. \\ &+\int \mathrm{d}\overline{k}'_\perp F_m(\overline{k}_\perp-\overline{k}'_\perp)F_m(\overline{k}'_\perp-\overline{k}_{i\perp})\left[\pm k_{mz}\hat{e}(\pm k_{mz})\cdot\tilde{\overline{A}}_{m,F_m}^{(1)}(\overline{k}'_\perp)\right. \\ &\left.\left.-\frac{k_\rho}{k_m}(\overline{k}_\perp-\overline{k}'_\perp)\cdot\tilde{\overline{B}}_{m,\perp,F_m}^{(1)}(\overline{k}'_\perp)\pm k_{mz}\hat{h}(\pm k_{mz})\cdot\tilde{\overline{B}}_{m,F_m}^{(1)}(\overline{k}'_\perp)\right]\right\} \end{aligned}$$

Now note that surface fields amplitudes $\tilde{\overline{A}}_{m,F_j}$ are deterministic functions, statistical average pass through and noting that for stationary process of the interfaces, second order moments of the surface are given by

$$\begin{aligned} \langle F_j^{(2)}(\overline{k}_\perp-\overline{k}_{\perp_i})\rangle=&\delta(\overline{k}_\perp-\overline{k}_{\perp_i})\int \mathrm{d}\overline{k}'_\perp W_j(\overline{k}'_\perp-\overline{k}_{\perp_i}) \\ \langle F_j(\overline{k}_\perp-\overline{k}'_\perp)F_j(\overline{k}'_\perp-\overline{k}_{\perp_i})\rangle=&\delta(\overline{k}_\perp-\overline{k}_{\perp_i})W_j(\overline{k}'_\perp-\overline{k}_{\perp_i}) \end{aligned} \tag{4.5.91}$$

and therefore, the averaged roughness terms can be simplified to

$$\begin{aligned} \langle u_m^{2e\pm}\rangle=&\delta(\overline{k}_\perp-\overline{k}_{\perp_i})\int \mathrm{d}\overline{k}'_\perp W_{m-1}(\overline{k}'_\perp-\overline{k}_{\perp_i})\left\{-\frac{1}{2}k_{mz}^2\left[\frac{k_{m-1}}{k_m}\hat{e}(\pm k_{mz})\cdot\overline{a}_{m-1}^{(0)}\right.\right. \\ &\left.+\hat{h}(\pm k_{mz})\cdot\overline{b}_{m-1}^{(0)}\right]+\left[\pm\frac{k_{m-1}}{k_m}k_{mz}\hat{e}(\pm k_{mz})\cdot\tilde{\overline{A}}_{m-1,F_{m-1}}^{(1)}(\overline{k}'_\perp)\right. \\ &\left.\left.-\frac{k_\rho}{k_m}(\overline{k}_\perp-\overline{k}'_\perp)\cdot\tilde{\overline{B}}_{m-1,\perp,F_{m-1}}^{(1)}(\overline{k}'_\perp)\pm k_{mz}\hat{h}(\pm k_{mz})\cdot\tilde{\overline{B}}_{m-1,F_{m-1}}^{(1)}(\overline{k}'_\perp)\right]\right\} \end{aligned} \tag{4.5.92}$$

$$\begin{aligned} \langle c_m^{2e\pm}\rangle=&\delta(\overline{k}_\perp-\overline{k}_{\perp_i})\int \mathrm{d}\overline{k}'_\perp W_m(\overline{k}'_\perp-\overline{k}_{\perp_i})e^{i\phi_m}\left\{-\frac{1}{2}k_{mz}^2\left[\hat{e}(\pm k_{mz})\cdot\overline{a}_m^{(0)}\right.\right. \\ &\left.+\hat{h}(\pm k_{mz})\cdot\overline{b}_m^{(0)}\right]+\left[\pm k_{mz}\hat{e}(\pm k_{mz})\cdot\tilde{\overline{A}}_{m,F_m}^{(1)}(\overline{k}'_\perp)\right. \\ &\left.\left.-\frac{k_\rho}{k_m}(\overline{k}_\perp-\overline{k}'_\perp)\cdot\tilde{\overline{B}}_{m,\perp,F_m}^{(1)}(\overline{k}'_\perp)\pm k_{mz}\hat{h}(\pm k_{mz})\cdot\tilde{\overline{B}}_{m,F_m}^{(1)}(\overline{k}'_\perp)\right]\right\} \end{aligned}$$

Therefore, propagation relation of the mean field between adjacent layers is given by

$$\begin{bmatrix}\langle A_{m,q}^{(2)}\rangle\\ \langle B_{m,p}^{(2)}\rangle\end{bmatrix}=\overline{\overline{P}}_{m,m-1}^{[2e]}\begin{bmatrix}\langle A_{m-1,q}^{(2)}\rangle\\ \langle B_{m-1,p}^{(2)}\rangle\end{bmatrix}+\langle\overline{U}_m^{[2e]}\rangle+\langle\overline{C}_m^{[2e]}\rangle \tag{4.5.93}$$

Using this relation between the adjacent surface fields, surface fields on the last layers can be related to those of the first interface through a recursive relation that can be obtained for an arbitrary $N$ by induction,

$$\begin{aligned}\begin{bmatrix}\langle A^{(2)}_{N-1,q}\rangle\\ \langle B^{(2)}_{N-1,p}\rangle\end{bmatrix}=&\overline{\overline{P}}^{[2e]}\begin{bmatrix}\langle A^{(2)}_{1,q}\rangle\\ \langle B^{(2)}_{1,p}\rangle\end{bmatrix}\\ &+\prod_{j=3}^{N-1}\overline{\overline{P}}^{[2e]}_{j,j-1}\Big(\langle\overline{U}^{[2e]}_{2}\rangle+\langle\overline{C}^{[2e]}_{2}\rangle\Big)\\ &+\prod_{j=4}^{N-1}\overline{\overline{P}}^{[2e]}_{j,j-1}\Big(\langle\overline{U}^{[2e]}_{3}\rangle+\langle\overline{C}^{[2e]}_{3}\rangle\Big)\\ &\vdots\\ &+\prod_{j=N-1}^{N-1}\overline{\overline{P}}^{[2e]}_{j,j-1}\Big(\langle\overline{U}^{[2e]}_{N-2}\rangle+\langle\overline{C}^{[2e]}_{N-2}\rangle\Big)\\ &+\langle\overline{U}^{[2e]}_{N-1}\rangle+\langle\overline{C}^{[2e]}_{N-1}\rangle\end{aligned}\tag{4.5.94}$$

where $\overline{\overline{P}}^{[2e]}=\prod_{j=2}^{N-1}\overline{\overline{P}}^{[2e]}_{j,j-1}$. Upon redefining the averaged vectors functions $\langle\overline{C}^{[2e]}_{m}\rangle$ and $\langle\overline{U}^{[2e]}_{m}\rangle$ through

$$\begin{aligned}\langle\overline{U}^{[2e]}_{m}\rangle=&\delta(\overline{k}_{\perp}-\overline{k}_{\perp_i})\int\mathrm{d}\overline{k}'_{\perp}W_{m-1}(\overline{k}'_{\perp}-\overline{k}_{\perp_i})\tilde{\overline{U}}^{[2e]}_{m}(\overline{k}'_{\perp})\\ \langle\overline{C}^{[2e]}_{m}\rangle=&\delta(\overline{k}_{\perp}-\overline{k}_{\perp_i})\int\mathrm{d}\overline{k}'_{\perp}W_{m}(\overline{k}'_{\perp}-\overline{k}_{\perp_i})\tilde{\overline{C}}^{[2e]}_{m}(\overline{k}'_{\perp})\end{aligned}\tag{4.5.95}$$

the relation between mean surface fields of the first and last interface can be written as

$$\begin{bmatrix}\langle A^{(2)}_{N-1,q}\rangle\\ \langle B^{(2)}_{N-1,p}\rangle\end{bmatrix}-\overline{\overline{P}}^{[2e]}\begin{bmatrix}\langle A^{(2)}_{1,q}\rangle\\ \langle B^{(2)}_{1,p}\rangle\end{bmatrix}=\delta(\overline{k}_{\perp}-\overline{k}_{\perp_i})\int\mathrm{d}\overline{k}'_{\perp}\overline{R}^{[2e]}(\overline{k}'_{\perp})$$

where $\overline{R}^{[2e]}(\overline{k}'_{\perp})$ is defined by

$$\begin{aligned}\overline{R}^{[2e]}(\overline{k}'_{\perp})=&+\prod_{j=3}^{N-1}\overline{\overline{P}}^{[2e]}_{j,j-1}\Big(\tilde{U}^{[2e]}_{2}(\overline{k}'_{\perp})W_1(\overline{k}'_{\perp}-\overline{k}_{\perp_i})+\tilde{\overline{C}}^{[2e]}_{2}(\overline{k}'_{\perp})W_2(\overline{k}'_{\perp}-\overline{k}_{\perp_i})\Big)\\ &+\prod_{j=4}^{N-1}\overline{\overline{P}}^{[2e]}_{j,j-1}\Big(\tilde{\overline{U}}^{[2e]}_{3}(\overline{k}'_{\perp})W_2(\overline{k}'_{\perp}-\overline{k}_{\perp_i})+\tilde{\overline{C}}^{[2e]}_{3}(\overline{k}'_{\perp})W_3(\overline{k}'_{\perp}-\overline{k}_{\perp_i})\Big)\\ &\vdots\\ &+\prod_{j=N-1}^{N-1}\overline{\overline{P}}^{[2e]}_{j,j-1}\Big(\tilde{\overline{U}}^{[2e]}_{N-2}(\overline{k}'_{\perp})W_{N-3}(\overline{k}'_{\perp}-\overline{k}_{\perp_i})+\tilde{\overline{C}}^{[2e]}_{N-2}(\overline{k}'_{\perp})W_{N-2}(\overline{k}'_{\perp}-\overline{k}_{\perp_i})\Big)\\ &+\tilde{\overline{U}}^{[2e]}_{N-1}(\overline{k}'_{\perp})W_{N-2}(\overline{k}'_{\perp}-\overline{k}_{\perp_i})+\tilde{\overline{C}}^{[2e]}_{N-1}(\overline{k}'_{\perp})W_{N-1}(\overline{k}'_{\perp}-\overline{k}_{\perp_i})\end{aligned}\tag{4.5.96}$$

On the other hand, two mean fields are also related together through the extinction relation of the first and last half spaces that upon taking statistical average yields,

$$\langle A_{1q}^{(2)}\rangle+\frac{k_{1z}}{k_1}\langle B_{1p}^{(2)}\rangle+\delta(\overline{k}_\perp-\overline{k}_{\perp_i})\int \mathrm{d}\overline{k}'_\perp W_1(\overline{k}'_\perp-\overline{k}_{\perp_i})\tilde{C}_{12}^{[2e]}(\overline{k}'_\perp)=0 \tag{4.5.97}$$

$$\frac{k_{N-1}}{k_N}\langle A_{N-1,q}^{(2)}\rangle-\frac{k_{Nz}}{k_N}\langle B_{N-1,p}^{(2)}\rangle+\delta(\overline{k}_\perp-\overline{k}_{\perp_i})\int \mathrm{d}\overline{k}'_\perp W_{N-1}(\overline{k}'_\perp-\overline{k}_{\perp_i})\tilde{C}_{N,N-1}^{[2e]}(\overline{k}'_\perp)=0$$

where the scalar spectral functions $\tilde{C}_{12}^{[2e]}$ and $\tilde{C}_{N,N-1}^{[2e]}$ are defined through,

$$\begin{aligned}\tilde{C}_{12}^{[2e]}(\overline{k}'_\perp)=&-\frac{1}{2}k_{1z}^2\left[\hat{e}(-k_{1z})\cdot\bar{a}_1^{(0)}+\hat{h}(-k_{1z})\cdot\bar{b}_1^{(0)}\right]\\&-k_{1z}\hat{e}(-k_{1z})\cdot\tilde{\overline{A}}_{1,F_1}^{(1)}(\overline{k}'_\perp)-\left(\frac{k_\rho}{k_1}(\overline{k}_\perp-\overline{k}'_\perp)+k_{1z}\hat{h}(-k_{1z})\right)\cdot\tilde{\overline{B}}_{1,F_1}^{(1)}(\overline{k}'_\perp)\\ \tilde{C}_{N,N-1}^{[2e]}(\overline{k}'_\perp)=&\Big\{-\frac{1}{2}k_{Nz}^2\left(\frac{k_{N-1}}{k_N}\hat{e}(k_{Nz})\cdot\bar{a}_{N-1}^{(0)}+\hat{h}(k_{Nz})\cdot\bar{b}_{N-1}^{(0)}\right)\\&+\frac{k_{N-1}}{k_N}k_{Nz}\hat{e}(k_{Nz})\cdot\tilde{\overline{A}}_{N-1,F_{N-1}}^{(1)}(\overline{k}'_\perp)\\&-\left(\frac{k_\rho}{k_N}(\overline{k}_\perp-\overline{k}'_\perp)-k_{Nz}\hat{h}(k_{Nz})\right)\cdot\tilde{\overline{B}}_{N-1,F_{N-1}}^{(1)}(\overline{k}'_\perp)\Big\}\end{aligned} \tag{4.5.98}$$

Therefore complete system of equations for the mean second order surface fields can be obtained as

$$\begin{bmatrix}1&\frac{k_{1z}}{k_1}&0&0\\0&0&\frac{k_{N-1}}{k_N}&-\frac{k_{Nz}}{k_N}\\-P_{11}^{[2e]}&-P_{12}^{[2e]}&1&0\\-P_{21}^{[2e]}&-P_{22}^{[2e]}&0&1\end{bmatrix}\begin{bmatrix}\langle A_{1q}^{(2)}\rangle\\\langle B_{1p}^{(2)}\rangle\\\langle A_{N-1,q}^{(2)}\rangle\\\langle B_{N-1,p}^{(2)}\rangle\end{bmatrix}=\delta(\overline{k}_\perp-\overline{k}_{\perp_i})\int \mathrm{d}\overline{k}'_\perp\begin{bmatrix}-\tilde{C}_{12}^{[2e]}W_1\\-\tilde{C}_{N,N-1}^{[2e]}W_{N-1}\\\tilde{R}^{2e}\end{bmatrix} \tag{4.5.99}$$

Since the right hand side of (4.5.99) has a delta function times a spectral integration of some functions, the individual solutions has the same for as the right hand side. Therefore, second order mean field exists in the specular spectral point. Calculation of TM field is also similar to the TE case. For TM part, the propagation matrix $\overline{\overline{P}}_{m,m-1}^{[2h]}$ and roughness vectors $\overline{U}_m^{[2h]}$ and $\overline{C}_m^{[2h]}$ are defined as

$$\begin{aligned}\overline{\overline{P}}_{m,m-1}^{[2h]}=&\begin{bmatrix}-\frac{k_{mz}}{k_m}&-1\\\frac{k_{mz}}{k_m}&-1\end{bmatrix}^{-1}\begin{bmatrix}e^{-i\phi_m}&0\\0&e^{i\phi_m}\end{bmatrix}\begin{bmatrix}-\frac{k_{m-1}}{k_m}\frac{k_{mz}}{k_m}&-1\\+\frac{k_{m-1}}{k_m}\frac{k_{mz}}{k_m}&-1\end{bmatrix}\\ \overline{U}_m^{[2h]}=&\begin{bmatrix}-\frac{k_{mz}}{k_m}&-1\\\frac{k_{mz}}{k_m}&-1\end{bmatrix}^{-1}\begin{bmatrix}e^{-i\phi_m}&0\\0&e^{i\phi_m}\end{bmatrix}\begin{bmatrix}u_m^{2h+}\\u_m^{2h-}\end{bmatrix}\\ \overline{C}_m^{[2h]}=&-\begin{bmatrix}-\frac{k_{mz}}{k_m}&-1\\\frac{k_{mz}}{k_m}&-1\end{bmatrix}^{-1}\begin{bmatrix}e^{-i\phi_m}&0\\0&e^{i\phi_m}\end{bmatrix}\begin{bmatrix}c_m^{2h+}\\c_m^{2h-}\end{bmatrix}\end{aligned} \tag{4.5.100}$$

By taking the statistical average of the surface fields, the average of the spectral functions $\langle u_m^{2h\pm}\rangle$ and $\langle c_m^{2h\pm}\rangle$ can be obtained as

$$\begin{aligned}\langle u_m^{2h+}\rangle=&\delta(\overline{k}_\perp-\overline{k}_{\perp_i})\int \mathrm{d}\overline{k}'_\perp W_{m-1}(\overline{k}'_\perp-\overline{k}_{\perp_i})\Bigg\{-\frac{1}{2}k_{mz}^2\Bigg[\frac{k_{m-1}}{k_m}\hat{h}(\pm k_{mz})\cdot\overline{a}_{m-1}^{(0)}\\ &-\hat{e}(\pm k_{mz})\cdot\overline{b}_{m-1}^{(0)}\Bigg]+\Bigg[-\frac{k_{m-1}}{k_m}\frac{k_\rho}{k_m}(\overline{k}_\perp-\overline{k}'_\perp)\cdot\tilde{\overline{A}}_{m-1,F_{m-1}}^{(1)}(\overline{k}'_\perp)\\ &\pm\frac{k_{m-1}}{k_m}k_{mz}\hat{h}(\pm k_{mz})\cdot\tilde{\overline{A}}_{m-1,F_{m-1}}^{(1)}(\overline{k}'_\perp)\mp k_{mz}\hat{e}(\pm k_{mz})\cdot\tilde{\overline{B}}_{m-1,F_{m-1}}^{(1)}(\overline{k}'_\perp)\Bigg]\Bigg\}\end{aligned}\tag{4.5.101}$$

$$\begin{aligned}\langle c_m^{2h\pm}\rangle=&\delta(\overline{k}_\perp-\overline{k}_{\perp_i})\int \mathrm{d}\overline{k}'_\perp W_m(\overline{k}'_\perp-\overline{k}_{\perp_i})e^{i\phi_m}\Bigg\{-\frac{1}{2}k_{mz}^2\Bigg[\hat{h}(\pm k_{mz})\cdot\overline{a}_m^{(0)}\\ &-\hat{e}(\pm k_{mz})\cdot\overline{b}_m^{(0)}\Bigg]+\Bigg[-\frac{k_\rho}{k_m}(\overline{k}_\perp-\overline{k}'_\perp)\cdot\tilde{\overline{A}}_{m,F_m}^{(1)}(\overline{k}'_\perp)\\ &\pm k_{mz}\hat{h}(\pm k_{mz})\cdot\tilde{\overline{A}}_{m,F_m}^{(1)}(\overline{k}'_\perp)\mp k_{mz}\hat{e}(\pm k_{mz})\cdot\tilde{\overline{B}}_{m,F_m}^{(1)}(\overline{k}'_\perp)\Bigg]\Bigg\}\end{aligned}$$

The linear system of equations or the second order mean fields can be obtained as

$$\begin{bmatrix}-\frac{k_{1z}}{k_1} & 1 & 0 & 0\\ 0 & 0 & -\frac{k_{N-1}}{k_N}\frac{k_{Nz}}{k_N} & -1\\ -P_{11}^{[2h]} & -P_{12}^{[2h]} & 1 & 0\\ -P_{21}^{[2h]} & -P_{22}^{[2h]} & 0 & 1\end{bmatrix}\begin{bmatrix}\langle A_{1p}^{(2)}\rangle\\ \langle B_{1q}^{(2)}\rangle\\ \langle A_{N-1,p}^{(2)}\rangle\\ \langle B_{N-1,q}^{(2)}\rangle\end{bmatrix}=\delta(\overline{k}_\perp-\overline{k}_{\perp_i})\int \mathrm{d}\overline{k}'_\perp\begin{bmatrix}-W_1\tilde{C}_{12}^{[2h]}\\ -W_{N-1}\tilde{C}_{N,N-1}^{[2h]}\\ \tilde{R}^{2h}\end{bmatrix}\tag{4.5.102}$$

where,

$$\begin{aligned}\langle\tilde{C}_{12}^{[2h]}\rangle=&-\frac{1}{2}k_{1z}^2\Big[\hat{e}(-k_{1z})\cdot\overline{b}_1^{(0)}-\hat{h}(-k_{1z})\cdot\overline{a}_1^{(0)}\Big]\\ &+\Big(\frac{k_\rho}{k_1}(\overline{k}_\perp-\overline{k}'_\perp)+k_{1z}\hat{h}(-k_{1z})\Big)\cdot\tilde{\overline{A}}_1^{(1)}(\overline{k}'_\perp)-k_{1z}\hat{e}(-k_{1z})\cdot\tilde{\overline{B}}_1^{(1)}(\overline{k}'_\perp)\\ \langle\tilde{C}_{N,N-1}^{[2h]}\rangle=&-\frac{1}{2}k_{Nz}^2\Big[\frac{k_{N-1}}{k_N}\hat{h}(k_{Nz})\cdot\overline{a}_{N-1}^{(0)}-\hat{e}(k_{Nz})\cdot\overline{b}_{N-1}^{(0)}\Big]\\ &-\frac{k_{N-1}}{k_N}\Big(\frac{k_\rho}{k_N}(\overline{k}_\perp-\overline{k}'_\perp)-k_{Nz}\hat{h}(k_{Nz})\Big)\cdot\tilde{\overline{A}}_{N-1}^{(1)}(\overline{k}'_\perp)-k_{Nz}\hat{e}(k_{Nz})\cdot\tilde{\overline{B}}_{N-1}^{(1)}(\overline{k}'_\perp)\Big]\end{aligned}\tag{4.5.103}$$

### 4.5.7 Second Order Scattered and Transmitted Fields

Once the second order surface fields are known by solving the linear system or the mean fields we are in position to evaluate mean scattered field into region 1 by applying the equivalence principle to region 1 up to the second order of surface height. Balancing the TE scattered field expression and inserting the zeroth and first order solution of the surface

fields and approximations of the scattering potential of the scattered field we arrive at

$$
\begin{aligned}
-2\frac{k_{1z}}{k_1}\hat{e}(k_{1z})\cdot\tilde{\overline{E}}_s^{(2)}(\overline{k})=&A_{1q}^{(2)}(\overline{k}_\perp)-\frac{k_{1z}}{k_1}B_{1p}^{(2)}(\overline{k}_\perp)-\frac{1}{2}k_{1z}^2F_1^{(2)}(\overline{k}_\perp-\overline{k}_{\perp_i})\hat{e}(k_{1z})\cdot\overline{a}_1^{(0)}\\
&+\int \mathrm{d}\overline{k}'_\perp\, k_{1z}F_1(\overline{k}_\perp-\overline{k}'_\perp)F_1(\overline{k}'_\perp-\overline{k}_{\perp_i})\hat{e}(k_{1z})\cdot\tilde{\overline{A}}_1^{(1)}(\overline{k}'_\perp)\\
&-\frac{k_\rho}{k_1}\int \mathrm{d}\overline{k}'_\perp F_1(\overline{k}_\perp-\overline{k}'_\perp)F_1(\overline{k}'_\perp-\overline{k}_{\perp_i})(\overline{k}_\perp-\overline{k}'_\perp)\cdot\tilde{\overline{B}}_1^{(1)}(\overline{k}'_\perp)\\
&-\frac{1}{2}k_{1z}^2F_1^{(2)}(\overline{k}_\perp-\overline{k}_{\perp_i})\hat{h}(k_{1z})\cdot\overline{b}_1^{(0)}\\
&+\int \mathrm{d}\overline{k}'_\perp\, k_{1z}F_1(\overline{k}_\perp-\overline{k}'_\perp)F_1(\overline{k}'_\perp-\overline{k}_{\perp_i})\hat{h}(k_{1z})\cdot\tilde{\overline{B}}_1^{(1)}(\overline{k}'_\perp)
\end{aligned}
\tag{4.5.104}
$$

The expression of the TE scattered field can be greatly simplified using the TE part of the second order extinction relation and utilizing symmetry properties of the polarization unit vectors. From the second order TE extinction relation of the surface fields in region 1 of (4.5.81) we have

$$
\begin{aligned}
&A_q^{(2)}(\overline{k}_\perp)-\frac{1}{2}k_z^2F^{(2)}(\overline{k}_\perp-\overline{k}_{\perp_i})\hat{e}(-k_z)\cdot\overline{a}^{(0)}\\
&\qquad+\int \mathrm{d}\overline{k}'_\perp\,(-)k_zF(\overline{k}_\perp-\overline{k}'_\perp)F(\overline{k}'_\perp-\overline{k}_{\perp_i})\hat{e}(-k_z)\cdot\tilde{\overline{A}}^{(1)}(\overline{k}'_\perp)\\
&+\frac{k_z}{k}B_p^{(2)}(\overline{k}_\perp)-\frac{k_\rho}{k}\int \mathrm{d}\overline{k}'_\perp F(\overline{k}_\perp-\overline{k}'_\perp)F(\overline{k}'_\perp-\overline{k}_{\perp_i})(\overline{k}_\perp-\overline{k}'_\perp)\cdot\tilde{\overline{B}}_\perp^{(1)}(\overline{k}'_\perp)\\
&\qquad-\frac{1}{2}k_z^2F^{(2)}(\overline{k}_\perp-\overline{k}_{\perp_i})\hat{h}(-k_z)\cdot\overline{b}^{(0)}\\
&\qquad+\int \mathrm{d}\overline{k}'_\perp(-)k_zF(\overline{k}_\perp-\overline{k}'_\perp)F(\overline{k}'_\perp-\overline{k}_{\perp_i})\hat{h}(-k_z)\cdot\tilde{\overline{B}}^{(1)}(\overline{k}'_\perp)=0
\end{aligned}
$$

This is the extinction of downward propagating wave in region 1. Changing the sign of the arguments of the polarization unit vectors according to the scattered field (transverse and $z$-components behave differently) we obtain,

$$
\begin{aligned}
-\frac{k_{1z}}{k_1}B_{1p}^{(2)}(\overline{k}_\perp)=&A_{1q}^{(2)}(\overline{k}_\perp)-\frac{1}{2}k_{1z}^2F_1^{(2)}(\overline{k}_\perp-\overline{k}_{\perp_i})\left(\hat{e}(k_{1z})\cdot\overline{a}_1^{(0)}-\hat{h}(k_{1z})\cdot\overline{b}_1^{(0)}\right)\\
&+\int \mathrm{d}\overline{k}'_\perp\,(-)k_{1z}F_1(\overline{k}_\perp-\overline{k}'_\perp)F_1(\overline{k}'_\perp-\overline{k}_{\perp_i})\hat{e}(k_{1z})\cdot\tilde{\overline{A}}_1^{(1)}(\overline{k}'_\perp)\\
&-\frac{k_\rho}{k_1}\int \mathrm{d}\overline{k}'_\perp F_1(\overline{k}_\perp-\overline{k}'_\perp)F_1(\overline{k}'_\perp-\overline{k}_{\perp_i})(\overline{k}_\perp-\overline{k}'_\perp)\cdot\tilde{\overline{B}}_{1\perp}^{(1)}(\overline{k}'_\perp)\\
&+\int \mathrm{d}\overline{k}'_\perp k_{1z}F_1(\overline{k}_\perp-\overline{k}'_\perp)F_1(\overline{k}'_\perp-\overline{k}_{\perp_i})\hat{h}(k_{1z})\cdot\tilde{\overline{B}}_{1\perp}^{(1)}(\overline{k}'_\perp)\\
&-\int \mathrm{d}\overline{k}'_\perp k_{1z}F_1(\overline{k}_\perp-\overline{k}'_\perp)F_1(\overline{k}'_\perp-\overline{k}_{\perp_i})\hat{h}(k_{1z})\cdot\hat{z}\tilde{B}_{1z}^{(1)}(\overline{k}'_\perp)
\end{aligned}
\tag{4.5.105}
$$

Upon substituting (4.5.105) into the scattered field expression, lots of cancellations occurs and it yields,

$$
\begin{aligned}
-\frac{k_{1z}}{k_1}\hat{e}(k_{1z})\cdot\tilde{\overline{E}}_s^{(2)}(\overline{k})=&A_{1q}^{(2)}(\overline{k}_\perp)-\frac{1}{2}k_{1z}^2F_1^{(2)}(\overline{k}_\perp-\overline{k}_{\perp_i})\hat{e}(k_{1z})\cdot\overline{a}_1^{(0)}\\
&+\int \mathrm{d}\overline{k}'_\perp F_1(\overline{k}_\perp-\overline{k}'_\perp)F_1(\overline{k}'_\perp-\overline{k}_{\perp_i})\left[k_{1z}\hat{h}(k_{1z})-\frac{k_\rho}{k_1}(\overline{k}_\perp-\overline{k}'_\perp)\right]\cdot\tilde{\overline{B}}_{1\perp}^{(1)}(\overline{k}'_\perp)
\end{aligned}
$$

From the first order solution of the surface fields, every component of the surface fields constitutes from the contributions of rough interfaces spectra. However, assuming uncorrelated interfaces, only correlated component of the surface field we gives a non-zero mean scattered field. Therefore, TE polarized mean scattered field can be written as

$$\hat{e}(k_{1z})\cdot\langle\tilde{\overline{E}}_s^{(2)}(\overline{k})\rangle=\delta(\overline{k}_\perp-\overline{k}_{\perp_i})\int \mathrm{d}\overline{k}'_\perp \sum_{j=1}^{N-1} S_{e,W_j}^{(2)}(\overline{k}'_\perp,\overline{k}_{i\perp})W_j(\overline{k}'_\perp-\overline{k}_{\perp_i}) \tag{4.5.106}$$

where for $j=1$,

$$S_{e,W_1}^{(2)}(\overline{k}'_\perp,\overline{k}_{i\perp})=-\frac{k_1}{k_{1z}}\Bigg[-\frac{1}{2}k_{1z}^2\hat{e}(k_{1z})\cdot\overline{a}_1^{(0)}+\left(k_{1z}\hat{h}(k_{1z})-\frac{k_\rho}{k_1}(\overline{k}_\perp-\overline{k}'_\perp)\right)\cdot\tilde{\overline{B}}_{1\perp,F_1}^{(1)}(\overline{k}'_\perp) + \tilde{A}_{1q,W_1}^{(2)}(\overline{k}_\perp)\Bigg] \tag{4.5.107}$$

and for $j\neq1$,

$$S_{e,W_j}^{(2)}(\overline{k}'_\perp,\overline{k}_{i\perp})=-\frac{k_1}{k_{1z}}\tilde{A}_{1q,W_j}^{(2)}(\overline{k}_\perp) \quad , \quad j=2,3,\ldots,N-1 \tag{4.5.108}$$

Notice that all of the surface fields orders (0,1,2) contribute to the second order scattered field. Following a similar procedure for the TM scattered mean field, we obtain

$$\hat{h}(k_{1z})\cdot\langle\tilde{\overline{E}}_s^{(2)}(\overline{k})\rangle=\delta(\overline{k}_\perp-\overline{k}_{\perp_i})\int \mathrm{d}\overline{k}'_\perp \sum_{j=1}^{N-1} S_{h,W_j}^{(2)}(\overline{k}'_\perp,\overline{k}_{i\perp})W_j(\overline{k}'_\perp-\overline{k}_{\perp_i}) \tag{4.5.109}$$

where different interfaces contribution in the second order mean TM scattered field amplitudes are given by

$$S_{h,W_1}^{(2)}(\overline{k}'_\perp,\overline{k}_{i\perp})=\frac{k_1}{k_{1z}}\Bigg[\left(\frac{k_\rho}{k_1}(\overline{k}_\perp-\overline{k}'_\perp)-k_{1z}\hat{h}(k_{1z})\right)\cdot\tilde{\overline{A}}_{1\perp,F_1}^{(1)}(\overline{k}'_\perp) - \frac{1}{2}k_{1z}^2\hat{e}(k_{1z})\cdot\overline{b}_1^{(0)}+\tilde{B}_{1q,W_1}^{(2)}(\overline{k}_\perp)\Bigg] \tag{4.5.110}$$

and,

$$S_{h,W_j}^{(2)}(\overline{k}'_\perp,\overline{k}_{i\perp})=\frac{k_1}{k_{1z}}\tilde{B}_{1q,W_j}^{(2)}(\overline{k}_\perp) \quad , \quad j=2,3,\ldots,N-1$$

In general, the second order scattered field representation in the spectral domain can be written as

$$\langle\tilde{\overline{E}}_s^{(2)}(\overline{k})\rangle=\delta(\overline{k}_\perp-\overline{k}_{\perp_i})\sum_{j=1}^{N-1}\int \mathrm{d}\overline{k}'_\perp\left[S_{e,W_j}^{(2)}(\overline{k}'_\perp,\overline{k}_{i\perp})\hat{e}(k_{iz})+S_{h,W_j}^{(2)}(\overline{k}'_\perp,\overline{k}_{i\perp})\hat{h}(k_{iz})\right]W_j \tag{4.5.111}$$

or in the spatial domain,

$$\langle\overline{E}_s^{(2)}(\overline{r})\rangle=e^{i\overline{k}_{i\perp}\cdot\overline{r}_\perp+ik_{iz}z}\sum_{j=1}^{N-1}\int \mathrm{d}\overline{k}'_\perp\left[S_{e,W_j}^{(2)}(\overline{k}'_\perp,\overline{k}_{i\perp})\hat{e}(k_{iz})+S_{h,W_j}^{(2)}(\overline{k}'_\perp,\overline{k}_{i\perp})\hat{h}(k_{iz})\right]W_j \tag{4.5.112}$$

Notice that the mean scattered field is propagating in the specular direction corresponds to the incident direction. The second order mean field solution does not have depolarized component in the scattered field. The integration over $\overline{k}'_{\perp}$ here should not misinterpreted as different directions in space that corresponds to an incoherent wave. The integration here s over the intermediate scattering directions that result in the mean field in direction $\overline{k}_{\perp}=\overline{k}_{i\perp}$. Similarly, mean second order transmitted field into region $N$ can be obtained as

$$\langle\overline{E}_t^{(2)}(\overline{k})\rangle=\delta(\overline{k}_{i\perp}-\overline{k}_{\perp_i})\sum_{j=1}^{N-1}\int \mathrm{d}\overline{k}'_{\perp}W_j(\overline{k}'_{\perp}-\overline{k}_{\perp_i})\Big[T_{e,W_j}^{(2)}(\overline{k}'_{\perp},\overline{k}_{i\perp})\hat{e}(-k_{Niz}) \\ +T_{h,W_j}^{(2)}(\overline{k}'_{\perp},\overline{k}_{i\perp})\hat{h}(-k_{Niz})\Big] \tag{4.5.113}$$

where contribution of the last interface ($j=N-1$) to the TM and TE transmitted mean field are given by

$$T_{h,W_{N-1}}^{(2)}(\overline{k}'_{\perp},\overline{k}_{i\perp})=\frac{k_N}{k_{Niz}}\Big\{-\tilde{B}_{N-1,q,W_{N-1}}^{(2)}(\overline{k}'_{\perp},\overline{k}_{i\perp})+\frac{1}{2}k_{Niz}^2\hat{e}(-k_{Niz})\cdot\overline{b}_{N-1}^{(0)} \\ -\frac{k_{N-1}}{k_N}\left(\frac{k_{i\rho}}{k_N}(\overline{k}_{i\perp}-\overline{k}'_{\perp})+k_{Niz}\hat{h}(-k_{Niz})\right)\cdot\tilde{\overline{A}}_{N-1,\perp,F_{N-1}}^{(1)}(\overline{k}'_{\perp})\Big\} \tag{4.5.114}$$

$$T_{e,W_{N-1}}^{(2)}(\overline{k}'_{\perp},\overline{k}_{i\perp})=\frac{k_N}{k_{Niz}}\Big\{\frac{k_{N-1}}{k_N}\tilde{A}_{N-1,q,W_{N-1}}^{(2)}(\overline{k}'_{\perp})-\frac{1}{2}\frac{k_{N-1}}{k_N}k_{Niz}^2\hat{e}(-k_{Niz})\cdot\overline{a}_{N-1}^{(0)} \\ -\left(\frac{k_{i\rho}}{k_N}(\overline{k}_{i\perp}-\overline{k}'_{\perp})+k_{Niz}\hat{h}(-k_{Niz})\right)\cdot\tilde{\overline{B}}_{N-1,\perp,F_{N-1}}^{(1)}(\overline{k}'_{\perp})\Big\}$$

and for other interfaces ($j\neq N-1$),

$$T_{h,W_{N-1}}^{(2)}(\overline{k}'_{\perp},\overline{k}_{i\perp})=-\frac{k_N}{k_{Niz}}\tilde{B}_{N-1,q,W_j}^{(2)}(\overline{k}'_{\perp}) \\ T_{e,W_j}^{(2)}(\overline{k}'_{\perp},\overline{k}_{i\perp})=\frac{k_{N-1}}{k_{Niz}}\tilde{A}_{N-1,q,W_j}^{(2)}(\overline{k}'_{\perp}) \tag{4.5.115}$$

The transmitted mean field can be converted to the spatial domain by inverse Fourier transform of

$$\langle\overline{E}_t^{(2)}(\overline{r})\rangle=\int \mathrm{d}\overline{k}_{\perp}\langle\tilde{\overline{E}}_t^{(2)}(\overline{k})\rangle e^{i\overline{k}_{\perp}\cdot\overline{r}_{\perp}-ik_{Nz}z} \\ =e^{i\overline{k}_{i\perp}\cdot\overline{r}_{\perp}-ik_{Niz}z}\sum_{j=1}^{N-1}\int \mathrm{d}\overline{k}'_{\perp}W_j(\overline{k}'_{\perp}-\overline{k}_{\perp_i})\Big[T_{e,W_j}^{(2)}(\overline{k}'_{\perp},\overline{k}_{i\perp})\hat{e}(-k_{Niz}) \\ +T_{h,W_j}^{(2)}(\overline{k}'_{\perp},\overline{k}_{i\perp})\hat{h}(-k_{Niz})\Big] \tag{4.5.116}$$

## 4.6 Scattered and Transmitted Power

The power density associated with the electromagnetic wave is carried by electric and magnetic fields that quantifies by the Poynting vector $\overline{S}$

$$\overline{S}=\frac{1}{2}\mathrm{Re}\Big(\overline{E}\times\overline{H}^*\Big) \tag{4.6.1}$$

where the real (time averaged) power is considered here. The power can be associated to the different orders of the electric field and magnetic field. Since electromagnetic fields are random quantities for the problem of interest, statistical average of power density is a proper quantity. Also, the power flow normal to the direction of the mean surface profile will be computed. Within SPM2 solution,

$$\langle \overline{S} \rangle = \frac{1}{2}\mathrm{Re}\left\langle \left(\overline{E}^{(0)}+\overline{E}^{(1)}+\overline{E}^{(2)}\right)\times\left(\overline{H}^{(0)}+\overline{H}^{(1)}+\overline{H}^{(2)}\right)^{*}\right\rangle \tag{4.6.2}$$

$$= \frac{1}{2}\mathrm{Re}\Big\{\overline{E}^{(0)}\times\overline{H}^{(0)*}+\overline{E}^{(0)}\times\langle\overline{H}^{(1)*}\rangle+\overline{E}^{(0)}\times\langle\overline{H}^{(2)*}\rangle + \langle\overline{E}^{(1)}\rangle\times\overline{H}^{(0)*}+\langle\overline{E}^{(1)}\times\overline{H}^{(1)*}\rangle+\langle\overline{E}^{(2)}\rangle\times\overline{H}^{(0)*}\Big\}$$

The first term in (4.6.2) is $\mathrm{Re}\langle\overline{E}_s^{(0)}\times\overline{H}_s^{(0)*}\rangle$ which reduces to $\mathrm{Re}[\overline{E}_s^{(0)}\times\overline{H}_s^{(0)*}]$ since the zeroth order solution is deterministic. It is exactly the reflected power from a layered medium with flat interfaces. Note that this term is the zeroth order term in the scattered power. The interaction of the zeroth order electric field with the first order magnetic field does not contribute to the average power transfer since the first order fields are zero mean processes, $\langle\overline{E}_s^{(1)}\times\overline{H}_s^{(0)*}\rangle=\langle\overline{E}_s^{(0)}\times\overline{H}_s^{(1)*}\rangle=0$. Thus there is no first order term in the scattered power; the first correction to the scattered power is at second order. Another term is $\langle\overline{E}_s^{(1)}\times\overline{H}_s^{(1)*}\rangle$, a product of two first order fields so it is a second order term in scattered power, and is non-zero. As mentioned earlier, first order scattered fields are incoherent; this term represents the second order incoherent power. This incoherent power is not concentrated in the specular direction, but rather exists in multiple scattered field directions. Another second order term in (4.6.2) is $\mathrm{Re}\langle\overline{E}_s^{(2)}\times\overline{H}_s^{(0)*}\rangle=\mathrm{Re}[\langle\overline{E}_s^{(2)}\rangle\times\overline{H}_s^{(0)*}]$, which coincides with the term $\mathrm{Re}\langle\overline{E}_s^{(2)}\times\overline{H}_s^{(0)*}\rangle$ in (4.6.2) . Since the averaged second order scattered field exists only in the specular direction (the same as zeroth order reflected field) this term called the *coherent reflected power correction*. The coherent scattered power (up to 2nd order) has two components, one is the zeroth order power and the coherent reflected power correction that comes from the average second order field. In (4.6.2), last term $\mathrm{Re}\langle\overline{E}_s^{(2)}\times\overline{H}_s^{(2)*}\rangle$ is of order of 4 that contributes to the higher order corrections. In the following discussion we will consider only second order corrections to the scattered and transmitted power. Therefore, to second order we have

$$\langle \overline{S} \rangle = \frac{1}{2}\mathrm{Re}\Big\{\overline{E}^{(0)}\times\overline{H}^{(0)*}+2\langle\overline{E}^{(2)}\rangle\times\overline{H}^{(0)*}+\langle\overline{E}^{(1)}\times\overline{H}^{(1)*}\rangle\Big\} \tag{4.6.3}$$

The second order mean scattered field is in the specular direction similar to the zeroth order fields. The first two terms in the power expansion of (4.6.3) are coherent power terms while the third term as we will see is proportional to the variance of the electric field and it is an incoherent power that on average has a distribution over all possible directions.

### 4.6.1 Coherent Scattered and Transmitted Powers

The coherent scattered power density that flows in $+\hat{z}$ direction has two components. One is the zeroth order power term that corresponds to the flat surface case, and another

component is the power carried by the zeroth order electric and second order magnetic field (and vice versa)

$$\langle \overline{S}_s^{(2)} \cdot \hat{z} \rangle_{\text{coh}} = \frac{1}{2} \text{Re} \Big\langle \overline{E}_s^{(0)}(\overline{r}) \times \overline{H}_s^{(2)*}(\overline{r}) + \overline{E}_s^{(2)}(\overline{r}) \times \overline{H}_s^{(0)*}(\overline{r}) \Big\rangle \cdot \hat{z} \tag{4.6.4}$$

or,

$$\langle \overline{S}_s^{(2)} \cdot \hat{z} \rangle_{\text{coh}} = \text{Re} \Big\langle \overline{E}_s^{(2)}(\overline{r}) \times \overline{H}_s^{(0)*}(\overline{r}) \Big\rangle \cdot \hat{z} = \text{Re} \Big( \Big\langle \overline{E}_s^{(2)}(\overline{r}) \Big\rangle \times \overline{H}_s^{(0)*}(\overline{r}) \cdot \hat{z} \Big) \tag{4.6.5}$$

Using the second order expansion of the scattered field, the second order coherent power density of the TE and TM channels can be obtained as

$$\langle \overline{S}_s^{(2)e} \cdot \hat{z} \rangle_{\text{coh}} = \frac{k_{1iz}}{k_1 \eta_1} \int \text{d}\overline{k}'_\perp \sum_{j=1}^{N-1} \text{Re} \Big[ S_e^{(0)*} S_{e,W_j}^{(2)}(\overline{k}'_\perp, \overline{k}_{i\perp}) \Big] W_j(\overline{k}'_\perp - \overline{k}_{\perp_i}) \tag{4.6.6}$$

$$\langle \overline{S}_s^{(2)h} \cdot \hat{z} \rangle_{\text{coh}} = \frac{k_{1iz}}{k_1 \eta_1} \int \text{d}\overline{k}'_\perp \sum_{j=1}^{N-1} \text{Re} \Big[ S_h^{(0)*} S_{h,W_j}^{(2)}(\overline{k}'_\perp, \overline{k}_{i\perp}) \Big] W_j(\overline{k}'_\perp - \overline{k}_{\perp_i})$$

where the zeroth order solution is taken to be

$$\overline{E}_s^{(0)}(\overline{r}) = e^{i\overline{k}_\perp \cdot \overline{r}_\perp + ik_{1iz}z} \Big[ S_e^{(0)} \hat{e}(k_{1iz}) + S_h^{(0)} \hat{h}(k_{1iz}) \Big] \tag{4.6.7}$$

$$\overline{H}_s^{(0)}(\overline{r}) = \frac{1}{\eta_1} e^{i\overline{k}_\perp \cdot \overline{r}_\perp + ik_{1iz}z} \Big[ -S_e^{(0)} \hat{h}(k_{1iz}) + S_h^{(0)} \hat{e}(k_{1iz}) \Big]$$

Note that the coherent power density does not include cross polarized component. Similarly, for the transmitted coherent power density into region $N$,

$$\langle \overline{S}_t^{(2)e} \cdot (-\hat{z}) \rangle_{\text{coh}} = \int \text{d}\overline{k}'_\perp \sum_{j=1}^{N-1} W_j(\overline{k}'_\perp - \overline{k}_{\perp_i}) \text{Re} \Big[ \frac{1}{\eta_N^*} T_{e,W_j}^{(2)}(\overline{k}'_\perp, \overline{k}_{i\perp}) T_e^{(0)*} \Big( \frac{k_{Niz}}{k_N} \Big)^* \Big] \tag{4.6.8}$$

$$\langle \overline{S}_t^{(2)h} \cdot (-\hat{z}) \rangle_{\text{coh}} = \int \text{d}\overline{k}'_\perp \sum_{j=1}^{N-1} W_j(\overline{k}'_\perp - \overline{k}_{\perp_i}) \text{Re} \Big[ \frac{1}{\eta_N^*} T_{h,W_j}^{(2)}(\overline{k}'_\perp, \overline{k}_{i\perp}) T_h^{(0)*} \Big( \frac{k_{Niz}}{k_N} \Big) \Big]$$

given the zeroth order transmitted electric and magnetic fields of,

$$\overline{E}_t^{(0)}(\overline{r}) = e^{i\overline{K}_{Ni} \cdot \overline{r}} \Big[ T_e^{(0)} \hat{e}(-k_{Niz}) + T_h^{(0)} \hat{h}(-k_{Niz}) \Big] \tag{4.6.9}$$

$$\overline{H}_t^{(0)}(\overline{r}) = \frac{1}{\eta_N} e^{i\overline{K}_{Ni} \cdot \overline{r}} \Big[ -T_e^{(0)} \hat{h}(-k_{Niz}) + T_h^{(0)} \hat{e}(-k_{Niz}) \Big]$$

It is possible to define the *coherent power spectral coefficients* $\mathcal{S}_{s,j}^{\text{coh}}$ and $\mathcal{S}_{t,j}^{\text{coh}}$ for the scattered and transmitted coherent powers (to be used in the next section) as

$$\langle \overline{S}_s^{\text{coh}} \cdot \hat{z} \rangle = \sum_{j=1}^{N-1} \int \text{d}\overline{k}_\perp W_j(\overline{k}_\perp - \overline{k}_{\perp_i}) \mathcal{S}_{s,j}^{\text{coh}}(\overline{k}_\perp) \tag{4.6.10}$$

$$\langle \overline{S}_t^{\text{coh}} \cdot \hat{z} \rangle = \sum_{j=1}^{N-1} \int \text{d}\overline{k}_\perp W_j(\overline{k}_\perp - \overline{k}_{\perp_i}) \mathcal{S}_{t,j}^{\text{coh}}(\overline{k}_\perp)$$

such that sum of spectral integration of the power spectral coefficients times the power spectral densities of the interfaces results in the corresponding power density.

### 4.6.2 Incoherent Scattered and Transmitted Power

Last term in the power expansion of (4.6.3) corresponds to the power carried by the first order electric and magnetic fields. However, the first order fields are zero mean but average of its square is not necessarily zero and is the second order moment of the scattered field. Since the first order scattered electric field is proportional to the surface spectrum, and for uncorrelated stationary surface profiles

$$\langle F_i(\overline{k}_\perp-\overline{k}_{\perp_i})F_j(\overline{k}'_\perp-\overline{k}_{\perp_i})\rangle=\delta_{ij}\delta(\overline{k}_\perp-\overline{k}'_\perp)W(\overline{k}_\perp-\overline{k}_{\perp_i}) \tag{4.6.11}$$

while for complex conjugated correlation,

$$\langle F_i(\overline{k}_\perp-\overline{k}_{\perp_i})F_j^*(\overline{k}'_\perp-\overline{k}_{\perp_i})\rangle=\delta_{ij}\delta(\overline{k}_\perp+\overline{k}'_\perp)W(\overline{k}_\perp-\overline{k}_{\perp_i}) \tag{4.6.12}$$

From the first order scattered field expression, the incoherent power can be computed as

$$\langle\overline{S}_s^{\rm inc}\cdot\hat{z}\rangle=\frac{1}{2k\eta}{\rm Re}\sum_{j=1}^{N-1}\int{\rm d}\overline{k}_\perp e^{i(k_z-k_z^*)z}W_j(\overline{k}_\perp-\overline{k}_{\perp_i})\left\{\left|S_{e,F_j}^{(1)}(\overline{k}_\perp)\right|^2k_{1z}^*+\left|S_{h,F_j}^{(1)}(\overline{k}_\perp)\right|^2k_{1z}\right\} \tag{4.6.13}$$

Notice that the polarization unit vector $\hat{e}(k_{1z})$ is always a real vector (even for a lossy medium) but $\hat{h}(k_{1z})$ can be complex in general (even for a lossless medium).

$$\begin{aligned}\hat{h}(k_{1z})&=-\frac{k_{1z}}{k_1}\hat{p}(\overline{k}_\perp)+\frac{k_\rho}{k_1}\hat{z}\\ \hat{h}^*(k_{1z})&=-\frac{k_{1z}^*}{k_1}\hat{p}(\overline{k}_\perp)+\frac{k_\rho}{k_1}\hat{z}\end{aligned} \tag{4.6.14}$$

so,

$$\hat{h}(k_{1z})\times\hat{h}^*(k_{1z})=-\frac{k_\rho}{k_1^2}(k_{1z}-k_{1z}^*)\hat{p}(\overline{k}_\perp)\times\hat{z} \tag{4.6.15}$$

which does not have $z$ component. Also, $\hat{e}(k_{1z})\times\hat{h}^*(k_{1z})=-\hat{k}^*$. Since propagating waves exist only when $|\overline{k}_\perp|\le k_1$ then for lossless region 1,

$$k_{1z}=k_{1z}^* \quad , \quad |\overline{k}_\perp|\le k_1 \tag{4.6.16}$$

and therefore,

$$\langle\overline{S}_s^{\rm inc}\cdot\hat{z}\rangle=\frac{1}{2k\eta}\sum_{j=1}^{N-1}\int_{|\overline{k}_\perp|\le k_1}{\rm d}\overline{k}_\perp k_{1z}W_j(\overline{k}_\perp-\overline{k}_{\perp_i})\left\{\left|S_{e,F_j}^{(1)}(\overline{k}_\perp)\right|^2+\left|S_{h,F_j}^{(1)}(\overline{k}_\perp)\right|^2\right\} \tag{4.6.17}$$

Similarly for the incoherent transmitted field we have

$$\langle\overline{S}_t^{\rm inc}\cdot(-\hat{z})\rangle=\frac{1}{2}\sum_{j=1}^{N-1}\int{\rm d}\overline{k}_\perp W_j(\overline{k}_\perp-\overline{k}_{\perp_i}){\rm Re}\left\{\frac{k_{2z}^*}{\eta_2^*k_2^*}\left|T_{e,F}^{(1)}(\overline{k}_\perp)\right|^2+\frac{k_{2z}}{k_2\eta_2^*}\left|T_{h,F}^{(1)}(\overline{k}_\perp)\right|^2\right\} \tag{4.6.18}$$

Note that in (4.6.18), the integrations are carried out over the propagating part of the spectrum since ${\rm Re}k_{1z}=0$ when $|\overline{k}_\perp|>k_1$. Thus, evanescent waves do not contribute to incoherent scattered power. On the other hand, for a general structure consisting of lossy materials, evanescent waves may contribute to the incoherent transmitted power. However, for the

lossless case, the transmitted power comes from only propagating part of the spectrum in region N. For the next section, we can define the *incoherent power spectral coefficients* $\mathcal{S}_{s,j}^{\rm inc}$ and $\mathcal{S}_{t,j}^{\rm inc}$ for the incident and transmitted incoherent powers as

$$\langle \overline{S}_s^{\rm inc} \cdot \hat{z} \rangle = \sum_{j=1}^{N-1} \int {\rm d}\overline{k}_\perp W_j(\overline{k}_\perp - \overline{k}_{\perp_i}) \mathcal{S}_{s,j}^{\rm inc}(\overline{k}_\perp) \tag{4.6.19}$$

$$\langle \overline{S}_t^{\rm inc} \cdot \hat{z} \rangle = \sum_{j=1}^{N-1} \int {\rm d}\overline{k}_\perp W_j(\overline{k}_\perp - \overline{k}_{\perp_i}) \mathcal{S}_{t,j}^{\rm inc}(\overline{k}_\perp)$$

such that sum of spectral integration of the power spectral coefficients times the power spectral densities of the interfaces results in the power density.

## 4.7 Strong Statement of Energy Conservation

It is well known that for a single rough surface, the second order perturbation theory obeys energy conservation [3]. This has typically been shown in the past by specifying the power spectral density, as for example a Gaussian or power law spectrum, and then performing numerical integrations over ${\rm d}k_x$ and ${\rm d}k_y$ to obtain the total reflectivity and transmissivity. For lossless media, the sum of the reflectivity and transmissivity is then shown to be unity, verifying energy conservation. In this section, we show that energy conservation in the SPM can also be shown through a "strong" condition in which it is not necessary to specify the spectral densities of any of the rough interfaces. The strong condition shows that the kernel function multiplying the spectral density of each rough interface obeys energy conservation for each value of $k_x$ and $k_y$. Numerical examples are shown for the case of a multi-layered medium with 50 rough interfaces to illustrate this condition. Note that the fact that the SPM2 conserves energy does not necessarily imply that its predictions of the reflected and transmitted powers are accurate. It has been shown in the literature that for the single interface case, the SPM2 prediction of emission fortuitously is a small surface slope, rather than small height, expansion. This greatly expands the domain of applicability of the method. However for the case of multiple layers, the fortuitous cancellation of height dependent terms is not obtained, so that the SPM2 prediction of total reflected powers should be expected to be applicable only in the limit of small interface heights compared to the electromagnetic wavelength. Energy conservation implies that for a *lossless* structure, the total scattered power (incoherent plus coherent part) emerging in the $\hat{z}$ direction plus the total transmitted power in region $N$ emerging in the $(-\hat{z})$ direction should be equal to the incident power impinging in the $(-\hat{z})$ direction.

$$\begin{aligned} &\left[\overline{S}_s^{(0)} + \langle \overline{S}_s^{(2),\rm coh} + \overline{S}_s^{(2),\rm inc} \rangle\right] \cdot \hat{z} \\ &+ \left[\overline{S}_t^{(0)} + \langle \overline{S}_t^{(2),\rm coh} + \overline{S}_t^{(2),\rm inc} \rangle\right] \cdot (-\hat{z}) = \overline{S}_{\rm i} \cdot (-\hat{z}) \end{aligned} \tag{4.7.1}$$

where $\overline{S}_{\rm i}$ is complex Poynting vector associated with the incident field. We know that the zeroth order solution is the exact solution of the problem when there is no roughness (flat boundaries), and therefore obeys energy conservation. This means

$$\overline{S}_s^{(0)} \cdot \hat{z} + \overline{S}_t^{(0)} \cdot (-\hat{z}) = \overline{S}_{\rm i} \cdot (-\hat{z}) \tag{4.7.2}$$

Using (4.7.2) in (4.7.1), the SPM2 solution conserves energy if

$$\langle \overline{S}_s^{(2),\mathrm{coh}} + \overline{S}_s^{(2),\mathrm{inc}} \rangle \cdot \hat{z} + \langle \overline{S}_t^{(2),\mathrm{coh}} + \overline{S}_t^{(2),\mathrm{inc}} \rangle \cdot (-\hat{z}) = 0 \tag{4.7.3}$$

Utilizing the power spectral coefficients (the kernel functions) energy is conserved if

$$\sum_{j=1}^{N-1} \int \mathrm{d}\overline{k}_\perp W_j(\overline{k}_\perp - \overline{k}_{i\perp}) \Big[ \mathcal{S}_{s,j}^{(2),\mathrm{inc}}(\overline{k}_\perp) + \mathcal{S}_{s,j}^{(2),\mathrm{coh}}(\overline{k}_\perp) + \mathcal{S}_{t,j}^{(2),\mathrm{inc}}(\overline{k}_\perp) + \mathcal{S}_{t,j}^{(2),\mathrm{coh}}(\overline{k}_\perp) \Big] = 0 \tag{4.7.4}$$

In this equation, there are $(a)$ a summation over all the roughness interfaces with each term in the summation a product of the spectral intensity of that interface and its corresponding kernel function, and $(b)$ integrations over $k_x$ and $k_y$. The usual process of showing energy conservation is to specify the spectral intensity of each interface followed by examination of the results of the double integrations over $k_x$ and $k_y$. This process is not necessary because energy conservation is satisfied for any arbitrary values of the surface power spectral densities. More precisely, since the $W_j$'s are independent functions, the coefficients of $W_j$ in the summand should be identically zero:

$$\int \mathrm{d}\overline{k}_\perp W_j(\overline{k}_\perp - \overline{k}_{i\perp}) \Big[ \mathcal{S}_{s,j}^{(2),\mathrm{inc}}(\overline{k}_\perp) + \mathcal{S}_{s,j}^{(2),\mathrm{coh}}(\overline{k}_\perp) + \mathcal{S}_{t,j}^{(2),\mathrm{inc}}(\overline{k}_\perp) + \mathcal{S}_{t,j}^{(2),\mathrm{coh}}(\overline{k}_\perp) \Big] = 0, \quad \forall j \tag{4.7.5}$$

Since expression (4.7.5) holds for arbitrary functions $W_j$, we must have

$$\mathcal{S}_{s,j}^{(2),\mathrm{inc}}(\overline{k}_\perp) + \mathcal{S}_{s,j}^{(2),\mathrm{coh}}(\overline{k}_\perp) + \mathcal{S}_{t,j}^{(2),\mathrm{inc}}(\overline{k}_\perp) + \mathcal{S}_{t,j}^{(2),\mathrm{coh}}(\overline{k}_\perp) = 0, \quad \forall j \,\&\, \forall \overline{k}_\perp \tag{4.7.6}$$

Equation (4.7.6) for all possible values of $j$ and $\overline{k}_\perp$ is the final "strong" condition of energy conservation. To illustrate SPM2 energy conservation, consider 50 layer structure with rough interfaces that is illuminated with a plane wave at normal incident angle. For permittivity and mean position of the layers we consider one realization of Gaussian correlated density fluctuations given in [41] and is depicted in Figure 4.2. Figure 4.3 plots for $k_y = 0$ the power spectral coefficients of $W_1(\overline{k}_\perp - \overline{k}_{i\perp})$ for the TE (right graph) and TM (left graph) plane wave excitations. Each graph contains 4 curves to account for the coherent and incoherent scattered and transmitted power spectral coefficients. These contributions are shown to sum up to zero for each $k_x$ and $k_y$ as expected, demonstrating (4.7.6) for $j = 1$. Figures 4.4 and 4.5 provide similar illustrations for the contributions of $W_{25}$ and $W_{50}$ respectively. Additional results not shown again verified energy conservation for the contributions of all of the medium interfaces.

## 4.8 Application 1: Brightness Temperature of Antarctic ice sheets

For a objects at physical temperature $T_0$, the emissivity $e_\beta$ is given by

$$e_\beta = \frac{T_\beta}{T_0} \tag{4.8.1}$$

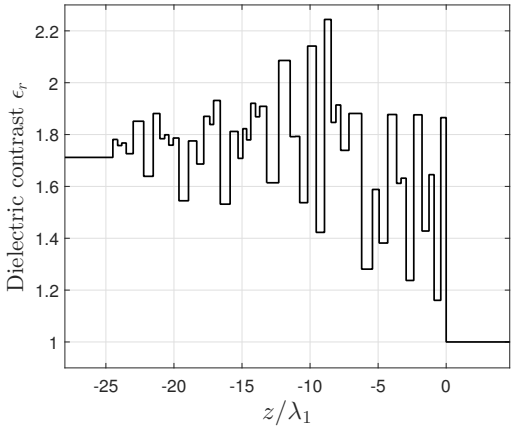


FIGURE 4.2: One realization of dielectric constants and corresponding mean position of the layers. $z>0$ corresponds to the first region (air).

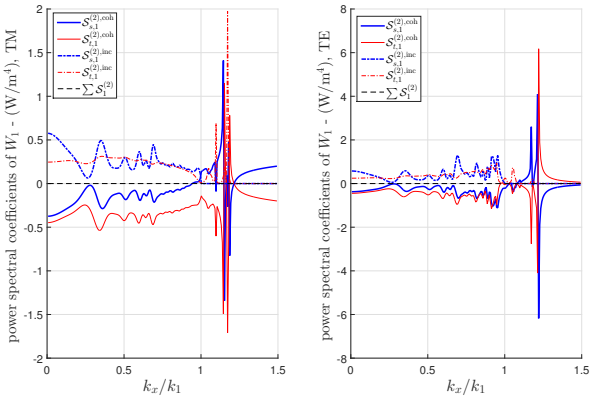


FIGURE 4.3: Power spectral coefficients of $W_1(\overline{k}_\perp - \overline{k}_{i\perp})$ as a function of $k_x$ for profile $k_y$=0 for 50 layer medium with permittivities and mean interface locations given by Figure 4.2. Right hand side and left hand side figures correspond to TE and TM excitation respectively.

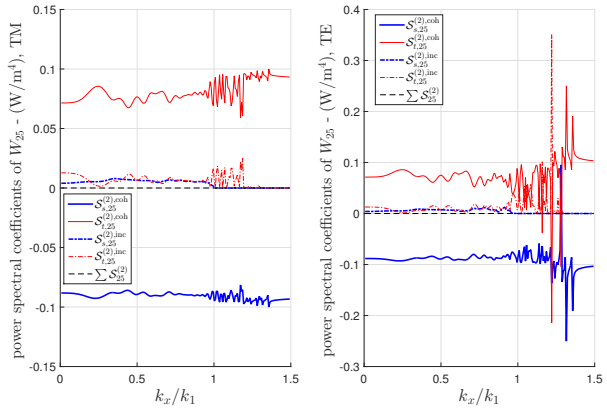


FIGURE 4.4: Power spectral coefficients of $W_{25}(\overline{k}_\perp - \overline{k}_{i\perp})$ as a function of $k_x$ for profile $k_y$=0 for 50 layer medium with permittivities and mean interface locations given by Figure 4.2. Right hand side and left hand side figures correspond to TE and TM excitation respectively.

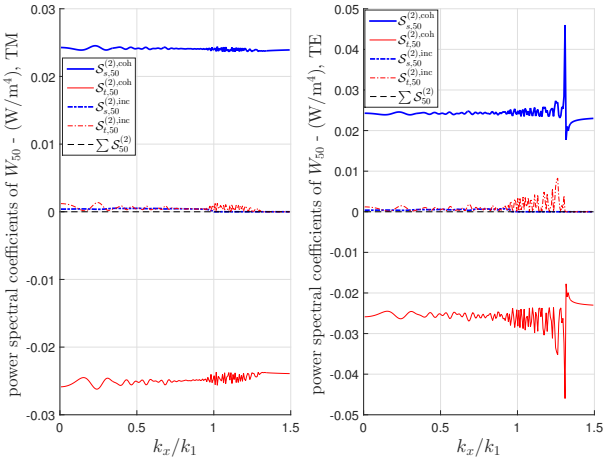


FIGURE 4.5: Power spectral coefficients of $W_{50}(\overline{k}_\perp - \overline{k}_{i\perp})$ as a function of $k_x$ for profile $k_y$=0 for 50 layer medium with permittivities and mean interface locations given by Figure 4.2. Right hand side and left hand side figures correspond to TE and TM excitation respectively.

where $T_\beta$ is the $\beta-$polarized brightness temperature of the object with ($\beta$=$H$,$V$). From reciprocity and for objects in thermal equilibrium, the emissivity of an object coincides with its absorptivity (the portion of power absorbed by the object). The emissivity of an object can then be computed from knowledge of the fraction of the incident power absorbed by the object. Since the sum of scattered and transmitted power is the total incident power, we can relate the emissivity of an object to its reflectivity as

$$e_\beta = t_\beta = 1 - r_\beta \tag{4.8.2}$$

In the Antarctic ice sheet , there are hundreds of layers of snow/ice with varying densities due to the accumulation pattern of falling snow. These density variations give rise

to the varying dielectric constants of the layers. Each interface is characterized by weak dielectric contrasts on either side of the rough interface. Although the contrast is weak, the total reflection by hundreds of interfaces causes a significant increase in reflectivity and a corresponding decrease in emissivity. The problem was analyzed previously with a multilayer model of flat interfaces [41]. Comparisons of the predictions of the flat surface model with 1.4 GHz microwave radiometer measurements of the Antarctic ice sheet showed that a reasonable match between model and measurement could be achieved for near nadir measurements in both polarizations, and for vertically polarized measurements at a variety of observation angles. However, the model was found to under-predict the measured data in horizontal polarization at larger incidence angles. In this section, we illustrate the application of the Multilayer SPM2 by including the effects of rough surfaces. A key question is whether the inclusion of surface roughness can increase the prediction of horizontally polarized brightness temperatures at larger incidence angles while leaving vertically polarized predictions relatively unaffected. A model for the Antarctic ice sheet is complicated and can contains up to thousands of layers. For this initial examination, we consider only a 20 layer structure to find the effect of roughness on the predicted brightness temperatures. We assume a Gaussian correlation function with RMS height $h$=1.5 cm and correlation length $l$=25 cm for all rough interfaces (note that this should satisfy the small height assumption at 1.4 GHz). All layers are assumed to have physical temperature $T_0$=228 K. In reality, the temperature of the Antarctic ice sheet varies with depth, but again we seek only an initial evaluation of the effect of surface roughness in this study. Monte Carlo simulations are used to generate random permittivities for each layer based on damped Gaussian correlated density fluctuation characterized by auto-covariance $\Delta^2=(0.18\text{g/cm}^3)^2$, correlation length $l$=10cm, and damping factor $\alpha$=3m (see [41]). For each random permittivity profile, we apply the SPM2 to calculate the emissivity. This is then repeated for realizations of the random permittivity. Note that this problem has 2 random processes involved, the random permittivity process, and the random roughness process. The Monte Carlo simulation is performed only over the permittivity process, because the SPM2 formulation has already analytically evaluated the ensemble average over surface roughness. The computation remains intensive as we need to average over $\mathcal{O}(1000)$ permittivity realizations, and for each realization , we need to compute all spectral coefficients over a finely discretized 2D $k_x$ and $k_y$ grid. Note that the ensemble average over the random permittivities can be performed again inside the integration over $k_x$ and $k_y$ by averaging the $S$ spectral functions over permittivity realizations. Figure 4.6 plots the simulated ice sheet brightness temperatures for the multilayer flat surface model and the multilayer rough surface model, both of which are averaged over 400 permittivity realizations. The results confirm that considering roughness effects can increase H-pol brightness temperatures at large observation angles while leaving V-pol brightness temperatures relatively unaffected. Further work is in process to model the rough surface effects on ice sheet emissions more realistically for comparison with radiometer measurements.

## 4.9 Application 2: photonic crystal of periodically alternating permittivities

Consider a photonic crystal of periodically alternating permittivities of larger dielectric contrast (Figure 4.8) that contains 50 independent Gaussian random rough interfaces. (i.e.

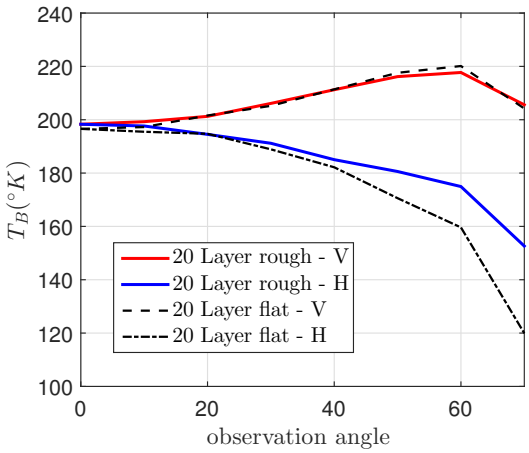


FIGURE 4.6: Brightness temperature of Antarctic ice sheets. Comparison of physical model based on Multilayer structure for both flat and rough interfaces. Considering roughness increases H-pol brightness temperatures while leaving V-pol brightness temperatures relatively unaffected.

it is not perfect periodic structure). In Figure 4.8, 20% of each period is filled by $\epsilon_r$=8.9 and the background is air. The band diagram of the corresponding infinite periodic structure with flat interfaces is shown in Figure 4.7; these results were calculated using a plane wave expansion approach [65, 76, 77]. In reality, all physical surfaces have roughness, which

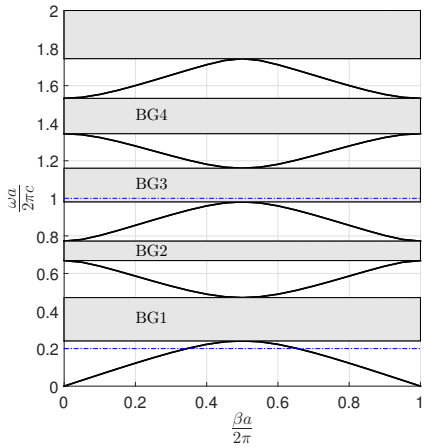


FIGURE 4.7: The band diagram of infinite photonic crystal of Figure 4.8 with flat interfaces.

could also be viewed as impurities in the crystal. In what follows, two particular case of the excitations one at the stop band and another at the pass band of the ideal structure with flat boundaries is simulated. Figure 4.9 shows the power spectral coefficients of $W_1$ for a normally incident plane wave excitation at normalized frequency of 1 ( which lies in the band gap of BG3 in Figure 4.7 shown by the dotted line), where the period of the structure is $a$=1 (Left and right plot correspond to TE and TM excitations respectively). The coherent transmitted spectral coefficient of $W_1$ is zero while the incoherent transmitted spectral

coefficient is non zero, indicating an imperfection in the periodic structure. The presence of rough surfaces at the boundaries cause leakage of the incoherent power (in all directions) to the structure. Figure 4.10 shows the spectral coefficients of $W_{50}$. It can be seen that for excitations in the band gap, the last rough interface has negligible contribution to the transmitted power compared to the upper rough interfaces. The contribution of the $j$-th rough interface to the incoherent transmitted power (that is $\mathcal{S}_{t,j}^{(2),\text{inc}}$) decays rapidly with increasing $j$. More generally, the transmitted and scattered power spectral coefficients again sum up to zero exactly for all $W_j$'s and for all points $\overline{k}_\perp$, again confirming SPM2 energy conservation. Note that for this structure that contains high contrast dielectric variation between adjacent layers, energy is conserved exactly by means of the strong condition (4.7.6) that shows SPM2 solution conserves energy not only for small dielectric contrast between adjacent layers but also for the case of larger dielectric contrasts. For excitations in the pass band regions, consider a normally incident plane wave at normalized frequency of 0.2. Figure 4.11 and 4.12 show the power spectral coefficients of $W_1$ and $W_{50}$ respectively for TE and TM excitations. Note that in contrast to the previous case of excitations in the stop region, in the pass band regions the contribution of each rough interface to the transmitted power (including incoherent and coherent) does not show rapid decay with $j$.

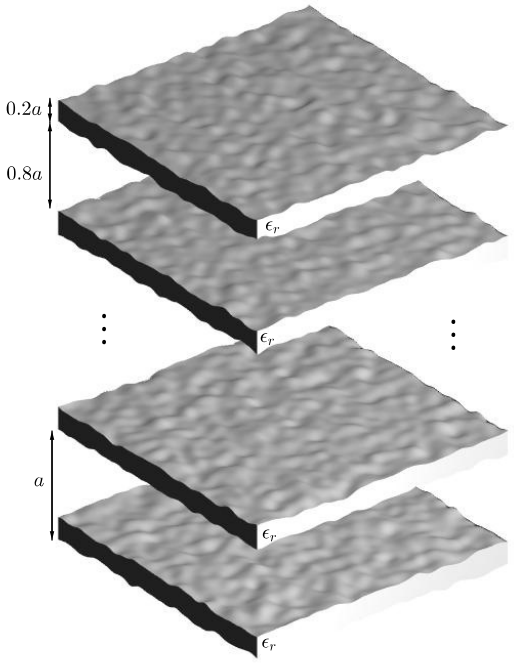


FIGURE 4.8: photonic crystal of periodically alternating permittivities with rough interfaces. Period of the structure is $a$ and 20% of each period filled with $\epsilon_r$=8.9 and the background is air.

## 4.10 Conclusions

In this chapter, we have derived a "strong" condition of energy conservation for the SPM2 with a large number of rough interfaces in a layered medium. The SPM2 kernel functions

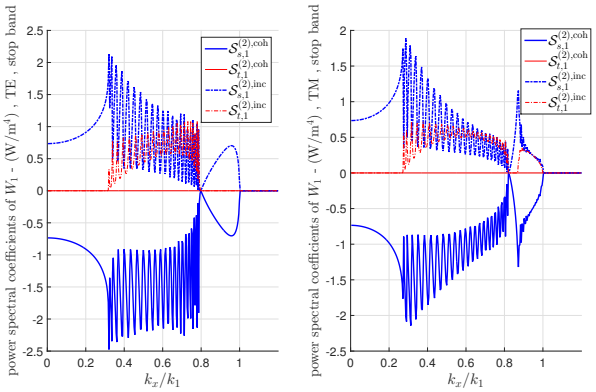


FIGURE 4.9: Power spectral coefficient of $W_1$ for the photonic crystal of Figure 4.8 as a function of $k_x$ for $k_y$=0. Excitation is at the band gap BG3 and normalized frequency of 1 (Figure 4.7). Left (Right) plot corresponds to TE (TM) excitation.

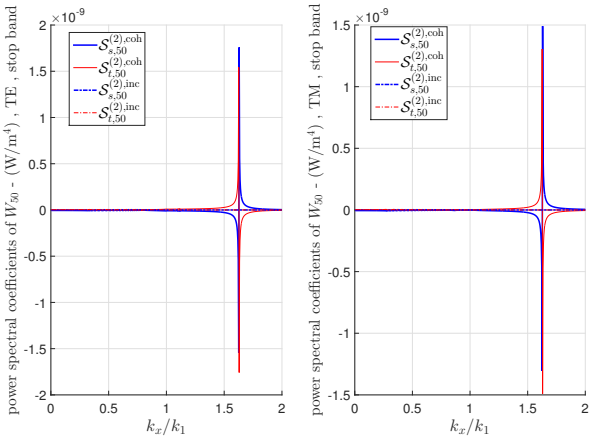


FIGURE 4.10: Power spectral coefficient of $W_{50}$ for the photonic crystal of Figure 4.8 as a function of $k_x$ for $k_y$=0. Excitation is at the band gap BG3 and normalized frequency of 1 (Figure 4.7). Left (Right) plot corresponds to TE (TM) excitation.

for the coherent and incoherent reflected and transmitted powers obey energy conservation irrespective of the roughness statistics. The SPM2 is therefore a useful method for computing layered rough medium emission in cases where there are a large number of rough interfaces characterized by small roughness for each interface. Applications of the method are in remote sensing and imaging, and in microwave, photonic, and photonic devices. Initial examples indicating the application of the approach to the prediction of layered medium brightness temperatures and to transmission in photonic crystals were also shown.

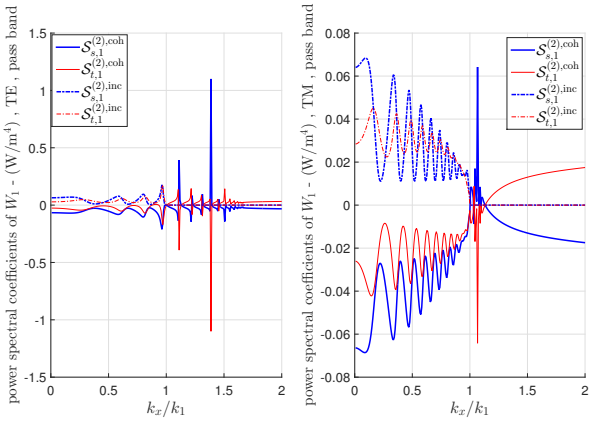


FIGURE 4.11: Power spectral coefficient of $W_1$ for the photonic crystal of Figure 4.8 as a function of $k_x$ for $k_y$=0. Excitation is at the bottom pass band at normalized frequency of 0.2 (Figure 4.7). Left (Right) plot corresponds to TE (TM) excitation.

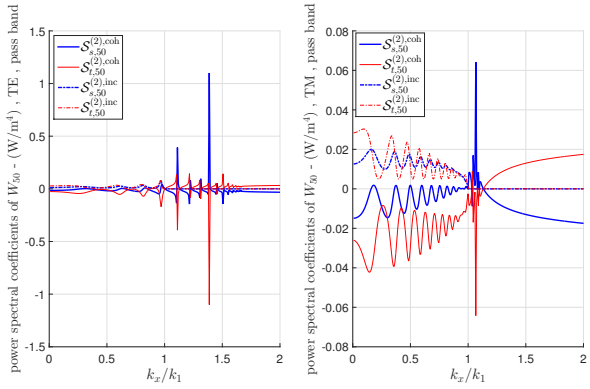


FIGURE 4.12: Power spectral coefficient of $W_{50}$ for the photonic crystal of Figure 4.8 as a function of $k_x$ for $k_y$=0. Excitation is at the bottom pass band at normalized frequency of 0.2 (Figure 4.7). Left (Right) plot corresponds to TE (TM) excitation.

# Chapter 5

# Scattering From 3D Layered Media with Periodic Random Rough interfaces, $T$-matrix Approach

## 5.1 Introduction

Scattering of electromagnetic waves from layered media with random rough interfaces has many applications in science and engineering [49, 70–72]. In particular, we are interested in multi-layered media with rough interfaces as a forward model of microwave remote sensing of ice sheets in the Arctic and Antarctica where snow accumulation causes multi-layer fluctuations of permittivity [41, 78, 79]. There are two types of randomness in this problem, a randomness in the rough interfaces and a randomness in the dielectric profile of the layered medium. A variety of techniques have been proposed to solve this problem that can generally be categorized into analytical, semi-analytical, and numerical approaches. Analytical methods are applicable only under certain approximations. For instance, the Small Perturbation Method (SPM) [29, 34, 38, 80**?** , 81] provides a closed form solution for the mean and variance of scattered field from a layered medium with random rough interfaces. The SPM2 is a low frequency approximation and is valid only for surfaces with electromagnetically small heights [35, 82]. Numerical methods such as the Method of Moments (MoM) and the Finite Element Method (FEM) are computationally intensive compared to the SPM for such a problem. Specially these methods are not suitable for the case of small dielectric contrast between layers, as the effect of small contrast between layers can fall beneath the discretization noise level.

For the case of layered media including random rough interfaces with small height, the SPM is the most favorable solution as it provides analytical expressions and more importantly, statistical averaging of the fields over surface randomness is included in the solution. However, it is shown that for the case of fluctuating permittivity in the layered media, which is the case in modeling slightly lossy layered random media, the SPM2 suffers from the presence of the waveguide modes in the spectral solution of the fields [79, 83]. Physically, in the presence of roughness, there are no waveguide modes, since waves can escape through the rough interface. However the SPM utilizes the zeroth order solution as the starting point of its iteration, and the zeroth order solution contains poles representing dielectric waveguide modes. The presence of these poles in the SPM2 can be treated using the Sommerfeld Integration Path (SIP) to find the total scattered and transmitted power (but not the bistatic pattern itself) [84]. However, there are situations (which are unavoidable for layered media with a fluctuating slightly lossy permittivity) where the

SPM2 solution results in a singular bistatic scattering pattern. Also, in the case of a random dielectric profile, the pole locations in the scattering pattern will change from one realization to the next. Although finding and working with such bistatic patterns is possible, it requires a very high level of accuracy to correctly capture the pole contributions.

To address these issues, we have developed a 3D $T$-Matrix solution for an arbitrary number of interfaces, surface profile functions, and dielectric profiles that provides a robust solution without the limitations of the SPM2. A T-matrix solution for layered media with 1D surfaces has been studied previously [85], but the 1D model does not include depolarization effects that in some situations are important [86]. One of the disadvantages of the $T$-Matrix method (and any other approach rather than analytical approaches) compared to the SPM is that a Monte Carlo simulation over interface realizations is necessary to obtain the mean and variance of the fields. From computational perspective, the T-matrix method has the advantage that its solution satisfies power conservation to a degree of accuracy that is not obtainable in other numerical approaches.

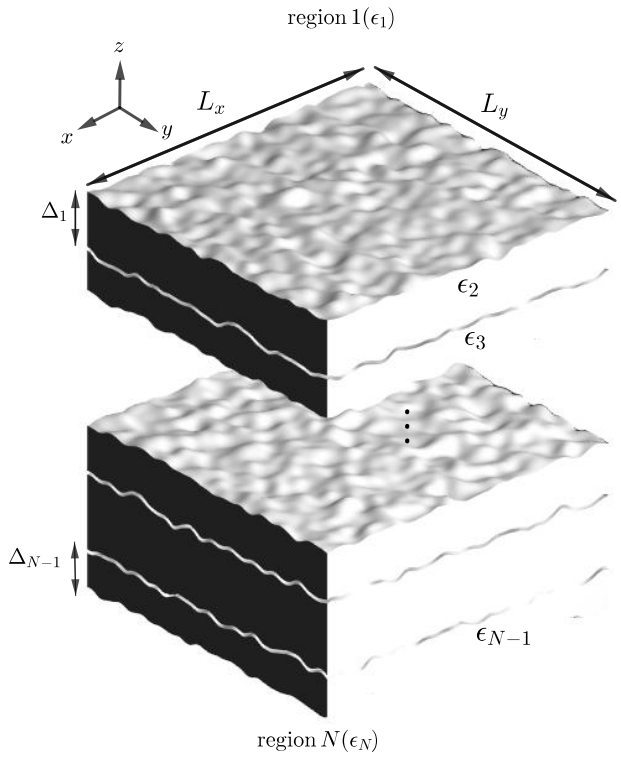


FIGURE 5.1: Geometry of the Layered media which is periodic along $x$ and $y$ directions with period of $L_x$, and $L_y$, respectively.

## 5.2 3D Periodic Green's function

Using Bloch theorem, it turns out that for the scattering problem from a surface which is periodic in two directions $x$ and $y$ with corresponding periods $L_x$ and $L_y$, we can condensate the spatial integration over the infinite surface into just one period if we replace the free

space Green's function $G(\overline{r},\overline{r}')$ with

$$G_p(\overline{r},\overline{r}')=\sum_{\overline{a}} G(\overline{r};\overline{r}'+\overline{a})e^{i\overline{k}_i\cdot\overline{a}} \tag{5.2.1}$$

where $\overline{a}=mL_x\hat{x}+nL_y\hat{y}$ is location of all lattice sites for $(m,n\in\mathbb{Z})$ This is just separating the so-called array factor of the elements (within the cells) from the scattering properties of a single lattice site. Therefore, the periodic Green's function accounts for the repetition of empty lattices. In order to perform the summation we can either use the plane wave expansion of the Green's function or a spatial representation of the free space Green's function. Starting from the wave equation for 3D scalar Green's function of free space

$$(\nabla^2+k_0^2)G(\overline{r},\overline{r}')=-\delta(\overline{r}-\overline{r}') \tag{5.2.2}$$

where $k_0$ is free space wavenumber. The solution of (5.2.2) can be obtained in spherical coordinate as $G(\overline{r},\overline{r}')=\exp(ik_0|\overline{r}-\overline{r}'|)/4\pi|\overline{r}-\overline{r}'|$. Upon inserting this solution in the expansion of the periodic Green's function (5.2.1),

$$G_p(\overline{r},\overline{r}')=\sum_{m,n}\frac{e^{ikR_{mn}}}{4\pi R_{mn}} \tag{5.2.3}$$

where, $R_{mn}=|\overline{r}-\overline{r}'-mL_x\hat{x}-nL_y\hat{y}|$. The series of (5.2.3) is a slowly convergent series, it is not an absolutely convergent series and computation of the periodic Green's function with (5.2.3) requires including large number of terms in the summation to get convergent results. If the medium of interest (background medium) is lossy with tangible amount of loss, then (5.2.3) is an exponentially convergent series and it provides a fast way of computing the periodic Green's function. However, this is not always the case and the spatial expansion is not a good candidate. Fourier expanding the Green's function in (5.2.2) results in the following spectral representation.

$$G(\overline{r},\overline{r}')=\int\frac{\mathrm{d}\overline{k}}{(2\pi)^3}\ \frac{1}{k_0^2-k^2}e^{i\overline{k}\cdot(\overline{r}-\overline{r}')} \tag{5.2.4}$$

where $k=|\overline{k}|$. This integral is not well defined unless for lossy medium to get the radiation poles off the real $k$ axis. For the lossless medium one can consider small amount of loss to move the poles from the real axis or use Sommerfeld integration path instead of real line. Both approaches result in the same answer. Evaluating the spectral integral over $k_z$ results in

$$G(\overline{r},\overline{r}')=\frac{i}{2}\int\frac{\mathrm{d}\overline{k}_\perp}{(2\pi)^2}\frac{1}{k_z}e^{i\overline{k}_\perp\cdot(\overline{\rho}-\overline{\rho}')+ik_z|z-z'|} \tag{5.2.5}$$

This is a plane wave representation of the scalar Green's function. Inserting this representation into the periodic Green's function summation and rearranging terms yields,

$$G_p(\overline{r},\overline{r}')=\frac{i}{2}\int\frac{\mathrm{d}\overline{k}_\perp}{(2\pi)^2}\frac{1}{k_z}e^{i\overline{k}_\perp\cdot(\overline{\rho}-\overline{\rho}')+ik_z|z-z'|}\sum_{m,n}e^{i(k_{ix}-k_x)mL_x+i(k_{iy}-k_y)nL_y} \tag{5.2.6}$$

In order to evaluate summations in the periodic Green's function we use the Fourier series expansion of the impulse train. For impulse train of period $L$ given by $p(x)=\sum_n\delta(x-nL)$, all of the Fourier components are equal to $1/L$ and thus,

$$p(x)=\frac{1}{L}\sum_{n=-\infty}^{\infty}e^{i\frac{2n\pi}{L}x}=\sum_{n=-\infty}^{\infty}\delta(x-nL) \tag{5.2.7}$$

By changing $L$ to $2\pi/L$ in this expression, the summation over $m,n$ can be written as

$$\sum_{m,n} e^{i(k_{ix}-k_x)mL_x+i(k_{iy}-k_y)nL_y} = \frac{(2\pi)^2}{L_xL_y} \sum_{n=-\infty}^{\infty} \delta\left(k_x - k_{ix} - \frac{2n\pi}{L_x}\right) \sum_{m=-\infty}^{\infty} \delta\left(k_y - k_{iy} - \frac{2m\pi}{L_y}\right) \tag{5.2.8}$$

Therefore, the periodic Green's function expression simplifies to

$$G_p(\overline{r},\overline{r}') = \frac{i}{2L_xL_y} \sum_{m,n} \frac{1}{k_z^{mn}} e^{i\overline{k}_\perp^{mn}\cdot(\overline{\rho}-\overline{\rho}')+ik_z^{mn}|z-z'|} \tag{5.2.9}$$

where

$$\overline{k}_\perp^{mn} = \left(k_{ix} + \frac{2m\pi}{L_x}\right)\hat{x} + \left(k_{iy} + \frac{2n\pi}{L_y}\right)\hat{y} \tag{5.2.10}$$

is the transverse wave vector of the $mn$-th Bloch modes and $\left(k_z^{mn}\right)^2 = k_0^2 - \left(k_\perp^{mn}\right)^2$. Note that the Bloch wave numbers $\overline{k}^{mn}$ are only dependent of the lattice period and the incident excitation wave vector.

## 5.3 Periodic Dyadic Green's function

Since the relation of the free space and periodic Green's function (5.2.1)is linear, the periodic dyadic Green's function $\overline{\overline{G}}_p(\overline{r},\overline{r}')$ can be obtained from

$$\overline{\overline{G}}_p(\overline{r},\overline{r}') = \left[\overline{\overline{I}} + \frac{\nabla\nabla}{k_0^2}\right] G_p(\overline{r},\overline{r}') \tag{5.3.1}$$

However, periodic scalar Green's function is written in terms of the upward and downward going plane waves (Bloch modes) which are eigen-functions of $\nabla$ operator.

$$G_p(\overline{r},\overline{r}') = \frac{i}{2L_xL_y} \sum_{m,n} \frac{1}{k_z^{mn}} \begin{cases} e^{i\overline{k}_+^{mn}\cdot(\overline{r}-\overline{r}')} & ,z>z' \\ \\ e^{i\overline{k}_-^{mn}\cdot(\overline{r}-\overline{r}')} & ,z<z' \end{cases} \tag{5.3.2}$$

where $\overline{k}_\pm^{mn} = \overline{k}_\perp^{mn} \pm k_z^{mn}\hat{z}$ and $\overline{k}_\perp^{mn}$ is the transverse Bloch wave number. Then, expression of the dyadic Green's function can be obtained as

$$\overline{\overline{G}}_p(\overline{r},\overline{r}') = \frac{i}{2L_xL_y} \sum_{m,n} \frac{1}{k_z^{mn}} \begin{cases} \left[\overline{\overline{I}} - \frac{\overline{k}_+^{mn}\overline{k}_+^{mn}}{k_0^2}\right] e^{i\overline{k}_+^{mn}\cdot(\overline{r}-\overline{r}')} & ,z>z' \\ \\ \left[\overline{\overline{I}} - \frac{\overline{k}_-^{mn}\overline{k}_-^{mn}}{k_0^2}\right] e^{i\overline{k}_-^{mn}\cdot(\overline{r}-\overline{r}')} & ,z<z' \end{cases} \tag{5.3.3}$$

For each upward and downward Floquet mode we can define an orthonormal coordinate system in the spectral space through,

$$\begin{aligned} \hat{e}_\pm^{mn} &= \frac{\overline{k}_\pm^{mn}\times\hat{z}}{|\overline{k}_\pm^{mn}\times\hat{z}|} = \frac{1}{k_\perp^{mn}}\left(k_y^n\hat{x} - k_x^m\hat{y}\right) \\ \hat{h}_\pm^{mn} &= \hat{e}_\pm^{mn}\times\hat{k}_\pm^{mn} = \mp\frac{k_z^{mn}}{kk_\perp^{mn}}\left(k_x^m\hat{x} + k_y^n\hat{y}\right) + \frac{k_\perp^{mn}}{k}\hat{z} \end{aligned} \tag{5.3.4}$$

Therefore triplet of $(\hat{h}_{\pm}^{mn},\hat{e}_{\pm}^{mn},\hat{k}_{\pm}^{mn})$ form a right handed system for each mode. Using this coordinate unit vectors we can write the periodic dyadic Green's function as

$$\overline{\overline{G}}_p(\overline{r},\overline{r}')=\frac{i}{2L_xL_y}\sum_{m,n}\frac{1}{k_z^{mn}}\begin{cases}\left[\hat{e}_+^{mn}\hat{e}_+^{mn}+\hat{h}_+^{mn}\hat{h}_+^{mn}\right]e^{i\overline{k}_+^{mn}\cdot(\overline{r}-\overline{r}')} & ,z>z'\\ \left[\hat{e}_-^{mn}\hat{e}_-^{mn}+\hat{h}_-^{mn}\hat{h}_-^{mn}\right]e^{i\overline{k}_-^{mn}\cdot(\overline{r}-\overline{r}')} & ,z<z'\end{cases} \tag{5.3.5}$$

## 5.4 Electric Field Integral Equation

### 5.4.1 Extinction of the Incident Field

Governing equation of the surface electric and magnetic fields over boundary of a homogeneous medium for arbitrary boundary surface $f_1(x,y)$ can be obtained from the Extinction theorem as

$$\overline{E}_{inc}(\overline{r})+\int_S \mathrm{d}S'\left\{ik_1\eta_1\overline{\overline{G}}_1(\overline{r},\overline{r}')\cdot\left[\hat{n}_1\times\overline{H}_1(\overline{r}')\right]+\nabla\times\overline{\overline{G}}_1(\overline{r},\overline{r}')\cdot\left[\hat{n}_1\times\overline{E}_1(\overline{r}')\right]\right\}=\begin{cases}0 & z<f_1\\ \overline{E}_1(\overline{r}) & z>f_1\end{cases}$$

Here, $\overline{E}_1(\overline{r})$ is the electric field in the region 1 (topmost medium), $\hat{n}_1$ is the local upward normal to the surface, and $k_1$ is the wavenumber in region 1. The surface integral is over the infinite surface $S$, while for a periodic surface, according to the Bloch theorem, surface fields have the same periodicity as the structure except the progressive phase shift related to the incident field. Now, the surface $S$ can be treated as an array of surfaces with dimension $L_x\times L_y$ and add their responses. This is exactly done by introducing the periodic Green's function into the picture. Using the periodic dyadic Green's function of region 1, $\overline{\overline{G}}_{1p}(\overline{r},\overline{r}')$, we can condensate the spatial integral over the infinite surface into a single cell

$$\int_{S_j}\mathrm{d}S'\overline{\overline{G}}_j(\overline{r};\overline{r}')[\cdot]=\int_{\mathrm{cell}}\mathrm{d}S'\overline{\overline{G}}_{jp}(\overline{r};\overline{r}')[\cdot] \tag{5.4.1}$$

The periodic Green's function includes the contributions of all radiators (scatterers) at different lattice sites.

$$\overline{E}_{inc}+\int_{\mathrm{cell}}\mathrm{d}S'\left\{ik_1\eta_1\overline{\overline{G}}_{1p}(\overline{r},\overline{r}')\cdot\left[\hat{n}_1\times\overline{H}_1(\overline{r}')\right]+\nabla\times\overline{\overline{G}}_{1p}(\overline{r},\overline{r}')\cdot\left[\hat{n}_1\times\overline{E}_1(\overline{r}')\right]\right\}=\begin{cases}0 & z<f_1\\ \overline{E}_1(\overline{r}) & z>f_1\end{cases} \tag{5.4.2}$$

Now, the observation point will be considered to be completely below the interface $z'=f_1(x',y')$ such for all of the points on the surface $z<z'$. This boundary that in not the actual boundary of the scatterer is known as the *Extended Boundary*. Upon defining the normalized surface fields $\overline{a}_1(\overline{r})$ and $\overline{b}_1(\overline{r})$ on the boundary surface to absorb the unit normal and surface measure on the boundary as

$$\begin{aligned}\mathrm{d}S\ \hat{n}_1\times\eta_1\overline{H}_1(\overline{r})&=\overline{a}_1(\overline{r})\mathrm{d}^2\overline{r}\\ \mathrm{d}S\ \hat{n}_1\times\overline{E}_1(\overline{r})&=\overline{b}_1(\overline{r})\mathrm{d}^2\overline{r}\end{aligned} \tag{5.4.3}$$

the extinction relation of the incident electric field will be obtained as

$$\overline{E}_{inc}(\overline{r})+\int_{\mathrm{cell}}\mathrm{d}^2\overline{r}'\left\{ik_1\overline{\overline{G}}_{1p}^{<}(\overline{r},\overline{r}')\cdot\overline{a}_1(\overline{r}')+\nabla\times\overline{\overline{G}}_{1p}^{<}(\overline{r},\overline{r}')\cdot\overline{b}_1(\overline{r}')\right\}=0\quad ,z<\min\ f_1(x,y) \tag{5.4.4}$$

where $\overline{\overline{G}}^{<}_{1p}(\overline{r},\overline{r}')$ is designated for periodic Green's function of region 1 when $z<z'$. For the plane wave expansion of the dyadic Green's function under the condition $z<\min f_1(x,y)$ we have

$$\overline{\overline{G}}^{<}_{1p}(\overline{r},\overline{r}')=\frac{i}{2L_xL_y}\sum_{m,n}\frac{1}{k_{1z}^{mn}}\left[\hat{e}_{1-}^{mn}\hat{e}_{1-}^{mn}+\hat{h}_{1-}^{mn}\hat{h}_{1-}^{mn}\right]e^{i\overline{k}_{1-}^{mn}\cdot(\overline{r}-\overline{r}')} \tag{5.4.5}$$

$$\nabla\times\overline{\overline{G}}^{<}_{1p}(\overline{r},\overline{r}')=-\frac{k_1}{2L_xL_y}\sum_{m,n}\frac{1}{k_{1z}^{mn}}\left[\hat{e}_{1-}^{mn}\hat{h}_{1-}^{mn}-\hat{h}_{1-}^{mn}\hat{e}_{1-}^{mn}\right]e^{i\overline{k}_{1-}^{mn}\cdot(\overline{r}-\overline{r}')}$$

Notice that by choosing the observation point somewhere that satisfies $z<\min f_1(x,y)$, the spectral expansion of the Green's function in terms of only downward propagating waves is possible. By this assumption we are neglecting propagation of the upward going waves in the extinction relation of (5.3.5). This assumption fails if the surface shape is such that allows for backward waves. Generally, if the slope of the surface is below an upper bound then, neglecting backward waves does not introduce any problem. However, if the surface has a large slope that allows presence of backward waves toward the surface, then it creates problems in determining surface fields as the surface fields cannot satisfy the proper boundary conditions. This assumption is known as *Extended Boundary Condition Method* which is essentially the same as the *Rayleigh Hypothesis* where later assumes the scattered field to be a superposition of only upward propagating waves. Substituting the periodic Green's function in the extinction equation of the incident field yields

$$\begin{aligned}\overline{E}_{inc}(\overline{r})-\frac{k_1}{2L_xL_y}\sum_{m,n}\frac{1}{k_{1z}^{mn}}\left[\hat{e}_{1-}^{mn}\hat{e}_{1-}^{mn}+\hat{h}_{1-}^{mn}\hat{h}_{1-}^{mn}\right]\cdot\int_{\text{cell}}\mathrm{d}^2\overline{r}'e^{i\overline{k}_{1-}^{mn}\cdot(\overline{r}-\overline{r}')}\overline{a}_1(\overline{r}') \\ -\frac{k_1}{2L_xL_y}\sum_{m,n}\frac{1}{k_{1z}^{mn}}\left[\hat{e}_{1-}^{mn}\hat{h}_{1-}^{mn}-\hat{h}_{1-}^{mn}\hat{e}_{1-}^{mn}\right]\cdot\int_{\text{cell}}\mathrm{d}^2\overline{r}'e^{i\overline{k}_{1-}^{mn}\cdot(\overline{r}-\overline{r}')}\overline{b}_1(\overline{r}')=\overline{0}\end{aligned} \tag{5.4.6}$$

This is the same as the extinction relation for an infinitely large surface that is obtained in Chap. 3. The transition from a system with a continuous spectrum to the corresponding discrete system with periodic boundary conditions can also be done using the general transformation between the discrete and continuous counterparts [87, 88]

$$\int\frac{\mathrm{d}^2k}{(2\pi)^2}[\cdot]\rightleftarrows\frac{1}{L_xL_y}\sum_{m,n}[\cdot] \tag{5.4.7}$$

Using this transformation, we can write the periodic dyadic Green's function directly from dyadic Green's function for non-periodic case. The summations in (5.4.6) can be written as a linear combination of downward going Bloch modes in region 1

$$\overline{E}_{inc}(\overline{r})+\sum_{m,n}\overline{D}_{mn}^{1,1}e^{i\overline{k}_{1-}^{mn}\cdot\overline{r}}=\overline{0} \tag{5.4.8}$$

where the amplitude of modes is given by,

$$\begin{aligned}\overline{D}_{mn}^{1,1}=-\frac{k_1}{2L_xL_y}\frac{1}{k_{1z}^{mn}}\Bigg\{&\left[\hat{e}_{1-}^{mn}\hat{e}_{1-}^{mn}+\hat{h}_{1-}^{mn}\hat{h}_{1-}^{mn}\right]\cdot\int_{\text{cell}}\mathrm{d}^2\overline{r}'e^{-i\overline{k}_{\perp}^{mn}\cdot\overline{r}'_{\perp}+ik_{1z}^{mn}f_1(\overline{r}'_{\perp})}\overline{a}_1(\overline{r}') \\ &+\left[\hat{e}_{1-}^{mn}\hat{h}_{1-}^{mn}-\hat{h}_{1-}^{mn}\hat{e}_{1-}^{mn}\right]\cdot\int_{\text{cell}}\mathrm{d}^2\overline{r}'e^{-i\overline{k}_{\perp}^{mn}\cdot\overline{r}'_{\perp}+ik_{1z}^{mn}f_1(\overline{r}'_{\perp})}\overline{b}_1(\overline{r}')\Bigg\}\end{aligned} \tag{5.4.9}$$

For an incident downward propagating plane wave of unit amplitude $\overline{E}_{inc}(\overline{r})=\hat{e}_ie^{i\overline{k}_i\cdot\overline{r}}$, it aligns with the direction of the zeroth order Bloch mode $(m,n)=(0,0)$. Considering orthogonality of the Bloch modes, $\overline{D}_{mn}^{1,1}=\overline{0}$ for all values of $m$, and $n$ except $\overline{D}_{00}^{1,1}=-\hat{e}_i$.

### 5.4.2 Extinction of Field Propagating in Region $j$

The extinction of the wave that propagates in region $j$ mandates that the propagation of the surface currents on the boundary of region $j$ using region $j$ Green's function vanishes for observation points outside region $j$. Mathematically,

$$\begin{aligned}0=&-\oint_{\partial V_j}\mathrm{d}S'\left\{ik_j\eta_j\overline{\overline{G}}_j(\overline{r},\overline{r}')\cdot[\hat{n}'\times\overline{H}_j(\overline{r}')]+\nabla\times\overline{\overline{G}}_j(\overline{r}',\overline{r})\cdot[\hat{n}'\times\overline{E}_j(\overline{r}')]\right\} \\ =&-\int_{S_{j-1}}\mathrm{d}S'\left\{ik_j\eta_j\overline{\overline{G}}_j(\overline{r},\overline{r}')\cdot[\hat{n}'_{j-1}\times\overline{H}_j(\overline{r}')]+\nabla\times\overline{\overline{G}}_j(\overline{r}',\overline{r})\cdot[\hat{n}'_{j-1}\times\overline{E}_j(\overline{r}')]\right\} \\ &+\int_{S_j}\mathrm{d}S'\left\{ik_j\eta_j\overline{\overline{G}}_j(\overline{r},\overline{r}')\cdot[\hat{n}'_j\times\overline{H}_j(\overline{r}')]+\nabla\times\overline{\overline{G}}_j(\overline{r}',\overline{r})\cdot[\hat{n}'_j\times\overline{E}_j(\overline{r}')]\right\}\end{aligned} \tag{5.4.10}$$

For the upper boundary at $z=-d_{j-1}+f_{j-1}(\overline{r}_\perp)$, we can define surface fields based on region $j-1$ fields (surface fields are continuous across the boundary) as

$$\begin{aligned}\mathrm{d}S'\hat{n}'_j\times\eta_{j-1}\overline{H}_j(\overline{r}')=\mathrm{d}S'\eta_{j-1}\hat{n}'_{j-1}\times\overline{H}_{j-1}(\overline{r}')=\mathrm{d}^2\overline{r}'_\perp\,\overline{a}_{j-1}(\overline{r}'_\perp) \\ \mathrm{d}S'\hat{n}'_j\times\overline{E}_j(\overline{r}')=\mathrm{d}S'\hat{n}'_{j-1}\times\overline{E}_{j-1}(\overline{r}')=\mathrm{d}^2\overline{r}'_\perp\,\overline{b}_{j-1}(\overline{r}'_\perp)\end{aligned} \tag{5.4.11}$$

and for second boundary $z=-d_j+f_j(\overline{r}_\perp)$ we use fields of region $j$ to define surface fields,

$$\begin{aligned}\mathrm{d}S'\hat{n}'_j\times\eta_j\overline{H}_j(\overline{r}')=\mathrm{d}^2\overline{r}'_\perp\,\overline{a}_j(\overline{r}'_\perp) \\ \mathrm{d}S'\hat{n}'_j\times\overline{E}_j(\overline{r}')=\mathrm{d}^2\overline{r}'_\perp\,\overline{b}_j(\overline{r}'_\perp)\end{aligned} \tag{5.4.12}$$

Note that normal vectors for upper and lower boundaries are different functions of position but we have absorbed their difference in unknown surface fields. For a Non-magnetic material case $k\eta=k_j\eta_j=k_{j-1}\eta_{j-1}=\omega\mu$, such that the surface field integral equation with observation point outside the region $j$ becomes,

$$\begin{aligned}0=&-\int_{z=-d_{j-1}+f_{j-1}(\overline{r}_\perp)}\mathrm{d}\overline{r}'_\perp\left\{ik_{j-1}\overline{\overline{G}}_j(\overline{r},\overline{r}')\cdot\overline{a}_{j-1}(\overline{r}'_\perp)]+\nabla\times\overline{\overline{G}}_j(\overline{r}',\overline{r})\cdot\overline{b}_{j-1}(\overline{r}'_\perp)\right\} \\ &+\int_{z=-d_j+f_j(\overline{r}_\perp)}\mathrm{d}\overline{r}'_\perp\left\{ik_j\overline{\overline{G}}_j(\overline{r},\overline{r}')\cdot\overline{a}_j(\overline{r}'_\perp)+\nabla\times\overline{\overline{G}}_j(\overline{r}',\overline{r})\cdot\overline{b}_j(\overline{r}'_\perp)\right\}\end{aligned} \tag{5.4.13}$$

Assuming the observation point is placed in the upper regions, and more over, over the extended boundary of $z=\max f_{j-1}$, in this case always $z>z'$ and we can expand dyadic periodic Green's function of region $j$ as

$$\begin{aligned}\overline{\overline{G}}^{>}_{jp}(\overline{r},\overline{r}')=&\frac{i}{2L_xL_y}\sum_{m,n}\frac{1}{k^{mn}_{jz}}\left[\hat{e}^{mn}_{j+}\hat{e}^{mn}_{j+}+\hat{h}^{mn}_{j+}\hat{h}^{mn}_{j+}\right]e^{i\overline{k}^{mn}_{j+}\cdot(\overline{r}-\overline{r}')} \\ \nabla\times\overline{\overline{G}}^{>}_{jp}(\overline{r},\overline{r}')=&-\frac{k_j}{2L_xL_y}\sum_{m,n}\frac{1}{k^{mn}_{jz}}\left[\hat{e}^{mn}_{j+}\hat{h}^{mn}_{j+}-\hat{h}^{mn}_{j+}\hat{e}^{mn}_{j+}\right]e^{i\overline{k}^{mn}_{j+}\cdot(\overline{r}-\overline{r}')}\end{aligned} \tag{5.4.14}$$

and noting that the spatial integrals are over a single cell, in accordance with introducing the periodic Green's function, we arrive at the following relation between the surface fields over the adjacent boundaries $j$ and $j-1$

$$\sum_{mn}\overline{U}^{j,j-1}_{mn}e^{i\overline{k}^{mn}_{j+}\cdot\overline{r}}=\overline{U}^{j,j}_{mn}e^{i\overline{k}^{mn}_{j+}\cdot\overline{r}} \tag{5.4.15}$$

where the amplitude of the upward propagating Bloch modes propagating in region $j$ and originated from the $j-1$ and $j$-th boundaries are given by

$$\overline{U}_{mn}^{j,j-1}=\frac{1}{k_{jz}^{mn}}e^{ik_{jz}^{mn}d_{j-1}}\Bigg\{\frac{k_{j-1}}{k_j}\left[\hat{e}_{j+}^{mn}\hat{e}_{j+}^{mn}+\hat{h}_{j+}^{mn}\hat{h}_{j+}^{mn}\right]\cdot\int_{\text{cell}}\mathrm{d}^2\overline{r}'e^{-i\overline{k}_{\perp}^{mn}\cdot\overline{r}'_{\perp}-ik_{jz}^{mn}f_{j-1}(\overline{r}'_{\perp})}\overline{a}_{j-1}(\overline{r}'_{\perp})$$
$$+\left[\hat{e}_{j+}^{mn}\hat{h}_{j+}^{mn}-\hat{h}_{j+}^{mn}\hat{e}_{j+}^{mn}\right]\cdot\int_{\text{cell}}\mathrm{d}^2\overline{r}'e^{-i\overline{k}_{\perp}^{mn}\cdot\overline{r}'_{\perp}-ik_{jz}^{mn}f_{j-1}(\overline{r}'_{\perp})}\overline{b}_{j-1}(\overline{r}'_{\perp})\Bigg\},$$
$$\overline{U}_{mn}^{j,j}=\frac{1}{k_{jz}^{mn}}e^{ik_{jz}^{mn}d_{j}}\Bigg\{\left[\hat{e}_{j+}^{mn}\hat{e}_{j+}^{mn}+\hat{h}_{j+}^{mn}\hat{h}_{j+}^{mn}\right]\cdot\int_{\text{cell}}\mathrm{d}^2\overline{r}'e^{-i\overline{k}_{\perp}^{mn}\cdot\overline{r}'_{\perp}-ik_{jz}^{mn}f_{j}(\overline{r}'_{\perp})}\overline{a}_{j}(\overline{r}'_{\perp})$$
$$+\left[\hat{e}_{j+}^{mn}\hat{h}_{j+}^{mn}-\hat{h}_{j+}^{mn}\hat{e}_{j+}^{mn}\right]\cdot\int_{\text{cell}}\mathrm{d}^2\overline{r}'e^{-i\overline{k}_{\perp}^{mn}\cdot\overline{r}'_{\perp}-ik_{jz}^{mn}f_{j}(\overline{r}'_{\perp})}\overline{b}_{j}(\overline{r}'_{\perp})\Bigg\}$$

and also from orthogonality of spatial harmonics

$$\overline{U}_{mn}^{j,j-1}=\overline{U}_{mn}^{j,j} \tag{5.4.16}$$

Similarly, we can obtain another independent integral equation for extinction of the downward propagating wave in region $j$. Placing the observation point on the extended boundary of

$$z=\min_{\overline{r}_{\perp}}\Big\{-d_j+f_j(\overline{r}_{\perp})\Big\} \tag{5.4.17}$$

ensures that always $z<z'$ an the dyadic periodic Green's function of region $j$ can be expanded in terms of only downward propagating plane waves as

$$\overline{\overline{G}}_{jp}^{<}(\overline{r},\overline{r}')=\frac{i}{2L_xL_y}\sum_{m,n}\frac{1}{k_{jz}^{mn}}\left[\hat{e}_{j-}^{mn}\hat{e}_{j-}^{mn}+\hat{h}_{j-}^{mn}\hat{h}_{j-}^{mn}\right]e^{i\overline{k}_{j-}^{mn}\cdot(\overline{r}-\overline{r}')} \tag{5.4.18}$$
$$\nabla\times\overline{\overline{G}}_{jp}^{<}(\overline{r},\overline{r}')=-\frac{k_j}{2L_xL_y}\sum_{m,n}\frac{1}{k_{jz}^{mn}}\left[\hat{e}_{j-}^{mn}\hat{h}_{j-}^{mn}-\hat{h}_{j-}^{mn}\hat{e}_{j-}^{mn}\right]e^{i\overline{k}_{j-}^{mn}\cdot(\overline{r}-\overline{r}')}$$

By inserting spectral expansion of (5.4.18) into extinction relation of (5.4.13), it can be written as a relation between the downward propagating waves in region $j$ that are originated from $j-1$ and $j$-th surface boundary, as

$$\sum_{m,n}\overline{D}_{mn}^{j,j-1}e^{i\overline{k}_{j-}^{mn}\cdot\overline{r}}=\sum_{m,n}\overline{D}_{mn}^{j,j}e^{i\overline{k}_{j-}^{mn}\cdot\overline{r}} \tag{5.4.19}$$

where the amplitude of the Bloch modes are given by

$$\overline{D}_{mn}^{j,j-1}=\frac{1}{k_{jz}^{mn}}e^{-ik_{jz}^{mn}d_{j-1}}\Bigg\{\frac{k_{j-1}}{k_j}\left[\hat{e}_{j-}^{mn}\hat{e}_{j-}^{mn}+\hat{h}_{j-}^{mn}\hat{h}_{j-}^{mn}\right]\cdot\int_{\text{cell}}\mathrm{d}^2\overline{r}'e^{-i\overline{k}_{\perp}^{mn}\cdot\overline{r}'_{\perp}+ik_{jz}^{mn}f_{j-1}(\overline{r}'_{\perp})}\overline{a}_{j-1}(\overline{r}'_{\perp}) \tag{5.4.20}$$
$$+\left[\hat{e}_{j-}^{mn}\hat{h}_{j-}^{mn}-\hat{h}_{j-}^{mn}\hat{e}_{j-}^{mn}\right]\cdot\int_{\text{cell}}\mathrm{d}^2\overline{r}'e^{-i\overline{k}_{\perp}^{mn}\cdot\overline{r}'_{\perp}+ik_{jz}^{mn}f_{j-1}(\overline{r}'_{\perp})}\overline{b}_{j-1}(\overline{r}'_{\perp})\Bigg\}$$
$$\overline{D}_{mn}^{j,j}=\frac{1}{k_{jz}^{mn}}e^{-ik_{jz}^{mn}d_{j}}\Bigg\{\left[\hat{e}_{j-}^{mn}\hat{e}_{j-}^{mn}+\hat{h}_{j-}^{mn}\hat{h}_{j-}^{mn}\right]\cdot\int_{\text{cell}}\mathrm{d}^2\overline{r}'e^{-i\overline{k}_{\perp}^{mn}\cdot\overline{r}'_{\perp}+ik_{jz}^{mn}f_{j}(\overline{r}'_{\perp})}\overline{a}_{j}(\overline{r}'_{\perp})$$
$$+\left[\hat{e}_{j-}^{mn}\hat{h}_{j-}^{mn}-\hat{h}_{j-}^{mn}\hat{e}_{j-}^{mn}\right]\cdot\int_{\text{cell}}\mathrm{d}^2\overline{r}'e^{-i\overline{k}_{\perp}^{mn}\cdot\overline{r}'_{\perp}+ik_{jz}^{mn}f_{j}(\overline{r}'_{\perp})}\overline{b}_{j}(\overline{r}'_{\perp})\Bigg\}$$

Note that the spatial integrals are performed over the primitive cell in accordance with introduction of the periodic Green's function. From the orthogonality of spatial harmonics over a cell, (5.4.19) yields the following propagation relation between adjacent surface fields

$$\overline{D}_{mn}^{j,j-1}=\overline{D}_{mn}^{j,j}. \tag{5.4.21}$$

### 5.4.3 Extinction of Field Propagating in Region $j$

Similarly, application of the extinction theorem to region $N$ results in

$$-\int_S \mathrm{d}S'\Big\{ik_N\eta_N\overline{\overline{G}}_N(\overline{r},\overline{r}')\cdot[\hat{n}'_N\times\overline{H}_N(\overline{r}')] \tag{5.4.22}$$
$$+\nabla\times\overline{\overline{G}}_N(\overline{r}',\overline{r})\cdot[\hat{n}'_N\times\overline{E}_N(\overline{r}')]\Big\}=\begin{cases}0 & z>-d_{N-1}+f_{N-1}(\overline{r}_\perp)\\ \overline{E}_N(\overline{r}) & z<-d_{N-1}+f_{N-1}(\overline{r}_\perp)\end{cases}$$

where $\overline{E}_N$ and $\overline{H}_N$ are electric and magnetic fields in region $N$ and $\overline{\overline{G}}_N$ is the free space dyadic Green's function with the wave number $k_N=\omega\sqrt{\mu_N\varepsilon_N}$. Utilizing continuity of the surface electric and magnetic fields over the boundary, we can substitute fields in region $N$ with those of region $N-1$. For non-magnetic materials $k_{N-1}\eta_{N-1}=k_N\eta_N$ and

$$\begin{aligned}k_N\overline{a}_N(\overline{r})&=k_{N-1}\overline{a}_{N-1}(\overline{r})\\ \overline{b}_N(\overline{r})&=\overline{b}_{N-1}(\overline{r})\end{aligned} \tag{5.4.23}$$

Following the same procedure and replacing the Green's function with periodic Green's function and putting the observation point in region $N-1$, we have

$$\int_{\text{cell}}\mathrm{d}^2\overline{r}'\Big\{ik_{N-1}\overline{\overline{G}}^{>}_{N-1,p}(\overline{r},\overline{r}')\cdot\overline{a}_{N-1}(\overline{r}')+\nabla\times\overline{\overline{G}}^{>}_{N-1,p}(\overline{r}',\overline{r})\cdot\overline{b}_{N-1}(\overline{r}')\Big\}=\overline{0} \tag{5.4.24}$$

Here,

$$\overline{\overline{G}}^{>}_{Np}(\overline{r},\overline{r}')=\frac{i}{2L_xL_y}\sum_{m,n}\frac{1}{k_{Nz}^{mn}}\left[\hat{e}_{N+}^{mn}\hat{e}_{N+}^{mn}+\hat{h}_{N+}^{mn}\hat{h}_{N+}^{mn}\right]e^{i\overline{k}_{N+}^{mn}\cdot(\overline{r}-\overline{r}')} \tag{5.4.25}$$
$$\nabla\times\overline{\overline{G}}^{>}_{Np}(\overline{r},\overline{r}')=-\frac{k_N}{2L_xL_y}\sum_{m,n}\frac{1}{k_{Nz}^{mn}}\left[\hat{e}_{N+}^{mn}\hat{h}_{N+}^{mn}-\hat{h}_{N+}^{mn}\hat{e}_{N+}^{mn}\right]e^{i\overline{k}_{N+}^{mn}\cdot(\overline{r}-\overline{r}')}$$

Notice that (5.4.24) is an exact integral equation for the surface fields. However, to be able to use the unidirectional plane wave expansions of the dyadic Green's function, the observation point should be placed on the extended boundary rather than the boundary itself. Substituting the periodic Green's function expressions in the extinction relation we arrive at the mode expansion in terms of the upward propagating modes in region $N$

$$\sum_{m,n}\overline{U}_{mn}^{N,N-1}e^{i\overline{k}_{N+}^{mn}\cdot\overline{r}}=\overline{0} \tag{5.4.26}$$

where the vector amplitude $\overline{U}_{mn}^{N}$ is given by

$$\overline{U}_{mn}^{N,N-1}=\frac{k_{N-1}}{k_N}\left[\hat{e}_{N+}^{mn}\hat{e}_{N+}^{mn}+\hat{h}_{N+}^{mn}\hat{h}_{N+}^{mn}\right]\cdot\int_{\text{cell}}\mathrm{d}^2\overline{r}'e^{-i\overline{k}_\perp^{mn}\cdot\overline{r}'_\perp-ik_{Nz}^{mn}f_{N-1}(\overline{r}'_\perp)}\overline{a}_{N-1}(\overline{r}') \tag{5.4.27}$$
$$+\left[\hat{e}_{N+}^{mn}\hat{h}_{N+}^{mn}-\hat{h}_{N+}^{mn}\hat{e}_{N+}^{mn}\right]\cdot\int_{\text{cell}}\mathrm{d}^2\overline{r}'e^{-i\overline{k}_\perp^{mn}\cdot\overline{r}'_\perp-ik_{Nz}^{mn}f_{N-1}(\overline{r}'_\perp)}\overline{b}_{N-1}(\overline{r}')$$

## 5.5 Surface Fields Solution

Recalling that the surface fields exist over the boundary surfaces i.e. $\hat{n}_j \cdot \overline{a}_j(\overline{r}_\perp) = \hat{n}_j \cdot \overline{b}_j(\overline{r}_\perp) = 0$ we have $a_{jz}(\overline{r}_\perp) = \nabla_\perp f_j \cdot \overline{a}_{j\perp}(\overline{r}_\perp)$ and therefore surface fields can be written in terms of its transverse component as

$$\overline{a}_j(\overline{r}_\perp) = \overline{a}_{j\perp}(\overline{r}_\perp) + \nabla_\perp f_j \cdot \overline{a}_{j\perp}(\overline{r}_\perp)\hat{z} \tag{5.5.1}$$

Now the vector unknowns contains two scalar variables. In order to convert the system of integral equations to a solvable system of equation, we use the reciprocal lattice vectors of the surface to expand vector surface fields which have the same periodicity as

$$\begin{aligned}
\overline{a}_{j\perp}(\overline{r}) &= \sum_{pq} \overline{\alpha}^j_{pq} e^{i\overline{k}^{pq}_\perp \cdot \overline{r}_\perp} = \sum_{pq} \overline{\alpha}^j_{pq} e^{i(k^p_x x + k^q_y y)} \\
\overline{b}_{j\perp}(\overline{r}) &= \sum_{pq} \overline{\beta}^j_{pq} e^{i\overline{k}^{pq}_\perp \cdot \overline{r}_\perp} = \sum_{pq} \overline{\beta}^j_{pq} e^{i(k^p_x x + k^q_y y)}
\end{aligned} \tag{5.5.2}$$

The Fourier series expansion of the transverse surface fields is based on the periodicity of the field quantities with the same period as the surface which is justified by the Bloch theorem. Inserting the transverse part of the surface fields into the complete expression of the surface fields (5.4.24) yields,

$$\begin{aligned}
\overline{a}_j(\overline{r}_\perp) &= \sum_{pq} \left[\overline{\alpha}^j_{pq} + \nabla_\perp f_j \cdot \overline{\alpha}^j_{pq}\hat{z}\right] e^{i\overline{k}^{pq}_\perp \cdot \overline{r}_\perp} \\
\overline{b}_j(\overline{r}_\perp) &= \sum_{pq} \left[\overline{\beta}^j_{pq} + \nabla_\perp f_j \cdot \overline{\beta}^j_{pq}\hat{z}\right] e^{i\overline{k}^{pq}_\perp \cdot \overline{r}_\perp}
\end{aligned} \tag{5.5.3}$$

Substituting the surface field expression in extinction relations in terms of the vector coefficients $\overline{D}_{mn}$ and $\overline{U}_{mn}$, results in

$$\begin{aligned}
\overline{D}^{1,1}_{mn} = &-\frac{k_1}{2L_xL_y}\frac{1}{k^{mn}_{1z}} \sum_{pq} \Bigg\{ \left[\hat{e}^{mn}_{1-}\hat{e}^{mn}_{1-} + \hat{h}^{mn}_{1-}\hat{h}^{mn}_{1-}\right] \cdot \left[\overline{\alpha}^1_{pq} - \frac{1}{k^{mn}_{1z}}(\overline{k}^{pq}_\perp - \overline{k}^{mn}_\perp)\cdot\overline{\alpha}^1_{pq}\hat{z}\right] \\
&+ \left[\hat{e}^{mn}_{1-}\hat{h}^{mn}_{1-} - \hat{h}^{mn}_{1-}\hat{e}^{mn}_{1-}\right] \cdot \left[\overline{\beta}^1_{pq} - \frac{1}{k^{mn}_{1z}}(\overline{k}^{pq}_\perp - \overline{k}^{mn}_\perp)\cdot\overline{\beta}^1_{pq}\hat{z}\right] \Bigg\} I^{pq-}_{mn}[1,1]
\end{aligned} \tag{5.5.4}$$

$$\begin{aligned}
\overline{U}^{j,j-1}_{mn} = &\frac{1}{k^{mn}_{jz}} e^{ik^{mn}_{jz} d_{m-1}} \sum_{pq} \Bigg\{ \frac{k_{j-1}}{k_j} \left[\hat{e}^{mn}_{j+}\hat{e}^{mn}_{j+} + \hat{h}^{mn}_{j+}\hat{h}^{mn}_{j+}\right] \cdot \left[\overline{\alpha}^{j-1}_{pq} + \frac{1}{k^{mn}_{jz}}(\overline{k}^{pq}_\perp - \overline{k}^{mn}_\perp)\cdot\overline{\alpha}^{j-1}_{pq}\hat{z}\right] \\
&+ \left[\hat{e}^{mn}_{j+}\hat{h}^{mn}_{j+} - \hat{h}^{mn}_{j+}\hat{e}^{mn}_{j+}\right] \cdot \left[\overline{\beta}^{j-1}_{pq} + \frac{1}{k^{mn}_{jz}}(\overline{k}^{pq}_\perp - \overline{k}^{mn}_\perp)\cdot\overline{\beta}^{j-1}_{pq}\hat{z}\right] \Bigg\} I^{pq+}_{mn}[j,j-1]
\end{aligned}$$

$$\begin{aligned}
\overline{U}^{j,j}_{mn} = &\frac{1}{k^{mn}_{jz}} e^{ik^{mn}_{jz} d_m} \sum_{pq} \Bigg\{ \left[\hat{e}^{mn}_{j+}\hat{e}^{mn}_{j+} + \hat{h}^{mn}_{j+}\hat{h}^{mn}_{j+}\right] \cdot \left[\overline{\alpha}^j_{pq} + \frac{1}{k^{mn}_{jz}}(\overline{k}^{pq}_\perp - \overline{k}^{mn}_\perp)\cdot\overline{\alpha}^j_{pq}\hat{z}\right] \\
&+ \left[\hat{e}^{mn}_{j+}\hat{h}^{mn}_{j+} - \hat{h}^{mn}_{j+}\hat{e}^{mn}_{j+}\right] \cdot \left[\overline{\beta}^j_{pq} + \frac{1}{k^{mn}_{jz}}(\overline{k}^{pq}_\perp - \overline{k}^{mn}_\perp)\cdot\overline{\beta}^j_{pq}\hat{z}\right] \Bigg\} I^{pq+}_{mn}[j,j]
\end{aligned}$$

$$
\begin{aligned}
\overline{D}^{j,j-1}_{mn} &= \frac{1}{k^{mn}_{jz}} e^{-ik^{mn}_{jz} d_{m-1}} \sum_{pq} \Bigg\{ \frac{k_{j-1}}{k_j} \left[ \hat{e}^{mn}_{j-} \hat{e}^{mn}_{j-} + \hat{h}^{mn}_{j-} \hat{h}^{mn}_{j-} \right] \cdot \left[ \overline{\alpha}^{j-1}_{pq} - \frac{1}{k^{mn}_{jz}} (\overline{k}^{pq}_{\perp} - \overline{k}^{mn}_{\perp}) \cdot \overline{\alpha}^{j-1}_{pq} \hat{z} \right] \\
&\quad + \left[ \hat{e}^{mn}_{j-} \hat{h}^{mn}_{j-} - \hat{h}^{mn}_{j-} \hat{e}^{mn}_{j-} \right] \cdot \left[ \overline{\beta}^{j-1}_{pq} - \frac{1}{k^{mn}_{jz}} (\overline{k}^{pq}_{\perp} - \overline{k}^{mn}_{\perp}) \cdot \overline{\beta}^{j-1}_{pq} \hat{z} \right] \Bigg\} I^{pq-}_{mn}[j,j-1] \\
\overline{D}^{j,j}_{mn} &= \frac{1}{k^{mn}_{jz}} e^{-ik^{mn}_{jz} d_{m}} \sum_{pq} \Bigg\{ \left[ \hat{e}^{mn}_{j-} \hat{e}^{mn}_{j-} + \hat{h}^{mn}_{j-} \hat{h}^{mn}_{j-} \right] \cdot \left[ \overline{\alpha}^{j}_{pq} - \frac{1}{k^{mn}_{jz}} (\overline{k}^{pq}_{\perp} - \overline{k}^{mn}_{\perp}) \cdot \overline{\alpha}^{j}_{pq} \hat{z} \right] \\
&\quad + \left[ \hat{e}^{mn}_{j-} \hat{h}^{mn}_{j-} - \hat{h}^{mn}_{j-} \hat{e}^{mn}_{j-} \right] \cdot \left[ \overline{\beta}^{j}_{pq} - \frac{1}{k^{mn}_{jz}} (\overline{k}^{pq}_{\perp} - \overline{k}^{mn}_{\perp}) \cdot \overline{\beta}^{j}_{pq} \hat{z} \right] \Bigg\} I^{pq-}_{mn}[j,j] \\
\overline{U}^{N,N-1}_{mn} &= \sum_{pq} \Bigg\{ \frac{k_{N-1}}{k_N} \left[ \hat{e}^{mn}_{N+} \hat{e}^{mn}_{N+} + \hat{h}^{mn}_{N+} \hat{h}^{mn}_{N+} \right] \cdot \left[ \overline{\alpha}^{N-1}_{pq} + \frac{1}{k^{mn}_{Nz}} (\overline{k}^{pq}_{\perp} - \overline{k}^{mn}_{\perp}) \cdot \overline{\alpha}^{N-1}_{pq} \hat{z} \right] \\
&\quad + \left[ \hat{e}^{mn}_{N+} \hat{h}^{mn}_{N+} - \hat{h}^{mn}_{N+} \hat{e}^{mn}_{N+} \right] \cdot \left[ \overline{\beta}^{N-1}_{pq} + \frac{1}{k^{mn}_{Nz}} (\overline{k}^{pq}_{\perp} - \overline{k}^{mn}_{\perp}) \cdot \overline{\beta}^{N-1}_{pq} \hat{z} \right] \Bigg\} I^{pq+}_{mn}[N,N-1]
\end{aligned}
\tag{5.5.5}
$$

where, the gradient term from the $z$ component of the surface fields in the integrand is simplified using by part integration and taking advantage of periodic boundary condition. Also the integrals $I^{pq\pm}_{mn}[j,j-1]$ and $I^{pq\pm}_{mn}[j,j]$ which correspond to the scattering potential of the rough boundaries are defined as

$$
\begin{aligned}
I^{pq\pm}_{mn}[j,j-1] &= \int_{\text{cell}} \mathrm{d}^2 \overline{r}' e^{i(\overline{k}^{pq}_{\perp} - \overline{k}^{mn}_{\perp}) \cdot \overline{r}'_{\perp} \mp i k^{mn}_{jz} f_{j-1}(\overline{r}'_{\perp})} \\
I^{pq\pm}_{mn}[j,j] &= \int_{\text{cell}} \mathrm{d}^2 \overline{r}' e^{i(\overline{k}^{pq}_{\perp} - \overline{k}^{mn}_{\perp}) \cdot \overline{r}'_{\perp} \mp i k^{mn}_{jz} f_{j}(\overline{r}'_{\perp})}
\end{aligned}
\tag{5.5.6}
$$

The involved matrices in the above equations are not full rank (rank of 2 in 3 dimensional space) and therefore can not be inverted in this form. Upon projecting the Bloch coefficients on the corresponding unit polarization vectors, the scalar equations will be obtained. From the extinction relation of the middle layers $2 \leq j \leq N-1$ as $\overline{U}^{j,j-1}_{mn} = \overline{U}^{j,j}_{mn}$, and $\overline{D}^{j,j-1}_{mn} = \overline{D}^{j,j}_{mn}$ the following scalar equations for the transverse component of the surface fields are obtained as

$$
\begin{aligned}
&\sum_{pq} \left\{ \frac{k_{j-1}}{k_j} \hat{e}^{mn}_{j+} \cdot \overline{\alpha}^{j-1}_{pq} + \hat{h}^{mn}_{j+} \cdot \overline{\beta}^{j-1}_{pq} + \frac{1}{k^{mn}_{jz}} \frac{k^{mn}_{\perp}}{k_j} (\overline{k}^{pq}_{\perp} - \overline{k}^{mn}_{\perp}) \cdot \overline{\beta}^{j-1}_{pq} \right\} I^{pq+}_{mn}[j,j-1] \\
&= e^{ik^{mn}_{jz} \Delta_j} \sum_{pq} \left\{ \hat{e}^{mn}_{j+} \cdot \overline{\alpha}^{j}_{pq} + \hat{h}^{mn}_{j+} \cdot \overline{\beta}^{j}_{pq} + \frac{1}{k^{mn}_{jz}} \frac{k^{mn}_{\perp}}{k_j} (\overline{k}^{pq}_{\perp} - \overline{k}^{mn}_{\perp}) \cdot \overline{\beta}^{j}_{pq} \right\} I^{pq+}_{mn}[j,j]
\end{aligned}
$$

$$
\begin{aligned}
&\sum_{pq} \left\{ \frac{k_{j-1}}{k_j} \left( \hat{h}^{mn}_{j+} \cdot \overline{\alpha}^{j-1}_{pq} + \frac{1}{k^{mn}_{jz}} \frac{k^{mn}_{\perp}}{k_j} (\overline{k}^{pq}_{\perp} - \overline{k}^{mn}_{\perp}) \cdot \overline{\alpha}^{j-1}_{pq} \right) - \hat{e}^{mn}_{j+} \cdot \overline{\beta}^{j-1}_{pq} \right\} I^{pq+}_{mn}[j,j-1] \\
&\quad = e^{ik^{mn}_{jz} \Delta_j} \sum_{pq} \left\{ \hat{h}^{mn}_{j+} \cdot \overline{\alpha}^{j}_{pq} + \frac{1}{k^{mn}_{jz}} \frac{k^{mn}_{\perp}}{k_j} (\overline{k}^{pq}_{\perp} - \overline{k}^{mn}_{\perp}) \cdot \overline{\alpha}^{j}_{pq} - \hat{e}^{mn}_{j+} \cdot \overline{\beta}^{j}_{pq} \right\} I^{pq+}_{mn}[j,j]
\end{aligned}
$$

$$\sum_{pq}\left\{\frac{k_{j-1}}{k_j}\hat{e}_{j-}^{mn}\cdot\overline{\alpha}_{pq}^{j-1}+\hat{h}_{j-}^{mn}\cdot\overline{\beta}_{pq}^{j-1}-\frac{1}{k_{jz}^{mn}}\frac{k_{\perp}^{mn}}{k_j}(\overline{k}_{\perp}^{pq}-\overline{k}_{\perp}^{mn})\cdot\overline{\beta}_{pq}^{j-1}\right\}I_{mn}^{pq-}[j,j-1]$$
$$=e^{-ik_{jz}^{mn}\Delta_j}\sum_{pq}\left\{\hat{e}_{j-}^{mn}\cdot\overline{\alpha}_{pq}^{j}+\hat{h}_{j-}^{mn}\cdot\overline{\beta}_{pq}^{j}-\frac{1}{k_{jz}^{mn}}\frac{k_{\perp}^{mn}}{k_j}(\overline{k}_{\perp}^{pq}-\overline{k}_{\perp}^{mn})\cdot\overline{\beta}_{pq}^{j}\right\}I_{mn}^{pq-}[j,j]$$

$$\sum_{pq}\left\{\frac{k_{j-1}}{k_j}\left(\hat{h}_{j-}^{mn}\cdot\overline{\alpha}_{pq}^{j-1}-\frac{1}{k_{jz}^{mn}}\frac{k_{\perp}^{mn}}{k_j}(\overline{k}_{\perp}^{pq}-\overline{k}_{\perp}^{mn})\cdot\overline{\alpha}_{pq}^{j-1}\right)-\hat{e}_{j-}^{mn}\cdot\overline{\beta}_{pq}^{j-1}\right\}I_{mn}^{pq-}[j,j-1]$$
$$=e^{-ik_{jz}^{mn}\Delta_j}\sum_{pq}\left\{\hat{h}_{j-}^{mn}\cdot\overline{\alpha}_{pq}^{j}-\frac{1}{k_{jz}^{mn}}\frac{k_{\perp}^{mn}}{k_j}(\overline{k}_{\perp}^{pq}-\overline{k}_{\perp}^{mn})\cdot\overline{\alpha}_{pq}^{j}-\hat{e}_{j-}^{mn}\cdot\overline{\beta}_{pq}^{j}\right\}I_{mn}^{pq-}[j,j]$$

Here $\Delta_j=d_j-d_{j-1}$. Expanding the unknown surface fields Fourier coefficients $\alpha$ and $\beta$ in terms of orthogonal unit vectors $\hat{u}$ and $\hat{v}$ (that are spanning $xy$ plane) as

$$\begin{aligned}\overline{\alpha}_{pq}^{j}&=\alpha_{pq}^{ju}\hat{u}+\alpha_{pq}^{jv}\hat{v}\\ \overline{\beta}_{pq}^{j}&=\beta_{pq}^{ju}\hat{u}+\beta_{pq}^{jv}\hat{v}\end{aligned}\tag{5.5.7}$$

the propagation relation between Fourier coefficients of the adjacent layers surface fields can be written in a matrix form as

$$\overline{\overline{F}}_{mn,pq}^{j}\overline{S}_{pq}^{j}=\overline{\overline{E}}_{mn,pq}^{j-1}\overline{S}_{pq}^{j-1}\tag{5.5.8}$$

where the surface field vector $\overline{S}_{pq}^{j}=[\alpha_{pq}^{ju},\alpha_{pq}^{jv},\beta_{pq}^{ju},\beta_{pq}^{jv}]^{\mathrm{T}}$ is the Fourier component of the surface fields on the $j$-th interface (a summation over $pq$ is assumed) and individual mode propagation matrices $\overline{\overline{F}}_{mn,pq}^{j},\overline{\overline{E}}_{mn,pq}^{j-1}$ are given by the components

$$E_{mn,pq}^{j-1}[11]=\left\{\frac{k_{j-1}}{k_j}\hat{e}_{j+}^{mn}\cdot\hat{u}\right\}I_{mn}^{pq+}[j,j-1]\tag{5.5.9}$$
$$E_{mn,pq}^{j-1}[12]=\left\{\frac{k_{j-1}}{k_j}\hat{e}_{j+}^{mn}\cdot\hat{v}\right\}I_{mn}^{pq+}[j,j-1]$$
$$E_{mn,pq}^{j-1}[13]=\left\{\hat{h}_{j+}^{mn}\cdot\hat{u}+\frac{1}{k_{jz}^{mn}}\frac{k_{\perp}^{mn}}{k_j}(\overline{k}_{\perp}^{pq}-\overline{k}_{\perp}^{mn})\cdot\hat{u}\right\}I_{mn}^{pq+}[j,j-1]$$
$$E_{mn,pq}^{j-1}[14]=\left\{\hat{h}_{j+}^{mn}\cdot\hat{v}+\frac{1}{k_{jz}^{mn}}\frac{k_{\perp}^{mn}}{k_j}(\overline{k}_{\perp}^{pq}-\overline{k}_{\perp}^{mn})\cdot\hat{v}\right\}I_{mn}^{pq+}[j,j-1]$$
$$F_{mn,pq}^{j}[11]=e^{ik_{jz}^{mn}\Delta_j}\left\{\hat{e}_{j+}^{mn}\cdot\hat{u}\right\}I_{mn}^{pq+}[j,j]$$
$$F_{mn,pq}^{j}[12]=e^{ik_{jz}^{mn}\Delta_j}\left\{\hat{e}_{j+}^{mn}\cdot\hat{v}\right\}I_{mn}^{pq+}[j,j]$$
$$F_{mn,pq}^{j}[13]=e^{ik_{jz}^{mn}\Delta_j}\left\{\hat{h}_{j+}^{mn}\cdot\hat{u}+\frac{1}{k_{jz}^{mn}}\frac{k_{\perp}^{mn}}{k_j}(\overline{k}_{\perp}^{pq}-\overline{k}_{\perp}^{mn})\cdot\hat{u}\right\}I_{mn}^{pq+}[j,j]$$
$$F_{mn,pq}^{j}[14]=e^{ik_{jz}^{mn}\Delta_j}\left\{\hat{h}_{j+}^{mn}\cdot\hat{v}+\frac{1}{k_{jz}^{mn}}\frac{k_{\perp}^{mn}}{k_j}(\overline{k}_{\perp}^{pq}-\overline{k}_{\perp}^{mn})\cdot\hat{v}\right\}I_{mn}^{pq+}[j,j]$$

$$F^{j}_{mn,pq}[21]=e^{ik^{mn}_{jz}\Delta_j}\left\{\hat{h}^{mn}_{j+}\cdot\hat{u}+\frac{1}{k^{mn}_{jz}}\frac{k^{mn}_{\perp}}{k_j}(\overline{k}^{pq}_{\perp}-\overline{k}^{mn}_{\perp})\cdot\hat{u}\right\}I^{pq+}_{mn}[j,j] \tag{5.5.10}$$

$$F^{j}_{mn,pq}[22]=e^{ik^{mn}_{jz}\Delta_j}\left\{\hat{h}^{mn}_{j+}\cdot\hat{v}+\frac{1}{k^{mn}_{jz}}\frac{k^{mn}_{\perp}}{k_j}(\overline{k}^{pq}_{\perp}-\overline{k}^{mn}_{\perp})\cdot\hat{v}\right\}I^{pq+}_{mn}[j,j]$$

$$F^{j}_{mn,pq}[23]=e^{ik^{mn}_{jz}\Delta_j}\left\{-\hat{e}^{mn}_{j+}\cdot\hat{u}\right\}I^{pq+}_{mn}[j,j]$$

$$F^{j}_{mn,pq}[24]=e^{ik^{mn}_{jz}\Delta_j}\left\{-\hat{e}^{mn}_{j+}\cdot\hat{v}\right\}I^{pq+}_{mn}[j,j]$$

$$E^{j-1}_{mn,pq}[21]=\left\{\frac{k_{j-1}}{k_j}\left(\hat{h}^{mn}_{j+}\cdot\hat{u}+\frac{1}{k^{mn}_{jz}}\frac{k^{mn}_{\perp}}{k_j}(\overline{k}^{pq}_{\perp}-\overline{k}^{mn}_{\perp})\cdot\hat{u}\right)\right\}I^{pq+}_{mn}[j,j-1] \tag{5.5.11}$$

$$E^{j-1}_{mn,pq}[22]=\left\{\frac{k_{j-1}}{k_j}\left(\hat{h}^{mn}_{j+}\cdot\hat{v}+\frac{1}{k^{mn}_{jz}}\frac{k^{mn}_{\perp}}{k_j}(\overline{k}^{pq}_{\perp}-\overline{k}^{mn}_{\perp})\cdot\hat{v}\right)\right\}I^{pq+}_{mn}[j,j-1]$$

$$E^{j-1}_{mn,pq}[23]=\left\{-\hat{e}^{mn}_{j+}\cdot\hat{u}\right\}I^{pq+}_{mn}[j,j-1]$$

$$E^{j-1}_{mn,pq}[24]=\left\{-\hat{e}^{mn}_{j+}\cdot\hat{v}\right\}I^{pq+}_{mn}[j,j-1]$$

$$F^{j}_{mn,pq}[31]=e^{-ik^{mn}_{jz}\Delta_j}\left\{\hat{e}^{mn}_{j-}\cdot\hat{u}\right\}I^{pq-}_{mn}[j,j] \tag{5.5.12}$$

$$F^{j}_{mn,pq}[32]=e^{-ik^{mn}_{jz}\Delta_j}\left\{\hat{e}^{mn}_{j-}\cdot\hat{v}\right\}I^{pq-}_{mn}[j,j]$$

$$F^{j}_{mn,pq}[33]=e^{-ik^{mn}_{jz}\Delta_j}\left\{\hat{h}^{mn}_{j-}\cdot\hat{u}-\frac{1}{k^{mn}_{jz}}\frac{k^{mn}_{\perp}}{k_j}(\overline{k}^{pq}_{\perp}-\overline{k}^{mn}_{\perp})\cdot\hat{u}\right\}I^{pq-}_{mn}[j,j]$$

$$F^{j}_{mn,pq}[34]=e^{-ik^{mn}_{jz}\Delta_j}\left\{\hat{h}^{mn}_{j-}\cdot\hat{v}-\frac{1}{k^{mn}_{jz}}\frac{k^{mn}_{\perp}}{k_j}(\overline{k}^{pq}_{\perp}-\overline{k}^{mn}_{\perp})\cdot\hat{v}\right\}I^{pq-}_{mn}[j,j]$$

$$E^{j-1}_{mn,pq}[31]=\left\{\frac{k_{j-1}}{k_j}\hat{e}^{mn}_{j-}\cdot\hat{u}\right\}I^{pq-}_{mn}[j,j-1] \tag{5.5.13}$$

$$E^{j-1}_{mn,pq}[32]=\left\{\frac{k_{j-1}}{k_j}\hat{e}^{mn}_{j-}\cdot\hat{v}\right\}I^{pq-}_{mn}[j,j-1]$$

$$E^{j-1}_{mn,pq}[33]=\left\{\hat{h}^{mn}_{j-}\cdot\hat{u}-\frac{1}{k^{mn}_{jz}}\frac{k^{mn}_{\perp}}{k_j}(\overline{k}^{pq}_{\perp}-\overline{k}^{mn}_{\perp})\cdot\hat{u}\right\}I^{pq-}_{mn}[j,j-1]$$

$$E^{j-1}_{mn,pq}[34]=\left\{\hat{h}^{mn}_{j-}\cdot\hat{v}-\frac{1}{k^{mn}_{jz}}\frac{k^{mn}_{\perp}}{k_j}(\overline{k}^{pq}_{\perp}-\overline{k}^{mn}_{\perp})\cdot\hat{v}\right\}I^{pq-}_{mn}[j,j-1]$$

$$F^{j}_{mn,pq}[41]=e^{-ik^{mn}_{jz}\Delta_j}\left\{\hat{h}^{mn}_{j-}\cdot\hat{u}-\frac{1}{k^{mn}_{jz}}\frac{k^{mn}_{\perp}}{k_j}(\overline{k}^{pq}_{\perp}-\overline{k}^{mn}_{\perp})\cdot\hat{u}\right\}I^{pq-}_{mn}[j,j] \tag{5.5.14}$$

$$F^{j}_{mn,pq}[42]=e^{-ik^{mn}_{jz}\Delta_j}\left\{\hat{h}^{mn}_{j-}\cdot\hat{v}-\frac{1}{k^{mn}_{jz}}\frac{k^{mn}_{\perp}}{k_j}(\overline{k}^{pq}_{\perp}-\overline{k}^{mn}_{\perp})\cdot\hat{v}\right\}I^{pq-}_{mn}[j,j]$$

$$F^{j}_{mn,pq}[43]=e^{-ik^{mn}_{jz}\Delta_j}\left\{-\hat{e}^{mn}_{j-}\cdot\hat{u}\right\}I^{pq-}_{mn}[j,j]$$

$$F^{j}_{mn,pq}[44]=e^{-ik^{mn}_{jz}\Delta_j}\left\{-\hat{e}^{mn}_{j-}\cdot\hat{v}\right\}I^{pq-}_{mn}[j,j]$$

$$E^{j-1}_{mn,pq}[41]=\left\{\frac{k_{j-1}}{k_j}\left(\hat{h}^{mn}_{j-}\cdot\hat{u}-\frac{1}{k^{mn}_{jz}}\frac{k^{mn}_{\perp}}{k_j}(\overline{k}^{pq}_{\perp}-\overline{k}^{mn}_{\perp})\cdot\hat{u}\right)\right\}I^{pq-}_{mn}[j,j-1]$$

$$E^{j-1}_{mn,pq}[42]=\left\{\frac{k_{j-1}}{k_j}\left(\hat{h}^{mn}_{j-}\cdot\hat{v}-\frac{1}{k^{mn}_{jz}}\frac{k^{mn}_{\perp}}{k_j}(\overline{k}^{pq}_{\perp}-\overline{k}^{mn}_{\perp})\cdot\hat{v}\right)\right\}I^{pq-}_{mn}[j,j-1]$$

$$E^{j-1}_{mn,pq}[43]=\left\{-\hat{e}^{mn}_{j-}\cdot\hat{u}\right\}I^{pq-}_{mn}[j,j-1]$$

$$E^{j-1}_{mn,pq}[44]=\left\{-\hat{e}^{mn}_{j-}\cdot\hat{v}\right\}I^{pq-}_{mn}[j,j-1]$$

Using the propagation matrix formalism, the surface fields on the last boundary can be related to those of the first boundary through,

$$\begin{aligned}\overline{S}^{N-1}_{pq}&=\left(\overline{\overline{F}}^{N-1}_{mn,pq}\right)^{-1}\overline{\overline{E}}^{N-2}_{mn,pq}\left(\overline{\overline{F}}^{N-2}_{mn,pq}\right)^{-1}\overline{\overline{E}}^{N-3}_{mn,pq}\cdots\left(\overline{\overline{F}}^{2}_{mn,pq}\right)^{-1}\overline{\overline{E}}^{1}_{mn,pq}\overline{S}^{1}_{pq}\\&:=\overline{\overline{D}}\,\overline{S}^{1}_{pq}\end{aligned} \tag{5.5.15}$$

Also from the extinction of incident field in region 1 we have

$$\overline{\overline{P}}^{1}_{mn,pq}\overline{S}^{1}_{pq}=\begin{bmatrix}\hat{e}^{mn}_{1-}\cdot\overline{D}^{1,1}_{mn}\\ \hat{h}^{mn}_{1-}\cdot\overline{D}^{1,1}_{mn}\end{bmatrix} \tag{5.5.16}$$

where the $2\times4$ mode matrix $\overline{\overline{P}}^{1}_{mn,pq}$ is given by its components as

$$\overline{\overline{P}}^{1}_{mn,pq}[11]=-\frac{k_1}{2L_xL_y}\frac{1}{k^{mn}_{1z}}\left\{\hat{e}^{mn}_{1-}\cdot\hat{u}\right\}I^{pq-}_{mn}[1,1] \tag{5.5.17}$$

$$\overline{\overline{P}}^{1}_{mn,pq}[12]=-\frac{k_1}{2L_xL_y}\frac{1}{k^{mn}_{1z}}\left\{\hat{e}^{mn}_{1-}\cdot\hat{v}\right\}I^{pq-}_{mn}[1,1]$$

$$\overline{\overline{P}}^{1}_{mn,pq}[13]=-\frac{k_1}{2L_xL_y}\frac{1}{k^{mn}_{1z}}\left\{\hat{h}^{mn}_{1-}\cdot\hat{u}-\frac{1}{k^{mn}_{1z}}\frac{k^{mn}_{\perp}}{k_1}(\overline{k}^{pq}_{\perp}-\overline{k}^{mn}_{\perp})\cdot\hat{u}\right\}I^{pq-}_{mn}[1,1]$$

$$\overline{\overline{P}}^{1}_{mn,pq}[14]=-\frac{k_1}{2L_xL_y}\frac{1}{k^{mn}_{1z}}\left\{\hat{h}^{mn}_{1-}\cdot\hat{v}-\frac{1}{k^{mn}_{1z}}\frac{k^{mn}_{\perp}}{k_1}(\overline{k}^{pq}_{\perp}-\overline{k}^{mn}_{\perp})\cdot\hat{v}\right\}I^{pq-}_{mn}[1,1]$$

$$\overline{\overline{P}}^{1}_{mn,pq}[21]=-\frac{k_1}{2L_xL_y}\frac{1}{k_{1z}^{mn}}\left\{\hat{h}_{1-}^{mn}\cdot\hat{u}-\frac{1}{k_{1z}^{mn}}\frac{k_{\perp}^{mn}}{k_1}(\overline{k}_{\perp}^{pq}-\overline{k}_{\perp}^{mn})\cdot\hat{u}\right\}I_{mn}^{pq-}[1,1] \tag{5.5.18}$$

$$\overline{\overline{P}}^{1}_{mn,pq}[22]=-\frac{k_1}{2L_xL_y}\frac{1}{k_{1z}^{mn}}\left\{\hat{h}_{1-}^{mn}\cdot\hat{v}-\frac{1}{k_{1z}^{mn}}\frac{k_{\perp}^{mn}}{k_1}(\overline{k}_{\perp}^{pq}-\overline{k}_{\perp}^{mn})\cdot\hat{v}\right\}I_{mn}^{pq-}[1,1]$$

$$\overline{\overline{P}}^{1}_{mn,pq}[23]=-\frac{k_1}{2L_xL_y}\frac{1}{k_{1z}^{mn}}\left\{-\hat{e}_{1-}^{mn}\cdot\hat{u}\right\}I_{mn}^{pq-}[1,1]$$

$$\overline{\overline{P}}^{1}_{mn,pq}[24]=-\frac{k_1}{2L_xL_y}\frac{1}{k_{1z}^{mn}}\left\{-\hat{e}_{1-}^{mn}\cdot\hat{v}\right\}I_{mn}^{pq-}[1,1]$$

Similarly, from the extinction of the wave in the last region,

$$\overline{\overline{P}}^{N}_{mn,pq}\overline{S}^{N-1}_{pq}=\overline{0} \tag{5.5.19}$$

where

$$\overline{\overline{P}}^{N}_{mn,pq}[11]=\left\{\frac{k_{N-1}}{k_N}\hat{e}_{N+}^{mn}\cdot\hat{u}\right\}I_{mn}^{pq+}[N,N-1] \tag{5.5.20}$$

$$\overline{\overline{P}}^{N}_{mn,pq}[12]=\left\{\frac{k_{N-1}}{k_N}\hat{e}_{N+}^{mn}\cdot\hat{v}\right\}I_{mn}^{pq+}[N,N-1]$$

$$\overline{\overline{P}}^{N}_{mn,pq}[13]=\left\{\hat{h}_{N+}^{mn}\cdot\hat{u}+\frac{1}{k_{Nz}^{mn}}\frac{k_{\perp}^{mn}}{k_N}(\overline{k}_{\perp}^{pq}-\overline{k}_{\perp}^{mn})\cdot\hat{u}\right\}I_{mn}^{pq+}[N,N-1]$$

$$\overline{\overline{P}}^{N}_{mn,pq}[14]=\left\{\hat{h}_{N+}^{mn}\cdot\hat{v}+\frac{1}{k_{Nz}^{mn}}\frac{k_{\perp}^{mn}}{k_N}(\overline{k}_{\perp}^{pq}-\overline{k}_{\perp}^{mn})\cdot\hat{v}\right\}I_{mn}^{pq+}[N,N-1]$$

$$\overline{\overline{P}}^{N}_{mn,pq}[21]=\left\{\frac{k_{N-1}}{k_N}\left(\hat{h}_{N+}^{mn}\cdot\hat{u}+\frac{1}{k_{Nz}^{mn}}\frac{k_{\perp}^{mn}}{k_N}(\overline{k}_{\perp}^{pq}-\overline{k}_{\perp}^{mn})\cdot\hat{u}\right)\right\}I_{mn}^{pq+}[N,N-1]$$

$$\overline{\overline{P}}^{N}_{mn,pq}[22]=\left\{\frac{k_{N-1}}{k_N}\left(\hat{h}_{N+}^{mn}\cdot\hat{v}+\frac{1}{k_{Nz}^{mn}}\frac{k_{\perp}^{mn}}{k_N}(\overline{k}_{\perp}^{pq}-\overline{k}_{\perp}^{mn})\cdot\hat{v}\right)\right\}I_{mn}^{pq+}[N,N-1]$$

$$\overline{\overline{P}}^{N}_{mn,pq}[23]=\left\{-\hat{e}_{N+}^{mn}\cdot\hat{u}\right\}I_{mn}^{pq+}[N,N-1]$$

$$\overline{\overline{P}}^{N}_{mn,pq}[24]=\left\{-\hat{e}_{N+}^{mn}\cdot\hat{v}\right\}I_{mn}^{pq+}[N,N-1]$$

Putting ll of the extinction relations together, the system of equations to determine the Fourier coefficients of the surface fields on the first and last boundary is given by

$$\begin{bmatrix}\overline{\overline{P}}^{1}_{mn,pq} & \overline{\overline{0}} \\ \overline{\overline{0}} & \overline{\overline{P}}^{N}_{mn,pq} \\ \overline{\overline{D}} & -\overline{\overline{I}}\end{bmatrix}\begin{bmatrix}\overline{S}^{1}_{pq} \\ \overline{S}^{N-1}_{pq}\end{bmatrix}=\begin{bmatrix}\hat{e}_{1-}^{mn}\cdot\overline{D}^{1,1}_{mn} \\ \hat{h}_{1-}^{mn}\cdot\overline{D}^{1,1}_{mn} \\ \overline{0}\end{bmatrix} \tag{5.5.21}$$

Once the Fourier coefficients of the surface fields on the first and last boundaries are determined through (5.5.21), the surface field on the other boundaries can be determined by using the propagation matrices.

## 5.6 Scattered Field

From the equivalence principle applied to region 1, for observation points in region 1 total electric field can be written as

$$\overline{E}_{inc}(\overline{r})+\int_S \mathrm{d}S'\Big\{ik_1\eta_1\overline{\overline{G}}_1(\overline{r},\overline{r}')\cdot[\hat{n}_1\times\overline{H}_1(\overline{r}')]+\nabla\times\overline{\overline{G}}_1(\overline{r},\overline{r}')\cdot[\hat{n}_1\times\overline{E}_1(\overline{r}')]\Big\}=\overline{E}_1(\overline{r}) \quad (5.6.1)$$

The second term is the scattered field and upon using the periodic dyadic Green's function spatial integrals become condensate to the primitive cell and

$$\overline{E}_s(\overline{r})=\int_{\text{cell}} \mathrm{d}^2\overline{r}'\Big\{ik_1\overline{\overline{G}}^{>}_{1p}(\overline{r},\overline{r}')\cdot\overline{a}_1(\overline{r}')+\nabla\times\overline{\overline{G}}^{>}_{1p}(\overline{r},\overline{r}')\cdot\overline{b}_1(\overline{r}')\Big\} \quad (5.6.2)$$

Upon considering the scattered field outside of the extended boundary at $z=\max f_1(\overline{r}_\perp)$, the dyadic Green's function can be expanded as

$$\overline{\overline{G}}^{>}_{1p}(\overline{r},\overline{r}')=\frac{i}{2L_xL_y}\sum_{m,n}\frac{1}{k_{1z}^{mn}}\Big[\hat{e}_{1+}^{mn}\hat{e}_{1+}^{mn}+\hat{h}_{1+}^{mn}\hat{h}_{1+}^{mn}\Big]e^{i\overline{k}_{1+}^{mn}\cdot(\overline{r}-\overline{r}')} \quad (5.6.3)$$

$$\nabla\times\overline{\overline{G}}^{>}_{p}(\overline{r},\overline{r}')=-\frac{k_1}{2L_xL_y}\sum_{m,n}\frac{1}{k_{1z}^{mn}}\Big[\hat{e}_{1+}^{mn}\hat{h}_{1+}^{mn}-\hat{h}_{1+}^{mn}\hat{e}_{1+}^{mn}\Big]e^{i\overline{k}_{1+}^{mn}\cdot(\overline{r}-\overline{r}')} \quad (5.6.4)$$

Substituting the periodic Green's function into the scattered field expression, results in an expansion of the scattered field in terms of upward propagating Bloch waves in region 1

$$\overline{E}_s(\overline{r})=\sum_{m,n}\overline{S}_{mn}e^{i\overline{k}_{1+}^{mn}\cdot\overline{r}} \quad (5.6.5)$$

where

$$\overline{S}_{mn}=-\frac{k_1}{2L_xL_y}\frac{1}{k_{1z}^{mn}}\Big[\hat{e}_{1+}^{mn}\hat{e}_{1+}^{mn}+\hat{h}_{1+}^{mn}\hat{h}_{1+}^{mn}\Big]\cdot\int_{\text{cell}}\mathrm{d}^2\overline{r}'e^{-i\overline{k}_{1+}^{mn}\cdot\overline{r}'}\overline{a}_1(\overline{r}') \quad (5.6.6)$$

$$-\frac{k_1}{2L_xL_y}\frac{1}{k_{1z}^{mn}}\Big[\hat{e}_{1+}^{mn}\hat{h}_{1+}^{mn}-\hat{h}_{1+}^{mn}\hat{e}_{1+}^{mn}\Big]\cdot\int_{\text{cell}}\mathrm{d}^2\overline{r}'e^{-i\overline{k}_{1+}^{mn}\cdot\overline{r}'}\overline{b}_1(\overline{r}') \quad (5.6.7)$$

Notice that (5.6.5) predict the scattered field to be expandable only in terms of the upward propagating waves (irrespective of whatever the surface profiles are) which is not generally true. one can imagine a surface that has such a curvature that allows backward propagating waves toward the surface. On the other side. the scattered field computed here is valid at points beyond the extended boundary and seems that the situation of the backward wave does not happen. However, the surface field are computed by the same assumption (extended boundary condition) and for a surface profile with large slopes, considered expansions cannot truly satisfy the boundary conditions and this would cause instability in the computation of the surface fields.

Using solution of surface field from extinction equation and substituting in relation of vector coefficient $\overline{S}_{mn}$, we have

$$\overline{S}_{mn}=-\frac{k_1}{2L_xL_y}\frac{1}{k_{1z}^{mn}}\sum_{pq}\Bigg\{\Big[\hat{e}_{1+}^{mn}\hat{e}_{1+}^{mn}+\hat{h}_{1+}^{mn}\hat{h}_{1+}^{mn}\Big]\cdot\Big[\overline{\alpha}^1_{pq}+\frac{1}{k_{1z}^{mn}}(\overline{k}_\perp^{pq}-\overline{k}_\perp^{mn})\cdot\overline{\alpha}^1_{pq}\hat{z}\Big] \quad (5.6.8)$$

$$+\Big[\hat{e}_{1+}^{mn}\hat{h}_{1+}^{mn}-\hat{h}_{1+}^{mn}\hat{e}_{1+}^{mn}\Big]\cdot\Big[\overline{\beta}^1_{pq}+\frac{1}{k_{1z}^{mn}}(\overline{k}_\perp^{pq}-\overline{k}_\perp^{mn})\cdot\overline{\beta}^1_{pq}\hat{z}\Big]\Bigg\}I_{mn}^{pq+}[1,1]$$

The term which consists of the gradient of the surface is integrated by part. The scattering potential integral for the scattered field from the first boundary in region 1 is defined as

$$I_{mn}^{pq+}[1,1]=\int_{\text{cell}}\mathrm{d}^2\overline{r}'e^{i(\overline{k}_\perp^{pq}-\overline{k}_\perp^{mn})\cdot\overline{r}'_\perp-ik_{1z}^{mn}f_1(\overline{r}'_\perp)} \tag{5.6.9}$$

$\overline{S}_{mn}$'s are the scattered electric field vector amplitude of Bloch modes labeled by $(m,n)$.

## 5.7 Transmitted Field

Similar to the scattered field case, the transmitted field into the region 1 can be find using equivalence principle applied to region $N$ as following

$$\overline{E}_t(\overline{r})=-\int_{\text{cell}}\mathrm{d}^2\overline{r}'\left\{ik_{N-1}\overline{\overline{G}}^{<}_{Np}(\overline{r},\overline{r}')\cdot\overline{a}_{N-1}(\overline{r}')+\nabla\times\overline{\overline{G}}^{<}_{Np}(\overline{r}',\overline{r})\cdot\overline{b}_{N-1}(\overline{r}')\right\}$$

where we have expressed surface fields in terms of region $N-1$ fields. Assuming observation point to be in region $N$ and upon insertion of the Green's function into transmitted field relation, it turns out that the transmitted field can be expanded in terms of the downward propagating waves in region $N$

$$\overline{E}_t(\overline{r})=\sum_{m,n}\overline{T}_{mn}e^{i\overline{k}_{N-}^{mn}\cdot\overline{r}} \tag{5.7.1}$$

where amplitude of the transmitted Bloch modes is given by

$$\begin{aligned}\overline{T}_{mn}=&\frac{k_{N-1}}{2L_xL_y}\frac{1}{k_{Nz}^{mn}}\left[\hat{e}_{N-}^{mn}\hat{e}_{N-}^{mn}+\hat{h}_{N-}^{mn}\hat{h}_{N-}^{mn}\right]\cdot\int_{\text{cell}}\mathrm{d}^2\overline{r}'e^{-i\overline{k}_{N-}^{mn}\cdot\overline{r}'}\overline{a}_{N-1}(\overline{r}')\\&+\frac{k_N}{2L_xL_y}\frac{1}{k_{Nz}^{mn}}\left[\hat{e}_{N-}^{mn}\hat{h}_{N-}^{mn}-\hat{h}_{N-}^{mn}\hat{e}_{N-}^{mn}\right]\cdot\int_{\text{cell}}\mathrm{d}^2\overline{r}'e^{-i\overline{k}_{N-}^{mn}\cdot\overline{r}'}\overline{b}_{N-1}(\overline{r}')\end{aligned}$$

Inserting the Fourier series representation of the surface fields into the equations and simplifying the integrals of the gradient of surface profile by a by part integration, we arrive at

$$\begin{aligned}\overline{T}_{mn}=&\frac{k_{N-1}}{2L_xL_y}\frac{1}{k_{Nz}^{mn}}e^{-ik_{Nz}^{mn}d_{N-1}}\sum_{pq}\left\{\left[\hat{e}_{N-}^{mn}\hat{e}_{N-}^{mn}+\hat{h}_{N-}^{mn}\hat{h}_{N-}^{mn}\right]\cdot\left[\overline{\alpha}_{pq}^{N-1}-\frac{1}{k_{Nz}^{mn}}(\overline{k}_\perp^{pq}-\overline{k}_\perp^{mn})\cdot\overline{\alpha}_{pq}^{N-1}\hat{z}\right]\right.\\&\left.+\frac{k_N}{k_{N-1}}\left[\hat{e}_{N-}^{mn}\hat{h}_{N-}^{mn}-\hat{h}_{N-}^{mn}\hat{e}_{N-}^{mn}\right]\cdot\left[\overline{\beta}_{pq}^{N-1}-\frac{1}{k_{Nz}^{mn}}(\overline{k}_\perp^{pq}-\overline{k}_\perp^{mn})\cdot\overline{\beta}_{pq}^{N-1}\hat{z}\right]\right\}I_{mn}^{pq-}[N,N-1]\end{aligned} \tag{5.7.2}$$

where

$$I_{mn}^{pq-}[N,N-1]=\int_{\text{cell}}\mathrm{d}^2\overline{r}'e^{i(\overline{k}_\perp^{pq}-\overline{k}_\perp^{mn})\cdot\overline{r}'_\perp+ik_{Nz}^{mn}f_{N-1}(\overline{r}'_\perp)} \tag{5.7.3}$$

Now we have the amplitude and polarization of each transmitted mode into region 1. Notice that the scattered field is evaluated from previously known surface fields and it does not require solving boundary value problems.

## 5.8 Scattered and Transmitted Power

For the scattered field in region 1 of $\overline{E}_s(\overline{r})=\sum_{m,n}\overline{S}_{mn}e^{i\overline{k}_{1+}^{mn}\cdot\overline{r}}$, associated magnetic field can be computed as

$$\overline{H}_s(\overline{r})=\frac{1}{\eta_1}\sum_{m,n}\left(\hat{k}_{1+}^{mn}\times\overline{S}_{mn}\right)\ e^{i\overline{k}_{1+}^{mn}\cdot\overline{r}} \tag{5.8.1}$$

Then, the complex poynting vector associated with scattered field is

$$\begin{aligned}\overline{S}_s(\overline{r})&=\frac{1}{2\eta}\overline{E}_s(\overline{r})\times\overline{H}_s^*(\overline{r}) \qquad (5.8.2)\\ &=\frac{1}{2\eta_1}\sum_{m,n}\sum_{p,q}\overline{S}_{mn}\times\left(\hat{k}_{1+}^{pq}\times\overline{S}_{pq}\right)^* e^{i(\overline{k}_\perp^{mn}-\overline{k}_\perp^{pq})\cdot\overline{r}_\perp}e^{i(k_{1z}^{mn}-k_{1z}^{pq*})z}\end{aligned}$$

Since Bloch modes are mutually orthogonal over surface of a cell, cross terms in the poynting vector do not contribute in the total scattered power. The complex scattered power in $z$ direction can be computed by integrating $\overline{S}_s$ over a cell

$$P_s=\frac{1}{2\eta_1}\sum_{m,n}\sum_{p,q}\overline{S}_{mn}\times\left(\hat{k}_{1+}^{pq}\times\overline{S}_{pq}\right)^*\cdot\hat{z}e^{i(k_{1z}^{mn}-k_{1z}^{pq*})z}\int\mathrm{d}^2\overline{r}_\perp\ e^{i(\overline{k}_\perp^{mn}-\overline{k}_\perp^{pq})\cdot\overline{r}_\perp} \tag{5.8.3}$$

whereas from orthogonality of the Bloch modes,

$$\int\mathrm{d}^2\overline{r}_\perp\ e^{i(\overline{k}_\perp^{mn}-\overline{k}_\perp^{pq})\cdot\overline{r}_\perp}=L_xL_y\delta_{mp}\delta_{nq} \tag{5.8.4}$$

that results in

$$\begin{aligned}P_s&=\frac{L_xL_y}{2\eta_1}\sum_{m,n}\overline{S}_{mn}\times\left(\hat{k}_{1+}^{mn}\times\overline{S}_{mn}\right)^*\cdot\hat{z}e^{-2\mathrm{Im}(k_{1z}^{mn})z} \qquad (5.8.5)\\ &=\frac{L_xL_y}{2\eta_1}\sum_{m,n}\left[|\overline{S}_{mn}|^2\hat{k}_{1+}^{mn*}-(\overline{S}_{mn}\cdot\hat{k}_{1+}^{mn*})\overline{S}_{mn}^*\right]\cdot\hat{z}e^{-2\mathrm{Im}(k_{1z}^{mn})z}\end{aligned}$$

If we are interested in lossless condition for region 0, then real power corresponds to the propagating modes only and then

$$\mathrm{Re}[P_s]=\frac{L_xL_y}{2\eta_1}\sum_{m,n}\mathrm{Re}\left(\frac{k_{1z}^{mn}}{k_1}\right)|\overline{S}_{mn}|^2 \tag{5.8.6}$$

Similarly, for the transmitted power in $(-\hat{z})$ direction we have

$$\mathrm{Re}[P_t]=\frac{L_xL_y}{2}\sum_{m,n}\mathrm{Re}\left(\frac{k_{Nz}^{mn}}{k_N\eta_N}\right)|\overline{T}_{mn}|^2 \tag{5.8.7}$$

The incident power associated with the incident plane wave in $(-\hat{z})$ direction can be obtained as

$$P_{\mathrm{inc}}=\int_{\mathrm{cell}}\mathrm{d}\overline{r}_\perp\frac{1}{2\eta_1}\cos\theta_i=\frac{L_xL_y}{2\eta_1}\cos\theta_i \tag{5.8.8}$$

Henceforth, the reflectivity and transmissivity of the surface can be computed as

$$\begin{aligned}R&=\sum_{m,n}\mathrm{Re}\left(\frac{k_{1z}^{mn}}{k_{iz}}\right)|\overline{S}_{mn}|^2 \qquad (5.8.9)\\ T&=\sum_{m,n}\mathrm{Re}\left(\frac{k_{Nz}^{mn}}{k_{iz}}\right)|\overline{T}_{mn}|^2\end{aligned}$$

## 5.9 Numerical Results and Comparison with SPM2 Solution

In order to verify the accuracy of the 3D $T$-Matrix method for a multi-layer case, we consider a lossless layered medium with dielectric constants given by $\epsilon_r$=(1,1.5,2,3,2) from the top, respectively. The interfaces are located at mean values of $d$=−(0,0.3,0.7,0.9)$\lambda_1$ where $\lambda_1$ is the wavelength in region 1 (the top half space). Parameters of the Gaussian rough interfaces include RMS height of $h_{\rm rms}$=0.03$\lambda_1$, correlation length of $\ell$=$\lambda_1$ which is considered the same for all of 4 uncorrelated and isotropic interfaces. The SPM2 solution is expected to be valid in this small RMS height regime [35]. We consider a periodic random surface of dimensions $L_x$=$L_y$=5$\lambda_1$≫$\ell$ in the $T$-matrix as well as SPM2 solution. In order to reach convergence, we average over 300 realizations of the surfaces (4 independent surfaces). It should be noted that this structure supports guided modes, and as a result the SPM2 power spectral kernels are singular and need to be treated carefully by the SIP [79, 84].

Figure 5.2 compares the $v$ and $h$ channel emissivities of the structure obtained by the SPM2 applied to a periodic surface of 5$\lambda_1$×5$\lambda_1$, and the $T$-matrix with that of flat surfaces. The maximum difference between the emissivities obtained by the two methods is always below 0.002 (corresponds to the relative error of less than 0.22%) for any polarization and observation angle. This represents a good agreement between the SPM2 and $T$-Matrix approaches in the small height regime [89, 90].

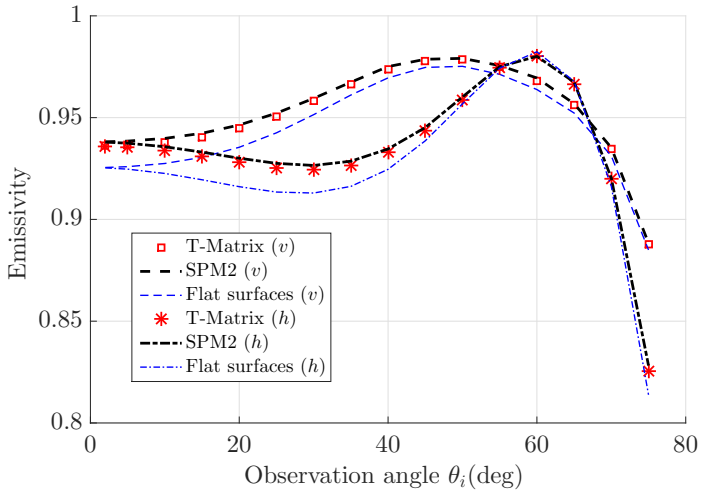


FIGURE 5.2: Emissivity of 5 layer structure of section 5.9 with rms height of $h$=0.03$\lambda_1$ for horizontal ($h$) and vertical ($v$) polarizations vs observation angle ($\theta_i$) obtained by the $T$-Matrix and periodic SPM2 compared to the flat surfaces response.

An important question regarding the implementation of the $T$-matrix method is how many modes should be included in Eq. (5.2.1). As one includes more evanescent modes, the condition number of the matrices in Eq. (**??**) becomes worse and after some point the solution is not possible. Although direct inversion has been used for all of the examples in this paper, ill-conditioned matrices involved in the problem can lead to divergent iterative procedure or numerical break-down in the case of direct inversion (for larger problem in

terms of included modes). This situation is more critical for larger RMS height when inclusion of more evanescent modes is necessary to account for the fields inside the grooves. In addition, for the case of large permittivity contrast between layers, capturing the propagating modes inside a high permittivity layer is required simultaneously with including more evanescent modes in layers with lower permittivity. This can be accounted as a limitation for the $T$-matrix method in the layered media scenario with high dielectric contrast between layers. A measure of the degree of accuracy of a solution is energy conservation. Although it cannot guarantee the correct solution, it is a necessary condition for a solution to be correct. Thus, we can increase the number of modes and monitor the energy conservation in the solution. For the cases where higher order evanescent modes must be included, preconditioning of matrices in Eq. (**??**) may be needed [85, 91, 92].

For the computation of emissivity in 5.2, the number of included modes in each direction is 13. The energy conservation criteria in this case is $1\pm10^{-4}$ which corresponds to error of 0.01%. During the Monte Carlo simulation over surfaces realizations it is necessary to be careful about adjacent interface intersections. Such cases violate the problem formulation assumptions in Eq. (5.2.2). The distance between the mean level of the interfaces considered above make this unlikely but not impossible. When running the simulation, cases having intersections between interfaces are discarded and excluded from further consideration.

For comparison of computational cost, the SPM which is an analytic solution, does not require intensive computations. On the other hand, a typical MoM solution does require more surface unknowns. For example, in the above problem of 4 surfaces of area $5\lambda_1\times5\lambda_1$ using discretization rule of 10 points/$\lambda$ the number of unknowns would be $N=50\times50\times\epsilon_r\times8\approx40{,}000$ just for one surface (last factor takes the polarization, and the electric and magnetic currents into account) and 160,000 for all 4 surfaces, while the $T$-matrix number of unknowns is around $N=1300$. Considering the orders of magnitudes difference in the number of unknowns, the $T-$matrix has lower cost than the MoM. Also, for such a slight dielectric contrast between the adjacent layers, the MoM solution suffers from the discretization noise such that energy conservation criteria would not be satisfactory. On the other hand, there are situations that the $T-$matrix as formulated in this paper does not work at all due to extremely ill-conditioned matrices. For example, in the sub wavelength periods or very high amplitude of the surface, the $T-$matrix solution break down numerically. For a sub wavelength structure, one can utilize the effective medium approximation or use the MoM solution.

In order to show the $T$-matrix solution in large RMS height regime, consider the same medium as discussed above with Gaussian surfaces of RMS height $0.08\lambda_1(k_{\max}h_{\rm rms}\approx0.5)$ which is out of the validity region of the SPM2. Also, the mean level of the interfaces is chosen to be at $d=-(0,0.6,1.4,2)\lambda_1$ to reduce possible interface intersections. Here the total number of included modes is $17\times17=289$, which leads to satisfaction of the energy conservation criteria to better than 0.1%. Figure 5.3 plots $h$ and $v$ channel emissivities of the structure obtained by the $T$-matrix and SPM2 compare to the flat surface case. As opposed to the small height example of Fig. 5.2, where the roughness increases the emission of the surface, here the presence of roughness cause a reduction in emission at observation angles less than 40°. The reason behind this is the structure with flat interfaces for this medium configuration is near the resonance condition. The presence of roughness then reduces transmission. For observation near grazing, the SPM2 solution for emissivity becomes close to the $T$-matrix for both polarizations.

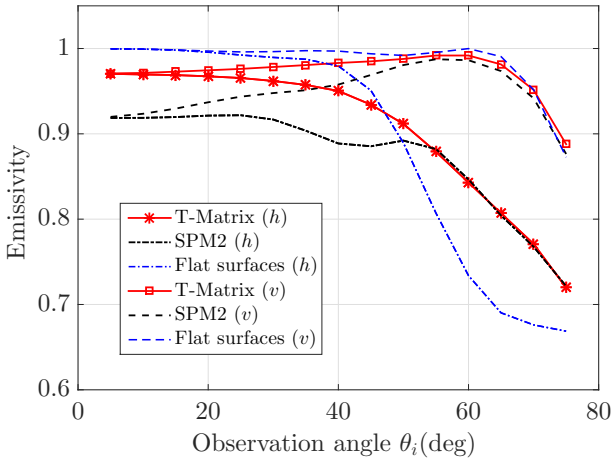


FIGURE 5.3: Emissivity of 5 layer structure of section 5.9 with rms height of $h$=0.08$\lambda_1$ for horizontal ($h$) and vertical ($v$) polarizations vs observation angle ($\theta_i$) obtained by the $T$-Matrix and periodic SPM2 compared to the flat surfaces response.

### 5.9.1 Bistatic Scattering Pattern

For a continuum spectrum of scattered waves, the bistatic scattering pattern $\sigma_s$ is defined as

$$P_s^{\alpha\beta}=\int_{(2\pi)}\mathrm{d}\Omega_s\sigma_s^{\alpha\beta}(\Omega_s,\Omega_i) \tag{5.9.1}$$

where $P_s^{\alpha\beta}$ is $\alpha-$polarized normalized scattered power when the surface is illuminated by a $\beta-$polarized incident field. For the set of discrete modes in the $T$-matrix, the normalized scattered power can be obtained by Eq. (5.4.6). In order to make a connection between these two cases when $L_x,L_y\gg\lambda$, note that for discrete modes,

$$\Delta k_{mx}=\frac{2\pi\Delta m}{L_x} \tag{5.9.2}$$

and one can approximate $\mathrm{d}k_x\approx 2\pi/L_x$ to go from discrete to continuum limit, or directly using the connection between discrete and continuous counterparts

$$\frac{1}{L_xL_y}\sum_{m,n}\Leftrightarrow\int\frac{\mathrm{d}^2\overline{k}_\perp}{(2\pi)^2}=\Big(\frac{k}{2\pi}\Big)^2\int\mathrm{d}\Omega_s\cos\theta_s \tag{5.9.3}$$

to find the incoherent reflectivity pattern as

$$\sigma_s(\Omega_s,\Omega_i)=\frac{k^2L_xL_y}{(2\pi)^2}\frac{\cos^2\theta_s}{\cos\theta_i}|\overline{S}_{mn}|^2 \tag{5.9.4}$$

Here, $k_x=k_1\sin\theta_s\cos\phi_s$ and $k_y=k_1\sin\theta_s\sin\phi_s$ are the Floquet wavenumber components for the scattered field given by Eq. (**??**). The relation between mode number $(m,n)$ and scattering direction $(\theta_s,\phi_s)$ can be written as $\tan\phi_s=k_{ny}/k_{mx}$ and $k_1^2\sin^2\theta_s=k_{mx}^2+k_{ny}^2$.

Note that the presence of the factor $\cos^2\theta_s$ mandates that $\sigma_s \to 0$ for $\theta_s \to \pm\pi/2$ which corresponds to the perimeter of the hemispheric plots (Fig. 5.4). However, due to the limited spatial resolution of the solution, $\theta_s = \pm\pi/2$ may not be achievable exactly over the $(\theta_s, \phi_s)$ grid for a given period of the surface.

Figure 5.4 and 5.5, compares co-polarized $\sigma_s^{hh}$ and cross-polarized $\sigma_s^{vh}$ bistatic reflectivity of the structure described in Section 5.9 with RMS height of $0.03\lambda_1$, obtained by the $T$-matrix and periodic SPM2, respectively. In order to increase the resolution of patterns, we consider interfaces of dimension $7\lambda \times 7\lambda$ and total number of $25 \times 25$ modes which leads to satisfaction of power conservation criteria better than $10^{-4}$. The incident field is an $h$-polarized (TE) plane wave at $\theta_i = 40^\circ$ (with respect to the $-z$ direction) and $\phi_i = 0^\circ$. The responses show good agreement in the forward scattering portion of the hemisphere, while more significant differences occur in the backscatter direction. The $T$-matrix method predicts higher reflectivity near backscattering direction while SPM2 concentrates more reflection near the forward scattering direction. In order to make a comparison between

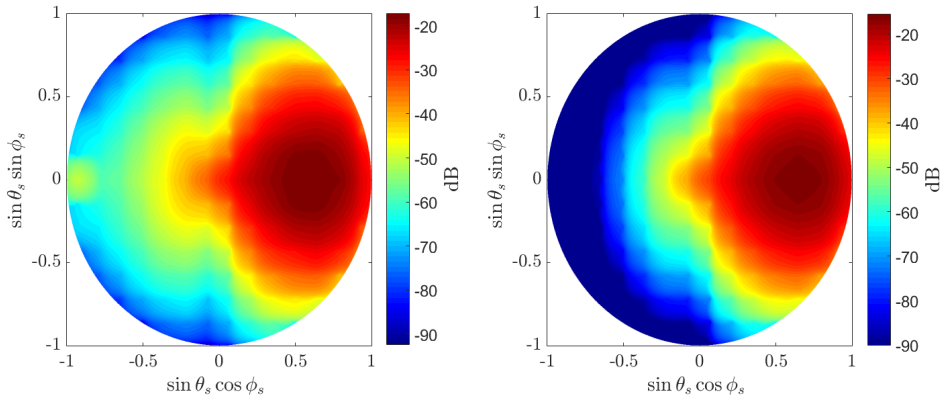


FIGURE 5.4: Co-polarized reflectivity pattern $\sigma_s^{hh}$ of the 5 layer structure described in section 5.9 for a TE-polarized incident field at $\theta_i = 40^\circ$, $\phi_i = 0^\circ$ obtained by the $T$-matrix (left) and SPM2 (right).

SPM2 and $T$-matrix for the case of anisotropic surfaces, we consider all of the interfaces for the structure in 5.9 to be a Gaussian surface with correlation length along $x$ and $y$ directions given by $\ell_x = 2\lambda_1$, and $\ell_y = \lambda_1$, respectively with RMS height of $h = 0.03\lambda_1$. Here, as opposed to the case of isotropic surface where the scattering pattern is independent of polar angle of incident $\phi_i$, scattering pattern depends on $\phi_i$ as well as $\theta_i$.

Figures. 5.6 and 5.7 compare the co-polarized and cross-polarized scattering pattern of the anisotropic surface for TE-polarized incident field at $\theta_i = 40^\circ$ and $\phi_i = 0$. SPM2 results in a very close pattern to that of $T$-matrix around the forward scattering portion of the hemisphere (although SPM2 gives 2 dB higher value at specular peak for co-pol) while it yields lower reflectivity ($\approx$60 dB lower) in backscattering portion of the hemisphere. Also, Figs. 5.8 and 5.9 compare the co-polarized and cross-polarized scattering pattern of the anisotropic surface for TE-polarized incident field at $\theta_i = 40^\circ$ and $\phi_i = 90^\circ$. The differences between both patterns are similar to that of $\phi_i = 0$. The present discrepancy in the backscattering portion of the hemispheric plot of reflectivity pattern between the SPM and the $T$-matrix solution can be explained as follows. In the the second order SPM, the reflectivity patten is proportional to the second moment of the surface (second order

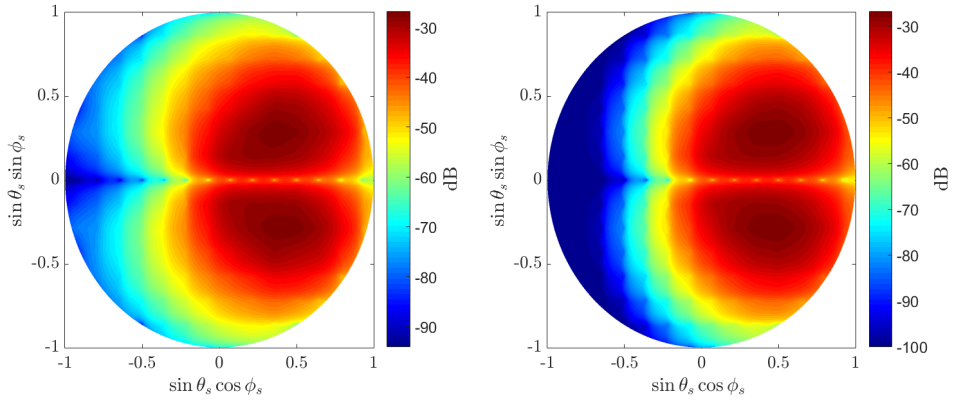


FIGURE 5.5: Cross-polarized reflectivity pattern $\sigma_s^{vh}$ of the 5 layer structure described in section 5.9 for a TE-polarized ($h-$pol) incident field at $\theta_i=40°$, $\phi_i=0°$ obtained by $T$-matrix (left) and SPM2 (right).

multiple scattering) while in actuality, the scattering process involves infinite orders of multiple scattering. Although in the perturbation solution the contribution of higher order terms decays with the powers of small roughness parameter, inclusion of higher order terms will broaden the spectrum of the scattered field. The $T$-matrix which in principle contains all orders of multiple scattering, yields more reflectivity than SPM2 in the backscattering direction.

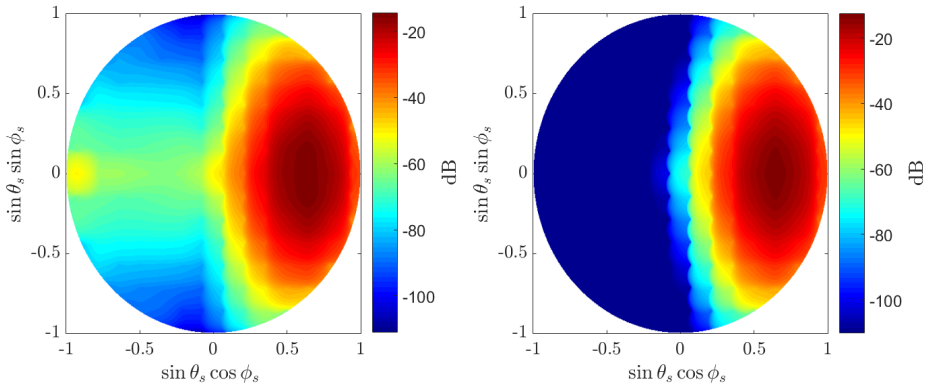


FIGURE 5.6: Co-polarized reflectivity pattern $\sigma_s^{hh}$ of the 5 layer structure including anisotropic interfaces ($\ell_x=2\ell_y=2\lambda_1$, $h_{\rm rms}=0.03\lambda_1$) for a TE-polarized ($h-$pol) incident field at $\theta_i=40°$, $\phi_i=0°$ obtained by the $T$-matrix (left) and SPM2 (right).

## 5.10 Conclusion

The problem of 3D electromagnetic scattering from a layered medium having 2D random rough interfaces was address in this paper using a T-matrix approach. The formulation is based on solving the coupled integral equation with a periodic Green's function kernel using the Floquet mode expansion. Comparison of the T-matrix results with the SPM2

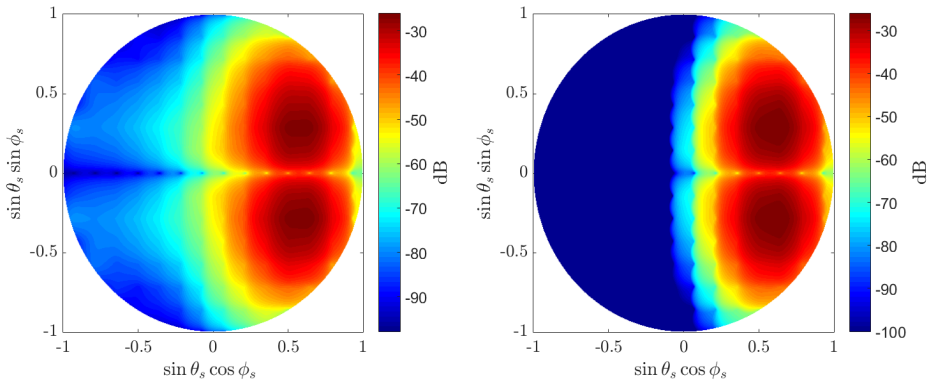


FIGURE 5.7: Cross-polarized reflectivity pattern $\sigma_s^{vh}$ of the 5 layer structure including anisotropic interfaces ($\ell_x = 2\ell_y = 2\lambda_1$, $h_{\rm rms} = 0.03\lambda_1$) for a TE-polarized ($h-$pol) incident field at $\theta_i = 40^\circ$, $\phi_i = 0^\circ$ obtained by the $T$-matrix (left) and SPM2 (right).

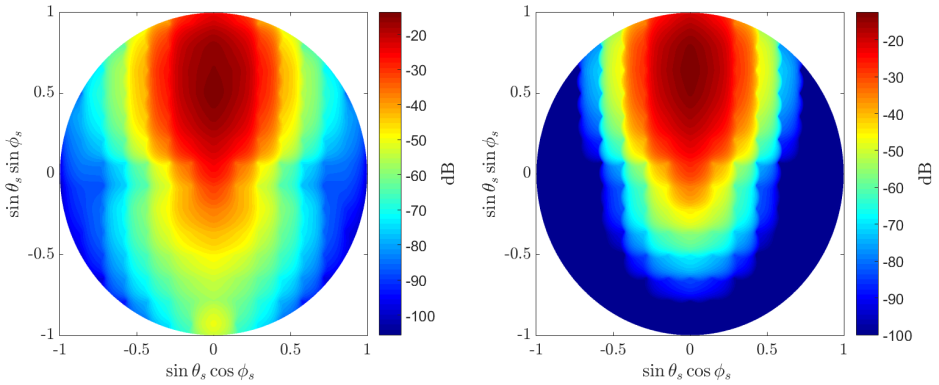


FIGURE 5.8: Co-polarized reflectivity pattern $\sigma_s^{hh}$ of the 5 layer structure including anisotropic interfaces ($\ell_x = 2\ell_y = 2\lambda_1$, $h_{\rm rms} = 0.03\lambda_1$) for a TE-polarized ($h-$pol) incident field at $\theta_i = 40^\circ$, $\phi_i = 90^\circ$ obtained by the $T$-matrix (left) and SPM2 (right).

is done for a 5 layered medium within the small height regime through the emissivity and co-polarized/cross-polarized bistatic reflectivity. The comparison shows a good agreement between the T-matrix and SPM2 methods in appropriate limits, and the ability of the T-matrix method to extend the computations beyond the limits of the SPM2. Also, the comparison of methods in the case of anisotropic surfaces show a close results near the forward scattering direction while there are significant differences near the backscattering direction.

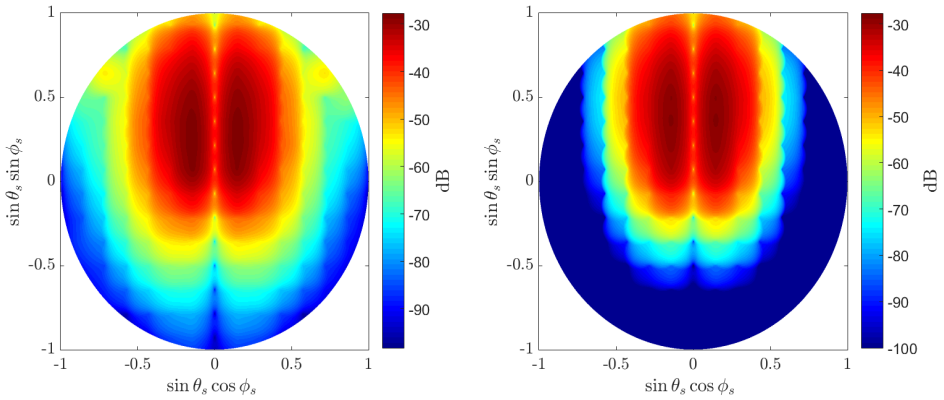


FIGURE 5.9: Cross-polarized reflectivity pattern $\sigma_s^{vh}(\theta_s,\phi_s)$ of the 5 layer structure including anisotropic interfaces ($\ell_x=2\ell_y=2\lambda_1$, $h_{\rm rms}=0.03\lambda_1$) for a TE-polarized ($h-$pol) incident field at $\theta_i=40^\circ$, $\phi_i=90^\circ$ obtained by the $T$-matrix (left) and SPM2 (right).

### 5.10.1 Special Case: Sinusoidal Periodic Surface

For the case of separable periodic surface where $f(x,y)=h(x)+g(y)$ the potential integrals of $I_{mn}^{pq}$ can be separated into one dimensional integrals,

$$\begin{aligned} I_{mn}^{pq} &= \int_{\rm cell} {\rm d}^2\overline{r}' e^{i(\overline{k}_\perp^{pq}-\overline{k}_\perp^{mn})\cdot\overline{r}'_\perp + ik_z^{mn}f(\overline{r}'_\perp)} \\ &= \int_{L_x}{\rm d}x' \int_{L_y}{\rm d}y' e^{i(k_x^p-k_x^m)x'} e^{i(k_y^q-k_y^n)y'} e^{ik_z^{mn}h(x)} e^{ik_z^{mn}g(y)} \\ &= I_x^{mp} I_y^{nq} \end{aligned} \tag{5.10.1}$$

where typical one dimensional integrals of the form

$$I_x^{mp} = \int_{L_x}{\rm d}x' e^{i(k_x^p-k_x^m)x'} e^{ik_z^{mn}h(x)} \tag{5.10.2}$$

which is the Fourier transform of the $\exp\left[ik_z^{mn}h(x)\right]$ evaluated at $k_x=k_x^p-k_x^m$. This integral can be computed in closed form for a sinusoidal surface of $f(x)=A\cos(2\pi x/L_x)$. For this surface,

$$\begin{aligned} I_x^{mp} &= \int_{L_x}{\rm d}x' e^{i(p-m)2\pi x'/L_x} e^{ik_z^{mn}A\cos(2\pi x/L_x)} \\ &= \int_0^{2\pi}{\rm d}\theta e^{i(p-m)\theta} e^{ik_z^{mn}A\cos\theta} \end{aligned} \tag{5.10.3}$$

This is an integral of the form,

$$I = \int_0^{2\pi}{\rm d}\theta\ e^{im\theta} e^{\pm i\alpha\cos\theta} \quad , \quad \alpha\in\mathbb{C}, m\in\mathbb{Z} \tag{5.10.4}$$

Form the integral representation of Bessel function of the first kind we have [93]

$$J_m(\alpha) = \frac{1}{2\pi}\int_0^{2\pi}{\rm d}\theta e^{i\alpha\sin\theta - im\theta} \tag{5.10.5}$$

changing dummy variable according to $\theta \to \pi/2 - \theta$ we have

$$2\pi J_m(\alpha) e^{im\pi/2} = \int_0^{2\pi} \mathrm{d}\theta e^{i\alpha\cos\theta + im\theta} \tag{5.10.6}$$

# Chapter 6

# Small Perturbation Method in Resonance Condition

## 6.1 Introduction

The small perturbation method has been studied for random rough surface scattering extensively [24, 29–39]. Recently, the method has been studied for multi-layered random rough surfaces [24, 30, 34] as an analytical method which has advantages over numerical methods for multiple rough interfaces. As the number of layers increases, Numerical methods become costly in CPU and memory. An application of the multi-layered medium is microwave remote sensing of ice sheets in the Arctic and Antarctica, where the snow layers have multi-layering of fluctuations of permittivity due to the snow accumulation patterns as well as rough interfaces between layers [41].

The small perturbation method must be carried out to the second order[24] for energy conservation in emissivity calculations. In carrying out the Small Perturbation Method, the higher order field is expressed in terms of a convolution of the layered medium Green's function with the lower order field, where the convolution is performed in the spectral domain. To calculate the emissivity, the energy is decomposed into the incoherent intensity and the coherent intensity followed by the spectral integration. In the incoherent intensity, integration is to be carried out over the visible radiation spectrum. However, In the coherent intensity, integration is to be carried out over the entire $k$ domain spectrum. In the case of a 1D rough surface with $z$ as the vertical direction and $x$ the horizontal direction (symmetry along $y$ direction), the spectral domain integrations that appear in the coherent and incoherent intensities are continuous integrals over $k_x$. However, in a layered dielectric structure, when a dielectric layer has higher dielectric constant than its surrounding media, discrete waveguide modes exist. Mathematically, the waveguide modes correspond to the poles in the Green's function, and lie on the real $k_x$ axis or close to the real $k_x$ axis for lossless and slightly lossy dielectric, respectively. In a multi-layered medium, it also becomes difficult to determine the location of these poles to set up an appropriate numerical integration grid. The existence of waveguide modes presents a difficulty for the implementation of the second order small perturbation method.

The case of waveguide modes in layered media has been addressed in the past for the higher orders of interaction [94–96]. In [94, 96], authors show that the waveguide modes can appear in the propagating part of the spectrum (Satellite Peaks) as a results of higher order of surface interaction. However, in second order perturbation waveguide poles are located in the evanescent part of the spectrum. In the case of random permittivity profile, when

SPM2 solution always has such singularities, we present a numerical approach to resolve the case of singular integrand appearing in power calculations of SPM2.

In this paper, we consider the second order small perturbation method for a layered geometry when the permittivity profile allows the existence of waveguide modes. Our proposed solution is analytical continuation of the integrands to the complex plane and use the Sommerfeld integration path (SIP) [97–99] to avoid possible poles on the real $k_x$ axis. Another advantage of using the SIP is that the pole locations do not need to be known to perform the integrations. The SIP is applied to the cases of lossy dielectrics, monotonic permittivity profiles, and permittivity profiles which support guided modes to show its robustness. It is also shown that the use of the Sommerfeld path presents no additional increase in CPU time versus integration over the real $k_x$ axis. We also compare the results with the T-matrix (Extended Boundary Condition) method [50] showing good agreement between our SPM2 alternative and the T-matrix method. The good agreement confirms the correctness of the method of the SIP in the presence of guided modes. The outline of the paper is as follows: In section 6.2, the formulation of SPM2 for a two layered media with random rough interfaces is derived in details using compact operator notations. This will help to explain the origin of the main problem which is singular behavior of SPM2 kernel functions. Then, we briefly discuss obtaining scattered field and scattered power in terms of surface fields. In section 6.4 the origin of pole singularities will be identified and an appropriate alternative path is introduced. Section 6.5 is dedicated to compare the SIP alternative to the T-matrix method. In the last section, comparison of the SIP alternative and the T-matrix method is given for the case of arbitrary number of layers with non-monotonic permittivity changes.

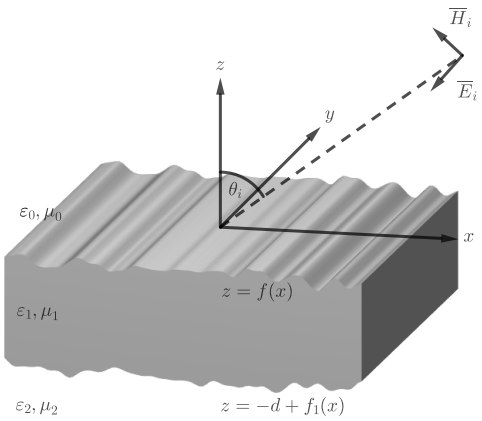


FIGURE 6.1: A dielectric slab sandwiched between to dielectric half spaces.

## 6.2 Problem Formulation

The small perturbation solution for the scattering of electromagnetic waves from multi-layer media with rough interfaces has been studied in detail in [24]. Here we formulate the

problem of a dielectric slab with two one-dimensional randomly rough surfaces, sandwiched between two semi-infinite dielectric media using a compact operator form which is more suitable for detection of the poles (Fig. 6.1). The formulation is based on the extinction theorem [3] and obtaining coupled surface integral equations for the surface fields on the interfaces. Application of the extinction theorem statement for region 0 in Fig. 6.1, results in

$$0=\psi_i(k_x)-\frac{i}{2k_z}\left[A_0(k_x)-ik_zB_0(k_x)+\int \mathrm{d}k'_x I_{00}^{-}(k_x,k'_x)\left\{A_0(k'_x)-B_0(k'_x)i\frac{k^2-k_xk'_x}{k_z}\right\}\right] \tag{6.2.1}$$

Here, $\psi_i(k_x)$ is the incident field ($\psi_i=E_{iy}$ and $\psi_i=H_{iy}$ for TE and TM polarizations, respectively) and $A(k_x)$ and $B(k_x)$ are spectral components of the surface magnetic and electric fields. On the first boundary, surface fields are defined as $a(x)\mathrm{d}x=\mathrm{d}l\hat{n}\cdot\nabla E_{0y}$ and $b(x)=E_{0y}(x)$ and related to the spectral fields by

$$\begin{aligned} a_0(x')&=\int \mathrm{d}k'_x A_0(k'_x)e^{ik'_x x'} \\ b_0(x')&=\int \mathrm{d}k'_x B_0(k'_x)e^{ik'_x x'} \end{aligned} \tag{6.2.2}$$

Also in (6.2.1), $I_{00}^{-}(k_x,k'_x)$ is the scattering potential due to the roughness of the first boundary described by $z=f_0(x)$ which is seen by downward propagating wave in the region 0 and is defined as

$$I_{00}^{-}(k_x,k'_x)=\frac{1}{2\pi}\int \mathrm{d}x' e^{-i(k_x-k'_x)x'}\left[e^{ik_zf_0(x')}-1\right] \tag{6.2.3}$$

Similarly, defining the surface fields $a_1(x)$ and $b_1(x)$ on the other boundary characterized by $z=f_1(x)-d$ and then applying the extinction theorem to region 1 and region 2, we can write an integral equation describing all of the surface unknowns in the spectral domain as

$$\overline{\overline{G}}_0(k_x)\overline{\psi}(k_x)+\int \mathrm{d}k'_x\ \overline{\overline{S}}(k_x,k'_x)\overline{\psi}(k'_x)=\overline{\psi}_i(k_x,k_{ix}) \tag{6.2.4}$$

Here $\overline{\psi}(k_x)=[A_0(k_x),B_0(k_x),A_1(k_x),B_1(k_x)]^T$ is the unknown surface field column vector and

$$\overline{\overline{G}}_0(k_x)=\begin{bmatrix} -\frac{i}{2k_z} & -\frac{1}{2} & 0 & 0 \\ \gamma_{01} & ik_{1z} & -e^{ik_{1z}d} & -ik_{1z}e^{ik_{1z}d} \\ \gamma_{01} & -ik_{1z} & -e^{-ik_{1z}d} & ik_{1z}e^{-ik_{1z}d} \\ 0 & 0 & \gamma_{12} & ik_{2z} \end{bmatrix} \tag{6.2.5}$$

is the propagator of the surface fields represented in the spectral domain corresponding to propagation of the fields inside the same layered media with flat interfaces. Also, the $\gamma_{ij}$'s are constant coefficients (coming from application of boundary conditions) which are $\gamma_{ij}=\mu_i/\mu_j$ and $\gamma_{ij}=\epsilon_i/\epsilon_j$ for TE and TM polarizations respectively. The presence of rough interfaces are described by the scattering operator $\overline{\overline{S}}(k_x,k'_x)$,

$$\overline{\overline{S}}(k_x,k'_x)=\begin{bmatrix} -\frac{i}{2k_z}I_{00}^{-} & -\frac{k^2-k_xk'_x}{2k_z^2}I_{00}^{-} & 0 & 0 \\ \gamma_{01}I_{10}^{+} & i\frac{k_1^2-k_xk'_x}{k_{1z}}I_{10}^{+} & -e^{ik_{1z}d}I_{11}^{+} & -e^{ik_{1z}d}i\frac{k_1^2-k_xk'_x}{k_{1z}}I_{11}^{+} \\ \gamma_{01}I_{10}^{-} & -i\frac{k_1^2-k_xk'_x}{k_{1z}}I_{10}^{-} & -e^{-ik_{1z}d}I_{11}^{-} & e^{-ik_{1z}d}i\frac{k_1^2-k_xk'_x}{k_{1z}}I_{11}^{-} \\ 0 & 0 & \gamma_{12}I_{21}^{+} & i\frac{k_2^2-k_xk'_x}{k_{2z}}I_{21}^{+} \end{bmatrix} \tag{6.2.6}$$

which is responsible for all orders of multiple scattering from each surface and also mutual interaction between the two boundaries. The scattering potential $I^{\pm}_{mn}(k_x,k'_x)$ has the following form

$$I^{\pm}_{mn}(k_x,k'_x)=\frac{1}{2\pi}\int \mathrm{d}x' e^{-i(k_x-k'_x)x'}\left[e^{\mp ik_{mz}f_n(x')}-1\right] \tag{6.2.7}$$

The integral equation of the surface fields can be cast into an operator equation (Lippmann-Schwinger equation) of the form,

$$G_0\psi+S\psi=\psi_i \tag{6.2.8}$$

where $S$ is the integral operator of the rough surface scattering. For small height where $||G_0||\gg||S||$, a formal solution can be obtained as

$$\psi=G_0^{-1}\sum_{n=0}^{\infty}\left[-G_0^{-1}S\right]^n\psi_i \tag{6.2.9}$$

$G_0^{-1}$ appears in all perturbation orders of the solution. As we will see, $G_0$ is singular at the internal resonance frequency $k_x$ that corresponds to the guided waves inside the dielectric slab with flat interfaces. At those values of $k_x$, $G_0$ is not invertible and make all of the perturbation orders of the solution singular. However, the solution to the Lippmann-Schwinger equation requires inversion of $(G_0+S)$ to obtain,

$$\psi=(G_0+S)^{-1}\psi_i \tag{6.2.10}$$

Even if $G_0$ is not an invertible operator at internal resonance frequencies, for a random interface, the operator $G_0+S$ is invertible with probability of 1. Therefore, the singularities in the solution is artificial and consequence of the iterative solution.

### 6.2.1 Perturbation solution of Surface field

In order to solve for the surface field $\overline{\psi}(k_x)$ we express it as a perturbation series

$$\overline{\psi}(k_x)=\overline{\psi}^{(0)}(k_x)+\overline{\psi}^{(1)}(k_x)+\overline{\psi}^{(2)}(k_x)+\cdots \tag{6.2.11}$$

and then iterate solution to find higher order surface fields.

#### Zeroth order solution

The zeroth order solution corresponds to the case of flat interfaces. The scattering potentials have been defined in such a way that they have no contribution to the zeroth order solution. In fact, if the waveguide modes exist for a particular configuration, they cannot be excited by an incident plane wave. Only a local source or perturbation such as a rough interface can excite the modes. The scattering operator kernel is zero up to the zeroth order

$$\overline{\overline{S}}^{(0)}(k_x,k'_x)=\overline{\overline{0}} \tag{6.2.12}$$

Thus, the zeroth order surface fields $\overline{\psi}^{(0)}(k_x)$ can be obtained easily from

$$\overline{\overline{G}}_0(k_x)\overline{\psi}^{(0)}(k_x)=\overline{\psi}_i(k_x,k_{ix})=-\delta(k_x-k_{ix})\begin{bmatrix}1 & 0 & 0 & 0\end{bmatrix}^T \tag{6.2.13}$$

Since the right hand side is non zero only for $k_x=k_{ix}$, equation (6.2.13) has a unique solution, if $\left|\overline{\overline{G}}_0(k_{ix})\right|\neq 0$

$$\overline{\psi}^{(0)}(k_x)=-\delta(k_x-k_{ix})\overline{\overline{G}}_0^{-1}(k_{ix})\overline{\psi}_i \tag{6.2.14}$$

Here we need to find how $\left|\overline{\overline{G}}_0(k_{ix})\right|$ behaves in order to examine the validity of solution(6.2.14). We will come back to this issue later in section (6.4).

**First order solution**

Balancing the integral equation of the surface fields to the first order we have ($\overline{\overline{G}}_0$ is non-perturbative )

$$\overline{\overline{G}}_0(k_x)\overline{\psi}^{(1)}(k_x)+\int \mathrm{d}k'_x\ \overline{\overline{S}}^{(1)}(k_x,k'_x)\overline{\psi}^{(0)}(k'_x)=0 \tag{6.2.15}$$

Using the zeroth order solution we have

$$\overline{\overline{G}}_0(k_x)\overline{\psi}^{(1)}(k_x)-\overline{\overline{S}}^{(1)}(k_x,k_{ix})\overline{\overline{G}}_0^{-1}(k_{ix})\overline{\psi}_i=0 \tag{6.2.16}$$

Now, if $\left|\overline{\overline{G}}_0(k_x)\right|\neq 0$ at a desired value of $k_x$, we can invert it to find

$$\overline{\psi}^{(1)}(k_x)=\overline{\overline{G}}_0^{-1}(k_x)\overline{\overline{S}}^{(1)}(k_x,k_{ix})\overline{\overline{G}}_0^{-1}(k_{ix})\overline{\psi}_i \tag{6.2.17}$$

However we will show that (see section 6.4) at a resonance condition when the permittivity of the slab ($\epsilon_1$) is larger than the surrounding medium ($\epsilon_0<\epsilon_1>\epsilon_2$), $\overline{\overline{G}}_0(k_x)$ is not invertible at the guided mode's cutoff frequency $k_x^g$, resulting in pole singularities in the spectral surface fields solution.

**Second order solution**

Balancing the integral equation of the surface fields to the second order results in

$$\overline{\overline{G}}_0(k_x)\overline{\psi}^{(2)}(k_x)+\int \mathrm{d}k'_x\ \overline{\overline{S}}^{(2)}(k_x,k'_x)\overline{\psi}^{(0)}(k'_x)+\int \mathrm{d}k'_x\ \overline{\overline{S}}^{(1)}(k_x,k'_x)\overline{\psi}^{(1)}(k'_x)=0 \tag{6.2.18}$$

By substituting the zeroth order solution we have

$$\overline{\overline{G}}_0(k_x)\overline{\psi}^{(2)}(k_x)-\overline{\overline{S}}^{(2)}(k_x,k_{ix})\overline{\overline{G}}_0^{-1}(k_{ix})\overline{\psi}_i+\int \mathrm{d}k'_x\ \overline{\overline{S}}^{(1)}(k_x,k'_x)\overline{\psi}^{(1)}(k'_x)=0 \tag{6.2.19}$$

Now if $\overline{\overline{G}}_0(k_x)$ is invertible, we can solve for second order fields as

$$\overline{\psi}^{(2)}(k_x)=\overline{\overline{G}}_0^{-1}(k_x)\overline{\overline{S}}^{(2)}(k_x,k_{ix})\overline{\overline{G}}_0^{-1}(k_{ix})\overline{\psi}_i-\overline{\overline{G}}_0^{-1}(k_x)\int \mathrm{d}k'_x\ \overline{\overline{S}}^{(1)}(k_x,k'_x)\overline{\psi}^{(1)}(k'_x) \tag{6.2.20}$$

Also substituting the first order surface fields of $\overline{\psi}^{(1)}(k_x)$, we obtain the second order solution as

$$\begin{aligned}\overline{\psi}^{(2)}(k_x)=&\overline{\overline{G}}_0^{-1}(k_x)\overline{\overline{S}}^{(2)}(k_x,k_{ix})\overline{\overline{G}}_0^{-1}(k_{ix})\overline{\psi}_i\\ &-\overline{\overline{G}}_0^{-1}(k_x)\int \mathrm{d}k'_x\ \overline{\overline{S}}^{(1)}(k_x,k'_x)\overline{\overline{G}}_0^{-1}(k'_x)\overline{\overline{S}}^{(1)}(k'_x,k_{ix})\overline{\overline{G}}_0^{-1}(k_{ix})\overline{\psi}_i\end{aligned} \tag{6.2.21}$$

## 6.3 Scattered and transmitted field

Using the spectral domain version of the equivalence principle applied to region 0 in Fig. 6.1, we can find the scattered field in region 0 as

$$\psi_s(k_x)=-\frac{i}{2k_z}\left[A_0(k_x)+ik_zB_0(k_x)+\int \mathrm{d}k'_x I^+_{00}(k_x,k'_x)\left\{A_0(k'_x)+B_0(k'_x)i\frac{k^2-k_xk'_x}{k_z}\right\}\right] \tag{6.3.1}$$

Here, $\psi_s=E_{sy}$ and $\psi_s=H_{sy}$ for TE and TM polarizations, respectively. The surface fields solution $A_0(k_x)$ and $B_0(k_x)$ are known up to the second order from the extinction equations. The scattering potential due to roughness of the first boundary experienced by the upward going wave in region 0 is

$$I^+_{00}(k_x,k'_x)=\frac{1}{2\pi}\int \mathrm{d}x' e^{-i(k_x-k'_x)x'}\left[e^{-ik_zf_0(x')}-1\right] \tag{6.3.2}$$

Similarly, the scattered field into region 2 (which is the transmitted field) can be obtained as

$$\psi_t(k_x)=\frac{i}{2k_{2z}}e^{-ik_{2z}d}\left[\gamma_{12}A_1(k_x)-ik_{2z}B_1(k_x)+\int \mathrm{d}k'_x I^-_{21}(k_x,k'_x)\left\{\gamma_{12}A_1(k'_x)-B_1(k'_x)i\frac{k_2^2-k_xk'_x}{k_{2z}}\right\}\right] \tag{6.3.3}$$

in terms of surface fields $A_1(k_x)$ and $B_1(k_x)$ which are defined on the second boundary. $I^-_{21}(k_x,k'_x)$ is the potential due to roughness of the second surface experienced by the downward traveling wave in region 2 and is given by

$$I^-_{21}(k_x,k'_x)=\frac{1}{2\pi}\int \mathrm{d}x' e^{-i(k_x-k'_x)x'}\left[e^{+ik_{2z}f_1(x')}-1\right] \tag{6.3.4}$$

If we define the scattered field column vector

$$\overline{\psi}_s(k_x)=\begin{bmatrix}\psi_s(k_x)\\ \psi_t(k_x)\end{bmatrix} \tag{6.3.5}$$

we can write relations (6.3.1) and (6.3.3) in a compact form

$$\overline{\psi}_s(k_x)=\overline{\overline{G}}^0_s(k_x)\overline{\psi}(k_x)+\int \mathrm{d}k'_x\ \overline{\overline{S}}_s(k_x,k'_x)\overline{\psi}(k'_x) \tag{6.3.6}$$

where $\overline{\overline{G}}^0_s(k_x)$ is the propagator of the scattered field in the layered media with flat interfaces and is given by

$$\overline{\overline{G}}^0_s(k_x)=\begin{bmatrix}-\frac{i}{2k_z} & \frac{1}{2} & 0 & 0\\ 0 & 0 & \frac{i}{2k_{2z}}e^{-ik_{2z}d}\gamma_{12} & \frac{1}{2}e^{-ik_{2z}d}\end{bmatrix} \tag{6.3.7}$$

$\overline{\overline{S}}_s(k_x,k'_x)$ is the scattering operator corresponding to the scattered field

$$\overline{\overline{S}}_s(k_x,k'_x)=\begin{bmatrix}-\frac{i}{2k_z}I^+_{00} & \frac{k^2-k_xk'_x}{2k_z^2}I^+_{00} & 0 & 0\\ 0 & 0 & \frac{i}{2k_{2z}}e^{-ik_{2z}d}\gamma_{12}I^-_{21} & e^{-ik_{2z}d}\frac{k_2^2-k_xk'_x}{2k_{2z}^2}I^-_{21}\end{bmatrix} \tag{6.3.8}$$

Now, we just need to insert the surface field solution into the governing relation of the scattered field (6.3.6)to find different orders of scattered fields.

### 6.3.1 Zeroth order scattered field

Balancing (6.3.6) up to the zeroth order, gives

$$\overline{\psi}_s^{(0)}(k_x)=\overline{\overline{G}}_s^0(k_x)\overline{\psi}^{(0)}(k_x) \tag{6.3.9}$$

Substituting the zeroth order solution of the surface fields 6.2.14 into (6.3.9) results in

$$\overline{\psi}_s^{(0)}(k_x)=-\delta(k_x-k_{ix})\overline{\overline{G}}_s^0(k_{ix})\overline{\overline{G}}_0^{-1}(k_{ix})\overline{\psi}_i \tag{6.3.10}$$

### 6.3.2 First order scattered field

Up to the first order of perturbation, the scattered field is

$$\overline{\psi}_s^{(1)}(k_x)=\overline{\overline{G}}_s^0(k_x)\overline{\psi}^{(1)}(k_x)+\int \mathrm{d}k'_x\ \overline{\overline{S}}_s^{(1)}(k_x,k'_x)\overline{\psi}^{(0)}(k'_x) \tag{6.3.11}$$

Using the zeroth and first order solution of the surface fields (6.2.14) and (6.2.17) we arrive at

$$\overline{\psi}_s^{(1)}(k_x)=\overline{\overline{G}}_s^0(k_x)\overline{\overline{G}}_0^{-1}(k_x)\overline{\overline{S}}^{(1)}(k_x,k_{ix})\overline{\overline{G}}_0^{-1}(k_{ix})\overline{\psi}_i-\overline{\overline{S}}_s^{(1)}(k_x,k_{ix})\overline{\overline{G}}_0^{-1}(k_{ix})\overline{\psi}_i \tag{6.3.12}$$

Now, we can split the scattering operators $\overline{\overline{S}}^{(1)}$ and $\overline{\overline{S}}_s^{(1)}$ into two parts, one corresponds to the effect of roughness due to the first boundary $\overline{\overline{S}}_{F_0}^{(1)}$ and the other due to the presence of the second boundary $\overline{\overline{S}}_{F_1}^{(1)}$. For $\overline{\overline{S}}_s^{(1)}(k_x,k_{ix})$, we can write it as

$$\overline{\overline{S}}_s^{(1)}(k_x,k_{ix})=\overline{\overline{S}}_{s,F_0}^{(1)}(k_x,k_{ix})F_0(k_x-k_{ix})+\overline{\overline{S}}_{s,F_1}^{(1)}(k_x,k_{ix})F_1(k_x-k_{ix}) \tag{6.3.13}$$

Here

$$\overline{\overline{S}}_{s,F_0}^{(1)}(k_x,k_{ix})=\begin{bmatrix}-\frac{1}{2} & -i\frac{k^2-k_xk_{ix}}{2k_z} & 0 & 0\\ 0 & 0 & 0 & 0\end{bmatrix} \tag{6.3.14}$$

$$\overline{\overline{S}}_{s,F_1}^{(1)}(k_x,k_{ix})=\begin{bmatrix}0 & 0 & 0 & 0\\ 0 & 0 & -\frac{1}{2}e^{-ik_{2z}d}\gamma_{12} & e^{-ik_{2z}d}i\frac{k_2^2-k_xk_{ix}}{2k_{2z}}\end{bmatrix} \tag{6.3.15}$$

and $F_j(k_x)$ is the Fourier Transform of the $j-$th surface boundary $f_j(x)$. Using this separation, we can divide the first order scattered field into contributions from each rough interface,

$$\overline{\psi}_s^{(1)}(k_x)=\overline{\psi}_{s,F_0}^{(1)}(k_x)F_0(k_x-k_{ix})+\overline{\psi}_{s,F_1}^{(1)}(k_x)F_1(k_x-k_{ix}) \tag{6.3.16}$$

where

$$\overline{\psi}_{s,F_j}^{(1)}(k_x)=\left[\overline{\overline{G}}_s^0(k_x)\overline{\overline{G}}_0^{-1}(k_x)\overline{\overline{S}}_{F_j}^{(1)}(k_x,k_{ix})-\overline{\overline{S}}_{s,F_j}^{(1)}(k_x,k_{ix})\right]\overline{\overline{G}}_0^{-1}(k_{ix})\overline{\psi}_i \quad ,j=0,1 \tag{6.3.17}$$

### 6.3.3 Second order scattered field

Balancing (6.3.6) up to the second order of perturbation yields the second order scattered field in terms of different orders (0, 1, 2) of the surface field solution as

$$\overline{\psi}_s^{(2)}(k_x)=\overline{\overline{G}}_s^0(k_x)\overline{\psi}^{(2)}(k_x)+\int \mathrm{d}k_x'\ \overline{\overline{S}}_s^{(2)}(k_x,k_x')\overline{\psi}^{(0)}(k_x')+\int \mathrm{d}k_x'\ \overline{\overline{S}}_s^{(1)}(k_x,k_x')\overline{\psi}^{(1)}(k_x') \quad (6.3.18)$$

Using the zeroth and first order surface fields solution of (6.2.14) and (6.2.17) we have

$$\begin{aligned}\overline{\psi}_s^{(2)}(k_x)=&\overline{\overline{G}}_s^0(k_x)\overline{\psi}^{(2)}(k_x)-\overline{\overline{S}}_s^{(2)}(k_x,k_{ix})\overline{\overline{G}}_0^{-1}(k_{ix})\overline{\psi}_i \\ &+\int \mathrm{d}k_x'\ \overline{\overline{S}}_s^{(1)}(k_x,k_x')\overline{\overline{G}}_0^{-1}(k_x')\overline{\overline{S}}^{(1)}(k_x',k_{ix})\overline{\overline{G}}_0^{-1}(k_{ix})\overline{\psi}_i\end{aligned} \quad (6.3.19)$$

Similar to the decomposition of the first order scattering operator in (6.3.13), the second order scattering operator is written as

$$\overline{\overline{S}}_s^{(2)}(k_x,k_{ix})=\overline{\overline{S}}_{s,F_0}^{(2)}(k_x,k_{ix})F_0^{(2)}(k_x-k_{ix})+\overline{\overline{S}}_{s,F_1}^{(2)}(k_x,k_{ix})F_1^{(2)}(k_x-k_{ix}) \quad (6.3.20)$$

$F_j^{(2)}(k_x-k_{ix})$ is the convolution of the $j$-th surface spectrum $F_j$ with itself, which is evaluated at $k_x-k_{ix}$. The marginal second order scattering operators corresponding to the scattered field are given by

$$\begin{aligned}\overline{\overline{S}}_{s,F_0}^{(2)}(k_x,k_{ix})&=\frac{1}{2}\begin{bmatrix}\frac{ik_z}{2} & -\frac{k^2-k_xk_{ix}}{2} & 0 & 0\\ 0 & 0 & 0 & 0\end{bmatrix} \\ \overline{\overline{S}}_{s,F_1}^{(2)}(k_x,k_{ix})&=\frac{1}{2}\begin{bmatrix}0 & 0 & 0 & 0\\ 0 & 0 & -\frac{ik_{2z}}{2}e^{-ik_{2z}d}\gamma_{12} & -e^{-ik_{2z}d}\frac{k_2^2-k_xk_{ix}}{2}\end{bmatrix}\end{aligned} \quad (6.3.21)$$

Thus, the second order scattered field becomes

$$\begin{aligned}\overline{\psi}_s^{(2)}(k_x)=&\overline{\overline{G}}_s^0(k_x)\overline{\psi}^{(2)}(k_x)-F_0^{(2)}(k_x-k_{ix})\overline{\overline{S}}_{s,F_0}^{(2)}(k_x,k_{ix})\overline{\overline{G}}_0^{-1}(k_{ix})\overline{\psi}_i \\ &-F_1^{(2)}(k_x-k_{ix})\overline{\overline{S}}_{s,F_1}^{(2)}(k_x,k_{ix})\overline{\overline{G}}_0^{-1}(k_{ix})\overline{\psi}_i \\ &+\int \mathrm{d}k_x'\ F_0(k_x-k_x')F_0(k_x'-k_{ix})\overline{\overline{S}}_{s,F_0}^{(1)}(k_x,k_x')\overline{\overline{G}}_0^{-1}(k_x')\overline{\overline{S}}_{F_0}^{(1)}(k_x',k_{ix})\overline{\overline{G}}_0^{-1}(k_{ix})\overline{\psi}_i \\ &+\int \mathrm{d}k_x'\ F_0(k_x-k_x')F_1(k_x'-k_{ix})\overline{\overline{S}}_{s,F_0}^{(1)}(k_x,k_x')\overline{\overline{G}}_0^{-1}(k_x')\overline{\overline{S}}_{F_1}^{(1)}(k_x',k_{ix})\overline{\overline{G}}_0^{-1}(k_{ix})\overline{\psi}_i \\ &+\int \mathrm{d}k_x'\ F_1(k_x-k_x')F_0(k_x'-k_{ix})\overline{\overline{S}}_{s,F_1}^{(1)}(k_x,k_x')\overline{\overline{G}}_0^{-1}(k_x')\overline{\overline{S}}_{F_0}^{(1)}(k_x',k_{ix})\overline{\overline{G}}_0^{-1}(k_{ix})\overline{\psi}_i \\ &+\int \mathrm{d}k_x'\ F_1(k_x-k_x')F_1(k_x'-k_{ix})\overline{\overline{S}}_{s,F_1}^{(1)}(k_x,k_x')\overline{\overline{G}}_0^{-1}(k_x')\overline{\overline{S}}_{F_1}^{(1)}(k_x',k_{ix})\overline{\overline{G}}_0^{-1}(k_{ix})\overline{\psi}_i\end{aligned} \quad (6.3.22)$$

Before proceeding further, we take the statistical average of the scattered field. The mean field expression can be derived with less effort, since averaging of statistical expressions in the scattered field can be simplified greatly using

$$\begin{aligned}\langle F^{(2)}(k_x-k_{ix})\rangle&=\delta(k_x-k_{ix})\int \mathrm{d}k_x' W(k_x'-k_{ix}) \\ \langle F(k_x-k_x')F(k_x'-k_{ix})\rangle&=\delta(k_x-k_{ix})W(k_x'-k_{ix})\end{aligned} \quad (6.3.23)$$

The only assumption made in deriving (6.3.23) is that the surface processes are assumed to be stationary. The second order spectral mean scattered field $\langle\overline{\psi}_s^{(2)}(k_x)\rangle$ can be decomposed into linear contributions from each boundary, that is

$$\langle\overline{\psi}_s^{(2)}(k_x)\rangle=\delta(k_x-k_{ix})\int \mathrm{d}k_x'\Big[\langle\overline{\psi}_s^{(2)}\rangle_{W_0}W_0(k_x'-k_{ix})+\langle\overline{\psi}_s^{(2)}\rangle_{W_1}W_1(k_x'-k_{ix})\Big] \tag{6.3.24}$$

where

$$\begin{aligned}\langle\overline{\psi}_s^{(2)}\rangle_{W_0}=\Bigg\{&\overline{\overline{G}}_s^0(k_{ix})\overline{\overline{G}}_0^{-1}(k_{ix})\Big[\overline{\overline{S}}_{F_0}^{(2)}(k_{ix},k_{ix})-\overline{\overline{S}}_{F_0}^{(1)}(k_{ix},k_x')\overline{\overline{G}}_0^{-1}(k_x')\overline{\overline{S}}_{F_0}^{(1)}(k_x',k_{ix})\Big]\\&-\overline{\overline{S}}_{s,F_0}^{(2)}(k_{ix},k_{ix})+\overline{\overline{S}}_{s,F_0}^{(1)}(k_{ix},k_x')\overline{\overline{G}}_0^{-1}(k_x')\overline{\overline{S}}_{F_0}^{(1)}(k_x',k_{ix})\Bigg\}\overline{\overline{G}}_0^{-1}(k_{ix})\overline{\psi}_i\end{aligned} \tag{6.3.25}$$

$$\begin{aligned}\langle\overline{\psi}_s^{(2)}\rangle_{W_1}=\Bigg\{&\overline{\overline{G}}_s^0(k_{ix})\overline{\overline{G}}_0^{-1}(k_{ix})\Big[\overline{\overline{S}}_{F_1}^{(2)}(k_{ix},k_{ix})-\overline{\overline{S}}_{F_1}^{(1)}(k_{ix},k_x')\overline{\overline{G}}_0^{-1}(k_x')\overline{\overline{S}}_{F_1}^{(1)}(k_x',k_{ix})\Big]\\&-\overline{\overline{S}}_{s,F_1}^{(2)}(k_{ix},k_{ix})+\overline{\overline{S}}_{s,F_1}^{(1)}(k_{ix},k_x')\overline{\overline{G}}_0^{-1}(k_x')\overline{\overline{S}}_{F_1}^{(1)}(k_x',k_{ix})\Bigg\}\overline{\overline{G}}_0^{-1}(k_{ix})\overline{\psi}_i\end{aligned} \tag{6.3.26}$$

Here we assume that the two surface processes $f_0(x)$ and $f_1(x)$ are uncorrelated.

### 6.3.4 Scattered and transmitted power

The scattered field in region 0 can be written in spatial coordinates as

$$\psi_s(\overline{r})=\int \mathrm{d}k_x\psi_s(k_x)e^{ik_xx+ik_zz} \tag{6.3.27}$$

For different orders of the scattered field we have

$$\begin{aligned}\psi_s^{(0)}(\overline{r})&=\psi_s^{(0)}(k_{ix})e^{ik_{ix}+ik_{iz}z}\\\psi_s^{(1)}(\overline{r})&=\int \mathrm{d}k_xe^{ik_xx+ik_zz}\Big[\psi_{s,F_0}^{(1)}(k_x)F_0(k_x-k_{ix})+\psi_{s,F_1}^{(1)}(k_x)F_1(k_x-k_{ix})\Big]\\\langle\psi_s^{(2)}(\overline{r})\rangle&=e^{ik_{ix}+ik_{iz}}\int \mathrm{d}k_x'\Big[\langle\psi_s^{(2)}\rangle_{W_0}W_0(k_x'-k_{ix})+\langle\psi_s^{(2)}\rangle_{W_1}W_1(k_x'-k_{ix})\Big]\end{aligned} \tag{6.3.28}$$

Here $\psi_s=E_{sy}$ is the $y-$component of the electric field associated with the scattered wave for TE polarized incident field. The case of TM-polarized excitation can be obtained using duality principle The mean scattered power density can be expressed in terms of the electric field as

$$\langle\overline{S}_s\cdot\hat{z}\rangle=-\frac{1}{2}\mathrm{Im}\left[\frac{1}{k\eta}\left\langle E_{sy}\frac{\partial E_{sy}^*}{\partial z}\right\rangle\right] \tag{6.3.29}$$

Noting that the first order scattered field has zero mean, the coherent power density flowing upward can be written as

$$\langle\overline{S}_s\cdot\hat{z}\rangle_{\mathrm{coh}}=\frac{1}{2}\mathrm{Re}\left[\frac{k_{iz}}{k\eta}\left(|E_{sy}^{(0)}|^2+2\langle E_{sy}^{(2)}\rangle E_{sy}^{(0)*}\right)\right] \tag{6.3.30}$$

then we can decompose the coherent scattered power into zeroth order and second order parts

$$\langle \overline{S}_s \cdot \hat{z} \rangle_{\text{coh}}^{(0)} = \frac{1}{2} \text{Re} \left[ \frac{k_{iz}}{k\eta} |E_{sy}^{(0)}|^2 \right] \tag{6.3.31}$$
$$\langle \overline{S}_s \cdot \hat{z} \rangle_{\text{coh}}^{(2)} = \text{Re} \left[ \frac{k_{iz}}{k\eta} \langle E_{sy}^{(2)} \rangle E_{sy}^{(0)*} \right]$$

The zeroth order scattered power is the power scattered by the same structure with flat boundaries. Using the second order mean scattered field 6.3.24 we have the coherent mean power density in $\hat{z}$ direction as

$$\begin{aligned} \langle \overline{S}_s \cdot \hat{z} \rangle_{\text{coh}}^{(2)} &= \int \text{d}k_x' \text{Re} \left[ \frac{k_{iz}}{k\eta} \psi_s^{(0)*}(k_{ix}) \left[ \langle \psi_s^{(2)} \rangle_{W_0} W_0(k_x' - k_{ix}) + \langle \psi_s^{(2)} \rangle_{W_1} W_1(k_x' - k_{ix}) \right] \right] \\ &= \sum_{j=0,1} \int \text{d}k_x' \Phi_{s,j}^{\text{coh}}(k_x') W_j(k_x' - k_{ix}) \end{aligned} \tag{6.3.32}$$

where we call $\Phi_{s,j}^{\text{coh}}(k_x')$, the $j-$th surface coherent scattered power spectral coefficient. The incoherent power originates from the first order scattered field

$$\langle \overline{S}_s \cdot \hat{z} \rangle_{\text{incoh}} = -\frac{1}{2} \text{Im} \left[ \frac{1}{k\eta} \left\langle E_{sy}^{(1)} \frac{\partial E_{sy}^{(1)*}}{\partial z} \right\rangle \right] = \frac{1}{2} \text{Re} \left[ \frac{k_z}{k\eta} \left\langle E_{sy}^{(1)} E_{sy}^{(1)*} \right\rangle \right] \tag{6.3.33}$$

However, assuming uncorrelated surface processes, we have

$$\langle \psi_s^{(1)}(\overline{r}) \psi_s^{(1)*}(\overline{r}) \rangle = \int \text{d}k_x \left[ |\psi_{s,F_0}^{(1)}(k_x)|^2 W_0(k_x - k_{ix}) + |\psi_{s,F_1}^{(1)}(k_x)|^2 W_1(k_x - k_{ix}) \right] \tag{6.3.34}$$

Therefore, the incoherent power density flowing in the $z$ direction can be written in terms of surface spectra

$$\langle \overline{S}_s \cdot \hat{z} \rangle_{\text{incoh}} = \frac{1}{2k\eta} \int \text{d}k_x \text{Re}(k_z) \left[ |\psi_{s,F_0}^{(1)}(k_x)|^2 W_0(k_x - k_{ix}) + |\psi_{s,F_1}^{(1)}(k_x)|^2 W_1(k_x - k_{ix}) \right] \tag{6.3.35}$$

and the transmitted power can be computed similarly. The connection between the spectral and spatial representation of the transmitted field into region 2 is as follows

$$\psi_t(\overline{r}) = \int \text{d}k_x \psi_t(k_x) e^{ik_x x - ik_{2z} z} \tag{6.3.36}$$

Following the same procedure as the scattered field, we have similar expression for the coherent and incoherent transmitted power densities along $(-\hat{z})$ direction

$$\langle \overline{S}_t \cdot \hat{z} \rangle_{\text{coh}}^{(2)} = \int \text{d}k_x' \text{Re} \left[ \frac{k_{2iz}}{k_2 \eta_2} \psi_t^{(0)*}(k_{ix}) \left[ \langle \psi_t^{(2)} \rangle_{W_0} W_0(k_x' - k_{ix}) + \langle \psi_t^{(2)} \rangle_{W_1} W_1(k_x' - k_{ix}) \right] \right] \tag{6.3.37}$$

$$\langle \overline{S}_t \cdot (-\hat{z}) \rangle_{\text{incoh}} = \frac{1}{2k\eta} \int \text{d}k_x \text{Re}(k_{2z}) \left[ |\psi_{t,F_0}^{(1)}(k_x)|^2 W_0(k_x - k_{ix}) + |\psi_{t,F_1}^{(1)}(k_x)|^2 W_1(k_x - k_{ix}) \right] \tag{6.3.38}$$

## 6.4 Waveguide modes and Sommerfeld integration path

In the case of resonance condition, when $\epsilon_0<\epsilon_1>\epsilon_2$, layered media can support guided modes at specific spectral frequencies $k_x^g$ for which $\left|\overline{\overline{G}}_0(k_x^g)\right|=0$. Surface field quantities which are governed by $\overline{\overline{G}}_0(k_x)$, will have pole singularities at $k_x=k_x^g$. The determinant of the flat surface layered media propagator $\overline{\overline{G}}_0(k_x)$ can be evaluated as

$$|\overline{\overline{G}}_0(k_x)|=\frac{-i}{k_z}e^{-ik_{1z}d}(\gamma_{01}k_z+k_{1z})(\gamma_{12}k_{1z}+k_{2z})\left[1+R_{01}(k_x)R_{12}(k_x)e^{2ik_{1z}d}\right] \tag{6.4.1}$$

where $k_{jz}^2+k_x^2=k_j^2$ and

$$\begin{aligned} R_{01}(k_x)&=\frac{\gamma_{01}k_z-k_{1z}}{\gamma_{01}k_z+k_{1z}} \\ R_{12}(k_x)&=\frac{\gamma_{12}k_{1z}-k_{2z}}{\gamma_{12}k_{1z}+k_{2z}} \end{aligned} \tag{6.4.2}$$

are electric field reflection coefficients from the two interfaces (assuming unbounded media). Also, $\gamma_{ij}=\epsilon_j/\epsilon_i$ for TM polarization and $\gamma_{ij}=\mu_j/\mu_i$ for a TE polarized wave. For simplicity, consider the case of TE polarized incident field and non-magnetic media. In this scenario, we do not have any depolarization and all of the field quantities preserve the incident polarization. In this case the determinant of $\overline{\overline{G}}_0(k_x)$ becomes

$$|\overline{\overline{G}}_0(k_x)|=\frac{-i}{k_z}e^{-ik_{1z}d}(k_z+k_{1z})(k_{1z}+k_{2z})\left[1+R_{01}(k_x)R_{12}(k_x)e^{2ik_{1z}d}\right] \tag{6.4.3}$$

The terms $(k_z+k_{1z})$ and $(k_{1z}+k_{2z})$ cannot be zero for distinct media (also, for the case of same media it will cancel out by the denominator). The only terms that can produce poles (eigenvalues of the propagator) comes from the expression

$$N(k_x)=1+R_{01}(k_x)R_{12}(k_x)e^{2ik_{1z}d} \tag{6.4.4}$$

For the lossless case and under guidance condition, $N(k_x)$ has real zeros at $k_x=k_x^g$ that will translate to real poles in the surface field solutions. These poles manifest themselves in both the first and second order surface fields.

In this situation, using the conventional definition of Fourier integrals to come back from spectral space to spatial space is illegal from a mathematical point of view. Computing the spectral integral over the real line contains only the principal value integral, and exact value of the integral is indefinite. Also from a physical point of view, singular behaviors should be investigated. On the other hand, a principal value integral has its own difficulties. First, we need to know the location of the poles which requires solving a nonlinear equation which is a time consuming task for real problems of random media with a large number of layers and ensemble of physical parameters, and second, when we know the poles' locations, it is necessary to use a dense numerical integration grid near the poles to capture the principal value integral correctly.

Instead of using spectral integrals over the real line, we will use the notion of analytic continuation of integrands and deform the path of integration into a Sommerfeld path alternative. This ensures definite values for the integrals and meaningful quantities in the

spectral domain. Therefore we need to formulate the problem by changing spectral integrals as

$$\int_{\mathbb{R}} \mathrm{d}k_x \Longrightarrow \int_{\mathrm{SIP}} \mathrm{d}k_x \tag{6.4.5}$$

In order to find the correct perturbed path of integration, or the Sommerfeld path of integration (SIP), we need to insert a small amount of loss such that propagating waves satisfy the radiation condition at infinity correctly. Then as the loss tends to zero we can identify the correct path of integration. Note that the SIP should work for a small loss condition, so this is our selection rule. In Fig. 6.2, with a small amount of loss, poles reside in the first quadrant (and also in the third quadrant). So for the lossless case, poles in the first quadrant merge to the real axis from the upper half plane. So, the appropriate SIP is passing through the second and fourth quadrants. Note also that branch cuts (compatible with the radiation condition) for a lossy problem start from the poles in the upper half plane and converge to the real axis. By this selection we avoid crossing any branch cuts.

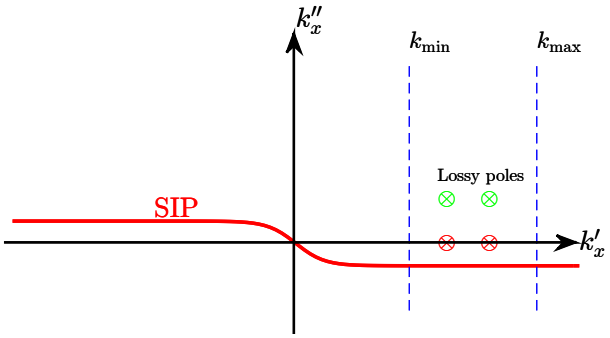


FIGURE 6.2: Appropriate Sommerfeld path of integration for the case of lossless layered dielectric media. SIP is chosen such that it does not pass over the poles or branch cuts of $k_{jz}$ $(j{=}0,1,2)$.

### 6.4.1 Sommerfeld Integration Path: Numerical Examples

In order to illustrate the concept, consider the special case of two layered media with lossless materials given by $\epsilon_0{=}\varepsilon_0$, $\epsilon_1{=}4\varepsilon_0$ and $\epsilon_2{=}2\varepsilon_0$ with separation of layers $d{=}0.7\lambda_0$ which can support a guided mode ($\lambda_0$ is free space wavelength). In this case we can find zeros of $N(k_x)$ numerically at $k_x{=}1.684k_0$ and $k_x{=}1.923k_0$. Both of the guided modes are evanescent in the $z$ direction in the upper and lower regions. For incoherent scattered and transmitted intensities, the averaged propagating power density (real part of the poynting vector) of Eqs. (6.3.35) and (6.3.38) are limited to the propagating part of the spectrum (because of $\mathrm{Re}(k_z)$ and $\mathrm{Re}(k_{2z})$ factors). In other words, the incoherent power spectral coefficients $(\Phi^{\mathrm{incoh}}_{s/t,j}(k_x))$ are only non-zero when $|k_x|{\leq}k_0$ and $|k_x|{<}k_2$ for reflected and transmitted power respectively. Thus, the poles at the eigen-mode frequencies $(k^g_x)$ do not appear in the incoherent part. This will happen only in the lossless case when $k_{jz}{=}\sqrt{k_j^2{-}k_x^2}$ is purely imaginary in the evanescent part of the spectrum $(|k_x|{>}k_j)$.

This is not the case with coherent intensities. Coherent intensities are not limited to propagating waves and they are non-zero over the whole spectrum. Therefore, we are faced with the guided modes singularities in the coherent part of the spectrum. In order to capture the total coherent power, theoretically, we need to integrate the coherent power spectral

coefficients up to infinity, but in practice, all of the surfaces are band limited in roughness and we only need to do integration over the spectrum up to some point ($k_{x,\max}$). Here we have two cases; 1 - The power spectral density of the surfaces $W_j(k_x)$, are very band-limited and decay quickly with increasing $k_x$ (very gentle surfaces with large correlation length). In this case we can put an appropriate cutoff for spectral quantities under the integrand ($k_{x,\max} \leq k_0$) and we are not worried about the poles which are always in the evanescent part of the spectrum. 2 - The power spectral densities of the surfaces do not decay rapidly enough (very rough surfaces with fast variations or small correlation length), so it may be necessary to continue integrating the coherent intensities to get a convergent result ($k_{x,\max} > k_0$). In this case the presence of the poles causes serious numerical problems in evaluating the spectral integrals [100, 101]. Figure 6.3, plots for power spectral coefficients

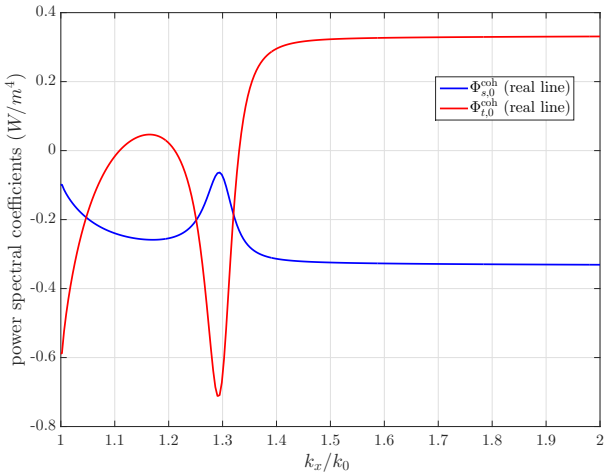


FIGURE 6.3: Coherent power spectral density of the first surface, for coherent scattered and transmitted power densities which are evaluated over the real $k_x$ axis. Physical parameters are $\epsilon_0 = \varepsilon_0, \epsilon_1 = 2\varepsilon_0, \epsilon_2 = 4\varepsilon_0$ and average distance between the surfaces is $0.7\lambda_0$ for the case of normal incidence. Coherent kernel functions $\Phi^{\text{coh}}_{s/t,j}(k_x)$, have no singularity in this case of monotonic dielectric variation.

of a two layer media with dielectric constant of (1,2,4) from top to bottom for normal incidence. Note that for the case of monotonic changes in permittivity, the coherent power spectral coefficients are smooth functions of $k_x$. On the other hand, Fig.6.4, plots the coherent power spectral coefficients of the first surface over the real line compared to the corresponding values over the SIP for dielectric constants of (1,4,2) from top to bottom. The integrands along the SIP are very gentle so the integrals can be computed accurately by a relatively coarse numerical integration grid. The price we pay is that we need to increase the integration interval over the SIP to get convergent results. On the other hand, in this way mesh refinement near poles is not necessary and a uniform grid works over the SIP. Choosing the parameters of the Sommerfeld path accordingly, one can greatly facilitate computation of spectral integrals.

Similarly, Fig. 6.5, plots the second surface power spectral coefficients over the real line and the SIP.

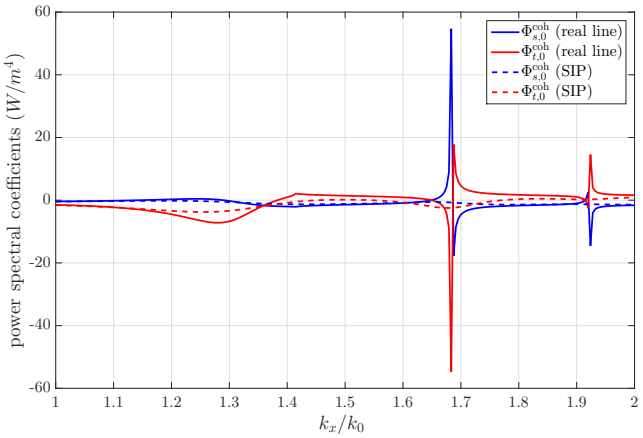


FIGURE 6.4: Coherent power spectral density of the first surface, for coherent scattered and transmitted power densities. Physical parameters are given in 6.4.1. Solid lines are power spectral densities evaluated over the real line which have singularities and cannot be integrated easily, while, dotted lines are the corresponding functions evaluated over the SIP. Variation of integrands is very gentle over the SIP compared to real line.

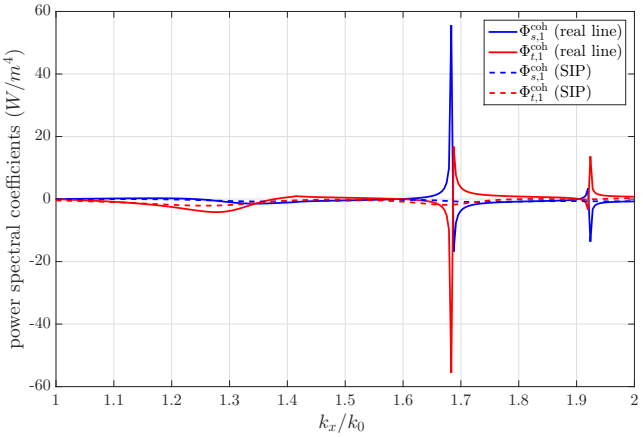


FIGURE 6.5: Coherent power spectral density of the second surface, for scattered and transmitted power. Physical parameters are given in 6.4.1. Solid lines, are power spectral densities evaluated over the real line which have singularities and cannot be integrated easily, while the dotted lines are the corresponding functions evaluated over the SIP. Variation of integrands is very gentle over the SIP compared to the real line.

### 6.4.2 SIP Implementation

Figure 6.6 shows a practical implementation of the SIP in the complex $k_x$-plane. Here, we need to choose appropriate values for the real cutoff wavenumber $k'_{x,\max}$ and the maximum deviation of path from the real axis $k''_{x,\max}$. The former is determined by how rapidly the power spectral densities of the surfaces $W_j(k_x)$ attenuate along the $k'_x$ axis. For the latter, in principle we can go up (down) the imaginary axis as high as we want. However, for practical cases taking $k''_{x,\max}$ in the order of $1/d$ ($d$ is the separation between the interfaces) results

in smooth kernel functions. Taking $k''_{x,\max}$ very large requires a larger integration domain $k'_{x,\max}$ to obtain convergent results. We need also to choose the discretization resolution

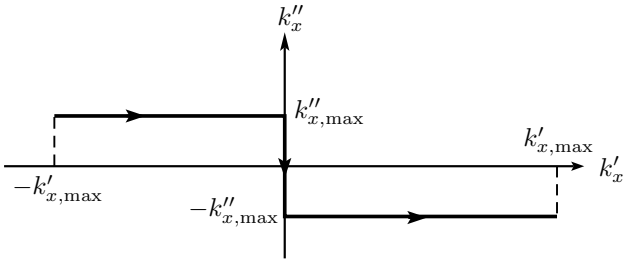


FIGURE 6.6: SIP in the complex $k_x$-plane.

along the real and imaginary axes. Since we do not use the pole locations, we can use a uniform numerical quadrature along the real $k_x$ axis with the grid spacing of $\Delta k'_x$. However For a uniform quadrature, the error term is negligible if

$$\Delta k'_x \ll k''_{x,\max} \tag{6.4.6}$$

For the examples in 6.4.1, we have used $k''_{x,\max}=\frac{0.2}{d}$ and $k'_{x,\max}=2\max\Big[k_0,k_1,k_2\Big]$. Also discretization steps along the real axis are chosen to be $\Delta k'_x=0.2k''_{x,\max}$. The cost for doing the spectral integral in the presence of guided modes using the SIP is not more than required in the regular case (which is the real line spectral integration).

## 6.5 Comparison with the T-matrix method

The T-Matrix method (also known as extended boundary condition method) is another powerful approach to compute electromagnetic scattering from random surfaces[50] . If the surface of interest is periodic, we can use Bloch modes as an expansion function for the surface fields. In this way, from the spectral point of view, there are only discrete values of propagation constants for the scattered and transmitted fields. For a sufficiently large period of the surface, the number of propagating Floquet modes becomes so large that it can be considered realistically as a continuous solution of an infinite surface. Thus, for large period surfaces, the T-Matrix solution coincides with the solution for an infinite surface problem. Apart from considering the finite period for the surfaces instead of infinite surfaces, the T-Matrix method has no approximation. In principle, it works for any surface height, correlation length and any dielectric constants, however, in practice it suffers from numerical issues for some cases (large RMS height, small correlation length and high dielectric contrast) and needs to be regularized.

For the first comparison, consider layered media with physical parameters of $\epsilon_0=\varepsilon_0$, $\epsilon_1=2\varepsilon_0$ and $\epsilon_2=4\varepsilon_0$ which is the case that cannot support guided modes. Boundary surfaces are considered to be Gaussian correlated, Gaussian random processes with statistical parameters given by $h_{\rm rms}=0.03\lambda_0$ and correlation length of $l=\lambda_0$ where $\lambda_0$ is the free space wavelength. For the T-matrix method we have generated an ensemble of Gaussian periodic random surfaces with Gaussian correlation function. It turns out that for the given physical parameters for the two layered structure, the solution converges after averaging over

≈50 realizations. In order to simulate an infinite surface, the period of the surface $L$ is selected as $L=20\lambda_0$). Each realization of the surface is characterized by 1024 samples (≈ 51 samples/$\lambda_0$) for highly accurate computation of integrals. Figure 6.7, compares emissiv-

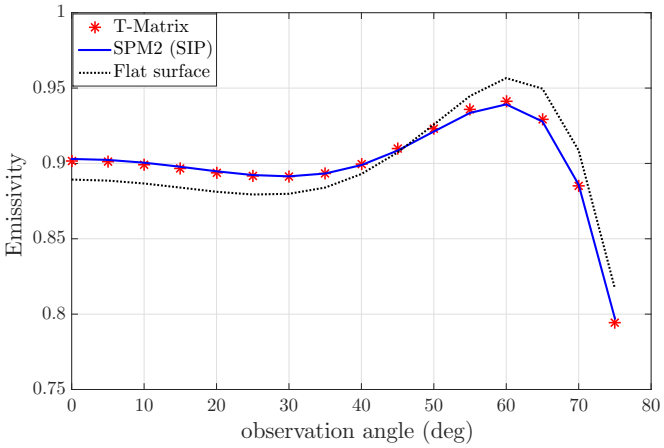


FIGURE 6.7: Emissivity of two layer media with permittivities of $\epsilon_0=\varepsilon_0$, $\epsilon_1=2\varepsilon_0$ and $\epsilon_2=4\varepsilon_0$ as a function of observation angle. Distance between two half spaces (region 1 thickness) is considered to be $d=0.7\lambda_0$. For this case where there is no supported guided mode inside the media, SPM2 results coincide with T-Matrix method solution. The dotted line corresponds to the flat boundary limit (presence of roughness smooths out coherence effect due to reflections from boundaries).

ity versus observation angle obtained by integrating SPM2 kernels over the SIP with the T-Matrix method solution and the case of zero RMS height (flat surfaces) for the regular case where there are no guided modes in the structure (permittivities are $\varepsilon_0$,$2\varepsilon_0$,$4\varepsilon_0$ from top). In this case, integrating over the SIP for SPM2 kernels gives the same results as the real line integration. For the regular cases (where no mode is supported within the slab), SPM2 kernel functions are smooth and integration over SIP and real line exactly coincide each other. We may conclude that for the regular case the SIP is a valid path of integration and results in correct evaluation of the spectral integrals. Comparison with flat surface emissivity also shows the level of accuracy of SPM2 in including the roughness effect.

As a second example, we consider the case where we encounter guided mode pole in the structure. In order to see how the SIP works in this case, consider the previous configuration with region 1 and 2 interchanged, i.e. $\epsilon_0=\varepsilon_0$, $\epsilon_1=4\varepsilon_0$ and $\epsilon_2=2\varepsilon_0$, with other physical parameters kept fixed. Here, this structure can support guided mode, and we have pole singularities in the kernel functions of scattered and transmitted powers. Figure 6.8, compares the T-Matrix solution of emissivity versus observation angle, with 1) SPM2 kernel functions integrated over an appropriate SIP , 2) SPM2 kernels integrated over the real line with 100 times finer grid, and 3) zero roughness limit (flat surfaces). Note that in both cases of real line and SIP integration, we did not use the location of the poles. As can be seen from Figs.6.7 and 6.8, the SIP not only works for the regular case, but also is successful in the presence of guided modes, while the real line integral yields erroneous predictions. This indicates that pole singularities can be avoided with only a moderate impact on the integration approach, while continued use of the real line even with very fine resolution remains problematic.

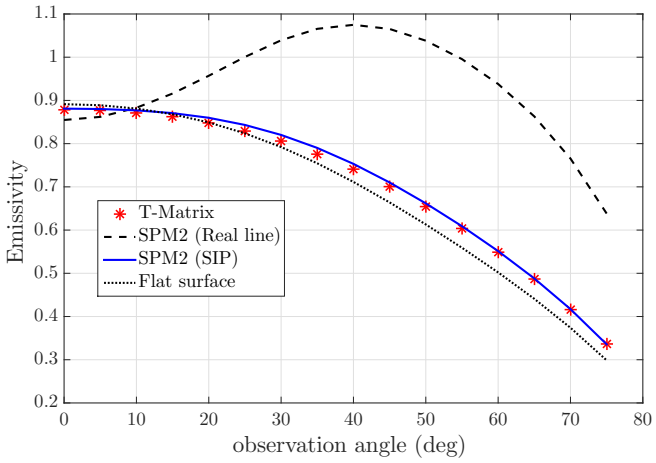


FIGURE 6.8: Emissivity of two layer media with permittivities of $\epsilon_0=\varepsilon_0$, $\epsilon_1=4\varepsilon_0$ and $\epsilon_2=2\varepsilon_0$ as a function of observation angle. Distance between two half spaces (thickness of region 1 ) is considered to be $d=0.7\lambda_0$. For this case where there are supported guided modes inside the media, emissivity obtained by integrating SPM2 power kernels over the SIP are in very good agreement with the T-Matrix method solution. Dashed line is corresponding to SPM2 integrated kernel functions over the real line with 100 times finer uniform grid. Real line integration despite 100 times higher computational cost results in non-physical results.

## 6.6 Extension to arbitrary number of Layers

Generalizing the approach to the multi-layer case is straightforward. In this case the integral equations which are related to the extinction of waves in the interior layers are homogeneous [24]. Then, homogeneous integral equations can be cast into recursive ladder propagation matrices for the surface fields over the rough boundaries. We do not repeat the procedure here and refer the reader to [24] for a detailed formulation of the problem using ladder operators.

In order to show the validity of the Sommerfeld alternative in multi-mode conditions in a multi-layer medium, consider a stack of 5 media separated by 4 random rough surfaces. We select the permittivity of the layers such that the structure supports guided modes. In this example permittivity of the layers is considered to be $\epsilon_0=\varepsilon_0,\epsilon_1=3\varepsilon_0,\epsilon_2=2\varepsilon_0,\epsilon_3=4\varepsilon_0$ and $\epsilon_4=2\varepsilon_0$. Separation distances between the mean positions of interfaces are $d_1=0.3\lambda_0,d_2=0.7\lambda_0$ and $d_3=0.8\lambda_0$. The T-matrix solution for this case which includes 4 uncorrelated surface processes (all of them Gaussian correlated with RMS height of $h=0.03\lambda_0$ and correlation length of $l=1\lambda_0$), requiring averaging over a larger number of realizations compared to the 2 layers case. Here, we used an ensemble of 200 realizations (each realization contains 4 uncorrelated surface boundaries) for the emissivity response to converge.

Figure 6.9 plots the emissivity of the 5 layer structure (with given physical parameters above) obtained by the SIP alternative in comparison with the T-matrix solution and zero RMS height (flat surface) limit. The differences between the flat interface case and rough interfaces are larger in this case compared to just two layers. This also shows that the SIP can capture the impact of multi-layer roughness.

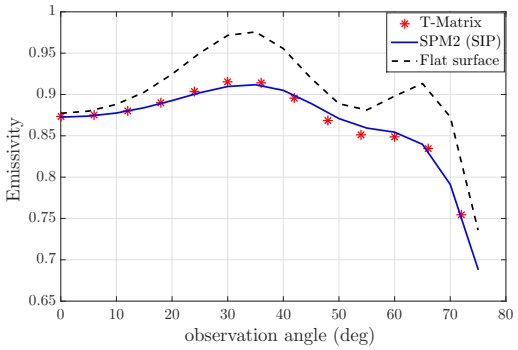


FIGURE 6.9: Emissivity of a 5 layer media with permittivities of $(1,3,2,4,2)\varepsilon_0$ from top to bottom, as a function of observation angle. Separations between the mean positions of interfaces are $d_1=0.3\lambda_0, d_2=0.7\lambda_0$ and $d_3=0.8\lambda_0$. For this case where there are many supported guided modes inside the media, emissivity obtained by integrating SPM2 power kernels over the SIP are in very good agreement with the T-Matrix method solution. Dashed line corresponds to the flat boundaries limit.

## 6.7 Conclusion

The application of SPM2 to multi-layer lossless structures (or with small amount of loss) with non-monotonic permittivity profiles, results in pole singularities in the integrands of the scattered power densities. It has been shown that we can compute power integrals very accurately at low cost using the Sommerfeld integration path alternative. The validity of the SIP approach for both monotonic and non-monotonic cases has been confirmed by comparing with the T-matrix method.

# Chapter 7

# Partially Coherent Cascading Scheme for Random Layered Media With Rough Interfaces

## 7.1 Introduction

Scattering of electromagnetic waves from layered media with random rough interfaces is an important problem in many applications in broad areas of science and engineering. The problem of scattering from rough interfaces has been studied extensively in physical modeling for remote sensing of the natural objects [102–106]. In particular, we are interested in multi-layered media with rough interfaces as a model for the microwave remote sensing of ice sheets in the Arctic and Antarctica [41, 78, 81, 84, 107, 108]. An ice sheet can be represented as a layered medium in which the permittivity (as well as the thickness) of a layer is a fluctuating function of depth due to the accumulation patterns of snow [41]. An additional statistical factor in the problem is presence of surface roughness at layer boundaries.

For a given dielectric constant profile in depth ($z$), the computation of electromagnetic wave scattering and emission can be solved in variety of ways [25, 30–32, 34, 38, 50, 80, 85, 109, 110]. However, in order to calculate the averaged quantities we need to run a Monte-Carlo simulation over realizations of the surface profiles. If the specifications of the problem are such that the Small Perturbation Method (SPM) [25, 35] is applicable, an analytical solution for the mean and variance of the fields is available that eliminates the need for Monte Carlo simulations [80].

Because the dielectric constant along $z$ is also random, a Monte-Carlo simulation over dielectric profile realizations is also required. Assuming that the number of layers ($N$) in the problem is very large, the number of required realizations to obtain a convergent solution can also be large (see **??**). Coherence properties of electromagnetic waves propagating in a random and turbulent atmosphere have been studied extensively [111–114]. The decay of coherence shown in these references suggests a method for enhancing efficiency in the computational of scattered fields [41]. In particular, if the dielectric profile has a finite correlation length along $z$, a wave propagating inside the layered medium will lose its phase coherency after traveling a distance of approximately the correlation length of the permittivity random process $\varepsilon(z)$. If the layered medium is therefore divided into blocks (Fig.7.1), each having a length larger than the correlation length of $\varepsilon(z)$, the fields within each block have some degree of coherency, and phase should be taken into account in the determination of the electromagnetic fields. However, it should also be reasonable to

model the fields in distinct blocks as having no phase relationships, so that the intensities, rather than fields, of adjacent blocks can be combined. Because Monte Carlo simulations of electromagnetic scattering or emission for a block having a smaller number of layers are known to converge more rapidly than those for a larger number of layers, this combined coherent-incoherent approach greatly reduces the number of required realizations to reach convergence. The cascading scheme for adjacent blocks can be developed based on power conservation arguments in two polarizations ($e$ or TE, and $h$ or TM).

In Section 7.2, a detailed definition of the problem is given, and Section 7.3 is dedicated to the scattering parameters within a block. In the next section, the method for cascading the intensities of two blocks is derived based on power conservation, and in Section 7.5 parameters of the equivalent block are extracted from the cascading equations. In the last section, the partially coherent developed is validated through numerical comparison between the coherent solution and an incoherent cascading of two blocks.

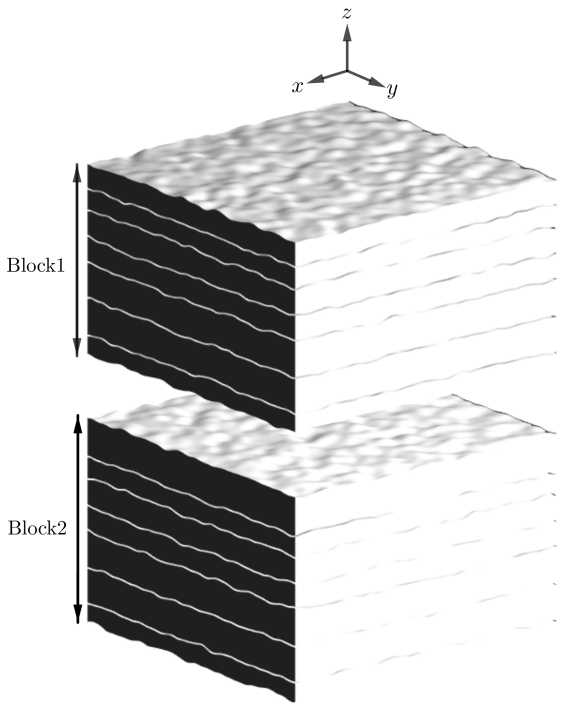


FIGURE 7.1: Two blocks of layered media with rough interfaces.

## 7.2 Problem statement

Consider the layered medium depicted in Fig. 7.1 in which the rough interfaces between layers are described as stationary and independent Gaussian processes having specified correlation functions; note that coordinate $z$ becomes more negative at greater depths within the ice sheet. The permittivity profile is also a stochastic process $\varepsilon(z)$ that is considered to be a Gaussian process with a Gaussian correlation function (other correlation function descriptions can also be used as long as they vanish for large separations). This

model can be considered a representation of an ice sheet. The ice sheet density (and associated permittivity) fluctuates in such a model [41] because of accumulation patterns of snowfall that contribute to the development of the ice sheet. For ice sheets, density fluctuations are expected to be smaller at greater depths where the pressure is higher; the variance of the permittivity can therefore be described as a damped Gaussian function along $z$. At coordinate $z=-H$ (below the ice sheet surface) the permittivity has an average of $\varepsilon(z)$ and a damped fluctuating part of $\delta\varepsilon(z)e^{z/\alpha}$ where

$$\langle\delta\varepsilon(z')\delta\varepsilon(z'-z)\rangle=\Delta^2 e^{-z^2/\ell_\varepsilon^2} \tag{7.2.1}$$

Here, $\alpha$ is the damping factor of the fluctuating part and $\Delta^2$ and $\ell_\varepsilon$ are the variance scale factor and correlation length of the permittivity profile, respectively. For a wave propagating between two points at distance $s\gg\ell_\varepsilon$, the permittivity is basically uncorrelated after this distance, and the wave acquires a random phase. When the phase becomes random, all the interference phenomena on average become zero, so that keeping track of the phase of the wave through the whole structure is unnecessary. If the structure is therefore divided into blocks with length $s\gg\ell_\varepsilon$ and the problem within a block solved coherently, we can cascade the intensities of adjacent blocks to obtain a solution for the entire layered medium. This idea has been implemented for the case of layered media with flat interfaces in [41], but the cost of averaging over dielectric realizations increases considerably when the interfaces have roughness.

## 7.3 Full Wave Solution within a Block

Consider a block of the layered medium of thickness $L_B$ which contains $N_B$ layers having rough interfaces. The electromagnetic response of this block can be characterized by its reflectivity and transmissivity pattern functions $\gamma_{\alpha\beta}(\theta_s,\phi_s;\theta_i,\phi_i)$ and $\xi_{\alpha\beta}(\theta_s,\phi_s;\theta_i,\phi_i)$ which are defined in terms of the corresponding vertical power flux densities as

$$\frac{\langle\overline{S}_s^{\alpha}\cdot\hat{z}\rangle}{\overline{S}_{\mathrm{i}}^{\beta}\cdot(-\hat{z})}=\int_{(2\pi)^+}\mathrm{d}\Omega_s\,\gamma_{\alpha\beta}(\theta_s,\phi_s;\theta_i,\phi_i) \tag{7.3.1}$$

$$\frac{\langle\overline{S}_t^{\alpha}\cdot(-\hat{z})\rangle}{\overline{S}_{\mathrm{i}}^{\beta}\cdot(-\hat{z})}=\int_{(2\pi)^-}\mathrm{d}\Omega_t\,\xi_{\alpha\beta}(\theta_t,\phi_t;\theta_i,\phi_i) \tag{7.3.2}$$

Here, $\beta$ and $\alpha$ are the source and response polarizations, and $\gamma_{\alpha\beta}$ and $\xi_{\alpha\beta}$ are the reflectivity and transmissivity of the block, respectively. The bracket $\langle\cdot\rangle$ denotes a statistical average over an ensemble of interface realizations.

### 7.3.1 Coherent Power

Coherent power contains zeroth order and second order terms. The zeroth order power does not depend on the statistic of the surfaces. However, the second order power term does. From the SPM2 solution of the coherent scattered power density,

$$\langle\overline{S}_s^{(2)e}\cdot\hat{z}\rangle_{\mathrm{coh}}=\frac{k_{1iz}}{k_1\eta_1}\int\mathrm{d}\overline{k}'_{\perp}\sum_{j=1}^{N-1}W_j(\overline{k}'_{\perp}-\overline{k}_{i\perp})\mathrm{Re}\Big[S_e^{(0)*}S_{e,W_j}^{(2)}(\overline{k}'_{\perp},\overline{k}_{i\perp})\Big] \tag{7.3.3}$$

$$\langle\overline{S}_s^{(2)h}\cdot\hat{z}\rangle_{\mathrm{coh}}=\frac{k_{1iz}}{k_1\eta_1}\int\mathrm{d}\overline{k}'_{\perp}\sum_{j=1}^{N-1}W_j(\overline{k}'_{\perp}-\overline{k}_{i\perp})\mathrm{Re}\Big[S_h^{(0)*}S_{h,W_j}^{(2)}(\overline{k}'_{\perp},\overline{k}_{i\perp})\Big]$$

From knowledge about the behavior of the power spectral coefficients, the dependence on azimuth angle is smooth. Therefore, in order to perform numerical integration, let us change spectral variable to spherical coordinates

$$\begin{aligned} k'_x &= k_1 \sin\theta'_k \cos\phi'_k \\ k'_y &= k_1 \sin\theta'_k \sin\phi'_k \end{aligned} \tag{7.3.4}$$

then $k_{1z}=k_1\cos\theta_k$. Also Jacobian of the transformation is

$$\mathrm{d}\overline{k}'_\perp = \mathrm{d}k'_x \mathrm{d}k'_y = k_1^2 \sin\theta'_k \cos\theta'_k \mathrm{d}\theta'_k \mathrm{d}\phi'_k = k_1^2 \cos\theta'_k \mathrm{d}\Omega'_k \tag{7.3.5}$$

As a result,

$$\begin{aligned} \langle \overline{S}_s^{(2)e} \cdot \hat{z} \rangle_{\mathrm{coh}} &= \frac{\cos\theta_i}{\eta_1} \int k_1^2 \cos\theta'_k \mathrm{d}\Omega'_k \sum_{j=1}^{N-1} W_j(\theta'_k, \phi'_k) \mathrm{Re}\left[ S_e^{(0)*} S_{e,W_j}^{(2)}(\theta'_k, \phi'_k) \right] \\ \langle \overline{S}_s^{(2)h} \cdot \hat{z} \rangle_{\mathrm{coh}} &= \frac{\cos\theta_i}{\eta_1} \int k_1^2 \cos\theta'_k \mathrm{d}\Omega'_k \sum_{j=1}^{N-1} W_j(\theta'_k, \phi'_k) \mathrm{Re}\left[ S_h^{(0)*} S_{h,W_j}^{(2)}(\theta'_k, \phi'_k) \right] \end{aligned} \tag{7.3.6}$$

On the other hand for incident power we have $\overline{S}_{\mathrm{i}}^{\beta} \cdot (-\hat{z}) = 1/2\eta_1 \cos\theta_i$. Therefore, normalized coherent reflectivity becomes

$$\begin{aligned} \frac{\langle \overline{S}_s^{(2)e} \cdot \hat{z} \rangle_{\mathrm{coh}}}{\overline{S}_{\mathrm{i}}^{\beta} \cdot (-\hat{z})} &= 2k_1^2 \int \mathrm{d}\Omega'_k \cos\theta'_k \sum_{j=1}^{N-1} W_j(\theta'_k, \phi'_k) \mathrm{Re}\left[ S_e^{(0)*} S_{e,W_j}^{(2)}(\theta'_k, \phi'_k) \right] \\ \frac{\langle \overline{S}_s^{(2)h} \cdot \hat{z} \rangle_{\mathrm{coh}}}{\overline{S}_{\mathrm{i}}^{\beta} \cdot (-\hat{z})} &= 2k_1^2 \int \mathrm{d}\Omega'_k \cos\theta'_k \sum_{j=1}^{N-1} W_j(\theta'_k, \phi'_k) \mathrm{Re}\left[ S_h^{(0)*} S_{h,W_j}^{(2)}(\theta'_k, \phi'_k) \right] \end{aligned} \tag{7.3.7}$$

Similarly for the transmitted power through the block, we can take

$$\begin{aligned} k'_x &= k_N \sin\theta'_k \cos\phi'_k \\ k'_y &= k_N \sin\theta'_k \sin\phi'_k \end{aligned} \tag{7.3.8}$$

Also Jacobian of the transformation is given by

$$\mathrm{d}\overline{k}'_\perp = \mathrm{d}k'_x \mathrm{d}k'_y = k_N^2 \sin\theta'_k \cos\theta'_k \mathrm{d}\theta'_k \mathrm{d}\phi'_k = k_N^2 \cos\theta'_k \mathrm{d}\Omega'_k \tag{7.3.9}$$

Assuming real permittivity for last layer (connecting layer), $\left(\frac{k_{Niz}}{k_N \eta_N}\right)^*$ is real and we have

$$\begin{aligned} \frac{\langle \overline{S}_t^{(2)e} \cdot (-\hat{z}) \rangle_{\mathrm{coh}}}{\overline{S}_{\mathrm{i}}^{\beta} \cdot (-\hat{z})} &= 2 \frac{\eta_1 \cos\theta_{Ni}}{\eta_N \cos\theta_i} k_N^2 \int \mathrm{d}\Omega'_k \cos\theta'_k \sum_{j=1}^{N-1} W_j(\theta'_k, \phi'_k) \mathrm{Re}\left[ T_{e,W_j}^{(2)}(\theta'_k, \phi'_k) T_e^{(0)*} \right] \\ \frac{\langle \overline{S}_t^{(2)h} \cdot (-\hat{z}) \rangle_{\mathrm{coh}}}{\overline{S}_{\mathrm{i}}^{\beta} \cdot (-\hat{z})} &= 2 \frac{\eta_1 \cos\theta_{Ni}}{\eta_N \cos\theta_i} k_N^2 \int \mathrm{d}\Omega'_k \cos\theta'_k \sum_{j=1}^{N-1} W_j(\theta'_k, \phi'_k) \mathrm{Re}\left[ T_{h,W_j}^{(2)}(\theta'_k, \phi'_k) T_h^{(0)*} \right] \end{aligned} \tag{7.3.10}$$

There is no depolarization effect in the coherent powers as it is proportional to the zeroth and second order fields that have no depolarization. In order to find the coherent reflectivity

and transmissivity functions, total coherent power density is normalized to the incident power density to get,

$$\frac{\langle \overline{S}_s^{(2)\alpha}\cdot\hat{z}\rangle_{\rm coh}}{\overline{S}_{\rm i}^{\beta}\cdot(-\hat{z})}+\frac{\langle \overline{S}_s^{(0)\alpha}\cdot\hat{z}\rangle_{\rm coh}}{\overline{S}_{\rm i}^{\beta}\cdot(-\hat{z})}=\int_{(2\pi)}{\rm d}\Omega_s\,\gamma_{\alpha\beta}^{\rm coh}(\theta_s,\phi_s;\theta_i,\phi_i) \tag{7.3.11}$$

$$\frac{\langle \overline{S}_t^{(2)\alpha}\cdot(-\hat{z})\rangle_{\rm coh}}{\overline{S}_{\rm i}^{\beta}\cdot(-\hat{z})}+\frac{\langle \overline{S}_t^{(0)\alpha}\cdot(-\hat{z})\rangle_{\rm coh}}{\overline{S}_{\rm i}^{\beta}\cdot(-\hat{z})}=\int_{(2\pi)}{\rm d}\Omega_t\,\xi_{\alpha\beta}^{\rm coh}(\theta_t,\phi_t;\theta_i,\phi_i)$$

Since the coherent power exists only in the specular direction (it is characterized by a number) and is concentrated in one direction, we have

$$\gamma_{\alpha\beta}^{\rm coh}(\theta_s,\phi_s;\theta_i,\phi_i)=\delta_{\alpha\beta}\delta(\phi_s-\phi_i)\delta(\cos\theta_s-\cos\theta_i) \tag{7.3.12}$$
$$\times\left[r_\alpha^{(0)}+2k_1^2\int{\rm d}\Omega_k'\cos\theta_k'\sum_{j=1}^{N-1}W_j(\theta_k',\phi_k'){\rm Re}\left[S_e^{(0)*}S_{e,W_j}^{(2)}(\theta_k',\phi_k')\right]\right]$$

and for coherent transmissivity function,

$$\xi_{\alpha\beta}^{\rm coh}(\theta_t,\phi_t;\theta_i,\phi_i)=\delta_{\alpha\beta}\delta(\phi_t-\phi_i)\delta(\cos\theta_t-\cos\theta_{it}) \tag{7.3.13}$$
$$\times\left[t_\alpha^{(0)}+2\frac{\eta_1\cos\theta_{Ni}}{\eta_N\cos\theta_i}k_N^2\int{\rm d}\Omega_k'\cos\theta_k'\sum_{j=1}^{N-1}W_j(\theta_k',\phi_k'){\rm Re}\left[T_{\alpha,W_j}^{(2)}(\theta_k',\phi_k')T_\alpha^{(0)*}\right]\right]$$

Notice that here, the angles $(\theta_k',\phi_k')$ are not observable angles. In fact these angles correspond to the intermediate scattering processes that results in the second order field (which is of the second order of multiple scattering).

### 7.3.2 Incoherent power

From the SPM2 solution of the layered media, the incoherent scattered and transmitted power densities are calculated as

$$\langle \overline{S}_s^{(2)}\cdot\hat{z}\rangle_{\rm inc}=\frac{1}{2k_1\eta_1}\int{\rm d}\overline{k}_\perp{\rm Re}(k_{1z})\left\{\sum_{j=1}^{N-1}\left[\left|S_{e,F_j}^{(1)}(\overline{k}_\perp)\right|^2+\left|S_{h,F_j}^{(1)}(\overline{k}_\perp)\right|^2\right]W_j(\overline{k}_\perp-\overline{k}_{i\perp})\right\}$$

$$\langle \overline{S}_t^{(2)}\cdot(-\hat{z})\rangle_{\rm inc}={\rm Re}\frac{1}{2\eta_N^*}\int{\rm d}\overline{k}_\perp\left\{\sum_{j=1}^{N-1}\left[\frac{k_{Nz}^*}{k_N^*}\left|T_{e,F_j}^{(1)}(\overline{k}_\perp)\right|^2+\frac{k_{Nz}}{k_N}\left|T_{h,F_j}^{(1)}(\overline{k}_\perp)\right|^2\right]W_j(\overline{k}_\perp-\overline{k}_{i\perp})\right\}$$

Notice that the incoherent power densities include cross polarized intensities for given polarization of incident field. For lossless connecting media, where $k_1$, and $k_N$ are real,only propagating part of the spectrum contributes to the incoherent power densities which is $|\overline{k}_\perp|\le k_1$ for scattered power and $|\overline{k}_\perp|\le k_N$ for the transmitted power. Therefore, the spectral integrals can be truncated just over the propagation band to yield

$$\langle \overline{S}_s^{(2)}\cdot\hat{z}\rangle_{\rm inc}=\frac{1}{2k_1\eta_1}\int_{|\overline{k}_\perp|\le k1}{\rm d}\overline{k}_\perp{\rm Re}(k_{1z})\left\{\sum_{j=1}^{N-1}\left[\left|S_{e,F_j}^{(1)}\right|^2+\left|S_{h,F_j}^{(1)}\right|^2\right]W_j(\overline{k}_\perp-\overline{k}_{i\perp})\right\} \tag{7.3.14}$$

$$\langle \overline{S}_t^{(2)}\cdot(-\hat{z})\rangle_{\rm inc}={\rm Re}\frac{1}{2\eta_N^*}\int_{|\overline{k}_\perp|\le k_N}{\rm d}\overline{k}_\perp\left\{\sum_{j=1}^{N-1}\left[\frac{k_{Nz}^*}{k_N^*}\left|T_{e,F_j}^{(1)}\right|^2+\frac{k_{Nz}}{k_N}\left|T_{h,F_j}^{(1)}\right|^2\right]W_j(\overline{k}_\perp-\overline{k}_{i\perp})\right\}$$

For the scattered power density upon change of the spectral integrations to the spherical coordinate it can be written as

$$\langle \overline{S}_s^{(2)} \cdot \hat{z} \rangle_{\text{inc}} = \frac{k_1^2}{2\eta_1} \int_0^{\pi/2} \mathrm{d}\theta_k \sin\theta_k \int_0^{2\pi} \mathrm{d}\phi_k \cos^2\theta_k \times \left\{ \sum_{j=1}^{N-1} \left[ \left| S_{e,F_j}^{(1)}(\theta_k,\phi_k) \right|^2 + \left| S_{h,F_j}^{(1)}(\theta_k,\phi_k) \right|^2 \right] W_j(\theta_k,\phi_k) \right\} \tag{7.3.15}$$

Also the incident power density is given by $\overline{S}_{\text{i}} \cdot (-\hat{z}) = \frac{1}{2\eta_1} \cos\theta_i$, therefore the total incoherent reflectivity of the structure becomes

$$\frac{\langle \overline{S}_s^{(2)} \cdot \hat{z} \rangle_{\text{inc}}}{\overline{S}_{\text{i}} \cdot (-\hat{z})} = \int_0^{\pi/2} \mathrm{d}\theta_k \sin\theta_k \int_0^{2\pi} \mathrm{d}\phi_k \frac{k_1^2 \cos^2\theta_k}{\cos\theta_i} \times \left\{ \sum_{j=1}^{N-1} \left[ \left| S_{e,F_j}^{(1)}(\theta_k,\phi_k) \right|^2 + \left| S_{h,F_j}^{(1)}(\theta_k,\phi_k) \right|^2 \right] W_j(\theta_k,\phi_k) \right\} \tag{7.3.16}$$

If we define bistatic reflectivity (differential reflectivity) as

$$\frac{\langle \overline{S}_s^{(2)\alpha} \cdot \hat{z} \rangle_{\text{inc}}}{\overline{S}_{\text{i}}^{\beta} \cdot (-\hat{z})} = \int_{(2\pi)^+} \mathrm{d}\Omega_s \, \gamma_{\alpha\beta}^{\text{inc}}(\theta_s,\phi_s;\theta_i,\phi_i) \tag{7.3.17}$$

then

$$\gamma_{e\alpha}^{\text{inc}}(\theta_s,\phi_s;\theta_i,\phi_i) = \frac{k_1^2 \cos^2\theta_s}{\cos\theta_i} \sum_{j=1}^{N-1} \left| S_{e\alpha,F_j}^{(1)}(\theta_s,\phi_s;\theta_i,\phi_i) \right|^2 W_j(\theta_s,\phi_s) \tag{7.3.18}$$

$$\gamma_{h\alpha}^{\text{inc}}(\theta_s,\phi_s;\pi-\theta_i,\phi_i) = \frac{k_1^2 \cos^2\theta_s}{\cos\theta_i} \sum_{j=1}^{N-1} \left| S_{h\alpha,F_j}^{(1)}(\theta_s,\phi_s;\theta_i,\phi_i) \right|^2 W_j(\theta_s,\phi_s)$$

Similar to the incoherent reflectivity, the incoherent transmissivity can be defined in a similar way,

$$\langle \overline{S}_t^{(2)} \cdot (-\hat{z}) \rangle_{\text{inc}} = \frac{k_N^2}{2\eta_N} \int_0^{\pi/2} \mathrm{d}\theta_k \sin\theta_k \int_0^{2\pi} \mathrm{d}\phi_k \cos^2\theta_k \sum_{j=1}^{N-1} W_j(\theta_k,\phi_k) \left[ \left| T_{e,F_j}^{(1)} \right|^2 + \left| T_{h,F_j}^{(1)} \right|^2 \right]$$

If we define bistatic transmissivity through

$$\frac{\langle \overline{S}_t^{(2)\alpha} \cdot (-\hat{z}) \rangle_{\text{inc}}}{\overline{S}_{\text{i}}^{\beta} \cdot (-\hat{z})} = \int_{(2\pi)^-} \mathrm{d}\Omega_t \, \xi_{\alpha\beta}^{\text{inc}}(\theta_t,\phi_t;\theta_i,\phi_i) \tag{7.3.19}$$

it yields

$$\xi_{e\alpha}^{\text{inc}}(\theta_t,\phi_t;\theta_i,\phi_i) = \frac{\eta_1}{\eta_N} \frac{k_N^2 \cos^2\theta_t}{\cos\theta_i} \sum_{j=1}^{N-1} W_j(\theta_t,\phi_t) \left| T_{e\alpha,F_j}^{(1)}(\theta_t,\phi_t;\theta_i,\phi_i) \right|^2 \tag{7.3.20}$$

$$\xi_{h\alpha}^{\text{inc}}(\theta_t,\phi_t;\theta_i,\phi_i) = \frac{\eta_1}{\eta_N} \frac{k_N^2 \cos^2\theta_t}{\cos\theta_i} \sum_{j=1}^{N-1} W_j(\theta_t,\phi_t) \left| T_{h\alpha,F_j}^{(1)}(\theta_t,\phi_t;\theta_i,\phi_i) \right|^2$$

Here, the coherent and incoherent responses are solutions of Maxwell's equations that originally account for the phase of the fields correctly; if the SPM solution is used, the physical parameters should fall into validity region of SPM. However, any exact solution for a block parameters can also be used as the approach does not rely on the SPM [3, 45].

Under an isotropic correlation function assumption for passive emission from the layered media, the intensity inside the layered media does not depends on $\phi$. Also in this situation the reflectivity and transmissivity of each block depends on $\phi_i$ and $\phi_s$ through their difference only $\phi_s-\phi_i$, and we can do the integration over $\phi_s$ to redefine the reduced reflectivity (and transmissivity) of the block $\gamma_{1u}^{\alpha\beta}(\theta_s,\theta_i)$ which is independent of azimuth angles as

$$\gamma_{1u}^{\alpha\beta}(\theta_s,\theta_i)=\int_0^{2\pi} \mathrm{d}\phi_s \ \gamma_{1u}^{\alpha\beta}(\theta_s,\theta_i;\phi_s-\phi_i) \tag{7.3.21}$$

As a result, the reflectivity of the first block when it is excited from the top can be written as

$$\gamma_{1u}^{\alpha\beta}(\mu_s,\mu_i)=\gamma_{1u}^{\alpha,\mathrm{coh}}\delta_{\alpha\beta}\delta(\mu_s-\mu_i)+\gamma_{1u}^{\alpha\beta,\mathrm{inc}}(\mu_s,\mu_i) \tag{7.3.22}$$

Here, $\mu_{i,s}=\cos\theta_{i,s}$. Following these procedures, all other scattering functions can similarly be cast into the same form as Eq. 7.3.22. If the problem is not isotropic or we are interested in active remote sensing (response due to an excitation at given incident angle $\theta_i,\phi_i$), the dependence of scattering functions on $\phi_i$ and $\phi_s$ should be preserved.

## 7.4 Incoherent Connection of Blocks

Processes representing the reflection and transmission of intensity between two blocks are depicted in Fig. 7.2. Assuming a $\beta-$ polarized intensity impinging on the first block in direction $\theta_i$, we have a diffuse upward scattered intensity $I_s(\theta_s)$ back into the top medium of block 1 and a transmitted intensity $I_t(\theta_t)$ down to bottom of the block 2. Between blocks there exist overall upward and downward going $\alpha-$polarized intensities in direction $\theta$ denoted by $I_u^\alpha(\theta)$ and $I_d^\alpha(\theta)$. If we can solve for the scattered and transmitted intensities In the presence of two blocks ($I_s^\alpha$ and $I_t^\alpha$ in Fig. 7.2), then the reflectivity $\tilde{\gamma}_u^{\alpha\beta}$ and transmissivity $\tilde{\xi}_u^{\alpha\beta}$ of the equivalent block when it is excited from the top ($u$) would be

$$\tilde{\gamma}_u^{\alpha\beta}(\theta_s,\theta_i)=\frac{I_s^\alpha(\theta_s)}{I_i^\beta(\theta_i)}, \quad \tilde{\xi}_u^{\alpha\beta}(\theta_t,\theta_i)=\frac{I_t^\alpha(\theta_t)}{I_i^\beta(\theta_i)} \tag{7.4.1}$$

In order to connect the intensities, the reflectivity and transmissivity of each block when the block is excited from the top as well as bottom is required (Fig. 7.2). When block 1 is excited from the top region, relevant scattering functions are $\gamma_{1,u}^{\alpha\beta}$ and $\xi_{1,u}^{\alpha\beta}$ and obtained by the coherent solution of block 1. By invoking energy conservation, the different intensities

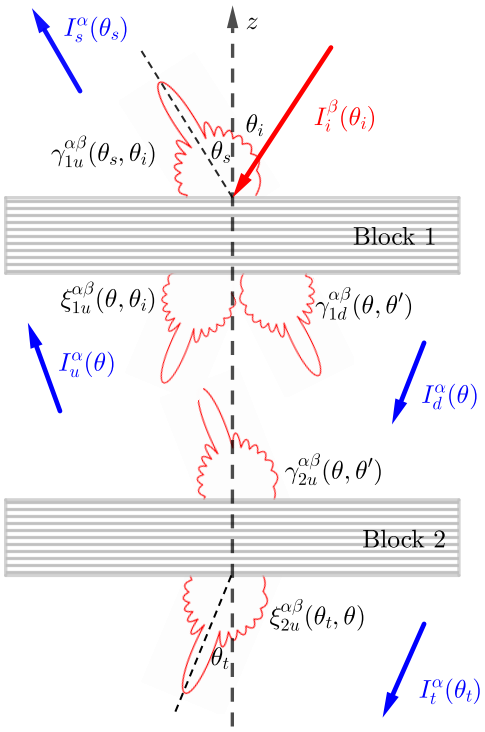


FIGURE 7.2: Incoherent connection of two blocks through the intensities. Overall upward and downward intensities in between blocks are $I_u^\alpha(\theta)$ and $I_d^\alpha(\theta)$, respectively.

are related through

$$
\begin{aligned}
I_s^\alpha(\mu) &= \sum_\beta \int_0^1 \mathrm{d}\mu' \left[\xi_{1d}^{\alpha\beta}(\mu,\mu') I_u^\beta(\mu') + \gamma_{1u}^{\alpha\beta}(\mu,\mu') I_i^\beta(\mu')\right] \\
I_d^\alpha(\mu) &= \sum_\beta \int_0^1 \mathrm{d}\mu' \left[\xi_{1u}^{\alpha\beta}(\mu,\mu') I_i^\beta(\mu') + \gamma_{1d}^{\alpha\beta}(\mu,\mu') I_u^\beta(\mu')\right] \\
I_u^\alpha(\mu) &= \sum_\beta \int_0^1 \mathrm{d}\mu' \, \gamma_{2u}^{\alpha\beta}(\mu,\mu') I_d^\beta(\mu') \\
I_t^\alpha(\mu) &= \sum_\beta \int_0^1 \mathrm{d}\mu' \; \xi_{2u}^{\alpha\beta}(\mu,\mu') I_d^\beta(\mu')
\end{aligned}
\tag{7.4.2}
$$

The system of equations (7.4.2) provides a direct determination of the coupling intensities on the left hand side given the intensities determined from a single block solution on the right hand side. Therefore the quantities on the left are directly determined from those on the right. For example, from Eq. 7.4.2, the total scattered $\alpha$-polarized intensity is a result of direct reflection of the incident intensity plus the transmission of upward going intensity $I_u^\beta$ through block 1 (from its bottom) by $\xi_{1d}^{\alpha\beta}$.

The energy conservation relations of Eqs. 7.4.2 constitute a system of coupled integral equations for $I_d$ and $I_u$. By eliminating $I_u$ we have

$$I_d^\alpha(\mu)=\sum_\beta \int_0^1 \mathrm{d}\mu' \xi_{1u}^{\alpha\beta}(\mu,\mu') I_i^\beta(\mu') \tag{7.4.3}$$
$$+\sum_{\beta,\eta} \int_0^1 \mathrm{d}\mu' \int_0^1 \mathrm{d}\mu'' \gamma_{1d}^{\alpha\beta}(\mu,\mu')\gamma_{2u}^{\beta\eta}(\mu',\mu'') I_d^\eta(\mu'')$$

The intermediate intensities $I_u$ and $I_d$ satisfy the multiple scattering equation Eq. 7.4.3. In order to solve it, we decompose each intensity in the problem into three terms, $I(\mu)=I^{(0)}(\mu)+I^{(1)}(\mu)+I^{(2)}(\mu)$ where the superscript shows total number of non-specular reflections and/or transmissions. The term with the (0) superscript corresponds to specular intensities that are related to specular reflection and transmission of the incident intensity from the boundaries of blocks. The first order intensity (1) contains just one bistatic (incoherent) reflection/transmission combined with specular reflection or transmission from other boundaries. The second order term (2) is a consequence of one bistatic reflection/transmission followed by another bistatic reflection/transmission. This expansion accounts for diffuse scattering up to the second order of diffuse multiple scattering and other higher order mechanisms can be neglected (as these are very small for the perturbative case). The system of Eq. 7.4.2 can then be solved for $I_u$ and $I_d$ by balancing orders of multiple scattering (collecting terms of the same order of diffuse scattering). Once the intermediate intensities are found, the reflected and transmitted intensities can be evaluated by the first and last relations of Eq. 7.4.2.

### 7.4.1 Zeroth Order Intensities

The zeroth order intensity is result of specular reflection at all of the boundaries. Balancing Eqs. (7.4.3) up to the zeroth order and noting that $I_i^\alpha(\mu)=I_i\delta(\mu-\mu_i)$, all the intensities become specular and

$$\begin{aligned}
I_s^{(0)\alpha}(\mu_s)&=\xi_{1d}^{\alpha,\mathrm{coh}}(\mu_s,\mu_I) I_u^{(0)\alpha}(\mu_I)+\gamma_{1u}^{\alpha,\mathrm{coh}}(\mu_s,\mu_i) I_i^\alpha(\mu_i) \\
I_d^{(0)\alpha}(\mu_I)&=\xi_{1u}^{\alpha,\mathrm{coh}}(\mu_I,\mu_i) I_i^\alpha+\gamma_{1d}^{\alpha,\mathrm{coh}}(\mu_I,\mu_I) I_u^{(0)\alpha}(\mu_I) \\
I_u^{(0)\alpha}(\mu_I)&=\gamma_{2u}^{\alpha,\mathrm{coh}}(\mu_I,\mu_I) I_d^{(0)\alpha}(\mu_I) \\
I_t^{(0)\alpha}(\mu_t)&=\xi_{2u}^{\alpha,\mathrm{coh}}(\mu_t,\mu_I) I_d^{(0)\alpha}(\mu_I)
\end{aligned} \tag{7.4.4}$$

where $\mu_I=\cos\theta_I$ and $\theta_I$ is the specular direction of propagation in the intermediate layer which is phased matched to the incident intensity in the direction $\theta_i$. From now on, when the argument of the coherent reflection/transmission is not mentioned explicitly, it is understood that it is evaluated in the corresponding specular direction. Note that the coherent reflection coefficients here include the reflection coefficient corrections due to the roughness of the blocks. Solving for the zeroth order intermediate intensities

$$I_d^{(0)\alpha}(\mu_I)=\frac{\xi_{1u}^{\alpha,\mathrm{coh}}(\mu_I,\mu_i)}{D^\alpha(\mu_I)} I_i^\alpha(\mu_i) \tag{7.4.5}$$

$$I_u^{(0)\alpha}(\mu_I)=\frac{\gamma_{2u}^{\alpha,\mathrm{coh}}(\mu_I,\mu_I)\xi_{1u}^{\alpha,\mathrm{coh}}(\mu_I,\mu_i)}{D^\alpha(\mu_I)} I_i^\alpha(\mu_i) \tag{7.4.6}$$

Here, $D^{\alpha}(\mu_I)=1-\gamma_{1d}^{\alpha,\mathrm{coh}}(\mu_I,\mu_I)\gamma_{2u}^{\alpha,\mathrm{coh}}(\mu_I,\mu_I)$ and is responsible for multiple reflections between the blocks.Then, the zeroth order reflected and transmitted intensities are given by

$$I_s^{(0)\alpha}=\left[\xi_{1d}^{\alpha,\mathrm{coh}}\frac{\gamma_{2u}^{\alpha,\mathrm{coh}}\xi_{1u}^{\alpha,\mathrm{coh}}}{D^{\alpha}}+\gamma_{1u}^{\alpha,\mathrm{coh}}\right]I_i^{\alpha} \tag{7.4.7}$$

$$I_t^{(0)\alpha}=\xi_{2u}^{\alpha,\mathrm{coh}}\frac{\xi_{1u}^{\alpha,\mathrm{coh}}}{D^{\alpha}}I_i^{\alpha}$$

This is identical to the traditional multi-layer Radiative Transfer solution [115].

### 7.4.2 First order intensities

Balancing (7.4.2) up to the first order terms for a general direction of $\mu$, we obtain

$$I_d^{(1)\alpha}(\mu)=\sum_{\beta}\int_0^1 \mathrm{d}\mu'\left[\gamma_{1d}^{\alpha\beta,\mathrm{inc}}(\mu,\mu')I_u^{(0)\beta}(\mu')+\gamma_{1d}^{\alpha,\mathrm{coh}}(\mu,\mu')I_u^{(1)\alpha}(\mu')+\xi_{1u}^{\alpha\beta,\mathrm{inc}}(\mu,\mu')I_i^{\beta}(\mu')\right] \tag{7.4.8}$$

$$I_u^{(1)\alpha}(\mu)=\sum_{\beta}\int_0^1 \mathrm{d}\mu'\left[\gamma_{2u}^{\alpha\beta,\mathrm{inc}}(\mu,\mu')I_d^{(0)\beta}(\mu')+\gamma_{2u}^{\alpha,\mathrm{coh}}(\mu,\mu')I_d^{(1)\alpha}(\mu')\right]$$

Using the fact that all of the zeroth order intensities are specular, the integrations can be performed to obtain

$$I_u^{(1)\alpha}(\mu)=\sum_{\beta}\left\{\gamma_{2u}^{\alpha\beta,\mathrm{inc}}(\mu,\mu_I)\frac{\xi_{1u}^{\beta,\mathrm{coh}}}{D^{\beta}(\mu_I)}+\frac{\gamma_{2u}^{\alpha,\mathrm{coh}}(\mu,\mu)}{D^{\alpha}(\mu)}\left[\xi_{1u}^{\alpha\beta,\mathrm{inc}}(\mu,\mu_i)+\frac{\xi_{1u}^{\beta,\mathrm{coh}}}{D^{\beta}(\mu_I)}\left(\gamma_{2u}^{\beta,\mathrm{coh}}\right.\right.\right. \tag{7.4.9}$$

$$\left.\left.\left.\times\gamma_{1d}^{\alpha\beta,\mathrm{inc}}(\mu,\mu_I)+\gamma_{1d}^{\alpha,\mathrm{coh}}(\mu,\mu)\gamma_{2u}^{\alpha\beta,\mathrm{inc}}(\mu,\mu_I)\right)\right]\right\}I_0^{\beta}$$

$$I_d^{(1)\alpha}(\mu)=\frac{1}{D^{\alpha}(\mu)}\sum_{\beta}\left[\xi_{1u}^{\alpha\beta,\mathrm{inc}}(\mu,\mu_i)+\frac{\xi_{1u}^{\beta,\mathrm{coh}}}{D^{\beta}(\mu_I)}\left(\gamma_{2u}^{\beta,\mathrm{coh}}\gamma_{1d}^{\alpha\beta,\mathrm{inc}}(\mu,\mu_I)\right.\right.$$

$$\left.\left.+\gamma_{1d}^{\alpha,\mathrm{coh}}(\mu,\mu)\gamma_{2u}^{\alpha\beta,\mathrm{inc}}(\mu,\mu_I)\right)\right]I_0^{\beta}$$

Inserting the first order intermediate intensities and balancing the scattered and transmitted intensity expression of Eq. 7.4.2 to the first order of multiple scattering gives

$$I_s^{(1)\alpha}(\mu)=\sum_{\beta}\left[\gamma_{1u}^{\alpha\beta,\mathrm{inc}}(\mu,\mu_i)+\xi_{1d}^{\alpha\beta,\mathrm{inc}}(\mu,\mu_I)\frac{\xi_{1u}^{\beta,\mathrm{coh}}\gamma_{2u}^{\beta,\mathrm{coh}}}{D^{\beta}}\right.$$

$$+\xi_{1d}^{\alpha,\mathrm{coh}}(\mu)\left\{\gamma_{2u}^{\alpha\beta,\mathrm{inc}}(\mu,\mu_I)\frac{\xi_{1u}^{\beta,\mathrm{coh}}}{D^{\beta}}+\frac{\gamma_{2u}^{\alpha,\mathrm{coh}}(\mu)}{D^{\alpha}(\mu)}\left[\xi_{1u}^{\alpha\beta,\mathrm{inc}}(\mu,\mu_i)+\frac{\xi_{1u}^{\beta,\mathrm{coh}}}{D^{\beta}}\left(\gamma_{2u}^{\beta,\mathrm{coh}}\gamma_{1d}^{\alpha\beta,\mathrm{inc}}(\mu,\mu_I)\right.\right.\right. \tag{7.4.10}$$

$$\left.\left.\left.\left.+\gamma_{1d}^{\alpha,\mathrm{coh}}(\mu)\gamma_{2u}^{\alpha\beta,\mathrm{inc}}(\mu,\mu_I)\right)\right]\right\}\right]I_0^{\beta}$$

$$I_t^{(1)\alpha}(\mu)=\sum_{\beta}\left[\xi_{2u}^{\alpha\beta,\mathrm{inc}}(\mu,\mu_I)\frac{\xi_{1u}^{\beta,\mathrm{coh}}}{D^{\beta}}+\frac{\xi_{2u}^{\alpha,\mathrm{coh}}(\mu)}{D^{\alpha}(\mu)}\left\{\xi_{1u}^{\alpha\beta,\mathrm{inc}}(\mu,\mu_i)\right.\right.$$

$$\left.\left.+\frac{\xi_{1u}^{\beta,\mathrm{coh}}}{D^{\beta}}\left(\gamma_{2u}^{\beta,\mathrm{coh}}\gamma_{1d}^{\alpha\beta,\mathrm{inc}}(\mu,\mu_I)+\gamma_{1d}^{\alpha,\mathrm{coh}}(\mu)\gamma_{2u}^{\alpha\beta,\mathrm{inc}}(\mu,\mu_I)\right)\right\}\right]I_0^{\beta} \tag{7.4.11}$$

Several mechanism of scattering involving combinations of coherent/incoherent scattering and transmission of intensity at the boundaries of the two blocks are apparent in these results, including 1- Diffuse scattering of the incident intensity by $\gamma_{1u}^{\alpha\beta,\text{inc}}(\mu,\mu_I)$; 2- Specular transmission through block 1 $\xi_{1u}^{\beta,\text{coh}}$ followed by another specular reflection off block 2 $\gamma_{2u}^{\beta,\text{coh}}$ and finally, diffuse transmission through block 1 to the direction $\mu$ by $\xi_{1d}^{\alpha\beta,\text{inc}}(\mu,\mu_I)$; 3- Specular transmission through block 1 $\xi_{1u}^{\beta,\text{coh}}$, diffuse reflection off block 2 $\gamma_{2u}^{\alpha\beta,\text{inc}}(\mu,\mu_I)$ followed by a specular transmission in direction $\mu$ to the top region $\xi_{1d}^{\alpha,\text{coh}}(\mu)$; 4- Diffuse transmission through block 1 by $\xi_{1u}^{\alpha\beta,\text{inc}}(\mu,\mu_i)$ , followed by specular reflection off block 2 $\xi_{2u}^{\alpha,\text{coh}}(\mu)$ and another specular transmission to the top region $\xi_{1d}^{\alpha,\text{coh}}(\mu)$; 5- Specular transmission through block 1 $\xi_{1u}^{\beta,\text{coh}}$, then a specular reflection off block 2 $\gamma_{2u}^{\beta\text{coh}}$ then a diffuse reflection off the bottom of block 1 $\gamma_{1d}^{\alpha\beta,\text{inc}}(\mu,\mu_I)$, followed by another specular reflection from block 2 $\gamma_{2u}^{\alpha,\text{coh}}(\mu)$ and finally, specular transmission through block 1 to the top region $\xi_{1d}^{\alpha,\text{coh}}(\mu)$; 6- The same process as 5 but here the intensity is reflected incoherently from block 2.

### 7.4.3 Second Order Intensities

Balancing Eq. 7.4.2 for the intermediate intensities $I_u$ and $I_d$ up to the second order of multiple scattering and substituting the specular scattering solution (zeroth order) we arrive at

$$I_d^{(2)\alpha}(\mu)=\frac{1}{D^\alpha(\mu)}\sum_\beta\int_0^1 \mathrm{d}\mu'\Bigg[\gamma_{1d}^{\alpha\beta,\text{inc}}(\mu,\mu')I_u^{(1)\beta}(\mu') + \gamma_{1d}^{\alpha,\text{coh}}(\mu,\mu)\gamma_{2u}^{\alpha\beta,\text{inc}}(\mu,\mu')I_d^{(1)\beta}(\mu')\Bigg] \tag{7.4.12}$$

$$I_u^{(2)\alpha}(\mu)=\frac{1}{D^\alpha(\mu)}\sum_\beta\int_0^1 \mathrm{d}\mu'\Bigg[\gamma_{2u}^{\alpha\beta,\text{inc}}(\mu,\mu')I_d^{(1)\beta}(\mu') + \gamma_{2u}^{\alpha,\text{coh}}(\mu,\mu)\gamma_{1d}^{\alpha\beta,\text{inc}}(\mu,\mu')I_u^{(1)\beta}(\mu')\Bigg] \tag{7.4.13}$$

Since the incident intensity does not enter into the second order multiple scattering directly, the second order equation of the intermediate intensities is symmetric under the transformation ($u\leftrightarrow d$) and (block 1$\leftrightarrow$block 2). The first order solution is known and it is not required to explicitly find $I_u^{(2)\alpha}(\mu)$ and $I_d^{(2)\alpha}(\mu)$. Instead the second order scattered intensity can be written in terms of the first order intermediate intensities,

$$I_s^{(2)\alpha}(\mu)=\sum_\beta\int_0^1 \mathrm{d}\mu'\,\xi_{1d}^{\alpha\beta,\text{inc}}(\mu,\mu')I_u^{(1)\beta}(\mu') + \frac{\xi_{1d}^{\alpha,\text{coh}}(\mu)}{D^\alpha(\mu)}\sum_\beta\int_0^1 \mathrm{d}\mu'\Bigg[\gamma_{2u}^{\alpha\beta,\text{inc}}(\mu,\mu')I_d^{(1)\beta}(\mu')+\gamma_{2u}^{\alpha,\text{coh}}(\mu)\gamma_{1d}^{\alpha\beta,\text{inc}}(\mu,\mu')I_u^{(1)\beta}(\mu')\Bigg] \tag{7.4.14}$$

and for the second order transmitted intensity

$$I_t^{(2)\alpha}(\mu)=\sum_\beta \int_0^1 \mathrm{d}\mu'\ \xi_{2u}^{\alpha\beta,\mathrm{inc}}(\mu,\mu')I_d^{(1)\beta}(\mu') \tag{7.4.15}$$
$$+\frac{\xi_{2u}^{\alpha,\mathrm{coh}}(\mu)}{D^\alpha(\mu)}\sum_\beta \int_0^1 \mathrm{d}\mu'\left[\gamma_{1d}^{\alpha\beta,\mathrm{inc}}(\mu,\mu')I_u^{(1)\beta}(\mu')+\gamma_{1d}^{\alpha,\mathrm{coh}}(\mu)\gamma_{2u}^{\alpha\beta,\mathrm{inc}}(\mu,\mu')I_d^{(1)\beta}(\mu')\right]$$

## 7.5 Equivalent Block parameters

After finding all scattered and transmitted intensities up to the second order, we can find the equivalent reflectivity and transmissivity of the combination of the two blocks.

### 7.5.1 Coherent Reflection and Transmission

By the way that the intensities are decomposed into different orders, only the zeroth order intensity is concentrated in the specular direction. Thus for the combination of two blocks, the overall reflectivity $\tilde{\gamma}_u^{\alpha,\mathrm{coh}}$ and transmissivity $\tilde{\xi}_u^{\alpha,\mathrm{coh}}$ when excited from the top can be found as

$$\tilde{\gamma}_u^{\alpha,\mathrm{coh}}=\frac{I_s^{(0)\alpha}}{I_0^\alpha}=\xi_{1d}^{\alpha,\mathrm{coh}}\frac{\xi_{1u}^{\alpha,\mathrm{coh}}\gamma_{2u}^{\alpha,\mathrm{coh}}}{1-\gamma_{1d}^{\alpha,\mathrm{coh}}\gamma_{2u}^{\alpha,\mathrm{coh}}}+\gamma_{1u}^{\alpha,\mathrm{coh}} \tag{7.5.1}$$
$$\tilde{\xi}_u^{\alpha,\mathrm{coh}}=\frac{I_t^{(0)\alpha}}{I_0^\alpha}=\xi_{2u}^{\alpha,\mathrm{coh}}\frac{\xi_{1u}^{\alpha,\mathrm{coh}}}{1-\gamma_{1d}^{\alpha,\mathrm{coh}}\gamma_{2u}^{\alpha,\mathrm{coh}}}$$

at zeroth order. Here all the single block coherent responses should be evaluated at the corresponding specular direction. In order to find equivalent coherent parameters when the combined block is excited from the bottom, $\tilde{\gamma}_d^{\alpha,\mathrm{coh}}$ and $\tilde{\xi}_d^{\alpha,\mathrm{coh}}$, we can make the changes $1u\Longleftrightarrow 2d$ and $2u\Longleftrightarrow 1d$ in the top excited parameters to obtain

$$\tilde{\gamma}_d^{\alpha,\mathrm{coh}}=\xi_{2u}^{\alpha,\mathrm{coh}}\frac{\xi_{2d}^{\alpha,\mathrm{coh}}\gamma_{1d}^{\alpha,\mathrm{coh}}}{1-\gamma_{1d}^{\alpha,\mathrm{coh}}\gamma_{2u}^{\alpha,\mathrm{coh}}}+\gamma_{2d}^{\alpha,\mathrm{coh}} \tag{7.5.2}$$
$$\tilde{\xi}_d^{\alpha,\mathrm{coh}}=\xi_{1d}^{\alpha,\mathrm{coh}}\frac{\xi_{2d}^{\alpha,\mathrm{coh}}}{1-\gamma_{1d}^{\alpha,\mathrm{coh}}\gamma_{2u}^{\alpha,\mathrm{coh}}}$$

Note that reciprocity mandates that $\xi_{1d}=\xi_{1u}$ and $\xi_{2d}=\xi_{2u}$ and for the equivalent block results $\tilde{\xi}_d^{\alpha,\mathrm{coh}}=\tilde{\xi}_u^{\alpha,\mathrm{coh}}$; this means that combined response satisfies reciprocity.

### 7.5.2 Incoherent Reflection and Transmission

Bistatic (diffuse) reflection and transmission are included in the first and second order intensity terms. Therefore the incoherent response of the equivalent block is

$$\tilde{\gamma}_u^{\alpha\beta,\mathrm{inc}}(\mu,\mu_i)=\frac{I_s^{(1)\alpha}(\mu)+I_s^{(2)\alpha}(\mu)}{I_0^\beta(\mu_i)} \tag{7.5.3}$$
$$\tilde{\xi}_u^{\alpha\beta,\mathrm{inc}}(\mu,\mu_i)=\frac{I_t^{(1)\alpha}(\mu)+I_t^{(2)\alpha}(\mu)}{I_0^\beta(\mu_i)}$$

In order to obtain the downward terms $\tilde{\gamma}_d^{\alpha\beta,\text{inc}}(\mu,\mu_i)$ and $\tilde{\xi}_d^{\alpha\beta,\text{inc}}(\mu,\mu_i)$ for the combined block, it suffices to change $1u \Longleftrightarrow 2d$ and $2u \Longleftrightarrow 1d$ in the expressions for the intensities.

## 7.6 Numerical Validation

Now, in order to implement the partially coherent approach for the rough layered media, consider two blocks, each of which includes $N_B=32$ layers (for each block the top and bottom half spaces are vacuum) with an average block length of $\overline{L}_B \approx 15\lambda_i$ and a Gaussian dielectric profile along $z$ where $\lambda_i$ is the free space wavelength. Parameters of the permittivity process are given by correlation length $\ell_\varepsilon = \lambda_i \ll \overline{L}_B$, variance scaling factor $\Delta=0.1$, damping factor $\alpha=30\lambda_i$ , and average dielectric constant of $\varepsilon_r=1.7$ for the given process in Eq. 7.2.1. A realization of the dielectric constant profile of the first block is depicted in Fig. 7.3.

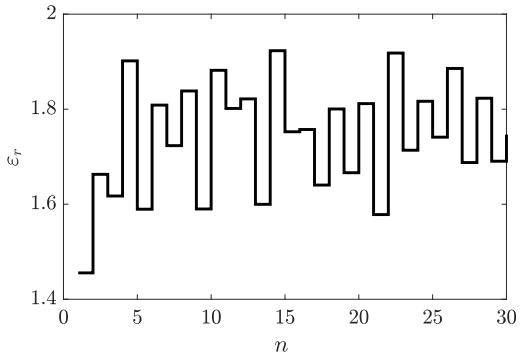


FIGURE 7.3: A realization of the dielectric constant profile of the first block.

Each rough interface is a Gaussian process $f(x,y)$ with correlation length of $\ell_s=1.5\lambda_i$ and RMS height of $h_s=0.03\lambda_i$. For the coherent solution of each block, the SPM2 is used as a full wave solution because the surface roughness satisfies the SPM criteria [25, 35]. The block reflectivities and transmissivities obtained by the SPM enter into the cascading procedure of Sec. 7.4. A detailed derivation of the SPM for a layered medium can be found in [80].

In order to evaluate the performance of the partially coherent cascading approach, we compare the incoherently combined solution of two blocks of 32 layers with the coherent response of the concatenated structure with 63 layers (two vacuum half spaces of the two blocks are merged together). A Monte-Carlo simulation over dielectric profiles is performed over 100 realizations for each block of 30 layers; for the concatenated block of 62 layers 900 realizations were used to reach the same level of convergence.

Figure 7.4 plots the specular reflectivity of the structure obtained by the full wave (coherent) solution of the structure versus the result of partially coherent cascading of the two blocks. Also the response of the media when all of the interfaces are flat is indicated in Fig. 7.4 that shows significance of surface roughness contribution in the specular reflectivities. The partially coherent cascading approach is in good agreement with the full wave solution for both polarizations. The difference between specular reflectivity obtained by partially coherent and the full wave solution (absolute error) is always less than $-20$ dB and is shown in Fig. 7.5. The small difference between two approaches is due to the residual randomness as well as the approximation made in neglecting the phase.

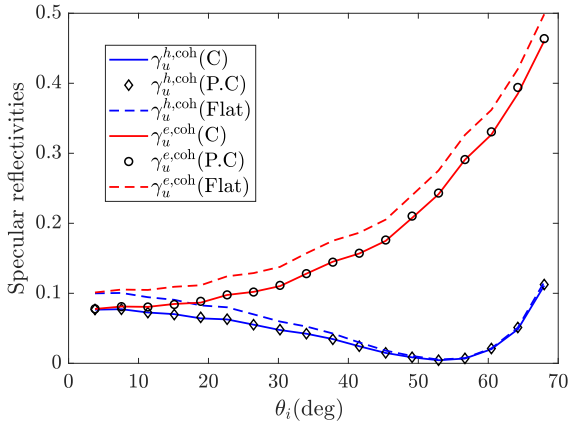


FIGURE 7.4: Specular reflectivity ($\gamma_u^{h,\mathrm{coh}}$) of the cascaded block with partially coherent approach (P.C) compared to coherent solution of reflectivity (C) versus incident angle when it is excited from the top for TE ($e$) and TM ($h$) polarizations.

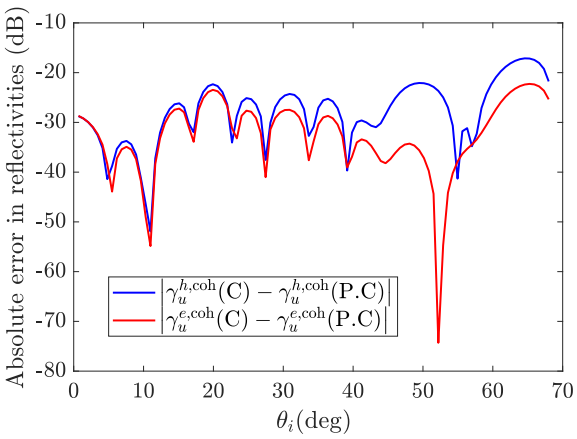


FIGURE 7.5: Absolute error in the specular reflectivity $\gamma_u^{h,\mathrm{coh}}$ of the cascaded block obtained by the partially coherent approach versus incident angle when the structure is excited from the top for TE ($e$) and TM ($h$) polarizations.

Figures 7.6, and 7.7 compare co-polarized $\gamma_u^{ee,\mathrm{inc}}(\theta_s,\theta_i)$ and cross-polarized $\gamma_u^{he,\mathrm{inc}}(\theta_s,\theta_i)$ bistatic reflectivity of the structure in dB obtained by the two methods (right: Partially coherent, left: Full wave) when excited from the top with a $e$-polarized (TE) plane wave in the direction $\theta_i$. Figures, 7.8, and 7.9 similarly compare co-polarized and cross-polarized responses in dB for $h$-polarized (TM) excitation.

The greatest discrepancy between the full wave and partially coherent bistatic solutions is observed for the co-polarized response of $\gamma_u^{ee,\mathrm{inc}}(\theta_s,\theta_i)$. The difference of partially coherent approach and the exact solution for TE bistatic co-polarized reflectivity is shown in Fig. 7.10 in dB. The absolute error in the pattern is approximately always less than -20 dB over all incident and scattered angles.

Regarding the computational cost, full wave solution for 63 layers approximately takes 8 times more CPU time than a block of length 32 layers. Including the fact that we need to solve for both top and bottom excitations for each block to cascade them, this gives a

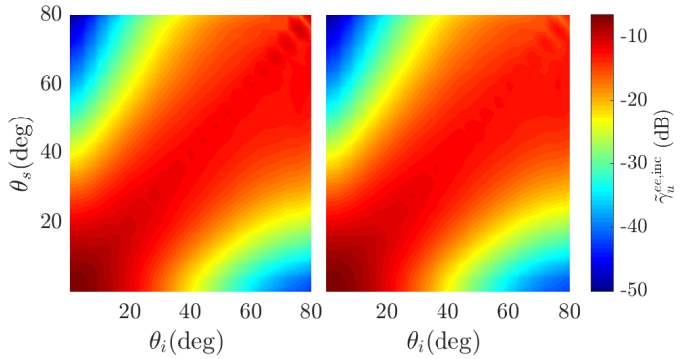


FIGURE 7.6: Bistatic (incoherent) co-polarized reflectivity $\gamma_u^{ee,\mathrm{inc}}(\theta_s,\theta_i)$ of the structure as a function of incident and scattered angles when it is excited by TE-polarized plane wave from the top. Cascaded block with partially coherent approach on the right compared to coherent solution on the left side.

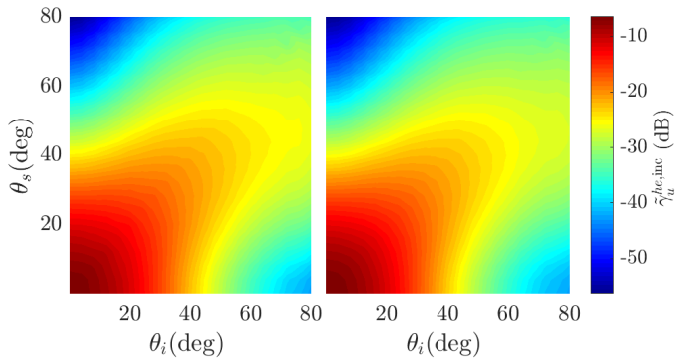


FIGURE 7.7: Bistatic (incoherent) cross-polarized reflectivity $\gamma_u^{he,\mathrm{inc}}(\theta_s,\theta_i)$ of the structure as a function of incident and scattered angles when it is excited by TE-polarized plane wave from the top. Cascaded block with partially coherent approach on the right compared to coherent solution on the left side.

factor of two in CPU time in favor of partially coherent approach for a single realization computation. Considering the required number of realizations to get convergent solution, the full wave solution is averaged over 900 realizations while partially coherent requires $2\times100$ realizations to converge (accounting for the top/bottom excitations separately). This also gives a factor of 3.5 in CPU time and totally there is a factor of 7 reduction in CPU time by using the partially coherent scheme for this particular example. For larger problems the difference in CPU time between the full wave and partially coherent cascading approach grows much faster [79, 116, 117].

Comparison of the bistatic and specular reflectivities shows that the partially coherent approach is applicable as a substitution for the full wave response with a lower computational cost and the same level of accuracy. It is worth mentioning that although the energy conservation relation (7.4.2) is used to connect the block responses, the method can be applied to lossy layered media as well, as long as the connecting layer between the blocks is lossless (this is where the energy conservation is invoked). In addition, this method can

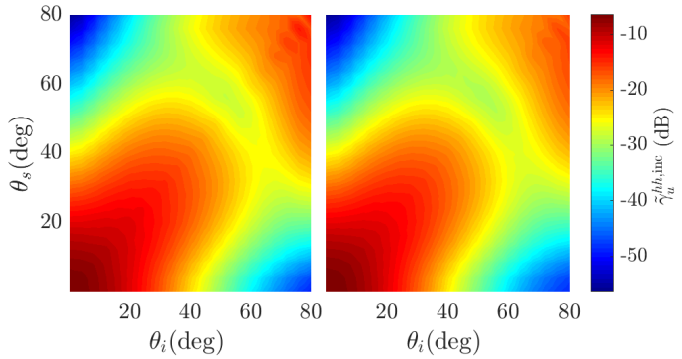


FIGURE 7.8: Bistatic (incoherent) co-polarized reflectivity $\gamma_u^{hh,\mathrm{inc}}(\theta_s,\theta_i)$ of the structure as a function of incident and scattered angles when it is excited by TM-polarized plane wave from the top. Cascaded block with partially coherent approach on the right compared to coherent solution on the left side.

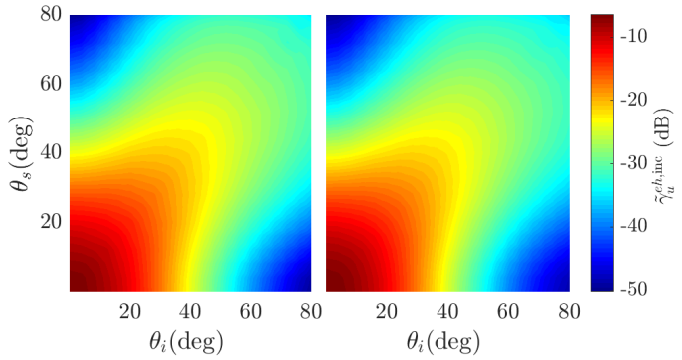


FIGURE 7.9: Bistatic (incoherent) cross-polarized reflectivity $\gamma_u^{eh,\mathrm{inc}}(\theta_s,\theta_i)$ of the structure as a function of incident and scattered angles when it is excited by TM-polarized plane wave from the top. Cascaded block with partially coherent approach on the right compared to coherent solution on the left side.

be recursively used to find the response of an arbitrary number of blocks.

## 7.7 Conclusion

The results of this chapter show that for the case of a layered medium in presence of randomness in the permittivity, the layered medium can be separated into blocks having lengths on the order of multiple correlation length of the permittivity random process. Solutions for the scattering and emission can then be performed by incoherently cascading the intensities of blocks without losing accuracy. This approach is efficient in the case of a layered media with large number of layers that possess fluctuating permittivity or other kind of randomness.

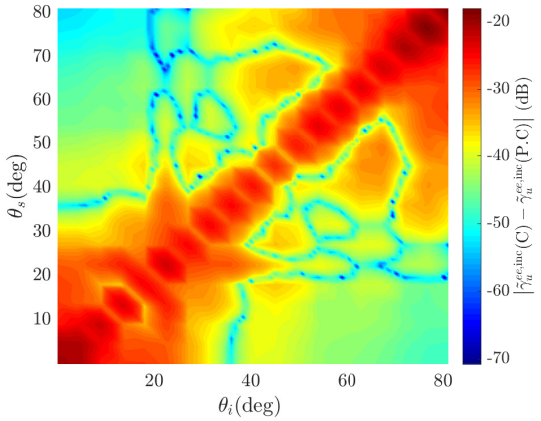


FIGURE 7.10: Absolute error in the bistatic (incoherent) co-polarized reflectivity $\gamma_u^{ee,\mathrm{inc}}(\theta_s,\theta_i)$ of the structure as a function of incident and scattered angles when it is excited by TE-polarized plane wave from the top, in dB.

# Chapter 8

# Fast and Broadband Computation of Green's Function in Cavity Resonator of Irregular Shape Using Imaginary Wave Number Extraction Technique

## 8.1 Introduction

The Green's function is a fundamental tool in analysis of every physical system and it provides an in depth insight to the dynamical behavior of the system. Based on this, obtaining the Green's function for a given system is as difficult as solving the problem directly. However, since the Green's function can determine response of the system to an arbitrary excitation it contains more informations about the system than the solution of the dynamical variable like the wave function. The Green's function is the collective response of all the resonant wave function in a unique way such that it is closely related to the spatial distribution of the density of states.

In particular, Green's function are important in electromagnetics as it provides the response for an arbitrary distribution of source. They are also useful for formulating the integral equations for various boundary value problems. Commonly used Green's functions include free space Green's functions, periodic Green's functions for empty periodic lattices, and Green's functions of regular geometry such as a sphere or cylinder, Green's functions of layered media, etc [118–121].

Recently we developed techniques of broad band Green's functions with low wavenumber extractions (BBGFL) that calculate Green's functions for more general irregular geometry and for periodic structures including the scatterers [122, 122].

For 2D waveguide and cavity problems, the essence of the BBGFL technique consists of 3 major steps. The first step is to start with the rectangular waveguide broadband Green's function. The hybrid representation of the rectangular waveguide Green's function consists of the sum of a low wavenumber extraction to accelerate the convergence of the modal expansion and the sum of modal terms, requiring much smaller number of modes to converge. In step 2, using the hybrid representation of the rectangular Greens function in a surface integral equation of irregular waveguide, a linear eigenvalue problem is formulated that rapidly calculate the modes of the irregular shaped waveguide. The modal functions of

the irregular shaped waveguide have a hybrid representation of the summation of boundary contributions and the modal expansions of the rectangular waveguide wave functions. The hybrid representation requires less number of modes in the modal expansion. In step 3, the Green's functions of irregular shaped waveguide are expressed as a hybrid representation of summation of a low wavenumber extraction part plus a spectral expansions in terms of the irregular shaped waveguide modes.

In this paper, the BBGFL technique is extended to 3D problems for the first time for irregular shaped cavity. In addition, instead of using low real wavenumber extraction, an imaginary wavenumber extraction is applied which is computationally more efficient and is also robust.

The Green's function of an irregular cavity resonator with perfect electric walls is studied. This irregularity in the geometry can be anything in general (defect in the surface boundary, loaded cavity etc.) In some cases, specially in designs, the behavior of the system response over a wide bandwidth is desired. This Green's function has many applications in designing the micro cavities [123], and irregular shaped quantum well [124, 125] where the density of surface states and spontaneous emission can be controlled by designing the Green's function.

The proposed method in this paper can provides the Green's function of the irregular cavity over a wide band of frequency with lower computational cost compare to the conventional approaches. In addition, this semi-analytical solution provides deeper insight and is better suited for manipulations and designs.

The method is based on a hybrid spatial-spectral eigen-function expansion with imaginary wave number extraction. The extraction at imaginary wave number captures the singularity of the Green's function such that the rest would have a regular characteristics even at the source location. In order to find the eigen-modes of the irregular cavity, a linear eigenvalue problem will be formulated that gives a hybrid spatial-spectral representation of the eigen-functions. The main point here is that this eigenvalue problem is linear (the involved operators are not function of eigenvalues). The method has been applied to variety of structure like Green's function in a waveguides with arbitrary cross section [126], Green's function for the photonic crystals and metamaterials including the scatterers (and also defects) [127, 128] where the Green's function is expressed in terms of the accelerated photonic bands eigen-functions.

Previously, people used different kinds of extractions. The BIRME method [129–131] uses the extraction of the static Green's function to accelerate convergence of eigen-function expansion; instead, the BBGFL [122, 132] uses extraction of the Green's function at a low but non-zero wave number $k_L$ to accelerate the convergence. It will be shown that the extraction of the Green's function at an imaginary wave number is superior to both DC and low wave number extractions.

## 8.2 Broadband Green's Function

### 8.2.1 Eigenfunction expansion of the Green's function

Consider the wave equation operator $\mathcal{L}=\nabla^2$ acting on Hilbert space $V$ with prescribed boundary conditions on $\mathcal{L}$ such that $\mathcal{L}$ is a self-adjoint (Hermitian) operator in $V$. For example radiation condition at infinity for unbounded space or Dirichlet/Neumann boundaries

for finite spaces make $\mathcal{L}$ Hermitian. The eigen-value equation reads

$$\nabla^2\psi_n = -k_n^2\psi_n \tag{8.2.1}$$

Here, $\psi$ is eigenfunction and $-k^2$ is corresponding eigenvalue (since $\nabla^2$ is a negative definite operator, the eigenvalues are chosen with an extra minus sign). According to the Storm-Liouvill theorem, eigenfunctions of this Hermitian operator are orthogonal with respect to the following inner product on $V$,

$$\langle\psi_m,\psi_n\rangle = \int_V \mathrm{d}\overline{r}\psi_m^*(\overline{r})\psi_n(\overline{r}) = \delta_{mn} \tag{8.2.2}$$

where we assumed that the eigenfunctions are normalized.The label $n$ here can be discrete or continuous, in case of continuous label, $\delta_{mn}$ should change into $\delta(m-n)$. These eigenfunctions can be used to expand functions within $V$ into Fourier-type expansions. If the delta function can be expanded in terms of the eigenfunctions, then any other function $f(\overline{r})$ in $V$ can be written in terms of the delta function

$$f(\overline{r}) = \int \mathrm{d}\overline{r}' f(\overline{r}')\delta(\overline{r}-\overline{r}') \tag{8.2.3}$$

So expanding the delta function is enough to expand any other function (which is more well-behaved than delta function). Consider the following expansion for the delta function,

$$\delta(\overline{r}-\overline{r}') = \sum_n C_n\psi_n(\overline{r}) \tag{8.2.4}$$

Upon using orthogonality of the eigenfunctions, it yields

$$\delta(\overline{r}-\overline{r}') = \sum_n \psi_n(\overline{r})\psi_n^*(\overline{r}') \tag{8.2.5}$$

Now, consider the scalar Green's function defined by

$$(\nabla^2+k_0^2)G(\overline{r},\overline{r}') = -\delta(\overline{r}-\overline{r}') \tag{8.2.6}$$

where $k_0=\omega\sqrt{\mu\varepsilon}$ is the wave number in the medium. By expanding the Green's function in terms of the eigenfunctions we find that

$$G(\overline{r},\overline{r}') = \sum_n \frac{1}{k_n^2-k_0^2}\psi_n(\overline{r})\psi_n^*(\overline{r}') \tag{8.2.7}$$

This expansion of the Green's function is called broad band because the dependence on the excitation frequency is simply in the denominator. The eigenfunctions and eigenvalues do not depend on the frequency or $k$. For the case of free space, one choice of the eigenfunctions are normalized plane waves

$$\psi_{\overline{k}}(\overline{r}) = \frac{1}{(2\pi)^{3/2}}e^{i\overline{k}\cdot\overline{r}} \tag{8.2.8}$$

and the Green's function expansion becomes [**?** ]

$$G(\overline{r},\overline{r}') = \frac{1}{(2\pi)^3}\int \mathrm{d}^3\overline{k}\frac{1}{k^2-k_0^2}e^{i\overline{k}\cdot(\overline{r}-\overline{r}')} \tag{8.2.9}$$

An important note here is that, even for a lossy medium this expansion is valid. Here we are using the eigenfunction of $-\nabla^2$ which is independent of the medium and physical properties. For lossy medium, the operator $-\nabla^2-k^2$ is no longer Hermitian and the eigenfunction overlap on each other as a result of spectral broadening, but herein we are taking the advantage of $\nabla^2$ eigenfunctions which are always mutually orthogonal.

### 8.2.2 Accelerating the Summation of eigenfunctions

Although the expansion of the Green's function is desired because of simple dependence on the frequency of excitation, the summation converges slowly.

$$G(\overline{r},\overline{r}')=\sum_{\alpha}\frac{1}{k_n^2-k_0^2}\psi_\alpha(\overline{r})\psi_\alpha^*(\overline{r}')\approx\sum_{\alpha}\frac{1}{k_\alpha^2-k_0^2} \tag{8.2.10}$$

it converges like $\mathcal{O}(k_\alpha^{-2})$ in amplitude. In the case of continuous spectrum in lossless free space

$$G(\overline{r},\overline{r}')=\frac{1}{(2\pi)^3}\int \mathrm{d}^3\overline{k}\,\frac{1}{k^2-k_0^2}e^{i\overline{k}\cdot(\overline{r}-\overline{r}')}\leq\frac{1}{(2\pi)^3}\int \mathrm{d}k\,\frac{k^2}{k^2-k_0^2} \tag{8.2.11}$$

The series of (8.2.10) is only conditionally convergent for a 3 dimensional problem since the summation $\sum_\alpha(k_\alpha^2-k_0^2)^{-1}$ is a divergent series (only for 1D the modal series is absolutely convergent). Therefore no error bound can be found for the convergence of (8.2.10) and in practice it cannot be used to compute the Green's function. In addition, since the Green's function has a discontinuous derivative at the source point, a well known Gibbs phenomena will happen in the summation near the source region.

However, the expansion of (8.2.10) is interesting as it depends on the frequency of excitation only through the denominator (the eigenfunctions do not depend on the excitation). If the eigenfunctions and resonant frequencies are known, in principle, the Green's function can be obtained over all frequency ranges by a simple calculation but poor convergence is still a serious problem. Thus we call this eigenfunction expansion as the *Broadband Green's function* which is not practical as given by (8.2.10), unless the convergence can be accelerated.

In order to increase the convergence rate of Eq. 8.4.3, the Green's function at an imaginary wave number $k=i\xi$ can be extracted from the original expansion. With the imaginary wave number extraction, the convergence of the regular shaped cavity Green's function expansion can be accelerated to the 4th order (the summand is proportional to $k_\alpha^{-4}$, asymptotically) and providing a *hybrid representation*

$$G^\Omega(\overline{r},\overline{r}';k)=G^\Omega(\overline{r},\overline{r}';i\xi)+\sum_{\alpha=1}^{M_\Omega}\left[\frac{k^2+\xi^2}{(k_\alpha^2-k^2)(k_\alpha^2+\xi^2)}\right]\psi_\alpha(\overline{r})\psi_\alpha^*(\overline{r}') \tag{8.2.12}$$

where the series is truncated at $\alpha=M_\Omega$. The series in (8.2.12) is absolutely convergent even at $\overline{r}=\overline{r}'$. The singular part of the Green's function is contained completely in the $G^\Omega(\overline{r},\overline{r}',i\xi)$. The summation now converges much faster than the original modal summation of (8.2.10) to the cost of computing $G^\Omega(\overline{r},\overline{r}',i\xi)$. We call this form as the *Hybrid Spatial-Spectral* representation as the fist and second terms are expressed in spatial and spectral domain, respectively. In general, the part of computing the Green's function at an imaginary wave number is not a time consuming task for several reasons. 1) It is only a one-time setup as it should be computed only one time in a broadband solution that potentially can have many frequency points, 2) At an imaginary wave number, oscillations will be replaced with exponential decay and all the numerical procedures are relaxed compared to the case of real frequency. The interaction matrices involved in the numerical methods (such as MoM) become real and sparse (banded). In addition, the numerical grid can be coarser for an imaginary wave number, 3) For some regular geometries (including rectangular) calculation

of $G^{\Omega}(\overline{r},\overline{r}',i\xi)$ can be done extremely fast by utilizing image sources to satisfy the boundary condition on the cavity walls. Method of images to compute $G^{\Omega}(\overline{r},\overline{r}',i\xi)$ is briefly discussed in the next section.

$$G(\overline{r},\overline{r}',k)=G(\overline{r},\overline{r}',i\xi)+\sum_{\alpha}\left[\frac{k^2+\xi^2}{(k_\alpha^2-k^2)(k_\alpha^2+\xi^2)}\right]\psi_\alpha(\overline{r})\psi_\alpha^*(\overline{r}') \tag{8.2.13}$$

We can move further to accelerate the eigenfunction expansion to the higher orders. Repeating the technique in Eq. (8.2.12) one more time yields

$$\begin{aligned}G^{\Omega}(\overline{r},\overline{r}',k)=&G^{\Omega}(\overline{r},\overline{r}',i\xi)-\frac{k^2+\xi^2}{2\xi}\frac{\partial}{\partial\xi}G^{\Omega}(\overline{r},\overline{r}',i\xi)\\&+(k^2+\xi^2)^2\sum_{\alpha=1}^{M_\Omega}\frac{\psi_\alpha(\overline{r})\psi_\alpha^*(\overline{r}')}{(k_\alpha^2+\xi^2)^2(k_\alpha^2-k^2)}\end{aligned} \tag{8.2.14}$$

This expansion is of 6th order in convergence with respect to $k_\alpha$. Computing the imaginary wave number derivative of $\partial_\xi G^{\Omega}(\overline{r},\overline{r}',i\xi)$ has the same procedure as $G^{\Omega}(\overline{r},\overline{r}',i\xi)$. The procedure of extraction can be continued to an arbitrary order (even order) of convergence at a cost of computing the higher order derivatives of the $G(\overline{r},\overline{r}';i\xi)$.

In order to show how the accelerated expansion facilitates computation of $G^{\Omega}(\overline{r},\overline{r}';k)$, we compare the 6th order expansion of (8.2.12) with the original expansion of (8.2.10) for the rectangular cavity of dimensions $L_x=L_y=L_z=L$ at the excitation frequency corresponds to $\lambda=0.93L$. The imaginary wave number extraction is done at $\xi=2/L$ (Selecting the imaginary wave number will be discussed later in Sec. 8.9). The Green's function is computed for the source located at $\overline{r}'=(L_x/4,L_y/4,L_z/4)$ over the plane of $z=0.45L_z$ (near the upper wall) inside the cavity. The original 2nd order expansion is evaluated by truncating the summation at $M_\Omega=300^3=2.7\times10^7$ in Eq. 8.2.10 while $M_\Omega=6^3$ terms are used in the 6th order expansion of Eq. 8.2.14. The absolute value of the Green's function obtained by 6th order expansion is plotted in Fig. 8.1 in logarithmic scale.

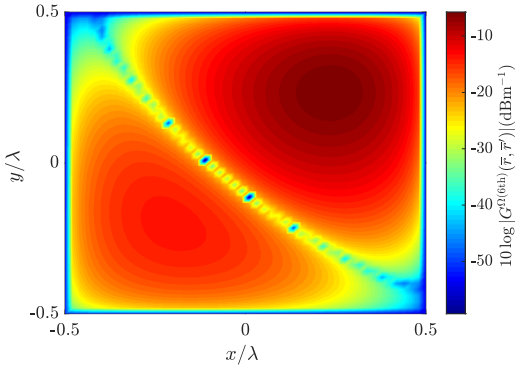


FIGURE 8.1: Scalar 3D Green's function inside a resonator of dimensions $L_x=L_y=L_z=L$ at wave length $\lambda\approx0.93L_x$ computed by the accelerated 6th order formula using $6^3$ terms, in dB scale for $\overline{r}'=(L_x/4,L_y/4,L_z/4)$ and $\overline{r}=(x,y,z=0.45L_z)$.

Figure. 8.2 also compare the Green's function obtained by 6th order and conventional 2nd order expansions. The maximum relative error is around $-60$ dB.

Regarding the comparison of CPU time of two summations, 6th order extracted sum (including calculation of $G^{\Omega}(\overline{r},\overline{r}';i\xi)$) takes about 0.6 CPU-ms while regular spectral 2nd

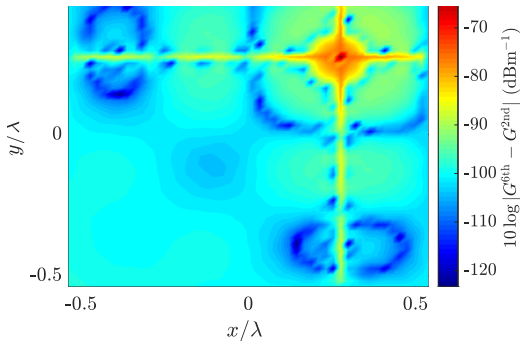


FIGURE 8.2: Absolute error of Green's function calculated by 6th order expansion using 6 modes in each direction respect to the 2nd order spectral expansion using 300 modes in each direction, in dB

expansion requires 2100 CPU-ms for computing the Green's function of the rectangular cavity per observation point, which is a factor of around 3500 in computation time.

Even computation of the regular shaped Green's function inside the cavity is useful in the potential formulation of the vector electromagnetic scattering formulation of some other irregular shaped variations of the rectangular cavity like loaded cavity [133] which will be discussed in the Appendix B.

## 8.3 Method of Images

The Green's function, which is the response of a point source inside a rectangular cavity can be calculated using the Image theorem. The hard boundaries of the cavity can be replaced by configuration of sources outside of the cavity (region of interest) to achieve required boundary conditions on the walls.

### 8.3.1 One Dimensional Green's function and Images

For a parallel plate structure, with a point source at $\overline{r}_0$, the Green's function can be expanded in terms of plane wave in $y$ and $z$ directions,

$$G(\overline{r},\overline{r}')=\int\frac{\mathrm{d}k_y}{2\pi}\int\frac{\mathrm{d}k_z}{2\pi}g(x,x',k_x)e^{ik_y(y-y')+ik_z(z-z')} \tag{8.3.1}$$

where the reduced $g(x,x',k_x)$ satisfies

$$\left(\frac{\mathrm{d}^2}{\mathrm{d}x^2}+k_x^2\right)g(x,x',k_x)=-\delta(x-x') \tag{8.3.2}$$

Subject to boundary conditions $g(x{=}0,a,x'){=}0$. This can be directly solved in a compact form.

$$g(x,x',k_x)=\begin{cases}A\sin k_x(a-x), & x>x'\\ \\ B\sin k_x x, & x<x'\end{cases} \tag{8.3.3}$$

where $A$ and $B$ are spatially constant. Continuity of the solution at $x=x'$ requires

$$A\sin k_x(a-x')-B\sin k_x x'=0 \tag{8.3.4}$$

Discontinuity of the derivative of the Green's function at $x=x'$ also gives

$$A\cos k_x(a-x')+B\cos k_x x'=\frac{1}{k_x} \tag{8.3.5}$$

Solving for $A$ and $B$ gives

$$g(x,x',k_x)=\frac{1}{k_x\sin(k_a a)}\begin{cases}\sin k_x(a-x)\sin k_x x', & x>x'\\ \\ \sin k_x x\sin k_x(a-x'), & x<x'\end{cases} \tag{8.3.6}$$

The Green's function has poles at the resonant frequencies of the structure $k_x a=n\pi$. In order to directly solve for the reduced Green's function, it can be equivalently expanded in terms of the eigenfunctions between the plates

$$g(x,x',k_x)=\sum_n A_n\sin k_{nx}x \tag{8.3.7}$$

where $k_{nx}=n\pi/a$. Upon expansion of the delta function in term of the same functions and substitution in one-dimensional wave equation,

$$g(x,x',k_x)=\frac{2}{a}\sum_n\frac{\sin k_{nx}x\ \sin k_{nx}x'}{k_x^2-k_{nx}^2} \tag{8.3.8}$$

The two solutions of the reduced Green's function are the same

$$\frac{2}{a}\sum_n\frac{\sin k_{nx}x\ \sin k_{nx}x'}{k_x^2-k_{nx}^2}=\frac{1}{k_x\sin(k_a a)}\sin k_x(a-x_>)\sin k_x x_< \tag{8.3.9}$$

where $x_>=x,x<=x'$ when $x>x'$ and vice versa. Notice that the reduced Green's function $g(x,x',k_x)$ is the field generated by a charge sheet of constant density at $x=x'$ between the parallel plates. Equation (8.3.9) is a summation identity that can be used to change the representation of the Green's function. Therefore, the complete Green's function becomes

$$G(\overline{r},\overline{r}')=\frac{2}{a}\sum_n\int\frac{\mathrm{d}k_y}{2\pi}\int\frac{\mathrm{d}k_z}{2\pi}e^{ik_y(y-y')+ik_z(z-z')}\frac{\sin k_{nx}x\ \sin k_{nx}x'}{k_x^2-k_{nx}^2} \tag{8.3.10}$$

One of the spectral integration can be performed due to the pole at resonance frequency $k_x=k_{nx}$. In order to perform the $k_z$ integral, there would be a pole at $k_{nz}=k^2-k_{nx}^2-k_y^2$ and another at complex conjugate place. Assuming infinitesimal physical loss ($\mathrm{Im}(k)>0$), for $z>z'$ we can close the contour of integration in complex $k_z$-plane upward

$$G(\overline{r},\overline{r}')=\frac{i}{a}\sum_n\int\frac{\mathrm{d}k_y}{2\pi}e^{ik_y(y-y')+ik_{nz}(z-z')}\frac{\sin k_{nx}x\ \sin k_{nx}x'}{2k_{nz}} \tag{8.3.11}$$

where $k_{nz}^2=k^2-k_{nx}^2-k_y^2$.

### One Dimensional Images

On the other side, 1D free Green's function (radiation of sheet of charge in free space) is solution of the one dimensional wave equation Eq. 8.3.2 with radiation boundary condition at infinity that gives

$$G_0(x,x')=\frac{i}{2k_x}e^{ik_x|x-x'|} \tag{8.3.12}$$

Each image charge, which is shown by dots (but they are charge sheets) will radiate with $G_0(x,x')$ such that collective response will construct $G(x,x',k_x)$. In order to construct the Dirichlet boundary condition on the plates, image charges placed one by one to make the wave function vanishes on both plates. The locations of actual charge $Q$ is given by $\overline{r}'=(x',y',z')$. The image charges with positive charge $+Q$ (red dots) should be placed at $\overline{r}''=(x'',y',z')$ where

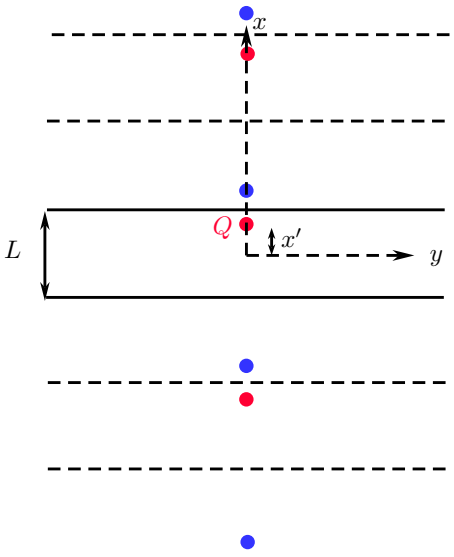


FIGURE 8.3: Images of point charge $Q$ between parallel plates.

$$x''=2L+x',-2L+x',4L+x',-4L+x',\cdots=(2n)L+x' \tag{8.3.13}$$

This set include the real charge itself. In addition, negative charges of $-Q$ (blue dots) should be placed at

$$x''=L-x',-L-x',3L-x',-3L-x',\cdots=(2n+1)L-x' \tag{8.3.14}$$

and $n\in\mathbb{Z}$. The Green function $g(x,x',k_x)$ that satisfies the Dirichlet boundary on the plates is the collective response of individual unit image sources

$$\begin{aligned}
G(x,x',k_x)&=\sum_{n+}G_0(x,x''_n,k_x)-\sum_{n-}G_0(x,x''_n,k_x)\\
&=\sum_n G_0\Big(x,2nL+x',k_x\Big)-\sum_n G_0\Big(x,(2n+1)L-x',k_x\Big)\\
&=\sum_n(-1)^{2n}G_0\Big(x,2nL+(-1)^{2n}x'\Big)+\sum_n(-1)^{2n+1}G_0\Big(x,(2n+1)L+(-1)^{2n+1}x'\Big)
\end{aligned}$$

Now we can combine the indices and write

$$G(\overline{r},\overline{r}';k_x)=\sum_n(-1)^n G_0\Big(x,nL+(-1)^n x';k_x\Big) \tag{8.3.15}$$

Since,

$$G_0(x,x';k_x)=\frac{i}{2k_x}e^{ik_x|x-x'|} \tag{8.3.16}$$

This expansion does not converge at all for lossless media while the spectral expansion of the Green's function is absolutely convergent. However, in a lossy medium or for an imaginary wave number, image charges expansion converges rapidly. For an imaginary wavenumber $k_x=i\xi_x$ and taking $x_n=nL+(-1)^n x'$ we have

$$G(x,x';i\xi_x)=\sum_n(-1)^n\frac{1}{2\xi_x}e^{-\xi_x|x-x_n|} \tag{8.3.17}$$

which is rapidly convergent with respect to the number of included images. The image expansion is compared to the spectral expansion of

$$G(x,x',k_x)=\frac{2}{L}\sum_n\frac{\sin k_{nx}x\ \sin k_{nx}x'}{k_x^2-k_{nx}^2} \tag{8.3.18}$$

for imaginary wave number $\xi=2\pi$ for plates separated by normalized distance $L_x=1$ (arbitrary unit) in Fig. 8.4. The source is located at $x'=L_x/4$ and the Green's function is plotted as a function of $x$. Modal summation of Eq. 8.3.18 is summed over 100 modes as a reference. The response of the source itself without considering any image source (Image $N=0$) as well as Green's function obtained by including just one image charge is plotted. The Green's function calculated by inclusion of just one image is exactly the same as modal summation with 100 terms.

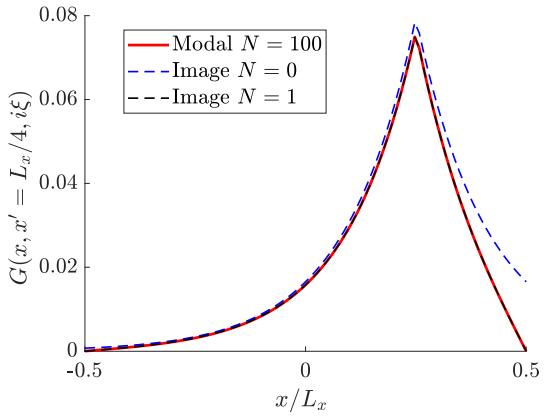


FIGURE 8.4: The 1D Green's function between parallel PEC plates calculated by modal summation (100 modes) and image method for an imaginary wave number $\xi_x=2\pi$.

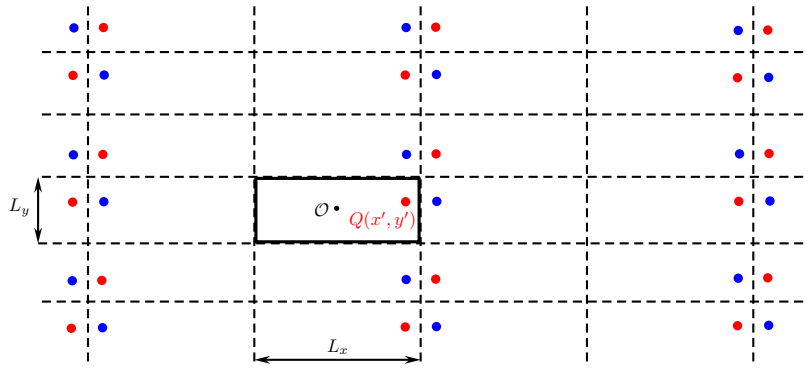


FIGURE 8.5: Images of point charge $Q$ between parallel plates.

### 8.3.2 Two Dimensional Images

For unit point source inside a rectangular waveguide, the Green's function can be obtained by considering image charges to be able to remove the boundaries. In fact the finite, and constraint problem of fields in the waveguide can be transformed into infinite unconstrained problem of radiation from image charges that produces the Dirichlet boundary condition on the walls. The array of image charges constitute a pseudo-periodic array of sources. The positive unit charge $Q(x',y')$ inside the waveguide is represented by a red point in Fig. 8.5. The image charges to make the wave function zero on the side walls of the wave guide include bunch of positive (red) and negative charges (blue). For $y=y'$ (the central row), the location of positive image charges is given by

$$x''=2mL_x+x' \tag{8.3.19}$$

where $m\in\mathbb{Z}$. Note that this also includes the real unit charge in addition to the image charges as they will be treated in the same way. Additionally, negative charges of $-Q$ (blue dots) should be placed at

$$x''=(2m+1)L_x-x' \tag{8.3.20}$$

At $y=L_y-y'$, location of positive and negative charges are reversed, i.e. positive charges are located at $x''=(2m+1)L_x-x'$ and negative charges at $x''=(2m)L_x+x'$. In general, the location of positive charges is given by

$$(x'',y'')=\Big(2mL_x+x',2nL_y+y'\Big),\Big((2m+1)L_x-x',(2n+1)L_y-y'\Big) \tag{8.3.21}$$

and for negative image charges

$$(x'',y'')=\Big((2m+1)L_x-x',2nL_y+y'\Big),\Big(2mL_x+x',(2n+1)L_y-y'\Big) \tag{8.3.22}$$

The collective response of the image charges as well as actual charge $Q$ leads to the 2D Green's function of

$$\begin{aligned} G(\overline{\rho},\overline{\rho}';k_\rho) &= \sum_{n+} G_0(\overline{\rho},\overline{\rho}_n'';k_\rho) - \sum_{n-} G_0(\overline{\rho},\overline{\rho}_n'';k_\rho) \\ &= \sum_{n,m} G_0\Big(\overline{\rho};2mL_x+x',2nL_y+y';k_\rho\Big) + \sum_{n,m} G_0\Big(\overline{\rho};(2m+1)L_x-x',(2n+1)L_y-y';k_\rho\Big) \\ &- \sum_{n,m} G_0\Big(\overline{\rho};(2m+1)L_x-x',2nL_y+y';k_\rho\Big) - \sum_{n,m} G_0\Big(\overline{\rho};2mL_x+x',(2n+1)L_y-y';k_\rho\Big) \end{aligned} \tag{8.3.23}$$

Here, $G_0(\overline{\rho},\overline{\rho}';k_\rho)$ is Green's function of a 2D free radiator with 2D wave number $k_\rho$ in space which is given by

$$G_0(\overline{\rho},\overline{\rho}';k_\rho) = \frac{i}{4} H_0^{(1)}\Big(k_\rho|\overline{\rho}-\overline{\rho}'|\Big) \tag{8.3.24}$$

Three dimensional Green's function $G_0(\overline{r},\overline{r}')$ for a point source radiator can be constructed for a 2D problem by a Fourier transform

$$G_0(\overline{r},\overline{r}') = \int \frac{\mathrm{d}k_z}{2\pi} G_0(\overline{\rho},\overline{\rho}';k_\rho) e^{ik_z(z-z')} \tag{8.3.25}$$

The image expansion (8.3.23) can be simplified to

$$G(\overline{\rho},\overline{\rho}';k_\rho) = \sum_{n,m} (-1)^{n+m} G_0\Big(\overline{\rho};mL_x+(-1)^m x',nL_y+(-1)^n y'\Big) \tag{8.3.26}$$

On the other side using the eigenfunction expansion we can derive a spectral expression for 2D Green's function. The result is

$$G(\overline{\rho},\overline{\rho}';k_\rho) = \frac{4}{L_x L_y} \sum_{m,n} \frac{\sin k_{mx}\Big(x+\frac{L_x}{2}\Big)\ \sin k_{mx}\Big(x'+\frac{L_x}{2}\Big) \sin k_{ny}\Big(y+\frac{L_y}{2}\Big)\ \sin k_{ny}\Big(y'+\frac{L_y}{2}\Big)}{k_\rho^2-(k_{mx}^2+k_{ny}^2)} \tag{8.3.27}$$

These two results are identical. The image expansion convergence is very poor for a lossless medium as the Hankel function for large distances decays like $(k_\rho\rho)^{-1/2}$. However, convergence rate of spectral expansion is independent of loss of the medium but the image expression which is in spatial domain depends on the propagation constant of the medium exponentially. In the case of lossy medium or at imaginary wave numbers, the spatial expansion converges rapidly while spectral expansion still converges poorly. For an imaginary wavenumber $k_\rho = i\xi_\rho$, and taking $\overline{\rho}_{mn} = (mL_x+(-1)^m x', nL_y+(-1)^n y')$ the image expression becomes

$$\begin{aligned} G(\overline{\rho},\overline{\rho}';i\xi_\rho) &= \frac{i}{4} \sum_{n,m} (-1)^{n+m} H_0^{(1)}\Big(i\xi_\rho|\overline{\rho}-\overline{\rho}_{mn}|\Big) \\ &= \frac{1}{2\pi} \sum_{n,m} (-1)^{n+m} K_0\Big(\xi_\rho|\overline{\rho}-\overline{\rho}_{mn}|\Big) \end{aligned} \tag{8.3.28}$$

which converges exponentially with number of images (distance). In order to evaluate performance of the image summation method for 2D Green's function, Fig. 8.6 plots the 2D

Green's function inside a rectangular waveguide of dimensions $L_x{=}L_y{=}1$ (arbitrary units) at imaginary wavenumber $k_\rho{=}2\pi i$. The 2D point source is located at $(x',y'){=}(L_x/4,L_y/4)$ and the response is plotted along $x$ for $y{=}L_y/3$. Modal summation is performed over 100 terms in each dimension ($10^4$ total terms). The images summation is also plotted for no image (the source itself, $N{=}0$) as well as including one cluster of 3 images. This shows that inclusion of just 3 image charges is enough to get convergent result by method of images while modal summation requires intensive computation. As the imaginary wave number becomes smaller in magnitude, the response would have a longer range and including higher number of image responses is required.

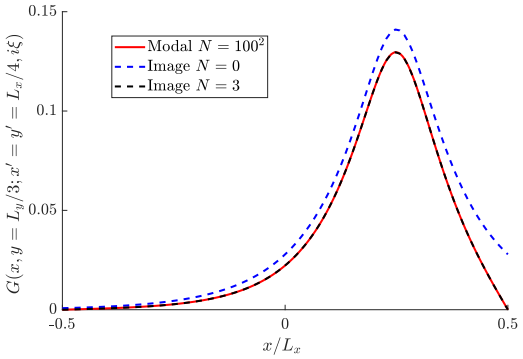


FIGURE 8.6: The 2D Green's function inside a rectangular waveguide calculated by modal summation ($100^2$ modes) and image method for an imaginary wave number $\xi{=}2\pi$.

### 8.3.3 Three Dimensional Image Charges

For the case of rectangular cavity, image charges should be placed in three dimensions and the Green's function of a point source inside the cavity with PEC walls can be obtained with the same token as

$$G(\overline{r},\overline{r}')=\sum_{n,m,p}(-1)^{n+m+p}G_0\Big(\overline{r};mL_x+(-1)^m x',nL_y+(-1)^n y',pL_z+(-1)^p z'\Big) \tag{8.3.29}$$

Here, $G_0\Big(\overline{r},\overline{r}'\Big)$ is Green's function of free point radiator

$$G_0\Big(\overline{r},\overline{r}'\Big)=\frac{e^{ik|\overline{r}-\overline{r}'|}}{4\pi|\overline{r}-\overline{r}'|} \tag{8.3.30}$$

and $G\Big(\overline{r},\overline{r}'\Big)$ is the Green's function of point source inside the cavity that satisfies the Dirichlet boundary condition. On the other hand, the spectral expansion of the Green's function inside the cavity is

$$G(\overline{r},\overline{r}')=\sum_{\alpha}\frac{1}{k_\alpha^2-k^2}\psi_\alpha(\overline{r})\psi_\alpha^*(\overline{r}') \tag{8.3.31}$$

where,

$$\psi_\alpha(\overline{r})=\sqrt{\frac{8}{L_xL_yL_z}}\sin\frac{m\pi}{L_x}\left(x+\frac{L_x}{2}\right)\sin\frac{n\pi}{L_y}\left(y+\frac{L_y}{2}\right)\sin\frac{p\pi}{L_z}\left(z+\frac{L_z}{2}\right) \tag{8.3.32}$$

The Image expansion do converge for 3D lossless case in contrast to 1D (does not converge) and 2D (very slow convergence) as the image response decays with $1/R$. On the other hand, spectral expansion is poorly convergent. In fact the triple summation

$$\sum_{m,n,p} \frac{1}{m^2+n^2+p^2} \tag{8.3.33}$$

is strictly divergent and even an error bound cannot be achieved for the partial summations. Therefore, for the lossless case image expression converges better than spectral expansion. However, for lossy media or for an imaginary wavenumber, the image expansion converges rapidly with including a few image sources. For an imaginary wavenumber $k=i\xi$ and taking $\overline{r}_{mnp}=\Big(mL_x+(-1)^m x', nL_y+(-1)^n y', pL_z+(-1)^p z'\Big)$

$$G(\overline{r},\overline{r}',i\xi)=\frac{1}{4\pi}\sum_{n,m,p}(-1)^{n+m+p}\frac{e^{-\xi|\overline{r}-\overline{r}_{mnp}|}}{|\overline{r}-\overline{r}_{mnp}|} \tag{8.3.34}$$

which decays very fast with number of images. Fig. 8.7 plots the 3D Green's function inside a rectangular cavity of dimensions $L_x=L_y=L_z=1$ (arbitrary units) at imaginary wavenumber $k=i\xi$. The point source is located at $(x',y',z')=(L_x/4,L_y/4,L_z/4)$ and the response is plotted along $x$ for $y=z=L_y/3$. The modal summation is performed over 100 terms in each dimension ($10^6$ total terms). The images summation is also plotted with inclusion of no image (the source itself, $N=0$) as well as including one cluster of 7 image charges around the primitive cell. The comparison shows that inclusion of just 7 image charges is enough to get convergent result by method of images while modal summation requires intensive computation. As the imaginary wave number becomes smaller in magnitude, the response would have a longer range and including higher number of image responses is required. In

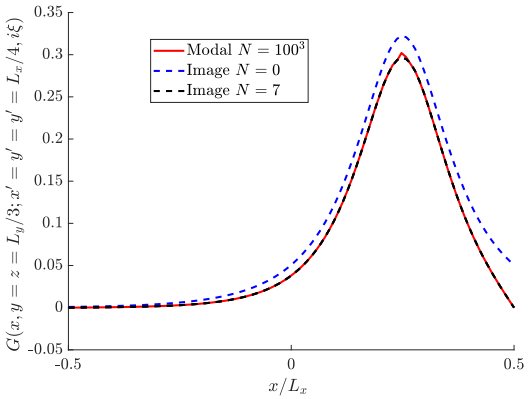


FIGURE 8.7: The 3D Green's function inside a rectangular cavity calculated by modal summation ($100^3$ modes) and image method for an imaginary wave number $\xi=2\pi$.

addition to the Green's function at imaginary wave number, the wave number derivative of the the Green's function is also require for 6th order convergence formulation. Using the image expression

$$\frac{\partial}{\partial\xi}G(\overline{r},\overline{r}',i\xi)=-\frac{1}{4\pi}\sum_{n,m,p}(-1)^{n+m+p}e^{-\xi|\overline{r}-\overline{r}_{mnp}|} \tag{8.3.35}$$

which is also exponentially convergent as a function of images positions.

## 8.4 Green's Function of the Regular Shape Cavity

The regular shaped cavity should be exactly solvable is one of the orthogonal coordinate systems. In a rectangular coordinate system, the eigen -functions of the wave equation for a perfect conductor rectangular cavity is given by

$$\psi_\alpha(\overline{r})=A\sin\frac{m\pi}{L_x}\left(x+\frac{L_x}{2}\right)\sin\frac{n\pi}{L_y}\left(y+\frac{L_y}{2}\right)\sin\frac{p\pi}{L_z}\left(z+\frac{L_z}{2}\right) \tag{8.4.1}$$

where the coordinates are defined such that $-L_j/2\leq r_j\leq L_j/2$. Normalization constant $A$ can be found to be $A=\sqrt{8/V}$ where $V$ is the volume of the cavity. The eigenvalues of the wave equation are labeled by discrete index $\alpha=(m,n,p)$ and given by $k_\alpha^2$ where

$$k_\alpha^2=\left(\frac{m\pi}{L_x}\right)^2+\left(\frac{n\pi}{L_y}\right)^2+\left(\frac{p\pi}{L_z}\right)^2 \tag{8.4.2}$$

The eigenfunction expansion of the Green function inside the cavity reads

$$G^\Omega(\overline{r},\overline{r}')=\sum_\alpha\frac{1}{k_\alpha^2-k_0^2}\psi_\alpha(\overline{r})\psi_\alpha^*(\overline{r}') \tag{8.4.3}$$

With the imaginary wave number extraction, the convergence of the regular shape Green's function expansion can be accelerated

$$G^\Omega(\overline{r},\overline{r}',k)=G^\Omega(\overline{r},\overline{r}',i\xi)-\frac{k^2+\xi^2}{2\xi}\frac{\partial}{\partial\xi}G^\Omega(\overline{r},\overline{r}',i\xi)+(k^2+\xi^2)^2\sum_\alpha\frac{\psi_\alpha(\overline{r})\psi_\alpha^*(\overline{r}')}{(k_\alpha^2+\xi^2)^2(k_\alpha^2-k^2)} \tag{8.4.4}$$

For the imaginary wave number, the first two terms can be calculated rapidly by using images sources,

$$\begin{aligned}G^\Omega(\overline{r},\overline{r}',i\xi)&=\sum_\alpha\frac{1}{k_\alpha^2+\xi^2}\psi_\alpha(\overline{r})\psi_\alpha^*(\overline{r}')\\&=\frac{1}{4\pi}\sum_{n,m,p}(-1)^{n+m+p}\frac{e^{-\xi|\overline{r}-\overline{r}_{mnp}|}}{|\overline{r}-\overline{r}_{mnp}|}\end{aligned} \tag{8.4.5}$$

and for the imaginary wave number derivative of the the Green's function

$$\begin{aligned}\frac{\partial}{\partial\xi}G^\Omega(\overline{r},\overline{r}',i\xi)&=\sum_\alpha\frac{-2\xi}{(k_\alpha^2+\xi^2)^2}\psi_\alpha(\overline{r})\psi_\alpha^*(\overline{r}')\\&=-\frac{1}{4\pi}\sum_{n,m,p}(-1)^{n+m+p}e^{-\xi|\overline{r}-\overline{r}_{mnp}|}\end{aligned} \tag{8.4.6}$$

Consider an empty cavity of dimensions $L_x=L_y=L_z=L$ at wavelength that $\lambda\approx1.08L$. The source point is located at $x'=y'=z'=L/4$ (the origin of the coordinate system at the center of cavity).

Here, the Green's function inside the rectangular cavity is computed by direct modal summation without any extraction of Eq. (8.4.3) and also using the accelerated 6th order formula of the Eq. (8.4.4) utilizing the image sources.

Figure 8.8 plots the Green function on the plane $z=L_z/3$ for a source located at $x'=y'=z'=L/4$ obtained by accelerated 6th order formula in a linear scale. The imaginary wave

number is chosen to be $\xi{=}k/\pi$ and total number of used image sources is 23. Also, in the 6th order expansion 6 terms are used in each direction (total number of terms: $6^3$). Figure. 8.9 also plots the Green's function in dB scale. In order to compare with a benchmark solution, the direct eigenfunction summation of Eq. (8.4.3) has been used with 300 terms in each direction (total of $2.7{\times}10^7$ terms in the summation) to obtain convergence up to $10^{-4}$ over all the points of observation plane. Figure. 8.10 compares plots the absolute error of the accelerated 6th order expression compared to the benchmark in $\mathrm{dBm}^{-1}$ scale. The absolute error is always less than 45 dB which is below the accuracy of direct expansion.

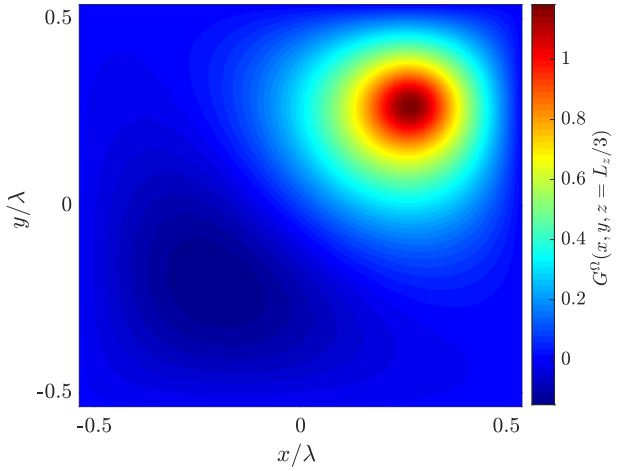


FIGURE 8.8: Scalar 3D Green's function inside a resonator of dimensions $L_x{=}L_y{=}L_z$ at wave length $\lambda{\approx}0.93L_x$ computed by the accelerated 6th order formula using $6^3$ terms.

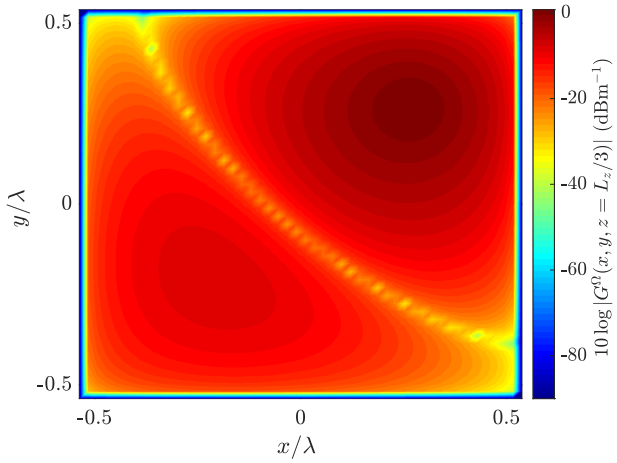


FIGURE 8.9: Scalar 3D Green's function inside a resonator of dimensions $L_x{=}L_y{=}L_z$ at wave length $\lambda{\approx}0.93L_x$ computed by the accelerated 6th order formula using $6^3$ terms, in dB scale ($\mathrm{dBm}^{-1}$)

Regarding the comparison of CPU time, 6th order extracted sum takes 0.6 CPU-ms while regular spectral expansion requires 2.1 CPU-s for computing the Green's function of

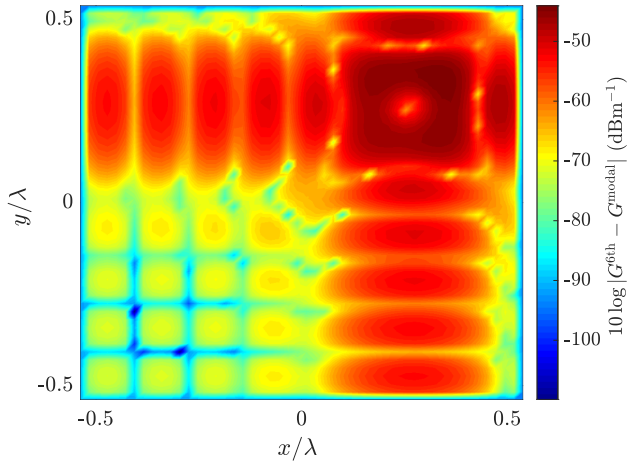


FIGURE 8.10: Absolute error of Green's function calculated by 6th order expansion using 6 modes in each direction respect to the direct modal expansion using 300 modes in each direction in dBm$^{-1}$

the rectangular cavity per observation point, which is a factor of around 3500 in computation time.

### 8.4.1 MoM to find $G^{\Omega}(\overline{r},\overline{r}'';k)$ using $G_0$ and comparison with 6th order expansion

The regular shaped cavity Green's function of $G^{\Omega}(\overline{r},\overline{r}'';k)$ satisfies the wave equation of

$$(\nabla^2+k^2)G^{\Omega}(\overline{r},\overline{r}'';k)=-\delta(\overline{r}-\overline{r}'') \quad , \quad G(\overline{r}\in\partial\Omega,\overline{r}'',k)=0 \tag{8.4.7}$$

On the other side, the free space Green's function $G_0(\overline{r},\overline{r}',k)$ also satisfies

$$(\nabla^2+k^2)G_0(\overline{r},\overline{r}';k)=-\delta(\overline{r}-\overline{r}') \quad , \tag{8.4.8}$$

subject to the radiation condition at infinity. Upon multiplying by $G_0(\overline{r},\overline{r}';k)$ and $G^{\Omega}(\overline{r},\overline{r}'';k)$, respectively and integrating the subtraction of both equation over the volume of $\Omega$ we have

$$\int_{\Omega}\mathrm{d}^3\overline{r}\Big[G^{\Omega}(\overline{r},\overline{r}'';k)\nabla^2G_0(\overline{r},\overline{r}';k)-G_0(\overline{r},\overline{r}';k)\nabla^2G^{\Omega}(\overline{r},\overline{r}'';k)\Big] \tag{8.4.9}$$
$$=\begin{cases} G_0(\overline{r}'',\overline{r}';k)-G^{\Omega}(\overline{r}',\overline{r}'';k) & \text{if:}\overline{r}',\overline{r}''\in\Omega \\ G_0(\overline{r}'',\overline{r}';k) & \text{if:}\overline{r}'\in\Omega,\overline{r}''\notin\Omega \\ -G^{\Omega}(\overline{r}',\overline{r}'';k) & \text{if:}\overline{r}''\in\Omega,\overline{r}'\notin\Omega \\ 0 & \text{if:}\overline{r}',\overline{r}''\notin\Omega \end{cases}$$

Converting the volume integration into surface integral over the boundary of the cavity and utilizing that $G^{\Omega}(\overline{r},\overline{r}'';k)$ vanishes on $\partial\Omega$, results in

$$-\oint_{\partial\Omega}\mathrm{d}SG_0(\overline{r},\overline{r}';k)\hat{n}\cdot\nabla G^{\Omega}(\overline{r},\overline{r}'';k)=\begin{cases} G_0(\overline{r}'',\overline{r}';k)-G^{\Omega}(\overline{r}',\overline{r}'';k) & \text{if:}\overline{r}',\overline{r}''\in\Omega \\ G_0(\overline{r}'',\overline{r}';k) & \text{if:}\overline{r}'\in\Omega,\overline{r}''\notin\Omega \\ -G^{\Omega}(\overline{r}',\overline{r}'';k) & \text{if:}\overline{r}''\in\Omega,\overline{r}'\notin\Omega \\ 0 & \text{if:}\overline{r}',\overline{r}''\notin\Omega \end{cases} \tag{8.4.10}$$

Upon letting $\overline{r}'\to\partial\Omega$ and interchanging $\overline{r}$ and $\overline{r}'$ we have

$$\int_{\partial\Omega}\mathrm{d}S' G_0(\overline{r},\overline{r}';k)\hat{n}'\cdot\nabla' G^{\Omega}(\overline{r}',\overline{r}'';k)=-G_0(\overline{r}'',\overline{r};k) \tag{8.4.11}$$

Taking the unknown surface current density $J(\overline{r}',\overline{r}'';k)=\hat{n}'\cdot\nabla' G^{\Omega}(\overline{r}',\overline{r}'';k)$ we have

$$\int_{\partial\Omega}\mathrm{d}S' G_0(\overline{r},\overline{r}';k)J(\overline{r}',\overline{r}'';k)=-G_0(\overline{r},\overline{r}'';k) \tag{8.4.12}$$

By expanding surface current in terms of local pulse basis functions as $J=\sum_{\overline{n}}1/\Delta S_{\overline{n}}J_{\overline{n}}P_{\overline{n}}(\overline{r}_{\overline{n}})$, over the elements $\partial\Omega=\sum_{\overline{n}}\sigma_{\overline{n}}$ the matrix equation is given by $\overline{\overline{Z}}\cdot\overline{J}=\overline{b}$ where

$$\begin{aligned} Z_{\overline{m},\overline{n}}&=\frac{1}{\Delta S_{\overline{n}}}\int_{\sigma_{\overline{n}}}\mathrm{d}S' G_0(\overline{r}_{\overline{m}},\overline{r}';k) \\ b_{\overline{m}}&=-G_0(\overline{r}_{\overline{m}},\overline{r}'';k) \end{aligned} \tag{8.4.13}$$

For non self patch elements ($\overline{m}\neq\overline{n}$),

$$Z_{\overline{m},\overline{n}}=G_0(\overline{r}_{\overline{m}},\overline{r}_{\overline{n}};k) \tag{8.4.14}$$

For self patch, the integrand is singular. We replace the patch area of $\sigma_{\overline{m}}$ with a circle of radius $R_{\overline{m}}$ that gives the same area as $\sigma_{\overline{m}}$

$$\begin{aligned} Z^{\mathrm{sing}}_{\overline{m},\overline{m}}&=\frac{1}{4\pi}\frac{1}{\Delta S_{\overline{m}}}\int_C \mathrm{d}S\frac{e^{ikr}}{r} \\ &=\frac{1}{2}\frac{1}{\Delta S_{\overline{m}}}\int_0^{R_{\overline{m}}}\mathrm{d}\rho e^{ik\rho} \\ &=-\frac{1}{2ik}\frac{1}{\Delta S_{\overline{m}}}\left[1-e^{ikR_{\overline{m}}}\right] \\ &=\frac{i}{2k}\frac{1}{\Delta S_{\overline{m}}}\left[1-e^{ik\sqrt{\Delta S_{\overline{m}}/\pi}}\right] \end{aligned} \tag{8.4.15}$$

After finding the surface current $J(\overline{r}',\overline{r}'';k)$, the Green's function can be obtained at any pair of points $(\overline{r},\overline{r}'')$ by the equivalence principle of Eq. 8.4.10 as

$$G^{\Omega}(\overline{r},\overline{r}'';k)=G_0(\overline{r},\overline{r}'';k)+\int_{\partial\Omega}\mathrm{d}S' G_0(\overline{r},\overline{r}';k)J(\overline{r}',\overline{r}'';k) \tag{8.4.16}$$

and in term of discretized surface current

$$G^{\Omega}(\overline{r},\overline{r}'';k)=G_0(\overline{r},\overline{r}'';k)+\sum_{\overline{n}}\frac{1}{\Delta S_{\overline{n}}}J_{\overline{n}}\int_{\sigma_{\overline{n}}}\mathrm{d}S' G_0(\overline{r},\overline{r}';k) \tag{8.4.17}$$

If observation point $\overline{r}$ is not on the boundary, then

$$G^{\Omega}(\overline{r},\overline{r}'';k)=G_0(\overline{r},\overline{r}'';k)+\sum_{\overline{n}}J_{\overline{n}}G_0(\overline{r},\overline{r}_{\overline{n}};k) \tag{8.4.18}$$

If the observation point coincide with the boundary surface element $\overline{m}$, then

$$G^{\Omega}(\overline{r},\overline{r}'';k)=G_0(\overline{r},\overline{r}'';k)+\sum_{\overline{n}\neq\overline{m}}\frac{1}{\Delta S_{\overline{n}}}J_{\overline{n}}\int_{\sigma_{\overline{n}}}\mathrm{d}S' G_0(\overline{r},\overline{r}';k)+\frac{i}{2k}\frac{J_{\overline{m}}}{\Delta S_{\overline{m}}}\left[1-e^{ik\sqrt{\Delta S_{\overline{m}}/\pi}}\right] \tag{8.4.19}$$

Figure 8.11 plots the Green's function of rectangular cavity of size $L_x=L_y=L_z=L$ for the source point at $x'=y'=z'=L/4$ at frequency corresponds to $\lambda=0.93L$ on the plane of $z=L_z/3$ computed by MoM over the walls of the rectangular cavity using $G_0(\overline{r},\overline{r}';k)$ as propagator of the SIE.

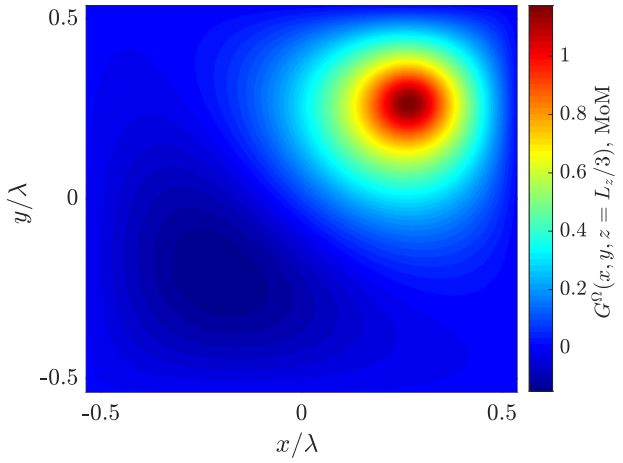


FIGURE 8.11: Scalar 3D Green's function inside a resonator of dimensions $L_x = L_y = L_z = L$ at wave length $\lambda \approx 0.93 L_x$ computed by the MoM over boundary of the rectangular cavity using $G_0(\overline{r}, \overline{r}', k)$

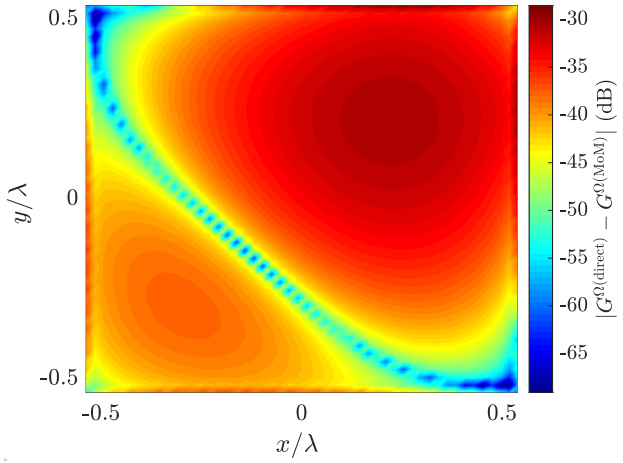


FIGURE 8.12: Absolute difference between MoM and 6th order spectral expansion for the scalar 3D Green's function inside a resonator of dimensions $L_x = L_y = L_z = L$ at wave length $\lambda \approx 0.93 L_x$ in dB.

## 8.5 Irregular Shape Cavity, Imaginary Wavenumber Extraction

Consider an irregular shaped cavity $S$. The procedure of constructing the Green's function of irregular shaped cavity $G^S(\overline{r}, \overline{r}'; k)$ is represented in the chart Fig. 8.13. Step 1 includes the hybrid representation of $G^{\Omega}(\overline{r}, \overline{r}'; k)$ which has been completed in the previous section. In the second step , the hybrid $G^{\Omega}(\overline{r}, \overline{r}'; k)$ is inserted into a surface integral equation of the irregular shaped cavity (described in sec. **??**) that yields a linear eigenvalue problem for the eigenvalue $q_\beta$ and the mode functions $\phi_\beta(\overline{r})$ where for the cavity $S$. The solution of $\phi_\beta(\overline{r})$ is a hybrid summation of the surface integral contribution and the modal expansion

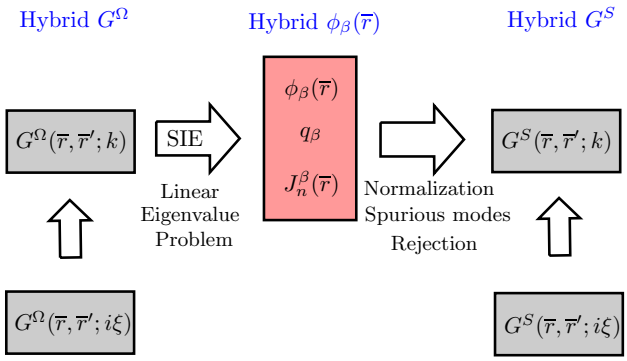


FIGURE 8.13: Procedure of construction of the irregular shaped cavity Green's function $G^S(\overline{r},\overline{r}';k)$.

in terms of $\psi_\alpha(\overline{r})$ of the rectangular cavity. In the last step $G^S(\overline{r},\overline{r}';k)$ is constructed using a hybrid representation of summation of imaginary wavenumber extraction $G^S(\overline{r},\overline{r}';k)$ and the modal expansion in terms of $\phi_\beta(\overline{r})$. This procedure will be described step by step here and in the next sections.

Here, in order to show the procedure of treating an irregular shaped cavity, we consider a rectangular cavity with a V-Groove of Fig. 8.14 as an example. Let's call the interior volume and the boundary surface of the cavity of the irregular shape $S$ and $\partial S$, respectively. . All of the steps and logics can be applied equivalently to the other geometries as well. The resonant wave function $\phi_\alpha(\overline{r})$ with resonant wave number $q_\alpha$ (In order to distinguish

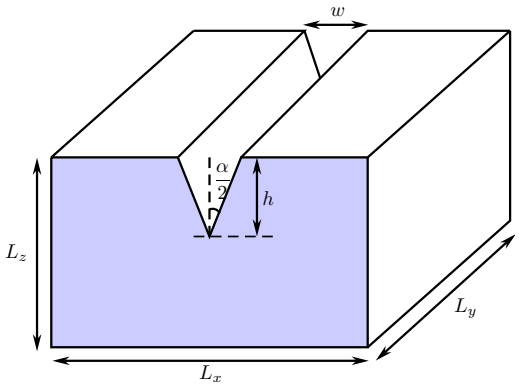


FIGURE 8.14: A rectangular cavity with a V-Groove.

between regular and irregular geometries, we will use this notation) inside the cavity satisfies the eigenvalue equation of

$$(\nabla^2+q_\alpha^2)\phi_\alpha(\overline{r})=0 \tag{8.5.1}$$

The eigenvalues $q_\alpha$ and eigenfunctions $\phi_\alpha(\overline{r})$ are functions of geometrical parameters but not the excitation frequency and are not known yet. The Green 's function at the excitation frequency $\omega$ that corresponds to excitation wave number $k=\omega\sqrt{\mu\varepsilon}$ inside the cavity, can be expanded in terms of the resonant modes as

$$G^S(\overline{r},\overline{r}';k)=\sum_\alpha \frac{1}{q_\alpha^2-k^2}\phi_\alpha(\overline{r})\phi_\alpha^*(\overline{r}') \tag{8.5.2}$$

Note that the resonant mode function $\phi_\alpha(\overline{r})$ does not depend on the frequency and this representation has a simple dependence on the excitation frequency. The problem with this expansion is that similar to the case of rectangular cavity, required number of terms to get a convergent Green's function with acceptable level of accuracy is large. Conventional way is to use the numerical methods like MoM to find the modes but computation cost would be expensive to solve for many modes. In particular, these numerical methods require a non-linear search to find the eigenvalues. Therefore, computing the Green's function using the modal expansion by computing the eigenfunctions directly is also computationally expensive. The spectral summation can be accelerated by Imaginary wave number extraction (similar to the rectangular cavity) to the 6th order convergence as

$$G^S(\overline{r},\overline{r}';k)=G^S(\overline{r},\overline{r}';i\xi)-\frac{k^2+\xi^2}{2\xi}\frac{\partial}{\partial\xi}G(\overline{r},\overline{r}';i\xi) \\ +(k^2+\xi^2)^2\sum_\beta\frac{\phi_\beta(\overline{r})\phi^*_\beta(\overline{r}')}{(q_\beta^2+\xi^2)^2(q_\beta^2-k^2)} \tag{8.5.3}$$

If the extracted terms can be determined with a low cost procedure, then at least this expansion would converge much faster (6th order instead of 2nd order). On the other hand, cost of computing the Green's function at imaginary wave number is lower than the computing the Green's function at a real wavenumber (reasons are mentioned in Sec. **??** ). Furthermore, for a broad band solution, the extracted terms need to be computed only one time at a fixed imaginary wave number $k=i\xi$.

The point of interest in the modal expansion is the broadband characteristic which is the simple dependence on the frequency through the denominator. However, it is important to find the resonant modes in a way that is independent of the excitation frequency. For example, one may use conventional MoM to find the resonant wave function $\phi_\beta(\overline{r})$ and sums up the spectral expansion. However, finding the resonant modes requires a fine sweep over frequency and in addition searching process is non-linear. Given these difficulties to find the mode functions, direct MoM solution for the Green's function at each frequency point is a more efficient approach.

In order to circumvent the required non-linear search and fine sweep over frequency to find the eigenvalues and eigenfunctions, a hybrid spatial-spectral linear eigenvalue problem will be developed in the next section.

## 8.6 Linear Eigenvalue Equation

### 8.6.1 Surface Integral Equation for The Resonant Modes

The resonant wave function $\phi(\overline{r})$ inside the irregular cavity satisfies the homogeneous wave equation

$$(\nabla^2+k^2)\phi(\overline{r})=0 \quad , \quad \phi(\overline{r}\in S)=0 \tag{8.6.1}$$

subject to Dirichlet boundary condition $\phi(\overline{r})=0$ for $\overline{r}\in S$. On the other side the Green's function at wave number $k$ in the corresponding regular shaped cavity $G^\Omega(\overline{r},\overline{r}')$ satisfies the inhomogeneous wave equation subject to boundary condition $G^\Omega(\overline{r},\overline{r}')=0$ for $\overline{r}\in\partial\Omega$ where $\partial\Omega$ is the boundary surface of the regular shaped (rectangular here) cavity,

$$(\nabla^2+k^2)G^\Omega(\overline{r},\overline{r}')=-\delta(\overline{r}-\overline{r}') \quad , \quad G^\Omega(\overline{r}\in\partial\Omega,\overline{r}')=0 \tag{8.6.2}$$

Upon multiplying Eq. (8.6.1) and Eq. (8.6.2) by $G^{\Omega}(\overline{r},\overline{r}')$ and $\phi(\overline{r})$, respectively and integrating the subtraction of both equation over the volume of $V$ we have

$$\int_V \mathrm{d}^3\overline{r}\left[G^{\Omega}(\overline{r},\overline{r}')\nabla^2\phi(\overline{r})-\phi(\overline{r})\nabla^2 G^{\Omega}(\overline{r},\overline{r}')\right]=\begin{cases}\phi(\overline{r}') & \text{if:}\overline{r}'\in V\\ 0 & \text{if:}\overline{r}'\notin V\end{cases} \tag{8.6.3}$$

Utilizing the Green's identity, volumetric integral can be converted into a surface integral over $S$,

$$\oint_S \mathrm{d}S\left[G^{\Omega}(\overline{r},\overline{r}')\hat{n}\cdot\nabla\phi(\overline{r})-\phi(\overline{r})\hat{n}\cdot\nabla G^{\Omega}(\overline{r},\overline{r}')\right]=\begin{cases}\phi(\overline{r}') & \text{if:}\overline{r}'\in V\\ 0 & \text{if:}\overline{r}'\notin V\end{cases} \tag{8.6.4}$$

Now, the resonant wave function $\phi(\overline{r})$ vanishes on the surface of the cavity and interchanging primed and unprimed coordinate

$$\oint_S \mathrm{d}S'\ G^{\Omega}(\overline{r},\overline{r}')\hat{n}'\cdot\nabla'\phi(\overline{r}')=\begin{cases}\phi(\overline{r}) & \text{if:}\overline{r}\in V\\ 0 & \text{if:}\overline{r}\notin V\end{cases} \tag{8.6.5}$$

The irregular cavity boundary $S$ can be decomposed into $S=S_{\Omega}+\sigma$ where $S_{\Omega}$ is the part of $S$ that overlap with $\partial\Omega$. The boundary surface $\sigma$ for the cavity of Fig. 8.14 is depicted in Fig. 8.15. Since $G^{\Omega}(\overline{r},\overline{r}')$ vanishes on $\partial\Omega$ and in particular on $S_{\Omega}$, the only non-zero part of the surface integral is

$$\int_{\sigma} \mathrm{d}S'\ G^{\Omega}(\overline{r},\overline{r}')\hat{n}'\cdot\nabla'\phi(\overline{r}')=\begin{cases}\phi(\overline{r}) & \text{if:}\overline{r}\in V\\ 0 & \text{if:}\overline{r}\notin V\end{cases} \tag{8.6.6}$$

Upon placing the observation point on the surface of the cavity and taking $J(\overline{r}')=\hat{n}'\cdot\nabla'\phi(\overline{r}')$ we have the surface integral equation

$$\int_{\sigma} \mathrm{d}S'\ G^{\Omega}(\overline{r},\overline{r}')J(\overline{r}')=0 \tag{8.6.7}$$

Notice that this is an integral equation counterpart of the differential eigenvalue equation of Eq. 8.6.1 and solutions are resonant wave functions $\phi_{\alpha}(\overline{r})$ with corresponding eigenvalue of $q_{\alpha}^2$.

### 8.6.2 Linear Eigen-value Equation Using The 4th Order Spectral Summation

The regular cavity Green's function $G^{\Omega}(\overline{r},\overline{r}';k)$ at excitation wave number $k$ can be written in terms of an accelerated modal expansion of

$$G^{\Omega}(\overline{r},\overline{r}',k)=G^{\Omega}(\overline{r},\overline{r}',i\xi)+\sum_{\alpha=1}^{M_{\Omega}}\left[\frac{k^2+\xi^2}{(k_{\alpha}^2-k^2)(k_{\alpha}^2+\xi^2)}\right]\psi_{\alpha}(\overline{r})\psi_{\alpha}^{*}(\overline{r}') \tag{8.6.8}$$

Here, $k_{\alpha}$ and $\psi_{\alpha}(\overline{r})$ are resonant frequencies and wave functions of the regular shaped cavity (rectangular), respectively. The summation is truncated at $M_{\Omega}$ such that the Green's function of the rectangular cavity is computed with desired level of accuracy. The Green's function at imaginary wave number is also calculated accurately with few terms in the

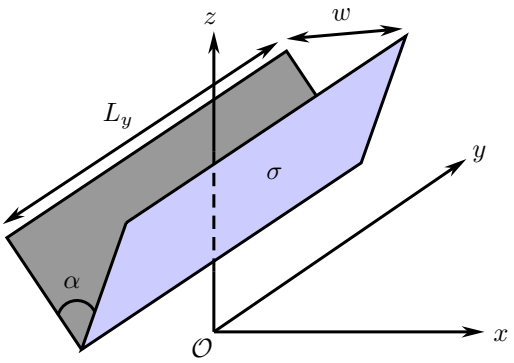


FIGURE 8.15: Boundary surface $\sigma$, the part of cavity surface which is not common with the corresponding regular shape cavity

image source expansion. Using the extracted expansion of Eq. 8.6.8 in the surface integral equation of Eq. 8.6.7 we have

$$\int_{\sigma} \mathrm{d}S' G^{\Omega}(\overline{r},\overline{r}',i\xi)J(\overline{r}')+\sum_{\alpha=1}^{M_{\Omega}}\left[\frac{k^2+\xi^2}{(k_{\alpha}^2-k^2)(k_{\alpha}^2+\xi^2)}\right]\psi_{\alpha}(\overline{r})\int_{\sigma}\mathrm{d}S'\psi_{\alpha}^{*}(\overline{r}')J(\overline{r}')=0 \tag{8.6.9}$$

Defining the projection of the surface current $J(\overline{r})$ on the $\psi_{\alpha}^{*}(\overline{r})$ together with frequency dependent terms as

$$c_{\alpha}=\frac{k^2+\xi^2}{k_{\alpha}^2-k^2}\int_{\sigma}\mathrm{d}S'\psi_{\alpha}^{*}(\overline{r}')J(\overline{r}') \tag{8.6.10}$$

the SIE becomes,

$$\int_{\sigma}\mathrm{d}S' G^{\Omega}(\overline{r},\overline{r}',i\xi)J(\overline{r}')+\sum_{\alpha=1}^{M_{\Omega}}\frac{1}{k_{\alpha}^2+\xi^2}\psi_{\alpha}(\overline{r})c_{\alpha}=0 \tag{8.6.11}$$

The surface current $J(\overline{r})$ can be discretized on the boundary surface $\sigma$ using a set of basis functions as

$$J(\overline{r})=\sum_{\overline{n}}\frac{1}{\Delta S_{\overline{n}}}J_{\overline{n}}P_{\overline{n}}(\overline{r}) \tag{8.6.12}$$

Here, $\overline{n}$ is a two dimensional index of the basis functions on the surface $\sigma$ and $\Delta S_{\overline{n}}$ is the area of the $\overline{n}$-th element. If we assume local pulse basis functions over the cell of $\sigma_{\overline{n}}$ and total number of the patches on $\sigma$ is $N_{\sigma}$

$$\sum_{\overline{n}}\frac{1}{\Delta S_{\overline{n}}}J_{\overline{n}}\int_{\sigma_{\overline{n}}}\mathrm{d}S' G^{\Omega}(\overline{r},\overline{r}',i\xi)+\sum_{\alpha=1}^{M_{\Omega}}\frac{1}{k_{\alpha}^2+\xi^2}\psi_{\alpha}(\overline{r})c_{\alpha}=0 \tag{8.6.13}$$

Now, using the delta function at $\overline{r}_{\overline{m}}$ to test the integral equation we have

$$\sum_{\overline{n}}Z_{\overline{m},\overline{n}}J_{\overline{n}}+\sum_{\alpha=1}^{M_{\Omega}}R_{\overline{m},\alpha}c_{\alpha}=0 \tag{8.6.14}$$

or in the matrix form $\overline{\overline{Z}}\cdot\overline{J}+\overline{\overline{R}}\cdot\overline{c}=0$. Here, the MoM impedance matrix elements $Z_{\overline{m},\overline{n}}$ and hybrid MoM-Modal matrix element $R_{\overline{m},\alpha}$ are given by

$$Z_{\overline{m},\overline{n}}=\frac{1}{\Delta S_{\overline{n}}}\int_{\sigma_{\overline{n}}}\mathrm{d}S' G^{\Omega}(\overline{r}_{\overline{m}},\overline{r}',i\xi)$$
$$R_{\overline{m},\alpha}=\frac{1}{k_\alpha^2+\xi^2}\psi_\alpha(\overline{r}_{\overline{m}}) \tag{8.6.15}$$

On the other side, the modal coefficients $c_\alpha$ can be discretized by the MoM scheme to give

$$c_\alpha=\frac{k^2+\xi^2}{k_\alpha^2-k^2}\sum_{\overline{n}}J_{\overline{n}}\psi_\alpha^*(\overline{r}_{\overline{n}}) \tag{8.6.16}$$
$$=\frac{(k^2+\xi^2)(k_\alpha^2+\xi^2)}{k_\alpha^2-k^2}\sum_{\overline{n}}J_{\overline{n}}R_{\overline{n},\alpha}^* \tag{8.6.17}$$

Where we have used definition of $R_{\overline{n},\alpha}$ in Eq. 8.6.15 and the fact that $\xi^2$ and $k_\alpha^2$ are real quantities. Rearranging the terms

$$\sum_{\overline{n}}J_{\overline{n}}R_{\overline{n},\alpha}^*=c_\alpha\left[\frac{1}{k^2+\xi^2}-\frac{1}{k_\alpha^2+\xi^2}\right] \tag{8.6.18}$$

Upon defining a diagonal matrix $\overline{\overline{D}}$ with $D_{\alpha\alpha}=(k_\alpha^2+\xi^2)^{-1}$ and taking $\lambda=(k^2+\xi^2)^{-1}$ we have

$$\overline{\overline{R}}^{\dagger}\cdot\overline{J}+\overline{\overline{D}}\cdot\overline{c}=\lambda\overline{c} \tag{8.6.19}$$

Using $\overline{\overline{Z}}\cdot\overline{J}+\overline{\overline{R}}\cdot\overline{c}=0$ to eliminate $\overline{J}$ by substituting $\overline{J}=-\overline{\overline{Z}}^{-1}\cdot\overline{\overline{R}}\cdot\overline{c}$ we have the linear eigenvalue equation of

$$\left(\overline{\overline{D}}-\overline{\overline{R}}^{\dagger}\cdot\overline{\overline{Z}}^{-1}\cdot\overline{\overline{R}}\right)\cdot\overline{c}=\lambda\overline{c} \tag{8.6.20}$$

This is the linear eigenvalue equation, where the eigenvalues determine the resonant wave number $k=q_\alpha$ and the eigenvectors $\overline{c}$ provides the projection coefficients of the resonant surface current $J(\overline{r})$ on the regular (rectangular) cavity wave functions $\psi_\alpha(\overline{r})$. In order to construct the Green's function of the irregular shaped cavity, eigenmodes of the cavity are required. The resonant wave functions $\phi_\beta(\overline{r})$ inside the cavity can be found by the equivalence principle of Eq. 8.6.6 where $\overline{r}\in V$

$$\int_\sigma \mathrm{d}S'\ G^{\Omega}(\overline{r},\overline{r}',k=q_\beta)J^\beta(\overline{r}')=\phi_\beta(\overline{r}) \tag{8.6.21}$$

Using the extracted expansion of the Green's function $G^{\Omega}(\overline{r},\overline{r}',q_\beta)$

$$\phi_\beta(\overline{r})=\sum_{\overline{n}}J_{\overline{n}}^\beta\frac{1}{\Delta S_{\overline{n}}}\int_{\sigma_{\overline{n}}}\mathrm{d}S' G^{\Omega}(\overline{r},\overline{r}',i\xi)+\sum_{\alpha=1}^{M_\Omega}\frac{1}{k_\alpha^2+\xi^2}\psi_\alpha(\overline{r})c_\alpha^\beta \tag{8.6.22}$$

where,

$$c_\alpha^\beta=\frac{q_\beta^2+\xi^2}{k_\alpha^2-q_\beta^2}\sum_{\overline{n}}J_{\overline{n}}^\beta\psi_\alpha^*(\overline{r}_{\overline{n}}) \tag{8.6.23}$$

$c_\alpha^\beta$ is the $\beta$-th eigenvector of the linear eigenvalue system of Eq. 8.6.20. Now, the wave functions $\phi_\beta(\overline{r})$ are known by Eq. 8.6.22.

### 8.6.3 Normalization of the Modes

The resonant wave functions $\phi_\beta(\overline{r})$ are related to the eigenvectors of the eigenvalue system of (8.6.20) and are known. However the wave functions obtained by (8.6.22) are arbitrary up to a multiplicative constant while in all of the spectral expansions of the Green's function it is assumed that the resonant wave functions are normalized with respect to the inner product induced by the wave equation. In order to use the spectral expansion of the Green's function, the wave functions $\phi_\beta(\overline{r})$ should be normalized over the volume of the cavity according to

$$\int_V \mathrm{d}^3\overline{r}\left|\phi_\beta(\overline{r})\right|^2=1 \quad , \quad \forall\beta$$

Normalizing the modes using this volume integration for each mode is a computationally expensive task. Instead each wave function $\phi_\beta$ can be expanded in terms of the regular shaped cavity wave functions $\psi_\alpha$ as they form a complete basis functions in $S\subseteq\Omega$

$$\phi_\beta(\overline{r})=\sum_{\alpha=1}^{\infty} d_\alpha^\beta\psi_\alpha(\overline{r})$$

Taking into account that $\left\{\psi_\alpha(\overline{r})\right\}_\alpha$ constitute an orthonormal set, normalization of the $\phi_\beta(\overline{r})$ requires that

$$\sum_\alpha\left|d_\alpha^\beta\right|^2=1$$

$\overline{\overline{d}}$ is the transformation matrix between two orthonormal sets $\{\phi_\beta\}_\beta$, and $\{\psi_\alpha\}_\alpha$ and therefore it should be a unitary transformation. Requirement of orthogonality of the columns of $\overline{\overline{d}}$ is always granted as $\{\phi_\beta(\overline{r})\}_\beta$ is an orthogonal set (for a lossless cavity). The transformation coefficients of $d_\alpha^\beta$ can be read from Eq. 8.6.22. Since we need to compute $|d_\alpha^\beta|^2$, substituting the conventional 2nd order spectral expansion of (8.4.3) into (8.6.22) results in the 4th order convergence in computation of $|d_\alpha^\beta|^2$ with respect to the mode number $\alpha$.

$$\phi_\beta(\overline{r})=\sum_{\alpha=1}^{\infty}\sum_{\overline{n}} J_{\overline{n}}^\beta\frac{1}{k_\alpha^2+\xi^2}\psi_\alpha(\overline{r})\psi_\alpha^*(\overline{r}_{\overline{n}})+\sum_{\alpha=1}^{M_\Omega}\frac{1}{k_\alpha^2+\xi^2}\psi_\alpha(\overline{r})c_\alpha^\beta$$

which results in

$$d_\alpha^\beta=\frac{1}{k_\alpha^2+\xi^2}\left(\sum_{\overline{n}} J_{\overline{n}}^\beta\psi_\alpha^*(\overline{r}_{\overline{n}})+c_\alpha^\beta\right)$$

or

$$d_\alpha^\beta=\begin{cases}\dfrac{1}{k_\alpha^2+\xi^2}\left(\dfrac{k_\alpha^2-q_\beta^2}{q_\beta^2+\xi^2}+1\right)c_\alpha^\beta, & 1\leq\alpha\leq M_\Omega\\[2ex] \dfrac{1}{k_\alpha^2+\xi^2}\displaystyle\sum_{\overline{n}} J_{\overline{n}}^\beta\psi_\alpha^*(\overline{r}_{\overline{n}}), & \alpha>M_\Omega\end{cases}$$

After finding the transformation coefficients $d_\alpha^\beta$ all of the surface currents $J^\beta(\overline{r})$ and wave functions $\phi_\beta(\overline{r})$ should be renormalized to $\sqrt{L^\beta}$ where

$$L_\beta = \sum_{\alpha=1}^{\infty} \left| d_\alpha^\beta \right|^2$$

### 8.6.4 Spurious Modes

The solution to the surface integral equation of (8.6.7), provides the resonant surface currents inside the irregular cavity of volume $V$. However, the resonant surface current of the complementary cavity of Fig. 8.16, $J^c(\overline{r})$ satisfies the same SIE as $J(\overline{r})$ of the cavity of Fig. 8.14 does,

$$\int_\sigma \mathrm{d}S' \; G^\Omega(\overline{r},\overline{r}') J^c(\overline{r}') = 0 \tag{8.6.24}$$

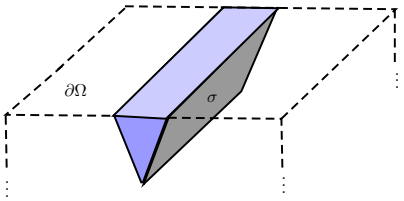


FIGURE 8.16: Complementary cavity with respect to the regular cavity bounded by $\partial\Omega$.

Although the complementary cavity surface current $J^c(\overline{r})$, satisfies the same surface integral equation as the surface current of the desired cavity, those are spurious solutions of the SIE.

The complementary cavity modes are not the only spurious solutions. A linear combination of cavity modes and complementary cavity modes is also an spurious mode. Figure. 8.17 shows a high order spurious mode that is linear combination of desired and complementary modes. Since the complementary cavity is smaller than the cavity itself, spurious modes appear among the high frequency modes.

In order to distinguish between real and spurious solutions, the extinction theorem for the cavity wave function can be used,

$$\int_\sigma \mathrm{d}S' \; G^\Omega(\overline{r},\overline{r}') \hat{n}' \cdot \nabla' \phi(\overline{r}') = \begin{cases} \phi(\overline{r}) & \text{if:} \overline{r} \in V \\ 0 & \text{if:} \overline{r} \notin V \end{cases} \tag{8.6.25}$$

The surface current that is related to the resonant wave functions of the desired cavity $\phi(\overline{r})$ will produce zero field outside of the cavity ($\overline{r} \notin V$). By evaluating the wave function at some sample points outside of the cavity we can throw away the spurious wave functions which have non-zero value outside the cavity.

## 8.7 MoM to find $G(\overline{r},\overline{r}';i\xi)$

After finding the resonant wave functions and wave numbers $\phi_\beta$ and $q_\beta$, we can directly plug them into the original spectral expansion of the second order convergence. However,

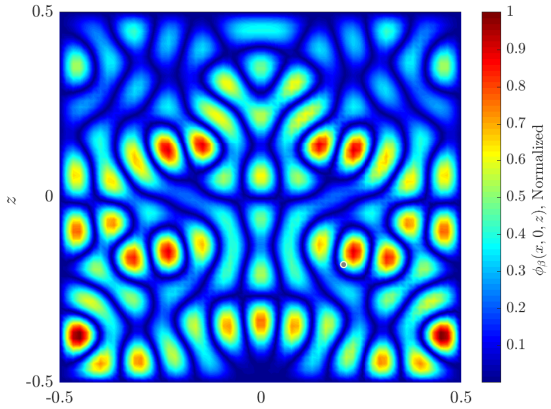


FIGURE 8.17: A spurious solution of the eigenfunction $\phi_\beta(\overline{r})$ of the irregular shaped cavity over $y$=0 plane. The wave function does not vanish outside of the cavity in the groove region.

the convergence is slow and in order to take the advantages of the fourth order expansion of $G(\overline{r},\overline{r}';i\xi)$ for the irregular shaped cavity which is given by

$$G(\overline{r},\overline{r}';k)=G(\overline{r},\overline{r}';i\xi)+\sum_\beta\left[\frac{k^2+\xi^2}{(q_\beta^2-k^2)(q_\beta^2+\xi^2)}\right]\phi_\beta(\overline{r})\phi_\beta^*(\overline{r}') \tag{8.7.1}$$

we need to find the Green's function of the irregular cavity at imaginary wave number $\xi$. Basically one may want to find the Green's function inside the cavity without going to the process of eigenfunction expansion and accelerating convergence of the summations. However, there are several reasons that applying MoM directly to find the Green's function is not efficient. First, at imaginary wave number, the matrix equations are very well behaved and sparse as the interaction is exponentially damped. Second, for a wide band solution (different $k$'s), $G(\overline{r},\overline{r}';i\xi)$ should be computed only one time at the imaginary wave number $\xi$. The regular cavity Green's function $G^\Omega(\overline{r},\overline{r}';i\xi)$ satisfies the inhomogeneous equation of

$$(\nabla^2-\xi^2)G^\Omega(\overline{r},\overline{r}';i\xi)=-\delta(\overline{r}-\overline{r}') \quad , \quad G^\Omega(\overline{r}\in\partial\Omega,\overline{r}')=0 \tag{8.7.2}$$

The irregular cavity Green's function at imaginary wave number of $G(\overline{r},\overline{r}'';i\xi)$ also satisfies the inhomogeneous equation of

$$(\nabla^2-\xi^2)G(\overline{r},\overline{r}'';i\xi)=-\delta(\overline{r}-\overline{r}'') \quad , \quad G(\overline{r}\in S,\overline{r}'',i\xi)=0 \tag{8.7.3}$$

Upon multiplying Eq. (8.7.2) and Eq. (8.7.3) by $G(\overline{r},\overline{r}';i\xi)$ and $G^\Omega(\overline{r},\overline{r}';i\xi)$, respectively and integrating the subtraction of both equation over the volume of $V$ we have

$$\int_V \mathrm{d}^3\overline{r}\left[G^\Omega(\overline{r},\overline{r}';i\xi)\nabla^2 G(\overline{r},\overline{r}'';i\xi)-G(\overline{r},\overline{r}'';i\xi)\nabla^2 G^\Omega(\overline{r},\overline{r}';i\xi)\right] \tag{8.7.4}$$

$$=\begin{cases} G(\overline{r}',\overline{r}'';i\xi)-G^\Omega(\overline{r}'',\overline{r}';i\xi) & \text{if:}\overline{r}',\overline{r}''\in V \\ G(\overline{r}',\overline{r}'';i\xi) & \text{if:}\overline{r}'\in V,\overline{r}''\notin V \\ -G^\Omega(\overline{r}',\overline{r}'';i\xi) & \text{if:}\overline{r}''\in V,\overline{r}'\notin V \\ 0 & \text{if:}\overline{r}',\overline{r}''\notin V \end{cases}$$

Converting the volume integration into surface integral over the boundary of the cavity and utilizing that $G(\overline{r},\overline{r}'';i\xi)$ vanishes on $S$ and $G^{\Omega}(\overline{r},\overline{r}';i\xi)$ also vanishes on $S-\sigma$,

$$\int_{\sigma} \mathrm{d}S G^{\Omega}(\overline{r},\overline{r}';i\xi)\hat{n}\cdot\nabla G(\overline{r},\overline{r}'';i\xi)=\begin{cases} G(\overline{r}',\overline{r}'';i\xi)-G^{\Omega}(\overline{r}'',\overline{r}';i\xi) & \text{if:}\overline{r}',\overline{r}''\in V \\ G(\overline{r}',\overline{r}'';i\xi) & \text{if:}\overline{r}'\in V,\overline{r}''\notin V \\ -G^{\Omega}(\overline{r}',\overline{r}'';i\xi) & \text{if:}\overline{r}''\in V,\overline{r}'\notin V \\ 0 & \text{if:}\overline{r}',\overline{r}''\notin V \end{cases} \tag{8.7.5}$$

Upon letting $\overline{r}'\to S$ and interchanging $\overline{r}$ and $\overline{r}'$ we have

$$\int_{\sigma} \mathrm{d}S' G^{\Omega}(\overline{r},\overline{r}';i\xi)\hat{n}'\cdot\nabla' G(\overline{r}',\overline{r}'';i\xi)=-G^{\Omega}(\overline{r},\overline{r}'';i\xi) \tag{8.7.6}$$

Taking the unknown surface current density $J(\overline{r}',\overline{r}'';i\xi)=\hat{n}'\cdot\nabla' G(\overline{r}',\overline{r}'';i\xi)$ we have

$$\int_{\sigma} \mathrm{d}S' G^{\Omega}(\overline{r},\overline{r}';i\xi) J(\overline{r}',\overline{r}'';i\xi)=-G^{\Omega}(\overline{r},\overline{r}'';i\xi) \tag{8.7.7}$$

By expanding surface current in terms of local pulse basis functions as $J=\sum_{\overline{n}} 1/\Delta S_{\overline{n}} J_{\overline{n}} P_{\overline{n}}(\overline{r}_{\overline{n}})$, the matrix equation is $\overline{\overline{Z}}\cdot\overline{J}=\overline{b}$ where

$$\begin{aligned} Z_{\overline{m},\overline{n}} &= \frac{1}{\Delta S_{\overline{n}}}\int_{\sigma_{\overline{n}}} \mathrm{d}S' G^{\Omega}(\overline{r}_{\overline{m}},\overline{r}';i\xi) \\ b_{\overline{m}} &= -G^{\Omega}(\overline{r}_{\overline{m}},\overline{r}'';i\xi) \end{aligned} \tag{8.7.8}$$

After finding the surface current $J(\overline{r}',\overline{r}'';i\xi)$, the Green's function can be obtained at any pair of points $(\overline{r},\overline{r}'')$ by the equivalence principle of Eq. 8.7.5 as

$$G(\overline{r},\overline{r}'';i\xi)=G^{\Omega}(\overline{r},\overline{r}'';i\xi)+\int_{\sigma} \mathrm{d}S' G^{\Omega}(\overline{r},\overline{r}';i\xi)\hat{n}'\cdot\nabla' G(\overline{r}',\overline{r}'';i\xi) \tag{8.7.9}$$

The matrix equation obtained by MoM is sparse and very well behaved. The interaction at imaginary wave number is exponentially damped and the impedance matrix is banded. In addition resonance does not occur at imaginary wave number and the system of equations has a very low condition number.

### Impedance matrix elements

For the problem of finding the Green's function at imaginary wave number $i\xi$ we need to compute the impedance matrix of

$$Z_{\overline{m},\overline{n}}=\frac{1}{\Delta S_{\overline{n}}}\int_{\sigma_{\overline{n}}} \mathrm{d}S' G^{\Omega}(\overline{r}_{\overline{m}},\overline{r}';i\xi) \tag{8.7.10}$$

Since $G^{\Omega}(\overline{r}_{\overline{m}},\overline{r}';i\xi)$ decays exponentially by distance and it is pretty uniform over a cell, non-self patch elements $\overline{m}\neq\overline{n}$ can be evaluated by center point approximation

$$Z_{\overline{m},\overline{n}}=G^{\Omega}(\overline{r}_{\overline{m}},\overline{r}_{\overline{n}};i\xi) \tag{8.7.11}$$

for the self patch elements, using the image expansion

$$G^{\Omega}(\overline{r},\overline{r}',i\xi)=\frac{1}{4\pi}\sum_{n,m,p}(-1)^{n+m+p}\frac{e^{-\xi|\overline{r}-\overline{r}_{mnp}|}}{|\overline{r}-\overline{r}_{mnp}|} \tag{8.7.12}$$

This expansion contains the contribution from the real source corresponds to $(m,n,p)=(0,0,0)$ and images charges. The only singular term is the contribution of the real source

$$Z_{\overline{m},\overline{m}}=\frac{1}{4\pi}\sum_{\substack{m,n,p\\(m,n,p\neq(0,0,0)}}(-1)^{n+m+p}\frac{e^{-\xi|\overline{r}_{\overline{m}}-\overline{r}_{mnp}|}}{|\overline{r}_{\overline{m}}-\overline{r}_{mnp}|}+\frac{1}{4\pi}\frac{1}{\Delta S_{\overline{m}}}\int_{\sigma_{\overline{m}}}\mathrm{d}S'\frac{e^{-\xi|\overline{r}_{\overline{m}}-\overline{r}'|}}{|\overline{r}_{\overline{m}}-\overline{r}'|} \tag{8.7.13}$$

In order to calculate the surface integral, we approximate the surface element $\sigma_{\overline{n}}$ (it can be any shape) with a circle centered at $\overline{r}_{\overline{m}}$ with the same area as $\sigma_n$. The radius of this circle would be $R_{\overline{m}}=\sqrt{\Delta S_{\overline{m}}/\pi}$. As long as the area of discretization element are small this is a valid approximation. Near the $\overline{m}$th patch, $\overline{r}'=\overline{r}_{\overline{m}}+\overline{r}$ and

$$\begin{aligned}Z^{\mathrm{sing}}_{\overline{m},\overline{m}}&=\frac{1}{4\pi}\frac{1}{\Delta S_{\overline{m}}}\int_C\mathrm{d}S\frac{e^{-\xi r}}{r}\\&=\frac{1}{2}\frac{1}{\Delta S_{\overline{m}}}\int_0^{R_{\overline{m}}}\mathrm{d}\rho e^{-\xi\rho}\\&=\frac{1}{2\xi}\frac{1}{\Delta S_{\overline{m}}}\left[1-e^{-\xi R_{\overline{m}}}\right]\\&=\frac{1}{2\xi}\frac{1}{\Delta S_{\overline{m}}}\left[1-e^{-\xi\sqrt{\Delta S_{\overline{m}}/\pi}}\right]\end{aligned} \tag{8.7.14}$$

Therefore, total self patch elements become

$$Z_{\overline{m},\overline{m}}=\frac{1}{4\pi}\sum_{\substack{m,n,p\\(m,n,p\neq(0,0,0)}}(-1)^{n+m+p}\frac{e^{-\xi|\overline{r}_{\overline{m}}-\overline{r}^{(\overline{m})}_{mnp}|}}{|\overline{r}_{\overline{m}}-\overline{r}^{(\overline{m})}_{mnp}|}+\frac{1}{2\xi}\frac{1}{\Delta S_{\overline{m}}}\left[1-e^{-\xi\sqrt{\Delta S_{\overline{m}}/\pi}}\right] \tag{8.7.15}$$

and for non-self patch elements

$$Z_{\overline{m},\overline{n}}=\frac{1}{4\pi}\sum_{m,n,p}(-1)^{n+m+p}\frac{e^{-\xi|\overline{r}_{\overline{m}}-\overline{r}^{(\overline{n})}_{mnp}|}}{|\overline{r}_{\overline{n}}-\overline{r}^{(\overline{n})}_{mnp}|} \tag{8.7.16}$$

where $\overline{r}^{(\overline{n})}_{mnp}$'s are position of images source when the real source is located at $\overline{r}=\overline{r}_{\overline{n}}$.

### 8.7.1 Additional MoM to find $\dfrac{\partial}{\partial\xi}G(\overline{r},\overline{r}';i\xi)$

Notice that the wavenumber derivative of the Green's function is independent of the value of the Green's function and requires a new SIE to be solved. The Green's function $G(\overline{r},\overline{r}'';i\xi)$ at imaginary wave number $i\xi$ is related to the regular Green's function $G^{\Omega}(\overline{r},\overline{r}'';i\xi)$ through

$$G(\overline{r},\overline{r}'';i\xi)=G^{\Omega}(\overline{r},\overline{r}'';i\xi)+\int_{\sigma}\mathrm{d}S'G^{\Omega}(\overline{r},\overline{r}';i\xi)\hat{n}'\cdot\nabla'G(\overline{r}',\overline{r}'';i\xi) \tag{8.7.17}$$

Applying the wavenumber derivative yields

$$\begin{aligned}\frac{\partial}{\partial\xi}G(\overline{r},\overline{r}'';i\xi)=\frac{\partial}{\partial\xi}G^{\Omega}(\overline{r},\overline{r}'';i\xi)&+\int_{\sigma}\mathrm{d}S'\frac{\partial}{\partial\xi}G^{\Omega}(\overline{r},\overline{r}';i\xi)\hat{n}'\cdot\nabla'G(\overline{r}',\overline{r}'';i\xi)\\&+\int_{\sigma}\mathrm{d}S'G^{\Omega}(\overline{r},\overline{r}';i\xi)\hat{n}'\cdot\nabla'\frac{\partial}{\partial\xi}G(\overline{r}',\overline{r}'';i\xi)\end{aligned} \tag{8.7.18}$$

Assuming we know the surface current $\hat{n}'\cdot\nabla' G(\overline{r}',\overline{r}'';i\xi)$ from the MoM solution in the previous section, it is not trivial that how it depends on he wave number to find

$$\frac{\partial}{\partial\xi}\hat{n}'\cdot\nabla' G(\overline{r}',\overline{r}'';i\xi) \tag{8.7.19}$$

from that. We can set up another MoM to find this new quantity. Taking derivative of the SIE with respect to wave number $\xi$ yields

$$\int_\sigma \mathrm{d}S' \frac{\partial}{\partial\xi} G^\Omega(\overline{r},\overline{r}';i\xi)\hat{n}'\cdot\nabla' G(\overline{r}',\overline{r}'';i\xi) + \int_\sigma \mathrm{d}S' G^\Omega(\overline{r},\overline{r}';i\xi)\hat{n}'\cdot\nabla' \frac{\partial}{\partial\xi} G(\overline{r}',\overline{r}'';i\xi) = -\frac{\partial}{\partial\xi} G^\Omega(\overline{r},\overline{r}'';i\xi) \tag{8.7.20}$$

The wave number derivative of the $G^\Omega(\overline{r},\overline{r}'';i\xi)$ can be easily calculated. Taking the surface current $J(\overline{r}',\overline{r}'';i\xi)=\hat{n}'\cdot\nabla' G(\overline{r}',\overline{r}'';i\xi)$ (which is now known by the previous MoM) and $J_\xi(\overline{r}',\overline{r}'';i\xi)=\hat{n}'\cdot\nabla'\partial_\xi G(\overline{r}',\overline{r}'';i\xi)$ we have the following matrix equation,

$$\overline{\overline{Z}}_\xi\cdot\overline{J}+\overline{\overline{Z}}\cdot\overline{J}_\xi=\overline{b}_\xi \tag{8.7.21}$$

that gives

$$\overline{J}_\xi=\overline{\overline{Z}}^{-1}\cdot\left(\overline{b}_\xi-\overline{\overline{Z}}_\xi\cdot\overline{J}\right) \tag{8.7.22}$$

where,

$$\begin{aligned} Z_{\overline{m},\overline{n}} &= \frac{1}{\Delta S_{\overline{n}}}\int_{\sigma_{\overline{n}}} \mathrm{d}S' G^\Omega(\overline{r}_{\overline{m}},\overline{r}';i\xi) \\ Z_{\xi,\overline{m},\overline{n}} &= \frac{1}{\Delta S_{\overline{n}}}\int_{\sigma_{\overline{n}}} \mathrm{d}S' \frac{\partial}{\partial\xi} G^\Omega(\overline{r}_{\overline{m}},\overline{r}';i\xi) \\ b_{\xi,\overline{m}} &= -\frac{\partial}{\partial\xi} G^\Omega(\overline{r}_{\overline{m}},\overline{r}'';i\xi) \end{aligned} \tag{8.7.23}$$

All of the impedance matrix elements can be calculated fast and analytically. Note that the wave number derivative of the Green's function is regular every where (even at the source point) for the $G^\Omega(\overline{r}_{\overline{m}},\overline{r}'';i\xi)$. We need this additional MoM to use the 6th order spectral expansion for the $G(\overline{r}',\overline{r}'';k)$.

## 8.8 Benchmark: Surface Integral Equation formulation of total Green's function

In order to verify the proposed approach, we compare the results with the benchmark solution using the usual approach of the SIE (pure MoM). The MoM solution will be used as the measure of the efficiency and accuracy of the proposed method. The MoM should be setup for one frequency at a time.

### 8.8.1 Irregular cavity Green's function by direct MoM using $G_0(\overline{r},\overline{r}';k)$

The irregular shaped cavity Green's function of $G(\overline{r},\overline{r}'';k)$ satisfies the wave equation of

$$(\nabla^2+k^2)G(\overline{r},\overline{r}'';k)=-\delta(\overline{r}-\overline{r}'') \quad , \quad G(\overline{r}\in S,\overline{r}'',k)=0 \tag{8.8.1}$$

On the other side, the free space Green's function $G_0(\overline{r},\overline{r}',k)$ also satisfies

$$(\nabla^2+k^2)G_0(\overline{r},\overline{r}';k)=-\delta(\overline{r}-\overline{r}') \quad , \tag{8.8.2}$$

Subject to the radiation condition at infinity. Upon multiplying by $G_0(\overline{r},\overline{r}';k)$ and $G(\overline{r},\overline{r}'';k)$, respectively and integrating the subtraction of both equation over the volume of $V$, converting the volume integration into surface integral over the boundary of the cavity and utilizing that $G(\overline{r},\overline{r}'';k)$ vanishes on $S$, it gives,

$$-\oint_S \mathrm{d}S G_0(\overline{r},\overline{r}';k)\hat{n}\cdot\nabla G(\overline{r},\overline{r}'';k)=\begin{cases} G_0(\overline{r}'',\overline{r}';k)-G(\overline{r}',\overline{r}'';k) & \text{if:}\overline{r}',\overline{r}''\in V \\ G_0(\overline{r}'',\overline{r}';k) & \text{if:}\overline{r}'\in V,\overline{r}''\notin V \\ -G(\overline{r}',\overline{r}'';k) & \text{if:}\overline{r}''\in V,\overline{r}'\notin V \\ 0 & \text{if:}\overline{r}',\overline{r}''\notin V \end{cases} \tag{8.8.3}$$

Upon letting $\overline{r}'\to S$ and interchanging $\overline{r}$ and $\overline{r}'$ we have

$$\oint_S \mathrm{d}S' G_0(\overline{r},\overline{r}';k)\hat{n}'\cdot\nabla' G(\overline{r}',\overline{r}'';k)=-G_0(\overline{r}'',\overline{r};k) \tag{8.8.4}$$

Taking the unknown surface current density $J(\overline{r}',\overline{r}'';k)=\hat{n}'\cdot\nabla' G(\overline{r}',\overline{r}'';k)$ we have

$$\oint_S \mathrm{d}S' G_0(\overline{r},\overline{r}';k)J(\overline{r}',\overline{r}'';k)=-G_0(\overline{r},\overline{r}'';k) \tag{8.8.5}$$

By expanding surface current in terms of local pulse basis functions as $J=\sum_{\overline{n}} 1/\Delta S_{\overline{n}} J_{\overline{n}} P_{\overline{n}}(\overline{r}_{\overline{n}})$, over the elements $\partial\Omega=\sum_{\overline{n}}\sigma_{\overline{n}}$ the matrix equation is $\overline{\overline{Z}}\cdot\overline{J}=\overline{b}$ where

$$\begin{aligned} Z_{\overline{m},\overline{n}} &= \frac{1}{\Delta S_{\overline{n}}}\int_{\sigma_{\overline{n}}} \mathrm{d}S' G_0(\overline{r}_{\overline{m}},\overline{r}';k) \\ b_{\overline{m}} &= -G_0(\overline{r}_{\overline{m}},\overline{r}'';k) \end{aligned} \tag{8.8.6}$$

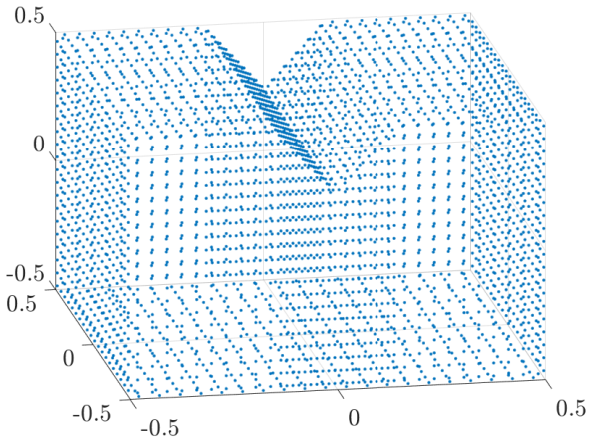


FIGURE 8.18: Discretization points on the irregular shaped cavity.

After finding the surface current $J(\overline{r}',\overline{r}'';k)$, the Green's function can be obtained at any pair of points $(\overline{r},\overline{r}'')$ by the equivalence principle of Eq. 8.7.5 as

$$G(\overline{r},\overline{r}'';k)=G_0(\overline{r},\overline{r}'';k)+\oint_S \mathrm{d}S' G_0(\overline{r},\overline{r}';k)J(\overline{r}',\overline{r}'';k) \tag{8.8.7}$$

and in term of discretized surface current

$$G(\overline{r},\overline{r}'';k)=G_0(\overline{r},\overline{r}'';k)+\sum_{\overline{n}}\frac{1}{\Delta S_{\overline{n}}}J_{\overline{n}}\int_{\sigma_{\overline{n}}}\mathrm{d}S' G_0(\overline{r},\overline{r}';k) \tag{8.8.8}$$

If observation point $\overline{r}$ is not on the boundary patch $\sigma_{\overline{n}}$, then

$$G(\overline{r},\overline{r}'';k)=G_0(\overline{r},\overline{r}'';k)+\sum_{\overline{n}}J_{\overline{n}}G_0(\overline{r},\overline{r}_{\overline{n}};k) \tag{8.8.9}$$

If the observation point coincide with the boundary surface element $\overline{m}$, then

$$G(\overline{r},\overline{r}'';k)=G_0(\overline{r},\overline{r}'';k)+\sum_{\overline{n}\neq\overline{m}}\frac{1}{\Delta S_{\overline{n}}}J_{\overline{n}}\int_{\sigma_{\overline{n}}}\mathrm{d}S' G_0(\overline{r},\overline{r}';k)+\frac{i}{2k}\frac{J_{\overline{m}}}{\Delta S_{\overline{m}}}\left[1-e^{ik\sqrt{\Delta S_{\overline{m}}/\pi}}\right] \tag{8.8.10}$$

### 8.8.2 Irregular cavity Green's function by MoM using $G^{\Omega}(\overline{r},\overline{r}';k)$

The regular cavity Green's function $G^{\Omega}(\overline{r},\overline{r}';i\xi)$ satisfies the inhomogeneous equation of

$$(\nabla^2+k^2)G^{\Omega}(\overline{r},\overline{r}';i\xi)=-\delta(\overline{r}-\overline{r}') \quad , \quad G^{\Omega}(\overline{r}\in\partial\Omega,\overline{r}')=0 \tag{8.8.11}$$

The irregular cavity Green's function of $G(\overline{r},\overline{r}'';k)$ also satisfies the inhomogeneous equation of

$$(\nabla^2+k^2)G(\overline{r},\overline{r}'';k)=-\delta(\overline{r}-\overline{r}'') \quad , \quad G(\overline{r}\in S,\overline{r}'',k)=0 \tag{8.8.12}$$

Upon multiplying Eq. (8.8.11) and Eq. (8.8.12) by $G(\overline{r},\overline{r}';k)$ and $G^{\Omega}(\overline{r},\overline{r}';k)$, respectively and integrating the subtraction of both equation over the volume of $V$, and converting the volume integration into surface integral over the boundary of the cavity and utilizing that $G(\overline{r},\overline{r}'';k)$ vanishes on $S$ and $G^{\Omega}(\overline{r},\overline{r}';k)$ also vanishes on $S-\sigma$,

$$\int_{\sigma}\mathrm{d}S G^{\Omega}(\overline{r},\overline{r}';k)\hat{n}\cdot\nabla G(\overline{r},\overline{r}'';k)=\begin{cases} G(\overline{r}',\overline{r}'';k)-G^{\Omega}(\overline{r}'',\overline{r}';k) & \text{if:}\overline{r}',\overline{r}''\in V \\ G(\overline{r}',\overline{r}'';k) & \text{if:}\overline{r}'\in V,\overline{r}''\notin V \\ -G^{\Omega}(\overline{r}',\overline{r}'';k) & \text{if:}\overline{r}''\in V,\overline{r}'\notin V \\ 0 & \text{if:}\overline{r}',\overline{r}''\notin V \end{cases} \tag{8.8.13}$$

Upon letting $\overline{r}'\to S$ and interchanging $\overline{r}$ and $\overline{r}'$ we have

$$\int_{\sigma}\mathrm{d}S' G^{\Omega}(\overline{r},\overline{r}';k)\hat{n}'\cdot\nabla' G(\overline{r}',\overline{r}'';k)=-G^{\Omega}(\overline{r},\overline{r}'';k) \tag{8.8.14}$$

Taking the unknown surface current density $J(\overline{r}',\overline{r}'';k)=\hat{n}'\cdot\nabla' G(\overline{r}',\overline{r}'';k)$ we have

$$\int_{\sigma}\mathrm{d}S' G^{\Omega}(\overline{r},\overline{r}';k)J(\overline{r}',\overline{r}'';k)=-G^{\Omega}(\overline{r},\overline{r}'';k) \tag{8.8.15}$$

By expanding surface current in terms of local pulse basis functions as $J=\sum_{\overline{n}} 1/\Delta S_{\overline{n}} J_{\overline{n}} P_{\overline{n}}(\overline{r}_{\overline{n}})$, the matrix equation is $\overline{\overline{Z}}\cdot\overline{J}=\overline{b}$ where

$$Z_{\overline{m},\overline{n}}=\frac{1}{\Delta S_{\overline{n}}}\int_{\sigma_{\overline{n}}} \mathrm{d}S' G^{\Omega}(\overline{r}_{\overline{m}},\overline{r}';k) \tag{8.8.16}$$

$$b_{\overline{m}}=-G^{\Omega}(\overline{r}_{\overline{m}},\overline{r}'';k) \tag{8.8.17}$$

After finding the surface current $J(\overline{r}',\overline{r}'';k)$, the Green's function can be obtained at any pair of points $(\overline{r},\overline{r}'')$ by the equivalence principle of Eq. 8.8.13 as

$$G(\overline{r},\overline{r}'';k)=G^{\Omega}(\overline{r},\overline{r}'';k)+\int_{\sigma} \mathrm{d}S' G^{\Omega}(\overline{r},\overline{r}';k)\hat{n}'\cdot\nabla' G(\overline{r}',\overline{r}'';k) \tag{8.8.18}$$

**Impedance matrix elements**

For the problem of finding the Green's function wave number $k$ we need to compute the impedance matrix of

$$Z_{\overline{m},\overline{n}}=\frac{1}{\Delta S_{\overline{n}}}\int_{\sigma_{\overline{n}}} \mathrm{d}S' G^{\Omega}(\overline{r}_{\overline{m}},\overline{r}';k) \tag{8.8.19}$$

Since $G^{\Omega}(\overline{r}_{\overline{m}},\overline{r}';k)$ decays exponentially by distance and it is pretty uniform over a cell, non-self patch elements $\overline{m}\neq\overline{n}$ can be evaluated by center point approximation

$$Z_{\overline{m},\overline{n}}=G^{\Omega}(\overline{r}_{\overline{m}},\overline{r}_{\overline{n}};k) \tag{8.8.20}$$

Using the 6th order spectral expansion,

$$G^{\Omega}(\overline{r},\overline{r}',k)=G^{\Omega}(\overline{r},\overline{r}',i\xi)-\frac{k^2+\xi^2}{2\xi}\frac{\partial}{\partial\xi}G^{\Omega}(\overline{r},\overline{r}',i\xi)+(k^2+\xi^2)^2\sum_{\alpha}\frac{\psi_{\alpha}(\overline{r})\psi_{\alpha}^{*}(\overline{r}')}{(k_{\alpha}^2+\xi^2)^2(k_{\alpha}^2-k^2)} \tag{8.8.21}$$

It can be observed that singularity at the source point contained in the first term (the imaginary wave number derivative is regular at $\overline{r}=\overline{r}'$) and the last term cannot rise in a singularity at the source point. Assuming $|\psi_{\alpha}(\overline{r})|\leq M$ (for rectangular cavity $M=\sqrt{8/V}$) and $k\neq k_{\alpha}$, at the source point $\overline{r}=\overline{r}'$ the last term would be a convergent series,

$$\sum_{\alpha}\frac{\psi_{\alpha}(\overline{r})\psi_{\alpha}^{*}(\overline{r})}{(k_{\alpha}^2+\xi^2)^2(k_{\alpha}^2-k^2)}\leq M^2\sum_{\alpha}\frac{1}{(k_{\alpha}^2+\xi^2)^2|k_{\alpha}^2-k^2|}<\infty \tag{8.8.22}$$

as for large values of $\alpha$, the tail is convergent. The singular term $G^{\Omega}(\overline{r},\overline{r}',i\xi)$ is computed using image expansion. The self patch impedance element would be

$$Z_{\overline{m},\overline{m}}=\frac{1}{\Delta S_{\overline{m}}}\int_{\sigma_{\overline{m}}} \mathrm{d}S' G^{\Omega}(\overline{r}_{\overline{m}},\overline{r}',i\xi)-\frac{k^2+\xi^2}{2\xi}\frac{\partial}{\partial\xi}G^{\Omega}(\overline{r}_{\overline{m}},\overline{r}_{\overline{m}},i\xi)+(k^2+\xi^2)^2\sum_{\alpha}\frac{\psi_{\alpha}(\overline{r}_{\overline{m}})\psi_{\alpha}^{*}(\overline{r}_{\overline{m}})}{(k_{\alpha}^2+\xi^2)^2(k_{\alpha}^2-k^2)} \tag{8.8.23}$$

The Green's function imaginary wave number $G^{\Omega}(\overline{r},\overline{r}',i\xi)$ is expressed in terms of image expansion

$$G^{\Omega}(\overline{r},\overline{r}',i\xi)=\frac{1}{4\pi}\sum_{n,m,p}(-1)^{n+m+p}\frac{e^{-\xi|\overline{r}-\overline{r}_{mnp}|}}{|\overline{r}-\overline{r}_{mnp}|} \tag{8.8.24}$$

This expansion contains the contribution from the real source corresponds to $(m,n,p)=(0,0,0)$ and images charges. The only singular term is the contribution of the real source

$$\frac{1}{\Delta S_{\overline{m}}}\int_{\sigma_{\overline{m}}} \mathrm{d}S' G^{\Omega}(\overline{r}_{\overline{m}},\overline{r}',i\xi)=\frac{1}{4\pi}\sum_{\substack{m,n,p\\(m,n,p)\neq(0,0,0)}}(-1)^{n+m+p}\frac{e^{-\xi|\overline{r}_{\overline{m}}-\overline{r}_{mnp}|}}{|\overline{r}_{\overline{m}}-\overline{r}_{mnp}|}+\frac{1}{4\pi}\frac{1}{\Delta S_{\overline{m}}}\int_{\sigma_{\overline{m}}}\mathrm{d}S'\frac{e^{-\xi|\overline{r}_{\overline{m}}-\overline{r}'|}}{|\overline{r}_{\overline{m}}-\overline{r}'|} \tag{8.8.25}$$

Therefore, total self patch elements become

$$Z_{\overline{m},\overline{m}}=\frac{1}{4\pi}\sum_{\substack{m,n,p\\(m,n,p\neq(0,0,0)}}(-1)^{n+m+p}\frac{e^{-\xi|\overline{r}_{\overline{m}}-\overline{r}^{(\overline{m})}_{mnp}|}}{|\overline{r}_{\overline{m}}-\overline{r}^{(\overline{m})}_{mnp}|}+\frac{1}{2\xi}\frac{1}{\Delta S_{\overline{m}}}\left[1-e^{-\xi\sqrt{\Delta S_{\overline{m}}/\pi}}\right] \tag{8.8.26}$$

$$-\frac{k^2+\xi^2}{2\xi}\frac{\partial}{\partial\xi}G^{\Omega}(\overline{r}_{\overline{m}},\overline{r}_{\overline{m}},i\xi)+(k^2+\xi^2)^2\sum_{\alpha}\frac{\psi_\alpha(\overline{r}_{\overline{m}})\psi^*_\alpha(\overline{r}_{\overline{m}})}{(k^2_\alpha+\xi^2)^2(k^2_\alpha-k^2)} \tag{8.8.27}$$

where $\overline{r}^{(\overline{m})}_{mnp}$'s are position of images source when the real source is located at $\overline{r}=\overline{r}_{\overline{m}}$.

## 8.9 Choosing the Imaginary Wave Number $\xi$

The imaginary wave number $\xi$ appears in two positions in the 6th order spectral expansion of (8.5.3). One is inside $G^S(\overline{r},\overline{r}';i\xi)$ and its derivative and the other one is in the summation as a factor of

$$F_\xi=\frac{(k^2+\xi^2)^2}{(q^2_\alpha+\xi^2)^2}.$$

The effect of $\xi$ in the Green's function $G^S(\overline{r},\overline{r}';i\xi)$ is that higher value of $\xi$ corresponds to shorter range of interaction and vice versa. For a short range interaction, computation of the Green's function is easier (the matrices are extremely sparse/number of image charges are very small in computation of $G^{\Omega}$ ) As $\xi$ increases, the contribution of the extraction terms decrease and in the limit of $\xi\to\infty$, $F_\xi\to 1$ and we recover the original second order spectral expansion. Therefore as $\xi$ increases, number of included modes in the 6th order spectral summation should increases accordingly.

In the limit of small $\xi$, imaginary wave number interactions are long range. If $\xi\ll k,q_\alpha$, the pre-factor $F_\xi$ tends to the factor of $(k/q_\alpha)^4$ that guarantee the 6th order convergence of the spectral expansion. However, for small $\xi$, calculation of the extracted terms is computationally more expensive because of long range interaction (in particular, in the image expansion, number of required image sources to get convergent response increases). The extracted term $G^S(\overline{r},\overline{r}';i\xi)$ mostly contributes in the source region as it is a short range propagator. The wave number derivative $\partial_\xi G^S(\overline{r},\overline{r}';i\xi)$ has a longer range than $G^S(\overline{r},\overline{r}';i\xi)$ itself but still is localized around the source region while the modal summation contains standing waves that can be present everywhere.

Therefore, choosing the imaginary wave number $\xi$ is also dependent on the physical size of the problem (excitation frequency).

TABLE 8.1: Resonant wave numbers of the rectangular ($k_\alpha$) and grooved ($q_\alpha$) cavities. Degeneracies are elevated by the broken symmetry of the cavity.

| $\alpha$ | 1 | 2 | 3 | 4 | 5 | 5 | 7 |
|---|---|---|---|---|---|---|---|
| $q_\alpha L$ | 5.78 | 7.75 | 7.94 | 8.47 | 9.47 | 9.57 | 10.07 |
| $k_\alpha L$ | 5.44 | 7.69 | 7.69 | 7.69 | 9.42 | 9.42 | 9.42 |

## 8.10 Numerical Example

In order to demonstrate the performance of the proposed method, the Green's function solution is compared with MoM solution for the grooved cavity of Fig. 8.14. The parameters of the cavity is given by $L_x{=}L_y{=}L_z{=}L$, $H{=}L/4$, $\alpha{=}60^\circ$ and the source is located at $\overline{r}'{=}L/4(1,1,1)$. For the extraction, we have selected $\xi{=}2/L$. We study the Green's function at several exciting wavelengths.

In order to calculate the broadband Green's function using the hybrid method, we need to select a discretization grid of the boundary surface (for the spatial part) and a truncation number ($M_\Omega$) for the number of included spectral modes in the hybrid formulation. The hybrid formulation is set up with $N{=}600$ unknowns on the whole surface of the cavity (100 points on the surface $\sigma$ for the hybrid eigenvalue problem) and inclusion of $M_\Omega{=}10^3$ spectral modes for the hybrid formulation.

On the other side, for the MoM solution, the computation grid size is strongly dependent on the frequency. For example, at $\lambda{=}0.93L$, MoM solution requires at least 2400 unknowns on the surface of the cavity to produces accurate results. This is more than the rule of thumb value of (10pts/$\lambda$) as resonance modes are involved here.

The first comparison is for exciting wavelength of $\lambda{=}0.93L$. The Green's function obtained by hybrid spatial-spectral formulation on the plane of $z{=}0$ is plotted in Fig. 8.19 (upper graph) together with the response obtained by MoM as a benchmark (lower graph). The two responses coincide each other with absolute error of less than $-32$ dB over all points of the observation grid. The absolute difference between two methods is plotted in Fig. 8.20 in logarithmic scale. The error can be reduced arbitrarily by increasing the number of included modes since the singularity in the source region is entirely captured in the imaginary wave number part.

The computational cost of the proposed method is comparable with that of single frequency MoM for $\lambda{=}0.93L$ while the hybrid method has absolute error of less than $-20$ over the continuous band from DC to $\lambda{=}0.23L$. Another advantage of spatial-spectral method is that it provides an analytical solution of the Green's function (apart from imaginary extractions which is constant over the frequency band) inside the cavity that can provides design insights.

The next comparison is for the exciting wavelength of $\lambda{=}0.43L$. Now the volume of the cavity is larger than $8\lambda^3$ which requires large number of surface unknowns. The solution using hybrid method is the same as previous example by only changing the value of $k$ in the last summation of (8.5.3). However, MoM solution requires more than $10^4$ unknown on the surface of the cavity to get the accurate results [134, 135]. The Green's function at this frequency obtained by hybrid and MoM method is depicted in Fig. 8.21 and corresponding absolute error of the hybrid method with respect to the MoM is shown

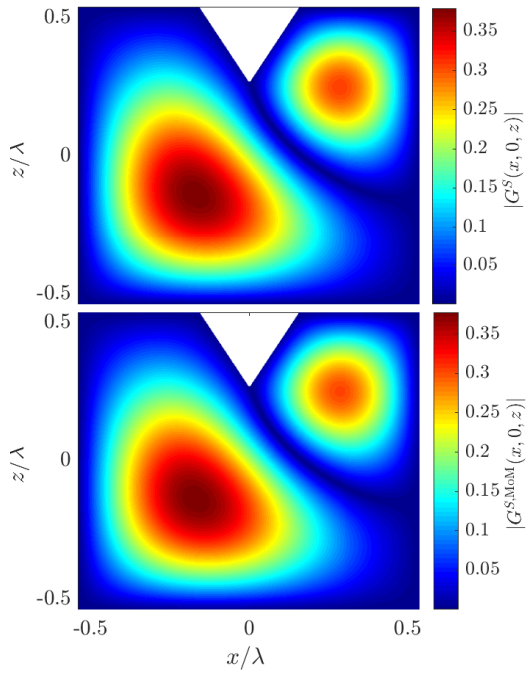


FIGURE 8.19: The Green's function $G^S(\overline{r},\overline{r}')$ at excitation wavelength $\lambda$=0.93$L$ for a point source at $\overline{r}'$=$L/4$(1,1,1) obtained by proposed method (top) against MoM solution (Bottom).

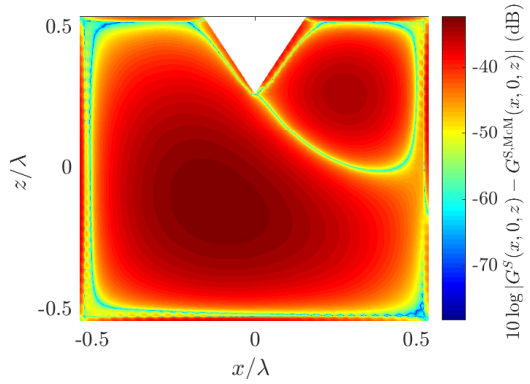


FIGURE 8.20: Absolute error in computation of the Green's function $G^S(\overline{r},\overline{r}')$ at excitation wavelength $\lambda$=0.93$L$ for a point source at $\overline{r}'$=$L/4$(1,1,1) respect to MoM solution.

in Fig. 8.22. As the last numerical example, Fig. 8.23 plot the Green's function observed on the line of $\overline{r}$=($x$,0,$z$=0.45$L$) with the source located at $\overline{r}'$=(1,1,1)$L/4$ for a decade of bandwidth ($0.4\leq\lambda/L\leq4$) computed by the hybrid method. The frequency points are chosen to not coincide exactly with the resonant frequencies. Notice that obtaining this broadband response does not requires additional computations.

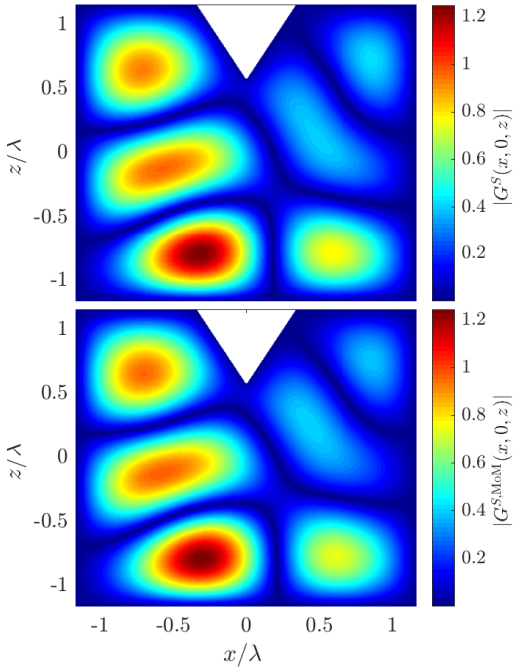


FIGURE 8.21: The Green's function $G^S(\overline{r},\overline{r}')$ at excitation wavelength $\lambda$=0.43$L$ for a point source at $\overline{r}'=L/4(1,1,1)$ obtained by proposed method (top) against MoM solution (Bottom).

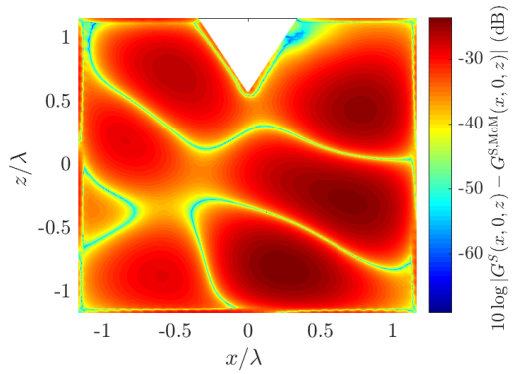


FIGURE 8.22: Absolute error in computation of the Green's function $G^S(\overline{r},\overline{r}')$ at excitation wavelength $\lambda$=0.43$L$ for a point source at $\overline{r}'=L/4(1,1,1)$ with respect to the MoM solution.

## 8.11 Finite element methods

Similar to the proposed method, the finite element methods are able to compute all of the resonant wave number and eigenmodes linearly. For the wave equation of $(\nabla^2+k^2)\psi=0$ results in linear system of type $\overline{\overline{A}}\cdot\overline{x}=k^2\overline{x}$. However, the proposed method has several advantages over finite element methods. The first advantage is that finite element method required volumetric discretization of the domain while the imaginary frequency surface integral equation formulate the problem in terms of surface unknowns that leads to additional

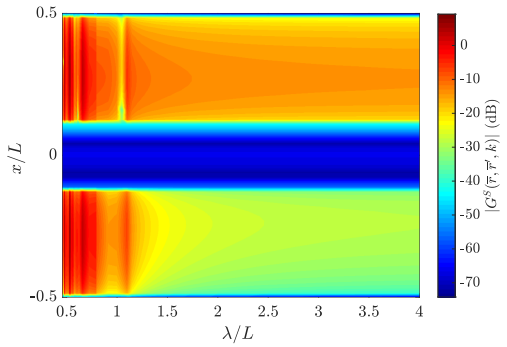


FIGURE 8.23: Broadband response of the Green's function for $\overline{r}=(x,0,z=0.45L)$ over a decade of bandwidth. Spectral lines are close to the resonant wavelengths.

factor of $N$ (typical number of unknown in one dimension) in number of unknowns.

The second advantage which is really sparkling is that in order to obtain the eigenmodes with finite element methods, the volumetric discretization size should be fine enough to capture the variation of modes. For high order modes this would impose a proportionally fine discretization of computational grid. However, the imaginary frequency surface integral equation is formulated for a fixed value of imaginary wavenumber $k=i\xi$ regardless of bandwidth of interest. Therefore high order modes are computed using the discretization as low order modes and because of imaginary wave number interaction the interaction matrices are sparse.

In order to realize this, consider a cubic cavity of size $(1\lambda)^3$ and assume that desired accuracy of computation of Green's function achieves with inclusion of 1000 modes in the 6th order expansion. For the imaginary wavenumber surface integral equation approach total number of unknowns on the surface would be (600) by taking $\xi=1/\lambda$ and assuming 10 pts/wavelength. However, for the finite element approach, in order to capture highest mode (corresponding to wavelength $\lambda/10$), number of volumetric unknowns would be $10^6$. For higher index of modes this will increase in power law.

# Chapter 9

# Fast and Broadband Computation of Dyadic Green's Function in Cavity Resonator Using Imaginary Wave Number Extraction Technique

## 9.1 Introduction

The Green's function is a fundamental tool in the analysis of every physical system and it provides an in-depth insight into the dynamical behavior of the system. Based on this, obtaining the Green's function for a given system is as difficult as solving the problem directly. However, since the Green's function can determine the response of the system to an arbitrary excitation it contains more information about the system than the solution of the dynamical variable like the wave function. The Green's function is the collective response of all the resonant wave functions in a unique way such that it is closely related to the spatial distribution of the density of states.

In particular, Green's function is of importance as it provides the response for an arbitrary distribution of the source. They are also useful for formulating the integral equations for various boundary value problems. Commonly used Green's functions include free-space Green's functions, periodic Green's functions for empty periodic lattices, and Green's functions of regular geometry such as a sphere or cylinder, Green's functions of layered media, etc [118–121].

The Green's function inside the cavity is also studied extensively [136–139]. In general for a cavity of regular shape (rectangular, cylindrical, ...), an expression for the Green's function can be found by either a spatial sum in terms of image sources [136] or a spectral sum in terms of the eigen-modes. Both of the pure spatial and spectral methods have slow convergence in terms of the number of included images/modes. While the spatial expansion can capture the singularity in the source region well, it has a slow convergence for the observation points far from the source. On the other side, spectral expansion does not converge in the proximity of the source as a consequence of the singular behavior of the Green's function. The famous Ewald's technique is about to obtain a hybrid spectral-spatial summation that has an exponential convergence rate [140–143] which is a successful technique of taking advantage of both spectral and spatial expansions. Another method based on

the Chebyshev polynomial approximation is reported [133] that provides an efficient way of evaluation of the Green's function in the rectangular cavity.

However, all of the mentioned methods are implemented for computation of the Green's function at a single frequency such that obtaining a broadband response required a frequency sweep. For the cavity Green's function, there are lots of resonance modes that require a fine frequency sweep to capture the resonances correctly. In this paper, a new approach of obtaining the dyadic Green's function inside the cavity based on imaginary wavenumber extraction is presented. The proposed approach can be used to evaluate the vector potential and electric field dyadic Green's function inside the rectangular cavity rapidly and over a broad range of frequency. This technique is previously applied to a variety of geometries including the Green's function of irregular shape waveguide [132], periodic structure including scatterers (photonic crystals) [126–128, 144], radiation from circuit boards [145], and scalar Green's function inside the cavity to capture the wideband behavior including the resonances. All prior published works are for the 2D case. In this paper, we treat the Dyadic Green's functions of the 3D cavity.

The method is a hybrid spatial-spectral method and from this point of view is similar to the Ewald method. For a given level of accuracy and even for response at one frequency, it can be faster than the Ewald method and it provides a broadband response over decades of bandwidth with an only one-time evaluation of the modes. The idea of extraction from the Green's function has been used and studied before. The BIRME method [129–131] is proposed with utilizing extraction of the corresponding static Green's function from itself to accelerate the spectral expansion. The BBGFL (broadband Green's function with low wavenumber extraction) method [122, 132] also uses the extraction of the Green's function at some low (close to DC but not necessarily DC) wave number. However, the imaginary wavenumber extraction is a superior approach as the extracted terms can be rapidly computed.

The logic behind the extraction techniques is separating the singular part of the Green's function and compute it by a different method (spatial series with an exponential convergence). The reduced Green's function after extraction, which represents a smooth function (it is regular even at the source point) will have a better convergence rate as it can be constructed by low-frequency spatial modes, in principle.

This paper has two main parts. The first part is devoted to the vector potential dyadic Green's function of the rectangular cavity. The different spatial and spectral representations are discussed in sec. 9.2. Several numerical examples has been brought to compare the accuracy of the proposed method and comparison of computation cost against the Ewald method. A broadband computation of the vector potential dyadic Green's function over two decades of bandwidth with 1000 resonant modes is also shown. In sec. 9.3, the electric field dyadic Green's function is studied. Spectral representation of the electric field dyadic Green's function is derived and imaginary wavenumber extraction is applied. Singularity of the dyadic Green's function is extracted in terms of static Green's function. A numerical example of evaluation of the dyadic Green's function with the proposed method is provided. Finally, a broadband evaluation of the electric field dyadic Green's function is performed in the last section.

## 9.2 Vector Potential Dyadic Green's Function

Under the Lorentz gauge, the vector potential $\overline{A}(\overline{r})$ satisfies the vector Helmholtz equation of

$$\nabla^2\overline{A}(\overline{r})+k^2\overline{A}(\overline{r})=-\mu\overline{J}(\overline{r}) \tag{9.2.1}$$

while the scalar potential satisfies

$$\nabla^2\phi(\overline{r})+k^2\phi(\overline{r})=-\frac{1}{\varepsilon}\rho(\overline{r}). \tag{9.2.2}$$

The electric field in terms of the potentials is expressed as $\overline{E}(\overline{r})=i\omega\overline{A}(\overline{r})-\nabla\phi(\overline{r})$ where $e^{-i\omega t}$ time dependence convention is used for harmonic fields throughout the text. On the surface of the cavity, tangential component of the electric field must vanish, i.e. $\hat{n}\times\left[i\omega\overline{A}(\overline{r})-\nabla\phi(\overline{r})\right]=0$. This imposes a boundary condition on both scalar and vector potentials, simultaneously. One choice is considering decoupled boundary conditions for vector and scalar potentials as $\hat{n}\times\overline{A}=0$ and $\hat{n}\times\nabla\phi=0$. The scalar potential itself also vanishes on the surface of the cavity and within the Lorenz gauge $\nabla\cdot\overline{A}=i\omega\mu\varepsilon\phi$ and thus $\nabla\cdot\overline{A}=0$ on the cavity surface. These are the boundary conditions to be satisfied by the vector potential and are less stronger than the general requirement of $\hat{n}\times\left[i\omega\overline{A}(\overline{r})-\nabla\phi(\overline{r})\right]=0$ over the walls of the cavity [146–151].

In order to integrate the wave equation of the vector potential , the vector potential dyadic Green's function $\overline{\overline{G}}_A(\overline{r},\overline{r}')$ can be introduced such that,

$$\nabla^2\overline{\overline{G}}_A(\overline{r},\overline{r}')+k^2\overline{\overline{G}}_A(\overline{r},\overline{r}')=-\overline{\overline{I}}\delta(\overline{r}-\overline{r}') \tag{9.2.3}$$

subject to the conditions $\hat{n}\times\overline{\overline{G}}_A=0$ and $\nabla\cdot\overline{\overline{G}}_A=0$ on the boundary of the cavity. Upon using the Green's identity for $\overline{A}$ and $\overline{\overline{G}}_A$, the vector potential can be written in terms of the current source as

$$\overline{A}(\overline{r})=\mu\int \mathrm{d}\overline{r}'\overline{\overline{G}}_A(\overline{r},\overline{r}')\cdot\overline{J}(\overline{r}') \tag{9.2.4}$$

The electric field can be obtained in terms of potentials (in Lorenz gauge) as

$$\begin{aligned}\overline{E}(\overline{r})&=i\omega\overline{A}(\overline{r})-\frac{1}{i\omega\mu\varepsilon}\nabla\nabla\cdot\overline{A}(\overline{r}) \\ &=i\omega\mu\left[\overline{\overline{I}}+\frac{\nabla\nabla}{k^2}\right]\cdot\int \mathrm{d}\overline{r}'\overline{\overline{G}}_A(\overline{r},\overline{r}')\cdot\overline{J}(\overline{r}')\end{aligned} \tag{9.2.5}$$

Now, the electric field dyadic Green's function can be identified as

$$\overline{\overline{G}}(\overline{r},\overline{r}')=\left[\overline{\overline{I}}+\frac{\nabla\nabla}{k^2}\right]\cdot\overline{\overline{G}}_A(\overline{r},\overline{r}'). \tag{9.2.6}$$

Notice that in (9.2.5), the differential operator $\nabla\nabla$ is supposed to operate on the result of the vector potential integration, but in order to get (9.2.6), order of the differentiation and integration operators are exchanged. If the vector potential integrand does not have second order derivative (around source point where $\overline{\overline{G}}_A$ is singular), exchanging the differentiation

and integration operators introduces a higher order singularity that has been studied extensively [152–155]. Note that the vector potential dyadic Green's function for a rectangular cavity is a diagonal dyadic, i.e.

$$\overline{\overline{G}}_A = G_A^{xx}\hat{x}\hat{x} + G_A^{yy}\hat{y}\hat{y} + G_A^{zz}\hat{z}\hat{z} \tag{9.2.7}$$

The vector potential dyadic Green's function and scalar Green's function are related through the gauge condition that is necessary for potentials to uniquely deliver the electromagnetic fields.

### 9.2.1 Image Expansion of the Vector Potential Dyadic Green's Function

Each component of the vector potential dyadic Green's function satisfies the scalar wave equation of,

$$\nabla^2 G_A^j(\overline{r},\overline{r}') + k^2 G_A^j(\overline{r},\overline{r}') = -\delta(\overline{r}-\overline{r}') \tag{9.2.8}$$

which is identical to the free space Green's function. The required boundary condition to be satisfied by $G_A^{xx}$ is the Dirichlet on the sidewalls and the Neumann on the end caps (with respect to $x$ direction). The collective response of the image sources with proper amplitude and location will produce the required boundary condition for different components of $\overline{\overline{G}}_A$ as

$$G_A^j(\overline{r},\overline{r}') = \sum_{n,m,p} (-1)^{m+n+p+s_j} G_0\Big(\overline{r};\overline{r}_{mnp}(\overline{r}')\Big) \tag{9.2.9}$$

where $s_j = m$ for $j = x$ and $\overline{r}_{mnp}(\overline{r}') = \Big(mL_x + (-1)^m x', nL_y + (-1)^n y', pL_z + (-1)^p z'\Big)$ represents the location of the image charges. The spatial expansion of (9.2.9) has a poor convergence and many terms should be included in the summation to get a convergent result.

### 9.2.2 Spectral Expansion With Imaginary Wave Number Extraction

Since the vector potential Green's function should satisfy the Dirichlet and Neumann conditions on the sidewalls and end caps, respectively, the eigenfunctions of the wave equation that satisfy the required boundary condition are of the form,

$$\begin{aligned}
\psi_{mnp}^x(\overline{r}) &= \sqrt{\frac{4(2-\delta_m)}{V}} \cos\frac{m\pi}{L_x}\left(x+\frac{L_x}{2}\right) \sin\frac{n\pi}{L_y}\left(y+\frac{L_y}{2}\right) \sin\frac{p\pi}{L_z}\left(z+\frac{L_z}{2}\right) \\
\psi_{mnp}^y(\overline{r}) &= \sqrt{\frac{4(2-\delta_n)}{V}} \sin\frac{m\pi}{L_x}\left(x+\frac{L_x}{2}\right) \cos\frac{n\pi}{L_y}\left(y+\frac{L_y}{2}\right) \sin\frac{p\pi}{L_z}\left(z+\frac{L_z}{2}\right) \\
\psi_{mnp}^z(\overline{r}) &= \sqrt{\frac{4(2-\delta_p)}{V}} \sin\frac{m\pi}{L_x}\left(x+\frac{L_x}{2}\right) \sin\frac{n\pi}{L_y}\left(y+\frac{L_y}{2}\right) \cos\frac{p\pi}{L_z}\left(z+\frac{L_z}{2}\right)
\end{aligned} \tag{9.2.10}$$

where $\psi_{mnp}^x$ is an eigenfunction of the wave equation that satisfies appropriate boundary conditions of $G_A^{xx}$ on the cavity walls. One may verify that the required boundary conditions of $\hat{n}\times\overline{\overline{G}}_A = 0$, and $\nabla\cdot\overline{\overline{G}}_A = 0$ is satisfied by these eigen-solutions. Also, the modes are

normalized such that each component of the vector potential dyadic Green's function can be written as

$$G_A^j(\overline{r},\overline{r}')=\sum_\alpha \frac{1}{k_\alpha^2-k^2}\psi_\alpha^j(\overline{r})\psi_\alpha^{j*}(\overline{r}') \tag{9.2.11}$$

Although this expansion of the Green's function is desired because of simple dependence on the frequency of excitation, the summation converges slowly.

$$G_A^j(\overline{r},\overline{r}')=\sum_\alpha \frac{1}{k_\alpha^2-k_0^2}\psi_\alpha(\overline{r})\psi_\alpha^*(\overline{r}')\approx\sum_\alpha \frac{1}{k_\alpha^2-k_0^2} \tag{9.2.12}$$

In the case of continuous spectrum in lossless free space,

$$G_A^j(\overline{r},\overline{r}')=\frac{1}{(2\pi)^3}\int \mathrm{d}^3\overline{k}\frac{1}{k^2-k_0^2}e^{i\overline{k}\cdot(\overline{r}-\overline{r}')}\le\frac{1}{(2\pi)^3}\int \mathrm{d}k\frac{k^2}{k^2-k_0^2}\to\infty \tag{9.2.13}$$

which shows that the summation is not absolutely convergent and has very poor convergence, mainly due to the singularity (sharp variations) of the Green's function. If we can somehow separate the singular part of the Green's function, then the leftover should have a better convergence rate. Assume that we extract the Green's function at another wave number $k=k_L$ from the desired Green's function. Since the eigenfunctions do not depend on the frequency of excitation, the expression reads

$$\begin{aligned} G_A^j(\overline{r},\overline{r}',k)-G_A^j(\overline{r},\overline{r}',k_L)&=\sum_\alpha\left[\frac{1}{k_\alpha^2-k^2}-\frac{1}{k_\alpha^2-k_L^2}\right]\psi_\alpha^j(\overline{r})\psi_\alpha^{j*}(\overline{r}') \\ &=\sum_\alpha\left[\frac{k^2-k_L^2}{(k_\alpha^2-k^2)(k_\alpha^2-k_L^2)}\right]\psi_\alpha^j(\overline{r})\psi_\alpha^{j*}(\overline{r}') \end{aligned} \tag{9.2.14}$$

or

$$G_A^j(\overline{r},\overline{r}',k)=G_A^j(\overline{r},\overline{r}',k_L)+\sum_\alpha\left[\frac{k^2-k_L^2}{(k_\alpha^2-k^2)(k_\alpha^2-k_L^2)}\right]\psi_\alpha^j(\overline{r})\psi_\alpha^{j*}(\overline{r}') \tag{9.2.15}$$

If we are able to compute the Green's function at single wave number $k_L$, then the Green's function at any other wavenumber $k$ will be calculated through the spectral summation where the summand decreases as $\mathcal{O}(k_\alpha^{-4})$ which is of fourth-order instead of $\mathcal{O}(k_\alpha^{-2})$. Now, if we take $k_L=i\xi$, an imaginary number, the extracted term which is the Green's function at imaginary wave number, is very well behaved (exponentially decaying with distance) and can be easily computed by spatial domain series (see appendix A),

$$G_A^j(\overline{r},\overline{r}',k)=G_A^j(\overline{r},\overline{r}',i\xi)+\sum_\alpha\left[\frac{k^2+\xi^2}{(k_\alpha^2-k^2)(k_\alpha^2+\xi^2)}\right]\psi_\alpha^j(\overline{r})\psi_\alpha^{j*}(\overline{r}') \tag{9.2.16}$$

We can proceed to further accelerate the spectral summation. The frequency dependent factor in the summand of (9.2.16) can be factorized as

$$\begin{aligned} \left[\frac{k^2+\xi^2}{(k_\alpha^2-k^2)(k_\alpha^2+\xi^2)}\right]&=\frac{k^2+\xi^2}{(k_\alpha^2+\xi^2)}\left[\frac{1}{k_\alpha^2-k^2}-\frac{1}{k_\alpha^2+\xi^2}\right]+\frac{k^2+\xi^2}{(k_\alpha^2+\xi^2)(k_\alpha^2+\xi^2)} \\ &=\frac{(k^2+\xi^2)^2}{(k_\alpha^2+\xi^2)^2(k_\alpha^2-k^2)}+\frac{k^2+\xi^2}{(k_\alpha^2+\xi^2)^2} \end{aligned} \tag{9.2.17}$$

where the last term can be written as

$$\frac{k^2+\xi^2}{(k_\alpha^2+\xi^2)^2}=\frac{k^2+\xi^2}{-2\xi}\frac{\partial}{\partial\xi}\frac{1}{(k_\alpha^2+\xi^2)} \tag{9.2.18}$$

which is proportional to the spectral coefficient of the Green's function expansion of (9.2.11) for $k=i\xi$. Therefore,

$$G_A^j(\overline{r},\overline{r}',k)=G_A^j(\overline{r},\overline{r}',i\xi)-\frac{k^2+\xi^2}{2\xi}\frac{\partial}{\partial\xi}G_A^j(\overline{r},\overline{r}',i\xi)+(k^2+\xi^2)^2\sum_\alpha\frac{\psi_\alpha^j(\overline{r})\psi_\alpha^{j*}(\overline{r}')}{(k_\alpha^2+\xi^2)^2(k_\alpha^2-k^2)} \tag{9.2.19}$$

This expansion is of the sixth order of convergence and converges with the inclusion of the few terms in the summation. Now, the spectral series in terms of eigenmodes converges much faster than the conventional eigenmode expansion of (9.2.11). There is an overall computational gain if the extracted terms $G^j(\overline{r},\overline{r}';i\xi)$ and $\partial_\xi G^j(\overline{r},\overline{r}';i\xi)$ at the imaginary wavenumber can be computed rapidly. The extracted terms can be computed by the image series which has an exponential convergence for imaginary wave numbers.

$$\begin{aligned} G_A^j(\overline{r},\overline{r}',i\xi)&=\sum_\alpha\frac{1}{k_\alpha^2+\xi^2}\psi_\alpha^j(\overline{r})\psi_\alpha^{j*}(\overline{r}') \\ &=\frac{1}{4\pi}\sum_{n,m,p}(-1)^{n+m+p+s_j}\frac{e^{-\xi|\overline{r}-\overline{r}_{mnp}|}}{|\overline{r}-\overline{r}_{mnp}|} \end{aligned} \tag{9.2.20}$$

where $s_j=m$ if $j=x$ and so on. Similarly, for the imaginary wave number derivative of the the Green's function

$$\begin{aligned} \frac{\partial}{\partial\xi}G_A^j(\overline{r},\overline{r}',i\xi)&=\sum_\alpha\frac{-2\xi}{(k_\alpha^2+\xi^2)^2}\psi_\alpha^j(\overline{r})\psi_\alpha^{j*}(\overline{r}') \\ &=-\frac{1}{4\pi}\sum_{n,m,p}(-1)^{n+m+p+s_j}e^{-\xi|\overline{r}-\overline{r}_{mnp}|} \end{aligned} \tag{9.2.21}$$

Note that for a wideband computation of the Green's function, the imaginary wavenumber extracted terms of (9.2.20), and (9.2.21) should be computed one time irrespective of the desired frequency bandwidth.

### 9.2.3 Ewald Summation Technique

The Ewald summation technique has been applied to the vector potential dyadic Green's function of the rectangular cavity [136, 137, 140, 141]. The derivation of the Ewald summation for the rectangular cavity here, closely follows that of [141] and center of coordinate system is shifted such that $0\leq x_j\leq L_j$. From the image expansion of the vector potential dyadic Green's function $G_A^{xx}$ we have

$$G_A^{xx}(\overline{r},\overline{r}')=\sum_{n,m,p}(-1)^{n+p}\frac{e^{ikR_{mnp}}}{4\pi R_{mnp}} \tag{9.2.22}$$

where $R_{mnp}=|\overline{r}-\overline{r}_{mnp}|$ and $\overline{r}_{mnp}$ is the location of image sources. The location of images dipoles constitute a periodic lattice in space with periods $2L_x$,$2L_y$, and $2L_z$ in $x$, $y$, and $z$ directions, respectively and each lattice site is occupied by a cluster of 8 dipoles. The series

of (9.2.22) does not reflect the periodicity of the problem explicitly. Instead, we can write the image expansion in terms of the response of a dipole cluster around the given lattice site. Within the primitive cell, upon defining

$$\begin{aligned} X_r &= x-(-1)^r x' \\ Y_s &= y-(-1)^s y' \\ Z_t &= z-(-1)^t z' \end{aligned}$$

where $r,s,t\in\{0,1\}$, and the distance between the image sources and the observation point can be written as

$$R_{mnp,rst}=\sqrt{(X_r+2mL_x)^2+(Y_s+2nL_y)^2+(Z_t+2pL_z)^2} \tag{9.2.23}$$

thus, the Green's function takes the form of

$$G_A^{xx}(\overline{r},\overline{r}';E)=\sum_{n,m,p}\sum_{r,s,t}(-1)^{s+t}\frac{e^{ikR_{mnp,rst}}}{4\pi R_{mnp,rst}} \tag{9.2.24}$$

This representation is equivalent to the original representation of (9.2.22). Following the Ewald approach, the Green's function is decomposed to two parts utilizing the error $\mathrm{erf}(x)$ and the complementary error functions $\mathrm{erfc}(x)$ that satisfy $\mathrm{erf}(x)+\mathrm{erfc}(x)=1$ (for any number $x$),

$$\begin{aligned} G_{A1}^{xx}(\overline{r},\overline{r}';E) &= \sum_{n,m,p}\sum_{r,s,t}(-1)^{s+t}\frac{e^{ikR_{mnp,rst}}}{4\pi R_{mnp,rst}}\mathrm{erfc}(ER_{mnp,rst}) \\ G_{A2}^{xx}(\overline{r},\overline{r}';E) &= \sum_{n,m,p}\sum_{r,s,t}(-1)^{s+t}\frac{e^{ikR_{mnp,rst}}}{4\pi R_{mnp,rst}}\mathrm{erf}(ER_{mnp,rst}) \end{aligned} \tag{9.2.25}$$

Here, $E$ is a free parameter (with the dimension of wave number) that controls the share of each summation in (9.2.25). Since $\mathrm{erfc}(x)\to 0$ as $x\to\infty$ exponentially, the first series is exponentially convergent. However, the second part is not affected by the error function at long distances and has a slow convergence. Using the Poisson summation formula of,

$$\sum_{mnp} f(\alpha m,\beta n,\gamma p)=\frac{1}{\alpha\beta\gamma}\sum_{mnp}F\left(\frac{2\pi m}{\alpha},\frac{2\pi n}{\beta},\frac{2\pi p}{\gamma}\right) \tag{9.2.26}$$

where $F(\overline{k})$ is the Fourier transform of the function $f(\overline{r})$, the second series can be transformed to a spectral sum of

$$G_{A2}^{xx}(\overline{r},\overline{r}';E)=\frac{1}{8V}\sum_{n,m,p}\sum_{r,s,t}(-1)^{s+t}\int \mathrm{d}\tilde{\overline{r}}e^{-i(k_{xm}\tilde{x}+k_{yn}\tilde{y}+k_{zp}\tilde{z})}\frac{e^{ikR_{rst}}}{4\pi R_{rst}}\mathrm{erf}(ER_{rst}) \tag{9.2.27}$$

where $R_{rst}=\sqrt{(X_r+\tilde{x})^2+(Y_s+\tilde{y})^2+(Z_t+\tilde{z})^2}$ and $k_{xm}=m\pi/L_x$ and so on. This integral can be computed analytically. First, let's shift the variables to get

$$G_{A2}^{xx}(\overline{r},\overline{r}';E)=\frac{1}{8V}\sum_{n,m,p}\sum_{r,s,t}(-1)^{s+t}e^{i(k_{xm}X_r+k_{yn}Y_s+k_{zp}Z_t)}\int \mathrm{d}\overline{r}e^{-i(k_{xm}x+k_{yn}y+k_{zp}z)}\frac{e^{ik|\overline{r}|}}{4\pi|\overline{r}|}\mathrm{erf}(E|\overline{r}|) \tag{9.2.28}$$

Now, since the integrand is only function of $|\overline{r}|$, upon switching to the Spherical coordinate with $z$ axis toward the direction of $(k_{mx},k_{ny},k_{pz})$ the integral becomes,

$$\begin{aligned} I&=\int \mathrm{d}\overline{r}e^{-i(k_{xm}x+k_{yn}y+k_{zp}z)}\frac{e^{ik|\overline{r}|}}{4\pi|\overline{r}|}\mathrm{erf}(E|\overline{r}|) \\ &=\int_0^\infty \mathrm{d}r\int_0^\pi \mathrm{d}\theta r^2\sin\theta e^{-ik_{mnp}r\cos\theta}\frac{e^{ikr}}{2r}\mathrm{erf}(Er) \\ &=\frac{2E}{k_{mnp}\sqrt{\pi}}\int_0^\infty \mathrm{d}re^{ikr}\frac{1}{2i}\left[e^{ik_{mnp}r}-e^{-ik_{mnp}r}\right]\int_0^r \mathrm{d}te^{-E^2t^2} \end{aligned} \tag{9.2.29}$$

The Fourier Transform of the function $e^{-E^2r^2}$ can be easily computed and from that, the Fourier transform of its integral can be found as

$$\int_0^\infty \mathrm{d}re^{ikr}\int_0^r \mathrm{d}te^{-E^2t^2}=\frac{i\sqrt{\pi}}{2kE}e^{-k^2/4E^2} \tag{9.2.30}$$

Therefore,

$$I(k_{mnp},E)=\frac{1}{2k_{mnp}}\left[\frac{1}{k+k_{mnp}}e^{-(k+k_{mnp})^2/4E^2}-\frac{1}{k-k_{mnp}}e^{-(k-k_{mnp})^2/4E^2}\right] \tag{9.2.31}$$

which has an exponential decay as a function of summation variables $m,n,p$. Therefore the second part of the Green's function becomes

$$G_{A2}^{xx}(\overline{r},\overline{r}';E)=\frac{1}{8V}\sum_{n,m,p}\sum_{r,s,t}(-1)^{s+t}e^{i(k_{xm}X_r+k_{yn}Y_s+k_{zp}Z_t)}I(k_{mnp},E) \tag{9.2.32}$$

This is an expansion in terms of the propagating waves which can be transformed to standing waves through,

$$\begin{aligned} \sum_r e^{ik_{xm}X_r}+\sum_r e^{-ik_{xm}X_r}&=e^{ik_{xm}(x-x')}+e^{ik_{xm}(x+x')}+e^{-ik_{xm}(x-x')}+e^{-ik_{xm}(x+x')} \\ &=2\cos k_{mx}(x-x')+2\cos k_{mx}(x+x')=4\cos k_{mx}x\cos k_{mx}x' \end{aligned} \tag{9.2.33}$$

except $m=0$ term which is simply equals to 2. The other terms can be treated similarly and finally,

$$G_{A2}^{xx}(\overline{r},\overline{r}';E)=\sum_{n,m,p}\psi_{mnp}^x(\overline{r})\psi_{mnp}^x(\overline{r}')I(k_{mnp},E) \tag{9.2.34}$$

where $\psi_{mnp}^x$ is the eigenfunction of wave equation that satisfies boundary condition of $G_A^{xx}$ over the cavity walls. The Ewald spectral summation is exactly the same as the conventional spectral expansion weighted by the spectral coefficient $I(k_{mnp},E)$. In the limit that $E\to 0$, $I\to 0$ and we recover pure spatial expansion (image expansion). On the other hand, when $E\to\infty$, $I$ becomes $(k_{mnp}^2-k^2)^{-1}$ and the spectral expansion of the Green's function is recovered.

As $E$ increases, the convergence of the spatial series improves while it slows down for the spectral series. We can find the value of $E$ that provides equal asymptotic convergence rates for both parts. An optimum selection of $E$ is given in the literature [141] as

$$E_o=\frac{\sqrt{\pi}}{2\sqrt[3]{V}} \tag{9.2.35}$$

that will be used in the future computations.

### 9.2.4 Numerical Validation

The Ewald technique provides an exponentially convergent series that results in highly accurate results. In this section, we use Ewald method with a relatively large number of included terms as a benchmark solution.

Consider an empty cavity of dimensions $L_x{=}L_y{=}L_z{=}L$ with perfect conductor walls. The source dipole is located at $\bar{r}'{=}(L_x/4,L_y/4,L_z/4)$.

In the first comparison, The excitation wavelength is selected to be $\lambda{=}0.93L$. The Green's function obtained by the imaginary extraction approach will be compared to that of Ewald summation for two settings; one is when acceptable maximum relative error is $10^{-5}$ and the other comparison is done when a highly accurate results with maximum relative error of $10^{-8}$ within the given observation grid, is required. With a fixed level of error, two approaches compare through the computation cost (All of the numerical routines are written by the same programmer and computed on the same machine). In [141], the Ewald technique was illustrated for a rectangular cavity with $L{=}0.3\lambda$.

#### First Comparison: Moderate Accuracy

Figure. 9.1 shows the $xx$ component of vector potential dyadic Green's function over the plane of $z{=}0$ inside the cavity computed by the 6th order convergent summation with imaginary wavenumber extraction. The maximum relative error with respect to the benchmark is less than $10^{-5}$ for all of the observation grid points. This result is obtained by including 10 modes (in each direction) in the 6th order summation and 5 clusters of image dipoles to compute the extracted terms with the computational time per observation point of 0.55 msec-CPU.

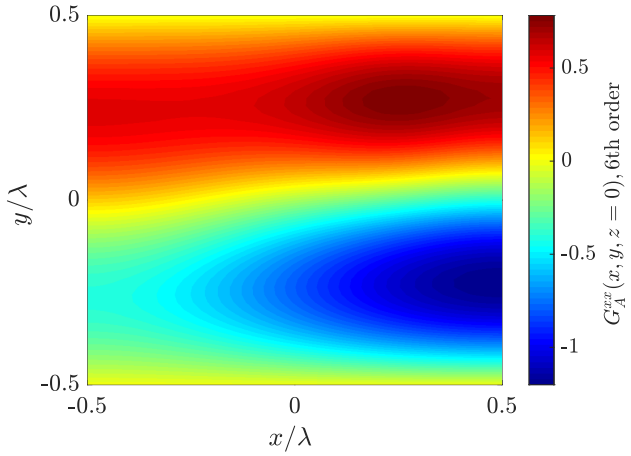


FIGURE 9.1: Vector potential Green's function $G_A^{xx}$ calculated by 6th order convergent spectral expansion, using 6 modes in each direction and $\xi{=}2/L$.

In order to obtain the same level of accuracy, the Ewald method is also evaluated to reach a relative error of $10^{-5}$. The CPU time for this method is 0.76 msec-CPU for evaluation of the dyadic Green's function at one point.

Figure. 9.2 plots the relative error of the 6th order method and Ewald method against the benchmark in dB.

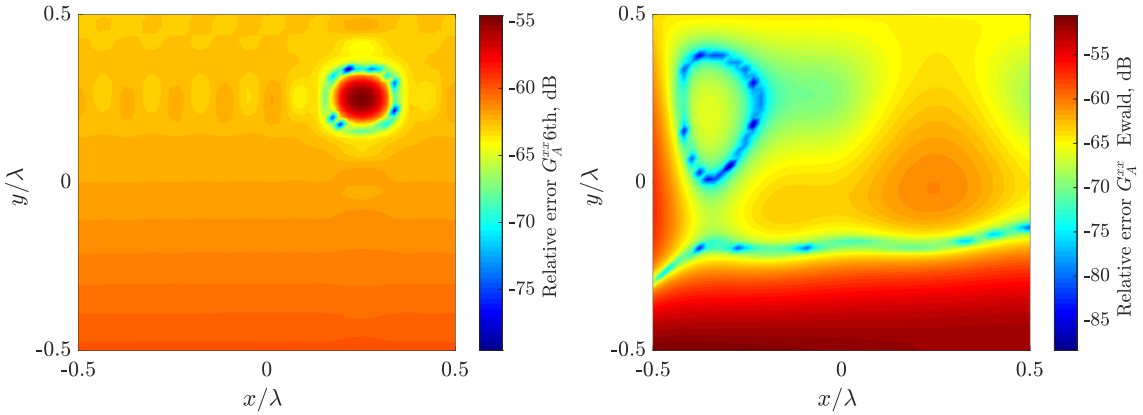


(A) 6th order Imaginary extraction (B) Ewald method

FIGURE 9.2: Relative error of 6th order convergent series and Ewald method against the benchmark.

TABLE 9.1: Computation cost of 6th order imaginary extraction technique against the Ewald method for different accuracies.

| Accuracy | Computation cost per point (CPU-msec) | |
|---|---|---|
| $10^{-5}$ | Ewald | 0.76 |
| | 6th | 0.55 |
| $10^{-8}$ | Ewald | 1.7 |
| | 6th | 8.2 |

**Second Comparison: Highly Accurate Results**

In this part, we set the acceptable error to $10^{-8}$ to compare the performance of two approaches. It is clear that the Ewald method performs better if a highly accurate result is desired. The convergence rate of the Ewald method is exponential while the imaginary extraction technique provides 6th order power-law convergence. In order to achieve the desired accuracy, the computation cost of the Ewald and imaginary extraction techniques are 1.7 and 8.2 msec-CPU per point, respectively. Therefore, if a very accurate value of the Green's function is required, the Ewald sum is superior from the computational cost standpoint.

However, the comparison of the results in Tab.9.1 is shown for a single frequency calculation. If a broadband solution of the dyadic Green's function is required, a very fine frequency sweep should be performed to capture individual resonance lines of the cavity (the resonance lines are closely spaced for a 3-dimensional cavity) that in turn leads to a large number of evaluations of the Green's function for different frequencies. For example, in order to find the Green's function of the cavity of dimension $L^3$ for excitation wavelengths

$\lambda$ from very long $\lambda \gg L$ to as small as $\lambda/L=0.2$, there are thousands of resonances. Accounting a few numbers of frequency points to capture a resonance in the Green's function correctly, the number of required frequency points would be several thousand. However, such a response can be obtained by a single run of the imaginary extraction. For the computational comparison of this wideband example (given required accuracy of $10^{-5}$), the expected cost of Ewald method is about $10{,}000 \times 0.76$ CPU.msec while for the imaginary extraction method it only takes 10 CPU.msec including the computation cost for a simple loop over frequency to evaluate the spectral coefficients.

Figure 9.3 plots the broadband Green's function for excitation wavelength $0.05 \leq \lambda/L \leq 5$ which is 2 decades of bandwidth obtained by imaginary wavenumber extraction technique with only one evaluation of the eigenmodes. The Green's function is shown over the line $x=z=0$ as a function of $L/\lambda$ for 130 frequency samples. The exact resonant frequencies are avoided as much as possible in plotting the broadband Green's function for a lossless cavity.

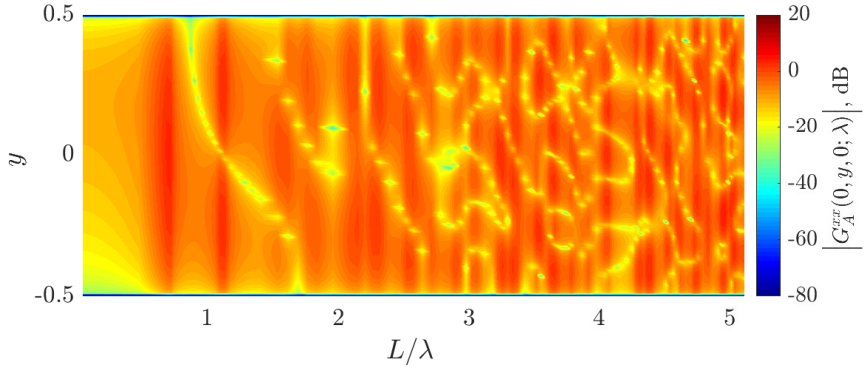


FIGURE 9.3: Vector potential Green's function $G_A^{xx}(0,y,0;\lambda)$ calculated by the 6th order convergent spectral expansion over two decades of bandwidth.

## 9.3 Electric Field Dyadic Green's Function

Given that we have the expression for the vector potential dyadic Green's function, one may calculate the electric field dyadic Green's function through Eq.(9.2.6). However, it is more insightful to begin with the electric field dyadic Green's function directly to have a better treatment of its singular behavior in the near field region. The electric field Green's function $\overline{\overline{G}}(\overline{r},\overline{r}')$ inside the cavity satisfies the vector wave equation of

$$\nabla \times \nabla \times \overline{\overline{G}}(\overline{r},\overline{r}') - k_0^2 \overline{\overline{G}}(\overline{r},\overline{r}') = \overline{\overline{I}}\delta(\overline{r}-\overline{r}') \tag{9.3.1}$$

subject to the Dirichlet boundary condition $\hat{n} \times \overline{\overline{G}}(\overline{r} \in \partial V, \overline{r}') = 0$. If we are able to find the vector eigenfunctions $\overline{F}_\alpha(\overline{r})$ that satisfy the homogeneous vector wave equation with eigenwavenumber $k_\alpha$ subject to the same type of boundary condition as imposed on the Green's function, i.e. $\hat{n} \times \overline{F}_\alpha(\overline{r} \in \partial V) = 0$ such that,

$$\nabla \times \nabla \times \overline{F}_\alpha(\overline{r}) - k_\alpha^2 \overline{F}_\alpha(\overline{r}) = 0 \tag{9.3.2}$$

then, an eigenmode expansion can be developed for the dyadic Green's function that satisfies the inhomogeneous vector wave equation. The vector eigenfunctions, which correspond to the Hermitian operator $\nabla\times\nabla\times-k^2$ (for real values of $k^2$ and given boundary conditions) constitute a complete and orthogonal basis that spans vector fields in the space that follow the same type of boundary conditions. The idea of completeness can be extended to include generalized functions as well. An eigenfunction expansion of the delta function (which satisfies the corresponding boundary condition on the wave equation operator) can be obtained as

$$\overline{\overline{I}}\delta(\overline{r}-\overline{r}')=\sum_{\alpha}\overline{F}_{\alpha}(\overline{r})\overline{F}_{\alpha}(\overline{r}') \tag{9.3.3}$$

where, it is assumed that the vector eigenfunctions are normalized according to

$$\int_{V}\mathrm{d}^3\overline{r}\overline{F}_{\alpha}(\overline{r})\cdot\overline{F}^{*}_{\beta}(\overline{r})=\delta_{\alpha\beta} \tag{9.3.4}$$

Upon expanding the dyadic Green's function in terms of vector eigenfunctions and substituting in the inhomogeneous vector wave equation of the dyadic Green's function we arrive at the similar expansion as the scalar case,

$$\overline{\overline{G}}(\overline{r},\overline{r}')=\sum_{\alpha}\frac{1}{k_{\alpha}^2-k_0^2}\overline{F}_{\alpha}(\overline{r})\overline{F}_{\alpha}(\overline{r}') \tag{9.3.5}$$

It is straight forward to verify that the following vector wave functions satisfy the homogeneous vector wave equation as well as the electric field boundary condition on the walls of the cavity.

$$\begin{aligned}
\overline{M}_{\alpha}(\overline{r})&=\nabla\times\left(\hat{z}\psi_{\alpha}^{M}(\overline{r})\right)\\
\overline{N}_{\alpha}(\overline{r})&=\frac{1}{k_{\alpha}}\nabla\times\nabla\times\left(\hat{z}\psi_{\alpha}^{N}(\overline{r})\right)\\
\overline{L}_{\alpha}(\overline{r})&=\nabla\left(\psi_{\alpha}^{L}(\overline{r})\right)
\end{aligned}$$

where,

$$\begin{aligned}
\psi_{\alpha}^{M}(\overline{r})&=\sqrt{\frac{8}{V}}\cos\frac{m\pi}{L_x}\left(x+\frac{L_x}{2}\right)\cos\frac{n\pi}{L_y}\left(y+\frac{L_y}{2}\right)\sin\frac{p\pi}{L_z}\left(z+\frac{L_z}{2}\right)\\
\psi_{\alpha}^{N}(\overline{r})&=\sqrt{\frac{8}{V}}\sin\frac{m\pi}{L_x}\left(x+\frac{L_x}{2}\right)\sin\frac{n\pi}{L_y}\left(y+\frac{L_y}{2}\right)\cos\frac{p\pi}{L_z}\left(z+\frac{L_z}{2}\right)\\
\psi_{\alpha}^{L}(\overline{r})&=\sqrt{\frac{8}{V}}\sin\frac{m\pi}{L_x}\left(x+\frac{L_x}{2}\right)\sin\frac{n\pi}{L_y}\left(y+\frac{L_y}{2}\right)\sin\frac{p\pi}{L_z}\left(z+\frac{L_z}{2}\right)
\end{aligned} \tag{9.3.6}$$

The transverse wave functions $\overline{M}_{\alpha}$ and $\overline{N}_{\alpha}$ are divergence free and with corresponding eigenvalues of

$$k_{\alpha}^2=\left(\frac{m\pi}{L_x}\right)^2+\left(\frac{n\pi}{L_y}\right)^2+\left(\frac{p\pi}{L_z}\right)^2 \tag{9.3.7}$$

The longitudinal wave functions $\overline{L}_\alpha$ are curl-free and span the degenerate eigenspace corresponding to the eigenvalue of $k{=}0$. Inclusion of the longitudinal wave functions are critical in the computation of the Green's function in the source region [156] and beyond that (as will be shown later). If we assume normalized eigenfunctions over the volume of the cavity, the dyadic Green's function can be written as

$$\overline{\overline{G}}(\overline{r},\overline{r}')=-\frac{1}{k_0^2}\sum_\alpha \overline{L}_\alpha(\overline{r})\overline{L}_\alpha(\overline{r}')+\sum_\alpha\left[\frac{\overline{M}_\alpha(\overline{r})\overline{M}_\alpha(\overline{r}')+\overline{N}_\alpha(\overline{r})\overline{N}_\alpha(\overline{r}')}{k_\alpha^2-k_0^2}\right] \tag{9.3.8}$$

Note that the vector wave functions are assumed to be normalized here.

### 9.3.1 Normalization of Vector Modes

By taking $k_x{=}m\pi/L_x, k_y{=}n\pi/L_y, k_z{=}p\pi/L_z$ and shifting the center of coordinate system for convenience we have,

$$\begin{aligned}\overline{M}_\alpha\cdot\overline{M}_\alpha&=\left(\nabla\psi_\alpha^M\times\hat{z}\right)\cdot\left(\nabla\psi_\alpha^M\times\hat{z}\right)=-\hat{z}\cdot\left[\nabla\psi_\alpha^M\times\left(\nabla\psi_\alpha^M\times\hat{z}\right)\right]\\&=\left[|\nabla\psi_\alpha^M|^2-|\nabla\psi_\alpha^M\cdot\hat{z}|^2\right]\\&=\frac{8}{V}\sin^2k_zz\left[k_x^2\sin^2k_xx\cos^2k_yy+k_y^2\cos^2k_xx\sin^2k_yy\right]\end{aligned} \tag{9.3.9}$$

Therefore,

$$\int_V \mathrm{d}\overline{r}\overline{M}_\alpha\cdot\overline{M}_\alpha=k_{\alpha\rho}^2\varepsilon_m\varepsilon_n\varepsilon_p \tag{9.3.10}$$

where $\varepsilon_n{=}1{+}\delta_n$ and $k_{\alpha\rho}^2{=}(k_x^2{+}k_y^2)$. Similarly,

$$\int_V \mathrm{d}\overline{r}\overline{N}_\alpha\cdot\overline{N}_\alpha=k_{\alpha\rho}^2\varepsilon_m\varepsilon_n\varepsilon_p \tag{9.3.11}$$

and for longitudinal wave functions,

$$\int_V \mathrm{d}\overline{r}\overline{L}_\alpha\cdot\overline{L}_\alpha=k_\alpha^2\varepsilon_m\varepsilon_n\varepsilon_p. \tag{9.3.12}$$

The dyadic Green's function in terms of unnormalized vector wave functions $\overline{M},\overline{N}$, and $\overline{L}$ becomes

$$\overline{\overline{G}}(\overline{r},\overline{r}')=-\frac{1}{k_0^2}\sum_\alpha\frac{1}{\varepsilon_m\varepsilon_n\varepsilon_p}\frac{1}{k_\alpha^2}\overline{L}_\alpha(\overline{r})\overline{L}_\alpha(\overline{r}')+\sum_\alpha\frac{1}{\varepsilon_m\varepsilon_n\varepsilon_p}\frac{1}{k_{\alpha\rho}^2}\left[\frac{\overline{M}_\alpha(\overline{r})\overline{M}_\alpha(\overline{r}')+\overline{N}_\alpha(\overline{r})\overline{N}_\alpha(\overline{r}')}{k_\alpha^2-k_0^2}\right] \tag{9.3.13}$$

### 9.3.2 Singularity Extraction

In order to extract the singularity of the dyadic Green's function, let's consider the asymptotic behavior of each terms as $\alpha\to\infty$. For $\overline{L}_\alpha$ term,

$$\lim_{\alpha\to\infty}\frac{1}{k_\alpha^2}\left|\overline{L}_\alpha(\overline{r})\overline{L}_\alpha(\overline{r}')\right|=\lim_{\alpha\to\infty}\frac{1}{k_\alpha^2}\left|\nabla\left(\psi_\alpha(\overline{r})\right)\nabla'\left(\psi_\alpha(\overline{r}')\right)\right|=\mathcal{O}(1) \tag{9.3.14}$$

which tends to a constant, but for $\overline{M}_\alpha$ and $\overline{N}_\alpha$ terms,

$$\lim_{\alpha\to\infty}\left|\frac{1}{k_{\alpha\rho}^2}\frac{\overline{M}_\alpha(\overline{r})\overline{M}_\alpha(\overline{r}')}{k_\alpha^2-k_0^2}\right|\approx\mathcal{O}\left(\frac{1}{k_\alpha^2}\right)$$
$$\lim_{\alpha\to\infty}\left|\frac{1}{k_{\alpha\rho}^2}\frac{\overline{N}_\alpha(\overline{r})\overline{N}_\alpha(\overline{r}')}{k_\alpha^2-k_0^2}\right|\approx\mathcal{O}\left(\frac{1}{k_\alpha^2}\right) \tag{9.3.15}$$

The first term does not represent a convergent series. Since the asymptotic spectral behavior tends to a constant value, it contains a delta function singularity in the spatial domain (which is known as the singularity of the dyadic Green's function [152–155]). For the free space dyadic Green's function expansion in terms of continuous spectrum of eigenfunctions, after evaluating one of the spectral integrations by contour integration technique, contribution of the $\overline{L}\overline{L}$ term includes a delta function singularity and an static pole term that exactly cancels the static pole hat arise from the $\overline{N}\overline{N}$ term [119, 121]. Therefore, the net contribution of the $\overline{L}\overline{L}$ term is just a delta function singularity at the source point. However, for the cavity Green's function where the modes are discrete, the $\overline{L}\overline{L}$ term similarly contains a delta function singularity at the source point and a static contribution that extends beyond the source point. The static pole does not appear hear either for $\overline{L}\overline{L}$ or $\overline{N}\overline{N}$ as a consequence of the discrete spectrum. Noting that $\psi_\alpha^L=\psi_\alpha$ is an eigenfunction of the scalar potential wave equation, the summation in the $\overline{L}\overline{L}$ part of the dyadic Green's function can be decomposed into two parts, one with all the indices non-zero and the other contains at least one zero index,

$$\overline{\overline{G}}(\overline{r},\overline{r}')\Big|_{LL}=-\frac{1}{k_0^2}\sum_{m,n,p\neq0}\frac{1}{k_\alpha^2-0^2}\nabla\nabla'\psi_\alpha(\overline{r})\psi_\alpha(\overline{r}')-\frac{1}{k_0^2}\sum_{\substack{m,n,p\\mnp=0}}\frac{1}{k_\alpha^2-0^2}\nabla\nabla'\psi_\alpha(\overline{r})\psi_\alpha(\overline{r}')\frac{1}{\varepsilon_m\varepsilon_n\varepsilon_p} \tag{9.3.16}$$

The second term is identically zero. By interchanging the summation and differential operators in the first summation symbolically (the singularity should be taken care of) as

$$\overline{\overline{G}}(\overline{r},\overline{r}')\Big|_{LL}=-\frac{1}{k_0^2}\nabla\nabla'\sum_{m,n,p\neq0}\frac{1}{k_\alpha^2-0^2}\psi_\alpha(\overline{r})\psi_\alpha(\overline{r}')=\frac{1}{k_0^2}\overline{\overline{G}}_L(\overline{r},\overline{r}') \tag{9.3.17}$$

where,

$$\overline{\overline{G}}_L(\overline{r},\overline{r}')=-\nabla\nabla'G_\phi(\overline{r},\overline{r}';k=0) \tag{9.3.18}$$

that corresponds to the derivative of the scalar Green's function $G_\phi(\overline{r},\overline{r}')$ of the cavity at DC. Notice that $\overline{\overline{G}}_L$ is a frequency-independent part of the dyadic Green's function $\overline{\overline{G}}$. Using the image expansion of the scalar Green's function of the cavity

$$G_\phi(\overline{r},\overline{r}';k=0)=\frac{1}{4\pi}\sum_{n,m,p}(-1)^{n+m+p}\frac{1}{|\overline{r}-\overline{r}_{mnp}(\overline{r}')|} \tag{9.3.19}$$

where $\overline{r}_{mnp}(\overline{r}')$ is the position of image sources. Taking $\overline{R}_{mnp}=\overline{r}-\overline{r}_{mnp}(\overline{r}')$, then the $x$-component of the posterior part of $\overline{\overline{G}}_L$ for $\overline{r}\neq\overline{r}'$ becomes

$$\overline{\overline{G}}_L(\overline{r},\overline{r}')\cdot\hat{x}=\frac{1}{4\pi}\sum_{m,n,p}(-1)^{n+p}\frac{1}{R_{mnp}^3}\left(3\hat{R}_{mnp}\hat{R}_{mnp}-\overline{\overline{I}}\right)\cdot\hat{x} \tag{9.3.20}$$

while for the $y$-component of the posterior part, $(-1)^{m+p}$ should be replaced in the summand and so on. This series converges much better than the image expansion of the dynamic dyadic Green's function. The image expansion of the dynamic dyadic Green's function is proportional to $R_{mnp}^{-1}$ while the DC part converges as $R_{mnp}^{-3}$ versus the number of included images. This term captures the near field singularity of the dyadic Green's function in the source region. All in all, the dyadic Green's function for $\overline{r}\neq\overline{r}'$ (apart from a delta function singularity at $\overline{r}=\overline{r}'$) can be written as

$$\overline{\overline{G}}(\overline{r},\overline{r}';k_0)=\frac{1}{k_0^2}\overline{\overline{G}}_L(\overline{r},\overline{r}')+\sum_\alpha \frac{1}{k_{\alpha\rho}^2}\frac{1}{\varepsilon_m\varepsilon_n\varepsilon_p}\left[\frac{\overline{M}_\alpha(\overline{r})\overline{M}_\alpha(\overline{r}')+\overline{N}_\alpha(\overline{r})\overline{N}_\alpha(\overline{r}')}{k_\alpha^2-k_0^2}\right] \tag{9.3.21}$$

In addition, a delta function singularity is buried in the definition of $\overline{\overline{G}}_L=-\nabla\nabla' G_\phi(\overline{r},\overline{r}';k=0)$ at $\overline{r}=\overline{r}'$. If we consider the image expansion of (9.3.19), singularity comes from the exciting dipole term $m=n=p=0$. Therefore, the delta function singularity would be the same as free space case. For $\overline{r}$ sufficiently close to $\overline{r}'$, the singular part $\overline{\overline{G}}_L^{\text{sing}}$ can be written as

$$\overline{\overline{G}}_L^{\text{sing}}(\overline{r},\overline{r}')=-\nabla\nabla'\frac{1}{4\pi|\overline{r}-\overline{r}'|}=\frac{1}{4\pi}\nabla\nabla\frac{1}{|\overline{r}-\overline{r}'|} \tag{9.3.22}$$

Applying the trace to both sides of (9.3.22) and noting that Tr $\nabla\nabla=\nabla^2$, it yields Tr $\overline{\overline{G}}_L^{\text{sing}}=-\delta(\overline{r}-\overline{r}')$. Since there is no preference between different directions near the source, $\overline{\overline{G}}_L^{\text{sing}}=-1/3\overline{\overline{I}}\delta(\overline{r}-\overline{r}')$ and the complete expansion of the dyadic Green's function that is valid everywhere reads,

$$\overline{\overline{G}}(\overline{r},\overline{r}';k_0)=-\frac{1}{3k_0^2}\overline{\overline{I}}\delta(\overline{r}-\overline{r}')+\frac{1}{k_0^2}\overline{\overline{G}}_L(\overline{r},\overline{r}')+\sum_\alpha \frac{1}{k_{\alpha\rho}^2}\frac{1}{\varepsilon_m\varepsilon_n\varepsilon_p}\left[\frac{\overline{M}_\alpha(\overline{r})\overline{M}_\alpha(\overline{r}')+\overline{N}_\alpha(\overline{r})\overline{N}_\alpha(\overline{r}')}{k_\alpha^2-k_0^2}\right] \tag{9.3.23}$$

### 9.3.3 Spectral Summation Acceleration

Following the imaginary wave number extraction of Eq. (9.2.14) and upon subtracting the dyadic Green's function at the imaginary wave number of $k=i\xi$ from itself yields,

$$\begin{aligned}\overline{\overline{G}}(\overline{r},\overline{r}';k)=&\overline{\overline{G}}(\overline{r},\overline{r}';i\xi)+\left(\frac{1}{k^2}+\frac{1}{\xi^2}\right)\overline{\overline{G}}_L(\overline{r},\overline{r}')\\&+\sum_\alpha \frac{1}{k_{\alpha\rho}^2\varepsilon_\alpha}\frac{k^2+\xi^2}{(k_\alpha^2-k^2)(k_\alpha^2+\xi^2)}\left[\overline{M}_\alpha(\overline{r})\overline{M}_\alpha(\overline{r}')+\overline{N}_\alpha(\overline{r})\overline{N}_\alpha(\overline{r}')\right]\end{aligned} \tag{9.3.24}$$

The DC term does not add any computational effort as it is frequency independent term. In (9.3.24), The imaginary wavenumber extracted term $\overline{\overline{G}}(\overline{r},\overline{r}';i\xi)$ will be computed by the image expansion which converges very fast in terms of included images (see Appendix A). The second term $\overline{\overline{G}}_L$ will be computed by the static image expansion (9.3.20) which converges much faster than dynamic image expansion. The modal series is now accelerated to the fourth-order of convergence with respect to $\alpha$. We can proceed to further accelerate

the summation by following the same procedure as the vector potential Green's function,

$$\overline{\overline{G}}(\overline{r},\overline{r}';k)=\overline{\overline{G}}(\overline{r},\overline{r}';i\xi)-\frac{k^2+\xi^2}{2\xi}\frac{\partial}{\partial\xi}\overline{\overline{G}}(\overline{r},\overline{r}';i\xi)+\left(\frac{1}{k^2}+\frac{1}{\xi^2}\right)\overline{\overline{G}}_L(\overline{r},\overline{r}')+\frac{k^2+\xi^2}{2\xi}\frac{\partial}{\partial\xi}\left(\frac{-1}{\xi^2}\right)\overline{\overline{G}}_L(\overline{r},\overline{r}')$$
$$+\sum_\alpha\frac{1}{k_{\alpha\rho}^2\varepsilon_\alpha}\frac{(k^2+\xi^2)^2}{(k_\alpha^2+\xi^2)^2(k_\alpha^2-k^2)}\left[\overline{M}_\alpha(\overline{r})\overline{M}_\alpha(\overline{r}')+\overline{N}_\alpha(\overline{r})\overline{N}_\alpha(\overline{r}')\right] \tag{9.3.25}$$

Again, since $\overline{\overline{G}}_L(\overline{r},\overline{r}')$ is frequency independent, it leads to a great simplification of the terms,

$$\overline{\overline{G}}(\overline{r},\overline{r}';k)=\overline{\overline{G}}(\overline{r},\overline{r}';i\xi)-\frac{k^2+\xi^2}{2\xi}\frac{\partial}{\partial\xi}\overline{\overline{G}}(\overline{r},\overline{r}';i\xi)+\frac{(k^2+\xi^2)^2}{k^2\xi^4}\overline{\overline{G}}_L(\overline{r},\overline{r}')$$
$$+\sum_\alpha\frac{1}{k_{\alpha\rho}^2\varepsilon_\alpha}\frac{(k^2+\xi^2)^2}{(k_\alpha^2+\xi^2)^2(k_\alpha^2-k^2)}\left[\overline{M}_\alpha(\overline{r})\overline{M}_\alpha(\overline{r}')+\overline{N}_\alpha(\overline{r})\overline{N}_\alpha(\overline{r}')\right]$$

This is the 6th order convergent spectral expansion of the dyadic Green's function of the rectangular cavity. It only remains to compute the imaginary wavenumber derivative of the dyadic Green's function. The image expansion of the dyadic Green's function of the rectangular cavity that is given in the appendix A can be used to find $\partial_\xi\overline{\overline{G}}(\overline{r},\overline{r}';i\xi)$. Note that for a wideband solution, the extracted terms with imaginary wavenumber as well as the static term $\overline{\overline{G}}_L$ should be evaluated only one time for a broadband frequency sweep.

Figure 9.4 plots the $xx$ component of the electric field dyadic Green's function of the cavity over the plane $z=0$ inside the cavity for the exciting wavelength of $\lambda=0.93L$. The source point and physical parameters are the same as the vector potential case in sec.9.2.4. A wideband evaluation of $G_{xx}$ is depicted in Fig. 9.5 with the observation points on the line $z=x=0$ in the cavity and the exciting wavelength in the range of $0.05\leq\lambda/L\leq5$. Notice that the difference between the vector potential $\overline{\overline{G}}_A$ and electric field $\overline{\overline{G}}$ dyadic Green's functions is dominant at low frequencies (near field). At high frequencies,

$$\overline{\overline{G}}(\overline{r},\overline{r}')=\left[\overline{\overline{I}}+\frac{\nabla\nabla}{k^2}\right]\cdot\overline{\overline{G}}_A(\overline{r},\overline{r}')\approx\overline{\overline{G}}_A(\overline{r},\overline{r}') \tag{9.3.26}$$

The difference between two dyadic Green's function is more pronounced around the source region where the electric field dyadic Green's function is hyper singular ($\propto1/R^3$).

### 9.3.4 Image Expansion of the Dyadic Green's Function

The free space Green's function $\overline{\overline{G}}_0(\overline{r},\overline{r}';k)$ at wavenumber $k$ that satisfies the vector wave equation of

$$\left(\nabla\times\nabla\times-k^2\right)\overline{\overline{G}}_0(\overline{r},\overline{r}';k)=\overline{\overline{I}}\delta(\overline{r}-\overline{r}') \tag{9.3.27}$$

subject to the radiation boundary condition at infinity, for $\overline{r}\neq\overline{r}'$ can be directly obtained by differentiating the scalar Green's function as

$$\overline{\overline{G}}_0(\overline{r},\overline{r}';k)=\left[\left(\frac{3}{k^2R^2}-\frac{3i}{kR}-1\right)\hat{R}\hat{R}+\left(-\frac{1}{k^2R^2}+\frac{i}{kR}+1\right)\overline{\overline{I}}\right]G_0(R;k) \tag{9.3.28}$$

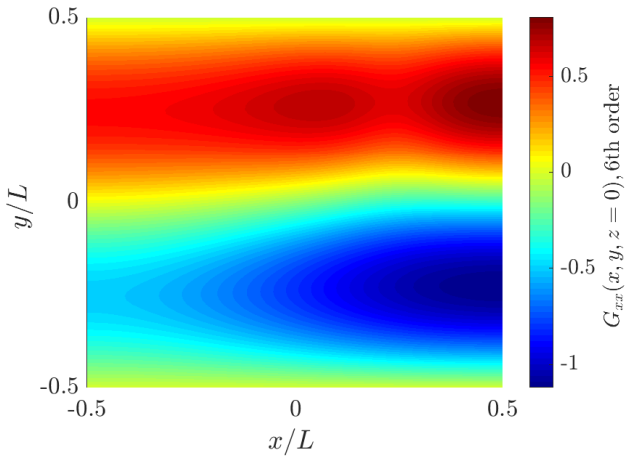


FIGURE 9.4: Electric field dyadic Green's function $G_{xx}(x,y,0)$ calculated by 6th order convergent spectral expansion for exciting wave length of $\lambda$=0.93$L$

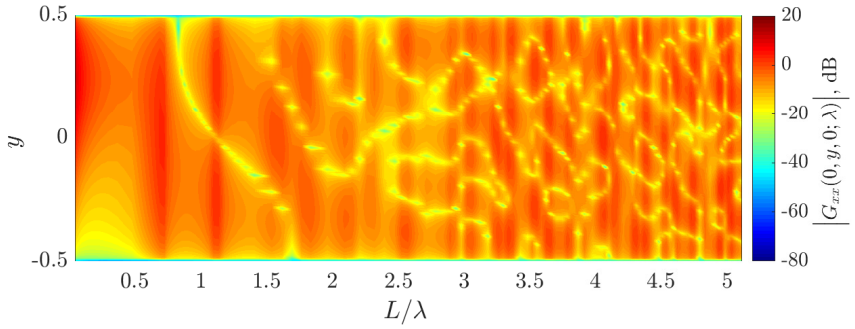


FIGURE 9.5: Electric field dyadic Green's function $G_{xx}(0,y,0;\lambda)$ calculated by 6th order convergent spectral expansion over two decades of bandwidth.

where, $G_0(R;k)=e^{ikR}/4\pi R$ is the scalar free space Green's function and $R=|\overline{r}-\overline{r}'|$. In order to obtain the cavity Green's function that satisfies the Dirichlet boundary condition on the walls, image sources should be placed all around the world in order to produce the response with vanishing tangential component over the walls. Once the boundary conditions are satisfied, presence of the walls does not have any additional effect on the fields and they can be removed. Figure. 9.6 shows a 2D profile ($xy$ plane) of the images dipoles around a cross-section of the cavity for a $x$-directed dipole in the cavity. Changing color from blue to red shows a flip in the sign of the dipole. For a $x-$ directed dipole with unit amplitude, the collective response of all the dipoles in Fig. 9.6 including the main dipole inside the cavity would be

$$\overline{\overline{G}}_{\perp}(\overline{r},\overline{r}')\cdot\hat{x}=\sum_{mn}(-1)^n\overline{\overline{G}}_0\Big(\overline{r};mL_x+(-1)^m x',nL_y+(-1)^n y',z'\Big)\cdot\hat{x}$$

Here, $\overline{\overline{G}}_{\perp}(\overline{r},\overline{r}')\cdot\hat{x}$ is the collective response of the image dipoles for a plane perpendicular to $z$ and the source dipole is located at $(x',y',z')$ inside the cavity and $(mL_x+(-1)^m x',nL_y+(-1)^n y',z')$ is the location of the image dipoles for 2D profile of Fig. 9.6 and $\overline{\overline{G}}_0$ is the free

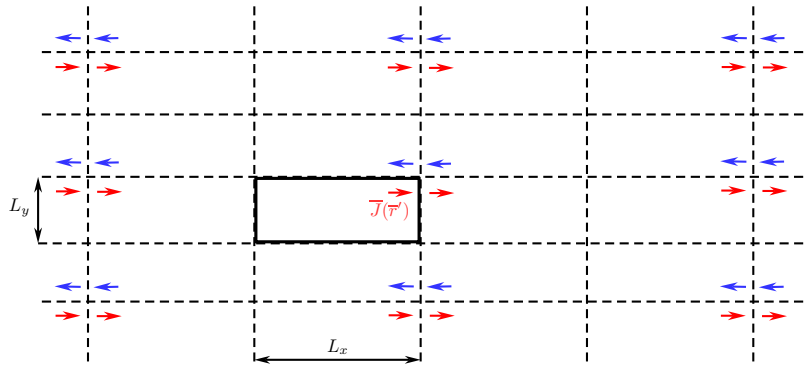


FIGURE 9.6: A profile of the images dipoles for a $x-$directed dipole current $\overline{J}$ in the cavity with PEC walls. change of color corresponds to a sign flip in the dipole moments.

space dyadic Green's function. Taking the other two walls into account, yields,

$$\begin{aligned}\overline{\overline{G}}(\overline{r},\overline{r}')\cdot\hat{x} &= \sum_{p}(-1)^{p}\overline{\overline{G}}_{\perp}(\overline{r},\overline{r}''_{p})\cdot\hat{x} \\ &= \sum_{m,n,p}(-1)^{n+p}\overline{\overline{G}}_{0}\Big(\overline{r};mL_x+(-1)^{m}x',nL_y+(-1)^{n}y',pL_z+(-1)^{p}z'\Big)\cdot\hat{x}\end{aligned} \tag{9.3.29}$$

This expansion for real values of $k$ has a good convergence in the near field region but far from the source, it has a very slow convergence rate that makes it not an attractive way of computing the cavity Green's function. However, for an imaginary wavenumber $k=i\xi$, it has an exponential convergence rate. In this case, the free space dyadic Green's function becomes

$$\overline{\overline{G}}_{0}(\overline{r},\overline{r}';i\xi)=\left[-\left(\frac{3}{Q^2}+\frac{3}{Q}+1\right)\hat{R}\hat{R}+\left(\frac{1}{Q^2}+\frac{1}{Q}+1\right)\overline{\overline{I}}\right]\frac{\xi e^{-Q}}{4\pi Q} \tag{9.3.30}$$

where $Q=\xi R$ and $R$ is the distance between the source and observation points. Similarly, for the wavenumber derivative of the dyadic Green's function, the image expansion of (9.3.29) can be evaluated with considering

$$\frac{\partial}{\partial\xi}\overline{\overline{G}}_{0}(\overline{r},\overline{r}';i\xi)=\frac{e^{-Q}}{4\pi}\left(\left[\left(\frac{6}{Q^3}+\frac{6}{Q^2}+\frac{3}{Q}+1\right)\hat{R}\hat{R}-\left(\frac{2}{Q^3}+\frac{2}{Q^2}+\frac{1}{Q}+1\right)\overline{\overline{I}}\right]\right) \tag{9.3.31}$$

that still is exponentially convergent.

## 9.4 Vector Potential Dyadic Green's Function For Cavity of Irregular Shape

The vector potential $\overline{A}(\overline{r})$ satisfies the wave equation of

$$(\nabla^2+k^2)\overline{A}(\overline{r})=-\mu\overline{J}(\overline{r}) \tag{9.4.1}$$

inside the cavity subject to boundary condition of $\hat{n}\times\overline{A}=0$, and $\nabla\cdot\overline{A}=0$ over the walls of the cavity. The free space Green's function for integration of the vector potential can be defined as

$$(\nabla^2+k^2)\overline{\overline{G}}_0(\overline{r},\overline{r}')=-\overline{\overline{I}}\delta(\overline{r}-\overline{r}') \tag{9.4.2}$$

such that in the free scatterer case,

$$\overline{A}(\overline{r})=\mu\int \mathrm{d}\overline{r}'\overline{\overline{G}}_0(\overline{r},\overline{r}')\cdot\overline{J}(\overline{r}') \tag{9.4.3}$$

or using the scalar Green's function $G_0(\overline{r},\overline{r}')$ it can be conventionally be written equivalently as

$$\overline{A}(\overline{r})=\mu\int \mathrm{d}\overline{r}'G_0(\overline{r},\overline{r}')\overline{J}(\overline{r}') \tag{9.4.4}$$

In order to construct the full Green's function of the vector potential wave equation, the vector wave equation can be rearranged in terms of its divergence for later ease,

$$\nabla\times\nabla\times\overline{A}(\overline{r})-\nabla\nabla\cdot\overline{A}(\overline{r})-k^2\overline{A}(\overline{r})=\mu\overline{J}(\overline{r}) \tag{9.4.5}$$

Corresponding dyadic Green's function that satisfies the same type of boundary condition can be defined in the same way as

$$\nabla\times\nabla\times\overline{\overline{G}}_A(\overline{r},\overline{r}')-\nabla\nabla\cdot\overline{\overline{G}}_A(\overline{r},\overline{r}')-k^2\overline{\overline{G}}_A(\overline{r},\overline{r}')=\overline{\overline{I}}\delta(\overline{r}-\overline{r}') \tag{9.4.6}$$

We do not assume any Specific boundary condition on $\overline{\overline{G}}_A$ for now. The free Green's function $\overline{\overline{G}}_0$ also can be written in the same form

$$\nabla\times\nabla\times\overline{\overline{G}}_0(\overline{r},\overline{r}')-\nabla\nabla\cdot\overline{\overline{G}}_0(\overline{r},\overline{r}')-k^2\overline{\overline{G}}_0(\overline{r},\overline{r}')=\overline{\overline{I}}\delta(\overline{r}-\overline{r}') \tag{9.4.7}$$

Where $\overline{\overline{G}}_0=\overline{\overline{I}}G_0$ and $G_0$ is the scalar Green's function. The surface integral equation for $\overline{A}$ can be obtained by post multiplying the dyadic Green's function with an arbitrary unit vector to get $\overline{G}_A=\overline{\overline{G}}_A(\overline{r},\overline{r}')\cdot\overline{\alpha}$. Upon multiplying (9.4.6) by $\overline{A}(\overline{r})$ from the left and (9.4.5) by $\overline{G}_A(\overline{r},\overline{r}')$ from the left side, and subtracting the results, we have

$$\nabla\times\nabla\times\overline{A}(\overline{r})\cdot\overline{G}_A(\overline{r},\overline{r}')-\overline{A}(\overline{r})\cdot\nabla\times\nabla\times\overline{G}_A(\overline{r},\overline{r}')-\Big(\nabla\nabla\cdot\overline{A}(\overline{r})\Big)\cdot\overline{G}_A(\overline{r},\overline{r}')+\overline{A}(\overline{r})\cdot\Big(\nabla\nabla\cdot\overline{G}_A(\overline{r},\overline{r}')\Big)$$
$$=\mu\overline{J}(\overline{r})\cdot\overline{G}_A(\overline{r},\overline{r}')-\overline{A}(\overline{r})\cdot\hat{\alpha}\delta(\overline{r}-\overline{r}') \tag{9.4.8}$$

The first two terms can be combined together to get (we always arrange vectors such that $\overline{G}_A$ stays on the right hand side of the expressions to be able to remove the arbitrary unit vector $\hat{\alpha}$ later)

$$\begin{aligned}I_1&=\nabla\times\nabla\times\overline{A}(\overline{r})\cdot\overline{G}_A(\overline{r},\overline{r}')-\overline{A}(\overline{r})\cdot\nabla\times\nabla\times\overline{G}_A(\overline{r},\overline{r}') \\ &=\Big[\nabla\cdot\Big((\nabla\times\overline{A})\times\overline{G}_A\Big)+\nabla\times\overline{A}\cdot\nabla\times\overline{G}_A\Big]-\Big[-\nabla\cdot\Big(\overline{A}\times\nabla\times\overline{G}_A\Big)+\nabla\times\overline{A}\cdot\nabla\times\overline{G}_A\Big] \\ &=\nabla\cdot\Big[\nabla\times\overline{A}\times\overline{G}_A+\overline{A}\times\nabla\times\overline{G}_A\Big]\end{aligned} \tag{9.4.9}$$

and for the second two terms,

$$\begin{aligned}I_2&=\overline{A}\cdot\Big(\nabla\nabla\cdot\overline{G}_A\Big)-\Big(\nabla\nabla\cdot\overline{A}\Big)\cdot\overline{G}_A \\ &=\Big[\nabla\cdot\Big(\overline{A}\nabla\cdot\overline{G}_A\Big)-\nabla\cdot\overline{A}\nabla\cdot\overline{G}_A\Big]-\Big[\nabla\cdot\Big(\nabla\cdot\overline{A}\overline{G}_A\Big)-\nabla\cdot\overline{A}-\nabla\cdot\overline{G}_A\Big] \\ &=\nabla\cdot\Big[\overline{A}\nabla\cdot\overline{G}_A-\nabla\cdot\overline{A}\overline{G}_A\Big]\end{aligned} \tag{9.4.10}$$

Integrating over the volume of the enclosure, $V$, and converting the volume integral to the surface integrals over the boundary surface, we arrive at

$$\int_{\partial V}\mathrm{d}S\;\hat{n}\cdot\Big[\nabla\times\overline{A}(\overline{r})\times\overline{G}_A(\overline{r},\overline{r}')+\overline{A}(\overline{r})\times\nabla\times\overline{G}_A(\overline{r},\overline{r}')\Big] \tag{9.4.11}$$
$$+\int_{\partial V}\mathrm{d}S\;\hat{n}\cdot\Big[\overline{A}(\overline{r})\nabla\cdot\overline{G}_A(\overline{r},\overline{r}')-\nabla\cdot\overline{A}(\overline{r})\overline{G}_A(\overline{r},\overline{r}')\Big]=\int_V\mathrm{d}\overline{r}\;\mu\overline{J}(\overline{r})\cdot\overline{G}_A(\overline{r},\overline{r}')+\begin{cases}-\overline{A}(\overline{r}')\cdot\hat{\alpha} & \overline{r}'\in V\\ 0 & \overline{r}'\notin V\end{cases}$$

The first integral can be altered to depends on the tangential surface field variables by permutations,

$$\int_{\partial V}\mathrm{d}S\;\Big[\Big(\hat{n}\times\nabla\times\overline{A}(\overline{r})\Big)\cdot\overline{G}_A(\overline{r},\overline{r}')+\Big(\hat{n}\times\overline{A}(\overline{r})\Big)\cdot\nabla\times\overline{G}_A(\overline{r},\overline{r}')\Big] \tag{9.4.12}$$
$$+\int_{\partial V}\mathrm{d}S\;\hat{n}\cdot\Big[\overline{A}(\overline{r})\nabla\cdot\overline{G}_A(\overline{r},\overline{r}')-\nabla\cdot\overline{A}(\overline{r})\overline{G}_A(\overline{r},\overline{r}')\Big]=\int_V\mathrm{d}\overline{r}\;\mu\overline{J}(\overline{r})\cdot\overline{G}_A(\overline{r},\overline{r}')+\begin{cases}-\overline{A}(\overline{r}')\cdot\hat{\alpha} & \overline{r}'\in V\\ 0 & \overline{r}'\notin V\end{cases}$$

Swapping the primed and unprimed coordinates gives

$$\int_{\partial V}\mathrm{d}S'\;\Big[\Big(\hat{n}'\times\nabla'\times\overline{A}(\overline{r}')\Big)\cdot\overline{G}_A(\overline{r}',\overline{r})+\Big(\hat{n}'\times\overline{A}(\overline{r}')\Big)\cdot\nabla'\times\overline{G}_A(\overline{r}',\overline{r})\Big] \tag{9.4.13}$$
$$+\int_{\partial V}\mathrm{d}S\;\hat{n}'\cdot\Big[\overline{A}(\overline{r}')\nabla'\cdot\overline{G}_A(\overline{r}',\overline{r})-\nabla\cdot\overline{A}(\overline{r}')\overline{G}_A(\overline{r}',\overline{r})\Big]=\int_V\mathrm{d}\overline{r}'\;\mu\overline{J}(\overline{r}')\cdot\overline{G}_A(\overline{r}',\overline{r})+\begin{cases}-\overline{A}(\overline{r})\cdot\hat{\alpha} & \overline{r}\in V\\ 0 & \overline{r}\notin V\end{cases}$$

Now, the Green's function has been kept on the right most position in the equations, we can remove the post factor of $\hat{\alpha}$ to get

$$\int_{\partial V} \mathrm{d}S' \left[\left(\hat{n}'\times\nabla'\times\overline{A}(\overline{r}')\right)\cdot\overline{\overline{G}}_A(\overline{r}',\overline{r})+\left(\hat{n}'\times\overline{A}(\overline{r}')\right)\cdot\nabla'\times\overline{\overline{G}}_A(\overline{r}',\overline{r})\right] \tag{9.4.14}$$
$$+\int_{\partial V} \mathrm{d}S\ \hat{n}'\cdot\left[\overline{A}(\overline{r}')\nabla'\cdot\overline{\overline{G}}_A(\overline{r}',\overline{r})-\nabla\cdot\overline{A}(\overline{r}')\overline{\overline{G}}_A(\overline{r}',\overline{r})\right]=\int_V \mathrm{d}\overline{r}'\ \mu\overline{J}(\overline{r}')\cdot\overline{\overline{G}}_A(\overline{r}',\overline{r})+\begin{cases}-\overline{A}(\overline{r}) & \overline{r}\in V\\ 0 & \overline{r}\notin V\end{cases}$$

This is the general Extinction theorem for the vector potential using a general vector potential Green's function $\overline{\overline{G}}_A$ that can satisfies any boundary condition. Similarly, it can be extended to SIE for the vector potential Green's function itself. Assuming $\overline{\overline{G}}_A(\overline{r},\overline{r}'')$ to be the vector potential dyadic Green's function inside the enclosure, the vector potential due to the current source $\overline{\overline{J}}(\overline{r})=\hat{\alpha}\delta(\overline{r}-\overline{r}'')$ gives $\overline{\overline{G}}_A(\overline{r},\overline{r}'')\cdot\hat{\alpha}$. If we use the propagator of the vector potential integral equation as $\overline{\overline{G}}^p_A(\overline{r},\overline{r}')$ to formulate the SIE we arrive at,

$$\int_{\partial V} \mathrm{d}S' \left[\left(\hat{n}'\times\nabla'\times\overline{\overline{G}}_A(\overline{r}',\overline{r}'')\cdot\hat{\alpha}\right)\cdot\overline{\overline{G}}^p_A(\overline{r}',\overline{r})+\left(\hat{n}'\times\overline{\overline{G}}_A(\overline{r}',\overline{r}'')\cdot\hat{\alpha}\right)\cdot\nabla'\times\overline{\overline{G}}^p_A(\overline{r}',\overline{r})\right] \tag{9.4.15}$$
$$+\int_{\partial V} \mathrm{d}S\ \hat{n}'\cdot\left[\overline{\overline{G}}_A(\overline{r}',\overline{r}'')\cdot\hat{\alpha}\nabla'\cdot\overline{\overline{G}}^p_A(\overline{r}',\overline{r})-\nabla\cdot\overline{\overline{G}}_A(\overline{r}',\overline{r}'')\cdot\hat{\alpha}\overline{\overline{G}}^p_A(\overline{r}',\overline{r})\right]$$
$$=\hat{\alpha}\cdot\overline{\overline{G}}^p_A(\overline{r},\overline{r}'')+\begin{cases}-\overline{\overline{G}}_A(\overline{r},\overline{r}'')\cdot\hat{\alpha} & \overline{r}\in V\\ 0 & \overline{r}\notin V\end{cases}$$

Different choices may be made for the propagator of the SIE to solve for the vector potential dyadic Green's function $\overline{\overline{G}}_A$. For the problem of the vector potential inside the cavity of perfect conductor walls, $\hat{n}\times\overline{\overline{G}}_A$ and $\nabla\cdot\overline{\overline{G}}_A$ vanish on the surface of the cavity and it reduces to

$$\int_{\partial V} \mathrm{d}S' \left[\left(\hat{n}'\times\nabla'\times\overline{\overline{G}}_A(\overline{r}',\overline{r}'')\cdot\hat{\alpha}\right)\cdot\overline{\overline{G}}^p_A(\overline{r}',\overline{r})+\hat{n}'\cdot\overline{\overline{G}}_A(\overline{r}',\overline{r}'')\cdot\hat{\alpha}\nabla'\cdot\overline{\overline{G}}^p_A(\overline{r}',\overline{r})\right] \tag{9.4.16}$$
$$=\hat{\alpha}\cdot\overline{\overline{G}}^p_A(\overline{r},\overline{r}'')+\begin{cases}-\overline{\overline{G}}_A(\overline{r},\overline{r}'')\cdot\hat{\alpha} & \overline{r}\in V\\ 0 & \overline{r}\notin V\end{cases}$$

Taking the surface field unknowns as

$$\begin{aligned}\overline{J}^{\alpha}(\overline{r}')&=\hat{n}'\times\nabla'\times\overline{\overline{G}}_A(\overline{r}',\overline{r}'')\cdot\hat{\alpha}\\ \sigma^{\alpha}(\overline{r}')&=\hat{n}'\cdot\overline{\overline{G}}_A(\overline{r}',\overline{r}'')\cdot\hat{\alpha}\end{aligned} \tag{9.4.17}$$

where $\overline{J}^{\alpha}$, and $\sigma^{\alpha}$ represent the tangential magnetic field and surface charge density over the surface of the cavity, respectively, the SIE becomes,

$$\int_{\partial V} \mathrm{d}S' \left[\overline{J}^{\alpha}(\overline{r}')\cdot\overline{\overline{G}}^p_A(\overline{r}',\overline{r})+\sigma^{\alpha}(\overline{r}')\nabla'\cdot\overline{\overline{G}}^p_A(\overline{r}',\overline{r})\right]=\hat{\alpha}\cdot\overline{\overline{G}}^p_A(\overline{r},\overline{r}'')+\begin{cases}-\overline{\overline{G}}_A(\overline{r},\overline{r}'')\cdot\hat{\alpha} & \overline{r}\in V\\ 0 & \overline{r}\notin V\end{cases} \tag{9.4.18}$$

Mapping the tangential component of the integral equation to the surface of the cavity and utilizing the boundary conditions,

$$\hat{n}\times\int_{\partial V}\mathrm{d}S'\ \left[\overline{J}^{\alpha}(\overline{r}')\cdot\overline{\overline{G}}_A^{p}(\overline{r}',\overline{r})+\sigma^{\alpha}(\overline{r}')\nabla'\cdot\overline{\overline{G}}_A^{p}(\overline{r}',\overline{r})\right]=\hat{n}\times\overline{\overline{G}}_A^{p}(\overline{r},\overline{r}'')\cdot\hat{\alpha} \tag{9.4.19}$$

We need to map the normal component of the integral equation to the surface as well to get enough number of equations for two unknown surface fields,

$$\int_{\partial V}\mathrm{d}S'\ \left[\overline{J}^{\alpha}(\overline{r}')\cdot\overline{\overline{G}}_A^{p}(\overline{r}',\overline{r})\cdot\hat{n}+\sigma^{\alpha}(\overline{r}')\nabla'\cdot\overline{\overline{G}}_A^{p}(\overline{r}',\overline{r})\cdot\hat{n}\right]=\hat{n}\cdot\overline{\overline{G}}_A^{p}(\overline{r},\overline{r}'')\cdot\hat{\alpha}+\begin{cases}-\sigma^{\alpha}(\overline{r}) & \overline{r}\in V\\ 0 & \overline{r}\notin V\end{cases} \tag{9.4.20}$$

where we have assumed that $\overline{\overline{G}}_A^{p}$ is a symmetric dyadic, $\overline{\overline{G}}_A^{p}(\overline{r},\overline{r}')=\left[\overline{\overline{G}}_A^{p}(\overline{r},\overline{r}')\right]^{\mathrm{T}}$. Noting that the second term of the integrand is singular and have a different value depending on $\overline{r}\to\partial S^{\pm}$, such that the right hand side value does not depend on whether the integral equation is mapped on $\partial S^{+}$ or $\partial S^{+}$. In terms of principal value integrals,

$$\mathcal{P}\int_{\partial V}\mathrm{d}S'\ \left[\overline{J}^{\alpha}(\overline{r}')\cdot\overline{\overline{G}}_A^{p}(\overline{r}',\overline{r})\cdot\hat{n}+\sigma^{\alpha}(\overline{r}')\nabla'\cdot\overline{\overline{G}}_A^{p}(\overline{r}',\overline{r})\cdot\hat{n}\right]=\hat{n}\cdot\overline{\overline{G}}_A^{p}(\overline{r},\overline{r}'')\cdot\hat{\alpha}-\frac{1}{2}\sigma^{\alpha}(\overline{r}) \tag{9.4.21}$$

### 9.4.1 SIE for $\overline{\overline{G}}_A$ with $\overline{\overline{G}}_0$ as a propagator

If we take $\overline{\overline{G}}_A^{p}(\overline{r},\overline{r}')=\overline{\overline{G}}_0(\overline{r},\overline{r}')=\overline{\overline{I}}G_0(\overline{r},\overline{r}')$, where $G_0(\overline{r},\overline{r}')$ is the free space scalar Green's function, $\overline{\overline{G}}_0(\overline{r},\overline{r}')=\overline{\overline{G}}_0^{\mathrm{T}}(\overline{r},\overline{r}')$. Furthermore, $\nabla'\cdot\overline{\overline{G}}_0(\overline{r}',\overline{r})=\nabla' G_0(\overline{r}',\overline{r})$ and the surface integral equations become

$$\begin{aligned}\hat{n}\times\int_{\partial S}\mathrm{d}S'\left\{G_0(\overline{r},\overline{r}')\overline{J}^{\alpha}(\overline{r}')+\nabla' G_0(\overline{r},\overline{r}')\sigma^{\alpha}(\overline{r}')\right\}&=\hat{n}\times\overline{\overline{G}}_0(\overline{r},\overline{r}'') \\ \mathcal{P}\int_{\partial S}\mathrm{d}S'\left\{G_0(\overline{r},\overline{r}')\hat{n}\cdot\overline{J}^{\alpha}(\overline{r}')+\hat{n}\cdot\nabla' G_0(\overline{r},\overline{r}')\sigma^{\alpha}(\overline{r}')\right\}&=\hat{n}\cdot\overline{\overline{G}}_0(\overline{r},\overline{r}'')\cdot\hat{\alpha}-\frac{1}{2}\sigma^{\alpha}(\overline{r})\end{aligned} \tag{9.4.22}$$

Expanding the unknown field over the walls of the cavity as

$$\begin{aligned}\overline{J}^{\alpha}(\overline{r}')&=\sum_{n'=1}^{N_J}J_{n'}^{\alpha}\overline{f}_{n'}(\overline{r}') \\ \sigma^{\alpha}(\overline{r}')&=\sum_{m'=1}^{M_\sigma}\sigma_{m'}^{\alpha}P_{m'}(\overline{r}')\end{aligned} \tag{9.4.23}$$

where $f_n(\overline{r}')$ is a linear RWG basis function attached to the $n$-th edge of the triangulation and is defined as

$$\overline{f}_n(\overline{r})=\begin{cases}\dfrac{L_n}{2A_n^+}\overline{\rho}_n^+(\overline{r}) & ,\overline{r}\in T_n^+\\[2ex] \dfrac{L_n}{2A_n^-}\overline{\rho}_n^-(\overline{r}) & ,\overline{r}\in T_n^-\end{cases} \tag{9.4.24}$$

where $L_n$ is the length of $n$-th edge and $A_n^{\pm}$ are area of triangles with common edge $n$. The vectors $\overline{\rho}_n^{\pm}(\overline{r})$ in $T_n^{\pm}$ are defined as

$$\begin{aligned}\overline{\rho}_n^+(\overline{r})&=\overline{v}_n^+-\overline{r}, \quad \overline{r}\in T_n^+\\ \overline{\rho}_n^-(\overline{r})&=\overline{r}-\overline{v}_n^-, \quad \overline{r}\in T_n^-\end{aligned} \tag{9.4.25}$$

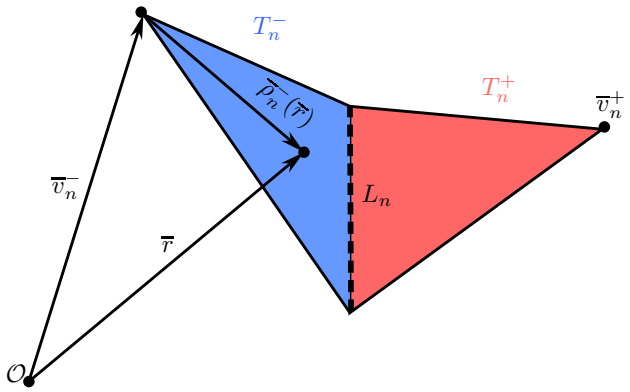


FIGURE 9.7: RWG basis function on the $n$-th edge.

Notice, given that $\overline{r}$ is on the surface of the object, $\overline{f}_n(\overline{r})$ is always in the tangent space of the object. If we use RWG function to test the SIE, it automatically picks up the tangential component.

In addition $P_n(\overline{r})$ is a pedestal scalar basis function over the $n$-th triangle. Inserting the expansion of unknown fields into the set of SIEs we have

$$\hat{n}\times\sum_{n'=1}^{N_J}J_{n'}^{\alpha}\int_{T_{n'}^{\pm}}\mathrm{d}S'G_0(\overline{r},\overline{r}')\overline{f}_{n'}(\overline{r}')+\hat{n}\times\sum_{m'=1}^{M_\sigma}\sigma_{m'}^{\alpha}\int_{T_{m'}}\nabla'G_0(\overline{r},\overline{r}')P_{m'}(\overline{r}')=\hat{n}\times\overline{\overline{G}}_0(\overline{r},\overline{r}'') \tag{9.4.26}$$

$$\sum_{n'=1}^{N_J}J_{n'}^{\alpha}\int_{T_{n'}^{\pm}}\mathrm{d}S'G_0(\overline{r},\overline{r}')\hat{n}\cdot\overline{f}_{n'}(\overline{r}')+\sum_{m'=1}^{M_\sigma}\sigma_{m'}^{\alpha}\int_{T_{m'}}\mathrm{d}S'\hat{n}\cdot\nabla'G_0(\overline{r},\overline{r}')P_{m'}(\overline{r}')=\hat{n}\cdot\overline{\overline{G}}_0(\overline{r},\overline{r}'')\cdot\hat{\alpha}-\frac{1}{2}\sigma^{\alpha}(\overline{r})$$

In order to test the SIE, we will test the vector SIE with RWG basis functions and the scalar SIE with pedestal basis $P_{m'}$.

$$\begin{aligned}&\sum_{n=1}^{N_J}J_{n'}^{\alpha}\int_{T_{n'}^{\pm}}\mathrm{d}S'\int_{T_n^{\pm}}\mathrm{d}SG_0(\overline{r},\overline{r}')\overline{f}_n(\overline{r})\cdot\overline{f}_{n'}(\overline{r}')+\sum_{m'=1}^{M_\sigma}\sigma_{m'}^{\alpha}\int_{T_{m'}}\mathrm{d}S'\int_{T_n^{\pm}}\mathrm{d}S\overline{f}_n(\overline{r})\cdot\nabla'G_0(\overline{r},\overline{r}')P_{m'}(\overline{r}')\\ &\qquad=\int_{T_n^{\pm}}\mathrm{d}S\overline{f}_n(\overline{r})\cdot\overline{\overline{G}}_0(\overline{r},\overline{r}'')\cdot\hat{\alpha}\end{aligned} \tag{9.4.27}$$

$$\sum_{n'=1}^{N_J} J_{n'}^{\alpha}\int_{T_{n'}^{\pm}} \mathrm{d}S'\int_{T_m} \mathrm{d}S P_m(\overline{r})G_0(\overline{r},\overline{r}')\hat{n}\cdot\overline{f}_{n'}(\overline{r}')+\sum_{m'=1}^{M_\sigma}\sigma_{m'}^{\alpha}\int_{T_{m'}} \mathrm{d}S'\int_{T_m} \mathrm{d}S P_m(\overline{r})\hat{n}\cdot\nabla' G_0(\overline{r},\overline{r}')P_{m'}(\overline{r}')$$
$$=\int_{T_m} \mathrm{d}S P_m(\overline{r})\hat{n}\cdot\overline{\overline{G}}_0(\overline{r},\overline{r}'')\cdot\hat{\alpha}-\frac{1}{2}\sigma^{\alpha}(\overline{r}) \tag{9.4.28}$$

Or in the matrix form,

$$\begin{aligned}\overline{\overline{Z}}_{JJ}\cdot\overline{J}+\overline{\overline{Z}}_{J\sigma}\cdot\overline{\sigma}&=\overline{b}_J\\ \overline{\overline{Z}}_{\sigma J}\cdot\overline{\sigma}+\overline{\overline{Z}}_{\sigma\sigma}\cdot\overline{\sigma}&=\overline{b}_\sigma\end{aligned} \tag{9.4.29}$$

where, the impedance matrix elements are given by

$$\begin{aligned}[Z_{JJ}]_{n,n'}&=\int_{T_{n'}^{\pm}}\mathrm{d}S'\int_{T_n^{\pm}}\mathrm{d}S G_0(\overline{r},\overline{r}')\overline{f}_n(\overline{r})\cdot\overline{f}_{n'}(\overline{r}')\\ [Z_{J\sigma}]_{n,m'}&=\int_{T_{m'}}\mathrm{d}S'\int_{T_n^{\pm}}\mathrm{d}S\overline{f}_n(\overline{r})\cdot\nabla' G_0(\overline{r},\overline{r}')P_{m'}(\overline{r}')\\ [Z_{\sigma J}]_{m,n'}&=\int_{T_{n'}^{\pm}}\mathrm{d}S'\int_{T_m}\mathrm{d}S P_m(\overline{r})G_0(\overline{r},\overline{r}')\hat{n}_m\cdot\overline{f}_{n'}(\overline{r}')\\ [Z_{\sigma\sigma}]_{m,m'}&=\int_{T_{m'}}\mathrm{d}S'\int_{T_m}\mathrm{d}S P_m(\overline{r})\left[\hat{n}_m\cdot\nabla' G_0(\overline{r},\overline{r}')+\frac{1}{2}\delta(\overline{r}-\overline{r}')\right]P_{m'}(\overline{r}')\end{aligned} \tag{9.4.30}$$

and,

$$\begin{aligned}[b_J]_n&=\int_{T_n^{\pm}}\mathrm{d}S\overline{f}_n(\overline{r})\cdot\overline{\overline{G}}_0(\overline{r},\overline{r}'')\cdot\hat{\alpha}\\ [b_\sigma]_m&=\int_{T_m}\mathrm{d}S P_m(\overline{r})\hat{n}\cdot\overline{\overline{G}}_0(\overline{r},\overline{r}'')\cdot\hat{\alpha}\end{aligned} \tag{9.4.31}$$

Once the surface field variables are obtained from the SIE, the vector potential dyadic Green's function can be evaluated through the extinction theorem of (9.4.18)

$$\begin{aligned}\overline{\overline{G}}_A(\overline{r},\overline{r}'')\cdot\alpha&=\overline{\overline{G}}_0(\overline{r},\overline{r}'')\cdot\alpha-\int_{\partial S}\mathrm{d}S'\left\{G_0(\overline{r},\overline{r}')\overline{J}^{\alpha}(\overline{r}',\overline{r}'')+\nabla' G_0(\overline{r},\overline{r}')\ \sigma^{\alpha}(\overline{r}',\overline{r}'')\right\}\\ &=\overline{\overline{G}}_0(\overline{r},\overline{r}'')\cdot\alpha-\int_{\partial S}\mathrm{d}S'\left\{G_0(\overline{r},\overline{r}')\overline{J}^{\alpha}(\overline{r}',\overline{r}'')-\nabla G_0(\overline{r},\overline{r}')\ \sigma^{\alpha}(\overline{r}',\overline{r}'')\right\}\end{aligned} \tag{9.4.32}$$

substituting the expansion of the surface fields into the dyadic Green's function

$$\overline{\overline{G}}_A(\overline{r},\overline{r}'')\cdot\alpha=\overline{\overline{G}}_0(\overline{r},\overline{r}'')\cdot\alpha-\sum_n J_n^{\alpha}\int_{T_n^{\pm}}\mathrm{d}S' G_0(\overline{r},\overline{r}')\overline{f}_n(\overline{r}')+\sum_m\sigma_m^{\alpha}\int_{T_m}\nabla G_0(\overline{r},\overline{r}')P_m(\overline{r}) \tag{9.4.33}$$

For the $\beta\alpha-$ component of the vector potential Green's function,

$$\hat{\beta}\cdot\overline{\overline{G}}_A(\overline{r},\overline{r}'')\cdot\alpha=\hat{\beta}\cdot\overline{\overline{G}}_0(\overline{r},\overline{r}'')\cdot\alpha-\sum_n J_n^{\alpha}\int_{T_n^{\pm}}\mathrm{d}S' G_0(\overline{r},\overline{r}')\hat{\beta}\cdot\overline{f}_n(\overline{r}')+\sum_m\sigma_m^{\alpha}\int_{T_m}\hat{\beta}\cdot\nabla G_0(\overline{r},\overline{r}')P_m(\overline{r}) \tag{9.4.34}$$

### Impedance Matrix Elements

The impedance matrix elements can be separated into singular and extracted parts through $\overline{\overline{Z}}=\overline{\overline{Z}}^{e}+\overline{\overline{Z}}^{s}$ where, the scalar Green's function can be factorized as

$$G_0(\overline{r},\overline{r}')=\Big[G_0(\overline{r},\overline{r}')-S(\overline{r},\overline{r}')\Big]+S(\overline{r},\overline{r}') \tag{9.4.35}$$

and

$$S(\overline{r},\overline{r}')=\frac{1}{4\pi}\left[\frac{1}{|\overline{r}-\overline{r}'|}-\frac{k^2}{2}|\overline{r}-\overline{r}'|\right] \tag{9.4.36}$$

Extraction of the first term involved in $S$ regularizes the Green's function at source point. However, the extracted Green's function is not differentiable at source point and numerical integration requires higher order quadratures. More importantly, for numerical integrations involving the gradient of the Green's function, the second order extraction is essential. Figure. 9.8 shows the extracted Green's function near the source region resulted from the first and second order extractions.

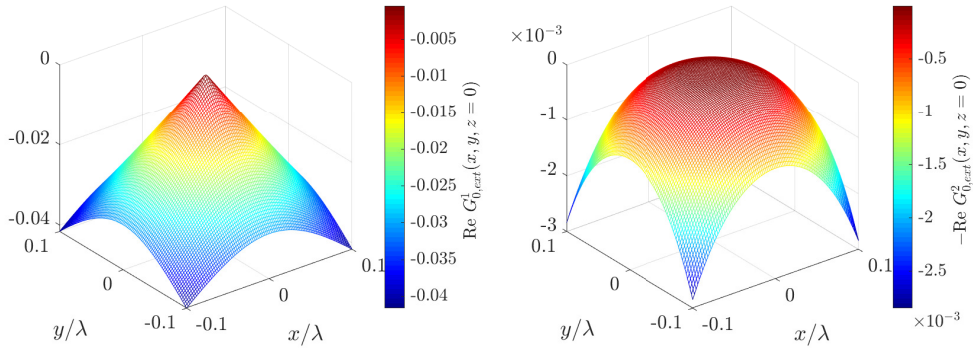


FIGURE 9.8: First and second order extracted scalar Green's function for the source at origin.

Figure. 9.9 plots $x$-component of the gradient of the scalar Green's function for a source located at the origin. Second order extraction results in a smooth behavior around the source point even for the gradient of Green's function.

Upon decomposition of the Green's function, the extracted impedance elements can be written as

$$[Z^e_{JJ}]_{n,n'}=\int_{T^{\pm}_{n'}}\mathrm{d}S'\int_{T^{\pm}_{n}}\mathrm{d}S G_{0,ext}(\overline{r},\overline{r}')\overline{f}_n(\overline{r})\cdot\overline{f}_{n'}(\overline{r}') \tag{9.4.37}$$

$$[Z^e_{J\sigma}]_{n,m'}=\frac{1}{A_{m'}}\int_{T_{m'}}\mathrm{d}S'\int_{T^{\pm}_{n}}\mathrm{d}S\overline{f}_n(\overline{r})\cdot\nabla' G_{0,ext}(\overline{r},\overline{r}')$$

$$[Z^e_{\sigma J}]_{m,n'}=\frac{1}{A_{m}}\int_{T^{\pm}_{n'}}\mathrm{d}S'\int_{T_{m}}\mathrm{d}S G_{0,ext}(\overline{r},\overline{r}')\hat{n}_m\cdot\overline{f}_{n'}(\overline{r}')$$

$$[Z^e_{\sigma\sigma}]_{m,m'}=\frac{1}{A_m A_{m'}}\mathcal{P}\int_{T_{m'}}\mathrm{d}S'\int_{T_m}\mathrm{d}S\ \hat{n}_m\cdot\nabla' G_{0,ext}(\overline{r},\overline{r}')$$

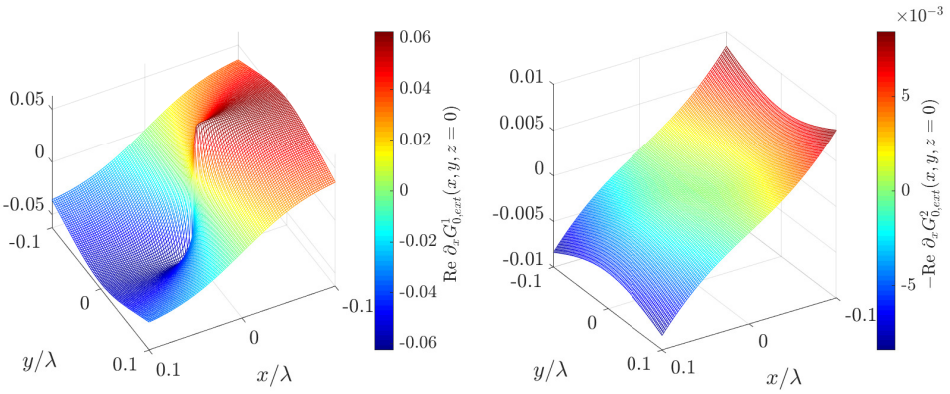


FIGURE 9.9: First and second order extraction of $x$-derivative scalar Green's function for the source at origin.

The second term can be integrated by part to give

$$[Z^e_{J\sigma}]_{n,m'} = -\frac{1}{A_{m'}}\int_{T_{m'}} \mathrm{d}S' \int_{T^\pm_n} \mathrm{d}S \overline{f}_n(\overline{r})\cdot\nabla G_{0,ext}(\overline{r},\overline{r}') \tag{9.4.38}$$
$$= \mp\frac{L_n}{A^\pm_n A_{m'}}\int_{T_{m'}} \mathrm{d}S' \int_{T^\pm_n} \mathrm{d}S G_{0,ext}(\overline{r},\overline{r}')$$

Note that the integral in the last impedance elements is a principal value integral and total diagonal contribution is associated with the singularity term $[Z_{\sigma\sigma}]_{m,m'}=1/(2A_m)$ for $m=m'$. The principal value integral is not singular away from the source point (which is excluded) it would be beneficial to still do the extraction for near terms. On the other hand, singular impedance elements can be written as

$$[Z^s_{JJ}]_{n,n'} = \int_{T^\pm_{n'}} \mathrm{d}S' \int_{T^\pm_n} \mathrm{d}S S(\overline{r},\overline{r}')\overline{f}_n(\overline{r})\cdot\overline{f}_{n'}(\overline{r}') \tag{9.4.39}$$
$$[Z^s_{J\sigma}]_{n,m'} = \frac{1}{A_{m'}}\int_{T_{m'}} \mathrm{d}S' \int_{T^\pm_n} \mathrm{d}S \overline{f}_n(\overline{r})\cdot\nabla' S(\overline{r},\overline{r}')$$
$$[Z^s_{\sigma J}]_{m,n'} = \frac{1}{A_m}\int_{T^\pm_{n'}} \mathrm{d}S' \int_{T_m} \mathrm{d}S S(\overline{r},\overline{r}')\hat{n}_m\cdot\overline{f}_{n'}(\overline{r}')$$
$$[Z^s_{\sigma\sigma}]_{m,m'} = \frac{1}{A_m A_{m'}}\mathcal{P}\int_{T_{m'}} \mathrm{d}S' \int_{T_m} \mathrm{d}S\ \hat{n}_m\cdot\nabla' S(\overline{r},\overline{r}')$$

The second line impedance elements can be simplified thanks to the symmetry of $S(\overline{r},\overline{r}')$. For $\overline{\overline{Z}}^s_{J\sigma}$ we have

$$[Z^s_{J\sigma}]_{n,m'} = -\frac{1}{A_{m'}}\int_{T_{m'}} \mathrm{d}S' \int_{T^\pm_n} \mathrm{d}S \overline{f}_n(\overline{r})\cdot\nabla S(\overline{r},\overline{r}') \tag{9.4.40}$$

while the integral over $T^\pm_n$ can be simplified as

$$\int_{T_n^\pm} \mathrm{d}S \overline{f}_n(\overline{r}) \cdot \nabla S(\overline{r},\overline{r}') = \oint_{\partial T_n^\pm} \mathrm{d}l \ \hat{n}_\partial^\pm \cdot \overline{f}_n(\overline{r}) S(\overline{r},\overline{r}') - \int_{T_n^\pm} \mathrm{d}S \nabla \cdot \overline{f}_n(\overline{r}) S(\overline{r},\overline{r}') \tag{9.4.41}$$
$$= \pm \frac{L_n}{A_n^\pm} \int_{T_n^\pm} \mathrm{d}S S(\overline{r},\overline{r}')$$

Therefore, the singular part of the impedance matrix elements can be expressed as

$$[Z_{JJ}^s]_{n,n'} = \frac{L_n L_{n'}}{4 A_n^\pm A_{n'}^\pm} \int_{T_{n'}^\pm} \mathrm{d}S' \int_{T_n^\pm} \mathrm{d}S S(\overline{r},\overline{r}') \overline{\rho}_n(\overline{r}) \cdot \overline{\rho}_{n'}(\overline{r}') \tag{9.4.42}$$
$$[Z_{J\sigma}^s]_{n,m'} = \mp \frac{L_n}{A_{m'} A_n^\pm} \int_{T_{m'}} \mathrm{d}S' \int_{T_n^\pm} \mathrm{d}S S(\overline{r},\overline{r}')$$
$$[Z_{\sigma J}^s]_{m,n'} = \frac{L_{n'}}{2 A_m A_{n'}^\pm} \int_{T_{n'}^\pm} \mathrm{d}S' \int_{T_m} \mathrm{d}S S(\overline{r},\overline{r}') \hat{n}_m \cdot \overline{\rho}_{n'}(\overline{r}')$$
$$[Z_{\sigma\sigma}^s]_{m,m'} = -\frac{1}{A_m A_{m'}} \mathcal{P} \int_{T_{m'}} \mathrm{d}S' \int_{T_m} \mathrm{d}S \ \hat{n}_m \cdot \nabla S(\overline{r},\overline{r}')$$

The inner integrals can be computed analytically []. After performing one integration, the outer integral would be a regular function and a low order quadrature can be used to compute the second integral over triangles.

### 9.4.2 SIE for $\overline{\overline{G}}_A$ with $\overline{\overline{G}}_A^{\Omega}$ as a propagator

If we take $\overline{\overline{G}}_A^{p}(\overline{r},\overline{r}')=\overline{\overline{G}}_A^{\Omega}(\overline{r},\overline{r}')$, which is the vector potential dyadic Green's function of the regular cavity (rectangular), the surface integral equations become,

$$\hat{n}\times\int_{\sigma}\mathrm{d}S'\left\{\overline{\overline{G}}_A^{\Omega}(\overline{r},\overline{r}')\cdot\overline{J}^{\alpha}(\overline{r}')+\nabla'\cdot\overline{\overline{G}}_A^{\Omega}(\overline{r},\overline{r}')\sigma^{\alpha}(\overline{r}')\right\}=\hat{n}\times\overline{\overline{G}}_A^{\Omega}(\overline{r},\overline{r}'')\cdot\hat{\alpha} \tag{9.4.43}$$

$$\int_{\sigma}\mathrm{d}S'\left\{\hat{n}\cdot\overline{\overline{G}}_A^{\Omega}(\overline{r},\overline{r}')\cdot\overline{J}^{\alpha}(\overline{r}')+\hat{n}\cdot[\nabla'\cdot\overline{\overline{G}}_A^{\Omega}(\overline{r},\overline{r}')]\sigma^{\alpha}(\overline{r}')\right\}=\hat{n}\cdot\overline{\overline{G}}_A^{\Omega}(\overline{r},\overline{r}'')\cdot\hat{\alpha}-\frac{1}{2}\sigma^{\alpha}(\overline{r})$$

where the surface integrals are reduced to the surface $\sigma=\partial S-\partial S\cap\partial\Omega$ using the boundary conditions imposed on $\overline{\overline{G}}_A^{\Omega}$. Expanding the unknown fields over the surface $\sigma$ and following the same procedure we obtain the matrix form of,

$$\begin{aligned}\overline{\overline{Z}}_{JJ}\cdot\overline{J}+\overline{\overline{Z}}_{J\sigma}\cdot\overline{\sigma}&=\overline{b}_J\\ \overline{\overline{Z}}_{\sigma J}\cdot\overline{\sigma}+\overline{\overline{Z}}_{\sigma\sigma}\cdot\overline{\sigma}&=\overline{b}_{\sigma}\end{aligned} \tag{9.4.44}$$

where,

$$\begin{aligned}[Z_{JJ}]_{n,n'}&=\int_{T_{n'}^{\pm}}\mathrm{d}S'\int_{T_n^{\pm}}\mathrm{d}S\overline{f}_n(\overline{r})\cdot\overline{\overline{G}}_A^{\Omega}(\overline{r},\overline{r}')\cdot\overline{f}_{n'}(\overline{r}')\\ [Z_{J\sigma}]_{n,m'}&=\int_{T_{m'}}\mathrm{d}S'\int_{T_n^{\pm}}\mathrm{d}S\overline{f}_n(\overline{r})\cdot[\nabla'\cdot\overline{\overline{G}}_A^{\Omega}(\overline{r},\overline{r}')]P_{m'}(\overline{r}')\\ [Z_{\sigma J}]_{m,n'}&=\int_{T_{n'}^{\pm}}\mathrm{d}S'\int_{T_m}\mathrm{d}SP_m(\overline{r})\hat{n}_m\cdot\overline{\overline{G}}_A^{\Omega}(\overline{r},\overline{r}')\cdot\overline{f}_{n'}(\overline{r}')\\ [Z_{\sigma\sigma}]_{m,m'}&=\int_{T_{m'}}\mathrm{d}S'\int_{T_m}\mathrm{d}SP_m(\overline{r})\left[\hat{n}_m\cdot[\nabla'\cdot\overline{\overline{G}}_A^{\Omega}(\overline{r},\overline{r}')]+\frac{1}{2}\delta(\overline{r}-\overline{r}')\right]P_{m'}(\overline{r}')\end{aligned} \tag{9.4.45}$$

and

$$\begin{aligned}[b_J]_n&=\int_{T_n^{\pm}}\mathrm{d}S\overline{f}_n(\overline{r})\cdot\overline{\overline{G}}_A^{\Omega}(\overline{r},\overline{r}'')\cdot\hat{\alpha}\\ [b_{\sigma}]_m&=\int_{T_m}\mathrm{d}SP_m(\overline{r})\hat{n}_m\cdot\overline{\overline{G}}_A^{\Omega}(\overline{r},\overline{r}'')\cdot\hat{\alpha}\end{aligned} \tag{9.4.46}$$

Once the surface field variables are obtained from the SIE, the vector potential dyadic Green's function can be evaluated as

$$\overline{\overline{G}}_A(\overline{r},\overline{r}'')\cdot\alpha=\overline{\overline{G}}_A^{\Omega}(\overline{r},\overline{r}')\cdot\alpha-\sum_n J_n^{\alpha}\int_{T_n^{\pm}}\mathrm{d}S'\overline{\overline{G}}_A^{\Omega}(\overline{r},\overline{r}')\cdot\overline{f}_n(\overline{r}')-\sum_m\sigma_m^{\alpha}\int_{T_m}\mathrm{d}S'\nabla'\cdot\overline{\overline{G}}_A^{\Omega}(\overline{r},\overline{r}')P_m(\overline{r}') \tag{9.4.47}$$

In addition to the Green's function itself, its imaginary wavenumber derivative is also required for the spectral expansion acceleration.

## 9.5 Impedance elements: Spectral and spatial expansion of the Green's function

Assuming the following expression for the vector potential Green's function of the regular geometry,

$$\overline{\overline{G}}_A^{\Omega}(\overline{r},\overline{r}';k)=\overline{\overline{G}}_A^{\Omega}(\overline{r},\overline{r}';i\xi)+\sum_{\alpha}\left[\frac{k^2+\xi^2}{(k_\alpha^2-k^2)(k_\alpha^2+\xi^2)}\right]\overline{A}_\alpha(\overline{r})\overline{A}_\alpha^*(\overline{r}') \tag{9.5.1}$$

in order to find the impedance matrix elements we need to evaluate $\nabla'\cdot\overline{\overline{G}}_A^{\Omega}(\overline{r},\overline{r}')$. Also, for the near field terms, the singularity of the dyadic Green's function need to be extracted before applying the quadrature. For the divergence of the Green's function, since the eigenfunctions are real (Hermitian boundaries), the Green's function is symmetric $\overline{\overline{G}}_A^{\Omega}(\overline{r},\overline{r}';k)=\overline{\overline{G}}_A^{\Omega}(\overline{r}',\overline{r};k)$ and $[\overline{\overline{G}}_A^{\Omega}]^{\mathrm{T}}=\overline{\overline{G}}_A^{\Omega}$, and therefore reciprocal.

The first term in the above expansion is calculated by the image expansion in our framework. For its $x$-component,

$$G_A^{xx}(\overline{r},\overline{r}';k)=\sum_{n,m,p}(-1)^{n+p}\frac{e^{ikR_{mnp}}}{4\pi R_{mnp}} \tag{9.5.2}$$

where $R_{mnp}=|\overline{r}-\overline{r}_{mnp}|$ and $\overline{r}_{mnp}=\Big(mL_x+(-1)^m x', nL_y+(-1)^n y', pL_z+(-1)^p z'\Big)$ is the location of image sources. For a rectangular cavity, $\overline{\overline{G}}_A^{\Omega}=G_A^{xx}\hat{x}\hat{x}+G_A^{yy}\hat{y}\hat{y}+G_A^{zz}\hat{z}\hat{z}$ and

$$\nabla'\cdot\overline{\overline{G}}_A^{\Omega}(\overline{r},\overline{r}')=\frac{\partial}{\partial x'}G_A^{xx}\hat{x}+\frac{\partial}{\partial y'}G_A^{yy}\hat{y}+\frac{\partial}{\partial z'}G_A^{zz}\hat{z} \tag{9.5.3}$$

According to image expansion, for the $x$-component of divergence of the Green's function

$$\begin{aligned}\frac{\partial}{\partial x'}G_A^{xx}(\overline{r},\overline{r}';k)&=\sum_{n,m,p}(-1)^{n+p}\frac{e^{ikR_{mnp}}}{4\pi R_{mnp}}\left(ik-\frac{1}{R_{mnp}}\right)\frac{\partial R_{mnp}}{\partial x'}\\&=\sum_{n,m,p}(-1)^{n+p+m+1}\frac{e^{ikR_{mnp}}}{4\pi R_{mnp}}\left(ik-\frac{1}{R_{mnp}}\right)\frac{x-x_{mnp}}{R_{mnp}}\end{aligned} \tag{9.5.4}$$

and therefore, for imaginary wavenumber $k=i\xi$

$$\nabla'\cdot\overline{\overline{G}}_A^{\Omega}(\overline{r},\overline{r}',i\xi)=\sum_{n,m,p}(-1)^{n+p+m}\frac{e^{-\xi R_{mnp}}}{4\pi R_{mnp}}\left(\xi+\frac{1}{R_{mnp}}\right)\frac{\overline{R}_{mnp}}{R_{mnp}} \tag{9.5.5}$$

which is rapidly convergent (and singular in source region). The near field singularity of the Green's function is contained entirely in the imaginary wave number part. In order to identify the type of singularity of $\overline{\overline{G}}_A^{\Omega}$, using the image expansion, the only singular term when $\overline{r}$ is close to $\overline{r}'$ comes from the actual source term ($m=n=p=0$). Therefore, in near

field regions, $\overline{\overline{G}}_A^{\Omega} \approx \overline{\overline{G}}_0 = \overline{\overline{I}} G_0$, where $G_0$ is the scalar Green's function. Therefore, second order order singularity extraction or the vector potential Green's function would be

$$\begin{aligned} \overline{\overline{G}}_A^{\Omega}(\overline{r},\overline{r}';k) &= \left[\overline{\overline{G}}_A^{\Omega}(\overline{r},\overline{r}';k) - \overline{\overline{I}} S(\overline{r},\overline{r}')\right] + \overline{\overline{I}} S(\overline{r},\overline{r}') \\ &= \overline{\overline{G}}_{A,ext}^{\Omega}(\overline{r},\overline{r}';k) + \overline{\overline{I}} S(\overline{r},\overline{r}') \end{aligned} \tag{9.5.6}$$

where

$$S(\overline{r},\overline{r}') = \frac{1}{4\pi}\left[\frac{1}{|\overline{r}-\overline{r}'|} - \frac{k^2}{2}|\overline{r}-\overline{r}'|\right] \tag{9.5.7}$$

This choice of extraction makes the extracted Green's function $\overline{\overline{G}}_{A,ext}^{\Omega}(\overline{r},\overline{r}';k)$ to be smooth (with continuous first derivative) everywhere. Similarly, for the divergence of the Green's function, the same extraction technique gives

$$\nabla' \cdot \overline{\overline{G}}_A^{\Omega}(\overline{r},\overline{r}';k) = \nabla' \cdot \overline{\overline{G}}_{A,ext}^{\Omega}(\overline{r},\overline{r}';k) - \nabla S(\overline{r},\overline{r}') \tag{9.5.8}$$

Figure. 9.10 shows $x$-component of the rectangular cavity Green's function and its divergence after the first order extraction (with source located at the origin). Divergence of the extracted Green's function is discontinuous at the source location. Using the second order extraction, divergence of Green's function becomes continuous as it is shown on Fig. 9.11. Note that the rectangular cavity Green's function has a smoother behavior near the source region compared to the free space propagator.

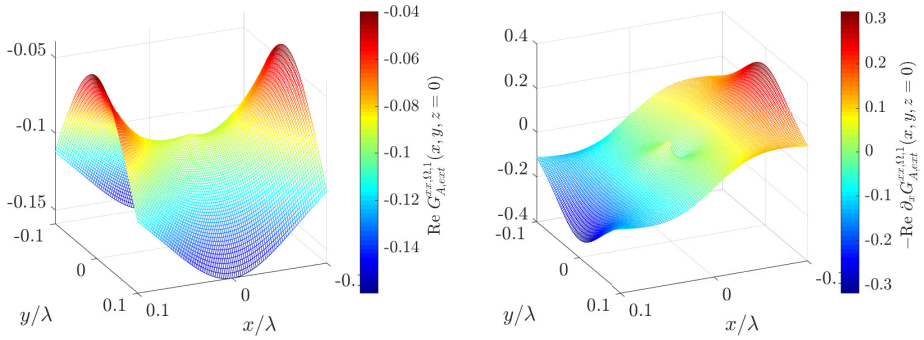


FIGURE 9.10: $x$-component of the rectangular cavity Green's function and its divergence after the first order extraction (source at the origin). Divergence of the extracted Green's function is discontinuous at the source location.

Based on this extraction scheme, the impedance elements can be separated into singular and extracted parts as $\overline{\overline{Z}} = \overline{\overline{Z}}^{e} + \overline{\overline{Z}}^{s}$, where

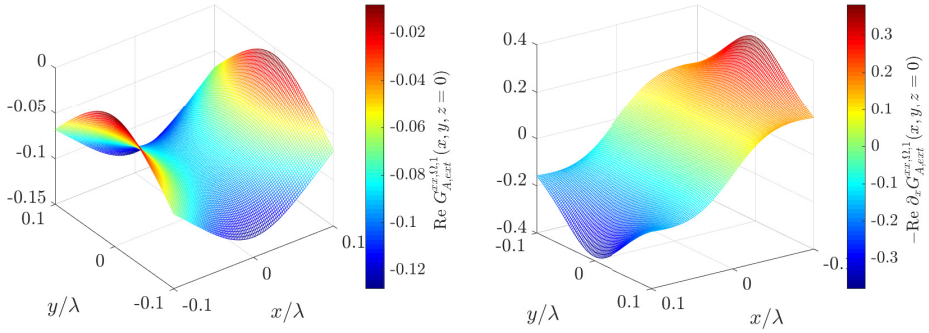


FIGURE 9.11: $x$-component of the rectangular cavity Green's function and its divergence after the second order extraction (source at the origin). Divergence of the extracted Green's function is now continuous at the source location.

$$[Z^e_{JJ}]_{n,n'} = \frac{L_n L_{n'}}{4A^\pm_n A^\pm_{n'}} \int_{T^\pm_{n'}} \mathrm{d}S' \int_{T^\pm_n} \mathrm{d}S \overline{\rho}_n(\overline{r}) \cdot \overline{\overline{G}}^{\Omega}_{A,ext}(\overline{r},\overline{r}') \cdot \overline{\rho}_{n'}(\overline{r}') \tag{9.5.9}$$

$$[Z^e_{J\sigma}]_{n,m'} = \frac{L_n}{2A^\pm_n A_{m'}} \int_{T_{m'}} \mathrm{d}S' \int_{T^\pm_n} \mathrm{d}S \overline{\rho}_n(\overline{r}) \cdot [\nabla' \cdot \overline{\overline{G}}^{\Omega}_{A,ext}(\overline{r},\overline{r}')]$$

$$[Z^e_{\sigma J}]_{m,n'} = \frac{L_{n'}}{2A_{n'} A_m} \int_{T^\pm_{n'}} \mathrm{d}S' \int_{T_m} \mathrm{d}S \hat{n}_m \cdot \overline{\overline{G}}^{\Omega}_{A,ext}(\overline{r},\overline{r}') \cdot \overline{\rho}_{n'}(\overline{r}')$$

$$[Z^e_{\sigma\sigma}]_{m,m'} = \frac{1}{A_m A_{m'}} \int_{T_{m'}} \mathrm{d}S' \mathcal{P} \int_{T_m} \mathrm{d}S \hat{n}_m \cdot [\nabla' \cdot \overline{\overline{G}}^{\Omega}_{A,ext}(\overline{r},\overline{r}')]$$

Note that the last integral is a principal value integral and for $m{=}m'$ element, $[Z_{\sigma\sigma}]_{m,m'} = 1/(2A_m)$.

For the singular impedance terms

$$[Z^s_{JJ}]_{n,n'} = \frac{L_n L_{n'}}{4A^\pm_n A^\pm_{n'}} \int_{T^\pm_{n'}} \mathrm{d}S' \int_{T^\pm_n} \mathrm{d}S \overline{\rho}_n(\overline{r}) \cdot \overline{\rho}_{n'}(\overline{r}') S(\overline{r},\overline{r}') \tag{9.5.10}$$

$$[Z^s_{J\sigma}]_{n,m'} = -\frac{L_n}{2A^\pm_n A_{m'}} \int_{T_{m'}} \mathrm{d}S' \int_{T^\pm_n} \mathrm{d}S \overline{\rho}_n(\overline{r}) \cdot \nabla S(\overline{r},\overline{r}')$$

$$[Z^s_{\sigma J}]_{m,n'} = \frac{L_{n'}}{2A_{n'} A_m} \int_{T^\pm_{n'}} \mathrm{d}S' \int_{T_m} \mathrm{d}S \hat{n}_m \cdot \overline{\rho}_{n'}(\overline{r}') S(\overline{r},\overline{r}')$$

$$[Z^s_{\sigma\sigma}]_{m,m'} = -\frac{1}{A_m A_{m'}} \int_{T_{m'}} \mathrm{d}S' \mathcal{P} \int_{T_m} \mathrm{d}S \hat{n}_m \cdot \nabla S(\overline{r},\overline{r}')$$

The second term can be integrated by part

$$\begin{aligned}
[Z^s_{J\sigma}]_{n,m'} &= -\frac{L_n}{2A^\pm_n A_{m'}} \int_{T_{m'}} \mathrm{d}S' \int_{T^\pm_n} \mathrm{d}S \overline{\rho}_n(\overline{r}) \cdot \nabla S(\overline{r},\overline{r}') \\
&= \frac{L_n}{2A^\pm_n A_{m'}} \int_{T_{m'}} \mathrm{d}S' \int_{T^\pm_n} \mathrm{d}S \nabla \cdot \overline{\rho}_n(\overline{r}) S(\overline{r},\overline{r}') \\
&= \mp \frac{L_n}{A^\pm_n A_{m'}} \int_{T_{m'}} \mathrm{d}S' \int_{T^\pm_n} \mathrm{d}S S(\overline{r},\overline{r}')
\end{aligned} \tag{9.5.11}$$

## 9.6 Vector potential vector modes

The vector potential $\overline{A}$ under the Lorenz gauge satisfies the inhomogeneous wave equation of

$$(\nabla^2+k^2)\overline{A}(\overline{r})=-\mu\overline{J}(\overline{r}) \tag{9.6.1}$$

subject to the boundary condition of $\hat{n}\times\overline{A}=0$ and $\nabla\cdot\overline{A}=0$ on the boundary of the cavity. The natural solution of the vector potential corresponds to the homogeneous wave equation of

$$(\nabla^2+k^2)\overline{\mathcal{A}}(\overline{r})=0 \tag{9.6.2}$$

where $\overline{\mathcal{A}}(\overline{r})$ is the vector potential mode inside the cavity which is subject to the boundary conditions of $\hat{n}\times\overline{\mathcal{A}}=0$ and $\nabla\cdot\overline{\mathcal{A}}=0$ over the walls of cavity. The eigenvalue $k^2$ is the resonant wave number inside the cavity for the vector potential. The wave equation of (9.6.2) alternatively can be rewritten as

$$\nabla\times\nabla\times\overline{\mathcal{A}}(\overline{r})-\nabla\nabla\cdot\overline{\mathcal{A}}(\overline{r})-k^2\overline{\mathcal{A}}(\overline{r})=0 \tag{9.6.3}$$

In order to formulate the surface integral equation for the mode functions $\overline{\mathcal{A}}(\overline{r})$, we can use the vector potential Green's function in free space $\overline{\overline{G}}_0(\overline{r},\overline{r}')=\overline{\overline{I}}G_0(\overline{r},\overline{r}')$ to formulate the integral equation for the resonant modes,

$$\nabla\times\nabla\times\overline{\overline{G}}_0(\overline{r},\overline{r}')-\nabla\nabla\cdot\overline{\overline{G}}_0(\overline{r},\overline{r}'')-k^2\overline{\overline{G}}_0(\overline{r},\overline{r}')=\overline{\overline{I}}\delta(\overline{r}-\overline{r}') \tag{9.6.4}$$

where $G_0$ is the scalar Green's function of free space. Another option is to use the vector potential Green's function of the corresponding regular cavity $\overline{\overline{G}}_A^{\Omega}(\overline{r},\overline{r}'')$(which is rectangular cavity here) that satisfies the same vector wave equation, namely,

$$\nabla\times\nabla\times\overline{\overline{G}}_A^{\Omega}(\overline{r},\overline{r}')-\nabla\nabla\cdot\overline{\overline{G}}_A^{\Omega}(\overline{r},\overline{r}'')-k^2\overline{\overline{G}}_A^{\Omega}(\overline{r},\overline{r}')=\overline{\overline{I}}\delta(\overline{r}-\overline{r}') \tag{9.6.5}$$

which satisfies the boundary conditions of $\hat{n}\times\overline{\overline{G}}_A^{\Omega}=0$ and $\nabla\cdot\overline{\overline{G}}_A^{\Omega}=0$ on the surface of the regular cavity, $\partial\Omega$. Using the extinction theorem obtained from (9.6.5) and (9.6.3), and utilizing the boundary conditions on the vector potential mode $\overline{\mathcal{A}}(\overline{r})$ inside the cavity yields,

$$\oint_{\partial S}\mathrm{d}S'\left\{\overline{\overline{G}}_A^{\Omega}(\overline{r},\overline{r}')\cdot\left[\hat{n}'\times\nabla'\times\overline{\mathcal{A}}(\overline{r}')\right]+\hat{n}'\cdot\overline{\mathcal{A}}(\overline{r}')\nabla'\cdot\overline{\overline{G}}_A^{\Omega}(\overline{r},\overline{r}')\right\}=\begin{cases}-\overline{\mathcal{A}}(\overline{r}) & \overline{r}\in S\\ 0 & \overline{r}\notin S\end{cases} \tag{9.6.6}$$

Mapping the tangential component of the integral equation over the surface and using the boundary conditions of $\overline{\overline{G}}_A^{\Omega}$ over $\partial\Omega$

$$\hat{n}\times\int_\sigma \mathrm{d}S'\left\{\overline{\overline{G}}_A^{\Omega}(\overline{r},\overline{r}')\cdot\overline{J}(\overline{r})+\nabla'\cdot\overline{\overline{G}}_A^{\Omega}(\overline{r},\overline{r}')\sigma(\overline{r}')\right\}=0 \tag{9.6.7}$$

where $\sigma(\overline{r}')=\hat{n}'\cdot\overline{\mathcal{A}}(\overline{r}')$, and $\overline{J}(\overline{r}')=\hat{n}'\times\nabla'\times\overline{\mathcal{A}}(\overline{r}')$ are the resonant surface charge and current densities over the walls of the cavity. The surface area $\sigma$, is the uncommon part of the irregular cavity surface $\partial S$ and the regular cavity surface $\partial\Omega$, i.e. $\sigma=\partial S-\partial S\cap\partial\Omega$.

In addition, mapping the normal component of the integral equation to the surface of the cavity provide us with another SIE,

$$\oint_{\partial S}\mathrm{d}S'\left\{\hat{n}\cdot\overline{\overline{G}}_A^{\Omega}(\overline{r},\overline{r}')\cdot\overline{J}(\overline{r}')+\hat{n}\cdot\left[\nabla'\cdot\overline{\overline{G}}_A^{\Omega}(\overline{r},\overline{r}')\right]\sigma(\overline{r}')\right\}=\begin{cases}-\sigma(\overline{r}) & \overline{r}\in S\\ 0 & \overline{r}\notin S\end{cases} \tag{9.6.8}$$

However it seems that the SIE depends on whether $\overline{r}$ goes to the surface from the interior or exterior region but it does not. The near field singular kernel of $\hat{n}\cdot\left[\nabla'\cdot\overline{\overline{G}}_A^{\Omega}(\overline{r},\overline{r}')\right]$ essentially has the same type of singularity as the free system $\hat{n}\cdot\left[\nabla'\cdot\overline{\overline{G}}_0(\overline{r},\overline{r}')\right]=-\hat{n}\cdot\nabla G_0(\overline{r},\overline{r}')$, which is know to produce a discontinuity in the surface integral of (9.6.8) that elevates the apparent ambiguity in the course of testing procedure. Therefore, for the principal value integral,

$$\mathcal{P}\oint_{\partial S}\mathrm{d}S'\left\{\hat{n}\cdot\overline{\overline{G}}_A^{\Omega}(\overline{r},\overline{r}')\cdot\overline{J}(\overline{r}')+\hat{n}\cdot\left[\nabla'\cdot\overline{\overline{G}}_A^{\Omega}(\overline{r},\overline{r}')\right]\sigma(\overline{r}')\right\}=-\frac{1}{2}\sigma(\overline{r}) \tag{9.6.9}$$

This time, since $\overline{J}$ is a tangential vector and $\overline{\overline{G}}_A^{\Omega}(\overline{r},\overline{r}')$ is a symmetric dyad, the first term vanishes over $\partial\Omega$ as $\hat{t}\cdot\overline{\overline{G}}_A^{\Omega}(\overline{r},\overline{r}')=\overline{\overline{G}}_A^{\Omega}(\overline{r},\overline{r}')\cdot\hat{t}=0$, where $\hat{t}$ is a tangential vector to the surface at $\overline{r}'$. The second term also vanishes over $\partial\Omega$ and we arrive at

$$\mathcal{P}\int_\sigma\mathrm{d}S'\left\{\hat{n}\cdot\overline{\overline{G}}_A^{\Omega}(\overline{r},\overline{r}')\cdot\overline{J}(\overline{r}')+\hat{n}\cdot\left[\nabla'\cdot\overline{\overline{G}}_A^{\Omega}(\overline{r},\overline{r}')\right]\sigma(\overline{r}')\right\}=-\frac{1}{2}\sigma(\overline{r}) \tag{9.6.10}$$

Therefore, the set of SIE's to be solved to find the vector potential mode functions are given by

$$\begin{aligned}&\hat{n}\times\int_\sigma\mathrm{d}S'\left\{\overline{\overline{G}}_A^{\Omega}(\overline{r},\overline{r}')\cdot\overline{J}(\overline{r}')+\nabla'\cdot\overline{\overline{G}}_A^{\Omega}(\overline{r},\overline{r}')\sigma(\overline{r}')\right\}=0\\ &\mathcal{P}\int_\sigma\mathrm{d}S'\left\{\hat{n}\cdot\overline{\overline{G}}_A^{\Omega}(\overline{r},\overline{r}')\cdot\overline{J}(\overline{r}')+\hat{n}\cdot\left[\nabla'\cdot\overline{\overline{G}}_A^{\Omega}(\overline{r},\overline{r}')\right]\sigma(\overline{r}')\right\}=-\frac{1}{2}\sigma(\overline{r})\end{aligned} \tag{9.6.11}$$

Once the surface current $\overline{J}(\overline{r})$ and surface charge density $\sigma(\overline{r})$ are in hand, the mode functions can be obtained from the extinction theorem of

$$\int_\sigma\mathrm{d}S'\left\{\overline{\overline{G}}_A^{\Omega}(\overline{r},\overline{r}')\cdot\overline{J}(\overline{r}')+\nabla'\cdot\overline{\overline{G}}_A^{\Omega}(\overline{r}',\overline{r})\sigma(\overline{r}')\right\}=\begin{cases}-\overline{\mathcal{A}}(\overline{r}) & \overline{r}\in S\\ 0 & \overline{r}\notin S\end{cases} \tag{9.6.12}$$

## 9.7 Linear Eigenvalue Problem

The vector potential dyadic Green's function of the regular shape cavity $\overline{\overline{G}}_A^{\Omega}$ can be written in terms of a hybrid spectral spatial expansion of

$$\overline{\overline{G}}_A^{\Omega}(\overline{r},\overline{r}';k)=\overline{\overline{G}}_A^{\Omega}(\overline{r},\overline{r}';i\xi)+\sum_{\alpha}\sum_{j=1}^{3}\Big[\frac{k^2+\xi^2}{(k_\alpha^2-k^2)(k_\alpha^2+\xi^2)}\Big]\overline{A}_{\alpha,j}(\overline{r})\overline{A}_{\alpha,j}^{*}(\overline{r}') \tag{9.7.1}$$

where $\overline{A}_{\alpha,j}$ is a vector mode of the vector potential in the cavity of the regular shape and $k_\alpha^2$ is the corresponding eigenvalue which are known. More specifically,

$$(\nabla^2+k_\alpha^2)\overline{A}_{\alpha,j}(\overline{r})=0 \tag{9.7.2}$$

where the eigenfunctions of the regular cavity for given eigenvalue of $k_\alpha^2$ includes 3 different eigenfunctions in different directions,

$$\overline{A}_{\alpha,x}(\overline{r})=\psi_\alpha^x(\overline{r})\hat{x} \tag{9.7.3}$$

and so on, which satisfy the boundary conditions of $\hat{n}\times\overline{A}_\alpha=0$ and $\nabla\cdot\overline{A}_\alpha=0$ on the surface of cavity ($\partial\Omega$). In what follows, we assume that for a given index $\alpha$ there are three different eigenfunctions. Using this expansion in the surface integral equations for the irregular cavity modes, we have

$$\hat{n}\times\Bigg\{\int_\sigma \mathrm{d}S'\Big\{\overline{\overline{G}}_A^{\Omega}(\overline{r},\overline{r}';i\xi)\cdot\overline{J}(\overline{r}')+\nabla'\cdot\overline{\overline{G}}_A^{\Omega}(\overline{r},\overline{r}',i\xi)\sigma(\overline{r}')\Big\} \tag{9.7.4}$$
$$+\sum_{\alpha}\sum_{j=1}^{3}\Big[\frac{k^2+\xi^2}{(k_\alpha^2-k^2)(k_\alpha^2+\xi^2)}\Big]\overline{A}_{\alpha j}(\overline{r})\int_\sigma \mathrm{d}S'\Big(\overline{A}_{\alpha j}(\overline{r}')\cdot\overline{J}(\overline{r}')+\nabla'\cdot\overline{A}_{\alpha j}(\overline{r}')\sigma(\overline{r}')\Big)\Bigg\}=0$$

$$\mathcal{P}\int_\sigma \mathrm{d}S'\Big\{\hat{n}\cdot\overline{\overline{G}}_A^{\Omega}(\overline{r},\overline{r}';i\xi)\cdot\overline{J}(\overline{r}')+\hat{n}\cdot\Big[\nabla'\cdot\overline{\overline{G}}_A^{\Omega}(\overline{r},\overline{r}';i\xi)\Big]\sigma(\overline{r}')\Big\} \tag{9.7.5}$$
$$+\sum_{\alpha}\sum_{j=1}^{3}\Big[\frac{k^2+\xi^2}{(k_\alpha^2-k^2)(k_\alpha^2+\xi^2)}\Big]\hat{n}\cdot\overline{A}_{\alpha j}(\overline{r})\int_\sigma \mathrm{d}S'\Big\{\overline{A}_{\alpha j}(\overline{r}')\cdot\overline{J}(\overline{r}')+\nabla'\cdot\overline{A}_{\alpha j}(\overline{r}')\sigma(\overline{r}')\Big\}=-\frac{1}{2}\sigma(\overline{r})$$

Upon expanding the surface fields in terms of the local basis functions as

$$\overline{J}(\overline{r}')=\sum_{n'}J_{n'}\overline{f}_{n'}(\overline{r}') \tag{9.7.6}$$
$$\sigma(\overline{r}')=\sum_{m'}\sigma_{m'}P_{m'}(\overline{r}')$$

where, $\overline{f}_n$ is the linear RWG basis function over the $n$-th edge and $P_m$ is a pulse over the triangle $T_m$, the SIE can be written as

$$\hat{n}\times\Bigg\{\sum_{n'}J_{n'}\int_{T^{\pm}_{n'}}\mathrm{d}S'\overline{\overline{G}}^{\Omega}_{A}(\overline{r},\overline{r}';i\xi)\cdot\overline{f}_{n'}(\overline{r}')+\sum_{m'}\sigma_{m'}\int_{T_{m'}}\mathrm{d}S'\nabla'\cdot\overline{\overline{G}}^{\Omega}_{A}(\overline{r},\overline{r}',i\xi)P_{m'}(\overline{r}') \qquad (9.7.7)$$
$$+\sum_{\alpha}\sum_{j}\frac{c^{J}_{\alpha j}+c^{\sigma}_{\alpha j}}{(k^{2}_{\alpha}+\xi^{2})}\overline{A}_{\alpha j}(\overline{r})\Bigg\}=0$$

$$\sum_{n'}J_{n'}\int_{T^{\pm}_{n'}}\mathrm{d}S'\hat{n}\cdot\overline{\overline{G}}^{\Omega}_{A}(\overline{r},\overline{r}';i\xi)\cdot\overline{f}_{n'}(\overline{r}')+\sum_{m'}\sigma_{m'}\int_{T_{m'}}\mathrm{d}S'\hat{n}\cdot\Big[\nabla'\cdot\overline{\overline{G}}^{\Omega}_{A}(\overline{r},\overline{r}';i\xi)\Big]P_{m'}(\overline{r}') \qquad (9.7.8)$$
$$+\sum_{\alpha}\sum_{j}\frac{c^{J}_{\alpha j}+c^{\sigma}_{\alpha j}}{(k^{2}_{\alpha}+\xi^{2})}\hat{n}\cdot\overline{A}_{\alpha j}(\overline{r})=-\frac{1}{2}\sigma(\overline{r})$$

where,

$$c^{J}_{\alpha j}=\frac{k^{2}+\xi^{2}}{(k^{2}_{\alpha}-k^{2})}\int_{\sigma}\mathrm{d}S'\overline{A}_{\alpha j}(\overline{r}')\cdot\overline{J}(\overline{r}') \qquad (9.7.9)$$
$$c^{\sigma}_{\alpha j}=\frac{k^{2}+\xi^{2}}{(k^{2}_{\alpha}-k^{2})}\int_{\sigma}\mathrm{d}S'\nabla'\cdot\overline{A}_{\alpha j}(\overline{r}')\sigma(\overline{r}')$$

We use the RWG basis function to test the vector SIE (first) and pulse basis functions to test the second SIE.

$$\sum_{n'}J_{n'}\int_{T^{\pm}_{n'}}\mathrm{d}S'\int_{T^{\pm}_{n}}\mathrm{d}S\overline{f}_{n}(\overline{r})\cdot\overline{\overline{G}}^{\Omega}_{A}(\overline{r},\overline{r}';i\xi)\cdot\overline{f}_{n'}(\overline{r}')$$
$$+\sum_{m'}\sigma_{m'}\int_{T^{\pm}_{n}}\mathrm{d}S\int_{T_{m'}}\mathrm{d}S'\overline{f}_{n}(\overline{r})\cdot\Big(\nabla'\cdot\overline{\overline{G}}^{\Omega}_{A}(\overline{r},\overline{r}';i\xi)\Big)P_{m'}(\overline{r}')$$
$$+\sum_{\alpha}\sum_{j}\frac{c^{J}_{\alpha j}+c^{\sigma}_{\alpha j}}{(k^{2}_{\alpha}+\xi^{2})}\int_{T^{\pm}_{n}}\mathrm{d}S\overline{f}_{n}(\overline{r})\cdot\overline{A}_{\alpha j}(\overline{r})=0$$

$$\sum_{n'}J_{n'}\int_{T^{\pm}_{n'}}\mathrm{d}S'\int_{T_{m}}\mathrm{d}SP_{m}(\overline{r})\hat{n}\cdot\overline{\overline{G}}^{\Omega}_{A}(\overline{r},\overline{r}';i\xi)\cdot\overline{f}_{n'}(\overline{r}')$$
$$+\sum_{m'}\sigma_{m'}\int_{T_{m'}}\mathrm{d}S'\int_{T_{m}}\mathrm{d}SP_{m}(\overline{r})\hat{n}\cdot\Big[\nabla'\cdot\overline{\overline{G}}^{\Omega}_{A}(\overline{r},\overline{r}';i\xi)\Big]P_{m'}(\overline{r}')$$
$$+\sum_{\alpha}\sum_{j}\frac{c^{J}_{\alpha j}+c^{\sigma}_{\alpha j}}{(k^{2}_{\alpha}+\xi^{2})}\int_{T_{m}}\mathrm{d}SP_{m}(\overline{r})\hat{n}\cdot\overline{A}_{\alpha j}(\overline{r})=-\frac{1}{2}\sigma(\overline{r})$$

That can be written in the matrix form of

$$\overline{\overline{Z}}^{JJ}\cdot\overline{J}+\overline{\overline{Z}}^{J\sigma}\cdot\overline{\sigma}+\overline{\overline{R}}\cdot(\overline{c}^{J}+\overline{c}^{\sigma})=0 \qquad (9.7.10)$$
$$\overline{\overline{Z}}^{\sigma J}\cdot\overline{J}+\overline{\overline{Z}}^{\sigma\sigma}\cdot\sigma+\overline{\overline{Q}}\cdot(\overline{c}^{J}+\overline{c}^{\sigma})=0$$

or

$$\begin{bmatrix} \overline{\overline{Z}}^{JJ} & \overline{\overline{Z}}^{J\sigma} \\ \overline{\overline{Z}}^{\sigma J} & \overline{\overline{Z}}^{\sigma\sigma} \end{bmatrix} \cdot \begin{bmatrix} \overline{J} \\ \overline{\sigma} \end{bmatrix} + \begin{bmatrix} \overline{\overline{R}} & \overline{\overline{R}} \\ \overline{\overline{Q}} & \overline{\overline{Q}} \end{bmatrix} \cdot \begin{bmatrix} \overline{c}^J \\ \overline{c}^\sigma \end{bmatrix} = 0 \tag{9.7.11}$$

where the impedance matrix elements are given by

$$\begin{aligned}
[Z^{JJ}]_{n,n'} &= \int_{T_n^\pm} \mathrm{d}S \int_{T_{n'}^\pm} \mathrm{d}S' \overline{f}_n(\overline{r}) \cdot \overline{\overline{G}}_A^\Omega(\overline{r},\overline{r}';i\xi) \cdot \overline{f}_{n'}(\overline{r}') \\
[Z^{J\sigma}]_{n,m'} &= \int_{T_n^\pm} \mathrm{d}S \int_{T_{m'}} \mathrm{d}S' \overline{f}_n(\overline{r}) \cdot \Big( \nabla' \cdot \overline{\overline{G}}_A^\Omega(\overline{r},\overline{r}';i\xi) \Big) P_{m'}(\overline{r}') \\
[Z^{\sigma J}]_{m,n'} &= \int_{T_m} \mathrm{d}S \int_{T_{n'}^\pm} \mathrm{d}S' P_m(\overline{r}) \hat{n}_m \cdot \overline{\overline{G}}_A^\Omega(\overline{r},\overline{r}';i\xi) \cdot \overline{f}_{n'}(\overline{r}') \\
[Z^{\sigma\sigma}]_{m,m'} &= \int_{T_m} \mathrm{d}S \int_{T_{m'}} \mathrm{d}S' P_m(\overline{r}) \hat{n}_m \cdot \Big[ \nabla' \cdot \overline{\overline{G}}_A^\Omega(\overline{r},\overline{r}';i\xi) + \frac{1}{2}\delta(\overline{r}-\overline{r}') \Big] P_{m'}(\overline{r}')
\end{aligned} \tag{9.7.12}$$

and

$$\begin{aligned}
[R]_{n\alpha j} &= \frac{1}{(k_\alpha^2+\xi^2)} \int_{T_n^\pm} \mathrm{d}S \overline{f}_n(\overline{r}) \cdot \overline{A}_{\alpha j}(\overline{r}) \\
[Q]_{m\alpha j} &= \frac{1}{(k_\alpha^2+\xi^2)} \int_{T_m} \mathrm{d}S P_m(\overline{r}) \hat{n}_m \cdot \overline{A}_{\alpha j}(\overline{r})
\end{aligned} \tag{9.7.13}$$

On the other hand, from the expression of $\overline{c}^J$ and $\overline{c}^\sigma$ we have

$$\begin{aligned}
c_{\alpha j}^J &= \frac{k^2+\xi^2}{(k_\alpha^2-k^2)} \sum_{n'} J_{n'} \int_{T_{n'}^\pm} \mathrm{d}S' \overline{A}_{\alpha j}(\overline{r}') \cdot \overline{f}_{n'}(\overline{r}') \\
c_{\alpha j}^\sigma &= \frac{k^2+\xi^2}{(k_\alpha^2-k^2)} \sum_{m'} \sigma_{m'} \int_{T_{m'}} \mathrm{d}S' \nabla' \cdot \overline{A}_{\alpha j}(\overline{r}') P_{m'}(\overline{r}')
\end{aligned} \tag{9.7.14}$$

Upon defining a new quantity

$$[S]_{m',\alpha j} = \frac{1}{(k_\alpha^2+\xi^2)} \int_{T_{m'}} \mathrm{d}S' \nabla' \cdot \overline{A}_{\alpha j}(\overline{r}') P_{m'}(\overline{r}') \tag{9.7.15}$$

the expression of $c_{\alpha j}^J$ and $c_{\alpha j}^\sigma$ can be rearranged as

$$\begin{aligned}
\sum_{n'} J_{n'} R_{n',\alpha j} &= \frac{(k_\alpha^2-k^2)}{(k_\alpha^2+\xi^2)(k^2+\xi^2)} c_{\alpha j}^J = \left[ \frac{1}{(k^2+\xi^2)} - \frac{1}{(k_\alpha^2+\xi^2)} \right] c_{\alpha j}^J \\
\sum_{m'} \sigma_{m'} S_{m',\alpha j} &= \frac{(k_\alpha^2-k^2)}{(k_\alpha^2+\xi^2)(k^2+\xi^2)} c_{\alpha j}^\sigma = \left[ \frac{1}{(k^2+\xi^2)} - \frac{1}{(k_\alpha^2+\xi^2)} \right] c_{\alpha j}^\sigma
\end{aligned} \tag{9.7.16}$$

By taking $D_{\alpha\alpha}=(k_\alpha^2+\xi^2)^{-1}$ and $\lambda=(k^2+\xi^2)^{-1}$ it can be written as

$$\begin{aligned}\overline{\overline{R}}^{\dagger}\cdot\overline{J}+\overline{\overline{D}}\cdot\overline{c}^{J}&=\lambda\overline{c}^{J}\\ \overline{\overline{S}}^{\dagger}\cdot\overline{\sigma}+\overline{\overline{D}}\cdot\overline{c}^{\sigma}&=\lambda\overline{c}^{\sigma}\end{aligned}\tag{9.7.17}$$

or

$$\begin{bmatrix}\overline{\overline{R}}^{\dagger} & \overline{\overline{0}}\\ \overline{\overline{0}} & \overline{\overline{S}}^{\dagger}\end{bmatrix}\begin{bmatrix}\overline{J}\\ \overline{\sigma}\end{bmatrix}+\begin{bmatrix}\overline{\overline{D}} & \overline{\overline{0}}\\ \overline{\overline{0}} & \overline{\overline{D}}\end{bmatrix}\begin{bmatrix}\overline{c}^{J}\\ \overline{c}^{\sigma}\end{bmatrix}=\lambda\begin{bmatrix}\overline{c}^{J}\\ \overline{c}^{\sigma}\end{bmatrix}\tag{9.7.18}$$

where we have combined two indices $j$ and $\alpha$ to be represented by $\alpha$. From the SIE,

$$\begin{bmatrix}\overline{J}\\ \overline{\sigma}\end{bmatrix}=-\begin{bmatrix}\overline{\overline{Z}}^{JJ} & \overline{\overline{Z}}^{J\sigma}\\ \overline{\overline{Z}}^{\sigma J} & \overline{\overline{Z}}^{\sigma\sigma}\end{bmatrix}^{-1}\cdot\begin{bmatrix}\overline{\overline{R}} & \overline{\overline{R}}\\ \overline{\overline{Q}} & \overline{\overline{Q}}\end{bmatrix}\cdot\begin{bmatrix}\overline{c}^{J}\\ \overline{c}^{\sigma}\end{bmatrix}\tag{9.7.19}$$

and eigenvalue problem takes the following form

$$-\begin{bmatrix}\overline{\overline{R}}^{\dagger} & \overline{\overline{0}}\\ \overline{\overline{0}} & \overline{\overline{S}}^{\dagger}\end{bmatrix}\begin{bmatrix}\overline{\overline{Z}}^{JJ} & \overline{\overline{Z}}^{J\sigma}\\ \overline{\overline{Z}}^{\sigma J} & \overline{\overline{Z}}^{\sigma\sigma}\end{bmatrix}^{-1}\cdot\begin{bmatrix}\overline{\overline{R}} & \overline{\overline{R}}\\ \overline{\overline{Q}} & \overline{\overline{Q}}\end{bmatrix}\cdot\begin{bmatrix}\overline{c}^{J}\\ \overline{c}^{\sigma}\end{bmatrix}+\begin{bmatrix}\overline{\overline{D}} & \overline{\overline{0}}\\ \overline{\overline{0}} & \overline{\overline{D}}\end{bmatrix}\begin{bmatrix}\overline{c}^{J}\\ \overline{c}^{\sigma}\end{bmatrix}=\lambda\begin{bmatrix}\overline{c}^{J}\\ \overline{c}^{\sigma}\end{bmatrix}\tag{9.7.20}$$

or

$$\overline{\overline{P}}\cdot\overline{c}=\lambda\overline{c}\tag{9.7.21}$$

where

$$\overline{\overline{P}}=-\begin{bmatrix}\overline{\overline{R}}^{\dagger} & \overline{\overline{0}}\\ \overline{\overline{0}} & \overline{\overline{S}}^{\dagger}\end{bmatrix}\begin{bmatrix}\overline{\overline{Z}}^{JJ} & \overline{\overline{Z}}^{J\sigma}\\ \overline{\overline{Z}}^{\sigma J} & \overline{\overline{Z}}^{\sigma\sigma}\end{bmatrix}^{-1}\cdot\begin{bmatrix}\overline{\overline{R}} & \overline{\overline{R}}\\ \overline{\overline{Q}} & \overline{\overline{Q}}\end{bmatrix}+\begin{bmatrix}\overline{\overline{D}} & \overline{\overline{0}}\\ \overline{\overline{0}} & \overline{\overline{D}}\end{bmatrix}\tag{9.7.22}$$

The eigenvalues provides the resonant wave numbers of the irregular cavity, namely $q_\beta$

$$\lambda=\frac{1}{q_\beta^2+\xi^2}\tag{9.7.23}$$

and the eigenvectors provides the projection coefficient of the corresponding resonant vector mode $\overline{\mathcal{A}}_\beta$ over the regular cavity modes $\overline{A}_\alpha$. For the resonant mode $\overline{\mathcal{A}}_\beta$,

$$-\overline{\mathcal{A}}_\beta(\overline{r})=\int_{\partial S}\mathrm{d}S'\left\{\overline{\overline{G}}_A^{\Omega}(\overline{r},\overline{r}')\cdot\overline{J}^{\beta}(\overline{r}')+\nabla'\cdot\overline{\overline{G}}_A^{\Omega}(\overline{r},\overline{r}')\sigma^{\beta}(\overline{r}')\right\}\tag{9.7.24}$$

Using the hybrid expansion of $\overline{\overline{G}}_A^{\Omega}$ we have

$$-\overline{\mathcal{A}}_\beta(\overline{r})=\int_{\partial S}\mathrm{d}S'\left\{\overline{\overline{G}}_A^{\Omega}(\overline{r},\overline{r}';i\xi)\cdot\overline{J}^\beta(\overline{r}')+\nabla'\cdot\overline{\overline{G}}_A^{\Omega}(\overline{r},\overline{r}',i\xi)\sigma^\beta(\overline{r}')\right\} \tag{9.7.25}$$
$$+\sum_\alpha\sum_j\left[\frac{k^2+\xi^2}{(k_\alpha^2-k^2)(k_\alpha^2+\xi^2)}\right]\overline{A}_{\alpha j}(\overline{r})\int_{\partial S}\mathrm{d}S'\left\{\overline{A}_{\alpha j}(\overline{r}')\cdot\overline{J}^\beta(\overline{r}')+\nabla'\cdot\overline{A}_{\alpha j}(\overline{r}')\sigma^\beta(\overline{r}')\right\}$$

or

$$-\overline{\mathcal{A}}_\beta(\overline{r})=\sum_{n'}J_{n'}^\beta\int_{T_{n'}^\pm}\mathrm{d}S'\overline{\overline{G}}_A^{\Omega}(\overline{r},\overline{r}';i\xi)\cdot\overline{f}_{n'}(\overline{r}')+\sum_{m'}\sigma_{m'}^\beta\int_{T_{m'}}\mathrm{d}S'\nabla'\cdot\overline{\overline{G}}_A^{\Omega}(\overline{r},\overline{r}',i\xi)P_{m'}(\overline{r}')\Big\} \tag{9.7.26}$$
$$+\sum_\alpha\sum_j\frac{1}{(k_\alpha^2+\xi^2)}\overline{A}_{\alpha j}(\overline{r})(c_{\alpha j}^{J\beta}+c_{\alpha j}^{\sigma\beta})$$

where projection of the irregular cavity's resonant surface fields on the regular cavity resonant modes are given by

$$c_{\alpha j}^{J\beta}=\frac{q_\beta^2+\xi^2}{(k_\alpha^2-q_\beta^2)}\sum_{n'}J_{n'}^\beta\int_{T_{n'}^\pm}\mathrm{d}S'\overline{A}_{\alpha j}(\overline{r}')\cdot\overline{f}_{n'}(\overline{r}') \tag{9.7.27}$$
$$c_{\alpha j}^{\sigma\beta}=\frac{q_\beta^2+\xi^2}{(k_\alpha^2-q_\beta^2)}\sum_{m'}\sigma_{m'}^\beta\int_{T_{m'}}\mathrm{d}S'\nabla'\cdot\overline{A}_{\alpha j}(\overline{r}')P_{m'}(\overline{r}')$$

$c_{\alpha j}^\beta$ is the $\beta$-th eigenvector of the linear eigenvalue system of (9.7.22). The resonant surface fields corresponding to the $\beta$-th mode can be obtained via

$$\begin{bmatrix}\overline{J}\\ \overline{\sigma}\end{bmatrix}=-\begin{bmatrix}\overline{\overline{Z}}^{JJ} & \overline{\overline{Z}}^{J\sigma}\\ \overline{\overline{Z}}^{\sigma J} & \overline{\overline{Z}}^{\sigma\sigma}\end{bmatrix}^{-1}\cdot\begin{bmatrix}\overline{\overline{R}} & \overline{\overline{R}}\\ \overline{\overline{Q}} & \overline{\overline{Q}}\end{bmatrix}\cdot\begin{bmatrix}\overline{c}^J\\ \overline{c}^\sigma\end{bmatrix} \tag{9.7.28}$$

The wave functions $\overline{\mathcal{A}}_\beta$ are known through (9.7.26). However, the wave functions obtained by (9.7.26) are arbitrary up to a multiplicative constant. In order to use the spectral expansion of the Green's function, the wave functions $\overline{\mathcal{A}}_\beta$ should be normalized over the volume of the cavity according to

$$\int_S\mathrm{d}^3\overline{r}\;\overline{\mathcal{A}}_\beta(\overline{r})\cdot\overline{\mathcal{A}}_\beta(\overline{r})=1\quad,\forall\beta \tag{9.7.29}$$

Normalizing the mode using this volume integration for each mode is a computationally expensive task. Instead each wave function $\overline{\mathcal{A}}_\beta(\overline{r})$ can be expanded in terms of the regular shaped cavity wave functions $\overline{A}_\alpha(\overline{r})$ as they form a complete set of functions inside $S\subseteq\Omega$

$$\overline{\mathcal{A}}_\beta(\overline{r})=\sum_\alpha d_\alpha^\beta\overline{A}_\alpha(\overline{r}) \tag{9.7.30}$$

Taking into account that $\{\overline{A}_\alpha\}_\alpha$ is an orthonormal set, $d_\alpha^\beta$ is a unitary transformation and therefore,

$$\sum_\alpha |d_\alpha^\beta|^2 = 1 \quad , \quad \forall \beta \tag{9.7.31}$$

The matrix coefficients $d_\alpha^\beta$ can be read from

$$-\overline{\mathcal{A}}_\beta(\overline{r}) = \sum_{n'} J_{n'}^\beta \int_{T_{n'}^\pm} \mathrm{d}S' \overline{\overline{G}}_A^\Omega(\overline{r},\overline{r}';i\xi)\cdot\overline{f}_{n'}(\overline{r}') + \sum_{m'} \sigma_{m'}^\beta \int_{T_{m'}} \mathrm{d}S' \nabla'\cdot\overline{\overline{G}}_A^\Omega(\overline{r},\overline{r}',i\xi) P_{m'}(\overline{r}') \tag{9.7.32}$$
$$+ \sum_\alpha \frac{1}{(k_\alpha^2+\xi^2)} \overline{A}_\alpha(\overline{r})(c_\alpha^{J\beta}+c_\alpha^{\sigma\beta})$$

Inserting the expression of the regular dyadic Green's function at imaginary wavenumber of $k=i\xi$ (second order form)

$$-\overline{\mathcal{A}}_\beta(\overline{r}) = \sum_\alpha \frac{1}{k_\alpha^2+\xi^2} \overline{A}_\alpha(\overline{r}) \Big\{ \sum_{n'} J_{n'}^\beta \int_{T_{n'}^\pm} \mathrm{d}S' \overline{A}_\alpha(\overline{r}')\cdot\overline{f}_{n'}(\overline{r}') + \sum_{m'} \sigma_{m'}^\beta \int_{T_{m'}} \mathrm{d}S' \nabla'\cdot\overline{A}_\alpha(\overline{r}') P_{m'}(\overline{r}') \tag{9.7.33}$$
$$+ (c_\alpha^{J\beta}+c_\alpha^{\sigma\beta}) \Big\}$$

Now, for the mode numbers $1 \le \alpha \le M_\Omega$,

$$d_\alpha^\beta = -\frac{1}{k_\alpha^2+\xi^2} \Big[ 1 + \frac{(k_\alpha^2-q_\beta^2)}{q_\beta^2+\xi^2} \Big] (c_\alpha^{J\beta}+c_\alpha^{\sigma\beta}) \tag{9.7.34}$$

and for $\alpha > M_\Omega$, $c_\alpha^\beta$ does not contribute (is not defined) and

$$d_\alpha^\beta = -\frac{1}{k_\alpha^2+\xi^2} \Big\{ \sum_{n'} J_{n'}^\beta \int_{T_{n'}^\pm} \mathrm{d}S' \overline{A}_\alpha(\overline{r}')\cdot\overline{f}_{n'}(\overline{r}') + \sum_{m'} \sigma_{m'}^\beta \int_{T_{m'}} \mathrm{d}S' \nabla'\cdot\overline{A}_\alpha(\overline{r}') P_{m'}(\overline{r}') \tag{9.7.35}$$
$$+ (c_\alpha^{J\beta}+c_\alpha^{\sigma\beta}) \Big\}$$

Once the coefficients $d_\alpha^\beta$ are known, the wave function $\overline{\mathcal{A}}_\beta$ can be normalized by $\sqrt{L_\beta}$ where,

$$L_\beta = \sum_\alpha |d_\alpha^\beta|^2 \tag{9.7.36}$$

# Chapter 10

# Casimir Self stress on Perfect Conductor Cylinder: A Semi-classical Electromagnetism Approach

## 10.1 Introduction

The Casimir stress on an object originated in the zero-point fluctuation of the quantum fields resulting from the nontrivial vacuum state of the quantum fields. In particular, changing vacuum energy can be happened as a result of external conditions, such as boundaries by introducing an object, background potentials, and curved space. The zero-point energy is an infinite quantity, physicists often discard the zero-point energy by redefining the energy reference point using normal ordering. It would be incorrect, however, to neglect the infinite zero-point energy found in the presence of material boundaries, for example, parallel metallic planes. The Casimir effect is fundamental because it is a manifestation of the zero-point fluctuations of the fields, which may have observable effects on all scales, from cosmological to nuclear. The Casimir effect has also been studied with the aid of source theory and radiative reaction, without any explicit reference to the zero-point energy fluctuations [157, 158]. The Casimir effect manifests itself in different area of physics including quantum electrodynamics, Cosmology,condensed matter (elucidation of the physical origin of sonoluminescence) theory of hadrons and so on.

Different methods are used for the Casimir effect calculations: the Green function formalism [159], stress-tensor method [160], multiple scattering expansion [161], zeta function regularization technique[162], heat-kernel series [163], direct mode summation with contour integration [164, 165], and numerical methods that is proposed for Casimir interaction between two arbitrary 3D objects [166]. In all the above-mentioned methods of computation of the Casimir effect, a vague point is the procedure of treatment of the divergences that appears in the formulations, where lack of a mathematically rigorous way of dealing with the infinite quantities apparently leads to different results in some cases [167]. On the other side, the numerical method in [166] developed to regularize the zero-point energy by normalizing the energy by that of separated objects that does not work for the self-stress calculations.

The Casimir self-stress on a cylindrical shell has been studied in 1981 by DeRaad and Milton [168] by the introduction of a frequency cutoff that vanishes rapidly enough to regularize the stress, but the final result is independent of the cutoff. Later on, a method

based on the mode by mode summation technique [169] proposed to obtain the zero-point energy and they used the Zeta function to regularize the energy for perfect conductor case and also the case with a uniform speed of light inside and outside of the cylinder. They examined the zero-point energy for a dilute dielectric limit (uniform speed of light) by perturbation and reported vanishingly small stress on a dilute dielectric tube [169] to the first order. The local and global Casimir energies for a semitransparent cylindrical shell is also studied for different strengths of the coupling [169] and for uniform speed of light inside and outside in [170] using the same approach as [168].

In this paper, we use a classical electrodynamic framework along with the fluctuation-dissipation theorem [171] to compute Casimir self-stress on a cylindrical shell similar to the original Lifshitz's approach [172]. The Dyadic Green's function formulation is obtained for a general dielectric cylinder but the stress calculation is performed for the perfect conductor case only. The main advantage of the semi-classical approach is to utilize mature classical electrodynamic resources and thinkings.

Invoking the superposition, one can decompose the Dyadic Green's function of the problem into two parts, free and scattered parts. The free part satisfies the source condition but not the boundary conditions. All of the electromagnetic properties of the medium are contained in the scattered part as the free part is a universal component of all propagators. One way of regularizing the zero-point energy is to remove the free part of the Green's function and work only with the scattered part. The free part of the Green's function is a hypersingular function at the source (where the stress is calculated on the body of the object) while the scattered part shows smoother behavior around the source (it is continuous with continuous derivative around the source while the free part is not), given that the physical parameters are smooth enough. For the planar geometry of parallel plates, the zero-point energy becomes regularized by removing the free part of the Green's function [15, 173]. However, as it is shown in this paper, subtraction of the background propagator in the cylindrical geometry does not remove the divergences in the stress tensor completely. The geometries with curved surfaces or intersecting planes introduce certain problems in the computation of vacuum energy [160, 161] as Curved surfaces alter the local density of modes and the vacuum energy in the region near the surface and the case of cylindrical geometry is more subtle that spherical or planar geometries [168]. In general, the change in mode density from the free-field case that occurs near the surface varies as the inverse of the radius of curvature [161].

The organization of the paper is as follows: The dyadic Green's function of the dielectric cylinder in terms of cylindrical waves are derived with details in the first section. The Green's function when the source is located outside of the cylinder is obtained based on the reciprocity from that of the source within the cylinder. Next, Maxwell's stress tensor is computed over the surface of the perfect conductor cylinder and frequency integrals are evaluated over imaginary frequencies using the Wick's rotation. In the last section, uniform asymptotic expansion is used to extract the reminding divergence in the stress expression and a value is assigned to this divergence with the help of zeta function.

## 10.2 Vector wave functions and free Cylindrical Dyadic Green's function

The vector wave functions can be obtained from the scalar eigen functions of the scalar wave equation. For a homogeneous wave equation of $(\nabla^2+k^2)\psi(\overline{r})=0$, the solutions that are finite at the origin have the form

$$\psi_n(\overline{r})=J_n(k_\rho\rho)e^{ik_z z}e^{in\phi} \tag{10.2.1}$$

where $k^2=k_\rho^2+k_z^2$ is the eigenvalue of the problem in free space. Since the problem is extended to infinity in both $z$ and $\rho$ directions, the wave number in these directions $k_\rho$,$k_z$ are continuous variables and a complete solution of the scalar wave equation can be written in the form of

$$\psi(\overline{r})=\sum_{n=-\infty}^{\infty}\int_{-\infty}^{\infty}\mathrm{d}k_z\int_0^{\infty}\mathrm{d}k_\rho A_n(k_\rho,k_z)J_n(k_\rho\rho)e^{ik_z z}e^{in\phi} \tag{10.2.2}$$

Orthogonality of partial wave functions $e^{ik_z z}$ is the origin of the Fourier transform,

$$\int_{-\infty}^{\infty}\mathrm{d}z\ e^{ik_z z}e^{-ik'_z z}=2\pi\delta(k_z-k'_z) \tag{10.2.3}$$

and orthogonality of the Bessel functions results in Hankel transform of

$$\int_0^{\infty}\rho\mathrm{d}\rho\ J_n(k_\rho\rho)J_n(k'_\rho\rho)=\frac{\delta(k_\rho-k'_\rho)}{k_\rho} \tag{10.2.4}$$

The vector wave functions can be constructed from the scalar wave function $\psi(\overline{r})$ by

$$\begin{aligned}\overline{L}(\overline{r})&:=\nabla\psi(\overline{r})\\ \overline{M}(\overline{r})&:=\nabla\times\Big(\hat{z}\psi(\overline{r})\Big)\\ \overline{N}(\overline{r})&:=\frac{1}{k}\nabla\times\nabla\times\Big(\hat{z}\psi(\overline{r})\Big)\end{aligned} \tag{10.2.5}$$

where the vector wave function are constructed by using the constant pilot vector $\hat{z}$. This choice results in wave functions with definite polarization states with respect to $z$ direction, namely TE and TM polarization defined with respect to $z$ direction. The vector wave functions $\overline{M}(\overline{r})$ and $\overline{N}(\overline{r})$ formally satisfy the homogeneous vector wave equation.

$$\nabla\times\nabla\times\begin{Bmatrix}\overline{M}(\overline{r})\\ \overline{N}(\overline{r})\end{Bmatrix}-k^2\begin{Bmatrix}\overline{M}(\overline{r})\\ \overline{N}(\overline{r})\end{Bmatrix}=0 \tag{10.2.6}$$

For instance, substituting $\overline{M}$ into the vector wave equation yields

$$\nabla\times\Big[\nabla\times\nabla\times\Big(\hat{z}\psi(\overline{r})\Big)-k^2\Big(\hat{z}\psi(\overline{r})\Big)\Big]=\nabla\times\overline{F} \tag{10.2.7}$$

where,

$$\begin{aligned}\overline{F}&=\nabla\times\nabla\times\Big(\hat{z}\psi(\overline{r})\Big)-k^2\Big(\hat{z}\psi(\overline{r})\Big)\\ &=\nabla\nabla\cdot\Big(\hat{z}\psi(\overline{r})\Big)-\hat{z}(\nabla^2+k^2)\psi(\overline{r})\end{aligned} \tag{10.2.8}$$

The first term is a gradient with zero curl and second term vanish from the scalar wave equation. $\overline{N}$ also satisfies the vector wave equation by a similar reasoning. The transverse wave functions $\overline{M},\overline{N}$ are related to each other by a curl,

$$\begin{aligned}\nabla\times\overline{N}&=\frac{1}{k}\nabla\times\nabla\times\overline{M}\\&=k\overline{M}\end{aligned}\tag{10.2.9}$$

therefore,

$$\begin{aligned}\overline{M}&=\frac{1}{k}\nabla\times\overline{N}\\\overline{N}&=\frac{1}{k}\nabla\times\overline{M}\end{aligned}\tag{10.2.10}$$

This also shows that both $\overline{M}$ and $\overline{N}$ wave functions are divergence free. They are neither enough for expansion of the electric field nor the dyadic Green's function of the electric field. From the vector wave equation for the electric field reads $-k^2\nabla\cdot\overline{E}(\overline{r})=i\omega\mu\nabla\cdot\overline{J}(\overline{r})$ which does not vanish in the source region. Therefore, the transverse wave functions are not complete for description of the electric field everywhere. In order to be able to have a complete expansion of the electric field, we need another wave function that at lease has a non-zero divergence. The vector wave function $\overline{L}(\overline{r}):=\nabla\psi(\overline{r})$ has this property. It is an eigenfunction of the wave equation with eigenvalue $k=0$.

### 10.2.1 Orthogonality relations

Before finding the orthogonality relation between the vector wave functions, lets find the explicit expression of the vector wave functions. Explicit expression of Different Cylindrical vector wave functions read,

$$\begin{aligned}\overline{L}_n(\overline{r})&=\hat{\rho}\frac{\mathrm{d}J_n(k_\rho\rho)}{\mathrm{d}\rho}e^{ik_zz}e^{in\phi}+\hat{\phi}\frac{in}{\rho}J_n(k_\rho\rho)e^{ik_zz}e^{in\phi}+\hat{z}ik_zJ_n(k_\rho\rho)e^{ik_zz}e^{in\phi}\\\overline{M}_n(\overline{r})&=-\hat{\phi}\frac{\mathrm{d}J_n(k_\rho\rho)}{\mathrm{d}\rho}e^{ik_zz}e^{in\phi}+\hat{\rho}\frac{in}{\rho}J_n(k_\rho\rho)e^{ik_zz}e^{in\phi}\\\overline{N}_n(\overline{r})&=\hat{\rho}\frac{ik_z}{k}\frac{\mathrm{d}J_n(k_\rho\rho)}{\mathrm{d}\rho}e^{ik_zz}e^{in\phi}-\hat{\phi}\frac{k_z}{k}\frac{n}{\rho}J_n(k_\rho\rho)e^{ik_zz}e^{in\phi}+\hat{z}\frac{k_\rho^2}{k}J_n(k_\rho\rho)e^{ik_zz}e^{in\phi}\end{aligned}\tag{10.2.11}$$

If we consider the eigenvalues of the problem as $k_z$, and $k_\rho$, the orthogonality between $\overline{F}_n(\overline{r};k_\rho,k_z)$ and $\overline{F'}_n(\overline{r};k'_\rho,k'_z)$ (eigenfunction corresponding with different eigenvalues) can be constructed as

$$\int\mathrm{d}^3\overline{r}\;\overline{F}_n(\overline{r};k_\rho,k_z)\cdot\overline{F'}_{-m}(\overline{r};-k'_\rho,-k'_z)\propto\delta(k_z-k'_z)\delta(k_\rho-k'_\rho)\delta_{nm}\tag{10.2.12}$$

Notice that all of the harmonics number $n$ for the same $k_z$ and $k_\rho$ constitute a degenerate eigen-space. We expect the presence of delta functions according to the Sturm-Liouville theory and the delta function is continuous since the $k_\rho$ and $k_z$ spectrum are continuous.

**Orthogonality of $\overline{L}$ functions**

Since, $J_{-n}(-x)=J_n(x)$ and $\overline{L}_n(\overline{r};k_\rho,k_z)\cdot\overline{L}_{-n'}(\overline{r};-k'_\rho,-k'_z)\propto e^{i(n-n')\phi}$, integration over $\phi$ results in

$$\int_{2\pi}\mathrm{d}\phi\overline{L}_n(\overline{r};k_\rho,k_z)\cdot\overline{L}_{-n}(\overline{r};-k'_\rho,-k'_z)=2\pi\Big[\frac{\mathrm{d}J_n(k_\rho\rho)}{\mathrm{d}\rho}\frac{\mathrm{d}J_n(k'_\rho\rho)}{\mathrm{d}\rho}+\Big[k_zk'_z+\Big(\frac{n}{\rho}\Big)^2\Big]J_n(k_\rho\rho)J_n(k'_\rho\rho)\Big]e^{i(k_z-k'_z)z} \tag{10.2.13}$$

We can express the Bessel function derivatives in terms of neighbor orders Bessel functions through

$$\frac{\mathrm{d}J_n(\xi)}{\mathrm{d}\xi}=\frac{1}{2}\Big[J_{n+1}(\xi)-J_{n-1}(\xi)\Big] \tag{10.2.14}$$

on the other hand different orders can be related by

$$J_n(\xi)=\frac{\xi}{2n}\Big[J_{n+1}(\xi)+J_{n-1}(\xi)\Big] \tag{10.2.15}$$

Therefore,

$$\int_{2\pi}\mathrm{d}\phi\overline{L}_n(\overline{r};k_\rho,k_z)\cdot\overline{L}_{-n}(\overline{r};-k'_\rho,-k'_z)=2\pi\Big[\frac{k_\rho k'_\rho}{2}\Big[J_{n+1}(k_\rho\rho)J_{n+1}(k'_\rho\rho)+J_{n-1}(k_\rho\rho)J_{n-1}(k'_\rho\rho)\Big]+k_zk'_zJ_n(k_\rho\rho)J_n(k'_\rho\rho)\Big]e^{i(k_z-k'_z)z} \tag{10.2.16}$$

Integration over $z$ also can be done easily and it gives a delta function of $\delta(k_z-k'_z)$. Using representation of delta function in terms of Bessel functions

$$\int\rho\mathrm{d}\rho J_n(k_\rho\rho)J_n(k'_\rho\rho)=\frac{\delta(k_\rho-k'_\rho)}{k_\rho} \tag{10.2.17}$$

we arrive at,

$$\int\mathrm{d}^3\overline{r}\overline{L}_n(\overline{r};k_\rho,k_z)\cdot\overline{L}_{-n}(\overline{r};-k'_\rho,-k'_z)=\frac{k^2}{k_\rho}(2\pi)^2\delta(k_z-k'_z)\delta(k_\rho-k'_\rho) \tag{10.2.18}$$

For different wave numbers $n$ in $\phi$ direction, the wave functions are orthogonal

$$\int_{2\pi}\mathrm{d}\phi e^{i(n-n')\phi}=2\pi\delta_{nn'} \tag{10.2.19}$$

The constraint of integer wave number $n$ in $\phi$ direction is the consequence of invoking single value constraint on the wave function. For geometries which $\phi$ cannot go over itself ($2\pi$ period), $n$ can be a real number in general but the wave functions are still orthogonal.

**Orthogonality of $\overline{M}$ functions**

Following a similar procedure and using the identities of the Bessel functions, we obtain

$$\int_{2\pi} \mathrm{d}\phi \overline{M}_n(\overline{r};k_\rho,k_z)\cdot\overline{M}_{-n}(\overline{r};-k'_\rho,-k'_z)=\Big[\frac{\mathrm{d}J_n(k_\rho\rho)}{\mathrm{d}\rho}\frac{\mathrm{d}J_n(k'_\rho\rho)}{\mathrm{d}\rho}+\Big(\frac{n}{\rho}\Big)^2 J_n(k_\rho\rho)J_n(k'_\rho\rho)\Big]2\pi e^{i(k_z-k'_z)z} \tag{10.2.20}$$

$$=\frac{k_\rho k'_\rho}{2}\Big[J_{n+1}(k_\rho\rho)J_{n+1}(k'_\rho\rho)+J_{n-1}(k_\rho\rho)J_{n-1}(k'_\rho\rho)\Big]2\pi e^{i(k_z-k'_z)z}$$

Therefore,

$$\int \mathrm{d}^3\overline{r}\overline{M}_n(\overline{r};k_\rho,k_z)\cdot\overline{M}_{-n'}(\overline{r};-k'_\rho,-k'_z)=k_\rho(2\pi)^2\delta(k_\rho-k'_\rho)\delta(k_z-k'_z)\delta_{nn'} \tag{10.2.21}$$

Similarly, for $\overline{N}$ functions,

$$\int \mathrm{d}^3\overline{r}\overline{N}_n(\overline{r};k_\rho,k_z)\cdot\overline{N}_{-n'}(\overline{r};-k'_\rho,-k'_z)=k_\rho(2\pi)^2\delta(k_z-k'_z)\delta(k_\rho-k'_\rho)\delta_{nn'} \tag{10.2.22}$$

**Mutual Orthogonality of $\overline{L}$, $\overline{M}$, and $\overline{N}$**

For different index of $n$, all of the vector wave functions are mutually orthogonal and this is clear from the $\phi$ dependent part. Therefore, it suffice to show the orthogonality of wave functions for the same index of $n$. For orthogonality of the $\overline{L}$ and $\overline{N}$ we have

$$\int \mathrm{d}\phi \overline{L}_n(\overline{r};k_\rho,k_z)\cdot\overline{N}_{-n}(\overline{r};-k_\rho,-k_z)=\Big[-\frac{ik'_z}{k}\frac{\mathrm{d}J_n(k_\rho\rho)}{\mathrm{d}\rho}\frac{\mathrm{d}J_n(k'_\rho\rho)}{\mathrm{d}\rho}-\frac{ik'_z}{k}\Big(\frac{n}{\rho}\Big)^2 J_n(k_\rho\rho)J_n(k'_\rho\rho) \tag{10.2.23}$$

$$+\frac{ik_zk'^2_\rho}{k}J_n(k_\rho\rho)J_n(k'_\rho\rho)\Big](2\pi)e^{i(k_z-k'_z)z}$$

Using Bessel functions identities, it can be written as

$$\int \mathrm{d}\phi \overline{L}_n(\overline{r};k_\rho,k_z)\cdot\overline{N}_{-n}(\overline{r};-k_\rho,-k_z)=\Big[-\frac{ik'_z}{k}\frac{k_\rho k'_\rho}{2}\Big[J_{n+1}(k_\rho\rho)J_{n+1}(k'_\rho\rho)+J_{n-1}(k_\rho\rho)J_{n-1}(k'_\rho\rho)\Big] \tag{10.2.24}$$

$$+\frac{ik_zk'^2_\rho}{k}J_n(k_\rho\rho)J_n(k'_\rho\rho)\Big](2\pi)e^{i(k_z-k'_z)z}$$

Integrating over whole space gives

$$\int \mathrm{d}^3\overline{r}\overline{L}_n(\overline{r};k_\rho,k_z)\cdot\overline{N}_{-n}(\overline{r};-k_\rho,-k_z)=\Big[-\frac{ik_zk_\rho^2}{k}+\frac{ik_zk'^2_\rho}{k}\Big](2\pi)\delta(k_z-k'_z)\frac{1}{k_\rho}\delta(k_\rho-k'_\rho)=0 \tag{10.2.25}$$

## 10.3 Free space dyadic Green's function expansion

The dyadic Green's function $\overline{\overline{G}}(\overline{r},\overline{r}')$ corresponding to the electric field that satisfies the vector wave equation of

$$\nabla\times\nabla\times\overline{E}(\overline{r})-k_0^2\overline{E}(\overline{r})=i\omega\mu\overline{J}(\overline{r}) \tag{10.3.1}$$

will satisfy the same vector wave equation with unit source of

$$\nabla\times\nabla\times\overline{\overline{G}}(\overline{r},\overline{r}')-k_0^2\overline{\overline{G}}(\overline{r},\overline{r}')=\overline{\overline{I}}\delta(\overline{r}-\overline{r}') \tag{10.3.2}$$

Here, $k_0=\omega\sqrt{\mu_0\varepsilon_0}$ is the wave number in the background medium which is unbounded free space. In order to solve for the dyadic Green's function, we use the completeness of the vector cylindrical wave functions and expand the dyadic Green's function in terms of vector wave functions,

$$\begin{aligned}\overline{\overline{G}}(\overline{r},\overline{r}')=\sum_\sigma\int_{-\infty}^{\infty}\mathrm{d}k_z\int_0^\infty\mathrm{d}k_\rho\Big[&\overline{M}_\sigma(\overline{r};k_\rho,k_z)\overline{A}_\sigma(k_\rho,k_z)+\overline{N}_\sigma(\overline{r};k_\rho,k_z)\overline{B}_\sigma(k_\rho,k_z)\\&+\overline{L}_\sigma(\overline{r};k_\rho,k_z)\overline{C}_\sigma(k_\rho,k_z)\Big]\end{aligned} \tag{10.3.3}$$

Substituting this expression into the vector wave equation of Green's function we arrive at

$$\begin{aligned}\overline{\overline{I}}\delta(\overline{r}-\overline{r}')=\sum_\sigma\int_{-\infty}^{\infty}\mathrm{d}k_z\int_0^\infty\mathrm{d}k_\rho\Big[&(k^2-k_0^2)\overline{M}_\sigma(\overline{r};k_\rho,k_z)\overline{A}_\sigma(k_\rho,k_z)\\&+(k^2-k_0^2)\overline{N}_\sigma(\overline{r};k_\rho,k_z)\overline{B}_\sigma(k_\rho,k_z)-k_0^2\overline{L}_\sigma(\overline{r};k_\rho,k_z)\overline{C}_\sigma(k_\rho,k_z)\Big]\end{aligned} \tag{10.3.4}$$

In order to find the generalized vector Fourier coefficients, for instance $\overline{A}_\sigma(k_\rho,k_z)$, we can multiply both sides by $\overline{M}_{-\sigma'}(\overline{r};-k_\rho',-k_z')$ and integrate over the whole space. Upon using the orthogonality of the vector wave functions

$$\overline{A}_\sigma(k_\rho,k_z)=\frac{1}{(2\pi)^2}\frac{\overline{M}_{-\sigma}(\overline{r}';-k_\rho,-k_z)}{k_\rho(k^2-k_0^2)} \tag{10.3.5}$$

Similarly,

$$\begin{aligned}\overline{B}_\sigma(k_\rho,k_z)&=\frac{1}{(2\pi)^2}\frac{\overline{N}_{-\sigma}(\overline{r}';-k_\rho,-k_z)}{k_\rho(k^2-k_0^2)}\\\overline{C}_\sigma(k_\rho,k_z)&=-\frac{1}{(2\pi)^2}k_\rho\frac{\overline{L}_{-\sigma}(\overline{r}';-k_\rho,-k_z)}{k^2k_0^2}\end{aligned} \tag{10.3.6}$$

Then the complete expression of the dyadic Green's function in terms of the cylindrical vector wave functions can be obtained as

$$\begin{aligned}\overline{\overline{G}}(\overline{r},\overline{r}')=\sum_{n=-\infty}^{\infty}\frac{1}{(2\pi)^2}\int_{-\infty}^{\infty}\mathrm{d}k_z\int_0^\infty\mathrm{d}k_\rho\Big[&\frac{\overline{M}_n(\overline{r};k_\rho,k_z)\overline{M}_{-n}(\overline{r}';-k_\rho,-k_z)}{k_\rho(k^2-k_0^2)}\\&+\frac{\overline{N}_n(\overline{r};k_\rho,k_z)\overline{N}_{-n}(\overline{r}';-k_\rho,-k_z)}{k_\rho(k^2-k_0^2)}-k_\rho\frac{\overline{L}_n(\overline{r};k_\rho,k_z)\overline{L}_{-n}(\overline{r}';-k_\rho,-k_z)}{k^2k_0^2}\Big]\end{aligned} \tag{10.3.7}$$

Here $k^2=k_\rho^2+k_z^2$ and there is no constraint on it. Until now, the vector wave functions with wave number $k$ are not actual wave propagating in the medium. We can make it actual waves in the medium by mandating $k=k_0$, but this cannot be done directly because of the presence of the poles at $k=\pm k_0$ in the dyadic Green's function. In order to convert the expansion into a mode expansion (where $\overline{M}$, $\overline{N}$, and $\overline{L}$ functions are actual propagating fields) we can perform the integration over $k_z$ to find mode propagating in $z$ direction (with

explicit dependence on $z$). Equivalently, we can perform integration over $k_\rho$ to find the mode expansion in $\rho$ direction. Since later on we are interested in the Green's function for medium which has discontinuity in the $\rho$ direction, it is preferable to have modes with explicit dependence on $\rho$ rather than $z$.

The terms involved in the spectral integrand include

$$\begin{aligned}
\overline{L}_n(\overline{r};k_\rho,k_z)\overline{L}_{-n}(\overline{r}';-k_\rho,-k_z)&=\nabla\nabla'\psi_n(\overline{r};k_\rho,k_z)\psi_{-n}(\overline{r}';-k_\rho,-k_z) \\
\overline{M}_n(\overline{r};k_\rho,k_z)\overline{M}_{-n}(\overline{r}';-k_\rho,-k_z)&=(\nabla\times\hat{z})(\nabla'\times\hat{z})\psi_n(\overline{r};k_\rho,k_z)\psi_{-n}(\overline{r}';-k_\rho,-k_z) \\
\overline{N}_n(\overline{r};k_\rho,k_z)\overline{N}_{-n}(\overline{r}';-k_\rho,-k_z)&=\frac{1}{k^2}(\nabla\times\nabla\times\hat{z})(\nabla'\times\nabla'\times\hat{z})\psi_n(\overline{r};k_\rho,k_z)\psi_{-n}(\overline{r}';-k_\rho,-k_z)
\end{aligned} \tag{10.3.8}$$

Here the scalar wave function is considered to be $\psi_n(\overline{r};k_\rho,k_z)=J_n(k_\rho\rho)e^{ik_zz}e^{in\phi}$. In order to write the dyadic Green's function as a cylindrical mode expansion with explicit dependence on $\rho$, we change the order of integration over $k_\rho$ and spatial derivatives. The integrals involve in this computation are of three forms,

$$\begin{aligned}
I_M&=\int_0^\infty \mathrm{d}k_\rho \frac{J_n(k_\rho\rho)J_n(k_\rho\rho')}{k_\rho(k^2-k_0^2)} \\
I_N&=\int_0^\infty \mathrm{d}k_\rho \frac{J_n(k_\rho\rho)J_n(k_\rho\rho')}{k^2k_\rho(k^2-k_0^2)} \\
I_L&=\int_0^\infty \mathrm{d}k_\rho k_\rho \frac{J_n(k_\rho\rho)J_n(k_\rho\rho')}{k^2k_0^2}
\end{aligned} \tag{10.3.9}$$

In order to use the complex integration techniques, we need to convert the integrations to integrals over the whole real line ($-\infty$ to $\infty$). Using the definition of Hankel functions,

$$J_n(\xi)=\mathrm{Re}\Big[H_n^{(1)}(\xi)\Big]=\frac{1}{2}\Big(H_n^{(1)}(\xi)+H_n^{(2)}(\xi)\Big) \tag{10.3.10}$$

Note that the Bessel function of $J_n(\xi)$ is regular at the origin (when $n\neq0$) while Hankel functions $H_n^{(1,2)}(\xi)$ have logarithmic singularity at the origin. The decomposition of Bessel functions in terms of Hankel functions will introduce a singularity at the origin which we should take care of that. In order to do so, we take the lower limit of the integral from $\delta$ instead of zero in a limiting process, i.e.

$$I_M=\frac{1}{2}\lim_{\delta\to0}\int_\delta^\infty \mathrm{d}k_\rho \frac{J_n(k_\rho\rho)H_n^{(1)}(k_\rho\rho')}{k_\rho(k^2-k_0^2)}+\frac{1}{2}\lim_{\delta\to0}\int_\delta^\infty \mathrm{d}k_\rho \frac{J_n(k_\rho\rho)H_n^{(2)}(k_\rho\rho')}{k_\rho(k^2-k_0^2)} \tag{10.3.11}$$

For real wavenumber $k_\rho$, $H_n^{(1)}(k_\rho\rho)$ represents the outgoing wave that satisfies the radiation condition while $H_n^{(2)}(k_\rho\rho)$ is an incoming wave toward the origin and does not fit the radiation condition. Using the reflection formula for Bessel and Hankel functions [93],

$$\begin{aligned}
J_n(e^{-i\pi}\xi)&=(-1)^nJ_n(\xi) \\
H_n^{(2)}(e^{-i\pi}\xi)&=-(-1)^nH_n^{(1)}(\xi)
\end{aligned} \tag{10.3.12}$$

and letting $k_\rho=e^{-i\pi}k_\rho$ in the second integral

$$\begin{aligned}
I_M&=\frac{1}{2}\lim_{\delta\to0}\int_\delta^\infty \mathrm{d}k_\rho \frac{J_n(k_\rho\rho)H_n^{(1)}(k_\rho\rho')}{k_\rho(k^2-k_0^2)}+\frac{1}{2}\lim_{\delta\to0}\int_{-\infty}^\delta \mathrm{d}k_\rho \frac{J_n(k_\rho\rho)H_n^{(1)}(k_\rho\rho')}{k_\rho(k^2-k_0^2)} \\
&=\frac{1}{2}\mathrm{PV}[0]\int_{-\infty}^\infty \mathrm{d}k_\rho \frac{J_n(k_\rho\rho)H_n^{(1)}(k_\rho\rho')}{k_\rho(k^2-k_0^2)}
\end{aligned} \tag{10.3.13}$$

This is a principal valve integral with respect to the present singularity of the Hankel func-

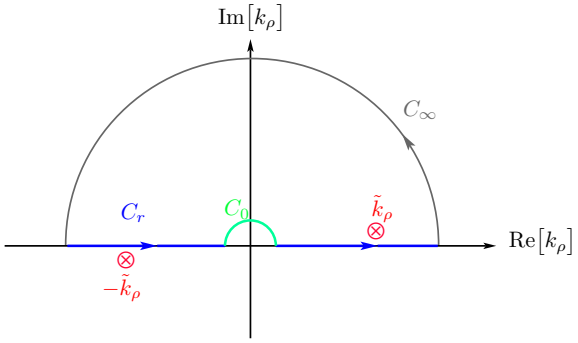


FIGURE 10.1: Contour of integration in $k_\rho$ plane.

tion at the origin at it is not ready to be converted to a complex integral. The contribution of this singularity can be found and add to the principal value integral to come up with a complete complex contour integral. Using small argument expansion of Bessel functions,

$$J_n(\xi)\approx\frac{1}{n!}\left(\frac{\xi}{2}\right)^n \tag{10.3.14}$$

and for $n\neq 0$

$$H_n^{(1)}(\xi)\approx -i\frac{(n-1)!}{\pi}\left(\frac{2}{\xi}\right)^n \tag{10.3.15}$$

then for $|k_\rho\rho|\ll 1, |k_\rho\rho'|\ll 1$ we have

$$J_n(k_\rho\rho)H_n^{(1)}(k_\rho\rho')=\frac{i}{n\pi}\left(\frac{\rho}{\rho'}\right)^n \tag{10.3.16}$$

The contribution of the simple pole at the origin can be computed using Residue theorem,

$$I_0=\frac{1}{2}\int_{C_0}\mathrm{d}k_\rho\frac{J_n(k_\rho\rho)H_n^{(1)}(k_\rho\rho')}{k_\rho(k^2-k_0^2)}=-\pi i\mathrm{Res}(k_\rho=0) \tag{10.3.17}$$

The minus sign accounts for clockwise path of integration near the origin and the pole contribution is divided by two because of half a circle path. Then,

$$\mathrm{Res}(k_\rho=0)=\lim_{k_\rho\to 0}\frac{1}{2}\frac{J_n(k_\rho\rho)H_n^{(1)}(k_\rho\rho')}{(k^2-k_0^2)}=\frac{1}{(k_z^2-k_0^2)}\frac{i}{2n\pi}\left(\frac{\rho}{\rho'}\right)^n \tag{10.3.18}$$

If we take $\tilde{k}_\rho^2=k_0^2-k_z^2$ then,

$$I_0=\frac{1}{2}\int_{C_0}\mathrm{d}k_\rho\frac{J_n(k_\rho\rho)H_n^{(1)}(k_\rho\rho')}{k_\rho(k^2-k_0^2)}=\frac{1}{\tilde{k}_\rho^2}\frac{1}{2n}\left(\frac{\rho}{\rho'}\right)^n \tag{10.3.19}$$

So the principal value integral can be converted into an integral over continuous contour of $C=C_r+C_0$ if we subtract the contribution of $C_0$

$$I_M=\frac{1}{2}\int_{C}\mathrm{d}k_\rho\frac{J_n(k_\rho\rho)H_n^{(1)}(k_\rho\rho')}{k_\rho(k^2-k_0^2)}-I_0 \tag{10.3.20}$$

In order to enclose contour at infinity note that from large argument asymptotic expansion,

$$\begin{aligned} J_n(k_\rho\rho)&\propto e^{ik_\rho\rho}+e^{-ik_\rho\rho} \\ H_n^{(1)}(k_\rho\rho')&\propto e^{ik_\rho\rho'} \end{aligned} \tag{10.3.21}$$

Therefore, when $k_\rho\to\infty$,

$$J_n(k_\rho\rho)H_n^{(1)}(k_\rho\rho')\propto Ae^{ik_\rho(\rho'+\rho)}+Be^{ik_\rho(\rho'-\rho)} \tag{10.3.22}$$

For $\rho'>\rho$ we can enclose the contour at infinity in upper half plane and the integral over $C_\infty$ has no contribution in this way. Now,

$$I_M=\frac{1}{2}\oint_{C+C_\infty}\mathrm{d}k_\rho\frac{J_n(k_\rho\rho)H_n^{(1)}(k_\rho\rho')}{k_\rho(k^2-k_0^2)}-I_0 \tag{10.3.23}$$

The integrand has two simple poles at $k_\rho=\pm\sqrt{k_0^2-k_z^2}=\pm\tilde{k}_\rho$ and one of them is located inside the contour (small loss in conjunction with radiation condition will pull the poles off the real axis). By the Residue theorem

$$I_M=\pi i\frac{J_n(\tilde{k}_\rho\rho)H_n^{(1)}(\tilde{k}_\rho\rho')}{2\tilde{k}_\rho^2}-I_0\quad,\quad\rho<\rho' \tag{10.3.24}$$

For the case of $\rho>\rho'$ we can enclose the contour in lower half plane and in general

$$I_M=\pi i\frac{J_n(\tilde{k}_\rho\rho_<)H_n^{(1)}(\tilde{k}_\rho\rho_>)}{2\tilde{k}_\rho^2}-\frac{1}{\tilde{k}_\rho^2}\frac{1}{2n}\left(\frac{\rho_<}{\rho_>}\right)^n \tag{10.3.25}$$

Similarly [119, 121],

$$\begin{aligned} I_N&=\frac{\pi i}{2\tilde{k}_\rho^2k_0^2}J_n(\tilde{k}_\rho\rho_<)H_n^{(1)}(\tilde{k}_\rho\rho_>)+\frac{\pi i}{2k_z^2k_0^2}J_n(ik_z\rho_<)H_n^{(1)}(ik_z\rho_>)-\frac{1}{\tilde{k}_\rho^2k_z^2}\frac{1}{2n}\left(\frac{\rho_<}{\rho_>}\right)^n \\ I_L&=\frac{\pi i}{2k_0^2}J_n(ik_z\rho_<)H_n^{(1)}(ik_z\rho_>) \end{aligned} \tag{10.3.26}$$

The result of $I_L$ is static in nature and comes from the presence of the term $1/k^2$ (pole at the origin). This static term will cancel the second term in the $I_N$ expression except for a delta function singularity. The last terms in the $I_M$ and $I_N$ also cancel each other such that the free dyadic Green's function can be written as

$$\overline{\overline{G}}(\overline{r},\overline{r}')=\sum_{n=-\infty}^{\infty}\frac{i}{8\pi}\int_{-\infty}^{\infty}\mathrm{d}k_z\frac{1}{k_\rho^2}\left[\overline{M}_n(\overline{r};k_z)\overline{M}_{-n}(\overline{r}';-k_z)+\overline{N}_n(\overline{r};k_z)\overline{N}_{-n}(\overline{r}';-k_z)\right]-\frac{\hat{\rho}\hat{\rho}}{k_0^2}\delta(\overline{r}-\overline{r}') \tag{10.3.27}$$

Now, for each mode with specified $k_z$, $k_\rho$ is fixed and its equal to $k_\rho=\sqrt{k_0^2-k_z^2}$. Also note that between $\rho$ and $\rho'$ whichever is larger should be constructed with the Hankel function.

**Singularity of the dyadic Green's function**

If we examine the integrands of the dyadic Green's functions with respect to $k_\rho$ (First evaluated the $k_\rho$ spectral integral and then $k_z$ integral)

$$\overline{\overline{G}}(\overline{r},\overline{r}')=\sum_{n=-\infty}^{\infty}\frac{1}{(2\pi)^2}\int_{-\infty}^{\infty}\mathrm{d}k_z\int_0^{\infty}\mathrm{d}k_\rho\Big[\frac{\overline{M}_n(\overline{r};k_\rho,k_z)\overline{M}_{-n}(\overline{r}';-k_\rho,-k_z)}{k_\rho(k^2-k_0^2)} \\ +\frac{\overline{N}_n(\overline{r};k_\rho,k_z)\overline{N}_{-n}(\overline{r}';-k_\rho,-k_z)}{k_\rho(k^2-k_0^2)}-k_\rho\frac{\overline{L}_n(\overline{r};k_\rho,k_z)\overline{L}_{-n}(\overline{r}';-k_\rho,-k_z)}{k^2k_0^2}\Big] \tag{10.3.28}$$

As $k_\rho\to\infty$, we expect that the term that contains Delta function to have a constant spectral content. By taking

$$I_M=\int_0^{\infty}\mathrm{d}k_\rho\frac{J_n(k_\rho\rho)J_n(k_\rho\rho')}{k_\rho(k^2-k_0^2)} \tag{10.3.29}$$
$$I_N=\int_0^{\infty}\mathrm{d}k_\rho\frac{J_n(k_\rho\rho)J_n(k_\rho\rho')}{k^2k_\rho(k^2-k_0^2)}$$
$$I_L=\int_0^{\infty}\mathrm{d}k_\rho k_\rho\frac{J_n(k_\rho\rho)J_n(k_\rho\rho')}{k^2k_0^2}$$

the differential operators involved in the vector wave functions in the limit of $k_\rho\to\infty$ are equivalent to [121]

$$(\nabla\times z)(\nabla'\times z)\approx\hat{\phi}\hat{\phi}\frac{\partial}{\partial\rho}\frac{\partial}{\partial\rho'}\approx\hat{\phi}\hat{\phi}\ k_\rho^2 \tag{10.3.30}$$
$$(\nabla\times(\nabla\times z))(\nabla'\times(\nabla'\times z))\approx\hat{z}\hat{z}\frac{\partial^2}{\partial\rho^2}\frac{\partial^2}{\partial\rho'^2}\approx\hat{z}\hat{z}\ k_\rho^4$$
$$\nabla\nabla'\approx\hat{\rho}\hat{\rho}\frac{\partial}{\partial\rho}\frac{\partial}{\partial\rho'}\approx\hat{\rho}\hat{\rho}\ k_\rho^2$$

Observing this asymptotic expansions, the $M$ and $N$ function integrals in the dyadic Green's function expansion do not have singularity in $k_\rho$ integral evaluation. For the $L$ term, the integrand does not vanish at $k_\rho\to\infty$. So this term would have a delta singular term. The integral of $I_L$ has been computed in the previous section as

$$I_L=\frac{\pi i}{2k_0^2}J_n(ik_z\rho_<)H_n^{(1)}(ik_z\rho_>) \tag{10.3.31}$$

This is not a differentiable function of $\rho$ and $\rho'$ near $\rho=\rho'$ that cause the singular behavior. The singular part of the Green's function becomes

$$\overline{\overline{G}}_{\mathrm{Sing}}(\overline{r},\overline{r}')=-\frac{\pi i}{2k_0^2}\sum_{n=-\infty}^{\infty}\frac{1}{(2\pi)^2}\int_{-\infty}^{\infty}\mathrm{d}k_z\nabla\nabla'\Big[J_n(ik_z\rho_<)H_n^{(1)}(ik_z\rho_>)e^{ik_z(z-z')}e^{in(\phi-\phi')}\Big] \tag{10.3.32}$$

But the singularity appears only in $\hat{\rho}\hat{\rho}$ component

$$\overline{\overline{G}}_{\mathrm{Sing}}(\overline{r},\overline{r}')=-\hat{\rho}\hat{\rho}\frac{\pi i}{2k_0^2}\sum_{n=-\infty}^{\infty}\frac{1}{(2\pi)^2}e^{in(\phi-\phi')}\int_{-\infty}^{\infty}\mathrm{d}k_z e^{ik_z(z-z')}\frac{\partial}{\partial\rho}\frac{\partial}{\partial\rho'}\Big[J_n(ik_z\rho_<)H_n^{(1)}(ik_z\rho_>)\Big] \tag{10.3.33}$$

Assume a constant source point $\rho'$. When $\rho>\rho'$

$$\frac{\partial}{\partial\rho}\Big[J_n(ik_z\rho_<)H_n^{(1)}(ik_z\rho_>)\Big]=\frac{\partial}{\partial\rho}\Big[J_n(ik_z\rho')H_n^{(1)}(ik_z\rho)\Big]=J_n(ik_z\rho')\frac{\mathrm{d}H_n^{(1)}(ik_z\rho)}{\mathrm{d}\rho} \quad (10.3.34)$$

but when $\rho<\rho'$

$$\frac{\partial}{\partial\rho}\Big[J_n(ik_z\rho_<)H_n^{(1)}(ik_z\rho_>)\Big]=\frac{\partial}{\partial\rho}\Big[J_n(ik_z\rho)H_n^{(1)}(ik_z\rho')\Big]=\frac{\mathrm{d}J_n(ik_z\rho)}{\mathrm{d}\rho}H_n^{(1)}(ik_z\rho') \quad (10.3.35)$$

The step change in the first derivative near $\rho=\rho'$ is

$$\Delta=J_n(ik_z\rho)\frac{\mathrm{d}H_n^{(1)}(ik_z\rho)}{\mathrm{d}\rho}-\frac{\mathrm{d}J_n(ik_z\rho)}{\mathrm{d}\rho}H_n^{(1)}(ik_z\rho)=\frac{2i}{\pi\rho} \quad (10.3.36)$$

where the Wronskian determinant has been used in the last equality. The second derivative with respect to $\rho$ gives a delta function of amplitude $\Delta$, but second derivative with respect to $\rho'$ gives delta function with amplitude of $-\Delta$. So

$$\begin{aligned}\overline{\overline{G}}_{\mathrm{Sing}}(\overline{r},\overline{r}')&=-\hat{\rho}\hat{\rho}\frac{\pi i}{2k_0^2}\sum_{n=-\infty}^{\infty}\frac{1}{(2\pi)^2}e^{in(\phi-\phi')}\int_{-\infty}^{\infty}\mathrm{d}k_z e^{ik_z(z-z')}\left(-\frac{2i}{\pi\rho}\right)\delta(\rho-\rho') \quad (10.3.37)\\ &=-\hat{\rho}\hat{\rho}\frac{1}{k_0^2}\frac{\delta(\rho-\rho')}{\rho}\delta(z-z')\delta(\phi-\phi')=-\frac{\hat{\rho}\hat{\rho}}{k_0^2}\delta(\overline{r}-\overline{r}')\end{aligned}$$

### 10.3.1 Dielectric cylinder dyadic Green's function

Now we have constructed the free space dyadic Green's function in the cylindrical coordinate, and it is possible to find the Green's function for the dielectric cylinder. Assuming the source is located inside the cylinder ($r\leq a$), then the objective is to find dyadic Green's functions of $\overline{\overline{G}}^{[11]}(\overline{r},\overline{r}')$ and $\overline{\overline{G}}^{[21]}(\overline{r},\overline{r}')$ for observation points inside and outside of the cylinder. Taking the linearity of the problem into account, we can construct the Green's functions

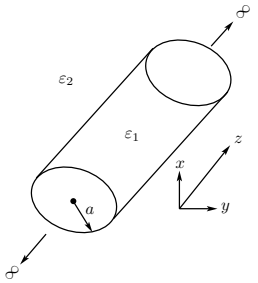


FIGURE 10.2: Geometry of the dielectric cylinder.

by superposition. If the space were to filled with $\varepsilon_1$ everywhere, then $\overline{\overline{G}}^{[11]}(\overline{r},\overline{r}')=\overline{\overline{G}}_1(\overline{r},\overline{r}')$ which is free space dyadic Green's function. Presence of the cylindrical boundary will cause reflections off the boundary into medium 1 as well as the field generated in the absence of the boundary. So, the free space Green's function should be corrected by a scattering part $\overline{\overline{G}}_S^{[11]}(\overline{r},\overline{r}')$ such that

$$\overline{\overline{G}}^{[11]}(\overline{r},\overline{r}')=\overline{\overline{G}}_1(\overline{r},\overline{r}')+\overline{\overline{G}}_S^{[11]}(\overline{r},\overline{r}') \quad (10.3.38)$$

and the Green's function of $\overline{\overline{G}}^{[21]}(\overline{r},\overline{r}')$ is consequence of transmission of the field through the boundary. It contains only scattering part and not the free space part,

$$\overline{\overline{G}}^{[21]}(\overline{r},\overline{r}')=\overline{\overline{G}}_S^{[21]}(\overline{r},\overline{r}') \tag{10.3.39}$$

In order to distinguish between the vector wave functions that are constructed from Bessel function and Hankel functions we will write the latter by a plus sign like $\overline{M}^+$ and $\overline{N}^+$. Therefore, free space Green's function in region 1 is

$$\overline{\overline{G}}_1(\overline{r},\overline{r}')=\sum_{n=-\infty}^{\infty}\frac{i}{8\pi}\int_{-\infty}^{\infty}\mathrm{d}k_z\frac{1}{k_{1\rho}^2}\begin{cases}\overline{M}_{1n}^+(\overline{r};k_z)\overline{M}_{1,-n}(\overline{r}';-k_z)+\overline{N}_{1n}^+(\overline{r};k_z)\overline{N}_{1,-n}(\overline{r}';-k_z)\\ \overline{M}_{1n}(\overline{r};k_z)\overline{M}_{1,-n}^+(\overline{r}';-k_z)+\overline{N}_{1n}(\overline{r};k_z)\overline{N}_{1,-n}^+(\overline{r}';-k_z)\end{cases}$$
$$-\frac{\hat{\rho}\hat{\rho}}{k_1^2}\delta(\overline{r}-\overline{r}')$$

For the scattered part of the Green's function $\overline{\overline{G}}_S^{[11]}(\overline{r},\overline{r}')$ (that is valid for $\rho>\rho'$) we consider the most general expansion that can match the boundary condition everywhere in primed coordinate (same dependence on the source coordinates as the exciting field)

$$\overline{\overline{G}}_S^{[11]}(\overline{r},\overline{r}')=\sum_{n=-\infty}^{\infty}\frac{i}{8\pi}\int_{-\infty}^{\infty}\mathrm{d}k_z\frac{1}{k_{1\rho}^2}\Big[\Big(A_n^{(11)}\overline{M}_{1n}(\overline{r};k_z)+B_n^{(11)}\overline{N}_{1n}(\overline{r};k_z)\Big)\overline{M}_{1,-n}(\overline{r}';-k_z)$$
$$+\Big(C_n^{(11)}\overline{N}_{1n}(\overline{r};k_z)+D_n^{(11)}\overline{M}_{1n}(\overline{r};k_z)\Big)\overline{N}_{1,n}(\overline{r}';-k_z)\Big] \tag{10.3.40}$$

The posterior part of the $\overline{\overline{G}}_S^{[11]}(\overline{r},\overline{r}')$ comes in accordance with the primary Green's function $\overline{\overline{G}}_1(\overline{r},\overline{r}')$ to match the boundary condition at the interface (which is $\rho>\rho'$ relation). Also anterior part should not contain any Hankel function as it is going to be evaluated inside the cylinder anywhere. Also, reflected wave contains depolarized component as it is the case for a dielectric cylinder. For $\overline{\overline{G}}_S^{[21]}(\overline{r},\overline{r}')$ we also take the following expression

$$\overline{\overline{G}}_S^{[21]}(\overline{r},\overline{r}')=\sum_{n=-\infty}^{\infty}\frac{i}{8\pi}\int_{-\infty}^{\infty}\mathrm{d}k_z\frac{1}{k_{1\rho}^2}\Big[\Big(A_n^{(21)}\overline{M}_{2n}^+(\overline{r};k_z)+B_n^{(21)}\overline{N}_{2n}^+(\overline{r};k_z)\Big)\overline{M}_{1,-n}(\overline{r}';-k_z)$$
$$+\Big(C_n^{(21)}\overline{N}_{2n}^+(\overline{r};k_z)+D_n^{(21)}\overline{M}_{2n}^+(\overline{r};k_z)\Big)\overline{N}_{1,-n}(\overline{r}';-k_z)\Big] \tag{10.3.41}$$

Again, the posterior part exactly follows the primary field to satisfies the boundary condition. Anterior art of the dyad is also consider that the co-polarize and cross polarized transmitted field should satisfy the radiation condition at infinity, and thats why they are taken wave function generated with Hankel function. It is clear that anterior part of $\overline{\overline{G}}_S^{[21]}(\overline{r},\overline{r}')$ is a wave that propagate in region 2 so the wave function written in the region 2.

### 10.3.2 Boundary conditions

The boundary condition on the posterior part of the dyadic Green's function has been applied in construction. On the other hand, the anterior part is the electric field within the observation medium

$$\overline{E}^{(j)}(\overline{r})=i\omega\mu\int \mathrm{d}^3\overline{r}'\overline{\overline{G}}^{[j1]}(\overline{r},\overline{r}')\cdot\overline{J}(\overline{r}') \tag{10.3.42}$$

and the magnetic field is give by

$$\overline{H}^{(j)}(\overline{r})=\frac{1}{i\omega\mu}\nabla\times\overline{E}^{(j)}(\overline{r})=\int \mathrm{d}^3\overline{r}'\nabla\times\overline{\overline{G}}^{[j1]}(\overline{r},\overline{r}')\cdot\overline{J}(\overline{r}') \tag{10.3.43}$$

and thus $\overline{\overline{G}}^{[j1]}(\overline{r},\overline{r}')$ should satisfy the electric field boundary condition across the interface. Taking the normal to the interface as $\hat{n}=\hat{\rho}$, then continuity of tangential electric and magnetic fields at $\rho=a$ mandate that

$$\begin{aligned}\hat{\rho}\times\left(\left[\overline{\overline{G}}_1(\overline{r},\overline{r}')+\overline{\overline{G}}_S^{[11]}(\overline{r},\overline{r}')\right]=\overline{\overline{G}}_S^{[21]}(\overline{r},\overline{r}')\right)\\ \hat{\rho}\times\nabla\times\left(\left[\overline{\overline{G}}_1(\overline{r},\overline{r}')+\overline{\overline{G}}_S^{[11]}(\overline{r},\overline{r}')\right]=\overline{\overline{G}}_S^{[21]}(\overline{r},\overline{r}')\right)\end{aligned} \tag{10.3.44}$$

Here, we consider non-magnetic materials. Defining the spectral components of the different dyadic Green's functions as

$$\overline{\overline{G}}(\overline{r},\overline{r}')=\sum_{n=-\infty}^{\infty}\frac{i}{8\pi}\int_{-\infty}^{\infty}\mathrm{d}k_z\frac{1}{k_{1\rho}^2}\tilde{\overline{\overline{G}}}_n(\overline{r},\overline{r}';k_z) \tag{10.3.45}$$

the boundary conditions will be translated to the corresponding constraint on the spectral components by virtue of the linearity.

$$\begin{aligned}\hat{\rho}\times\left[A_n^{(11)}\overline{M}_{1n}(\overline{r})+B_n^{(11)}\overline{N}_{1n}(\overline{r})+\overline{M}_{1n}^{+}(\overline{r})=A_n^{(21)}\overline{M}_{2n}^{+}(\overline{r})+B_n^{(21)}\overline{N}_{2n}^{+}(\overline{r})\right]\\ \hat{\rho}\times\left[C_n^{(11)}\overline{N}_{1n}(\overline{r})+D_n^{(11)}\overline{M}_{1n}(\overline{r})+\overline{N}_{1n}^{+}(\overline{r})=C_n^{(21)}\overline{N}_{2n}^{+}(\overline{r})+D_n^{(21)}\overline{M}_{2n}^{+}(\overline{r})\right]\end{aligned} \tag{10.3.46}$$

$$\begin{aligned}\hat{\rho}\times k_1\left[A_n^{(11)}\overline{N}_{1n}(\overline{r})+B_n^{(11)}\overline{M}_{1n}(\overline{r})+\overline{N}_{1n}^{+}(\overline{r})\right]=\hat{\rho}\times k_2\left[A_n^{(21)}\overline{N}_{2n}^{+}(\overline{r})+B_n^{(21)}\overline{M}_{2n}^{+}(\overline{r})\right]\\ \hat{\rho}\times k_1\left[C_n^{(11)}\overline{M}_{1n}(\overline{r})+D_n^{(11)}\overline{N}_{1n}(\overline{r})+\overline{M}_{1n}^{+}(\overline{r})\right]=\hat{\rho}\times k_2\left[C_n^{(21)}\overline{M}_{2n}^{+}(\overline{r})+D_n^{(21)}\overline{N}_{2n}^{+}(\overline{r})\right]\end{aligned} \tag{10.3.47}$$

where

$$\begin{aligned}\overline{N}_j(\overline{r})=\frac{1}{k_j}\nabla\times\overline{M}_j(\overline{r})\\ \overline{M}_j(\overline{r})=\frac{1}{k_j}\nabla\times\overline{N}_j(\overline{r})\end{aligned} \tag{10.3.48}$$

is used to replace the derivatives. The terms that contains derivatives should be evaluated at the interface $\rho{=}a$ after differentiation. The boundary equations can be separated into two parts and expressed in the matrix form as

$$\overline{\overline{M}}_1 \begin{bmatrix} A_n^{(11)} \\ B_n^{(11)} \\ A_n^{(21)} \\ B_n^{(21)} \end{bmatrix} = \begin{bmatrix} -\frac{\mathrm{d}H_n^{(1)}(k_{1\rho}\rho)}{\mathrm{d}\rho} \\ -\frac{nk_z}{a} H_n^{(1)}(k_{1\rho}a) \\ 0 \\ -k_{1\rho}^2 H_n^{(1)}(k_{1\rho}a) \end{bmatrix} \tag{10.3.49}$$

and

$$\overline{\overline{M}}_1 \begin{bmatrix} D_n^{(11)} \\ C_n^{(11)} \\ D_n^{(21)} \\ C_n^{(21)} \end{bmatrix} = \begin{bmatrix} -\frac{nk_z}{k_1 a} H_n^{(1)}(k_{1\rho}a) \\ -k_1 \frac{\mathrm{d}H_n^{(1)}(k_{1\rho}\rho)}{\mathrm{d}\rho} \\ -\frac{k_{1\rho}^2}{k_1} H_n^{(1)}(k_{1\rho}a) \\ 0 \end{bmatrix} \tag{10.3.50}$$

where,

$$\overline{\overline{M}}_1 = \begin{bmatrix} \frac{\mathrm{d}J_n(k_{1\rho}\rho)}{\mathrm{d}\rho} & \frac{nk_z}{k_1 a} J_n(k_{1\rho}a) & -\frac{\mathrm{d}H_n^{(1)}(k_{2\rho}\rho)}{\mathrm{d}\rho} & -\frac{nk_z}{k_2 a} H_n^{(1)}(k_{2\rho}a) \\ \frac{nk_z}{a} J_n(k_{1\rho}a) & k_1 \frac{\mathrm{d}J_n(k_{1\rho}\rho)}{\mathrm{d}\rho} & -\frac{nk_z}{a} H_n^{(1)}(k_{2\rho}a) & -k_2 \frac{\mathrm{d}H_n^{(1)}(k_{2\rho}\rho)}{\mathrm{d}\rho} \\ 0 & \frac{k_{1\rho}^2}{k_1} J_n(k_{1\rho}a) & 0 & -\frac{k_{2\rho}^2}{k_2} H_n^{(1)}(k_{2\rho}a) \\ k_{1\rho}^2 J_n(k_{1\rho}a) & 0 & -k_{2\rho}^2 H_n^{(1)}(k_{2\rho}a) & 0 \end{bmatrix} \tag{10.3.51}$$

## 10.4 Dyadic Green's function when source is outside of the cylinder

Assuming the source is located outside of the cylinder ($r{\geq}a$), then the objective is to find dyadic Green's functions of $\overline{\overline{G}}^{[22]}(\overline{r},\overline{r}')$ and $\overline{\overline{G}}^{[12]}(\overline{r},\overline{r}')$ for observation points inside and outside of the cylinder. Taking the linearity of the problem into account, we can construct

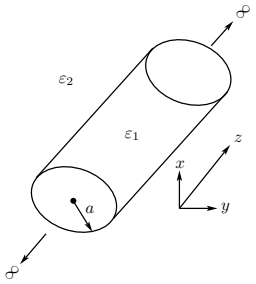


FIGURE 10.3: Geometry of the dielectric cylinder.

the Green's functions by superposition. If the space were to filled with $\varepsilon_2$ everywhere, then $\overline{\overline{G}}^{[22]}(\overline{r},\overline{r}')=\overline{\overline{G}}_2(\overline{r},\overline{r}')$ which is free space dyadic Green's function. Presence of the cylindrical boundary will cause reflections off the boundary into medium 2 as well as the field generated

in the absence of the boundary. So, the free space Green's function should be corrected by a scattering part $\overline{\overline{G}}_S^{[22]}(\overline{r},\overline{r}')$ such that

$$\overline{\overline{G}}^{[22]}(\overline{r},\overline{r}')=\overline{\overline{G}}_2(\overline{r},\overline{r}')+\overline{\overline{G}}_S^{[22]}(\overline{r},\overline{r}') \tag{10.4.1}$$

and the Green's function of $\overline{\overline{G}}^{[12]}(\overline{r},\overline{r}')$ is consequence of transmission of the field through the boundary. It contains only scattering part and not the free space part,

$$\overline{\overline{G}}^{[12]}(\overline{r},\overline{r}')=\overline{\overline{G}}_S^{[12]}(\overline{r},\overline{r}') \tag{10.4.2}$$

In order to distinguish between the vector wave functions that are constructed from Bessel function and Hankel functions we will write the latter by a plus sign like $\overline{M}^+$ and $\overline{N}^+$. Therefore, free space Green's function in region 1 is

$$\overline{\overline{G}}_2(\overline{r},\overline{r}')=\sum_{n=-\infty}^{\infty}\frac{i}{8\pi}\int_{-\infty}^{\infty}\mathrm{d}k_z\frac{1}{k_{2\rho}^2}\begin{cases}\overline{M}_{2n}^+(\overline{r};k_z)\overline{M}_{2,-n}(\overline{r}';-k_z)+\overline{N}_{2n}^+(\overline{r};k_z)\overline{N}_{2,-n}(\overline{r}';-k_z)\\ \\ \overline{M}_{2n}(\overline{r};k_z)\overline{M}_{2,-n}^+(\overline{r}';-k_z)+\overline{N}_{2n}(\overline{r};k_z)\overline{N}_{2,-n}^+(\overline{r}';-k_z)\end{cases}$$
$$-\frac{\hat{\rho}\hat{\rho}}{k_2^2}\delta(\overline{r}-\overline{r}')$$

where the top relation corresponds to $\rho>\rho'$ case. For the scattered part of the Green's function $\overline{\overline{G}}_S^{[22]}(\overline{r},\overline{r}')$ we consider the most general expansion that can match the boundary condition everywhere in primed coordinate (same dependence on the source coordinates as the exciting field)

$$\overline{\overline{G}}_S^{[22]}(\overline{r},\overline{r}')=\sum_{n=-\infty}^{\infty}\frac{i}{8\pi}\int_{-\infty}^{\infty}\mathrm{d}k_z\frac{1}{k_{2\rho}^2}\Big[\Big(A_n^{(22)}\overline{M}_{2n}^+(\overline{r};k_z)+B_n^{(22)}\overline{N}_{2n}^+(\overline{r};k_z)\Big)\overline{M}_{2,-n}^+(\overline{r}';-k_z) \tag{10.4.3}$$

$$+\Big(C_n^{(22)}\overline{N}_{2n}^+(\overline{r};k_z)+D_n^{(22)}\overline{M}_{2n}^+(\overline{r};k_z)\Big)\overline{N}_{2,n}^+(\overline{r}';-k_z)\Big] \tag{10.4.4}$$

The posterior part of the $\overline{\overline{G}}_S^{[22]}(\overline{r},\overline{r}')$ comes in accordance with the primary Green's function $\overline{\overline{G}}_2(\overline{r},\overline{r}')$ to match the boundary condition at the interface (which is $\rho<\rho'$ relation). Also anterior part is constructed by Hankel functions to satisfies the radiation condition at infinity. Also, reflected wave contains depolarized component as it is the case for a dielectric cylinder. For $\overline{\overline{G}}_S^{[12]}(\overline{r},\overline{r}')$ we also take the following expression

$$\overline{\overline{G}}_S^{[12]}(\overline{r},\overline{r}')=\sum_{n=-\infty}^{\infty}\frac{i}{8\pi}\int_{-\infty}^{\infty}\mathrm{d}k_z\frac{1}{k_{2\rho}^2}\Big[\Big(A_n^{(12)}\overline{M}_{1n}(\overline{r};k_z)+B_n^{(12)}\overline{N}_{1n}(\overline{r};k_z)\Big)\overline{M}_{2,-n}^+(\overline{r}';-k_z) \tag{10.4.5}$$

$$+\Big(C_n^{(12)}\overline{N}_{1n}(\overline{r};k_z)+D_n^{(12)}\overline{M}_{1n}(\overline{r};k_z)\Big)\overline{N}_{2,-n}^+(\overline{r}';-k_z)\Big] \tag{10.4.6}$$

Again, the posterior part exactly follows the primary field to satisfies the boundary condition. Anterior art of the dyad is also consider that the co-polarize and cross polarized

transmitted field should be regular at the origin, and thats why they are taken wave function generated with Bessel function. It is clear that anterior part of $\overline{\overline{G}}_S^{[12]}(\overline{r},\overline{r}')$ is a wave that propagate in region 1 so the wave functions in the anterior part are written using wave propagating in the region 1.

### 10.4.1 Boundary conditions

The boundary condition on the posterior part of the dyadic Green's function has been applied in construction. On the other hand, the anterior part is the electric field within the observation medium

$$\overline{E}^{(j)}(\overline{r})=i\omega\mu\int \mathrm{d}^3\overline{r}'\overline{\overline{G}}^{[j2]}(\overline{r},\overline{r}')\cdot\overline{J}(\overline{r}') \tag{10.4.7}$$

and the magnetic field is

$$\overline{H}^{(j)}(\overline{r})=\frac{1}{i\omega\mu}\nabla\times\overline{E}^{(j)}(\overline{r})=\int \mathrm{d}^3\overline{r}'\nabla\times\overline{\overline{G}}^{[j2]}(\overline{r},\overline{r}')\cdot\overline{J}(\overline{r}') \tag{10.4.8}$$

and thus $\overline{\overline{G}}^{[j2]}(\overline{r},\overline{r}')$ should satisfy the electric field boundary condition across the interface. Following the same procedure as interior problem, the Green's function coefficients can be obtained from,

$$\overline{\overline{M}}_2\begin{bmatrix}A_n^{(22)}\\B_n^{(22)}\\A_n^{(12)}\\B_n^{(12)}\end{bmatrix}=\begin{bmatrix}-\frac{\mathrm{d}J_n(k_{2\rho}\rho)}{\mathrm{d}\rho}\\-\frac{nk_z}{a}J_n(k_{2\rho}a)\\0\\-k_{2\rho}^2J_n(k_{2\rho}a)\end{bmatrix} \tag{10.4.9}$$

and,

$$\overline{\overline{M}}_2\begin{bmatrix}D_n^{(22)}\\C_n^{(22)}\\D_n^{(12)}\\C_n^{(12)}\end{bmatrix}=\begin{bmatrix}-\frac{nk_z}{k_2a}J_n(k_{2\rho}a)\\-k_2\frac{\mathrm{d}J_n(k_{2\rho}\rho)}{\mathrm{d}\rho}\\-\frac{k_{2\rho}^2}{k_2}J_n(k_{2\rho}a)\\0\end{bmatrix} \tag{10.4.10}$$

where,

$$\overline{\overline{M}}_2=\begin{bmatrix}\frac{\mathrm{d}H_n^{(1)}(k_{2\rho}\rho)}{\mathrm{d}\rho} & \frac{nk_z}{k_2a}H_n^{(1)}(k_{2\rho}a) & -\frac{\mathrm{d}J_n(k_{1\rho}\rho)}{\mathrm{d}\rho} & -\frac{nk_z}{k_1a}J_n(k_{1\rho}a)\\ \frac{nk_z}{a}H_n^{(1)}(k_{2\rho}a) & k_2\frac{\mathrm{d}H_n^{(1)}(k_{2\rho}\rho)}{\mathrm{d}\rho} & -\frac{nk_z}{a}J_n(k_{1\rho}a) & -k_1\frac{\mathrm{d}J_n(k_{1\rho}\rho)}{\mathrm{d}\rho}\\ 0 & \frac{k_{2\rho}^2}{k_2}H_n^{(1)}(k_{2\rho}a) & 0 & -\frac{k_{1\rho}^2}{k_1}J_n(k_{1\rho}a)\\ k_{2\rho}^2H_n^{(1)}(k_{2\rho}a) & 0 & -k_{1\rho}^2J_n(k_{1\rho}a) & 0\end{bmatrix} \tag{10.4.11}$$

The solution to this system of equations can be obtained from the problem of source inside the cylinder with $1\rightarrow2$ and Bessel functions become Hankel functions. The matrices $\overline{\overline{M}}_1$ and $\overline{\overline{M}}_2$ has the same form except exchanging the medium ($1\leftrightarrow2$) and transforming the Hankel function to Bessel function and vice versa which is manifestation of the Reciprocity.

## 10.5 Casimir Force calculation using the scattered wave Green's function

By adding the polarization source $\overline{P}$ (which arise from the fluctuating electromagnetic fields everywhere even at vacuum and zero temperature) to the Maxwell's equations, one can solve for the excited fields in the medium and then find the desired stress on the object of interest.

$$\begin{aligned}\nabla\times\overline{E}&=i\omega\mu\overline{H}\\ \nabla\times\overline{H}&=-i\omega\epsilon\overline{E}-i\omega\overline{P}\end{aligned} \tag{10.5.1}$$

However, it can be shown that evaluation of Maxwell's stress tensor is possible without finding the fields in the medium explicitly. Instead of finding electromagnetic field in the medium, it is possible to introduce boundary condition of the problem into the scenario through the Green's function of the corresponding problem. This is not strange as the Green's function contains all details of the physical problem. This method has the advantage of separating statistical properties of the fluctuating sources from deterministic procedure of solving a boundary value problem to find the Green's function.

Vector wave equation for electric field with fluctuating polarization $\overline{P}$ as a source is given by

$$\nabla\times\nabla\times\overline{E}-\omega^2\mu\epsilon\overline{E}=\omega^2\mu\overline{P} \tag{10.5.2}$$

In order to solve wave equation, we introduce corresponding dyadic Green's function $\overline{\overline{G}}(\overline{r},\overline{r}')$ which satisfies the same vector wave equation

$$\nabla\times\nabla\times\overline{\overline{G}}(\overline{r},\overline{r}')-\omega^2\mu\epsilon\overline{\overline{G}}(\overline{r},\overline{r}')=\overline{\overline{I}}\delta(\overline{r}-\overline{r}') \tag{10.5.3}$$

Also $\overline{\overline{G}}(\overline{r},\overline{r}')$ satisfies the same boundary condition as the electric field. With this informations, we can find the electric field directly with the help of dyadic Green's function

$$\overline{E}(\overline{r})=\omega^2\mu\int \mathrm{d}\overline{r}'\overline{\overline{G}}(\overline{r},\overline{r}')\cdot\overline{P}(\overline{r}') \tag{10.5.4}$$

The power spectral density of the electric field can be obtained as

$$\left\langle\overline{E}(\overline{r},\omega)\overline{E}(\overline{r}',\omega')^*\right\rangle=(\omega^2\mu)(\omega'^2\mu)\int \mathrm{d}\overline{s}'\int \mathrm{d}\overline{s}\overline{\overline{G}}(\overline{r},\overline{s},\omega)\cdot\left\langle\overline{P}(\overline{s})\overline{P}(\overline{s}')^*\right\rangle\cdot\overline{\overline{G}}^*(\overline{s}',\overline{r}',\omega') \tag{10.5.5}$$

Upon using the Rytov relation for the power spectral density of the noise polarization [171, 172],

$$\left\langle\overline{P}(\overline{s})\overline{P}(\overline{s}')^*\right\rangle=\frac{\hbar\varepsilon_0}{\pi}\coth\left(\frac{\hbar\omega}{2k_BT}\right)\mathrm{Im}\epsilon(\overline{s},\omega)\delta(\overline{s}-\overline{s}')\delta(\omega-\omega')\overline{\overline{I}} \tag{10.5.6}$$

we have

$$\left\langle\overline{E}(\overline{r},\omega)\overline{E}(\overline{r}',\omega)^*\right\rangle=(\omega^2\mu)^2\frac{\hbar\varepsilon_0}{\pi}\coth\left(\frac{\hbar\omega}{2k_BT}\right)\int \mathrm{d}\overline{s}\ \mathrm{Im}\epsilon(\overline{s},\omega)\overline{\overline{G}}(\overline{r},\overline{s},\omega)\cdot\overline{\overline{G}}^*(\overline{s},\overline{r}',\omega')\delta(\omega-\omega') \tag{10.5.7}$$

Using the complex reciprocity relation of Chapter 1, the dyadic Green's function $\overline{\overline{G}}$ satisfies the following integral equation

$$\int \mathrm{d}\bar{s}\ (\omega^2\mu_0\epsilon_0)\mathrm{Im}\epsilon(\bar{s},\omega)\overline{\overline{G}}(\bar{r},\bar{s},\omega)\cdot\overline{\overline{G}}^*(\bar{s},\bar{r}',\omega')=\mathrm{Im}\ \overline{\overline{G}}(\bar{r},\bar{r}',\omega) \tag{10.5.8}$$

Therefore, the power spectral density of the electric field can be simplified to

$$\left\langle \overline{E}(\bar{r},\omega)\overline{E}(\bar{r}',\omega')^*\right\rangle=(\omega^2\mu)\frac{\hbar}{\pi}\coth\left(\frac{\hbar\omega}{2k_BT}\right)\mathrm{Im}\overline{\overline{G}}(\bar{r},\bar{r}',\omega)\delta(\omega-\omega') \tag{10.5.9}$$

Similarly, contribution of the magnetic field into the stress tensor can be characterized by the power spectral density of the magnetic field which can be obtained from the Maxwell's equations,

$$\left\langle \overline{H}(\bar{r},\omega)\overline{H}(\bar{r}',\omega')^*\right\rangle=\frac{\hbar}{\pi\mu}\coth\left(\frac{\hbar\omega}{2k_BT}\right)\delta(\omega-\omega')\nabla\times\mathrm{Im}\overline{\overline{G}}(\bar{r},\bar{r}',\omega)\times\nabla' \tag{10.5.10}$$

The averaged time domain expressions for the real fields at $t=0$ (for stationary field processes) can be obtained as

$$\begin{aligned}\left\langle \overline{E}(\bar{r})\overline{E}(\bar{r}')\right\rangle&=\frac{\mu\hbar}{\pi}\int_0^\infty \mathrm{d}\omega\ \omega^2\coth\left(\frac{\hbar\omega}{2k_BT}\right)\mathrm{Im}\overline{\overline{G}}(\bar{r},\bar{r}',\omega)\\ \left\langle \overline{H}(\bar{r})\overline{H}(\bar{r}')\right\rangle&=\frac{\hbar}{\mu\pi}\int_0^\infty \mathrm{d}\omega\ \coth\left(\frac{\hbar\omega}{2k_BT}\right)\nabla\times\mathrm{Im}\overline{\overline{G}}(\bar{r},\bar{r}',\omega)\times\nabla'\end{aligned} \tag{10.5.11}$$

Based on the linearity of the problem, the Green's function can be always decomposed to a bulk part $\overline{\overline{G}}^{(0)}(\bar{r},\bar{r}')$ which is responsible for radiation in free space (solution of inhomogeneous wave equation subject to radiation condition), and an scattered part $\overline{\overline{G}}^{(s)}(\bar{r},\bar{r}')$ which is solution of homogeneous wave equation (divergence free part) and is required for satisfaction of border conditions of the full Green's function. As it can be seen from the construction of the total Green's function by superposition approach, the free part does not depends in the geometry of the problem and corresponds to the zero point energy of the background. This term does not contribute to the self stress on the body of interest (virtual work is identically zero). On the other side, although the stress is a quadratic function of the field amplitude, it depends on the Green's function through a linear relation that allows us to remove the bulk contribution without changing the stress. Although removing the free Green's function contribution completely removes the divergence in the Casimir stress in the planar case, it will be shown that after subtraction of bulk response in cylindrical geometry, the Casimir stress is still divergent and need additional treatments.

$$\langle\overline{\overline{T}}(\bar{r})\rangle=\varepsilon\langle\overline{E}(\bar{r})\overline{E}(\bar{r})\rangle+\mu\langle\overline{H}(\bar{r})\overline{H}(\bar{r})\rangle-\frac{1}{2}\overline{\overline{I}}\left[\varepsilon\langle\overline{E}(\bar{r})\cdot\overline{E}(\bar{r})\rangle+\mu\langle\overline{H}(\bar{r})\cdot\overline{H}(\bar{r})\rangle\right] \tag{10.5.12}$$

Since $\mathrm{Tr}\left(\overline{E}(\bar{r})\overline{E}(\bar{r})\right)=\overline{E}(\bar{r})\cdot\overline{E}(\bar{r})$, the stress tensor can be written as

$$\langle\overline{\overline{T}}(\bar{r})\rangle=\lim_{\bar{r}\to\bar{r}'}\left[\overline{\overline{Q}}(\bar{r},\bar{r}')-\frac{1}{2}\mathrm{Tr}\overline{\overline{Q}}(\bar{r},\bar{r}')\right] \tag{10.5.13}$$

where

$$\overline{\overline{Q}}(\overline{r},\overline{r}')=\frac{\hbar}{\pi}\int_0^\infty \mathrm{d}\omega\left[\frac{\omega^2}{c^2}\mathrm{Im}\overline{\overline{G}}^s(\overline{r},\overline{r}')+\nabla\times\mathrm{Im}\overline{\overline{G}}^s(\overline{r},\overline{r}')\times\nabla'\right] \tag{10.5.14}$$

The integration over the frequency can be deformed to the imaginary axis by virtue of analyticity of the retarded Green's function over the upper half plane of $\omega-$plane. For the first term,

$$\begin{aligned}\int_0^\infty \mathrm{d}\omega\ \omega^2\mathrm{Im}\overline{\overline{G}}^s(\overline{r},\overline{r}')&=\frac{1}{2i}\int_0^\infty \mathrm{d}\omega\ \omega^2\left[\overline{\overline{G}}^s(\overline{r},\overline{r}';\omega)-\overline{\overline{G}}^{s*}(\overline{r},\overline{r}';\omega)\right]\\&=\frac{1}{2i}\int_0^\infty \mathrm{d}\omega\ \omega^2\left[\overline{\overline{G}}^s(\overline{r},\overline{r}';\omega)-\overline{\overline{G}}^s(\overline{r},\overline{r}';-\omega)\right]\\&=\frac{1}{2i}\int_0^\infty \mathrm{d}\omega\ \omega^2\overline{\overline{G}}^s(\overline{r},\overline{r}';\omega)-\frac{1}{2i}\int_0^\infty \mathrm{d}\omega\ \omega^2\overline{\overline{G}}^s(\overline{r},\overline{r}';-\omega)\end{aligned} \tag{10.5.15}$$

where we have used the Hermitian property of the Green's function $\overline{\overline{G}}^{s*}(\overline{r},\overline{r}';\omega)=\overline{\overline{G}}^s(\overline{r},\overline{r}';-\omega)$ (which corresponds to a real function in time domain). Changing the integration variable $\omega\to-\omega$ in the second integral,

$$\begin{aligned}\int_0^\infty \mathrm{d}\omega\ \omega^2\mathrm{Im}\overline{\overline{G}}^s(\overline{r},\overline{r}')&=\frac{1}{2i}\int_0^\infty \mathrm{d}\omega\ \omega^2\overline{\overline{G}}^s(\overline{r},\overline{r}';\omega)+\frac{1}{2i}\int_0^{-\infty} \mathrm{d}\omega\ \omega^2\overline{\overline{G}}^s(\overline{r},\overline{r}';\omega)\\&=\frac{1}{2i}\left(\int_0^\infty+\int_0^{-\infty}\right)\mathrm{d}\omega\ \omega^2\overline{\overline{G}}^s(\overline{r},\overline{r}';\omega)\end{aligned} \tag{10.5.16}$$

Now, according to the Causality principle for the retarded Green's function $\overline{\overline{G}}(\overline{r},\overline{r}';t,t')$, we should have [12, 174]

$$\overline{\overline{G}}(\overline{r},\overline{r}';t,t')=0\qquad\text{for}\quad t<t' \tag{10.5.17}$$

Herein, $t$, and $t'$ refer to the observation and excitation times, respectively. The Green's function $\overline{\overline{G}}(\overline{r},\overline{r}';t,t')$ is stationary in time and depends on $t$ and $t'$ through $t-t'$ and is related to it's frequency domain counterpart by

$$\overline{\overline{G}}(\overline{r},\overline{r}';t,t')=\int \mathrm{d}\omega\ \overline{\overline{G}}(\overline{r},\overline{r}';\omega)e^{-i\omega(t-t')} \tag{10.5.18}$$

The asymptotic behavior of the Green's function as $\omega\to\infty$ can be obtained from the vector wave equation

$$\nabla\times\nabla\times\overline{\overline{G}}(\overline{r},\overline{r}';\omega)-\omega^2\mu\varepsilon\overline{\overline{G}}(\overline{r},\overline{r}';\omega)=\overline{\overline{I}}\delta(\overline{r}-\overline{r}') \tag{10.5.19}$$

thus,

$$\overline{\overline{G}}(\overline{r},\overline{r}';\omega)\approx-\frac{c^2}{\omega^2}\overline{\overline{I}}\delta(\overline{r}-\overline{r}')\quad\text{as}\quad\omega\to\infty \tag{10.5.20}$$

The singularity only happens for the primary part of the Green's function and the scattering part is always regular at $\overline{r}=\overline{r}'$. With the knowledge of this asymptotic behavior, the dyadic Green's function satisfies the Jordan's lemma on a path at infinity and the inverse Fourier

transform over real axis can be written in terms of a contour integral over upper half plane of the complex $\omega$-plane. Then, it shows that for $t<t'$, the following complex integral vanishes,

$$\int_{C^+} \mathrm{d}\omega \overline{\overline{G}}(\overline{r},\overline{r}';\omega)e^{-i\omega(t-t')}=0 \tag{10.5.21}$$

where $C^+$ is a contour that include the real $\omega$ axis and closes in the upper half plane on $\omega$ at infinity. This result also shows that the dyadic Green's function $\overline{\overline{G}}(\overline{r},\overline{r}';\omega)$ does not have any singularity in the upper half plane of the complex $\omega$ plane. Therefore, it is possible to

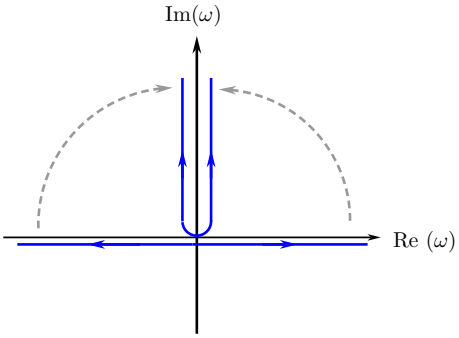


FIGURE 10.4: Deformation of contour of integration in the complex $\omega$-plane

deform the contour of integration from real axis to the imaginary axis without crossing any singularity. Taking $\omega=i\zeta$ over the imaginary axis of the complex $\omega$-plane, we have

$$\int_0^\infty \mathrm{d}\omega\ \omega^2 \mathrm{Im}\overline{\overline{G}}^s(\overline{r},\overline{r}';\omega)=-\int \mathrm{d}\zeta\ \zeta^2\overline{\overline{G}}^s(\overline{r},\overline{r}';i\zeta) \tag{10.5.22}$$

Similarly,

$$\begin{aligned}\int_0^\infty \mathrm{d}\omega\ \mathrm{Im}\overline{\overline{G}}^s(\overline{r},\overline{r}';\omega)&=\frac{1}{2i}\int_0^\infty \mathrm{d}\omega\ \overline{\overline{G}}^s(\overline{r},\overline{r}';\omega)+\frac{1}{2i}\int_0^{-\infty} \mathrm{d}\omega\ \overline{\overline{G}}^s(\overline{r},\overline{r}';\omega) \\ &=\frac{1}{2i}\left(\int_0^\infty+\int_0^{-\infty}\right)\mathrm{d}\omega\ \overline{\overline{G}}^s(\overline{r},\overline{r}';\omega)\end{aligned} \tag{10.5.23}$$

After a wick's rotation $\omega=i\zeta$ in Fig. 10.4 for both semi infinite contours we have

$$\int_0^\infty \mathrm{d}\omega\ \mathrm{Im}\overline{\overline{G}}^s(\overline{r},\overline{r}';\omega)=\frac{1}{2i}\left(\int_0^\infty+\int_0^\infty\right)i\mathrm{d}\zeta\ \overline{\overline{G}}^s(\overline{r},\overline{r}';i\zeta)=\int_0^\infty \mathrm{d}\zeta\ \overline{\overline{G}}^s(\overline{r},\overline{r}';i\zeta) \tag{10.5.24}$$

and then upon applying curls from both sides we arrive at

$$\int_0^\infty \mathrm{d}\omega\ \nabla\times\mathrm{Im}\overline{\overline{G}}^s(\overline{r},\overline{r}';\omega)\times\nabla'=\int_0^\infty \mathrm{d}\zeta\ \nabla\times\overline{\overline{G}}^s(\overline{r},\overline{r}';i\zeta)\times\nabla' \tag{10.5.25}$$

The stress tensor can be expressed as

$$\overline{\overline{T}}=\lim_{\overline{r}\to\overline{r}'}\left[\overline{\overline{Q}}(\overline{r},\overline{r}')-\frac{1}{2}\mathrm{Tr}\overline{\overline{Q}}(\overline{r},\overline{r}')\right] \tag{10.5.26}$$

where

$$\overline{\overline{Q}}=\frac{\hbar}{\pi}\int_0^\infty \mathrm{d}\zeta\left[-\frac{\zeta^2}{c^2}\overline{\overline{G}}^s(\overline{r},\overline{r}';i\zeta)+\nabla\times\overline{\overline{G}}^s(\overline{r},\overline{r}';i\zeta)\times\nabla'\right] \tag{10.5.27}$$

## 10.6 Calculating the Stress Tensor

### 10.6.1 Stress contribution from fields inside the cylinder

The scattering part of the dyadic Green's function for source and observation points inside a finite cylinder of radius $a$ has been derived as

$$\overline{\overline{G}}_S^{[11]}(\overline{r},\overline{r}')=\sum_{n=-\infty}^{\infty}\frac{i}{8\pi}\int_{-\infty}^{\infty}\mathrm{d}k_z\frac{1}{k_{1\rho}^2}\Big[\Big(A_n^{(11)}\overline{M}_{1n}(\overline{r};k_z)+B_n^{(11)}\overline{N}_{1n}(\overline{r};k_z)\Big)\overline{M}_{1,-n}(\overline{r}';-k_z) \tag{10.6.1}$$
$$+\Big(C_n^{(11)}\overline{N}_{1n}(\overline{r};k_z)+D_n^{(11)}\overline{M}_{1n}(\overline{r};k_z)\Big)\overline{N}_{1,-n}(\overline{r}';-k_z)\Big]$$

or using the spectral component of the dyadic Green's function

$$\overline{\overline{G}}_{S,n}^{[11]}(\overline{r},\overline{r}';k_z)=\Big(A_n^{(11)}\overline{M}_{1n}(\overline{r};k_z)+B_n^{(11)}\overline{N}_{1n}(\overline{r};k_z)\Big)\overline{M}_{1,-n}(\overline{r}';-k_z) \tag{10.6.2}$$
$$+\Big(C_n^{(11)}\overline{N}_{1n}(\overline{r};k_z)+D_n^{(11)}\overline{M}_{1n}(\overline{r};k_z)\Big)\overline{N}_{1,-n}(\overline{r}';-k_z)$$

where the spatial domain counterpart can be written as

$$\overline{\overline{G}}_S^{[11]}(\overline{r},\overline{r}')=\sum_{n=-\infty}^{\infty}\frac{i}{8\pi}\int_{-\infty}^{\infty}\mathrm{d}k_z\frac{1}{k_{1\rho}^2}\overline{\overline{G}}_{S,n}^{[11]}(\overline{r},\overline{r}';k_z) \tag{10.6.3}$$

For the propagator of the magnetic field, if we define the scattering dyadic Green's function of $\overline{\overline{K}}_S^{[11]}(\overline{r},\overline{r}')$ as

$$\overline{\overline{K}}_S^{[11]}(\overline{r},\overline{r}')=\frac{1}{k_1^2}\nabla\times\overline{\overline{G}}_S^{[11]}(\overline{r},\overline{r}')\times\nabla' \tag{10.6.4}$$

then, the spectral components of the $\overline{\overline{K}}$ can be obtained as

$$\overline{\overline{K}}_{S,n}^{[11]}(\overline{r},\overline{r}';k_z)=\Big(A_n^{(11)}\overline{N}_{1n}(\overline{r};k_z)+B_n^{(11)}\overline{M}_{1n}(\overline{r};k_z)\Big)\overline{N}_{1,-n}(\overline{r}';-k_z) \tag{10.6.5}$$
$$+\Big(C_n^{(11)}\overline{M}_{1n}(\overline{r};k_z)+D_n^{(11)}\overline{N}_{1n}(\overline{r};k_z)\Big)\overline{M}_{1,-n}(\overline{r}';-k_z)$$

In order to calculate the $\hat{\rho}\hat{\rho}$ component of the stress tensor, we use the cylindrical coordinate unit vectors $\hat{\rho},\hat{\phi},\hat{z}$ to expand the components of the dyadic Green's function and find the trace. Because we are interested in the $\rho\rho$ component of the stress tensor $T_{\rho\rho}$,

$$\hat{\rho}\cdot\overline{\overline{G}}_{S,n}^{[11]}(\overline{r},\overline{r}';k_z)\cdot\hat{\rho}=\Big(A_n^{(11)}M_{1n}^{\rho}(\overline{r};k_z)+B_n^{(11)}N_{1n}^{\rho}(\overline{r};k_z)\Big)M_{1,-n}^{\rho}(\overline{r}';-k_z) \tag{10.6.6}$$
$$+\Big(C_n^{(11)}N_{1n}^{\rho}(\overline{r};k_z)+D_n^{(11)}M_{1n}^{\rho}(\overline{r};k_z)\Big)\overline{N}_{1,-n}^{\rho}(\overline{r}';-k_z)$$

And also the trace of the electric field dyadic Green's function is given by

$$\begin{aligned}\text{Tr }\overline{\overline{G}}^{[11]}_{S,n}(\overline{r},\overline{r}';k_z)=&A_n^{(11)}\Big[M^{\rho}_{1n}M^{\rho}_{1,-n}+M^{\phi}_{1n}M^{\phi}_{1,-n}+M^{z}_{1n}M^{z}_{1,-n}\Big]+B_n^{(11)}\Big[N^{\rho}_{1n}M^{\rho}_{1,-n}+N^{\phi}_{1n}M^{\phi}_{1,-n}\\&+N^{z}_{1n}(\overline{r})M^{z}_{1,-n}\Big]+C_n^{(11)}\Big[N^{\rho}_{1n}N^{\rho}_{1,-n}+N^{\phi}_{1n}N^{\phi}_{1,-n}+N^{z}_{1n}N^{z}_{1,-n}\Big]\\&+D_n^{(11)}\Big[M^{\rho}_{1n}\overline{N}^{\rho}_{1,-n}+M^{\phi}_{1n}\overline{N}^{\phi}_{1,-n}+M^{z}_{1n}\overline{N}^{z}_{1,-n}\Big]\end{aligned}$$

then,

$$\begin{aligned}&\hat{\rho}\cdot\overline{\overline{G}}^{[11]}_{S,n}(\overline{r},\overline{r}';k_z)\cdot\hat{\rho}-\frac{1}{2}\text{Tr }\overline{\overline{G}}^{[11]}_{S,n}(\overline{r},\overline{r}';k_z)\\&\quad=\frac{1}{2}\Big(A_n^{(11)}\Big[M^{\rho}_{1n}M^{\rho}_{1,-n}-M^{\phi}_{1n}M^{\phi}_{1,-n}-M^{z}_{1n}M^{z}_{1,-n}\Big]+B_n^{(11)}\Big[N^{\rho}_{1n}M^{\rho}_{1,-n}\\&\quad-N^{\phi}_{1n}M^{\phi}_{1,-n}-N^{z}_{1n}(\overline{r})M^{z}_{1,-n}\Big]+C_n^{(11)}\Big[N^{\rho}_{1n}N^{\rho}_{1,-n}-N^{\phi}_{1n}N^{\phi}_{1,-n}-N^{z}_{1n}N^{z}_{1,-n}\Big]\\&\quad+D_n^{(11)}\Big[M^{\rho}_{1n}\overline{N}^{\rho}_{1,-n}-M^{\phi}_{1n}\overline{N}^{\phi}_{1,-n}-M^{z}_{1n}\overline{N}^{z}_{1,-n}\Big]\Big)\\&\quad=:Q_E\end{aligned}$$

where $Q_E$ is the electric field contribution to the stress tensor. Similarly, for $\overline{\overline{K}}$ we have,

$$\begin{aligned}&\hat{\rho}\cdot\overline{\overline{K}}^{[11]}_{S,n}(\overline{r},\overline{r}';k_z)\cdot\hat{\rho}-\frac{1}{2}\text{Tr }\overline{\overline{K}}^{[11]}_{S,n}(\overline{r},\overline{r}';k_z)\\&\quad=\frac{1}{2}\Big(A_n^{(11)}\Big[N^{\rho}_{1n}N^{\rho}_{1,-n}-N^{\phi}_{1n}N^{\phi}_{1,-n}-N^{z}_{1n}N^{z}_{1,-n}\Big]+B_n^{(11)}\Big[M^{\rho}_{1n}N^{\rho}_{1,-n}-M^{\phi}_{1n}N^{\phi}_{1,-n}\\&\quad-M^{z}_{1n}(\overline{r})N^{z}_{1,-n}\Big]+C_n^{(11)}\Big[M^{\rho}_{1n}M^{\rho}_{1,-n}-M^{\phi}_{1n}M^{\phi}_{1,-n}-M^{z}_{1n}M^{z}_{1,-n}\Big]\\&\quad+D_n^{(11)}\Big[N^{\rho}_{1n}\overline{M}^{\rho}_{1,-n}-N^{\phi}_{1n}\overline{M}^{\phi}_{1,-n}-N^{z}_{1n}\overline{M}^{z}_{1,-n}\Big]\Big)\\&\quad=:Q_H\end{aligned}$$

and $Q_H$ is the magnetic field contribution to the stress tensor. Using components of the vector wave functions, and by taking $\overline{r}=\overline{r}'$, we would have

$$\begin{aligned}\Big[N^{\rho}_{1n}N^{\rho}_{1,-n}-N^{\phi}_{1n}N^{\phi}_{1,-n}-N^{z}_{1n}N^{z}_{1,-n}\Big]&=\Big(\frac{k_z^2}{k^2}\Big[\frac{\mathrm{d}J_n(k_\rho\rho)}{\mathrm{d}\rho}\Big]^2-\frac{n^2k_z^2}{k^2\rho^2}[J_n(k_\rho\rho)]^2-\frac{k_\rho^4}{k^2}[J_n(k_\rho\rho)]^2\Big)\\\Big[M^{\rho}_{1n}M^{\rho}_{1,-n}-M^{\phi}_{1n}M^{\phi}_{1,-n}-M^{z}_{1n}M^{z}_{1,-n}\Big]&=\Big(\frac{n^2}{\rho^2}[J_n(k_\rho\rho)]^2-\Big[\frac{\mathrm{d}J_n(k_\rho\rho)}{\mathrm{d}\rho}\Big]^2\Big)\\\Big[M^{\rho}_{1n}N^{\rho}_{1,-n}-M^{\phi}_{1n}N^{\phi}_{1,-n}-M^{z}_{1n}N^{z}_{1,-n}\Big]&=\frac{nk_z}{k\rho}J_n(k_\rho\rho)\frac{\mathrm{d}J_{-n}(k_\rho\rho)}{\mathrm{d}\rho}-\frac{nk_z}{k\rho}J_{-n}(k_\rho\rho)\frac{\mathrm{d}J_n(k_\rho\rho)}{\mathrm{d}\rho}=0\\\Big[N^{\rho}_{1n}\overline{M}^{\rho}_{1,-n}-N^{\phi}_{1n}\overline{M}^{\phi}_{1,-n}-N^{z}_{1n}\overline{M}^{z}_{1,-n}\Big]&=\frac{nk_z}{k\rho}J_{-n}(k_\rho\rho)\frac{\mathrm{d}J_n(k_\rho\rho)}{\mathrm{d}\rho}-\frac{nk_z}{k\rho}J_n(k_\rho\rho)\frac{\mathrm{d}J_{-n}(k_\rho\rho)}{\mathrm{d}\rho}=0\end{aligned}$$

Then using vanishing components, the $\rho\rho$ component of the stress tensor arose from the fields inside the cylinder depends can be expressed as

$$T_{\rho\rho}=-\frac{i\hbar}{8\pi^2c^2}\int_0^\infty \mathrm{d}\zeta\ \zeta^2\sum_{n=-\infty}^{\infty}\int_{-\infty}^{\infty}\mathrm{d}k_z\frac{1}{k_{1\rho}^2}\Big[Q_E(i\zeta)+Q_H(i\zeta)\Big] \tag{10.6.7}$$

where the total contribution of the electric and magnetic field is given by

$$\begin{aligned} Q_{\text{Total}}(\omega)&=Q_E+Q_H \\ &=\frac{1}{2}\Big(A_n^{(11)}+C_n^{(11)}\Big)\Bigg\{\Big[N_{1n}^{\rho}N_{1,-n}^{\rho}-N_{1n}^{\phi}N_{1,-n}^{\phi}-N_{1n}^{z}N_{1,-n}^{z}\Big] \\ &\qquad+\Big[M_{1n}^{\rho}M_{1,-n}^{\rho}-M_{1n}^{\phi}M_{1,-n}^{\phi}-M_{1n}^{z}M_{1,-n}^{z}\Big]\Bigg\} \end{aligned} \tag{10.6.8}$$

Noting that the integrand of the stress depends on $k_z$ through a quadratic form, then the integral can be simplified to

$$T_{\rho\rho}=-\frac{i\hbar}{4\pi^2c^2}\int_0^\infty \mathrm{d}\zeta\ \zeta^2\sum_{n=-\infty}^{\infty}\int_{0}^{\infty}\mathrm{d}k_z\frac{1}{k_{1\rho}^2}\Big[Q_E(i\zeta)+Q_H(i\zeta)\Big] \tag{10.6.9}$$

### 10.6.2 Perfect conductor limit $\varepsilon_2\to\infty$

In the limit of the perfect conductor in the region 2

$$\begin{aligned} \xi_2&=k_{2\rho}a=a\sqrt{k_2^2-k_z^2} \\ \xi_1&=k_{1\rho}a=a\sqrt{k_1^2-k_z^2} \end{aligned} \tag{10.6.10}$$

Then $\xi_1/\xi_2\to 0$ for any finite value of $k_z$. Also,

$$\frac{\xi_1 k_2^2}{\xi_2 k_1^2}\to\frac{k_2^2}{k_1^2}\frac{\xi_1}{k_2 a}=k_2\frac{k_{1\rho}}{k_1^2}\to\infty \tag{10.6.11}$$

and

$$\frac{\xi_1^2 k_2}{\xi_2^2 k_1}\to\frac{k_{1\rho}^2 k_2}{k_2^2 k_1}=\frac{k_{1\rho}^2}{k_2 k_1}\to 0 \tag{10.6.12}$$

Using asymptotic forms of the Hankel function for large arguments we obtain,

$$\begin{aligned} C_n^{(11)}&=-\frac{H_n^{(1)}(\xi_1)}{J_n(\xi_1)} \\ A_n^{(11)}&=-\frac{H_n^{'(1)}(\xi_1)}{J_n'(\xi_1)} \end{aligned} \tag{10.6.13}$$

The coefficients $B_n$ and $D_n$ in the limit of $k_2\to\infty$ become zero. Total contribution of the electric and magnetic field inside the cylinder in the radial stress can be written as

$$T_{\rho\rho}=-\frac{i\hbar}{4\pi^2c^2}\int_0^\infty \mathrm{d}\zeta\ \zeta^2\sum_{n=-\infty}^{\infty}\int_{0}^{\infty}\mathrm{d}k_z\frac{1}{k_{1\rho}^2}Q_{\text{Total}}(\omega) \tag{10.6.14}$$

$$Q_{\text{Total}}(\omega)=-\frac{1}{2}\left(\frac{H_n^{(1)}(\xi_1)}{J_n(\xi_1)}+\frac{H_n^{'(1)}(\xi_1)}{J_n'(\xi_1)}\right)\frac{k_{1\rho}^2}{k_1^2}\left\{-k_{1\rho}^2\left[\frac{\mathrm{d}J_n(k_{1\rho}\rho)}{k_{1\rho}\mathrm{d}\rho}\right]^2+\left(\frac{n^2}{\rho^2}-k_{1\rho}^2\right)J_n^2(k_{1\rho}\rho)\right\} \tag{10.6.15}$$

### 10.6.3 Imaginary Frequency

The dyadic Green's function is analytic over the complex $\omega-$plane and by applying a wick rotation we can write the frequency integral over $\omega$ as an integral over the imaginary axis of $\omega=i\zeta$ where,

$$k^2=\omega^2\mu\varepsilon=-\frac{\zeta^2}{c^2} \tag{10.6.16}$$

and also under transformation, $k_\rho$ becomes,

$$k_\rho=\sqrt{k^2-k_z^2}=\sqrt{-\frac{\zeta^2}{c^2}-k_z^2}=\pm i\sqrt{\frac{\zeta^2}{c^2}+k_z^2} \tag{10.6.17}$$

and as a result, all of the Bessel and Hankel functions becomes the modified Bessel and modified Hankel functions, respectively. The sign of $k_\rho$ should be selected in accordance with the radiation boundary condition. The outgoing cylindrical waves are proportional to

$$H_n^{(1)}(k_\rho\rho)\propto e^{ik_\rho\rho}\quad,\quad\text{as}\quad\rho\to\infty \tag{10.6.18}$$

Then radiation condition mandates that $\mathrm{Im}(k_\rho)>0$ and thus,

$$k_\rho=i\sqrt{\frac{\zeta^2}{c^2}+k_z^2} \tag{10.6.19}$$

On the other hand using the relation between the Bessel and modified Bessel functions

$$\begin{aligned}J_n(i\xi)&=i^nI_n(\xi)\\ H_n^{(1)}(i\xi)&=\frac{2}{\pi}(-i)^{n+1}K_n(\xi)\end{aligned} \tag{10.6.20}$$

Here, $I_n(\xi)$ and $K_n(\xi)$ are modified Bessel function of the first and second kind, respectively. For derivative of the modified Bessel functions,

$$\begin{aligned}J_n'(i\xi)&=i^{n-1}I_n'(\xi)\\ H_n^{'(1)}(i\xi)&=\frac{2}{\pi}(-i)^{n+2}K_n'(\xi)\end{aligned} \tag{10.6.21}$$

then the ratio of the Bessel and Hankel functions for imaginary frequencies will give additional factor of $i$!

$$\begin{aligned}\frac{H_n^{(1)}(i\xi)}{J_n(i\xi)}&=-i\frac{2}{\pi}(-1)^n\frac{K_n(\xi)}{I_n(\xi)}\\ \frac{H_n^{'(1)}(i\xi)}{J_n'(i\xi)}&=-i\frac{2}{\pi}(-1)^n\frac{K_n'(\xi)}{I_n'(\xi)}\end{aligned} \tag{10.6.22}$$

and thus the overall result of the stress is real as expected. For an imaginary frequency $k_{1\rho}$ is pure imaginary and taking $k_{1\rho}a=i\xi$ we have

$$k_{1\rho}^2a^2=-\xi^2 \tag{10.6.23}$$

and the stress integral can be rewritten as

$$T_{\rho\rho}=-\frac{\hbar}{4\pi^3a^2}\int_0^\infty \mathrm{d}\zeta \sum_{n=-\infty}^{\infty}(-1)^n\int_0^\infty \mathrm{d}k_z\left(\frac{K_n(\xi)}{I_n(\xi)}+\frac{K_n'(\xi)}{I_n'(\xi)}\right)\left\{\xi^2\left[J_n'(i\xi)\right]^2+\left(n^2+\xi^2\right)J_n^2(i\xi)\right\} \tag{10.6.24}$$

Now, since the integrand only depends on $k_z$ and $\zeta$ through the quadratic form of $\xi=a\sqrt{k_z^2+\kappa^2}$, lets take $\kappa=\zeta/c$ and make the following change of variables

$$\begin{aligned}\kappa a&=\xi\cos\alpha\\ k_z a&=\xi\sin\alpha\end{aligned} \tag{10.6.25}$$

here, $0\le\xi<\infty$ and $0\le\alpha\le\pi/2$ and the integral becomes

$$\int_0^\infty \mathrm{d}\zeta\int_0^\infty \mathrm{d}k_z=\frac{c}{a^2}\int_0^\infty \mathrm{d}(\kappa a)\int_0^\infty \mathrm{d}(k_z a)=\frac{c}{a^2}\int_0^\infty \mathrm{d}\xi\,\xi\int_0^{\pi/2}\mathrm{d}\alpha=\frac{\pi c}{2a^2}\int_0^\infty \mathrm{d}\xi\,\xi \tag{10.6.26}$$

as the integrand does not depend on $\alpha$. With this definition

$$k_1^2=\frac{\omega^2}{c^2}=-\frac{\zeta^2}{c^2}=-\kappa^2 \tag{10.6.27}$$

Therefore, the self stress becomes

$$T_{\rho\rho}=-\frac{\hbar c}{8\pi^2a^4}\sum_{n=-\infty}^{\infty}\int_0^\infty \mathrm{d}\xi\;\xi\left(\frac{K_n(\xi)}{I_n(\xi)}+\frac{K_n'(\xi)}{I_n'(\xi)}\right)\left\{-\xi^2{I_n'}^2(\xi)+\left(n^2+\xi^2\right)I_n^2(\xi)\right\} \tag{10.6.28}$$

The integral is independent of physical dimension $a$ and the pre-factor correctly has dimension of the mechanical pressure.

### 10.6.4 Stress contribution from fields outside the cylinder

For the stress calculations outside of the cylinder, the relevant Green's function is $\overline{\overline{G}}_S^{[22]}(\overline{r},\overline{r}')$ that should be inserted into the stress expressions.

$$\overline{\overline{G}}_S^{[22]}(\overline{r},\overline{r}')=\sum_{n=-\infty}^{\infty}\frac{i}{8\pi}\int_{-\infty}^{\infty}\mathrm{d}k_z\frac{1}{k_{2\rho}^2}\Big[\Big(A_n^{(22)}\overline{M}_{2n}^{+}(\overline{r};k_z)+B_n^{(22)}\overline{N}_{2n}^{+}(\overline{r};k_z)\Big)\overline{M}_{2,-n}^{+}(\overline{r}';-k_z) \tag{10.6.29}$$

$$+\Big(C_n^{(22)}\overline{N}_{2n}^{+}(\overline{r};k_z)+D_n^{(22)}\overline{M}_{2n}^{+}(\overline{r};k_z)\Big)\overline{N}_{2,n}^{+}(\overline{r}';-k_z)\Big]$$

However, in order to obtain contribution of the fields outside of cylinder it suffice to replace all of the Hankel functions with Bessel function and vice versa in the inside contribution,

$$T_{\rho\rho}^{\mathrm{out}}=-\frac{\hbar c}{8\pi^2a^4}\sum_{n=-\infty}^{\infty}\int_0^\infty \mathrm{d}\xi\;\xi\left(\frac{I_n(\xi)}{K_n(\xi)}+\frac{I_n'(\xi)}{K_n'(\xi)}\right)\left\{-\xi^2\left[K_n'(\xi)\right]^2+\left(n^2+\xi^2\right)K_n^2(\xi)\right\} \tag{10.6.30}$$

Here, we have taken $k_2=k_1=k$ which corresponds to the stress on a conductor shell in the free space.

### 10.6.5 Asymptotic expansion of the integrand

From the asymptotic expansion of modified Bessel and Hankel function for large arguments for a fixed value of $n$,

$$\begin{aligned} I_n(\xi) &\approx \frac{e^{\xi}}{\sqrt{2\pi\xi}}\left[1-\frac{\mu-1}{8\xi}\right] \\ K_n(\xi) &\approx \sqrt{\frac{\pi}{2\xi}}e^{-\xi}\left[1+\frac{\mu-1}{8\xi}\right] \end{aligned} \tag{10.6.31}$$

and for derivative of the modified Bessel function,

$$\begin{aligned} I'_n(\xi) &\approx \frac{e^{\xi}}{\sqrt{2\pi\xi}}\left[1-\frac{\mu+3}{8\xi}\right] \\ K'_n(\xi) &\approx -\sqrt{\frac{\pi}{2\xi}}e^{-\xi}\left[1+\frac{\mu+3}{8\xi}\right] \end{aligned} \tag{10.6.32}$$

For the inside stress integrand, as $\xi\to\infty$ we have

$$\frac{K_n(\xi)}{I_n(\xi)}+\frac{K'_n(\xi)}{I'_n(\xi)} \approx 2\pi(\Delta-\delta)e^{-2\xi} \approx -\frac{\pi}{\xi}e^{-2\xi} \tag{10.6.33}$$

where $\delta=(\mu+3)/8\xi$ and $\Delta=(\mu-1)/8\xi$ and thus $\delta-\Delta=1/2\xi$. In addition,

$$\left\{-\xi^2 {I'_n}^2(\xi)+\left(n^2+\xi^2\right)I_n^2(\xi)\right\} \approx \xi^2\left[-{I'_n}^2(\xi)+I_n^2(\xi)\right] \approx \frac{2}{\pi}\xi e^{\xi}(\delta-\Delta)=\frac{1}{2\pi}e^{2\xi} \tag{10.6.34}$$

and the integrand of the stress from field inside of the cylinder for a fixed value of $n$ asymptotes to

$$\mathcal{T}^{\text{in}}_{\xi\to\infty}=-1/2 \tag{10.6.35}$$

Similarly, for the outside stress integrand, as $\xi\to\infty$ we have

$$\mathcal{T}^{\text{out}}_{\xi\to\infty}=-1/2 \tag{10.6.36}$$

Each of the contributions into the stress tensor results in a divergent values, just considering the frequency integral (sum over harmonics intensify the divergence).

## 10.7 Total stress on the Cylindrical shell

Total stress exerted on the perfect conductor shell is the difference of pressure from the fields inside and outside of the cylinder. Consider the Cylindrical shell depicted in Fig. 10.5. For an object with boundary surface of $S$, total electromagnetic force can be written as

$$\overline{F}^{\text{Net}}=\oint_S \mathrm{d}S\ \overline{\overline{T}}\cdot\hat{n} \tag{10.7.1}$$

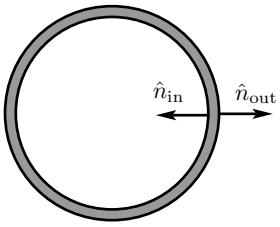


FIGURE 10.5: Normal to the cylinder

where $\overline{\overline{T}}$ is the Maxwell stress tensor and $\hat{n}$ is the normal to the body of object. Assuming we have the stress tensor inside and outside of the cylinder, the surface $S$ would be total interior and exterior surfaces of the shell and the net normal pressure (Force per unit area) is given by

$$T_{\rho\rho}^{\text{Net}} = \hat{\rho} \cdot \left( \overline{\overline{T}}^{\text{in}} \cdot \hat{n}_{\text{in}} + \overline{\overline{T}}^{\text{out}} \cdot \hat{n}_{\text{out}} \right) = - \left( T_{\rho\rho}^{\text{in}} - T_{\rho\rho}^{\text{out}} \right) \tag{10.7.2}$$

$$T_{\rho\rho}^{\text{Net}} = \frac{\hbar c}{8\pi^2 a^4} \sum_{n=-\infty}^{\infty} F_n^{\text{Net}} \tag{10.7.3}$$

where,

$$\begin{aligned} F_n^{\text{net}} = & \int_0^\infty \mathrm{d}\xi \; \xi^3 \left\{ - \left( \frac{K_n(\xi)}{I_n(\xi)} + \frac{K_n'(\xi)}{I_n'(\xi)} \right) {I_n'}^2(\xi) + \left( \frac{I_n(\xi)}{K_n(\xi)} + \frac{I_n'(\xi)}{K_n'(\xi)} \right) {K_n'}^2(\xi) \right\} \\ & + \int_0^\infty \mathrm{d}\xi \; \xi (n^2 + \xi^2) \left\{ \left( \frac{K_n(\xi)}{I_n(\xi)} + \frac{K_n'(\xi)}{I_n'(\xi)} \right) {I_n}^2(\xi) - \left( \frac{I_n(\xi)}{K_n(\xi)} + \frac{I_n'(\xi)}{K_n'(\xi)} \right) {K_n}^2(\xi) \right\} \end{aligned} \tag{10.7.4}$$

The first term can be simplified as

$$\begin{aligned} -\left( \frac{K_n}{I_n} + \frac{K_n'}{I_n'} \right) {I_n'}^2 + \left( \frac{I_n}{K_n} + \frac{I_n'}{K_n'} \right) {K_n'}^2 &= -\frac{1}{I_n} \left( K_n {I_n'}^2 + K_n' I_n' I_n \right) + \frac{1}{K_n} \left( I_n {K_n'}^2 + I_n' K_n' K_n \right) \\ &= \frac{1}{I_n K_n} \left( -K_n^2 {I_n'}^2 - I_n I_n' K_n K_n' + I_n^2 {K_n'}^2 + I_n I_n' K_n K_n' \right) \\ &= \frac{1}{I_n K_n} \left( I_n^2 {K_n'}^2 - K_n^2 {I_n'}^2 \right) \end{aligned} \tag{10.7.5}$$

Similarly, the second term can be written as

$$\begin{aligned} \left( \frac{K_n}{I_n} + \frac{K_n'}{I_n'} \right) {I_n}^2 - \left( \frac{I_n}{K_n} + \frac{I_n'}{K_n'} \right) {K_n}^2 &= \frac{1}{I_n'} \left( K_n I_n I_n' + K_n' I_n^2 \right) - \frac{1}{K_n'} \left( I_n' {K_n}^2 + I_n K_n K_n' \right) \\ &= \frac{1}{I_n' K_n'} \left( I_n I_n' K_n K_n' + I_n^2 {K_n'}^2 - {I_n'}^2 {K_n}^2 - I_n I_n' K_n K_n' \right) \\ &= \frac{1}{I_n' K_n'} \left( I_n^2 {K_n'}^2 - K_n^2 {I_n'}^2 \right) \end{aligned} \tag{10.7.6}$$

Therefore,

$$F_n^{\text{net}}=\int_0^\infty \mathrm{d}\xi\ \xi^3(I_n^2K_n'^2-K_n^2I_n'^2)\Big(\frac{1}{I_nK_n}+\frac{1}{I_n'K_n'}\Big)+n^2\int_0^\infty \mathrm{d}\xi\ \xi(I_n^2K_n'^2-K_n^2I_n'^2)\Big(\frac{1}{I_n'K_n'}\Big) \tag{10.7.7}$$

Now, for fixed $n$, the asymptotic behavior of the integrand vanishes up to the first order. In other words, two partial stresses from inside and outside fields regularize the total stress but as will be shown the stress expression is still divergent. In addition, the asymptotic behavior of the Bessel function for large argument and fixed order is not useful here as the summation index can be also large. Therefore we need to extract the divergence of the stress that is valid for all the ranges of the argument $\xi$ for large values of $n$. This is where the uniform asymptotic expansion proves useful.

## 10.8 Uniform asymptotic expansion

In order to evaluate the asymptotic behavior of the stress integrals, one may want to use the asymptote of the Bessel function as $\xi\to\infty$ for a fixed value of $n$. However, this is not valid when $n$ goes to infinity. Another alternative is considering the asymptote of the Bessel functions when $n\to\infty$ but this is not valid for all ranges of $\xi$. When, $n\to\infty$, these expansion hold uniformly with respect to $x$ [93],

$$\begin{aligned} I_n(nx)&=\frac{1}{\sqrt{2\pi n}}\frac{e^{n\eta}}{(1+x^2)^{1/4}}\Big(1+\sum_{k=1}\frac{u_k(t)}{n^k}\Big) \\ K_n(nx)&=\sqrt{\frac{\pi}{2n}}\frac{e^{-n\eta}}{(1+x^2)^{1/4}}\Big(1+\sum_{k=1}(-)^k\frac{u_k(t)}{n^k}\Big) \end{aligned} \tag{10.8.1}$$

and for their derivatives

$$\begin{aligned} I_n'(nx)&=\frac{1}{\sqrt{2\pi n}}\frac{(1+x^2)^{1/4}}{x}e^{n\eta}\Big(1+\sum_{k=1}\frac{v_k(t)}{n^k}\Big) \\ K_n'(nx)&=-\sqrt{\frac{\pi}{2n}}\frac{(1+x^2)^{1/4}}{x}e^{-n\eta}\Big(1+\sum_{k=1}(-)^k\frac{v_k(t)}{n^k}\Big) \end{aligned} \tag{10.8.2}$$

Here,

$$\begin{aligned} \eta&=\sqrt{1+x^2}+\ln\frac{x}{1+\sqrt{1+x^2}} \\ t&=\frac{1}{\sqrt{1+x^2}} \end{aligned} \tag{10.8.3}$$

For square of the Bessel functions, up to the first order of the uniform expansion we have

$$
\begin{aligned}
I_n^2(nx) &= \frac{1}{2\pi n}\frac{e^{2n\eta}}{(1+x^2)^{1/2}}\Big(1+2u_1/n\Big) \\
I_n'^{\,2}(nx) &= \frac{1}{2\pi n}\frac{(1+x^2)^{1/2}}{x^2}e^{2n\eta}\Big(1+2v_1/n\Big) \\
K_n^2(nx) &= \frac{\pi}{2n}\frac{e^{-2n\eta}}{(1+x^2)^{1/2}}\Big(1-2u_1/n\Big) \\
K_n'^{\,2}(nx) &= \frac{\pi}{2n}\frac{(1+x^2)^{1/2}}{x^2}e^{-2n\eta}\Big(1-2v_1/n\Big)
\end{aligned}
\tag{10.8.4}
$$

Then for $n\to\infty$, leading order approximation reads

$$
I_n^2K_n'^{\,2}-K_n^2I_n'^{\,2}\approx-\frac{1}{4n^2x^2}\Big[(1+2v_1/n)(1-2u_1/n)-(1+2u_1/n)(1-2v_1/n)\Big]\approx-\frac{1}{n^3x^2}(v_1-u_1)
\tag{10.8.5}
$$

$$
\begin{aligned}
I_nK_n &= \frac{1}{2n}\frac{1}{(1+x^2)^{1/2}}\Big(1+\frac{2u_2-u_1^2}{n^2}\Big) \\
I_n'K_n' &= -\frac{1}{2n}\frac{(1+x^2)^{1/2}}{x^2}\Big(1+\frac{2v_2-v_1^2}{n^2}\Big)
\end{aligned}
\tag{10.8.6}
$$

or

$$
\begin{aligned}
\frac{1}{I_nK_n} &= 2n(1+x^2)^{1/2}\Big(1-\frac{2u_2-u_1^2}{n^2}\Big) \\
\frac{1}{I_n'K_n'} &= -2n\frac{x^2}{(1+x^2)^{1/2}}\Big(1-\frac{2v_2-v_1^2}{n^2}\Big)
\end{aligned}
\tag{10.8.7}
$$

Taking $\xi=ny$ in the expression of stress summand $F_n^{\rm net}$, the stress integrand would be ready for application of uniform expansions.

$$
F_n(n\to\infty)=n^4\int_0^\infty \mathrm{d}y\; y(K_n^2I_n'^{\,2}-I_n^2K_n'^{\,2})\left\{y^2\frac{1}{I_nK_n}+(y^2+1)\frac{1}{I_n'K_n'}\right\}
\tag{10.8.8}
$$

Now, the argument of the Bessel functions is $ny$ and we can use the uniform expansions here,

$$
\begin{aligned}
y^2\frac{1}{I_nK_n}+(y^2+1)\frac{1}{I_n'K_n'} &\approx 2n\xi^2(1+y^2)^{1/2}\left[\Big(1-\frac{2u_2-u_1^2}{n^2}\Big)-\Big(1-\frac{2v_2-v_1^2}{n^2}\Big)\right] \\
&= \frac{2}{n}y^2(1+y^2)^{1/2}\Big[2(v_2-u_2)+(u_1^2-v_1^2)\Big]
\end{aligned}
\tag{10.8.9}
$$

$$
I_n^2K_n'^{\,2}-K_n^2I_n'^{\,2}\approx-\frac{1}{4n^2y^2}\Big[(1+2v_1/n)(1-2u_1/n)-(1+2u_1/n)(1-2v_1/n)\Big]\approx-\frac{1}{n^3y^2}(v_1-u_1)
\tag{10.8.10}
$$

therefore, the asymptotic expansion of the integrand would be

$$F_n(n\to\infty)=-2\int_0^\infty \mathrm{d}y\ y(1+y^2)^{1/2}\left[2(v_2-u_2)+(u_1^2-v_1^2)\right](v_1-u_1) \tag{10.8.11}$$

Note that $u$ and $v$ are functions of $y$. If $t=1/\sqrt{1+y^2}$

$$\begin{aligned} u_1(t)&=\frac{3t-5t^3}{24} \\ u_2(t)&=\frac{81t^2-462t^4+385t^6}{1152} \end{aligned} \tag{10.8.12}$$

$$\begin{aligned} v_1(t)&=\frac{-9t+7t^3}{24} \\ v_2(t)&=\frac{-135t^2+594t^4-455t^6}{1152} \end{aligned} \tag{10.8.13}$$

Therefore,

$$\left[2(v_2-u_2)+(u_1^2-v_1^2)\right](v_1-u_1)=\frac{1}{4}t^3(t^2-1)(-1+4t^2-3t^4) \tag{10.8.14}$$

Taking into account that $t^2=1/(1+y^2)$, gives

$$\begin{aligned} F_n(n\to\infty)&=-2\int_0^\infty \mathrm{d}y\ y(1+y^2)^{1/2}\left[2(v_2-u_2)+(u_1^2-v_1^2)\right](v_1-u_1) \\ &=-\frac{1}{2}\int_0^\infty \mathrm{d}y\ \frac{y}{(1+y^2)}\frac{-y^2}{(1+y^2)}\frac{-y^4+2y^2}{(1+y^2)^2} \\ &=-\frac{1}{2}\int_0^\infty \mathrm{d}y\ \frac{y^5(y^2-2)}{(1+y^2)^4} \end{aligned} \tag{10.8.15}$$

$$T_{\rho\rho}^{\mathrm{Net}}=\frac{\hbar c}{8\pi^2a^4}\left[\sum_{n=-\infty}^{\infty}\left(F_n^{\mathrm{Net}}-F_\infty\right)+\sum_{n=-\infty}^{\infty}F_\infty\right] \tag{10.8.16}$$

The last term is infinite. We can assign a finite value to this summation by Zeta function regularization

$$\begin{aligned} \sum_{n=-\infty}^{\infty}F_\infty&=F_\infty\sum_{n=-\infty}^{\infty}n^0 \\ &=\lim_{s\to0^+}\left[-\frac{1}{2}\int_0^\infty \mathrm{d}y\ \frac{y^{5-s}(y^2-2)}{(1+y^2)^4}\Big[2\zeta(s)+1\Big]\right] \end{aligned} \tag{10.8.17}$$

For $s>0$ the integral is convergent and by taking $1+y^2=t^2$

$$\begin{aligned} \lim_{s\to0^+}\int_0^\infty \mathrm{d}y\ \frac{y^{5-s}(y^2-2)}{(1+y^2)^4}&=\lim_{s\to0^+}\int_1^\infty \mathrm{d}t\ \frac{t(t^2-1)^2(t^2-3)(t^2-1)^{-s/2}}{t^8} \\ &=\lim_{s\to0^+}\int_1^\infty \mathrm{d}t\ \frac{t(t^2-1)^2(t^2-3)t^{-s}}{t^8} \\ &=\lim_{s\to0^+}\int_1^\infty \mathrm{d}t\ t^{-(1+s)}+\int_1^\infty \mathrm{d}t\Big[-\frac{5}{t^3}+\frac{7}{t^5}-\frac{3}{t^7}\Big] \end{aligned} \tag{10.8.18}$$

$$\int_1^\infty \mathrm{d}t\Big[-\frac{5}{t^3}+\frac{7}{t^5}-\frac{3}{t^7}\Big]=-\frac{5}{4} \tag{10.8.19}$$

therefore,

$$\lim_{s\to 0^+}\int_0^\infty \mathrm{d}y\ \frac{y^{5-s}(y^2-2)}{(1+y^2)^4}=\lim_{s\to 0^+}\Big[\frac{1}{s}-\frac{5}{4}\Big] \tag{10.8.20}$$

$$\begin{aligned}\sum_{n=-\infty}^{\infty} F_\infty &= -\frac{1}{2}\lim_{s\to 0^+}\Big[\frac{1}{s}-\frac{5}{4}\Big]\Big[2\zeta(s)+1\Big] \\ &= -\frac{1}{2}\lim_{s\to 0^+}\Big[\frac{1}{s}-\frac{5}{4}\Big]\Big[2\zeta'(s)s\Big]=-\zeta'(0)=\frac{1}{2}\ln(2\pi)\end{aligned} \tag{10.8.21}$$

where the second equality is result of formal definition of the derivative of the Zeta function at $s=0$. As $s\to 0$

$$\zeta'(s)=\frac{\zeta(s)-\zeta(0)}{s} \tag{10.8.22}$$

using $\zeta(0)=-1/2$ we have $2\zeta(s)+1=2\zeta'(s)s$.

$$\begin{aligned}T^{\mathrm{Net}}_{\rho\rho} &= \frac{\hbar c}{8\pi^2 a^4}\left[\sum_{n=-\infty}^{\infty}\Big(F_n^{\mathrm{Net}}-F_\infty\Big)+\frac{1}{2}\ln(2\pi)\right] \\ &= \frac{\hbar c}{8\pi^2 a^4}\left[\sum_{n=-\infty}^{\infty}\tilde{F}_n+\frac{1}{2}\ln(2\pi)\right]\end{aligned} \tag{10.8.23}$$

Where $\tilde{F}_n$ is the renormalized stress term.

$$\begin{aligned}\tilde{F}_n=&\int_0^\infty \mathrm{d}\xi\ \xi^3(I_n^2 {K'_n}^2-K_n^2 {I'_n}^2)\Big(\frac{1}{I_nK_n}+\frac{1}{I'_nK'_n}\Big)+n^2\int_0^\infty \mathrm{d}\xi\ \xi(I_n^2 {K'_n}^2-K_n^2 {I'_n}^2)\Big(\frac{1}{I'_nK'_n}\Big) \\ &+\frac{1}{2}\int_0^\infty \mathrm{d}y\ \frac{y^5(y^2-2)}{(1+y^2)^4}\end{aligned} \tag{10.8.24}$$

For $n\neq 0$ we should change back to $y=\xi/n$ in the last added integral that results in

$$\begin{aligned}\tilde{F}_{n\neq 0}=&\int_0^\infty \mathrm{d}\xi\ \xi^3(I_n^2 {K'_n}^2-K_n^2 {I'_n}^2)\Big(\frac{1}{I_nK_n}+\frac{1}{I'_nK'_n}\Big)+n^2\int_0^\infty \mathrm{d}\xi\ \xi(I_n^2 {K'_n}^2-K_n^2 {I'_n}^2)\Big(\frac{1}{I'_nK'_n}\Big) \\ &+\frac{1}{2}\int_0^\infty \mathrm{d}\xi\ \frac{\xi^5(\xi^2-2n^2)}{(n^2+\xi^2)^4}\end{aligned} \tag{10.8.25}$$

$$\tilde{F}_{n\neq 0}=\int_0^\infty \mathrm{d}\xi\ \left\{\xi(I_n^2 {K'_n}^2-K_n^2 {I'_n}^2)\left[\xi^2\Big(\frac{1}{I_nK_n}+\frac{1}{I'_nK'_n}\Big)+n^2\Big(\frac{1}{I'_nK'_n}\Big)\right]+\frac{\xi^5(\xi^2-2n^2)}{2(n^2+\xi^2)^4}\right\} \tag{10.8.26}$$

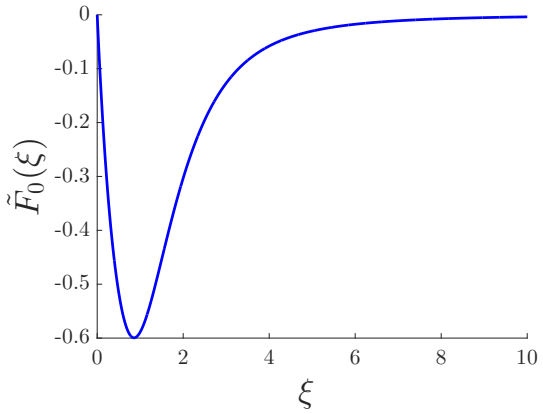


FIGURE 10.6: Zeroth harmonic to the stress contribution

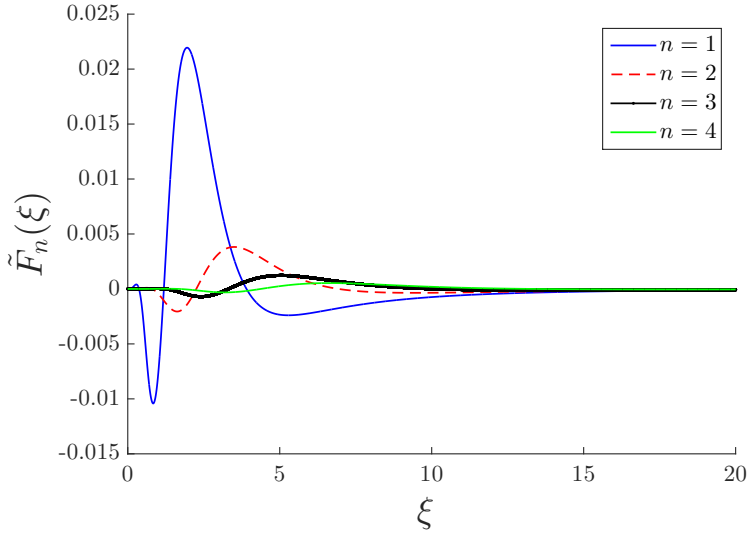


FIGURE 10.7: First four harmonic contribution to the stress

$$\tilde{F}_{n=0}=\int_0^\infty \mathrm{d}\xi\,\left\{\xi(I_n^2 K_n'^{\,2}-K_n^2 I_n'^{\,2})\left[\xi^2\left(\frac{1}{I_n K_n}+\frac{1}{I_n' K_n'}\right)+n^2\left(\frac{1}{I_n' K_n'}\right)\right]+\frac{\xi^5(\xi^2-2)}{2(1+\xi^2)^4}\right\} \tag{10.8.27}$$

The total stress on the cylinder is

$$T_{\rho\rho}^{\mathrm{Net}}=\frac{\hbar c}{8\pi^2 a^4}\left[\tilde{F}_0+2\sum_{n=1}^{\infty}\tilde{F}_n+\frac{1}{2}\ln(2\pi)\right] \tag{10.8.28}$$

Numerical integration gives

$$\tilde{F}_0=8\pi(-0.051857)$$
$$2\sum_{n=1}^{\infty}\tilde{F}_n=8\pi(0.001744)$$

Therefore, total stress would be

$$T_{\rho\rho}=\frac{\hbar c}{\pi a^4}\left(-0.051857+0.001744+\frac{1}{16\pi}\ln(2\pi)\right)=\frac{\hbar c}{\pi a^4}(-0.01355) \tag{10.8.29}$$

which is the same as Milton's result [159, 168].

# Appendix A: Scalar Green's Function in Different Dimensions

For a 3 dimensional problem that involve the 3D wave equation operator, like determining the scalar potential $\phi(\overline{r})$ in terms of the given source function (charge density) of $S(\overline{r})$ that follows

$$(\nabla^2+k^2)\phi(\overline{r})=-S(\overline{r}) \tag{.0.30}$$

subject to radiation condition at infinity. In order to find the potential everywhere for an arbitrary source function, the Green's function $G_{3\mathrm{D}}(\overline{r},\overline{r}')$ of the wave equation operator $(\nabla^2+k^2)$ with unit source can be solved in spherical coordinate to yield the closed form solution of

$$G_{3\mathrm{D}}(\overline{r},\overline{r}')=\frac{e^{ik|\overline{r}-\overline{r}'|}}{4\pi|\overline{r}-\overline{r}'|} \tag{.0.31}$$

and the solution of the scalar potential for given forcing function can be obtained as

$$\phi(\overline{r})=\int \mathrm{d}^3\overline{r}' G_{3\mathrm{D}}(\overline{r},\overline{r}')S(\overline{r}') \tag{.0.32}$$

The 3D scalar Green's function of (.0.31), represent a spherical wave emanating from the point source. Now, if we assume that the charge density $S(\overline{r})$ is uniform along a direction in space (say $z$) and depends only on $\overline{\rho}$, where $\overline{r}=(\overline{\rho},z)$, then, the scalar potential can be written as

$$\phi(\overline{r})=\int \mathrm{d}^2\overline{\rho}' S(\overline{\rho}')\Big[\int_{-\infty}^{\infty} \mathrm{d}z' G_{3\mathrm{D}}(\overline{r},\overline{r}')\Big] \tag{.0.33}$$

According to reciprocity, the Green's function is symmetric under $z\leftrightarrow z'$ and the integration can be perform over $z$, equally. In order to evaluate the integration over $z$, introducing Fourier transform pair of

$$\begin{aligned} G(z-z';\overline{\rho},\overline{\rho}')&=\int \frac{\mathrm{d}k_z}{2\pi} G(k_z;\overline{\rho},\overline{\rho}')e^{ik_z(z-z')} \\ G(k_z;\overline{\rho},\overline{\rho}')&=\int \mathrm{d}z G(z-z';\overline{\rho},\overline{\rho}')e^{-ik_z(z-z')} \end{aligned} \tag{.0.34}$$

and substituting in the scalar wave equation for the Green's function, it yields

$$(\nabla_\rho^2+k_\rho^2)G(k_z;\overline{\rho},\overline{\rho}')=-\delta(\overline{\rho}-\overline{\rho}') \tag{.0.35}$$

where $k_\rho^2=k^2-k_z^2$, and the differential equation can be solved directly in the cylindrical coordinate and accepts the solution of

$$G(k_z;\overline{\rho},\overline{\rho}')=\frac{i}{4}H_0^{(1)}\Big(k_\rho|\overline{\rho}-\overline{\rho}'|\Big) \tag{.0.36}$$

Which is the solution of 2D wave equation with unit source subject to the Sommerfeld radiation condition. Upon evaluating the Fourier transform of (.0.52) at $k_z{=}0$ it yields the expression of the desired integral. Therefore,

$$\frac{i}{4}H_0^{(1)}\Big(k|\overline{\rho}-\overline{\rho}'|\Big):=G_{2\mathrm{D}}(\overline{\rho},\overline{\rho}')=\int\limits_{-\infty}^{\infty}\mathrm{d}z'G_{3\mathrm{D}}(\overline{r},\overline{r}') \tag{.0.37}$$

Therefore, the wave function associated with the source $S(\overline{\rho})$ that does not depend on $z$ can be written as

$$\phi(\overline{\rho})=\int\mathrm{d}^2\overline{\rho}'G_{2\mathrm{D}}(\overline{\rho},\overline{\rho}')S(\overline{\rho}') \tag{.0.38}$$

That also shows that the field does not depends on $z$ as well.This source function is description of a line charge along $z$ and the 2D Green's function describes a cylindrical wave emanating from the axis of the charge density. Now, if we assume that the source function is only function of one variable, say $x$, then the potential can be computed as

$$\phi(x)=\int\limits_{-\infty}^{\infty}\mathrm{d}x'S(x')\Big[\int\limits_{-\infty}^{\infty}\mathrm{d}y'G_{2\mathrm{D}}(\overline{\rho},\overline{\rho}')\Big] \tag{.0.39}$$

Following the same procedure to compute the integral of the 2D Green's function with respect to $y'$, the Fourier transform of the 2D Green's function with respect to $y$, $G_{2\mathrm{D}}(k_y;x,x')$ satisfies,

$$\left(\frac{\mathrm{d}^2}{\mathrm{d}x^2}+k_x^2\right)G_{2\mathrm{D}}(k_y;x,x')=-\delta(x-x') \tag{.0.40}$$

Subject to radiation condition and here, $k_x^2{=}k^2{-}k_y^2$. The solution can be obtained by solving the differential equation directly,

$$G_{2\mathrm{D}}(k_y;x,x')=\frac{i}{2k_x}e^{ik_x|x-x'|} \tag{.0.41}$$

By taking $k_y{=}0$ in the Fourier transform the integral with respect to $y'$ can be computed as

$$\int\limits_{-\infty}^{\infty}\mathrm{d}y'G_{2\mathrm{D}}(\overline{\rho},\overline{\rho}'):=G_{1\mathrm{D}}(x,x')=\frac{i}{2k}e^{ik|x-x'|} \tag{.0.42}$$

which is defined as one dimensional Green's function. The source that is independent of the $y,z$ describe a sheet of charge and (.0.42) simply predict its radiation as one dimensional upward and downward propagating Cartesian plane waves away from the sheet.

Putting everything together, we have the following identity between Green's functions in various dimensions,

$$\frac{i}{2k}e^{ik|x-x'|}=\int\limits_{-\infty}^{\infty}\mathrm{d}y\frac{i}{4}H_0^{(1)}\Big(k_\rho|\overline{\rho}-\overline{\rho}'|\Big)=\int\limits_{-\infty}^{\infty}\mathrm{d}y\int\limits_{-\infty}^{\infty}\mathrm{d}z\frac{e^{ik|\overline{r}-\overline{r}'|}}{4\pi|\overline{r}-\overline{r}'|} \tag{.0.43}$$

# Appendix B: Spectral Expansion of Dyadic Green's Function

## Plane Wave Expansion of the Scalar Free Green's Function

Let's first consider the free scalar Green's function $G(\overline{r},\overline{r}')$ that satisfies the scalar wave equation, can be expanded as a sum of Cartesian plane wave by a 3D Fourier integral representation

$$G(\overline{r},\overline{r}')=\int \frac{\mathrm{d}^3\overline{k}}{(2\pi)^3}\, e^{i\overline{k}\cdot\overline{r}}G(\overline{k}) \tag{.0.44}$$

Substituting this expansion into the wave equation $(\nabla^2+k_0^2)G(\overline{r},\overline{r}')=-\delta(\overline{r}-\overline{r}')$ and using the completeness relation of plane waves as

$$\delta(\overline{r}-\overline{r}')=\int \frac{\mathrm{d}^3\overline{k}}{(2\pi)^3}\, e^{i\overline{k}\cdot(\overline{r}-\overline{r}')} \tag{.0.45}$$

yields the spectral content of the Green's function as

$$G(\overline{r},\overline{r}')=\int \frac{\mathrm{d}^3\overline{k}}{(2\pi)^3}\frac{e^{i\overline{k}\cdot(\overline{r}-\overline{r}')}}{k^2-k_0^2} \tag{.0.46}$$

Here, $k^2=\overline{k}\cdot\overline{k}$ and $\overline{k}$ is an arbitrary vector in the spectral space and therefore $e^{i\overline{k}\cdot\overline{r}}$ is not necessarily a plane wave propagating in space as it does not satisfy the dispersion relation of the free space $\overline{k}\cdot\overline{k}=\omega^2\mu\varepsilon$ in general. However, the poles in the integrand corresponds to a propagating mode with $k=k_0$. In general wave vector $\overline{k}$ has 3D degrees of freedom but in order to have a wave that is consistent with the Maxwell's equations, $\overline{k}$ should be on the dispersion sphere. This would reduce the degrees of freedom in a plane wave to 2. By integration over one of dimensions, say $k_z$ which consists of the following integral

$$I=\int_{-\infty}^{\infty}\mathrm{d}k_z\,\frac{e^{ik_z(z-z')}}{k_z^2-k_p^2}\quad ,k_p^2=k_0^2-k_x^2-k_y^2 \tag{.0.47}$$

the additional degree of freedom can be removed. The integral $I$ can be evaluated by complex integration over a contour that includes the real line in the complex $k_z-$plane. Noting that if $\mathrm{Im}(k_z)=0$ the integral is undefined over the real axis. So, In order to ensure the radiation condition, we assume that there is small amount of loss in medium for the purpose of integration (After integration we allow the medium be lossless). The radiation condition mandates that $\mathrm{Im}(k_z)>0$ in order to have finite field quantities as $z\to\infty$.

For $z>z'$, proper contour of integration $\gamma_u$ is depicted in Fig. 8. The integrand over the semicircle in the upper half plane goes to zero when $z>z'$ as the semicircle radius goes

to infinity. Choosing the proper contour make the integrand to be ready for application of the Jordan's lemma (The integral over the semi-circle at infinity is zero)

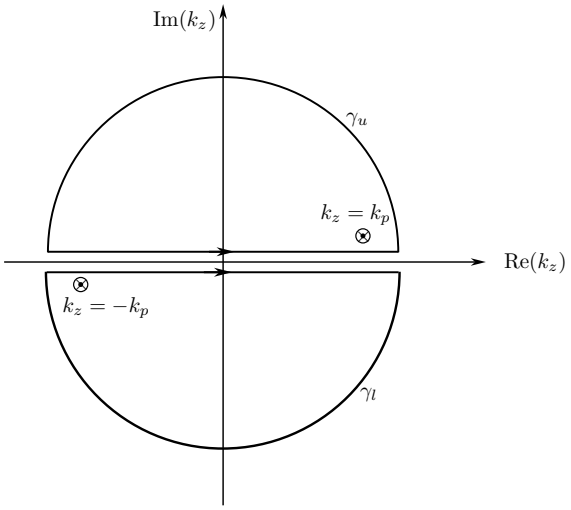


FIGURE 8: Proper contour of integration on complex $k_z$ plane. For $z>z'$ ($z<z'$) the integrand satisfies the radiation condition on $\gamma_u$ ($\gamma_l$).

The integrand has only one singular point at $k_z=k$ within the contour of integration. Using the Residue theorem , for $z>z'$ we have [60],

$$I=\int_{-\infty}^{\infty} \mathrm{d}k_z \ \frac{e^{ik_z(z-z')}}{k_z^2-k_p^2}=\oint_{\gamma_u} \mathrm{d}k_z \ \frac{e^{ik_z(z-z')}}{k_z^2-k_p^2}=2\pi i\frac{e^{ik_p(z-z')}}{2k_p} \tag{.0.48}$$

Similarly, for $z<z'$, the proper contour of integration is $\gamma_l$ that results in

$$I=\int_{-\infty}^{\infty} \mathrm{d}k_z \ \frac{e^{ik_z(z-z')}}{k_z^2-k_p^2}=\oint_{\gamma_l} \mathrm{d}k_z \ \frac{e^{ik_z(z-z')}}{k_z^2-k_p^2}=2\pi i\frac{e^{-ik_p(z-z')}}{-2k_p}\times(-1)=2\pi i\frac{e^{-ik_p(z-z')}}{2k_p} \tag{.0.49}$$

Recent results can be combined in a more compact form

$$\int_{-\infty}^{\infty} \mathrm{d}k_z \ \frac{e^{ik_z(z-z')}}{k_z^2-k_p^2}=2\pi i\frac{e^{ik_p|z-z'|}}{2k_p} \tag{.0.50}$$

Note that $k_z$ is not an independent variable anymore. Replacing $k_p$ with $k_z$ and remembering that $k_z=(k_0^2-k_x^2-k_y^2)^{1/2}$,

$$G(\overline{r},\overline{r}')=\frac{i}{2}\int \frac{\mathrm{d}^2\overline{k}_\perp}{(2\pi)^2} \ e^{i\overline{k}_\perp\cdot(\overline{r}_\perp-\overline{r}'_\perp)}\frac{e^{ik_z|z-z'|}}{k_z} \tag{.0.51}$$

This is the plane wave expansion of the scalar Green's function in term of scalar plane waves with definite wave number along $z$ direction.

## Plane Wave Expansion of the Dyadic Green's Function

The dyadic Green's function in free space can be obtained from the scalar Green's function through,

$$\overline{\overline{G}}(\overline{r},\overline{r}')=\left[\overline{\overline{I}}+\frac{\nabla\nabla}{k_0^2}\right]G(\overline{r},\overline{r}') \tag{.0.52}$$

Notice that the relation (.0.52) is only valid for determination of the free space dyadic Green's function from the scalar one. For bounded regions, although (.0.52) satisfies the vector wave equation, it may not satisfy the border conditions of the electric field. In order to obtain such representation for dyadic Green's function of free space, $\nabla\nabla=\hat{x}_i\hat{x}_j\partial_i\partial_j$ should operate on $G(\overline{r}-\overline{r}')$. However,due to the presence of $|z-z'|$ function in the exponent of the integrand, which is not a differentiable function, there would be a discontinuity at $z=z'$ (source point) in the first derivative of $G(\overline{r}-\overline{r}')$, i.e $\partial_z g(\overline{r}-\overline{r})$,

$$\frac{\partial}{\partial z}G(\overline{r}-\overline{r})=-\frac{1}{2}\mathrm{sgn}(z-z')\int\frac{\mathrm{d}^2\overline{k}_\perp}{(2\pi)^2}\;e^{i\overline{k}_\perp\cdot(\overline{r}_\perp-\overline{r}'_\perp)}e^{ik_z|z-z'|} \tag{.0.53}$$

where $\mathrm{sgn}(\cdot)$ is the sign function. This is always the case for the Green's function in the source region that the second derivative is singular. As a consequence, $\partial_z^2 G(\overline{r}-\overline{r}')$ has a delta function singularity at $z=z'$. Taking the second derivative gives with respect to $z$ yields

$$\begin{aligned}\frac{\partial^2}{\partial z^2}g(\overline{r},\overline{r}')=&-\frac{1}{2}\left[\frac{\partial}{\partial z}\mathrm{sgn}(z-z')\right]\int\frac{\mathrm{d}^2\overline{k}_\perp}{(2\pi)^2}\;e^{i\overline{k}_\perp\cdot(\overline{r}_\perp-\overline{r}'_\perp)}e^{ik_z|z-z'|}\\&-\frac{i}{2}\mathrm{sgn}(z-z')^2\int\frac{\mathrm{d}^2\overline{k}_\perp}{(2\pi)^2}\;k_z e^{i\overline{k}_\perp\cdot(\overline{r}_\perp-\overline{r}'_\perp)}e^{ik_z|z-z'|}\end{aligned}$$

Here, $\mathrm{sgn}(z-z')^2=1$ and $\partial_z\mathrm{sgn}(z-z')=2\delta(z-z')$. The second term is regular and the singular part of the dyadic Green's function is given by

$$\overline{\overline{G}}_{\text{Singular}}=\frac{\hat{z}\hat{z}}{k_0^2}\frac{\partial^2 g(\overline{r}-\overline{r}')}{\partial z^2}=-\frac{\hat{z}\hat{z}}{k_0^2}\delta(z-z')\int\frac{\mathrm{d}^2\overline{k}_\perp}{(2\pi)^2}\;e^{i\overline{k}_\perp\cdot(\overline{r}_\perp-\overline{r}'_\perp)}=-\frac{\hat{z}\hat{z}}{k_0^2}\delta(\overline{r}-\overline{r}') \tag{.0.54}$$

The singular part of the dyadic Green's function found to be proportional to $\hat{z}\hat{z}$. This is the direct consequence of performing the $k_z$ spectral integral first that resulted in plane waves with definite wave number along $z$ direction. Now, the singularity is extracted and we can perform differentiation without being worried about singularity at the source point. Since the plane waves are eigenfunction of $\nabla$, operation of $\nabla$ on the eigenfunctions can be replaced by its eigenvalue $i\overline{k}$. Therefore,

$$\overline{\overline{G}}^{\gtrless}(\overline{r},\overline{r}')=-\frac{\hat{z}\hat{z}}{k_0^2}\delta(\overline{r}-\overline{r}')+\frac{i}{2}\int\frac{\mathrm{d}^2\overline{k}_\perp}{(2\pi)^2}\;\frac{1}{k_z}\left[\overline{\overline{I}}-\hat{k}^{\pm}\hat{k}^{\pm}\right]e^{i\overline{k}^{\pm}\cdot(\overline{r}-\overline{r}')} \tag{.0.55}$$

Where the upward/downward propagating wave vectors are defined as $\overline{k}^{\pm}=k_x\hat{x}+k_y\hat{y}\pm k_z\hat{z}$.

The Dirac delta function term is known as the singularity of the Green's function and and it is important in calculating the fields in the source region. It is closely related to the

hyper-singularity of the dyadic Green's function and principal value exclusion volume in the spatial domain. With a spectral expansion of the dyadic Green's function, the singular part comes out as according to the spectral expansion that is used. The dyad $\overline{\overline{I}}-\hat{k}^{\pm}\hat{k}^{\pm}$ is a transverse dyad (with respect to propagation direction). We can define horizontal (TE) and vertical (TM) polarizations unit vector for specific propagation direction $\hat{k}$ as follows

$$\hat{e}(\pm k_z)=\frac{\hat{k}^{\pm}\times\hat{z}}{|\hat{k}\times\hat{z}|}=\frac{k_y\hat{x}-k_x\hat{y}}{\sqrt{k_x^2+k_y^2}}=\frac{1}{k_\rho}(k_y\hat{x}-k_x\hat{y})$$
$$\hat{h}(\pm k_z)=\hat{e}(\pm k_z)\times\hat{k}^{\pm}=\mp\frac{k_z}{kk_\rho}(k_y\hat{x}+k_y\hat{y})+\frac{k_\rho}{k}\hat{z}$$

Note that $\hat{e}(k_z)$ does not depend on $k_z$, hence $\hat{e}(-k_z)=\hat{e}(k_z)$. These unit vectors are natural as if the electric field is polarized along $\hat{e}(k_z)$ and the wave is propagating along $\overline{k}^{+}$, then $\hat{h}(k_z)$ would show the direction of magnetic field. A complete set of orthonormal vectors $\left(\hat{h},\hat{e},\hat{k}\right)$, can be used to expand the unit dyad,

$$\overline{\overline{I}}-\hat{k}^{\pm}\hat{k}^{\pm}=\hat{h}(\pm k_z)\hat{h}(\pm k_z)+\hat{e}(\pm k_z)\hat{e}(\pm k_z) \tag{.0.56}$$

Substitution recent representation into (.0.55) gives [60]

$$\overline{\overline{G}}(\overline{r},\overline{r}')=-\frac{\hat{z}\hat{z}}{k_0^2}\delta(\overline{r}-\overline{r}')+\frac{i}{2(2\pi)^2}\int \mathrm{d}^2\overline{k}_\perp\,\frac{1}{k_z}\begin{cases}\left[\hat{h}(+k_z)\hat{h}(+k_z)+\hat{e}(+k_z)\hat{e}(+k_z)\right]e^{i\overline{k}^{+}\cdot(\overline{r}-\overline{r}')} & z>z'\\ \left[\hat{h}(-k_z)\hat{h}(-k_z)+\hat{e}(-k_z)\hat{e}(-k_z)\right]e^{i\overline{k}^{-}\cdot(\overline{r}-\overline{r}')} & z<z'\end{cases} \tag{.0.57}$$

This is complete expansion of the free dyadic Green's function in terms of the polarized plane waves.

# Appendix C: Extinction Theorem

The Extinction theorem is the basis of the integral equation formalism for electromagnetic scattering and propagation in terms of equivalent surface fields. Assume a homogeneous scatterer with material properties of $\mu_1,\varepsilon_1$ that occupies region $V_1$ of space as depicted in Fig. 9. The scatterer is illuminated by a current element $\overline{J}(\overline{r})$ with support in the region $V$. Here, the entire space is decompose to $V_1$ and $V$ such that, $V_1 \cup V = \mathbb{R}^3$.

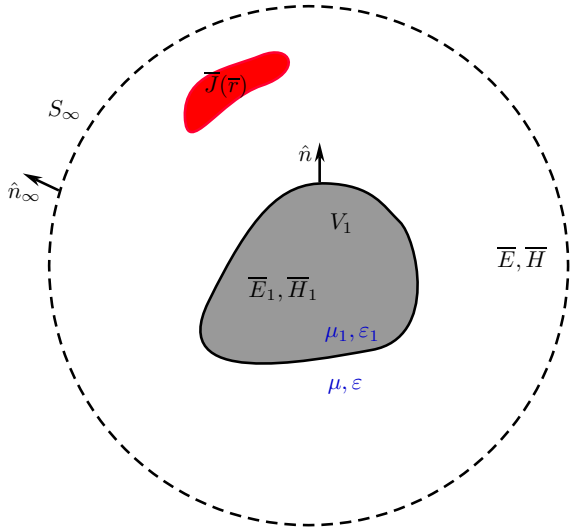


FIGURE 9: The scatterer in the background medium which is illuminated by the current source $\overline{J}(\overline{r})$.

Assume that the solution of the Maxwell's equations in both regions are given by $(\overline{E},\overline{H})$ and $(\overline{E}_1,\overline{H}_1)$. Outside of the scatterer in region $V$, the electric field $\overline{E}(\overline{r})$ satisfies the vector wave equation with wavenumber $k$ as

$$\nabla\times\nabla\times\overline{E}(\overline{r})-k^2\overline{E}(\overline{r})=i\omega\mu\overline{J}(\overline{r}) \tag{.0.58}$$

where $k^2=\omega^2\mu\varepsilon$. Free dyadic Green's function with wave number $k$ also satisfies the wave equation of the same kind,

$$\nabla\times\nabla\times\overline{\overline{G}}(\overline{r},\overline{r}')-k^2\overline{\overline{G}}(\overline{r},\overline{r}')=\overline{\overline{I}}\delta(\overline{r}-\overline{r}') \tag{.0.59}$$

subject to the radiation condition at infinity. Multiplying Eq.(.0.58) by $\overline{\overline{G}}(\overline{r},\overline{r}')$ from right hand side and Eq.(.0.59) by $\overline{E}(\overline{r})$ from left hand side and upon subtracting those and integrating the result over volume $V$ we arrive at,

$$\int_V \mathrm{d}^3\overline{r}\left[\nabla\times\nabla\times\overline{E}(\overline{r})\cdot\overline{\overline{G}}(\overline{r},\overline{r}')-\overline{E}(\overline{r})\cdot\nabla\times\nabla\times\overline{\overline{G}}(\overline{r},\overline{r}')\right] \tag{.0.60}$$
$$=i\omega\mu\int_V \mathrm{d}^3\overline{r}\,\overline{J}(\overline{r})\cdot\overline{\overline{G}}(\overline{r},\overline{r}')-\begin{cases}\overline{E}(\overline{r}') & \overline{r}'\in V\\ \overline{0} & \overline{r}'\notin V\end{cases}$$

The first term on the right hand side is the electric field radiated from the source $\overline{J}(\overline{r})$ in free space and is independent of the boundaries. Let's call it the incident field $\overline{E}_{\mathrm{inc}}$,

$$\overline{E}_{\mathrm{inc}}(\overline{r}')=i\omega\mu\int_V \mathrm{d}^3\overline{r}\,\overline{J}(\overline{r})\cdot\overline{\overline{G}}(\overline{r},\overline{r}')=i\omega\mu\int_V \mathrm{d}^3\overline{r}\,\overline{\overline{G}}(\overline{r}',\overline{r})\cdot\overline{J}(\overline{r}) \tag{.0.61}$$

where the reciprocity relation of the free dyadic Green's function is used. If we perform integration by part on the second term in the bracket twice with the help of vector identity $\nabla\cdot(\overline{A}\times\overline{B})=\overline{B}\cdot\nabla\times\overline{A}-\overline{A}\cdot\nabla\times\overline{B}$, (.0.60) can be written as

$$\overline{E}_{\mathrm{inc}}(\overline{r}')-\oint_{\partial V}\mathrm{d}S\hat{n}\cdot\left[\overline{E}(\overline{r})\times\nabla\times\overline{\overline{G}}(\overline{r},\overline{r}')+\nabla\times\overline{E}(\overline{r})\times\overline{\overline{G}}(\overline{r},\overline{r}')\right]=\begin{cases}\overline{E}(\overline{r}') & \overline{r}'\in V\\ \overline{0} & \overline{r}'\notin V\end{cases} \tag{.0.62}$$

Here, $\hat{n}$ is the unit normal on the surface of volume $V$ that points out of $V$. Now, the closed boundary of $V$ contains two surfaces; one is $\partial V_1$ and the other surface is a surface at infinitely $S_\infty$ that entirely encompass $V$, as depicted in Fig. 9. Because all the sources are localized inside the volume $V$, the radiation condition mandates that fields decay faster than $1/r$ as $r\to\infty$ and therefore,

$$\oint_{S_\infty}\mathrm{d}S\hat{n}_\infty\cdot\left[\overline{E}(\overline{r})\times\nabla\times\overline{\overline{G}}(\overline{r},\overline{r}')+\nabla\times\overline{E}(\overline{r})\times\overline{\overline{G}}(\overline{r},\overline{r}')\right]=0 \tag{.0.63}$$

(There is another way of incorporating the incident field by assuming that the source of incident field is infinitely far away, and starting with homogeneous wave equation for the electric field. In this case, by assuming the scatterer to disappear, the boundary integral over $C_\infty$ yields the incident field.) Therefore,

$$\overline{E}_{\mathrm{inc}}(\overline{r}')+\oint_{\partial V_1}\mathrm{d}S\hat{n}\cdot\left[\overline{E}(\overline{r})\times\nabla\times\overline{\overline{G}}(\overline{r},\overline{r}')+\nabla\times\overline{E}(\overline{r})\times\overline{\overline{G}}(\overline{r},\overline{r}')\right]=\begin{cases}\overline{E}(\overline{r}') & \overline{r}'\in V\\ \overline{0} & \overline{r}'\notin V\end{cases} \tag{.0.64}$$

Here the normal $\hat{n}$ points out out of the scatterer (is opposite to the normal vector in the Gauss's theorem). Using the Maxwell's equations to insert in the magnetic field gives,

$$\overline{E}_{\mathrm{inc}}(\overline{r}')+\oint_{\partial V_1}\mathrm{d}S\hat{n}\cdot\left[\overline{E}(\overline{r})\times\nabla\times\overline{\overline{G}}(\overline{r},\overline{r}')+i\omega\mu\overline{H}(\overline{r})\times\overline{\overline{G}}(\overline{r},\overline{r}')\right]=\begin{cases}\overline{E}(\overline{r}') & \overline{r}'\in V\\ \overline{0} & \overline{r}'\notin V\end{cases} \tag{.0.65}$$

Permutation of the triple products in the bracket reveal electric and magnetic surface current terms,

$$\hat{n}\cdot\overline{E}(\overline{r})\times\nabla\times\overline{\overline{G}}(\overline{r},\overline{r}')=\Big[\hat{n}\times\overline{E}(\overline{r})\Big]\cdot\nabla\times\overline{\overline{G}}(\overline{r},\overline{r}') \tag{.0.66}$$
$$\hat{n}\cdot\overline{H}(\overline{r})\times\overline{\overline{G}}(\overline{r},\overline{r}')=\Big[\hat{n}\times\overline{H}(\overline{r})\Big]\cdot\overline{\overline{G}}(\overline{r},\overline{r}')$$

Note that all the operations should be performed on the anterior part of the Green's function and it should always stay on the right hand side of the terms. Substituting the surface currents back to the integral equation of Eq. .0.65 and interchanging the prin=med and unprimed coordinates, we arrive at

$$\overline{E}_{\rm inc}(\overline{r})+\oint_{\partial V_1}{\rm d}S'\Big\{\Big[\hat{n}'\times\overline{E}(\overline{r}')\Big]\cdot\nabla'\times\overline{\overline{G}}(\overline{r}',\overline{r}) \tag{.0.67}$$
$$+i\omega\mu\Big[\hat{n}'\times\overline{H}(\overline{r}')\Big]\cdot\overline{\overline{G}}(\overline{r}',\overline{r})\Big\}=\begin{cases}\overline{E}(\overline{r}) & \overline{r}\in V\\ \overline{0} & \overline{r}\notin V\end{cases}$$

Using the reciprocity of the free space Green's function $\overline{\overline{G}}(\overline{r},\overline{r}')=\overline{\overline{G}}^{\rm T}(\overline{r}',\overline{r})$ and,

$$\nabla'\times\overline{\overline{G}}(\overline{r}',\overline{r})=\nabla' g(\overline{r}',\overline{r})\times\overline{\overline{I}}=-\nabla g(\overline{r}',\overline{r})\times\overline{\overline{I}} \tag{.0.68}$$

and also noting that any dyadic of the form $\overline{A}\times\overline{\overline{I}}$ is antisymmetric, we have

$$\Big[\nabla'\times\overline{\overline{G}}(\overline{r}',\overline{r})\Big]^{\rm T}=\nabla g(\overline{r}',\overline{r})\times\overline{\overline{I}}=\nabla g(\overline{r},\overline{r}')\times\overline{\overline{I}}=\nabla\times\overline{\overline{G}}(\overline{r},\overline{r}') \tag{.0.69}$$

Utilizing these symmetry relations in the integral equation of Eq. (.0.67) yields

$$\overline{E}_{\rm inc}(\overline{r})+\oint_{\partial V_1}{\rm d}S'\Big\{\nabla\times\overline{\overline{G}}(\overline{r},\overline{r}')\cdot\Big[\hat{n}'\times\overline{E}(\overline{r}')\Big] \tag{.0.70}$$
$$+i\omega\mu\overline{\overline{G}}(\overline{r},\overline{r}')\cdot\Big[\hat{n}'\times\overline{H}(\overline{r}')\Big]\Big\}=\begin{cases}\overline{E}(\overline{r}) & \overline{r}\in V\\ \overline{0} & \overline{r}\notin V\end{cases}$$

This is the statement of the Extinction theorem. The surface fields $\hat{n}'\times\overline{E}(\overline{r}')$ and $\hat{n}'\times\overline{H}(\overline{r}')$ on the surface of the scatterer are unknown, but extinction theorem provides an integral equation for the surface fields on the scatterer. If the surface fields on the scatterer are known (After solving the integral equation on the surface of the scatterer) upper relation of Eq. (.0.70) can be used to propagate the surface fields by the exterior region Green's function $\overline{\overline{G}}(\overline{r},\overline{r}')$ to find the scattered field everywhere $\overline{r}\in V$. For $\overline{r}\in V$ the scattered field is

$$\overline{E}_{\rm s}(\overline{r})=\oint_{\partial V_1}{\rm d}S'\Big\{\nabla\times\overline{\overline{G}}(\overline{r},\overline{r}')\cdot\Big[\hat{n}'\times\overline{E}(\overline{r}')\Big]+i\omega\mu\overline{\overline{G}}(\overline{r},\overline{r}')\cdot\Big[\hat{n}'\times\overline{H}(\overline{r}')\Big]\Big\} \tag{.0.71}$$

where the total field in $V$ is written as $E(\overline{r})=\overline{E}_{\rm inc}(\overline{r})+\overline{E}_{\rm s}(\overline{r})$. However, If the Green's function of exterior medium $\overline{\overline{G}}(\overline{r},\overline{r}')$ will be used to propagate the surface field on the object

to point $\overline{r}\in V_1$ inside of the scatterer, resulted field would exactly cancel the incident field or extincts the incident field. The integral equation Eq. (.0.70) is called the *Extinction theorem* based on this observation. Sometimes the lower relation of (.0.70) is called the *Equivalence Principle* or *Huygens Principle* [60, 175].

Although the total field inside the scatterer is not zero, the wave with number $k$ cannot be present in the scatterer with wavenumber $k_1$. This fact can be viewed from a different perspective; incident field with wave number $k$ will propagate with wave number $k$ in the scatterer. A scattered field with wave number $k$ will be excited inside the scatterer to exactly extinguish the presence of incident field. In order to get the correct field $(\overline{E}_1,\overline{H}_1)$ inside the scatterer, $\overline{\overline{G}}_1(\overline{r},\overline{r}')$ should be used to propagate the surface fields.

Before moving forward, It is interesting to consider the case when there is no scatterer in the medium. In this case the medium is homogeneous everywhere. Imagine an arbitrary volume $V_1$ with closed surface $\partial V_1$ in space and apply the Extinction theorem. Herein, the total electric field everywhere is the incident field $\overline{E}_{\rm inc}(\overline{r})$ and,

$$\oint_{\partial V_1} \mathrm{d}S' \Big\{ \nabla\times\overline{\overline{G}}(\overline{r},\overline{r}')\cdot\Big[\hat{n}'\times\overline{E}_{\rm inc}(\overline{r}')\Big] + i\omega\mu\overline{\overline{G}}(\overline{r},\overline{r}')\cdot\Big[\hat{n}'\times\overline{H}_{\rm inc}(\overline{r}')\Big]\Big\} = \begin{cases} \overline{0} & \overline{r}\notin V_1 \\ -\overline{E}_{\rm inc}(\overline{r}) & \overline{r}\in V_1 \end{cases} \tag{.0.72}$$

Propagation of the surface fields $\hat{n}'\times\overline{E}_{\rm inc}(\overline{r}')$ and $\hat{n}'\times\overline{H}_{\rm inc}(\overline{r}')$ over an arbitrary and imaginary closed surface in the homogeneous medium results zero field outside and $-\overline{E}_{\rm inc}(\overline{r})$ inside the imaginary surface.

**Conclusion:**

The Extinction theorem can be written for the scattered surface fields $\hat{n}\times\overline{E}_s(\overline{r})$ and $\hat{n}\times\overline{H}_s(\overline{r})$ instead of total fields as

$$\oint_{\partial V_1} \mathrm{d}S' \Big\{ \nabla\times\overline{\overline{G}}(\overline{r},\overline{r}')\cdot\Big[\hat{n}'\times\overline{E}_s(\overline{r}')\Big] + i\omega\mu\overline{\overline{G}}(\overline{r},\overline{r}')\cdot\Big[\hat{n}'\times\overline{H}_s(\overline{r}')\Big]\Big\} = \begin{cases} \overline{E}_s(\overline{r}) & \overline{r}\in V \\ \overline{0} & \overline{r}\notin V \end{cases} \tag{.0.73}$$

Another version of the Extinction can be find by considering the fields inside the scatterer. The electric field $\overline{E}_1(\overline{r})$ inside the scatterer satisfies the homogeneous vector wave equation with wavenumber $k_1=\omega\sqrt{\mu_1\varepsilon_1}$

$$\nabla\times\nabla\times\overline{E}_1(\overline{r}) - k_1^2\overline{E}_1(\overline{r}) = 0 \tag{.0.74}$$

Here it is assumed that there is no impressed source of the electromagnetic fields inside the scatterer. Free dyadic Green's function inside the scatterer also satisfies the wave equation of the same kind with wavenumber $k_1$ and unit source,

$$\nabla\times\nabla\times\overline{\overline{G}}_1(\overline{r},\overline{r}') - k_1^2\overline{\overline{G}}_1(\overline{r},\overline{r}') = \overline{\overline{I}}\delta(\overline{r}-\overline{r}') \tag{.0.75}$$

Following the same procedure as exterior region (but integrating over the volume of the scatterer) we will arrive at

$$-\oint_{\partial V_1} \mathrm{d}S' \left\{ \nabla \times \overline{\overline{G}}_1(\overline{r},\overline{r}') \cdot \left[ \hat{n}' \times \overline{E}_1(\overline{r}') \right] + i\omega\mu \overline{\overline{G}}_1(\overline{r},\overline{r}') \cdot \left[ \hat{n}' \times \overline{H}_1(\overline{r}') \right] \right\} = \begin{cases} \overline{E}_1(\overline{r}) & \overline{r} \in V_1 \\ \overline{0} & \overline{r} \notin V_1 \end{cases} \tag{.0.76}$$

The minus sign appears here as the result of change in the direction of normal vector. The Extinction theorem applied to the volume of the scatterer reveals that propagation of the surface fields over the boundary with the scatterer's Green's function $\overline{\overline{G}}_1(\overline{r},\overline{r}')$ into the scatterer, gives the field inside the scatterer $\overline{E}_1$. However, if the surface fields will be propagated outside of the scatterer with $\overline{\overline{G}}_1(\overline{r},\overline{r}')$ the results is null, while if instead $\overline{\overline{G}}(\overline{r},\overline{r}')$ will be used as a propagator, the result is the scattered field.

# Bibliography


[1] Vladyslav A Golyk, Matthias Krüger, and Mehran Kardar. Heat radiation from long cylindrical objects. *Physical Review E*, 85(4):046603, 2012.

[2] FSS Rosa, DAR Dalvit, and PW Milonni. Electromagnetic energy, absorption, and casimir forces: Uniform dielectric media in thermal equilibrium. *Physical Review A*, 81(3):033812, 2010.

[3] L Tsang and J A Kong. Scattering of electromagnetic waves, vol. 3: Advanced topics. In *Scattering of Electromagnetic Waves, Vol. 3: Advanced Topics*. Wiley Interscience, 2001.

[4] L Tsang, J A Kong, and Kung Hau Ding. Scattering of electromagnetic waves, vol. 1: Theories and applications. Wiley Interscience, 2001.

[5] Andrei V Shchegrov, Karl Joulain, Rémi Carminati, and Jean-Jacques Greffet. Near-field spectral effects due to electromagnetic surface excitations. *Physical Review Letters*, 85(7):1548, 2000.

[6] Karl Joulain, Jean-Philippe Mulet, François Marquier, Rémi Carminati, and Jean-Jacques Greffet. Surface electromagnetic waves thermally excited: Radiative heat transfer, coherence properties and casimir forces revisited in the near field. *Surface Science Reports*, 57(3-4):59–112, 2005.

[7] Evgeny Mikhailovich Lifshitz, LP Pitaevskii, and VB Berestetskii. Landau and lifshitz course of theoretical physics. *Statistical physics*, 5, 1980.

[8] Stephen J Blundell and Katherine M Blundell. *Concepts in thermal physics*. OUP Oxford, 2009.

[9] JB Pendry. Radiative exchange of heat between nanostructures. *Journal of Physics: Condensed Matter*, 11(35):6621, 1999.

[10] Lukas Novotny and Bert Hecht. *Principles of nano-optics*. Cambridge university press, 2012.

[11] Gerald D Mahan. *Condensed matter in a nutshell*, volume 8. Princeton University Press, 2011.

[12] Lev Davidovich Landau, JS Bell, MJ Kearsley, LP Pitaevskii, EM Lifshitz, and JB Sykes. *Electrodynamics of continuous media*, volume 8. elsevier, 2013.

[13] Venkataraman Balakrishnan. Fluctuation-dissipation theorems from the generalised langevin equation. *Pramana*, 12(4):301–315, 1979.

[14] Rep Kubo. The fluctuation-dissipation theorem. *Reports on progress in physics*, 29 (1):255, 1966.

[15] William MR Simpson and Ulf Leonhardt. *Forces of the quantum vacuum: An Introduction to Casimir Physics*. World Scientific Publishing Company, 2015.

[16] Charles-Antoine Guérin, Boris Gralak, and Adriaan Tip. Singularity of the dyadic green's function for heterogeneous dielectrics. *Physical Review E*, 75(5):056601, 2007.

[17] Weng Cho Chew, WE Sha, and Qi I Dai. Green's dyadic, spectral function, local density of states, and fluctuation dissipation theorem. *arXiv preprint arXiv:1505.01586*, 2015.

[18] DVHM Polder and M Van Hove. Theory of radiative heat transfer between closely spaced bodies. *Physical Review B*, 4(10):3303, 1971.

[19] Jackson J Loomis and Humphrey J Maris. Theory of heat transfer by evanescent electromagnetic waves. *Physical Review B*, 50(24):18517, 1994.

[20] Jean-Jacques Greffet and Manuel Nieto-Vesperinas. Field theory for generalized bidirectional reflectivity: derivation of helmholtz's reciprocity principle and kirchhoff's law. *JOSA A*, 15(10):2735–2744, 1998.

[21] Shurun Tan, Mustafa Aksoy, Marco Brogioni, Giovanni Macelloni, Michael Durand, Kenneth C Jezek, Tian-Lin Wang, Leung Tsang, Joel T Johnson, Mark R Drinkwater, et al. Physical models of layered polar firn brightness temperatures from 0.5 to 2 ghz. *IEEE Journal of Selected Topics in Applied Earth Observations and Remote Sensing*, 8(7):3681–3691, 2015.

[22] G Picard, Ludovic Brucker, A Roy, F Dupont, M Fily, A Royer, and C Harlow. Simulation of the microwave emission of multi-layered snowpacks using the dense media radiative transfer theory: the dmrt-ml model. 2013.

[23] Andreas Wiesmann and Christian Mätzler. Microwave emission model of layered snowpacks. *Remote Sensing of Environment*, 70(3):307–316, 1999.

[24] Mohammadreza Sanamzadeh, Leung Tsang, Joel T Johnson, Robert J Burkholder, and Shurun Tan. Scattering of electromagnetic waves from 3d multilayer random rough surfaces based on the second-order small perturbation method: energy conservation, reflectivity, and emissivity. *JOSA A*, 34(3):395–409, 2017.

[25] Mohammadreza Sanamzadeh, Leung Tsang, and Joel T Johnson. 3-d electromagnetic scattering from multilayer dielectric media with 2-d random rough interfaces using $t$-matrix approach. *IEEE Transactions on Antennas and Propagation*, 67(1):495–503, 2019.

[26] Shurun Tan. Multiple volume scattering in random media and periodic structures with applications in microwave remote sensing and wave functional materials. 2016.

[27] Kenneth C Jezek. Airborne and space-borne remote sensing of cryosphere. In *Earth System Monitoring*, pages 7–34. Springer, 2013.

[28] Giovanni Macelloni, Marco Brogioni, Simone Pettinato, Renato Zasso, Andrea Crepaz, Jonathan Zaccaria, Boris Padovan, and Mark Drinkwater. Ground-based l-band emission measurements at dome-c antarctica: The domex-2 experiment. *IEEE Transactions on Geoscience and Remote Sensing*, 51(9):4718–4730, 2013.

[29] A Tabatabaeenejad and M Moghaddam. Bistatic scattering from three-dimensional layered rough surfaces. *IEEE Transactions on Geoscience and Remote Sensing*, 44 (8):2102–2114, 2006.

[30] Imperatore P, A Iodice, and D Riccio. Electromagnetic wave scattering from layered structures with an arbitrary number of rough interfaces. *IEEE Transactions on Geoscience and Remote Sensing*, 47(4):1056–1072, 2009.

[31] Hasan Zamani, Ahad Tavakoli, and Mojtaba Dehmollaian. Second-order perturbative solution of scattering from two rough surfaces with arbitrary dielectric profiles. *IEEE Transactions on Antennas and Propagation*, 63(12):5767–5776, 2015.

[32] H Zamani, A Tavakoli, and M Dehmollaian. Scattering from layered rough surfaces: Analytical and numerical investigations. *IEEE Transactions on Geoscience and Remote Sensing*, 54(6):3685 – 3696, 2016.

[33] RJ Burkholder, JT Johnson, M Sanamzadeh, L Tsang, and S Tan. Microwave thermal emission characteristics of a two-layer medium with rough interfaces using the second-order small perturbation method. *IEEE Geoscience and Remote Sensing Letters*, 14 (10):1780–1784, 2017.

[34] Wu C and X Zhang. Second-order perturbative solutions for 3-d electromagnetic radiation and propagation in a layered structure with multilayer rough interfaces. *IEEE Journal of Selected Topics in Applied Earth Observations and Remote Sensing*, 8(1):180–194, 2015.

[35] A Tabatabaeenejad and M Moghaddam. Study of validity region of small perturbation method for two-layer rough surfaces. *IEEE Geoscience and Remote Sensing Letter*, 7(2):319–323, 2010.

[36] J T Johnson. Third-order small-perturbation method for scattering from dielectric rough surfaces. *Journal of the Optical Society of America A*, 16(11):2720–2736, 1999.

[37] Demir M A and J T Johnson. Fourth and higher-order small perturbation solution for scattering from dielectric rough surfaces. *Journal of the Optical Society of America A*, 20(12):2330–2337, 2003.

[38] M A Demir, J T Johnson, and T J Zajdel. A study of the fourth-order small perturbation method for scattering from two-layer rough surfaces. *IEEE Transactions on Geoscience and Remote Sensing*, 50(9):3374–3382, 2012.

[39] Tianlin Wang, Leung Tsang, Joel T Johnson, and Shurun Tan. Scattering and transmission of waves in multiple random rough surfaces: Energy conservation studies with the second order small perturbation method. *PIER*, 157:1–20, 2016.

[40] Weng Cho Chew, Eric Michielssen, JM Song, and Jian-Ming Jin. *Fast and efficient algorithms in computational electromagnetics*. Artech House, Inc., 2001.

[41] S Tan, M Aksoy, M Brogioni, G Macelloni, M Durand, K C Jezek, T L Wang, L Tsang, J T Johnson, M R Drinkwater, and L Brucker. Physical models of layered polar firn brightness temperatures from 0.5 to 2 ghz. *IEEE Journal of Selected Topics in Applied Earth Observations and Remote Sensing*, 8(7):3681–3691, 2015.

[42] K S Chen, T D Wu, L Tsang, Qin Li, J C Shi, and A K Fung. Emission of rough surfaces calculated by the integral equation method with comparison to three-dimensional moment method simulations. *IEEE Trans. Geoscience and Remote Sensing*, 41(1):90–101, 2003.

[43] Demir M A, J T Johnson, and T J Zajdel. A study of the fourth-order small perturbation method for scattering from two-layer rough surfaces. *IEEE Transactions on Geoscience and Remote Sensing*, 50(9):3374–3382, 2012.

[44] A Maradudin and E Méndez. Light scattering from randomly rough surfaces. *Science Progress*, 90(4):161–221, 2007.

[45] L Tsang and J A Kong. In *Scattering of Electromagnetic Waves, Vol. 2: Numerical Simulations*. Wiley Interscience, 2001.

[46] Huang S and L Tsang. Electromagnetic scattering of randomly rough soil surfaces based on numerical solutions of maxwell equations in three-dimensional simulations using a hybrid uv/pbtg/smcg method. *IEEE Transactions on Geoscience and Remote Sensing*, 50(10):4025–4035, 2012.

[47] Weng Cho Chew, Mei Song Tong, and Bin Hu. Integral equation methods for electromagnetic and elastic waves. *Synthesis Lectures on Computational Electromagnetics*, 3(1):1–241, 2008.

[48] Kamal Sarabandi and Tsenchieh Chiu. Electromagnetic scattering from slightly rough surfaces with inhomogeneous dielectric profiles. *IEEE Transactions on Antennas and Propagation*, 45(9):1419–1430, 1997.

[49] S Huang, H Wang, K Ding, and L Tsang. Subwavelength imaging enhancement through a three-dimensional plasmon superlens with rough surface. *Optics Letters*, 37(8):1295, 2012.

[50] X Duan and M Moghaddam. 3-d vector electromagnetic scattering from arbitrary random rough surfaces using stabilized extended boundary condition method for remote sensing of soil moisture. *IEEE Transactions on Geoscience and Remote Sensing*, 50(1):87 – 103, 2011.

[51] C Chan, S Lou, L Tsang, and J Kong. Electromagnetic scattering of waves by random rough surface: A finite-difference time-domain approach. *Microwave and Optical Technology Letters*, 4(9):355–359, 1991.

[52] Max Born and Emil Wolf. *Principles of optics: electromagnetic theory of propagation, interference and diffraction of light*. Elsevier, 2013.

[53] ML Burrows. Equivalence of the rayleigh solution and the extended-boundary-condition solution for scattering problems. *Electronics Letters*, 5(12):277–278, 1969.

[54] RHT Bates. Rayleigh hypothesis, the extended-boundary condition and point matching. *Electronics Letters*, 5(25):654–655, 1969.

[55] S Savaidis, P Frangos, DL Jaggard, and K Hizanidis. Scattering from fractally corrugated surfaces with use of the extended boundary condition method. *JOSA A*, 14 (2):475–485, 1997.

[56] PC Waterman. Scattering by periodic surfaces. *The Journal of the Acoustical Society of America*, 57(4):791–802, 1975.

[57] Leung Tsang, Jin Au Kong, and Robert T Shin. Theory of microwave remote sensing. 1985.

[58] RF Millar. The rayleigh hypothesis and a related least-squares solution to scattering problems for periodic surfaces and other scatterers. *Radio Science*, 8(8-9):785–796, 1973.

[59] Benjamin Gallinet, Andreas M Kern, and Olivier JF Martin. Accurate and versatile modeling of electromagnetic scattering on periodic nanostructures with a surface integral approach. *JOSA A*, 27(10):2261–2271, 2010.

[60] Kamal Sarabandi. Electromagnetic scattering lecture notes (eecs 730). 2016.

[61] MG Moharam and Thomas K Gaylord. Diffraction analysis of dielectric surface-relief gratings. *JOSA*, 72(10):1385–1392, 1982.

[62] GM Whitman, DM Leskiw, and F Schwering. Rigorous theory of scattering by perfectly conducting periodic surfaces with trapezoidal height profile. te and tm polarization. *JOSA*, 70(12):1495–1503, 1980.

[63] JA DeSanto. Scattering from a perfectly reflecting arbitrary periodic surface: An exact theory. *Radio Science*, 16(6):1315–1326, 1981.

[64] A Voronovich. Small-slope approximation for electromagnetic wave scattering at a rough interface of two dielectric half-spaces. *Waves in random media*, 4(3):337–368, 1994.

[65] J Joannopoulos. Photonic crystals. Princeton University Press, 2008.

[66] Felix Bloch. Über die quantenmechanik der elektronen in kristallgittern. *Zeitschrift für physik*, 52(7-8):555–600, 1929.

[67] Kamal Sarabandi. Electromagnetic scattering from vegetation canopies, phd thesis. 1991.

[68] RF Millar. On the rayleigh assumption in scattering by a periodic surface. In *Mathematical Proceedings of the Cambridge Philosophical Society*, volume 65, pages 773–791. Cambridge University Press, 1969.

[69] A Zayats, I Smolyaninov, and A Maradudin. Nano-optics of surface plasmon polaritons. *Physics Reports*, 408(3-4):131–314, 2005.

[70] Ping Yang, G Kattawar, Gang Hong, P Minnis, and Yongxiang Hu. Uncertainties associated with the surface texture of ice particles in satellite-based retrieval of cirrus clouds&x2014;part i: Single-scattering properties of ice crystals with surface roughness. *IEEE Transactions on Geoscience and Remote Sensing*, 46(7):1940–1947, 2008.

[71] S Biehs and J Greffet. Influence of roughness on near-field heat transfer between two plates. *Phys. Rev. B*, 82(24), 2010.

[72] Leung Tsang, Xiaoxiong Gu, and H Braunisch. Effects of random rough surface on absorption by conductors at microwave frequencies. *IEEE Microwave and Wireless Components Letters*, 16(4):221–223, 2006.

[73] Pinel N, J T Johnson, and C Bourlier. A geometrical optics model of three dimensional scattering from a rough layer with two rough surfaces. *IEEE Transactions on Antennas and Propagation*, 58(3):809–816, 2010.

[74] Jian-Ming Jin. *Theory and computation of electromagnetic fields*. John Wiley & Sons, 2011.

[75] Petr Beckmann and Andre Spizzichino. The scattering of electromagnetic waves from rough surfaces. *Norwood, MA, Artech House, Inc., 1987, 511 p.*, 1987.

[76] J Winn, Y Fink, S Fan, and J Joannopoulos. Omnidirectional reflection from a one-dimensional photonic crystal. *Optics Letters*, 23(20):1573, 1998.

[77] D Smith, S McCall, P Platzman, R Dalichaouch, N Kroll, and S Schultz. Photonic band structure and defects in one and two dimensions. *Optical Society of America B*, 10(2):314, 1993.

[78] L Tsang, S Tan, M Sanamzadeh, JT Johnson, KC Jezek, and MT Durand. Ultra-wideband radiometry remote sensing of polar ice sheet temperature profile, sea ice and terrestrial snow thickness: Forward modeling and data analysis. In *AGU Fall Meeting Abstracts*, 2017.

[79] Mohammadreza Sanamzadeh, Leung Tsang, and Joel T Johnson. A partial coherent model of brightness temperatures of polar ice sheets at l band incorporating multi-layer roughness effects based on spm2 theory. In *Geoscience and Remote Sensing Symposium (IGARSS), 2017 IEEE International*, pages 2832–2835. IEEE, 2017.

[80] Mohammadreza Sanamzadeh, Leung Tsang, Joel T. Johnson, Robert J. Burkholder, and Shurun Tan. Scattering of electromagnetic waves from 3d multilayer random rough surfaces based on the second-order small perturbation method: energy conservation, reflectivity, and emissivity. *J. Opt. Soc. Am. A*, 34(3):395–409, Mar 2017. doi: 10.1364/JOSAA.34.000395. URL `http://josaa.osa.org/abstract.cfm?URI=josaa-34-3-395`.

[81] RJ Burkholder, JT Johnson, M Sanamzadeh, L Tsang, and S Tan. Microwave thermal emission characteristics of a two-layer medium with rough interfaces using the second-order small perturbation method. *IEEE Geoscience and Remote Sensing Letters*, 14 (10):1780–1784, 2017.

[82] Pasquale Imperatore, Antonio Iodice, Matteo Pastorino, and Nicolas Pinel. Modelling scattering of electromagnetic waves in layered media: An up-to-date perspective. *International Journal of Antennas and Propagation*, 2017, 2017.

[83] Angela Piegari and François Flory. *Optical thin films and coatings: From materials to applications*. Elsevier, 2013.

[84] Mohammadreza Sanamzadeh, Leung Tsang, Joel Tidmore Johnson, Robert J Burkholder, and Shurun Tan. Electromagnetic scattering from one dimensional random rough surfaces of dielectric layered media with waveguide modes using second order small perturbation method. *Progress In Electromagnetics Research*, 80:1–17, 2018.

[85] C-H Kuo and Mahta Moghaddam. Scattering from multilayer rough surfaces based on the extended boundary condition method and truncated singular value decomposition. *IEEE Transactions on antennas and propagation*, 54(10):2917–2929, 2006.

[86] Joel T Johnson, Leung Tsang, Robert T Shin, K Pak, Chi H Chan, Akira Ishimaru, and Yasuo Kuga. Backscattering enhancement of electromagnetic waves from two-dimensional perfectly conducting random rough surfaces: A comparison of monte carlo simulations with experimental data. *IEEE Transactions on Antennas and Propagation*, 44(5):748, 1996.

[87] Julius Adams Stratton. *Electromagnetic theory*. John Wiley & Sons, 2007.

[88] Donald G Dudley. *Mathematical foundations for electromagnetic theory*. IEEE press New York, 1994.

[89] Mohammadreza Sanamzadeh, Leung Tsang, and Joel T Johnson. 3-d electromagnetic scattering from multilayer dielectric media with 2-d random rough interfaces using t-matrix approach. *IEEE Transactions on Antennas and Propagation*, 67(1):495–503, 2018.

[90] Mohammadreza Sanamzadeh, Leung Tsang, and Joel Johnson. Electromagnetic scattering from multi-layer dielectric media with 3d random rough interfaces using translation matrix approach. In *2018 IEEE International Symposium on Antennas and Propagation & USNC/URSI National Radio Science Meeting*, pages 1337–1338. IEEE, 2018.

[91] JT Johnson and RT Kong. Scattering and thermal emission from a two dimensional periodic surface. *Progress In Electromagnetics Research*, 15:303–333, 1997.

[92] Xueyang Duan and Mahta Moghaddam. 3-d vector electromagnetic scattering from arbitrary random rough surfaces using stabilized extended boundary condition method for remote sensing of soil moisture. *IEEE Transactions on Geoscience and Remote Sensing*, 50(1):87–103, 2012.

[93] Milton Abramowitz and Irene A Stegun. *Handbook of mathematical functions: with formulas, graphs, and mathematical tables*, volume 55. Courier Corporation, 1965.

[94] J. A. Sánchez-Gil, A. A. Maradudin, Jun Q. Lu, V. D. Freilikher, M. Pustilnik, and I. Yurkevich. Scattering of electromagnetic waves from a bounded medium with a random surface. *Phys. Rev. B*, 50:15353–15368, Nov 1994. doi: 10.1103/PhysRevB.50.15353. URL `https://link.aps.org/doi/10.1103/PhysRevB.50.15353`.

[95] V. Freilikher, M. Pustilnik, and I. Yurkevich. Wave scattering from a bounded medium with disorder. *Physics Letters A*, 193(5):467 – 470, 1994. ISSN 0375-9601. doi: https://doi.org/10.1016/0375-9601(94)90541-X. URL `http://www.sciencedirect.com/science/article/pii/037596019490541X`.

[96] A. Piegari and F. Flory. In *Optical thin films and coatings: From materials to applications*. Woodhead Publishing Elsevier , Cambridge, 2013.

[97] Juan R Mosig and Alejandro Alvarez Melcón. Green's functions in lossy layered media: Integration along the imaginary axis and asymptotic behavior. *IEEE Transactions on Antennas and Propagation*, 51(12):3200–3208, 2003.

[98] PB Katehi and NG Alexopoulos. Real axis integration of sommerfeld integrals with applications to printed circuit antennas. *Journal of Mathematical Physics*, 24(3): 527–533, 1983.

[99] Tie Jun Cui and Weng Cho Chew. Fast evaluation of sommerfeld integrals for em scattering and radiation by three-dimensional buried objects. *IEEE Transactions on Geoscience and Remote Sensing*, 37(2):887–900, 1999.

[100] Leung Tsang. Near-field radiation from microstrip lines. *Microwave and Optical Technology Letters*, 19(3):176–184, 1998.

[101] Amit Hochman and Yehuda Leviatan. A numerical methodology for efficient evaluation of 2d sommerfeld integrals in the dielectric half-space problem. *IEEE Transactions on Antennas and Propagation*, 58(2):413–431, 2009.

[102] Joel T Johnson, Jin A Kong, Robert T Shin, David H Staelin, Kevin O'Neill, and AW Lananick. Third stokes parameter emission from a periodic water surface. *IEEE transactions on geoscience and remote sensing*, 31(5):1066–1080, 1993.

[103] GV Rozhnov. Electromagnetic scattering from statistically rough sourfaces. *Sov. Phys. JETP*, 67:240–247, 1988.

[104] W Peake. Interaction of electromagnetic waves with some natural surfaces. *IRE Transactions on Antennas and Propagation*, 7(5):324–329, 1959.

[105] Joel T Johnson, Robert T Shin, Jin Au Kong, Leung Tsang, and Kyung Pak. A numerical study of ocean polarimetric thermal emission. *IEEE transactions on geoscience and remote sensing*, 37(1):8–20, 1999.

[106] SV Nghiem, ME Veysoglu, JA Kong, RT Shin, K O'Neill, and AW Lohanick. Polarimetric passive remote sensing of a periodic soil surface: microwave measurements and analysis. *Journal of electromagnetic waves and applications*, 5(9):997–1005, 1991.

[107] K C Jezek, J T Johnson, M R Drinkwater, G Macelloni, L Tsang, M Aksoy, and M Durand. Radiometric approach for estimating relative changes in intraglacier average temperature. *IEEE Transactions on Geoscience and Remote Sensing*, 53(1): 134–143, 2015.

[108] Murat E Veysoglu, HA Yueh, RT Shin, and JA Kong. Polarimetric passive remote sensing of periodic surfaces. *Journal of Electromagnetic Waves and Applications*, 5 (3):267–280, 1991.

[109] Zahn D, K Sarabandi, K F Sabet, and J Harvey. Numerical simulation of scattering from rough surfaces: A wavelet-based approach. *IEEE Transactions on Antennas and Propagation*, 48(2):246–253, Feb 2000.

[110] GV Rozhnov. Electromagnetic-wave diffraction by multilayer media with rough interfaces. *Sov. Phys. JETP*, 69(3):646–651, 1989.

[111] Emil Wolf. Unified theory of coherence and polarization of random electromagnetic beams. *Physics letters A*, 312(5-6):263–267, 2003.

[112] Hema Roychowdhury, Sergey A Ponomarenko, and Emil Wolf*. Change in the polarization of partially coherent electromagnetic beams propagating through the turbulent atmosphere. *Journal of Modern Optics*, 52(11):1611–1618, 2005.

[113] Jani Tervo, Tero Setälä, and Ari T Friberg. Degree of coherence for electromagnetic fields. *Optics express*, 11(10):1137–1143, 2003.

[114] David Paganin and Keith A Nugent. Noninterferometric phase imaging with partially coherent light. *Physical review letters*, 80(12):2586, 1998.

[115] Bagley J Q, L Tsang, K H Ding, and A Ishimaru. Optical transmission through a plasmon film lens with small roughness: Enhanced spatial resolution of images of single source and multiple sources. *Optical Society of America B*, 28(7):1766–1777, 2011.

[116] Mohammadreza Sanamzadeh and Leung Tsang. A partially coherent approach for scattering of electromagnetic waves from random layered media with 3d rough interfaces. In *2019 USNC-URSI Radio Science Meeting (Joint with AP-S Symposium)*, pages 89–90. IEEE, 2019.

[117] Mohammadreza Sanamzadeh, Leung Tsang, and Joel T Johnson. Scattering and emission of electromagnetic waves from random layered media with random rough interfaces; a partially coherent cascading approach. In *IEEE Transactions on Antennas and Propagation, Accepted for publication*. IEEE, 2019.

[118] Chen-To Tai. *Dyadic Green functions in electromagnetic theory*. Institute of Electrical & Electronics Engineers (IEEE), 1994.

[119] Robert E Collin. Field theory of guided waves. 1960.

[120] Leopold B Felsen and Nathan Marcuvitz. *Radiation and scattering of waves*, volume 31. John Wiley & Sons, 1994.

[121] Weng Cho Chew. *Waves and fields in inhomogeneous media*. IEEE press, 1995.

[122] Leung Tsang, Kung-Hau Ding, Tien-Hao Liao, and Shaowu Huang. Modeling of scattering in arbitrary-shape waveguide using broadband green's function with higher order low wavenumber extractions. *IEEE Transactions on Electromagnetic Compatibility*, 60(1):16–25, 2017.

[123] Simon Félix, Mark Asch, Marcel Filoche, and Bernard Sapoval. Localization and increased damping in irregular acoustic cavities. *Journal of sound and vibration*, 299 (4-5):965–976, 2007.

[124] B Sapoval, S Russ, and JN Chazalviel. Eigenstates in irregular quantum wells: application to porous silicon. *Journal of Physics: Condensed Matter*, 8(34):6235, 1996.

[125] Ernst Jan R Vesseur, F Javier García de Abajo, and Albert Polman. Broadband purcell enhancement in plasmonic ring cavities. *Physical Review B*, 82(16):165419, 2010.

[126] Shurun Tan and Leung Tsang. Efficient broadband evaluations of lattice green's functions via imaginary wavenumber components extractions. *Progress In Electromagnetics Research*, 164:63–74, 2019.

[127] Shurun Tan and Leung Tsang. Green's functions, including scatterers, for photonic crystals and metamaterials. *JOSA B*, 34(7):1450–1458, 2017.

[128] Shurun Tan and Leung Tsang. Scattering of waves by a half-space of periodic scatterers using broadband green's function. *Optics letters*, 42(22):4667–4670, 2017.

[129] Paolo Arcioni, Maurizio Bozzi, Marco Bressan, Giuseppe Conciauro, and Luca Perregrini. The bi-rme method: An historical overview. In *2014 International Conference on Numerical Electromagnetic Modeling and Optimization for RF, Microwave, and Terahertz Applications (NEMO)*, pages 1–4. IEEE, 2014.

[130] Maurizio Bozzi, Luca Perregrini, and Ke Wu. Modeling of conductor, dielectric, and radiation losses in substrate integrated waveguide by the boundary integral-resonant mode expansion method. *IEEE Transactions on Microwave Theory and Techniques*, 56(12):3153–3161, 2008.

[131] Marco Guglielmi, Roberto Sorrentino, and Giuseppe Conciauro. *Advanced Modal Analysis: CAD Techniques for Waveguide Components and Filter*. John Wiley & Sons, Inc., 1999.

[132] Leung Tsang and Shaowu Huang. Broadband green's function with low wavenumber extraction for arbitrary shaped waveguide and applications to modeling of vias in finite power/ground plane. *Prog. Electromagn. Res.*, 152:105–125, 2015.

[133] Amir Borji and Safieddin Safavi-Naeini. Rapid calculation of the green's function in a rectangular enclosure with application to conductor loaded cavity resonators. *IEEE transactions on microwave theory and techniques*, 52(7):1724–1731, 2004.

[134] Mohammadreza Sanamzadeh and Leung Tsang. Fast and broadband computation of green's function in cavity resonator of irregular shape using imaginary wave number extraction technique. *Journal of Optical Society of America, Accepted for publication*, 2019.

[135] Mohammadreza Sanamzadeh and Leung Tsang. Fast and broad band calculation of the dyadic green's function in the rectangular cavity; an imaginary wave number extraction technique. *Progress In Electromagnetics Research*, 96:243–258, 2019.

[136] Filippo Marliani and A Ciccolella. Computationally efficient expressions of the dyadic green's function for rectangular enclosures. *Progress In Electromagnetics Research*, 31:195–223, 2001.

[137] Myun-Joo Park and Sangwook Nam. Rapid summation of the green's function for the rectangular waveguide. *IEEE transactions on microwave theory and techniques*, 46(12):2164–2166, 1998.

[138] Rodolfo Araneo and Giampiero Lovat. An efficient mom formulation for the evaluation of the shielding effectiveness of rectangular enclosures with thin and thick apertures. *IEEE transactions on Electromagnetic Compatibility*, 50(2):294–304, 2008.

[139] David A Hill. *Electromagnetic fields in cavities: deterministic and statistical theories*, volume 35. John Wiley & Sons, 2009.

[140] Francisco Javier Perez Soler, Fenando D Quesada Pereira, David Cañete Rebenaque, Alejandro Alvarez Melcon, and Juan R Mosig. A novel efficient technique for the calculation of the green's functions in rectangular waveguides based on accelerated series decomposition. *IEEE transactions on antennas and propagation*, 56(10):3260–3270, 2008.

[141] Myun-Joo Park. Accelerated summation of the green's function for the rectangular cavity. *IEEE Microwave and Wireless Components Letters*, 19(5):260–262, 2009.

[142] Michael E Gruber and Thomas F Eibert. A hybrid ewald-spectral cavity green's function boundary element method with spectral domain acceleration for modeling of over-moded cavities. *IEEE Transactions on Antennas and Propagation*, 63(6): 2627–2635, 2015.

[143] Salvatore Campione and Filippo Capolino. Ewald method for 3d periodic dyadic green's functions and complex modes in composite materials made of spherical particles under the dual dipole approximation. *Radio science*, 47(06):1–11, 2012.

[144] Leung Tsang and Shurun Tan. Calculations of band diagrams and low frequency dispersion relations of 2d periodic dielectric scatterers using broadband green's function with low wavenumber extraction (bbgfl). *Optics Express*, 24(2):945–965, 2016.

[145] Shaowu Huang and Leung Tsang. Fast electromagnetic analysis of emissions from printed circuit board using broadband green's function method. *IEEE Transactions on Electromagnetic Compatibility*, 58(5):1642–1652, 2016.

[146] Jie Li, Xin Fu, and Balasubramaniam Shanker. Decoupled potential integral equations for electromagnetic scattering from dielectric objects. *IEEE Transactions on Antennas and Propagation*, 67(3):1729–1739, 2018.

[147] Qin S Liu, Li Jun Jiang, Sheng Sun, Qi Dai, and Weng Cho Chew. Theory of potential-based integral-form a-$\phi$ formulation in electromagnetic applications. In *2018 Progress in Electromagnetics Research Symposium (PIERS-Toyama)*, pages 2280–2286. IEEE, 2018.

[148] Reid K McCargar. An implicit gauge condition for auxiliary potentials in inhomogeneous media. *IEEE Transactions on Antennas and Propagation*, 66(5):2684–2685, 2018.

[149] Qin S Liu, Sheng Sun, Qi I Dai, Weng Cho Chew, and Li Jun Jiang. Theory of characteristic modes based on potential-based integral equation. In *2016 URSI International Symposium on Electromagnetic Theory (EMTS)*, pages 292–295. IEEE, 2016.

[150] Timothy M Philip and Matthew J Gilbert. Theory of ac quantum transport with fully electrodynamic coupling. *Journal of Computational Electronics*, 17(3):934–948, 2018.

[151] Weng Cho Chew, Aiyin Y Liu, Carlos Salazar-Lazaro, and Wei EI Sha. Quantum electromagnetics: A new look—part i. *IEEE Journal on Multiscale and Multiphysics Computational Techniques*, 1:73–84, 2016.

[152] Weng Cho Chew. Some observations on the spatial and eigenfunction representations of dyadic green's functions (electromagnetic theory). *IEEE transactions on antennas and propagation*, 37(10):1322–1327, 1989.

[153] J Wang. A unified and consistent view on the singularities of the electric dyadic green's function in the source region. *IEEE Transactions on Antennas and Propagation*, 30 (3):463–468, 1982.

[154] Arthur D Yaghjian. Electric dyadic green's functions in the source region. *Proceedings of the IEEE*, 68(2):248–263, 1980.

[155] WA Johnson, AQ Howard, and DG Dudley. On the irrotational component of the electric green's dyadic. *Radio Science*, 14(6):961–967, 1979.

[156] Yahya Rahmat-Samii. On the question of computation of the dyadic green's function at the source region in waveguides and cavities (short papers). *IEEE Transactions on Microwave Theory and Techniques*, 23(9):762–765, 1975.

[157] Julian Schwinger, Lester L DeRaad Jr, and Kimball A Milton. Casimir effect in dielectrics. *Annals of Physics*, 115(1):1–23, 1978.

[158] Peter W Milonni. *The quantum vacuum: an introduction to quantum electrodynamics*. Academic press, 2013.

[159] Kimball A Milton, Lester L DeRaad Jr, and Julian Schwinger. Casimir self-stress on a perfectly conducting spherical shell. *Annals of Physics*, 115(2):388–403, 1978.

[160] David Deutsch and P Candelas. Boundary effects in quantum field theory. *Physical Review D*, 20(12):3063, 1979.

[161] Roger Balian and Bertrand Duplantier. Electromagnetic waves near perfect conductors. ii. casimir effect. *Annals of Physics*, 112(1):165–208, 1978.

[162] S Leseduarte and August Romeo. Complete zeta-function approach to the electromagnetic casimir effect for spheres and circles. *annals of physics*, 250(2):448–484, 1996.

[163] Michael Bordag, E Elizalde, and K Kirsten. Heat kernel coefficients of the laplace operator on the d-dimensional ball. *Journal of Mathematical Physics*, 37(2):895–916, 1996.

[164] G Lambiase and VV Nesterenko. Quark mass correction to the string potential. *Physical Review D*, 54(10):6387, 1996.

[165] VV Nesterenko and IG Pirozhenko. Justification of the zeta function renormalization in rigid string model. *Journal of Mathematical Physics*, 38(12):6265–6280, 1997.

[166] MT Homer Reid, Alejandro W Rodriguez, Jacob White, and Steven G Johnson. Efficient computation of casimir interactions between arbitrary 3d objects. *Physical review letters*, 103(4):040401, 2009.

[167] Siddhartha Sen. A calculation of the casimir force on a circular boundary. *Journal of Mathematical Physics*, 22(12):2968–2973, 1981.

[168] Lester L DeRaad Jr and Kimball A Milton. Casimir self-stress on a perfectly conducting cylindrical shell. *Annals of Physics*, 136(2):229–242, 1981.

[169] AV Nesterenko and VV Nesterenko. Mode by mode summation for the zero point electromagnetic energy of an infinite solid cylinder. *Physical Review D*, 59:105009.

[170] Iver Brevik and GH Nyland. Casimir force on a dielectric cylinder. *Annals of Physics*, 230(2):321–342, 1994.

[171] Sergei M Rytov, Yurii A Kravtsov, and Valeryan I Tatarskii. Principles of statistical radiophysics. 4. wave propagation through random media. *Principles of statistical radiophysics. 4. Wave propagation through random media., by Rytov, SM; Kravtsov, YA; Tatarskii, VI. Springer, Berlin (Germany, FR), 1989, 198 p., ISBN 3-540-17828-7,*, 1989.

[172] Evgenni Mikhailovich Lifshitz, M Hamermesh, et al. The theory of molecular attractive forces between solids. In *Perspectives in Theoretical Physics*, pages 329–349. Elsevier, 1992.

[173] William MR Simpson. *Surprises in theoretical Casimir physics: quantum forces in inhomogeneous media*. Springer, 2014.

[174] Lev Davidovich Landau. *The classical theory of fields*, volume 2. Elsevier, 2013.

[175] Jin Au Kong. *Theory of electromagnetic waves*. New York, Wiley-Interscience, 1975.